Diversity of Secondary Structure in Catalytic Peptides with β-Turn-Biased Sequences

Anthony J. Metrano, Nadia C. Abascal,

Brandon Q. Mercado, Eric K. Paulson, Anna E. Hurtley, and Scott J. Miller*

Department of Chemistry, Yale University, New Haven, CT 06520-8107, United States

*E-mail: scott.miller@yale.edu

Supporting Information

Table of Contents

I. General Information

Room temperature (rt) is defined as 21–23 °C. All reagents were purchased from commercial suppliers and used without further purification, unless otherwise noted. Methylene chloride (CH_2Cl_2) and toluene (PhMe) were obtained from a Seca Solvent System by GlassContour, in which the solvent was dried over alumina and dispensed under an atmosphere of argon. All other solvents were purchased from commercial suppliers and used without further purification.

Routine ^{1}H-NMR spectra were recorded on Agilent 500 and 600 MHz spectrometers at ambient temperature unless otherwise noted. NMR solvents, chloroform-*d*, benzene-d_6, methanol-d_4, acetone-d_6, and dimethylsulfoxide-d_6, were purchased from Cambridge Isotope Laboratories and used without further purification. *d*-Chloroform was stored at ambient temperature over 4 Å molecular sieves, and benzene-d_6, methanol-d_4, dimethylsulfoxide-d_6 ampules were used immediately after opening. Spectra were processed with MestReNova 10.0.2 using the automatic phasing and Bernstein (third order) polynomial baseline correction capabilities. Splitting was determined using the automatic multiplet analysis function with intervention as necessary. Spectral data are reported as follows: chemical shift (multiplicity [singlet (s), doublet (d), triplet (t), quartet (q), pentet (p), multiplet (m), doublet of doublets (dd), doublet of doublet of doublets (ddd), doublet of triplet of doublets (dtd), doublet of triplets (dt), triplet of doublets (td), etc.], coupling constant, integration). Chemical shifts are reported in ppm (δ), and coupling constants are reported in Hz. ^{1}H-Resonances are referenced to solvent residual peaks for $CDCl_3$ (7.26 ppm) and C_6D_6 (7.16 ppm).[1] Routine ^{13}C-NMR spectra were recorded on Agilent 500 or 600 MHz spectrometers with protons fully decoupled. ^{13}C-Resonances are reported in ppm relative to solvent residual peaks for $CDCl_3$ (77.2 ppm) or C_6D_6 (128.1 ppm).[1]

Samples for high-resolution liquid chromatography-mass spectrometry (HRMS) were submitted to the Mass Spectrometry Laboratory at the University of Illinois at Urbana-Champaign. Data were acquired on a Waters Synapt G2-Si instrument equipped with an ESI detector. For crude analysis, ultra-high-performance liquid chromatography-mass spectrometry (UPLC/MS) was performed on a Waters Acquity UPLC/MS instrument equipped with a reverse-phase BEH C18 column (1.7 μm particle size, 2.1 x 50 mm), a dual atmospheric pressure chemical ionization (API)/electrospray ionization (ESI) mass spectrometry detector, and a photodiode array detector.

Analytical thin-layer chromatography (TLC) was performed using 60 Å Silica Gel F_{254} pre-coated plates (0.25 mm thickness). TLC plates were visualized by irradiation with a UV lamp. R_f values are reported. Normal-phase flash chromatography was performed using a Biotage Isolera One purification system equipped with a 10, 25, or 50 g SNAP Ultra (HP Sphere, 25 μm silica) cartridge and an appropriate EtOAc/hexanes linear gradient in the mobile phase. Reverse-phase column chromatography was performed using a Biotage Isolera One purification system equipped with a 60 or 120 g SNAP-C18 column and an appropriate MeOH/H_2O linear gradient in the mobile phase. Normal-phase high-performance liquid chromatography (HPLC)

was performed using an Agilent 1100 series instrument equipped with a diode array detector and columns (chiral supports) from Daicel Chemical Industries (Chiralcel OJ-H).

II. Solution Phase Peptide Synthesis and Characterization

A. General Remarks

The solution phase peptide synthesis of catalysts **3**–**33** was accomplished using the *N*-*tert*-butoxycarbonyl (Boc) protecting group strategy.[2] Boc-L-β-Dimethylaminoalanine (**S7**, Boc-Dmaa-OH) was synthesized according to a literature procedure.[3] All other amino acid residues and coupling reagents were purchased from commercial suppliers. Once synthesized, peptides were stored at 0 °C to prevent epimerization and other adverse side-reactivity. Yields are not optimized.

B. Representative Synthesis of Dimethylamide-Containing Peptide 3

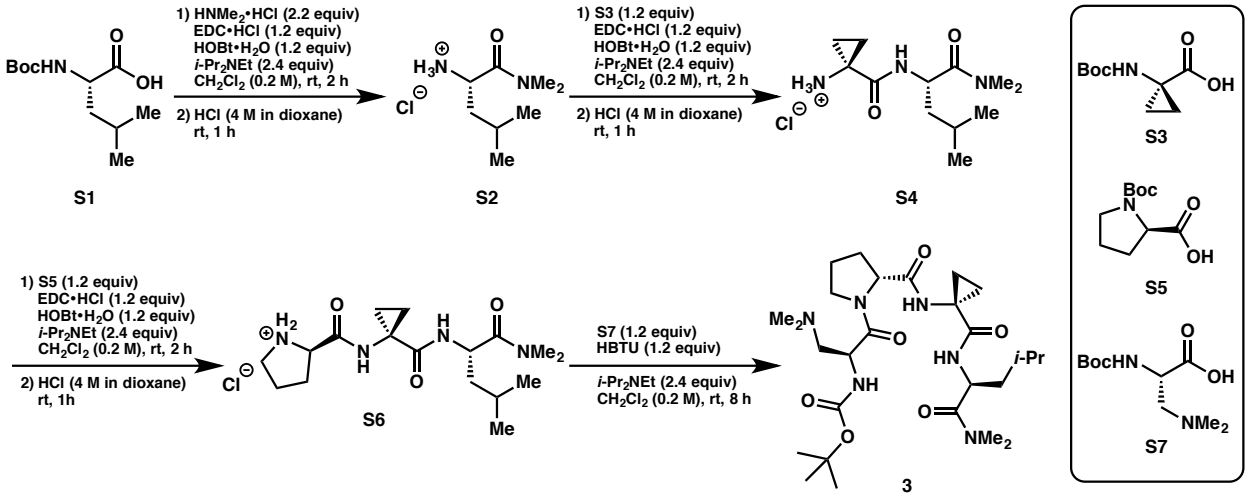

Installation of Dimethyl Amide Cap: Boc-Leu-OH•H_2O (**S1**, 499 mg, 2.00 mmol), dimethylamine hydrochloride (359 mg, 4.40 mmol), and HOBt•H_2O (368 mg, 2.40 mmol) were added to a round bottom flask equipped with a magnetic stir bar. The solid mixture was dissolved in CH_2Cl_2 (10 mL, 0.2 M w.r.t. **S1**), and EDC•HCl (460 mg, 2.40 mmol) was added. The resulting solution was allowed to stir at rt as *i*-Pr_2NEt (0.84 mL, 4.80 mmol) was added slowly, causing the cloudy solution to clarify. The pale yellow reaction solution was allowed to stir at rt for about 2 h, after which the solution was poured into a separatory funnel, diluted to 30 mL with additional CH_2Cl_2, and washed with approximately 25 mL of 10% aqueous (w/v) citric acid. The organic layer was separated and subsequently washed with 25 mL each of saturated aqueous $NaHCO_3$ and brine. The organics were dried over anhydrous Na_2SO_4, filtered, and concentrated *in vacuo* to provide a clear, pale yellow oil (517 mg, > 99% crude yield). The identity of Boc-Leu-NMe_2 was confirmed by UPLC/MS. **MS:** Exact mass calculated for $[C_{13}H_{26}N_2O_3 + H]^+$ requires *m/z* = 259.2. Found 259.2 (ESI+).

Deprotection 1: Crude Boc-Leu-NMe_2 was then treated with 6 mL of 4.0 M HCl in 1,4-dioxane to cleave the Boc group. The resulting pale yellow solution was allowed to stir at rt for 1 h before HCl and 1,4-dioxane were removed *in vacuo*. Residual 1,4-dioxane was removed by co-

evaporation with CH_2Cl_2 to provide 389 mg (> 99% crude yield) of **S2** as a foam, which was dried thoroughly under reduced pressure before being carried forward to the next coupling step.

Peptide Coupling 1: To a flask containing H-Leu-NMe_2•HCl (**S2**, 389 mg, 2.00 mmol) was added Boc-Acpc-OH (**S3**, 483 mg, 2.20 mmol), HOBt•H_2O (368 mg, 2.40 mmol), and a magnetic stir bar. The solid mixture was dissolved in dry CH_2Cl_2 (10 mL, 0.2 M w.r.t. **S2**), and EDC•HCl (460 mg, 2.40 mmol) was then added. The resulting solution was allowed to stir at rt as *i*-Pr_2NEt (0.84 mL, 4.8 mmol) was added slowly. The deep yellow reaction solution was allowed to stir at rt for 2 h, after which the solution was poured into a separatory funnel, diluted to 30 mL with additional CH_2Cl_2, and washed with 25 mL of 10% aqueous (w/v) citric acid. The organic layer was separated and subsequently washed with 25 mL each of saturated aqueous $NaHCO_3$ and brine. The organics were dried over anhydrous Na_2SO_4, filtered, and concentrated *in vacuo* to provide a white foam (739 mg, > 99% crude yield). The identity of Boc-Acpc-Leu-NMe_2 was confirmed by UPLC-MS. **MS:** Exact mass calculated for $[C_{17}H_{31}N_3O_4 + H]^+$ requires *m/z* = 342.2. Found 342.3 (ESI+).

Deprotection 2: Deprotection of the crude dipeptide Boc-Acpc-Leu-NMe_2 was accomplished in the same manner as described in Deprotection 1 (*vide supra*) to provide **S4** (556 mg, 2.00 mmol) as a white foam.

Peptide Coupling 2: To a flask containing H-Acpc-Leu-NMe_2•HCl (**S4**, 556 mg, 2.00 mmol) was added Boc-D-Pro-OH (**S3**, 517 mg, 2.20 mmol), HOBt•H_2O (368 mg, 2.40 mmol), and a magnetic stir bar. The solid mixture was dissolved in dry CH_2Cl_2 (10 mL, 0.2 M w.r.t. **S4**), and EDC•HCl (460 mg, 2.4 mmol) was then added. The resulting solution was allowed to stir at rt as *i*-Pr_2NEt (0.84 mL, 4.8 mmol) was added slowly. The deep yellow reaction solution was allowed to stir at rt for 2 h, after which the solution was poured into a separatory funnel, diluted to 30 mL with additional CH_2Cl_2, and washed with 25 mL of 10% aqueous (w/v) citric acid. The organic layer was separated and subsequently washed with 25 mL each of saturated aqueous $NaHCO_3$ and brine. The organics were dried over anhydrous Na_2SO_4, filtered, and concentrated *in vacuo* to provide a white foam (873 mg, > 99% crude yield). The identity of Boc-D-Pro-Acpc-Leu-NMe_2 was confirmed by UPLC-MS. **MS:** Exact mass calculated for $[C_{22}H_{38}N_4O_5 + H]^+$ requires *m/z* = 439.3. Found 439.4 (ESI+).

Deprotection 3: Deprotection of the crude tripeptide Boc-D-Pro-Acpc-Leu-NMe_2 was accomplished in the same manner as described in Deprotection 1 (*vide supra*) to provide **S6** (750 mg, 2.0 mmol) as an off-white foam.

Peptide Coupling 3: To a flask containing H-D-Pro-Acpc-Leu-NMe_2•HCl (**S6**, 750 mg, 2.0 mmol) was added Boc-Dmaa-OH (**S7**, 511 mg, 2.20 mmol) and a magnetic stir bar. The solid mixture was dissolved in CH_2Cl_2 (10 mL, 0.2 M w.r.t. **S6**), and HBTU (910 mg, 2.4 mmol) was then added to the stirring solution at rt. Next, *i*-Pr_2NEt (0.84 mL, 4.8 mmol) was added slowly. The deep yellow/brown reaction solution was allowed to stir at rt for 8 h, after which the solution was poured into a separatory funnel, diluted to 30 mL with additional CH_2Cl_2, and washed twice with about 25 mL of saturated aqueous $NaHCO_3$. The organic layer was separated and

subsequently washed with 20 mL of brine. The organics were dried over anhydrous Na_2SO_4, filtered, and concentrated *in vacuo* to provide a deep yellow oil. The crude product was loaded onto a Biotage Isolera One purification system for reverse-phase column chromatography (120 g column, 30-100% MeOH/H_2O over 16 column volumes with 3 column volume pre- and post-run equilibrations, 45 mLmin^{-1} flow, collection λ = 210 nm, monitored λ = 254 nm, 16 x 150 mm test tubes with 20 mL fractions). Fractions were pooled, concentrated *in vacuo*, and dried thrice azeotropically with CH_2Cl_2 to provide Boc-Dmaa-D-Pro-Acpc-Leu-NMe_2 (**3**, 667 mg, 60% yield) as a white foam.

C. Representative Synthesis of Methyl Ester-Containing Peptide 4

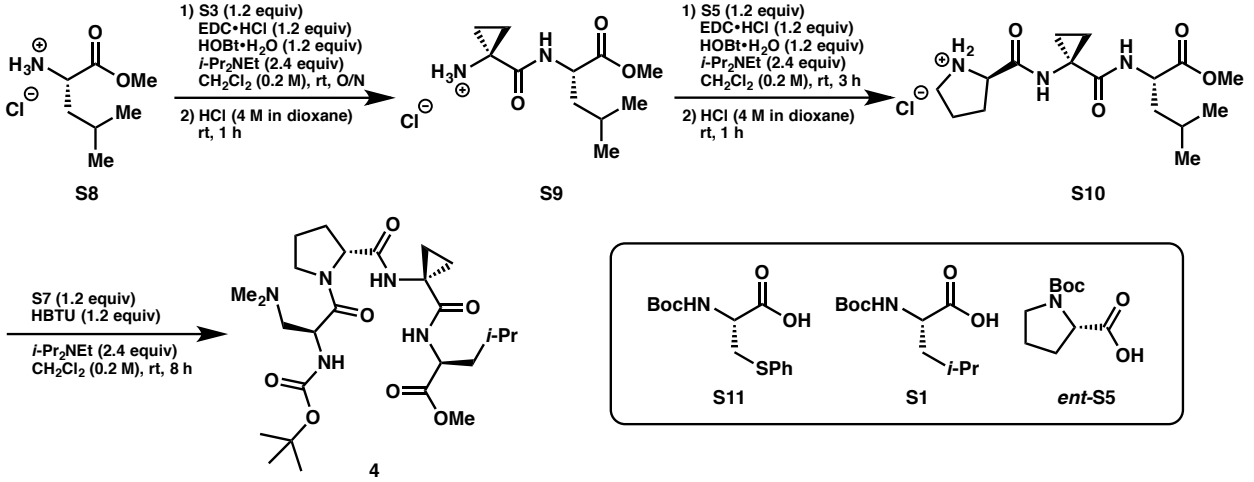

Peptide Coupling 1: To a flask containing H-Leu-OMe•HCl (**S8**, 362 mg, 2.00 mmol) was added Boc-Acpc-OH (**S3**, 483 mg, 2.40 mmol), HOBt•H_2O (368 mg, 2.40 mmol), and a magnetic stir bar. The solid mixture was dissolved in dry CH_2Cl_2 (10 mL, 0.2 M w.r.t. **S8**), and EDC•HCl (460 mg, 2.4 mmol) was then added. The resulting solution was allowed to stir at rt as *i*-Pr_2NEt (0.84 mL, 4.8 mmol) was added slowly. The clear, colorless reaction solution was allowed to stir at rt for overnight, after which the solution was poured into a separatory funnel, diluted to 30 mL with additional CH_2Cl_2, and washed with 25 mL of 10% aqueous (w/v) citric acid. The organic layer was separated and subsequently washed with 25 mL each of saturated aqueous $NaHCO_3$ and brine. The organics were dried over anhydrous Na_2SO_4, filtered, and concentrated *in vacuo* to provide an off-white waxy solid (772 mg, > 99% crude yield). The identity of Boc-Acpc-Leu-OMe was confirmed by UPLC-MS. **MS:** Exact mass calculated for $[C_{16}H_{28}N_2O_5 + H]^+$ requires *m/z* = 329.2. Found 329.3 (ESI+).

Deprotection 1: Crude Boc-Acpc-Leu-OMe was then treated with 6 mL of 4.0 M HCl in 1,4-dioxane to cleave the Boc group. The resulting pale yellow solution was allowed to stir at rt for 1 h, before HCl and 1,4-dioxane were removed *in vacuo*. Residual 1,4-dioxane was removed by co-evaporation with CH_2Cl_2 to provide 530 mg (> 99% crude yield) of **S9** as a white foam, which was dried thoroughly under reduced pressure before being carried forward to the next coupling step.

Peptide Coupling 2: To a flask containing H-Acpc-Leu-OMe•HCl (**S9**, 530 mg, 2.0 mmol) was added Boc-D-Pro-OH (**S5**, 517 mg, 2.20 mmol), HOBt•H_2O (368 mg, 2.40 mmol), and a magnetic stir bar. The solid mixture was dissolved in dry CH_2Cl_2 (10.0 mL, 0.20 M w.r.t. **S9**), and EDC•HCl (460 mg, 2.40 mmol) was then added. The resulting solution was allowed to stir at rt as *i*-Pr_2NEt (0.84 mL, 4.80 mmol) was added slowly. The clear, pale yellow reaction solution was allowed to stir at rt for 3 h, after which the solution was poured into a separatory funnel, diluted to 30 mL with additional CH_2Cl_2, and washed with 25 mL of 10% aqueous (w/v) citric acid. The organic layer was separated and subsequently washed with 25 mL each of saturated aqueous $NaHCO_3$ and brine. The organics were dried over anhydrous Na_2SO_4, filtered, and concentrated *in vacuo* to provide a white foam (851 mg, 1.86 mmol, 93% crude yield). The identity of Boc-D-Pro-Acpc-Leu-OMe was confirmed by UPLC-MS. **MS:** Exact mass calculated for $[C_{21}H_{35}N_3O_6 + H]^+$ requires *m/z* = 426.3. Found 426.4 (ESI+). ***Note:** To access peptides **15**, **21**, and **30**, Boc-Pro-OH (***ent*-S5**) was coupled to **S9** instead of **S5** using an otherwise identical procedure.

Deprotection 2: Deprotection of the crude tripeptide Boc-D-Pro-Acpc-Leu-OMe was accomplished in the same manner as described in Deprotection 1 (*vide supra*) to provide 672 mg of **S10** (1.86 mmol, > 99% crude yield) as an off-white foam.

Peptide Coupling 3: To a flask containing H-D-Pro-Acpc-Leu-OMe•HCl (**S10**, 672 mg, 1.86 mmol) was added Boc-Dmaa-OH (**S7**, 518 mg, 2.23 mmol) and a magnetic stir bar. The solid mixture was dissolved in CH_2Cl_2 (9.3 mL, 0.20 M w.r.t. **S10**), and HBTU (846 mg, 2.23 mmol) was then added to the stirring solution at rt. Next, *i*-Pr_2NEt (0.78 mL, 4.46 mmol) was added slowly. The deep yellow reaction solution was allowed to stir at rt for 8 h, after which the solution was poured into a separatory funnel, diluted to 30 mL with additional CH_2Cl_2, and washed twice with about 25 mL of saturated aqueous $NaHCO_3$. The organic layer was separated and subsequently washed with 20 mL of brine. The organics were dried over anhydrous Na_2SO_4, filtered, and concentrated *in vacuo* to provide a deep yellow oil. The crude product was loaded onto a Biotage Isolera One purification system for reverse-phase column chromatography (120 g column, 30-100% MeOH/H_2O over 16 column volumes with 3 column volume pre- and post-run equilibrations, 45 $mLmin^{-1}$ flow, collection λ = 210 nm, monitored λ = 254 nm, 16 x 150 mm test tubes with 20 mL fractions). Fractions were pooled, concentrated *in vacuo*, and dried thrice azeotropically with CH_2Cl_2 to provide Boc-Dmaa-D-Pro-Acpc-Leu-OMe (**4l**, 759 mg, 76% yield) as a white foam. ***Note:** To access peptides **5** and **23**, Boc-Cys(Ph)-OH (**S11**) was coupled to **S10** instead of **S7** using a procedure identical to Peptide Coupling 2 (EDC/HOBt instead of HBTU). To access peptide **6**, Boc-Leu-OH (**S1**) was coupled to **S10** instead of **S7** using an otherwise identical procedure.

D. Characterization of Peptides

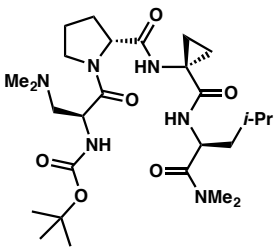

Boc-Dmaa-D-Pro-Acpc-Leu-NMe$_2$ (3): White foamy solid, 60% overall yield from **S1** using the dimethyl amide procedure.[4] **^{1}H-NMR** (500 MHz, $CDCl_3$): δ 7.55 (d, *J* = 8.5 Hz, 1H), 7.16 (s, 1H), 6.48 (d, *J* = 6.3 Hz, 1H), 4.92 (td, *J* = 8.6, 5.1 Hz, 1H), 4.39 (q, *J* = 7.1 Hz, 1H), 4.36 (dd, *J* = 7.6, 4.1 Hz, 1H), 4.03–3.91 (m, 1H), 3.60 (dt, *J* = 9.9, 6.8 Hz, 1H), 3.10 (s, 3H), 2.91 (s, 3H), 2.72 (dd, *J* = 12.3, 7.6 Hz, 1H), 2.46 (dd, *J* = 12.3, 7.2 Hz, 1 H), 2.26 (s, 6H), 2.16–2.10 (m, 3H), 1.99–1.90 (m, 1H), 1.73–1.61 (m, 2H), 1.55–1.46 (m, 3H), 1.40 (s, 9H), 0.97 (dq, *J* = 6.3, 3.2 Hz, 2H), 0.92 (dd, *J* = 9.4, 6.4 Hz, 6H). **^{13}C-NMR** (126 MHz, $CDCl_3$): δ 172.5, 172.3, 171.5, 171.1, 156.5, 79.9, 76.9, 61.3, 60.1, 50.6, 47.7, 47.5, 45.9, 41.8, 37.3, 36.0, 34.6, 28.9, 28.5, 25.1, 24.7, 23.4, 22.4, 17.2, 17.1. **HRMS:** Exact mass calculated for $[C_{27}H_{48}N_6O_6 + H]^+$ requires *m/z* = 553.3714. Found 553.3709 (ESI+).

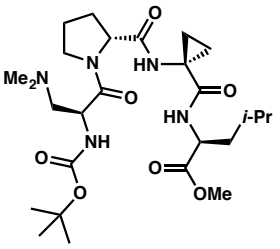

Boc-Dmaa-D-Pro-Acpc-Leu-OMe (4): White foamy solid, 76% overall yield from **S8** using the methyl ester procedure.[5] **^{1}H-NMR** (500 MHz, $CDCl_3$): δ 7.64 (s, 1H), 7.40 (d, *J* = 7.7 Hz, 1H), 5.78 (s, 1H), 4.48 (ddd, *J* = 9.0, 7.6, 5.3 Hz, 1H), 4.40 (dd, *J* = 8.5, 4.3 Hz, 1H), 4.34–4.22 (m, 1H), 4.00 (dt, *J* = 9.9, 6.3 Hz, 1H), 3.68 (s, 3H), 3.58 (dt, *J* = 9.7, 7.5 Hz, 1H), 2.67 (t, *J* = 11.1 Hz, 1H), 2.48–2.35 (m, 1H), 2.28 (s, 6H), 2.18 (dq, *J* = 12.9, 8.2 Hz, 1H), 2.13–2.02 (m, 1H), 2.02–1.89 (m, 2H), 1.71 (ddt, *J* = 13.8, 6.7, 5.0 Hz, 3H), 1.60 (tt, *J* = 9.9, 5.3 Hz, 1H), 1.41 (s, 9H), 1.31–1.27 (m, 1H), 1.02–0.93 (m, 2H), 0.90 (dd, *J* = 9.6, 6.2 Hz, 6H). **^{13}C-NMR** (126 MHz, $CDCl_3$): δ 173.5, 172.3, 171.5, 171.2, 156.7, 80.7, 61.7, 59.4, 51.9, 51.6, 50.8, 47.9, 45.7, 41.3, 34.6, 29.5, 28.5, 28.4, 24.8, 24.8, 23.0, 22.0, 17.1, 16.8. **HRMS:** Exact mass calculated for $[C_{26}H_{45}N_5O_7 + H]^+$ requires *m/z* = 540.3397. Found 540.3394 (ESI+).

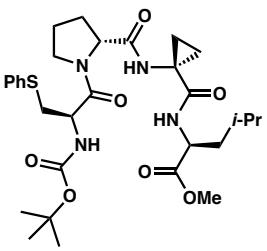

Boc-Cys(Ph)-D-Pro-Acpc-Leu-OMe (5): Pale yellow powder, 84% overall yield from **S8** using the methyl ester procedure. **^{1}H-NMR** (500 MHz, $CDCl_3$): δ 7.50 (d, *J* = 8.2 Hz, 1H), 7.39 (d, *J* = 7.6 Hz, 2H), 7.31 (t, *J* = 7.6 Hz, 2H), 7.22 (t, *J* = 7.3 Hz, 1H), 6.97 (bs, 1H), 5.80 (d, *J* = 6.4 Hz, 1H), 4.59 (dt, *J* = 14.1, 7.0 Hz, 1H), 4.45 (q, *J* = 6.7 Hz, 1H), 4.18 (dd, *J* = 8.2, 4.6 Hz, 1H), 3.82–3.73 (m, 1H), 3.69 (s, 2H), 3.51–3.42 (m, 1H), 3.30 (dd, *J* = 13.7, 8.1 Hz, 1H), 3.17 (dd, *J* = 13.7, 6.3 Hz, 1H), 2.13–2.03 (m, 1H), 2.03–1.92 (m, 2H), 1.92–1.81 (m, 1H), 1.78–1.68 (m, 2H), 1.68–1.57 (m, 2H), 1.50–1.35 (m, 10H), 1.00–0.86 (m, 9H). **^{13}C-NMR** (151 MHz, $CDCl_3$): δ 174.0, 172.3, 171.4, 170.9, 156.1, 134.9, 129.5, 129.3, 126.9, 80.7, 61.6, 52.2, 52.1, 51.3, 47.8, 41.3, 35.1, 34.6, 29.2, 28.4, 25.0, 24.8, 23.1, 22.0, 17.3, 17.2. **HRMS:** Exact mass calculated for $[C_{30}H_{44}N_4O_7S + H]^+$ requires *m/z* = 605.3009. Found 605.3007 (ESI+).

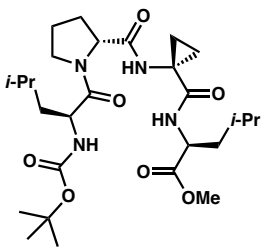

Boc-Leu-D-Pro-Acpc-Leu-OMe (6): White powder, 44% overall yield from **S8** using the methyl ester procedure. **^{1}H-NMR** (500 MHz, $CDCl_3$): δ 7.46 (d, *J* = 7.9 Hz, 1H), 7.30 (bs, 1H), 5.28 (bd, *J* = 6.0 Hz, 1H), 4.52 (ddd, *J* = 9.2, 7.7, 5.3 Hz, 1H), 4.41 (dd, *J* = 8.5, 4.3 Hz, 1H), 4.28 (dt, *J* = 8.5, 5.6 Hz, 1H), 4.03 (dt, *J* = 9.7, 6.3 Hz, 1H), 3.69 (s, 3H), 3.55 (dt, *J* = 9.8, 7.4 Hz, 1H), 2.20 (dq, *J* = 12.9, 8.2 Hz, 1H), 2.14–2.05 (m, 1H), 2.04–1.96 (m, 2H), 1.78–1.65 (m, 4H), 1.65–1.46 (m, 3H), 1.46–1.43 (m, 1H), 1.42 (s, 9H), 1.36 (dd, *J* = 10.2, 4.2 Hz, 1H), 1.02–0.93 (m, 7H), 0.92 (dd, *J* = 10.1, 6.3 Hz, 6H). **^{13}C-NMR** (151 MHz, $CDCl_3$): δ 173.7, 172.7, 171.7, 156.9, 110.2, 80.8, 61.5, 52.1, 51.6, 51.2, 47.7, 41.1, 40.4, 34.7, 29.4, 28.4, 24.9, 24.8, 24.8, 23.4, 23.0, 22.2, 21.9, 17.6, 17.1. **HRMS:** Exact mass calculated for $[C_{27}H_{46}N_4O_7 + H]^+$ requires *m/z* = 539.3445. Found 539.3446 (ESI+).

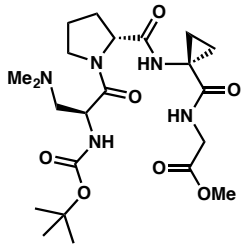

Boc-Dmaa-D-Pro-Acpc-Gly-OMe (7): White, foamy solid, 44% overall yield from **S8** using the methyl ester procedure.[4,5] **^{1}H-NMR** (500 MHz, $CDCl_3$): δ 7.73 (s, 1H), 7.52 (t, *J* = 5.7 Hz, 1H), 5.69 (s, 1H), 4.49 (t, *J* = 6.3 Hz, 1H), 4.32– 4.23 (m, 1H), 4.07–3.93 (m, 3H), 3.71 (s, 3H), 3.57 (q, *J* = 8.2 Hz, 1H), 2.67 (t, *J* = 11.0 Hz, 1H), 2.37 (dd, *J* = 12.5, 4.9 Hz, 1H), 2.27 (s, 6H), 2.20–2.10 (m, 2H), 1.99 (p, *J* = 7.0 Hz, 2H), 1.75–1.67 (m, 1H), 1.40 (s, 9H), 1.37–1.29 (m, 1H), 1.06–0.93 (m, 2H). **^{13}C-NMR** (126 MHz, $CDCl_3$): δ 172.1, 172.0, 171.4, 170.1, 156.5, 110.0, 80.6, 61.4, 58.9, 52.0, 50.7, 47.7, 45.4, 41.8, 34.5, 29.2, 28.2, 24.6, 17.0, 16.7. **HRMS:** Exact mass calculated for $[C_{22}H_{37}N_5O_7 + H]^+$ requires *m/z* = 484.2771. Found 484.2768 (ESI+).

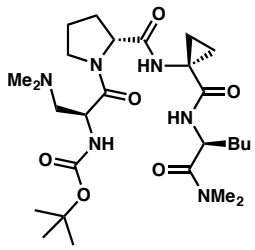

Boc-Dmaa-D-Pro-Acpc-Nle-NMe$_2$ (8): White solid, 53% overall yield from **S1** using the dimethyl amide procedure.[4] **^{1}H-NMR** (500 MHz, $CDCl_3$): δ 7.55 (d, *J* = 8.3 Hz, 1H), 7.21 (s, 1H), 6.45 (d, *J* = 6.2 Hz, 1H), 4.84 (td, *J* = 7.9, 6.2 Hz, 1H), 4.43–4.29 (m, 2H), 3.91 (dt, *J* = 10.5, 5.7 Hz, 1H), 3.60 (dt, *J* = 9.9, 6.9 Hz, 1H), 3.08 (s, 3H), 2.92 (s, 3H), 2.71 (dd, *J* = 12.3, 7.3 Hz, 1H), 2.47 (dd, *J* = 12.3, 7.4 Hz, 1H), 2.26 (s, 6H), 2.18–2.12 (m, 1H), 2.11–2.00 (m, 2H), 1.99–1.90 (m, 1H), 1.83–1.72 (m, 1H), 1.72–1.63 (m, 1H), 1.54–1.46 (m, 2H), 1.39 (s, 9H), 1.35–1.20 (m, 4H), 1.04–0.91 (m, 2H), 0.89–0.82 (m, 3H). **^{13}C-NMR** (126 MHz, $CDCl_3$): δ 172.4, 172.0, 171.5, 171.0, 156.5, 79.9, 61.3, 60.1, 50.7, 49.3, 47.5, 45.9, 37.4, 35.9, 34.6, 32.5, 28.8, 28.5, 27.7, 25.1, 22.7, 17.3, 17.0, 14.1. **HRMS:** Exact mass calculated for $[C_{27}H_{48}N_6O_6 + H]^+$ requires *m/z* = 553.3714. Found 553.3707 (ESI+).

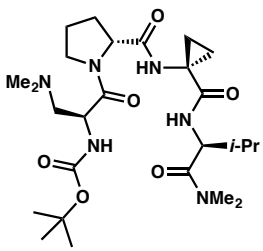

Boc-Dmaa-D-Pro-Acpc-Val-NMe$_2$ (9): White solid, 54% overall yield from **S1** using the dimethyl amide procedure.[4,5] **^{1}H-NMR** (500 MHz, $CDCl_3$): δ 7.45 (d, *J* = 8.7 Hz, 1H), 7.28 (s, 1H), 6.40 (bs, 1H), 4.62 (t, *J* = 8.5 Hz, 1H), 4.40 (dd, *J* = 7.6, 4.5 Hz, 1H), 4.36 (q, *J* = 7.0 Hz, 1H), 3.97–3.87 (m, 1H), 3.59 (dt, *J* = 10.0, 6.9 Hz, 1H), 3.12 (s, 3H), 2.92 (s, 3H), 2.73–2.59 (m, 1H), 2.52 (dd, *J* = 12.4, 7.8 Hz, 1H), 2.26 (s, 6H), 2.22–2.13 (m, 1H), 2.13–2.02 (m, 3H), 2.01–1.87 (m, 1H), 1.55 (dt, *J* = 10.1, 3.5 Hz, 1H), 1.48–1.40 (m, 1H), 1.38 (s, 9H), 1.01–0.93 (m, 5H), 0.89 (d, *J* = 6.7 Hz, 3H). **^{13}C-NMR** (126

MHz, $CDCl_3$): δ 172.4, 171.8, 171.6, 171.4, 156.6, 79.9, 61.4, 59.9, 54.7, 50.7, 47.5, 45.9, 37.6, 35.8, 34.6, 31.3, 28.9, 28.4, 25.0, 19.5, 18.7, 17.4, 17.0. **HRMS:** Exact mass calculated for $[C_{26}H_{46}N_6O_6 + H]^+$ requires *m/z* = 539.3557. Found 539.3555 (ESI+).

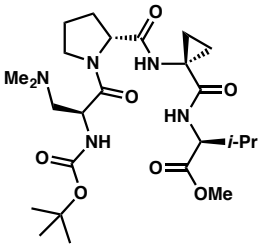

Boc-Dmaa-D-Pro-Acpc-Val-OMe (10): White solid, 56% overall yield from **S8** using the methyl ester procedure.[5] **^{1}H-NMR** (500 MHz, $CDCl_3$): δ 7.12–6.95 (m, 2H), 5.77 (s, 1H), 4.52–4.42 (m, 2H), 4.39 (td, *J* = 7.2, 5.3 Hz, 1H), 3.98–3.81 (m, 1H), 3.69 (s, 3H), 3.61–3.47 (m, 1H), 2.59 (d, *J* = 6.9 Hz, 1H), 2.34–2.22 (m, 6H), 2.21–2.11 (m, 1H), 2.11–2.03 (m, 1H), 2.03–1.92 (m, 2H), 1.50 (d, *J* = 7.3 Hz, 6H), 1.41 (s, 9H), 0.93 (dd, *J* = 6.9, 4.6 Hz, 6H). **^{13}C-NMR** (126 MHz, $CDCl_3$): δ 174.4, 172.8, 171.2, 170.7, 155.9, 110.2, 80.0, 61.4, 59.8, 57.6, 57.4, 51.9, 50.9, 47.6, 45.7, 31.4, 28.5, 25.8, 25.6, 24.9, 19.2, 18.2. **HRMS:** Exact mass calculated for $[C_{25}H_{43}N_5O_7 + H]^+$ requires *m/z* = 526.3241. Found 526.3240 (ESI+).

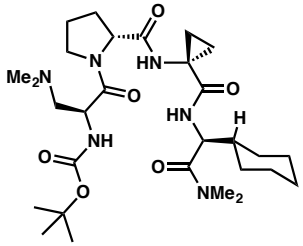

Boc-Dmaa-D-Pro-Acpc-Chg-NMe_2 (11): White solid, 61% overall yield from **S1** using the dimethyl amide procedure.[4] **^{1}H-NMR** (500 MHz, $CDCl_3$): δ 7.48 (d, *J* = 8.7 Hz, 1H), 7.18 (s, 1H), 6.56 (d, *J* = 6.5 Hz, 1H), 4.66 (t, *J* = 8.5 Hz, 1H), 4.50–4.29 (m, 2H), 3.88 (dt, *J* = 10.8, 6.0 Hz, 1H), 3.59 (dt, *J* = 9.8, 6.6 Hz, 1H), 3.10 (s, 3H), 2.91 (s, 3H), 2.85–2.63 (m, 1H), 2.44 (dd, *J* = 12.3, 7.1 Hz, 1H), 2.25 (s, 6H), 2.22–1.98 (m, 3H), 1.98–1.89 (m, 1H), 1.90–1.75 (m, 2H), 1.76–1.56 (m, 4H), 1.54–1.43 (m, 2H), 1.38 (s, 9H), 1.33–1.04 (m, 3H), 1.04–0.81 (m, 4H). **^{13}C-NMR** (126 MHz, $CDCl_3$): δ 172.4, 171.7, 171.4, 171.3, 156.5, 79.8, 61.2, 60.0, 53.9, 50.6, 47.4, 45.9, 40.6, 37.7, 35.8, 34.6, 29.8, 28.8, 28.8, 28.4, 26.4, 26.2, 26.1, 25.1, 17.4, 17.0. **HRMS:** Exact mass calculated for $[C_{29}H_{50}N_6O_6 + H]^+$ requires *m/z* = 579.3870. Found 579.3860 (ESI+).

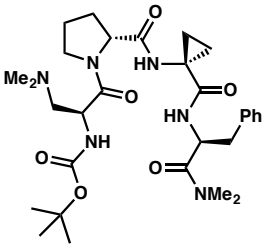

Boc-Dmaa-D-Pro-Acpc-Phe-NMe_2 (12): White, foamy solid, 30% overall yield from **S1** using the dimethyl amide procedure.[4–6] **^{1}H-NMR** (500 MHz, $CDCl_3$): δ 7.69 (d, *J* = 8.2 Hz, 1H), 7.37 (s, 1H), 7.27–7.14 (m, 5H), 6.52 (d, *J* = 6.0 Hz, 1H), 5.03 (ddd, *J* = 9.3, 8.2, 5.8 Hz, 1H), 4.46–4.38 (m, 2H), 3.92 (dd, *J* = 8.1, 6.6 Hz, 1H), 3.61 (dt, *J* = 9.7, 7.0 Hz, 1H), 3.11 (dd, *J* = 13.0, 9.4 Hz, 1H), 3.02 (dd, *J* = 13.0, 5.8 Hz, 1H), 2.77 (s, 3H), 2.73 (dd, *J* = 12.8 Hz, 1H), 2.62 (s, 3H), 2.60–2.49 (m, 1H), 2.29 (s, 6H), 2.17–2.08 (m, 2H), 2.08–2.00 (m, 1H), 2.00–1.91 (m, 1H), 1.53–1.43 (m, 2H), 1.39 (s, 9H), 1.04–0.95 (m, 1H), 0.97–0.91 (m, 1H). **^{13}C-NMR** (126 MHz, $CDCl_3$): δ 172.6, 171.7, 171.4, 171.0, 156.6, 137.1, 129.5, 128.4, 126.8, 80.0, 61.4, 59.9, 50.8, 50.7, 47.6, 45.9, 39.2, 37.0, 35.7, 34.6, 28.9, 28.4, 25.0, 17.3, 17.2. **HRMS:** Exact mass calculated for $[C_{30}H_{46}N_6O_6 + H]^+$ requires *m/z* = 587.3557. Found 587.3551 (ESI+).

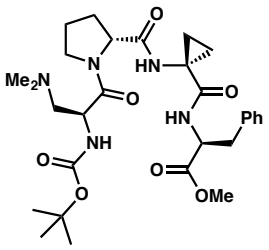

Boc-Dmaa-D-Pro-Acpc-Phe-OMe (13): White foamy solid, 7% overall yield from **S8** using the methyl ester procedure.[5] **^{1}H-NMR** (600 MHz, $CDCl_3$): δ 7.61 (s, 1H), 7.51 (d, *J* = 7.5 Hz, 1H), 7.30–7.22 (m, 3H), 7.22–7.15 (m, 2H), 5.73 (s, 1H), 4.70 (q, *J* = 7.2 Hz, 1H), 4.43 (t, *J* = 6.2 Hz, 1H), 4.31–4.25 (m, 1H), 4.03–3.95 (m, 1H), 3.61 (s, 3H), 3.56 (q, *J* = 8.2 Hz, 1H), 3.15–3.07 (m, 2H), 2.66 (t, *J* = 11.1 Hz, 1H), 2.45–2.36 (m, 1H), 2.28 (s, 6H), 2.19–2.11 (m, 2H), 2.01–1.91 (m, 2H), 1.69–1.57 (m, 1H), 1.42 (s, 9H), 1.37–1.30 (m, 1H), 1.01–0.95 (m, 2H). **^{13}C-NMR** (151 MHz, $CDCl_3$): δ 172.2, 172.2, 171.5, 171.3, 156.7, 137.0, 129.6, 128.4, 126.7, 80.7, 61.6, 59.4, 54.7, 52.0, 50.7, 47.8, 45.7, 38.4, 34.6, 29.4, 28.4, 24.7, 17.3, 17.1. **HRMS:** Exact mass calculated for $[C_{29}H_{43}N_5O_7 + H]^+$ requires *m/z* = 574.3241. Found 574.3235 (ESI+).

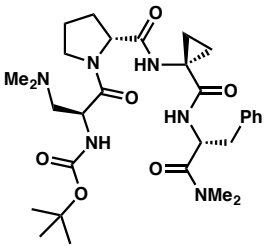

Boc-Dmaa-D-Pro-Acpc-D-Phe-NMe$_2$ (14): White, foamy solid, 56% overall yield from **S1** using the dimethyl amide procedure.[4] **^{1}H-NMR** (500 MHz, $CDCl_3$): δ 7.60 (d, *J* = 7.9 Hz, 1H), 7.50 (s, 1H), 7.24–7.23 (m, 4H), 7.18 (dq, *J* = 8.5, 3.8 Hz, 1H), 5.92 (d, *J* = 4.4 Hz, 1H), 4.98 (ddd, *J* = 9.4, 7.9, 4.7 Hz, 1H), 4.49–4.47 (m, 1H), 4.33 (dt, *J* = 9.5, 5.3 Hz, 1H), 4.11–3.81 (m, 1H), 3.56 (q, *J* = 8.1 Hz, 1H), 3.11 (dd, *J* = 13.0, 9.5 Hz, 1H), 2.93 (dd, *J* = 12.9, 4.6 Hz, 1H), 2.81 (s, 3H), 2.63 (dd, *J* = 12.4, 9.1 Hz, 1H), 2.59 (s, 3H), 2.47 (dd, *J* = 12.5, 5.9 Hz, 1H), 2.25 (s, 6H), 2.23–2.21 (m, 1H), 2.14–1.84 (m, 3H), 1.65–1.51 (m, 1H), 1.47–1.43 (m, 1H), 1.39 (s, 9H), 1.13–0.89 (m, 2H). **^{13}C-NMR** (126 MHz, $CDCl_3$): δ 172.3, 171.4, 171.1, 170.7, 156.4, 137.5, 129.8, 128.3, 126.6, 80.2, 61.3, 59.7, 51.4, 50.8, 47.6, 45.7, 39.5, 36.9, 35.7, 34.8, 29.0, 28.5, 24.9, 17.2. **HRMS:** Exact mass calculated for $[C_{30}H_{46}N_6O_6 + H]^+$ requires *m/z* = 587.3557. Found 587.3549 (ESI+).

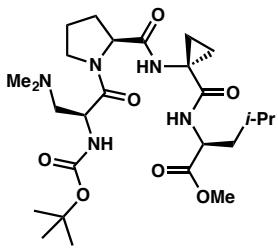

Boc-Dmaa-Pro-Acpc-Leu-OMe (15): White, foamy solid, 72% overall yield from **S8** using the methyl ester procedure.[5] **^{1}H-NMR** (600 MHz, $CDCl_3$): δ 7.94 (s, 1H), 7.38 (d, *J* = 8.1 Hz, 1H), 5.38–5.20 (m, 1H), 4.66 (q, *J* = 7.4 Hz, 1H), 4.59–4.42 (m, 2H), 3.92 (m, 1H), 3.70 (s, 3H), 3.66–3.55 (m, 1H), 2.91–2.54 (m, 2H), 2.34–2.31 (m, 7H), 1.94–1.99 (m, 3H), 1.76–1.62 (m, 3H), 1.42 (s, 11H), 1.00 (ddd, *J* = 10.1, 7.7, 4.8 Hz, 1H), 0.94 (dd, *J* = 10.9, 6.0 Hz, 6H), 0.82–1.79 (m, 1H). **^{13}C-NMR** (151 MHz, $CDCl_3$): δ 173.1, 172.0, 171.7, 155.3, 80.4, 62.2, 61.3, 52.3, 51.6, 50.7, 48.2, 46.7, 41.3, 34.6, 29.4, 28.5, 28.4, 25.3, 24.9, 23.0, 22.0, 17.5, 16.9. **HRMS:** Exact mass calculated for $[C_{26}H_{45}N_5O_7 + H]^+$ requires *m/z* = 540.3397. Found 540.3387 (ESI+).

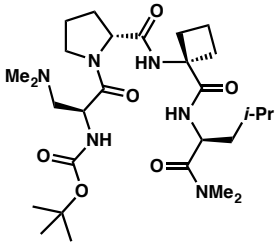

Boc-Dmaa-D-Pro-Acbc-Leu-NMe$_2$ (16): White solid, 39% overall yield from **S1** using the dimethyl amide procedure. **^{1}H-NMR** (500 MHz, $CDCl_3$): δ 7.24 (s, 1H), 7.15 (d, *J* = 8.8 Hz, 1H), 6.37 (s, 1H), 4.99 (td, *J* = 8.9, 5.0 Hz, 1H), 4.56 – 4.35 (m, 2H), 3.84 (brs, 1H), 3.58 (q, *J* = 8.0 Hz, 1H), 3.11 (s, 3H), 2.90 (s, 3H), 2.87 – 2.77 (m, 2H), 2.63 – 2.51 (m, 2H), 2.37 (s, 5H), 2.31 – 2.21 (m, 2H), 2.19 – 2.07 (m, 3H), 2.07 – 1.91 (m, 4H), 1.70 – 1.52 (m, 2H), 1.49 (d, *J* = 4.8 Hz, 1H), 1.41 (s, 9H), 0.93 (dd,

J = 26.5, 6.4 Hz, 6H). **^{13}C-NMR** (126 MHz, $CDCl_3$): δ 172.9, 172.3, 170.9, 156.0, 79.8, 60.9, 59.8, 59.4, 50.6, 47.4, 47.1, 45.7, 42.1, 37.3, 35.9, 32.3, 31.1, 28.5, 28.3, 25.0, 24.8, 23.4, 22.3, 16.0. **HRMS:** Exact mass calculated for $[C_{28}H_{50}N_6O_6 + H]^+$ requires *m/z* = 567.3870. Found 567.3859 (ESI+).

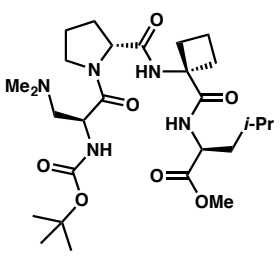

Boc-Dmaa-D-Pro-Acbc-Leu-OMe (17): White solid, 70% overall yield from **S8** using the methyl ester procedure.[1] **^{1}H-NMR** (600 MHz, $CDCl_3$): δ 7.47 (s, 1H), 7.05 (d, *J* = 7.9 Hz, 1H), 5.75 (brs, 1H), 4.56–4.49 (m, 1H), 4.47–4.42 (m, 1H), 4.32 (s, 1H), 3.97 (s, 1H), 3.67 (s, 3H), 3.56 (q, *J* = 8.2 Hz, 1H), 2.86–2.77 (m, 1H), 2.67–2.58 (m, 1H), 2.37–2.18 (m, 9H), 2.15–1.87 (m, 7H), 1.72–1.53 (m, 3H), 1.39 (s, 9H), 0.90 (dd, *J* = 6.4, 1.2 Hz, 6H). **^{13}C-NMR** (151 MHz, $CDCl_3$): δ 173.5, 173.4, 170.8, 156.1, 80.3, 77.4, 77.2, 76.9, 61.1, 59.5, 59.3, 52.0, 51.0, 50.9, 47.7, 45.6, 41.3, 31.6, 31.5, 29.0, 28.6, 28.5, 24.8, 24.8, 23.0, 22.0, 15.9. **HRMS:** Exact mass calculated for $[C_{27}H_{47}N_5O_7 + H]^+$ requires *m/z* = 554.3554. Found 554.3571 (ESI+).

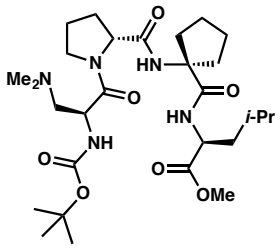

Boc-Dmaa-D-Pro-Cle-Leu-OMe (18): White, foamy solid, 30% overall yield from **S8** using the methyl ester procedure. **^{1}H-NMR** (500 MHz, $CDCl_3$): δ 7.16 (d, *J* = 8.1 Hz, 1H), 7.00 (s, 1H), 5.79 (brs, 1H), 4.56 (td, *J* = 8.7, 5.4 Hz, 1H), 4.40 (dd, *J* = 7.8, 3.7 Hz, 2H), 3.91 (s, 1H), 3.67 (s, 3H), 3.60–3.54 (m, 1H), 2.63 (s, 2H), 2.41–2.17 (m, 9H), 2.08–1.88 (m, 5H), 1.85–1.71 (m, 2H), 1.71–1.55 (m, 5H), 1.42 (s, 9H), 0.91 (dd, *J* = 6.4, 1.5 Hz, 6H). **^{13}C-NMR** (126 MHz, $CDCl_3$): δ 186.1, 174.0, 173.8, 170.9, 156.0, 80.2, 67.2, 61.4, 52.0, 51.0, 50.9, 47.7, 45.7, 41.3, 37.3, 37.2, 28.7, 28.5, 24.9, 24.9, 24.8, 24.6, 23.1, 22.0. **HRMS:** Exact mass calculated for $[C_{28}H_{49}N_5O_7 + H]^+$ requires *m/z* = 568.3710. Found 568.3697 (ESI+).

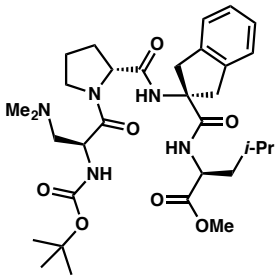

Boc-Dmaa-D-Pro-Aic-Leu-OMe (19): White, foamy solid, 74% overall yield from **S8** using the methyl ester procedure.[5] **^{1}H-NMR** (500 MHz, $CDCl_3$): δ 7.24–7.18 (m, 2H), 7.18–7.10 (m, 4H), 5.73 (brs, 1H), 4.72–4.49 (m, 1H), 4.35 (dd, *J* = 8.1, 3.8 Hz, 1H), 4.30 (dt, *J* = 9.0, 5.2 Hz, 1H), 3.81–3.73 (m, 2H), 3.69–3.63 (m, 4H), 3.50 (q, *J* = 7.8 Hz, 1H), 3.43 (d, *J* = 16.8 Hz, 1H), 3.26 (d, *J* = 16.7 Hz, 1H), 2.64–2.46 (m, 2H), 2.29 (s, 6H), 2.19–2.07 (m, 1H), 2.05–1.94 (m, 1H), 1.94–1.83 (m, 2H), 1.79–1.57 (m, 3H), 1.47 (s, 9H), 0.93 (dd, *J* = 6.3, 2.7 Hz, 6H). **^{13}C-NMR** (126 MHz, $CDCl_3$): δ 173.6, 172.9, 171.3, 171.0, 156.0, 140.8, 140.5, 126.8, 126.7, 124.6, 80.2, 67.4, 61.3, 59.6, 52.0, 51.3, 51.0, 47.6, 45.6, 43.7, 43.6, 41.2, 28.7, 28.6, 24.9, 24.8, 23.1, 22.0. **HRMS:** Exact mass calculated for $[C_{32}H_{49}N_5O_7 + H]^+$ requires *m/z* = 616.3710. Found 616.3706 (ESI+).

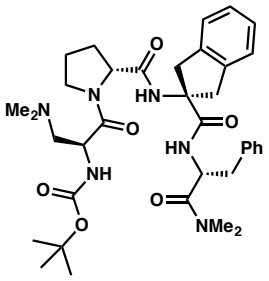

Boc-Dmaa-D-Pro-Aic-D-Phe-NMe$_2$ (20): White, foamy solid, 54% overall yield from **S1** using the dimethyl amide procedure.[6] **^{1}H-NMR** (500 MHz, $CDCl_3$): δ 7.53 (d, *J* = 8.1 Hz, 1H), 7.32 (s, 1H), 7.26–7.18 (m, 4H), 7.21–7.14 (m, 1H), 7.17–7.09 (m, 4H), 5.88 (d, *J* = 5.5 Hz, 1H), 5.02 (q, *J* = 7.6 Hz, 1H), 4.44–4.38 (m, 1H), 4.36 (q, *J* = 6.9 Hz, 1H), 3.84–3.75 (m, 1H), 3.68 (d, *J* = 16.7 Hz, 1H), 3.61 (d, *J* = 16.6 Hz, 1H), 3.52 (q, *J* = 7.9 Hz, 1H), 3.35 (d, *J* = 16.7 Hz, 1H), 3.28 (d, *J* = 16.6 Hz, 1H), 3.00–2.93 (m, 2H), 2.80 (s, 3H), 2.68 (m, 1H), 2.59 (s, 3H), 2.56–2.49 (m, 2H), 2.24 (s, 6H), 2.19–2.11 (m, 1H), 2.03–1.93 (m, 2H), 1.92–1.85 (m, 1H), 1.39 (s, 9H). **^{13}C-NMR** (126 MHz, $CDCl_3$): δ 172.7, 171.6, 171.3, 171.1, 156.0, 140.7, 140.0, 137.2, 129.6, 128.3, 126.8, 126.7, 126.7, 124.6, 124.4, 110.1, 80.0, 67.2, 61.0, 60.0, 51.1, 50.8, 47.5, 45.7, 44.2, 43.3, 39.2, 37.0, 35.8, 28.7, 28.4, 24.8. **HRMS:** Exact mass calculated for $[C_{36}H_{50}N_6O_6 + H]^+$ requires *m/z* = 663.3870. Found 663.3885 (ESI+).

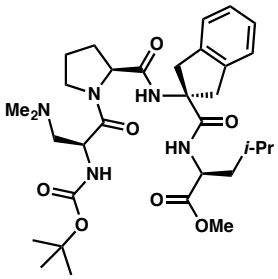

Boc-Dmaa-Pro-Aic-Leu-OMe (21): White, foamy solid, 75% overall yield from **S8** using the methyl ester procedure.[5] NMR Spectra show conformational isomerism (~20% minor conformer in $CDCl_3$). **Major Rotamer (80%): ^{1}H-NMR** (500 MHz, $CDCl_3$): δ 7.33 (d, *J* = 8.0 Hz, 1H), 7.22 (s, 1H), 7.18–7.07 (m, 4H), 5.31 (d, *J* = 6.8 Hz, 1H), 4.57–4.50 (m, 1H), 4.48–4.42 (m, 2H), 3.80–3.74 (m, 1H), 3.74 (d, *J* = 16.6 Hz, 1H), 3.69 (s, 3H), 3.61 (d, *J* = 16.5 Hz, 1H), 3.57–3.50 (m, 1H), 3.39 (d, *J* = 21.3 Hz, 1H), 3.26 (d, *J* = 16.5 Hz, 1H), 2.54–2.43 (m, 2H), 2.25 (s, 6H), 2.12–2.00 (m, 2H), 1.97–1.86 (m, 2H), 1.68–1.51 (m, 3H), 1.49–1.36 (s, 9H), 0.92 (dd, *J* = 8.2, 5.8 Hz, 6H). **^{13}C-NMR** (126 MHz, $CDCl_3$): δ 173.3, 173.0, 171.8, 171.4, 155.6, 140.7, 139.9, 127.0, 126.9, 124.7, 124.5, 80.1, 67.4, 61.4, 60.8, 52.1, 51.4, 47.8, 46.1, 43.8, 43.1, 41.2, 32.0, 28.4, 28.1, 25.2, 25.0, 23.0, 22.0. **Minor Rotamer (20%): ^{1}H-NMR** (500 MHz, $CDCl_3$): δ 7.44 (s, 1H), 7.25–7.23 (m, 1H), 7.18–7.07 (m, 4H), 5.49 (d, *J* = 5.5 Hz, 1H), 4.65 (td, 8.9, *J* = 5.0 Hz, 1H), 4.58–4.50 (m, 1H), 4.49–4.41 (m, 1H), 3.98 (d, *J* = 16.8 Hz, 1H), 3.65 (s, 3H), 3.47–3.41 (m, 1H), 3.30 (d, *J* = 16.9 Hz, 1H), 3.26–3.22 (m, 1H), 3.23–3.18 (m, 1H), 2.58 (dd, *J* = 12.7, 8.9 Hz, 1H), 2.43–2.33 (m, 2H), 2.26 (s, 6H), 1.99–1.85 (m, 2H), 1.75 (dt, *J* = 13.8, 7.1 Hz, 1H), 1.69–1.57 (m, 2H), 1.54 (dd, 8.5, *J* = 5.0 Hz, 1H), 1.46 (s, 9H), 1.44–1.36 (m, 1H), 0.95–0.89 (m, 3H), 0.87 (d, *J* = 6.3, 3H). **^{13}C-NMR** (126 MHz, $CDCl_3$): δ 173.9, 172.3, 171.8, 171.0, 156.9, 141.5, 138.9, 127.2, 126.7, 124.7, 124.5, 80.5, 67.9, 61.1, 60.2, 52.1, 51.7, 50.7, 46.6, 45.9, 44.1, 42.4, 41.1, 32.0, 28.6, 25.0, 22.8, 22.2, 21.9. **HRMS:** Exact mass calculated for $[C_{32}H_{49}N_5O_7 + H]^+$ requires *m/z* = 616.3710. Found 616.3702 (ESI+).

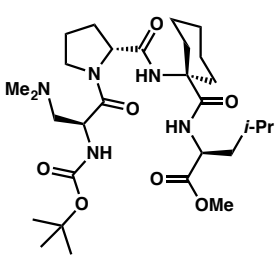

Boc-Dmaa-D-Pro-Achc-Leu-OMe (22): White, foamy solid, 25% overall yield from **S8** using the methyl ester procedure. **^{1}H-NMR** (500 MHz, $CDCl_3$): δ 7.10 (d, *J* = 8.2 Hz, 1H), 6.90 (s, 1H), 5.72 (brs, 1H), 4.57 (td, *J* = 8.7, 5.4 Hz, 1H), 4.51–4.37 (m, 2H), 4.03–3.89 (m, 1H), 3.66 (s, 3H), 3.62–3.51 (m, 1H), 2.58 (s, 2H), 2.30 (d, *J* = 15.1 Hz, 7H), 2.20–1.95 (m, 5H), 1.92–1.72 (m, 2H), 1.72–1.51 (m, 6H), 1.41 (s, 9H), 1.45–1.19 (m, 3H), 0.91 (d, *J* = 6.4 Hz, 6H). **^{13}C-NMR** (126 MHz, $CDCl_3$): δ 174.5,

173.9, 172.0, 170.5, 155.8, 80.0, 61.4, 60.3, 59.8, 52.0, 50.8, 50.7, 47.6, 45.7, 41.4, 32.0, 31.6, 28.5, 28.4, 25.3, 25.0, 24.9, 23.1, 21.9, 21.7, 21.6. **HRMS:** Exact mass calculated for $[C_{29}H_{51}N_5O_7 + H]^+$ requires *m/z* = 582.3867. Found 582.3858 (ESI+).

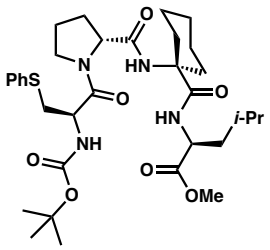

Boc-Cys(Ph)-D-Pro-Achc-Leu-OMe (23): Yellow/orange powder, 68% overall yield from **S8** using the methyl ester procedure. **^{1}H-NMR** (500 MHz, $CDCl_3$): δ 7.40 (d, *J* = 7.7 Hz, 2H), 7.31 (t, *J* = 7.6 Hz, 2H), 7.21 (t, *J* = 7.5 Hz, 2H), 4.72–4.53 (m, 2H), 4.26 (dd, *J* = 7.7, 3.9 Hz, 1H), 3.68 (s, 4H), 3.46 (q, *J* = 7.4 Hz, 1H), 3.24 (ddd, *J* = 40.0, 13.7, 7.0 Hz, 2H), 2.24–2.02 (m, 4H), 2.01–1.78 (m, 4H), 1.70–1.57 (m, 7H), 1.42 (s, 9H), 1.34–1.15 (m, 4H), 0.92 (t, *J* = 6.1 Hz, 6H). **^{13}C-NMR** (151 MHz, $CDCl_3$): δ 174.2, 174.1, 170.7, 170.6, 144.0, 135.5, 129.3, 129.3, 126.6, 80.2, 61.4, 60.6, 52.3, 52.0, 50.6, 47.6, 41.3, 35.5, 32.8, 31.0, 28.5, 28.5, 28.4, 25.2, 25.2, 24.9, 23.2, 21.9, 21.6, 21.4. **HRMS:** Exact mass calculated for $[C_{33}H_{50}N_4O_7S + H]^+$ requires *m/z* = 647.3478. Found 647.3464 (ESI+).

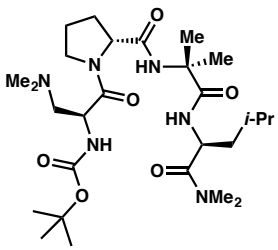

Boc-Dmaa-D-Pro-Aib-Leu-NMe$_2$ (24): White, foamy solid, 66% overall yield from **S1** using the dimethyl amide procedure.[5] **^{1}H-NMR** (500 MHz, $CDCl_3$): δ 7.19 (d, *J* = 8.9 Hz, 1H), 6.88 (s, 1H), 6.44 (d, *J* = 6.6 Hz, 1H), 4.97 (td, *J* = 9.0, 4.8 Hz, 1H), 4.43 (q, *J* = 7.1 Hz, 1H), 4.36 (dd, *J* = 7.7, 4.0 Hz, 1H), 3.82 (td, *J* = 7.6, 4.6 Hz, 1H), 3.56 (dt, *J* = 9.8, 7.0 Hz, 1H), 3.10 (s, 3H), 2.90 (s, 3H), 2.85–2.67 (m, 1H), 2.42 (dd, *J* = 12.2, 7.2 Hz, 1H), 2.29 (s, 6H), 2.28–2.18 (m, 1H), 2.17–2.02 (m, 1H), 1.98–1.85 (m, 2H), 1.68–1.56 (m, 2H), 1.51 (s, 3H), 1.48 (dd, *J* = 8.9, 5.8 Hz, 1H), 1.44 (s, 3H), 1.41 (s, 9H), 0.92 (dd, *J* = 21.4, 6.3 Hz, 6H). **^{13}C-NMR** (126 MHz, $CDCl_3$): δ 173.9, 172.4, 171.2, 170.9, 155.9, 79.5, 61.2, 60.1, 57.2, 50.6, 47.4, 47.1, 45.8, 42.1, 37.3, 35.9, 28.5, 28.1, 27.3, 25.1, 24.8, 24.2, 23.4, 22.3. **HRMS:** Exact mass calculated for $[C_{27}H_{50}N_6O_6 + H]^+$ requires *m/z* = 555.3870. Found 555.3869 (ESI+).

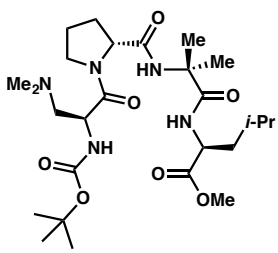

Boc-Dmaa-D-Pro-Aib-Leu-OMe (25): White, foamy solid, 72% overall yield from **S8** using the methyl ester procedure.[5] **^{1}H-NMR** (500 MHz, $CDCl_3$): δ 7.08 (d, *J* = 8.2 Hz, 1H), 6.95 (s, 1H), 5.72 (s, 1H), 4.55 (td, *J* = 8.6, 5.5 Hz, 1H), 4.43–4.29 (m, 2H), 3.96–3.85 (m, 1H), 3.67 (s, 3H), 3.60–3.47 (m, 1H), 2.54 (d, *J* = 7.3 Hz, 2H), 2.28 (s, 6H), 2.27–2.19 (m, 1H), 2.08 (ddd, *J* = 11.4, 6.1, 2.6 Hz, 1H), 2.03–1.89 (m, 2H), 1.69–1.55 (m, 3H), 1.48 (d, *J* = 2.3 Hz, 6H), 1.41 (s, 9H), 0.91 (d, *J* = 6.4 Hz, 6H). **^{13}C-NMR** (126 MHz, $CDCl_3$): δ 174.3, 173.8, 171.3, 170.6, 155.9, 110.2, 80.0, 61.3, 59.8, 57.3, 52.0, 51.0, 50.9, 47.6, 45.7, 41.4, 28.5, 25.8, 25.5, 24.9, 24.9, 23.1, 22.0. **HRMS:** Exact mass calculated for $[C_{26}H_{47}N_5O_7 + H]^+$ requires *m/z* = 542.3554. Found 542.3543 (ESI+).

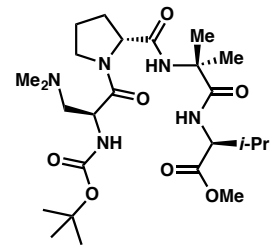

Boc-Dmaa-D-Pro-Aib-Val-OMe (26): White, foamy solid, 56% overall yield from **S8** using the methyl ester procedure.[5] **^{1}H-NMR** (500 MHz, $CDCl_3$): δ 7.12–6.95 (m, 2H), 5.77 (brs, 1H), 4.52–4.42 (m, 2H), 4.39 (td, *J* = 7.2, 5.3 Hz, 1H), 3.98–3.81 (m, 1H), 3.69 (s, 3H), 3.61–3.47 (m, 1H), 2.64–2.54 (m, 2H), 2.31 (s, 6H), 2.29–2.21 (m, 1H), 2.20–1.91 (m, 4H),

1.50 (d, *J* = 7.3 Hz, 6H), 1.41 (s, 9H), 0.93 (dd, *J* = 6.9, 4.6 Hz, 6H). **^{13}C-NMR** (126 MHz, $CDCl_3$): δ 174.4, 172.8, 171.2, 170.7, 155.9, 110.2, 80.0, 61.4, 59.8, 57.6, 57.4, 51.9, 50.9, 47.6, 45.7, 31.4, 28.5, 25.8, 25.6, 24.9, 19.2, 18.2. **HRMS:** Exact mass calculated for $[C_{25}H_{45}N_5O_7 + H]^+$ requires *m/z* = 528.3397. Found 528.3398 (ESI+).

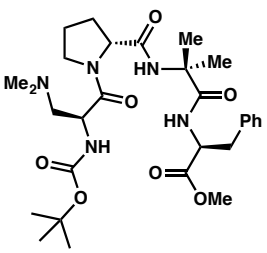

Boc-Dmaa-D-Pro-Aib-Phe-OMe (27): White, foamy solid, 8–23% overall yield from **S8** using the methyl ester procedure.[4–7] **^{1}H-NMR** (600 MHz, $CDCl_3$): δ 7.28–7.26 (m, 2H), 7.22–7.16 (m, 3H), 7.11 (d, *J* = 8.0 Hz, 1H), 6.90 (s, 1H), 5.71 (brs, 1H), 4.81 (app q, *J* = 7.1 Hz, 1H), 4.44–4.34 (m, 2H), 3.92–3.84 (m, 1H), 3.64 (s, 3H), 3.58–3.51 (m, 1H), 3.23–3.01 (m, 2H), 2.58–2.48 (m, 2H), 2.28 (s, 6H), 2.29–2.19 (m, 1H), 2.13–2.03 (m, 1H), 2.02–1.90 (m, 2H), 1.61 (s, 2H), 1.48 (s, 3H), 1.42 (s, 9H), 1.37 (s, 3H). **^{13}C-NMR** (151 MHz, $CDCl_3$): δ 174.1, 172.6, 171.3, 170.8, 155.9, 136.8, 129.5, 128.5, 126.9, 79.9, 61.1, 59.9, 57.2, 53.6, 52.2, 50.9, 47.5, 45.8, 38.2, 28.5, 28.4, 26.1, 24.9, 24.9. **HRMS:** Exact mass calculated for $[C_{29}H_{45}N_5O_7 + H]^+$ requires *m/z* = 576.3397. Found 576.3389 (ESI+).

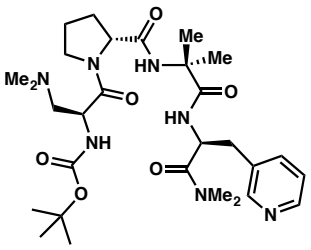

Boc-Dmaa-D-Pro-Aib-3-Pal-NMe$_2$ (28): White, foamy solid, 26% overall yield from **S1** using the dimethyl amide procedure.[5] **^{1}H-NMR** (500 MHz, $CDCl_3$): δ 8.48 (d, *J* = 2.1 Hz, 1H), 8.41 (dd, *J* = 4.9, 1.6 Hz, 1H), 7.58 (dt, *J* = 7.8, 2.0 Hz, 1H), 7.49 (d, *J* = 8.9 Hz, 1H), 7.18 (dd, *J* = 7.8, 4.9 Hz, 1H), 6.95 (s, 1H), 6.52 (d, *J* = 7.0 Hz, 1H), 5.07 (dt, *J* = 8.9, 7.5 Hz, 1H), 4.46 (q, *J* = 7.2 Hz, 1H), 4.31 (dd, *J* = 8.0, 4.4 Hz, 1H), 3.78 (ddd, *J* = 10.1, 7.3, 5.4 Hz, 1H), 3.59 (dt, *J* = 10.0, 6.9 Hz, 1H), 3.09–2.98 (m, 2H), 2.92 (s, 3H), 2.86 (s, 3H), 2.84–2.79 (m, 1H), 2.45 (dd, *J* = 12.3, 6.8 Hz, 1H), 2.28 (s, 6H), 2.17–2.10 (m, 1H), 2.10–2.03 (m, 1H), 2.02–1.95 (m, 1H), 1.94–1.85 (m, 1H), 1.45 (s, 3H), 1.40 (s, 9H), 1.22 (s, 3H). **^{13}C-NMR** (126 MHz, $CDCl_3$): δ 173.7, 171.4, 171.1, 170.7, 156.0, 150.9, 147.9, 137.1, 133.0, 123.4, 79.7, 61.2, 60.3, 57.3, 50.5, 49.5, 47.5, 45.8, 37.3, 36.0, 35.7, 28.5, 26.9, 25.1, 24.2. **HRMS:** Exact mass calculated for $[C_{29}H_{47}N_7O_6 + H]^+$ requires *m/z* = 590.3666. Found 590.3658 (ESI+).

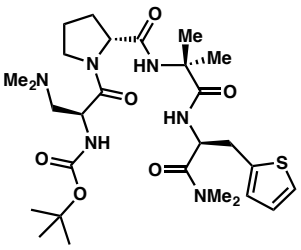

Boc-Dmaa-D-Pro-Aib-2-Thi-NMe$_2$ (29): Off-white, foamy solid, 30% overall yield from **S1** using the dimethyl amide procedure.[5] **^{1}H-NMR** (500 MHz, $CDCl_3$): δ 7.39 (d, *J* = 8.7 Hz, 1H), 7.10 (dd, *J* = 5.0, 1.3 Hz, 1H), 6.89–6.82 (m, 3H), 6.45 (d, *J* = 6.7 Hz, 1H), 5.10 (dt, *J* = 8.6, 7.1 Hz, 1H), 4.43 (q, *J* = 7.1 Hz, 1H), 4.33 (dd, *J* = 7.9, 4.1 Hz, 1H), 3.86–3.76 (m, 1H), 3.57 (dt, *J* = 9.6, 6.9 Hz, 1H), 3.29 (dd, *J* = 14.6, 7.7 Hz, 1H), 3.20 (dd, *J* = 14.5, 6.8 Hz, 1H), 2.92 (s, 3H), 2.85 (s, 3H), 2.75 (dd, *J* = 12.3, 7.3 Hz, 1H), 2.43 (dd, *J* = 12.3, 7.2 Hz, 1H), 2.27 (s, 6H), 2.22–2.15 (m, 1H), 2.13–2.03 (m, 1H), 1.99–1.85 (m, 2H), 1.48 (s, 3H), 1.40 (s, 9H), 1.34 (s, 3H). **^{13}C-NMR** (126 MHz, $CDCl_3$): δ 173.7, 171.3, 171.1, 170.9, 156.0, 139.2, 126.9, 126.4, 124.3, 79.6, 61.1, 60.1, 57.2, 50.6, 50.1, 47.4, 45.9, 37.3, 35.9, 32.8, 28.5, 28.3, 27.0, 25.0, 24.1. **HRMS:** Exact mass calculated for $[C_{28}H_{46}N_6O_6S + H]^+$ requires *m/z* = 595.3278. Found 595.3278 (ESI+).

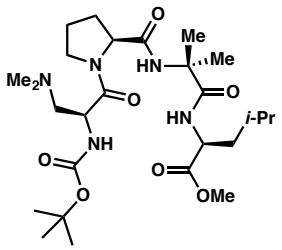

Boc-Dmaa-Pro-Aib-Leu-OMe (30): White, foamy solid, 76% overall yield from **S8** using the methyl ester procedure.[5] NMR Spectra show conformational isomerism (~25% minor conformer in $CDCl_3$). **Major Conformer (75%):** **^{1}H-NMR** (500 MHz, $CDCl_3$): δ 7.16 (d, *J* = 8.0 Hz, 1H), 7.09 (d, *J* = 8.7 Hz, 1H), 6.95 (s, 1H), 5.33 (brs, 1H), 4.55–4.47 (m, 3H), 3.80 (q, *J* = 8.2 Hz, 1H), 3.69 (s, 3H), 3.62–3.57 (m, 1H), 2.71–2.59 (m, 1H), 2.59–2.49 (s, 1H), 2.27 (s, 6H), 2.22–2.15 (m, 1H), 2.11–2.01 (m, 2H), 2.01–1.94 (m, 1H), 1.68–1.54 (m, 3H), 1.49 (s, 3H), 1.48 (s, 3H), 1.42 (s, 9H), 0.92 (dd, *J* = 6.2, 3.5 Hz, 6H). **^{13}C-NMR** (126 MHz, $CDCl_3$): δ 174.2, 173.5, 171.9, 170.9, 155.6, 80.1, 61.4, 61.0, 57.5, 52.1, 51.1, 50.6, 47.8, 46.2, 41.5, 32.1, 28.5, 28.1, 25.7, 25.2, 25.0, 23.0, 22.1. **Minor Conformer (25%):** **^{1}H-NMR** (500 MHz, $CDCl_3$): 7.13 (s, 1H), 7.09 (d, *J* = 8.7 Hz, 1H), 5.47 (bs, 1H), 4.62 (td, *J* = 8.9, 5.2 Hz, 1H), 4.58–4.54 (m, 5 H), 4.44 (q, *J* = 7.6 Hz, 3H), 3.85–3.80 (m, 1H), 3.67–3.61 (m, 1H), 2.64–2.54 (m, 1H), 2.40 (dd, *J* = 12.6, 6.5 Hz, 2H), 2.12–1.97 (m, 2H), 1.96–1.92 (m, 1H), 1.83–1.71 (m, 1H), 1.69–1.53 (m, 3H), 1.52 (s, 3H), 1.51 (s, 3H), 1.41 (s, 9H), 0.95–0.92 (m, 3H), 0.87 (d, *J* = 6.5 Hz, 3H). **^{13}C-NMR** (126 MHz, $CDCl_3$): δ 174.1, 174.0, 172.2, 170.6, 156.5, 80.3, 61.2, 60.4, 57.4, 52.1, 51.6, 51.2, 50.6, 47.0, 45.9, 42.4, 32.2, 28.6, 25.8, 25.6, 24.1, 22.9, 22.2. **HRMS:** Exact mass calculated for $[C_{26}H_{47}N_5O_7 + H]^+$ requires *m/z* = 542.3554. Found 542.3555 (ESI+).

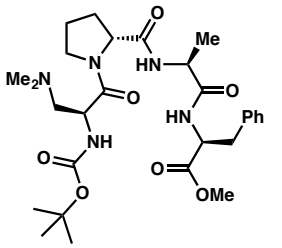

Boc-Dmaa-D-Pro-Ala-Phe-OMe (31): Off-white, foamy solid, uncalculated yield from **S8** using the methyl ester procedure (1.00 mmol scale).[5] **^{1}H-NMR** (600 MHz, $CDCl_3$): δ 7.29–7.09 (m, 6H), 7.05 (d, *J* = 7.5 Hz, 1H), 5.83 (d, *J* = 5.5 Hz, 1H), 4.80 (q, *J* = 6.9 Hz, 1H), 4.49–4.44 (m, 1H), 4.37 (td, *J* = 7.3, 5.2 Hz, 2H), 3.83–3.77 (m, 1H), 3.64 (s, 3H), 3.53 (q, *J* = 8.1 Hz, 1H), 3.17–3.04 (m, 2H), 2.77 (s, 2H), 2.59–2.47 (m, 1H), 2.27 (s, 6H), 2.24–2.18 (m, 1H), 2.04–1.88 (m, 2H), 1.41 (s, 9H), 1.31 (d, *J* = 7.3 Hz, 3H). **^{13}C-NMR** (151 MHz, $CDCl_3$): δ 172.3, 172.1, 171.7, 170.7, 155.9, 136.4, 129.4, 128.5, 126.9, 80.0, 60.8, 59.8, 53.3, 52.3, 50.7, 49.6, 47.3, 45.7, 38.0, 28.9, 28.4, 24.6, 17.3. **HRMS:** Exact mass calculated for $[C_{28}H_{43}N_5O_7 + H]^+$ requires *m/z* = 562.3241. Found 562.3237 (ESI+).

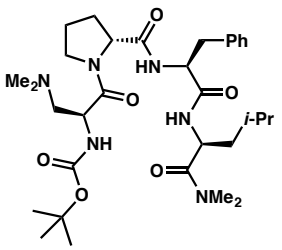

Boc-Dmaa-D-Pro-Phe-Leu-NMe$_2$ (32): White, foamy solid, 85% overall yield from **S1** using the dimethyl amide procedure.[5] **^{1}H-NMR** (500 MHz, $CDCl_3$): δ 7.42 (d, *J* = 9.0 Hz, 1H), 7.30–7.12 (m, 6H), 6.78 (d, *J* = 8.2 Hz, 1H), 6.72 (d, *J* = 9.2 Hz, 1H), 5.01 (td, *J* = 9.4, 4.5 Hz, 1H), 4.77–4.63 (m, 1H), 4.57–4.40 (m, 1H), 4.40–4.20 (m, 1H), 3.83–3.67 (m, 1H), 3.66–3.42 (m, 1H), 3.24 (dd, *J* = 14.0, 7.1 Hz, 1H), 3.12 (s, 3H), 3.07 (dd, *J* = 14.0, 5.0 Hz, 1H), 2.90 (s, 3H), 2.89–2.80 (m, 1H), 2.24 (s, 6H), 2.22–2.07 (m, 2H), 1.94–1.82 (m, 2H), 1.63 (ddd, *J* = 13.8, 9.7, 4.5 Hz, 1H), 1.51–1.41 (m, 2H), 1.41 (s, 9H), 0.90 (dd, *J* = 39.4, 6.4 Hz, 6H). **^{13}C-NMR** (126 MHz, $CDCl_3$): δ 172.0, 171.3, 171.1, 170.1, 156.0, 136.8, 129.5, 128.7, 127.1, 79.5, 60.7, 60.6, 54.5, 50.2, 47.3, 46.8, 45.9, 41.6, 37.3, 35.9, 28.5, 28.1, 25.2, 24.4, 23.4, 22.2. **HRMS:** Exact mass calculated for $[C_{32}H_{52}N_6O_6 + H]^+$ requires *m/z* = 617.4027. Found 617.4023 (ESI+).

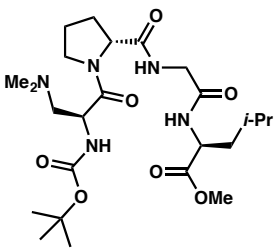

Boc-Dmaa-D-Pro-Gly-Leu-OMe (33): White, foamy solid, 24% overall yield from **S8** using the methyl ester procedure. **^{1}H-NMR** (500 MHz, $CDCl_3$): δ 7.67 (s, 1H), 7.18 (d, *J* = 8.1 Hz, 1H), 5.84 (s, 1H), 4.60–4.46 (m, 2H), 4.34 (d, *J* = 8.2 Hz, 1H), 4.12 (dd, *J* = 17.0, 7.5 Hz, 1H), 4.03 (s, 1H), 3.70 (s, 3H), 3.67–3.51 (m, 2H), 2.73 (s, 1H), 2.48 (s, 1H), 2.33 (s, 6H), 2.28–2.14 (m, 2H), 2.13–1.93 (m, 2H), 1.73–1.56 (m, 3H), 1.41 (s, 9H), 0.91 (t, *J* = 6.4 Hz, 6H). **^{13}C-NMR** (126 MHz, $CDCl_3$): δ 173.3, 171.7, 171.2, 169.2, 156.7, 80.9, 61.6, 59.4, 52.1, 50.9, 47.9, 45.7, 43.4, 41.2, 29.4, 28.4, 24.8, 24.8, 23.0, 21.9. **HRMS:** Exact mass calculated for $[C_{24}H_{43}N_5O_7 + H]^+$ requires *m/z* = 514.3241. Found 514.3260 (ESI+).

NOTE: Spectra of **21** and **30** were also acquired in methanol-d_4, acetone-d_6, and dimethylsulfoxide-d_6. The integrations of the major and minor peaks changed, providing evidence that the species are indeed conformers/rotamers.

NOTE: Peptides **34**–**37** were not synthesized herein. Their previously reported X-ray crystal structures were used to supplement our analyses.[8–11]

E. ^{1}H- & ^{13}C-NMR Spectra of Peptides 3–33

Peptide 3

^{1}H-NMR (500 MHz, $CDCl_3$)

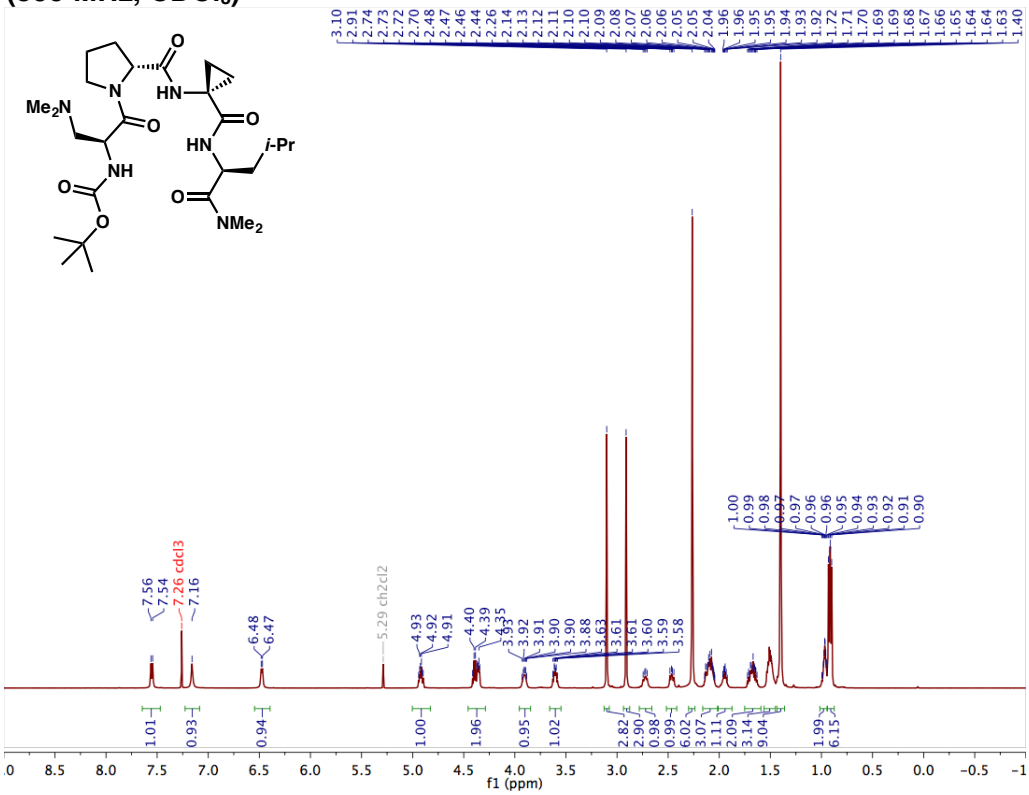

^{13}C-NMR (126 MHz, $CDCl_3$)

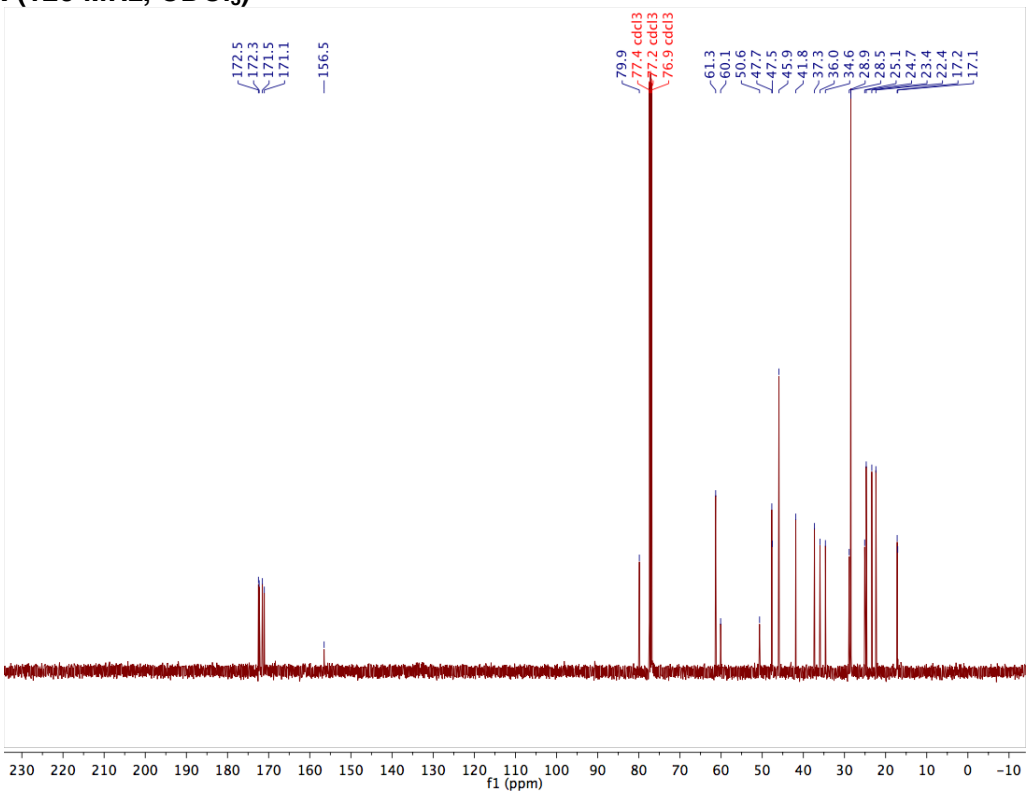

Peptide 4

^{1}H-NMR (500 MHz, $CDCl_3$)

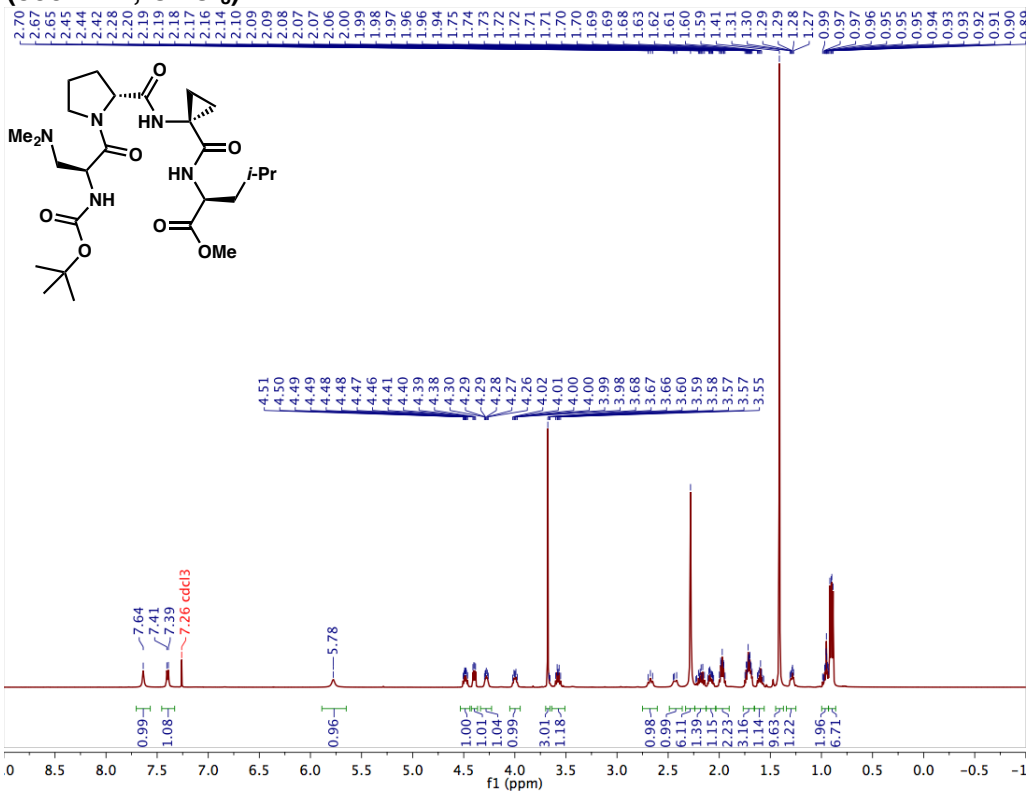

^{13}C-NMR (126 MHz, $CDCl_3$)

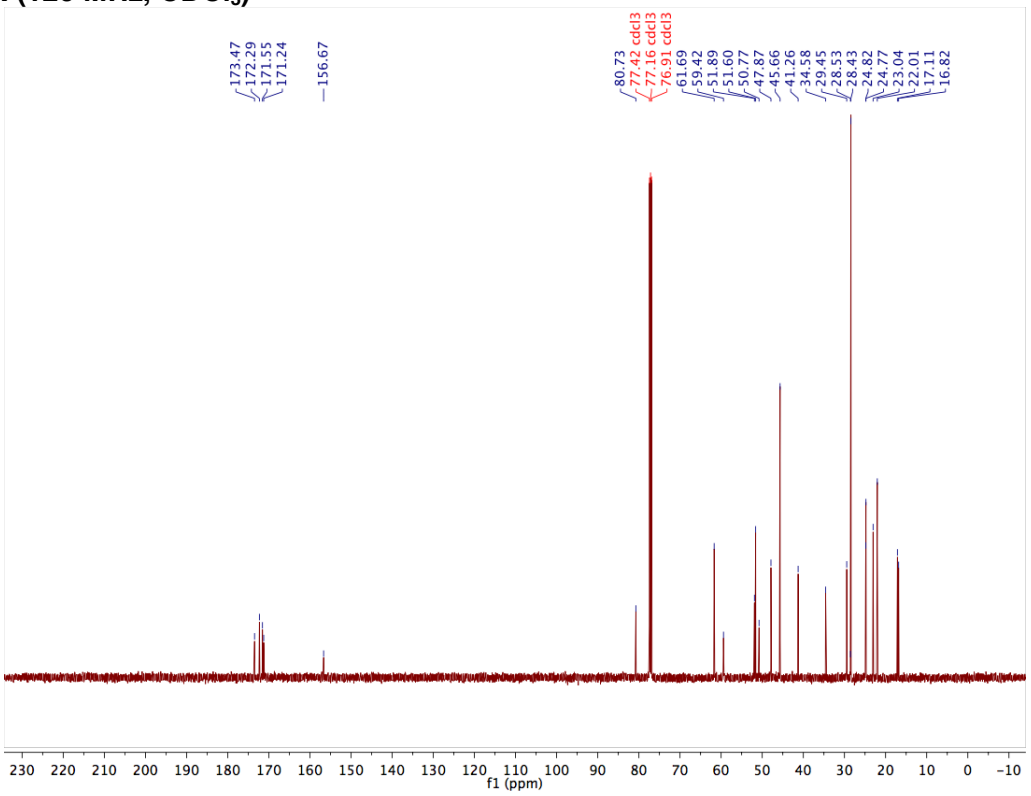

Peptide 5

^{1}H-NMR (500 MHz, $CDCl_3$)

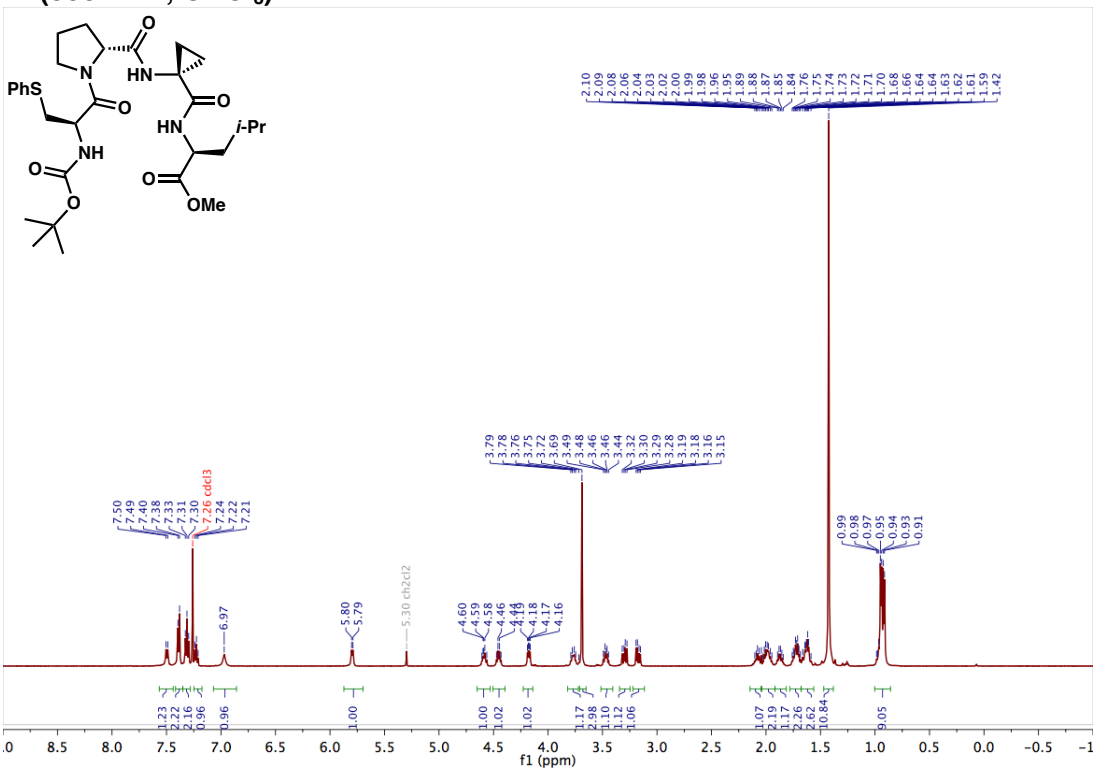

^{13}C-NMR (151 MHz, $CDCl_3$)

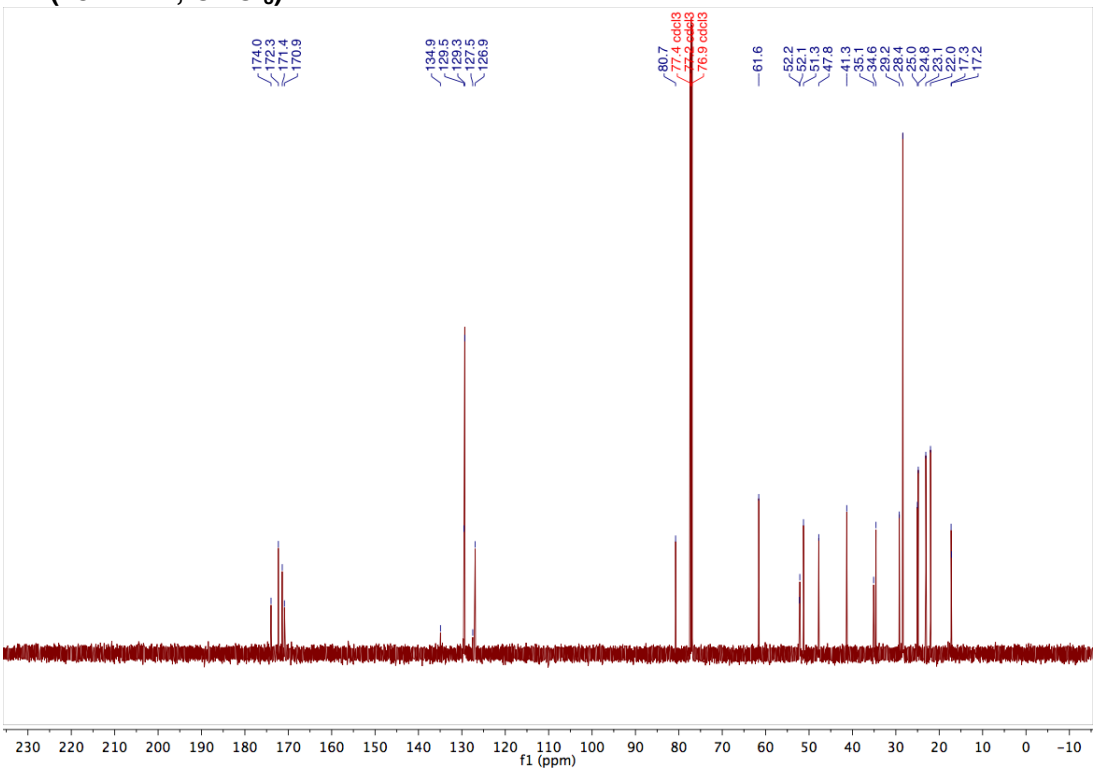

Peptide 6

^{1}H-NMR (500 MHz, $CDCl_3$)

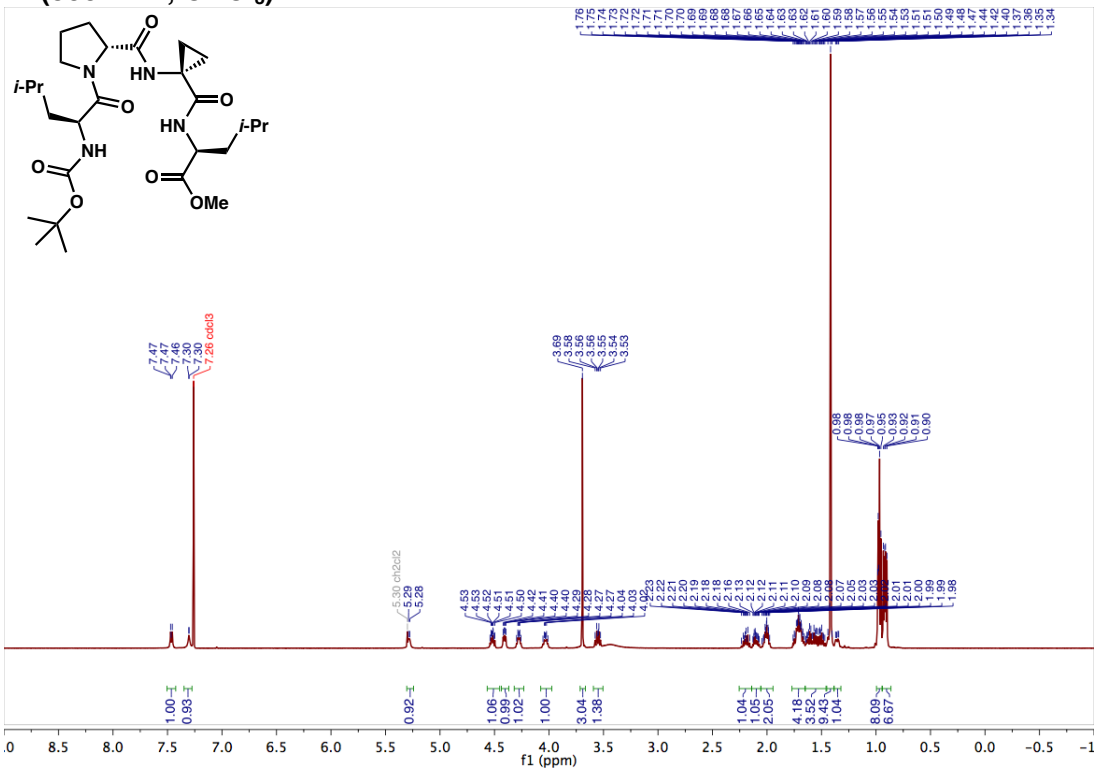

^{13}C-NMR (151 MHz, $CDCl_3$)

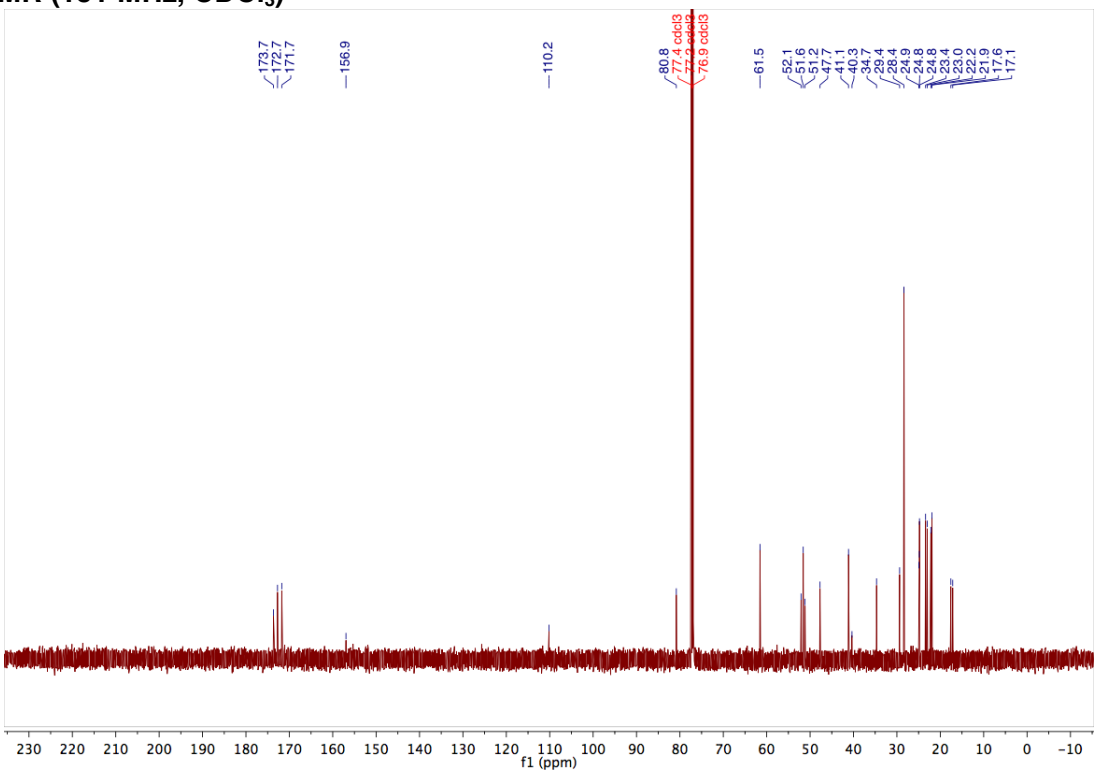

Peptide 7

^{1}H-NMR (500 MHz, $CDCl_3$)

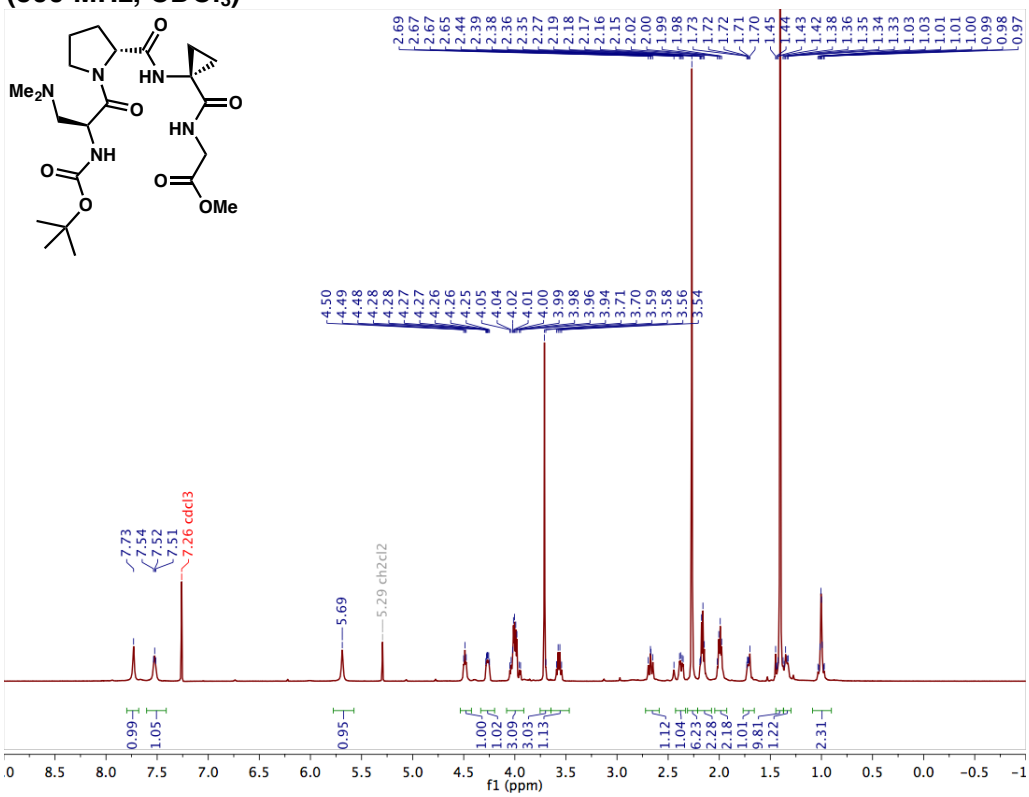

^{13}C-NMR (126 MHz, $CDCl_3$)

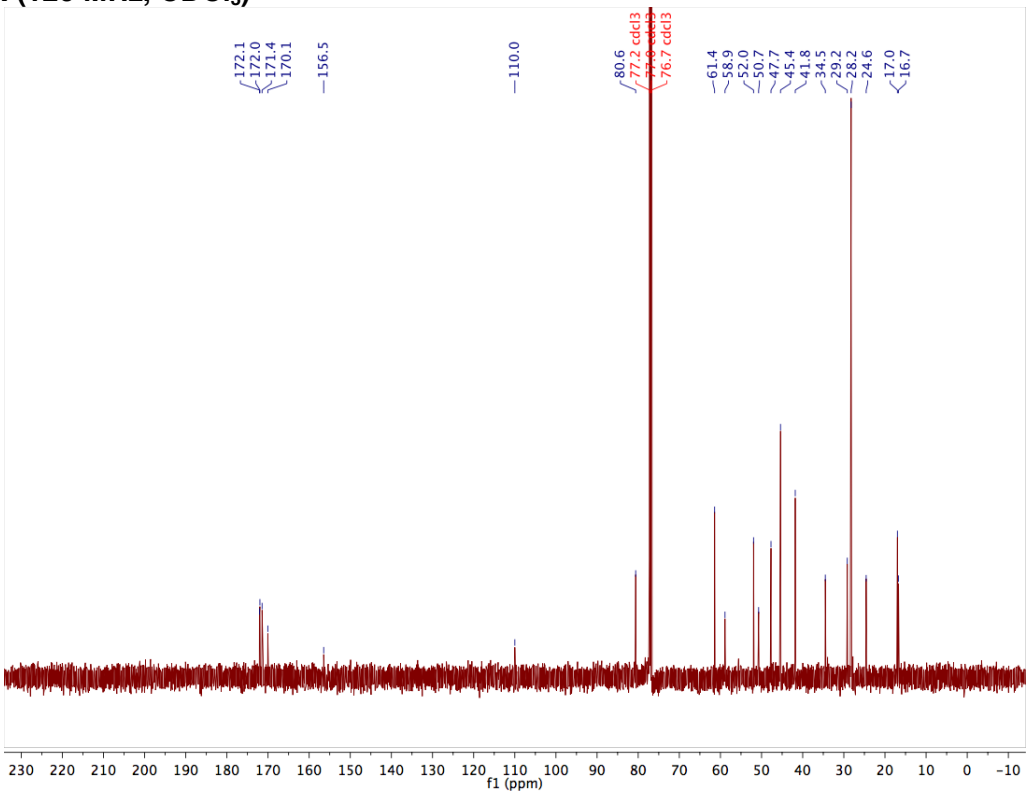

Peptide 8

^{1}H-NMR (500 MHz, $CDCl_3$)

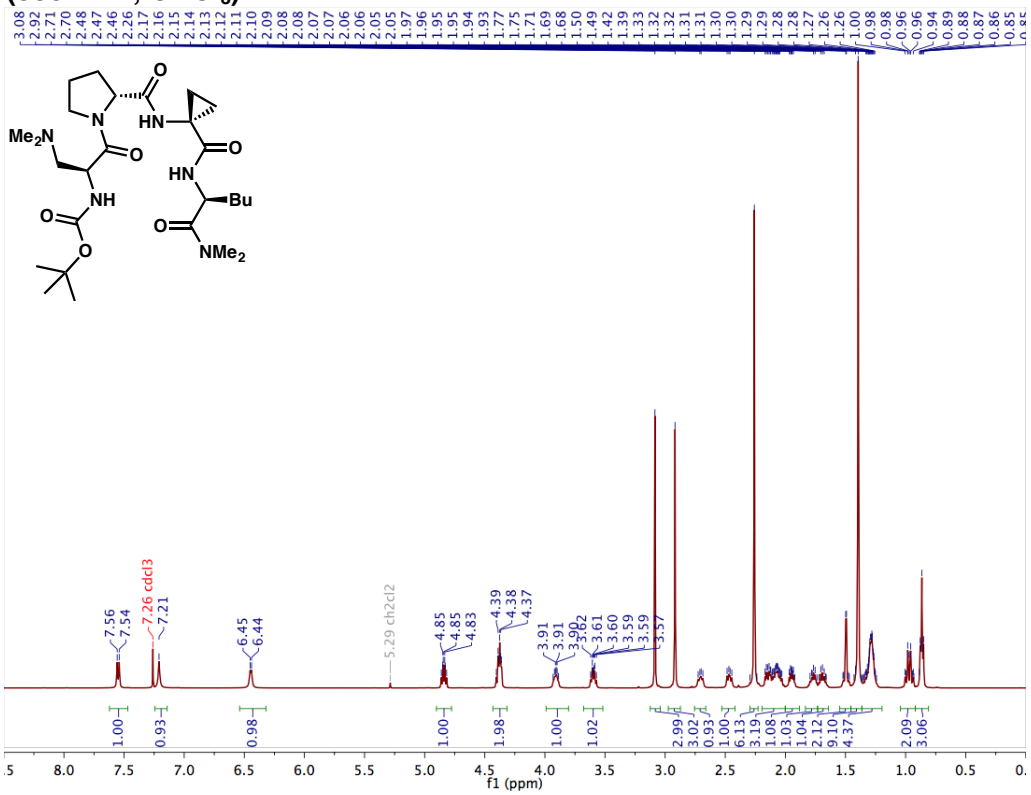

^{13}C-NMR (126 MHz, $CDCl_3$)

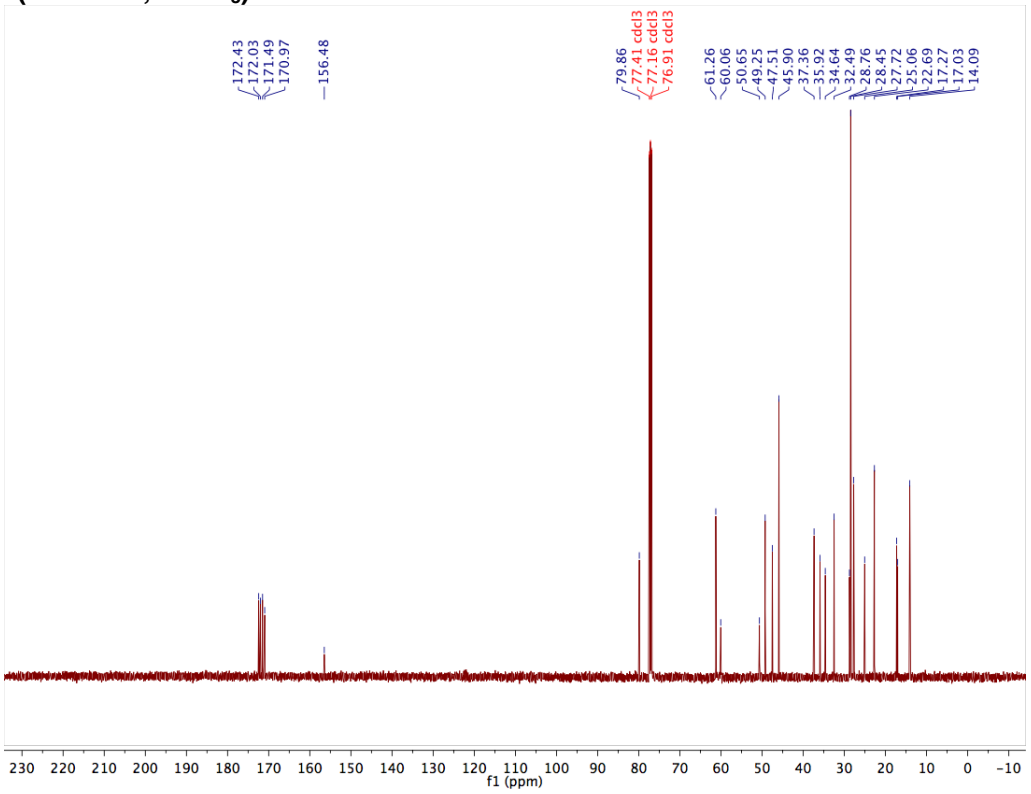

Peptide 9

^{1}H-NMR (500 MHz, $CDCl_3$)

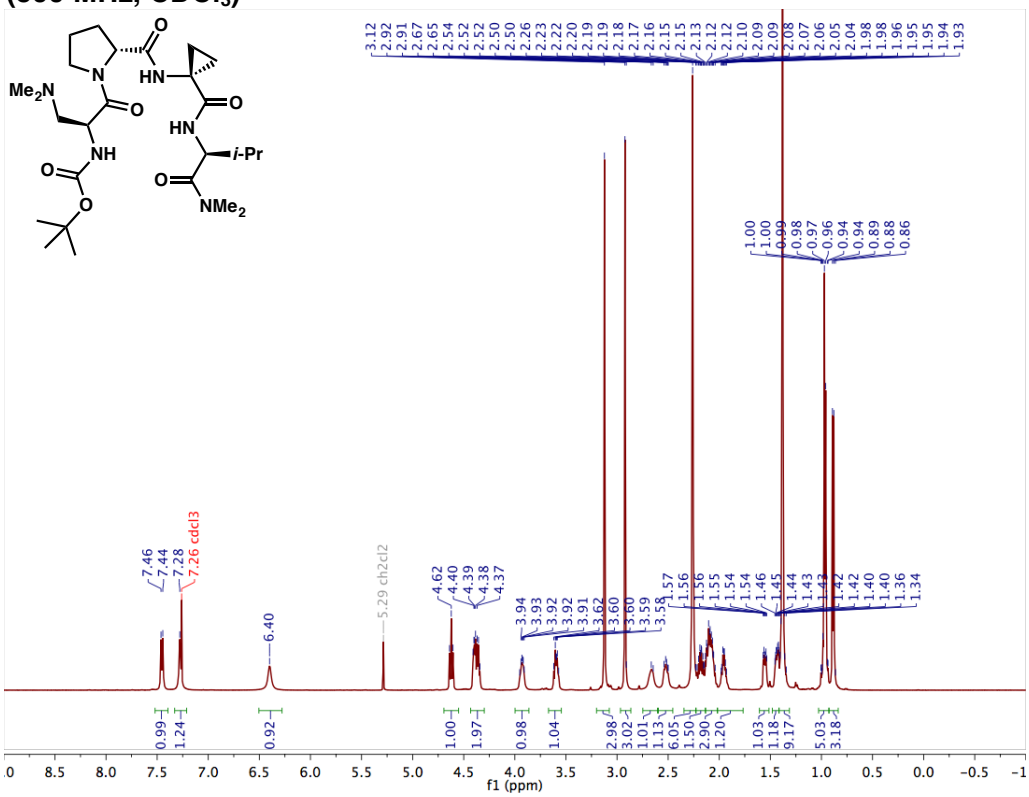

^{13}C-NMR (126 MHz, $CDCl_3$)

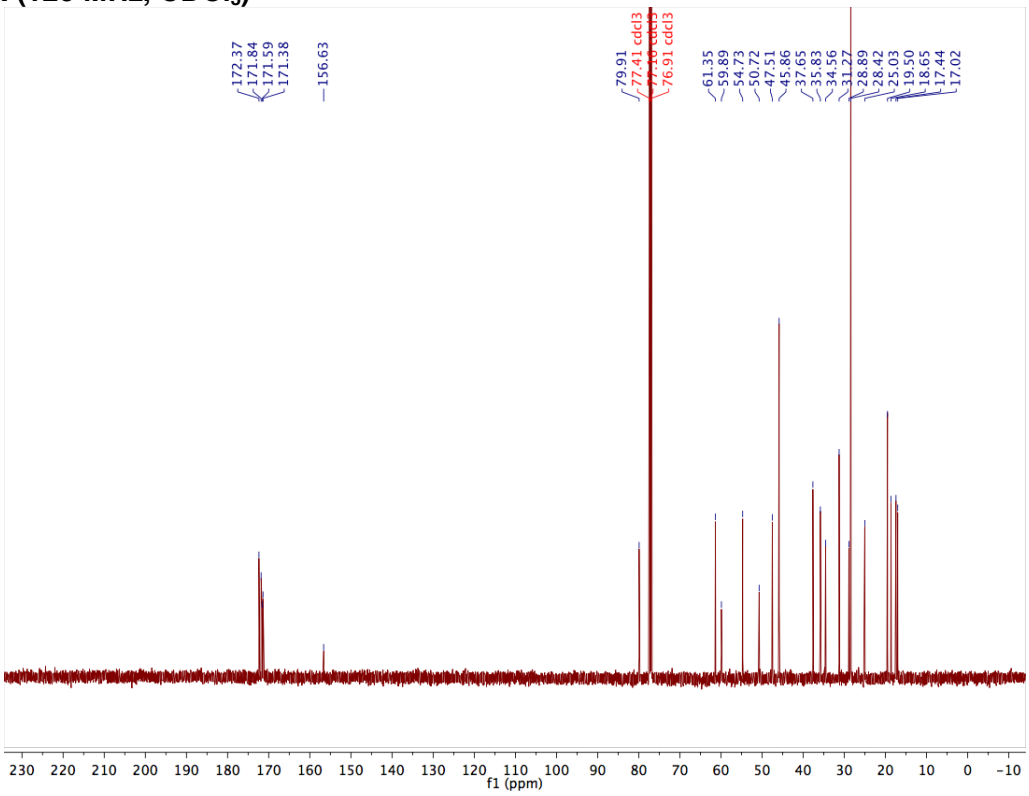

Peptide 10

^{1}H-NMR (500 MHz, $CDCl_3$)

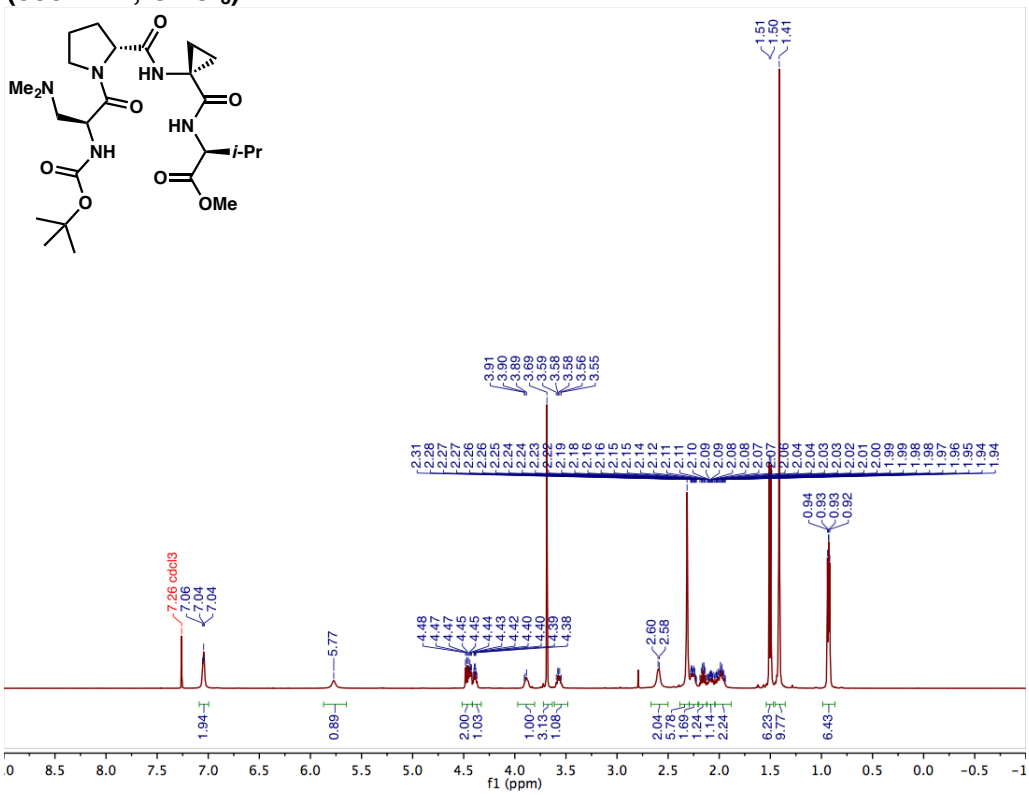

^{13}C-NMR (126 MHz, $CDCl_3$)

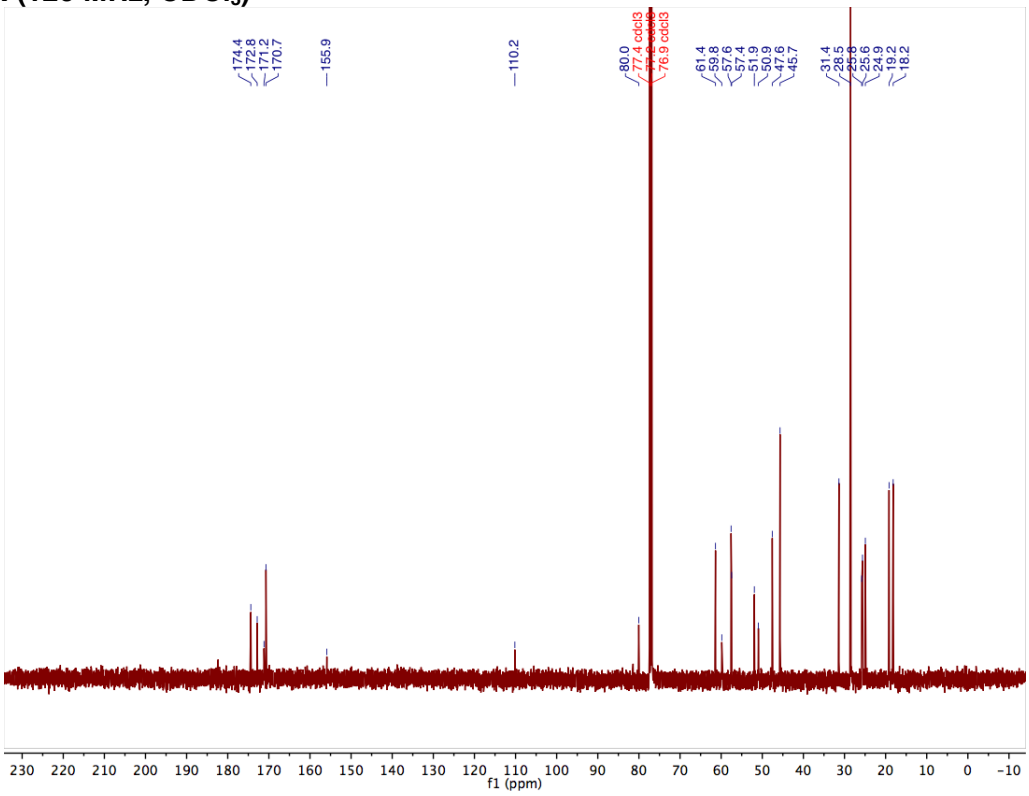

Peptide 11

^{1}H-NMR (500 MHz, $CDCl_3$)

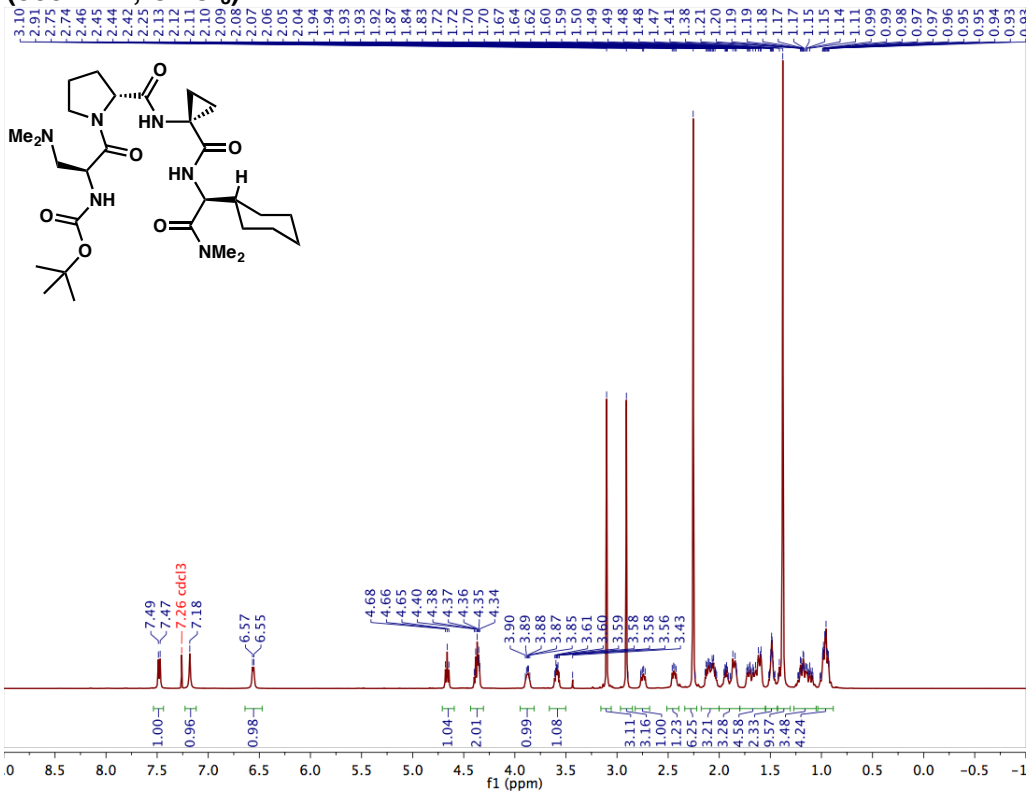

^{13}C-NMR (126 MHz, $CDCl_3$)

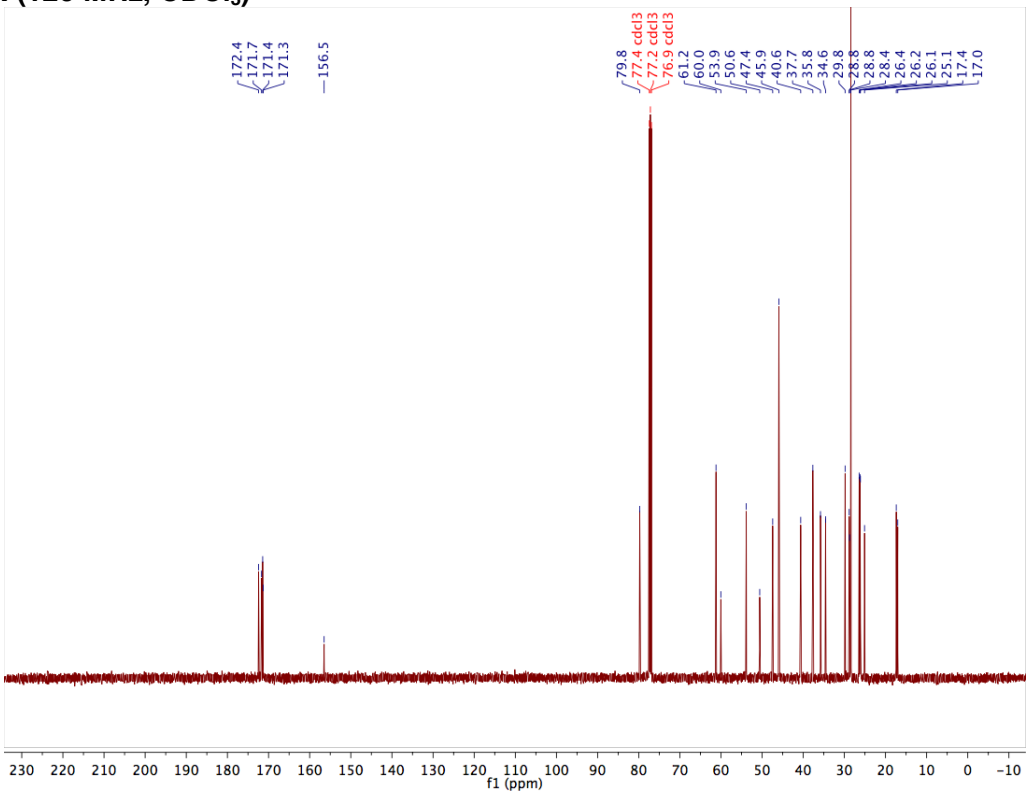

Peptide 12

^{1}H-NMR (500 MHz, $CDCl_3$)

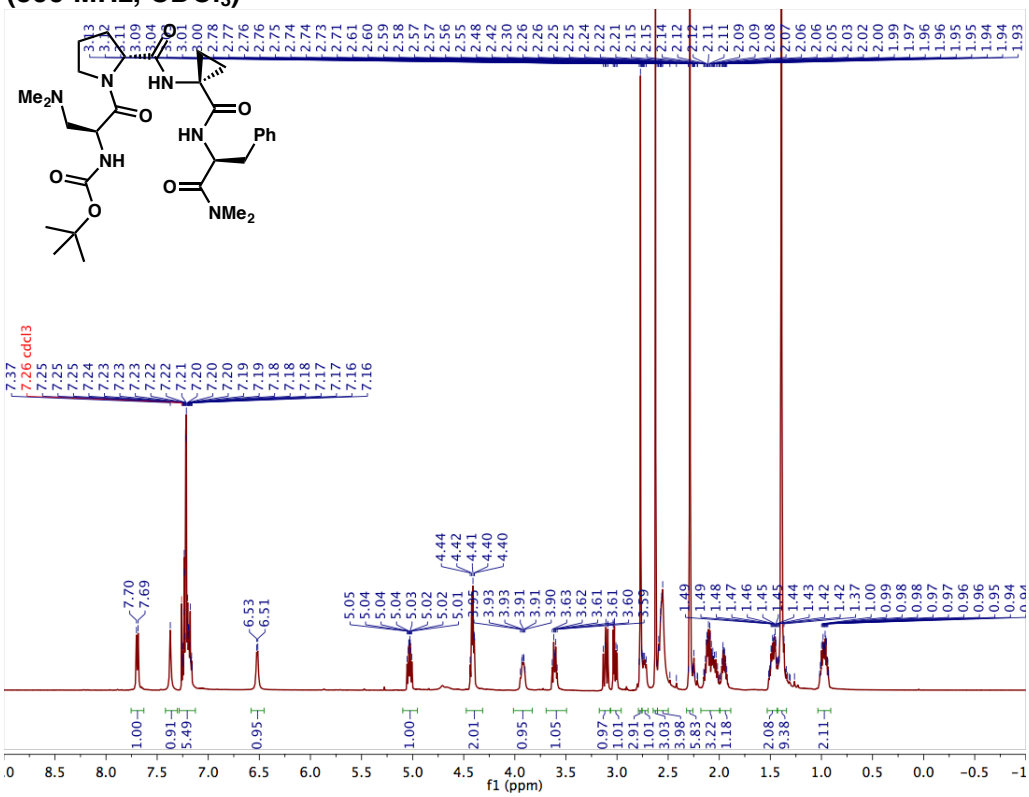

^{13}C-NMR (126 MHz, $CDCl_3$)

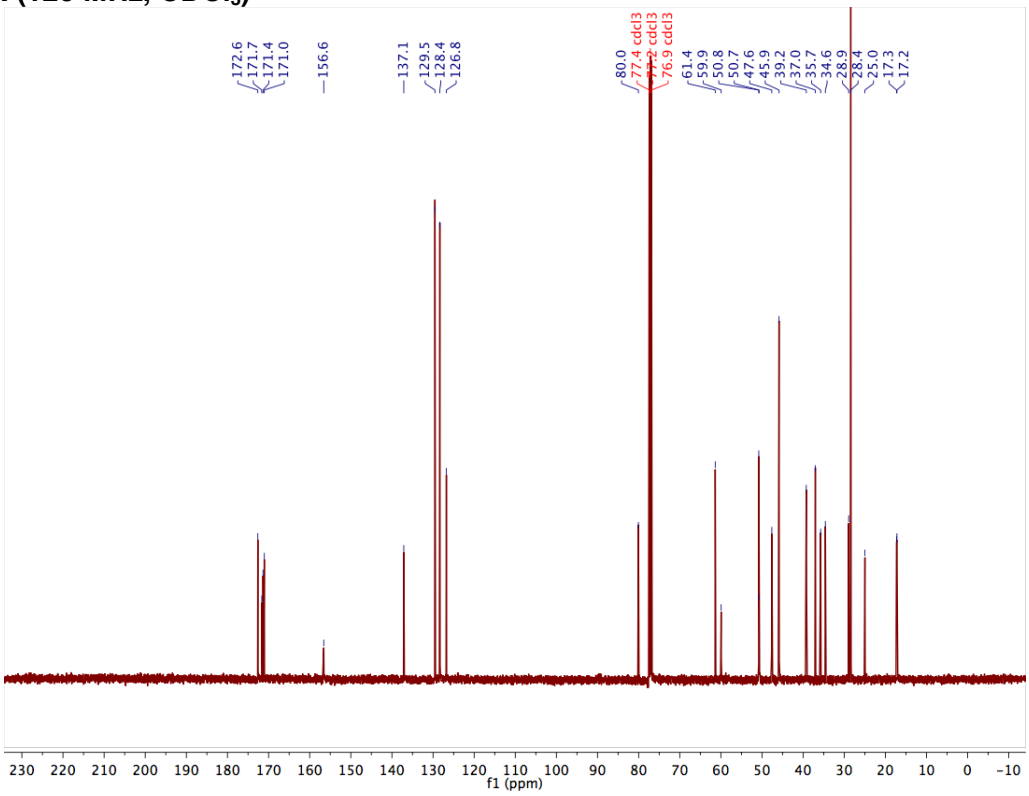

Peptide 13

^{1}H-NMR (600 MHz, $CDCl_3$)

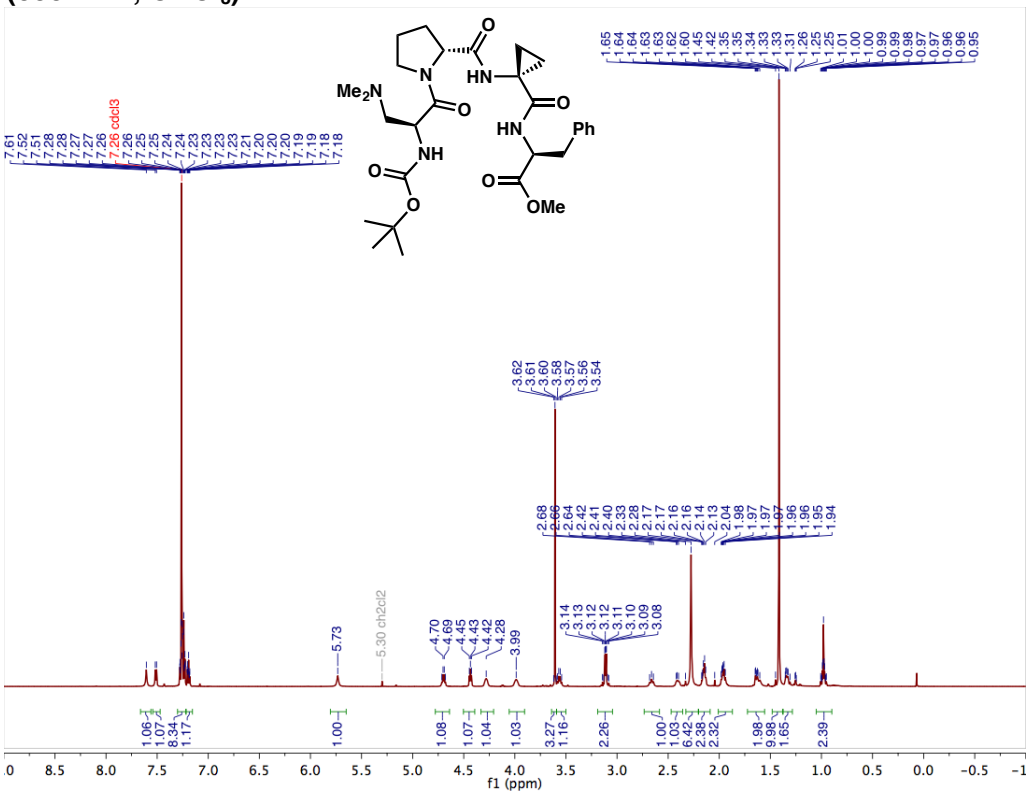

^{13}C-NMR (151 MHz, $CDCl_3$)

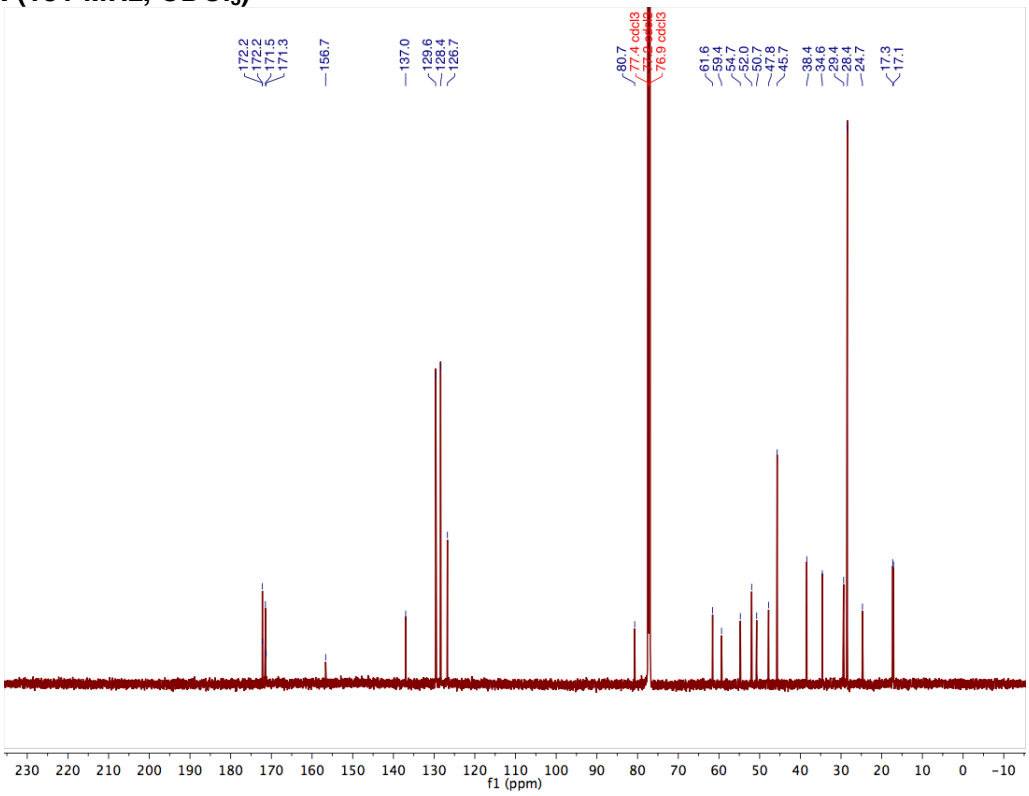

Peptide 14

^{1}H-NMR (500 MHz, $CDCl_3$)

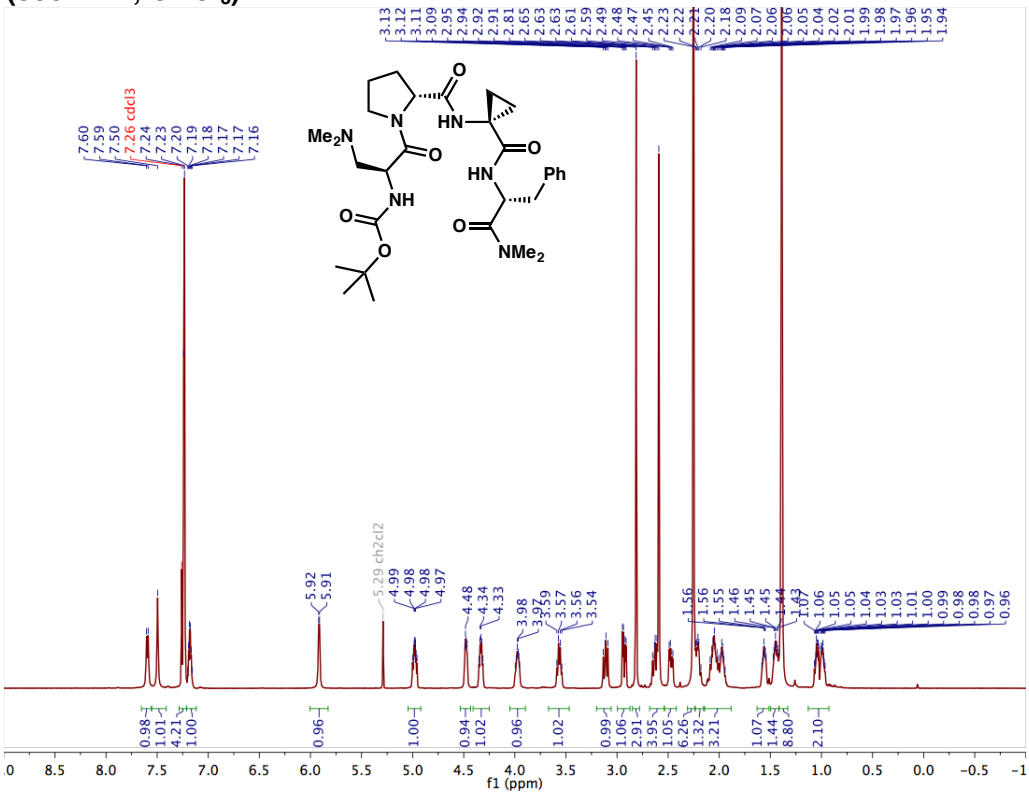

^{13}C-NMR (126 MHz, $CDCl_3$)

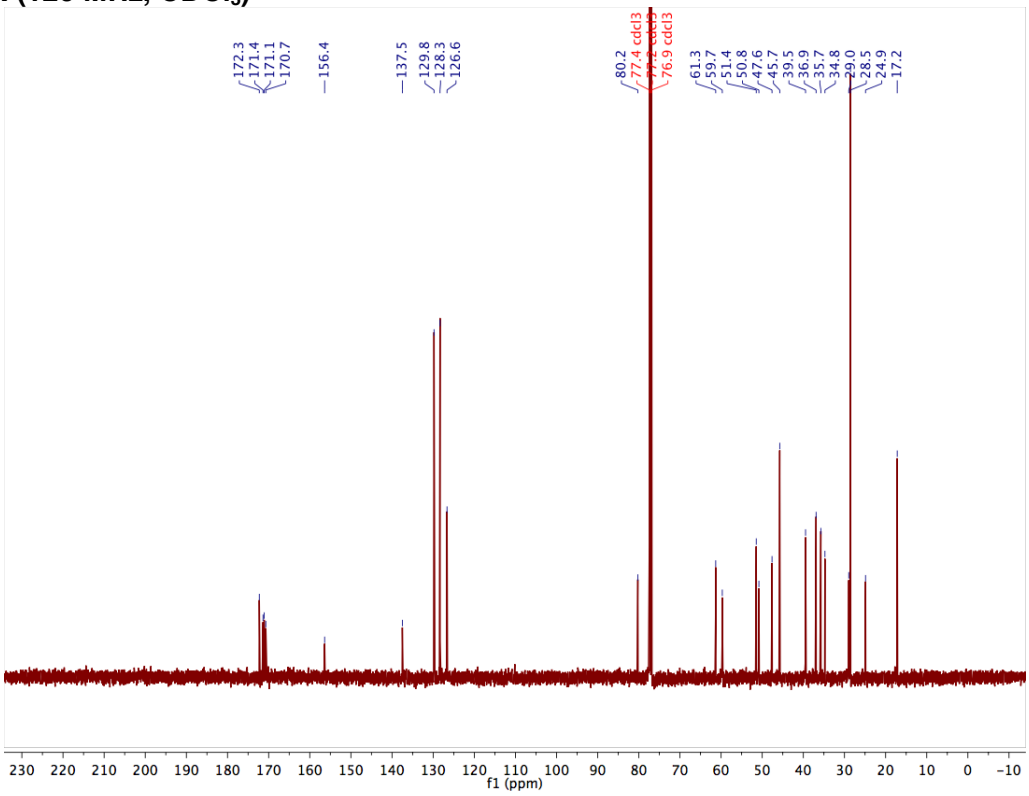

Peptide 15

^{1}H-NMR (600 MHz, $CDCl_3$)

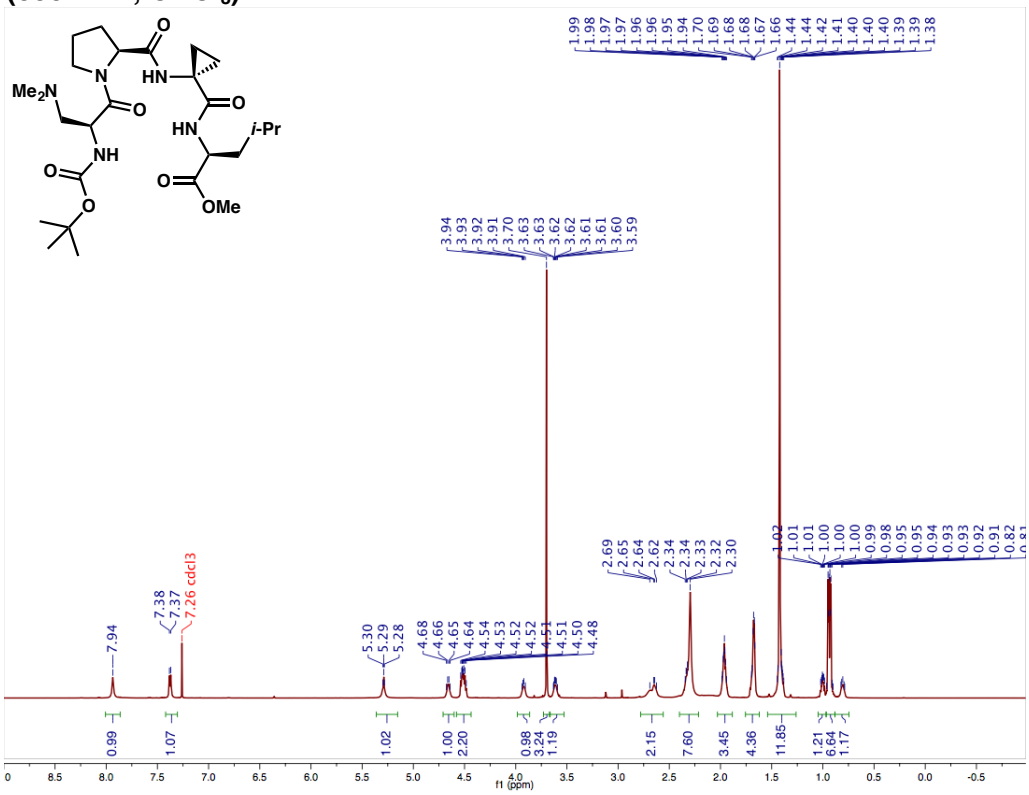

^{13}C-NMR (151 MHz, $CDCl_3$)

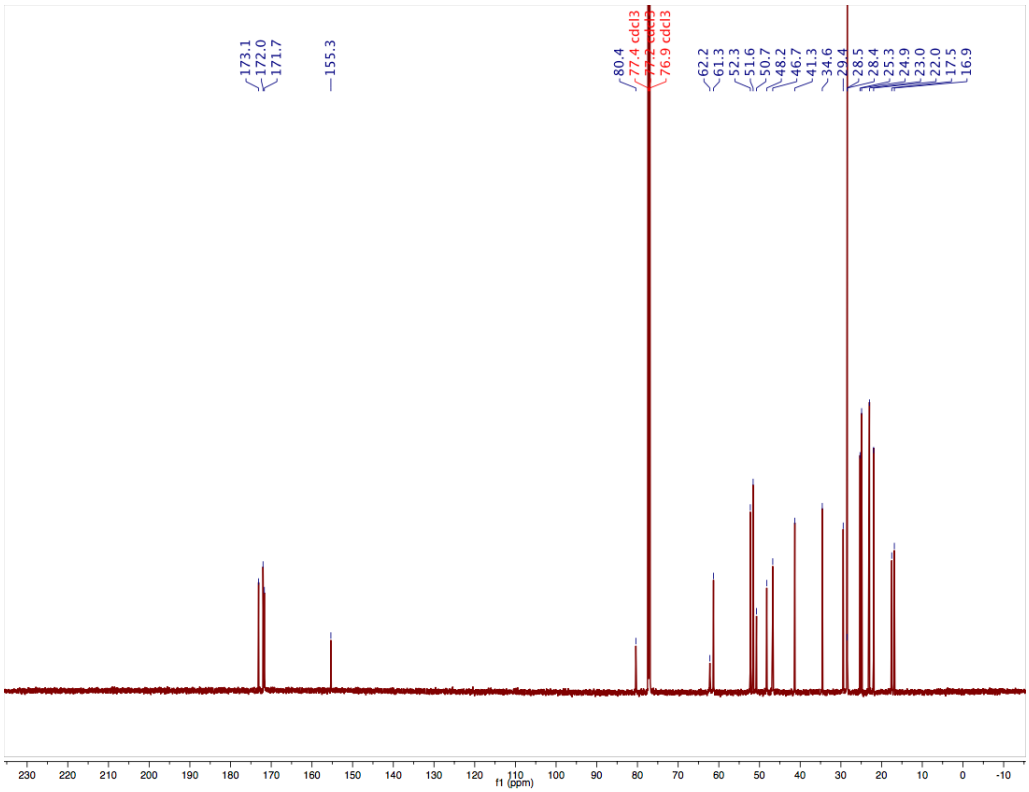

Peptide 16

^{1}H-NMR (500 MHz, $CDCl_3$)

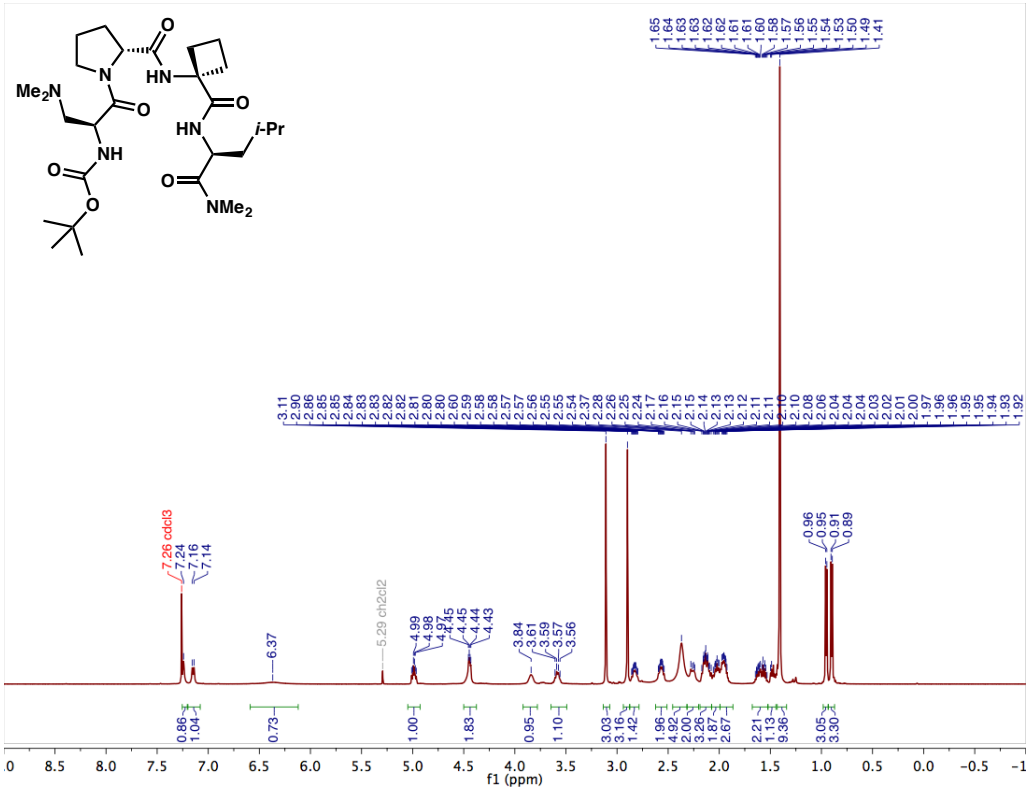

^{13}C-NMR (126 MHz, $CDCl_3$)

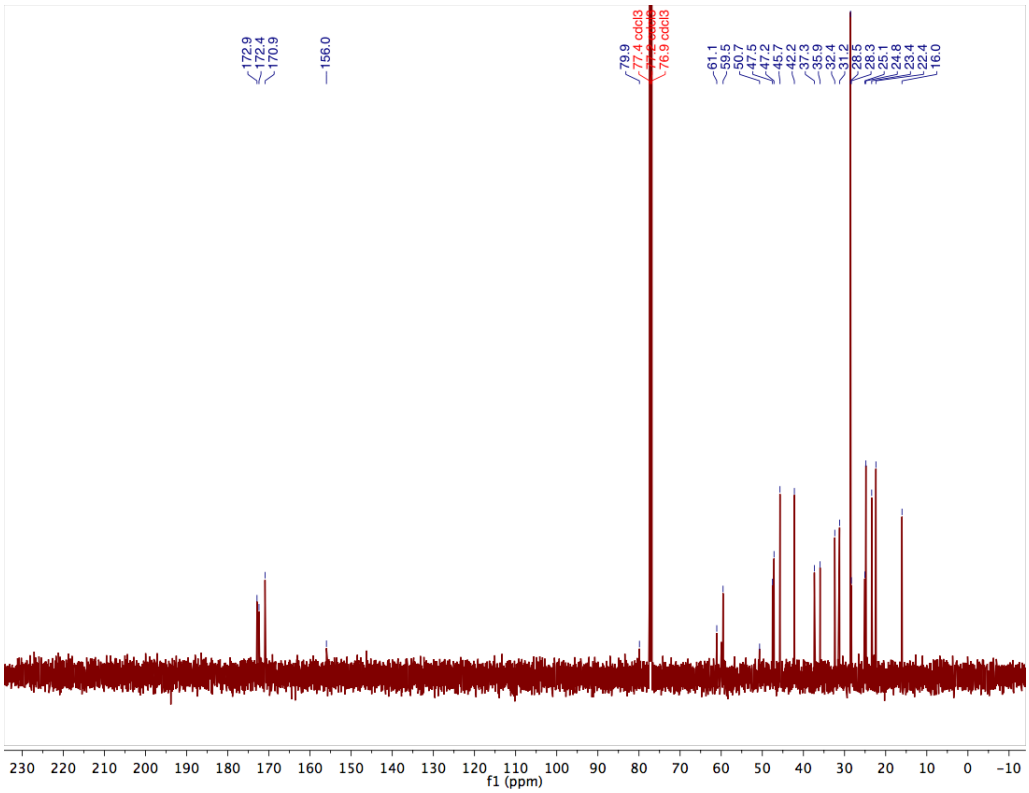

Peptide 17

^{1}H-NMR (600 MHz, $CDCl_3$)

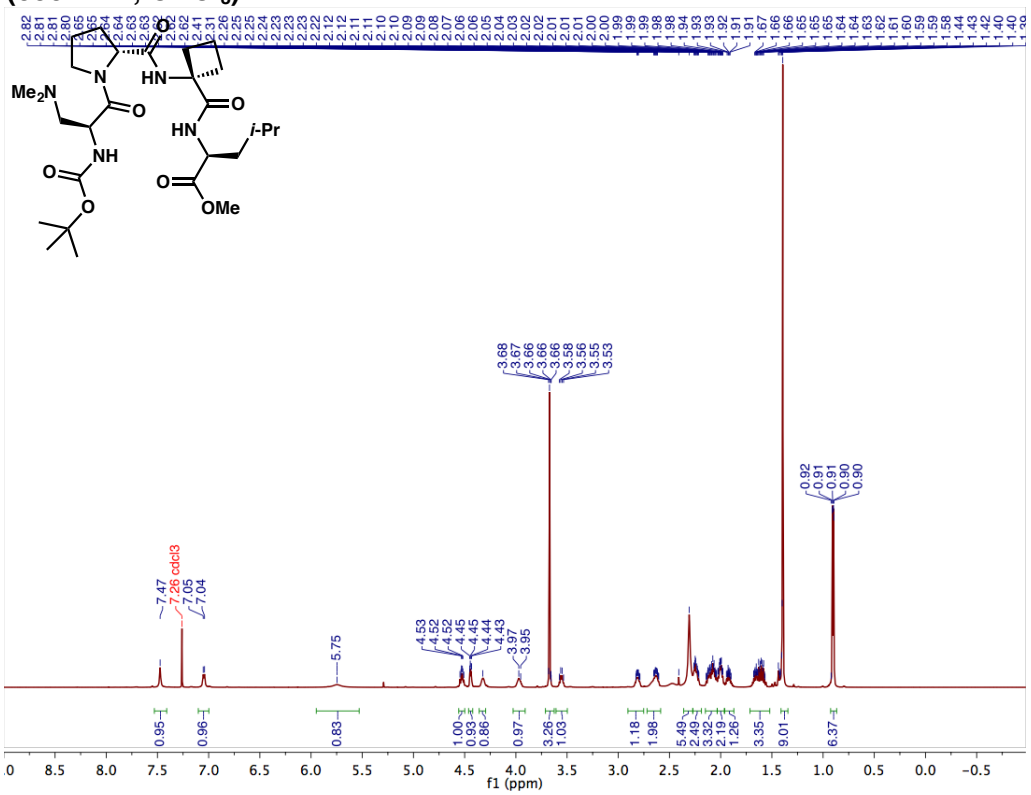

^{13}C-NMR (151 MHz, $CDCl_3$)

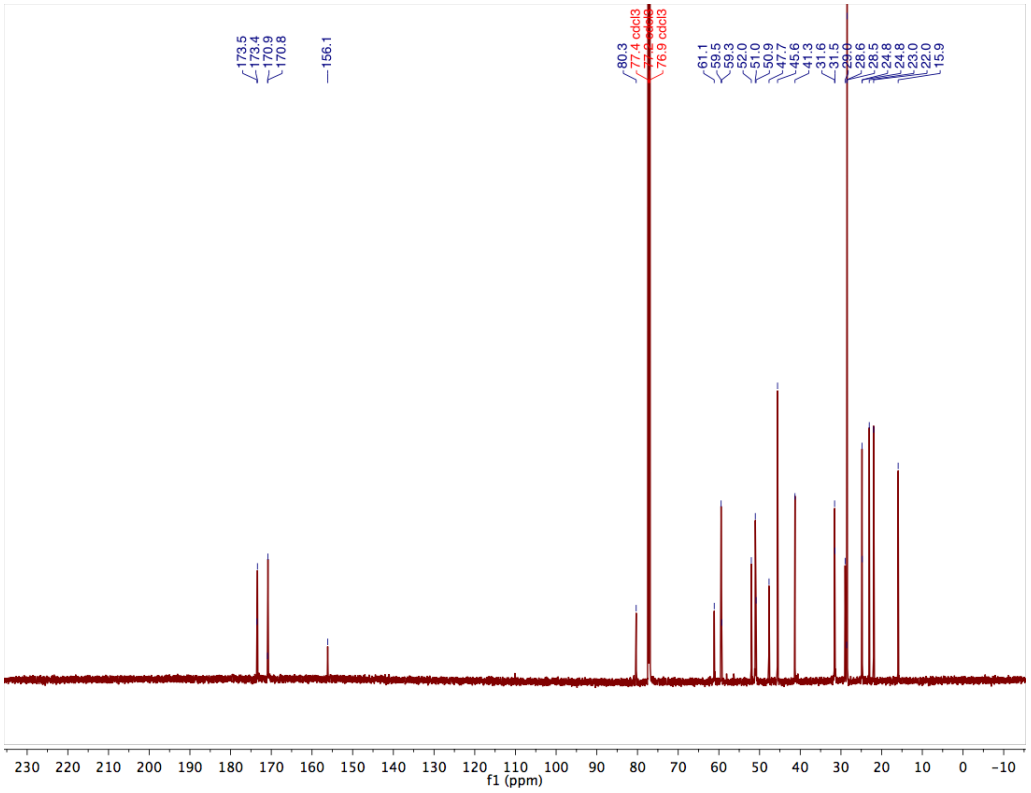

Peptide 18

^{1}H-NMR (500 MHz, $CDCl_3$)

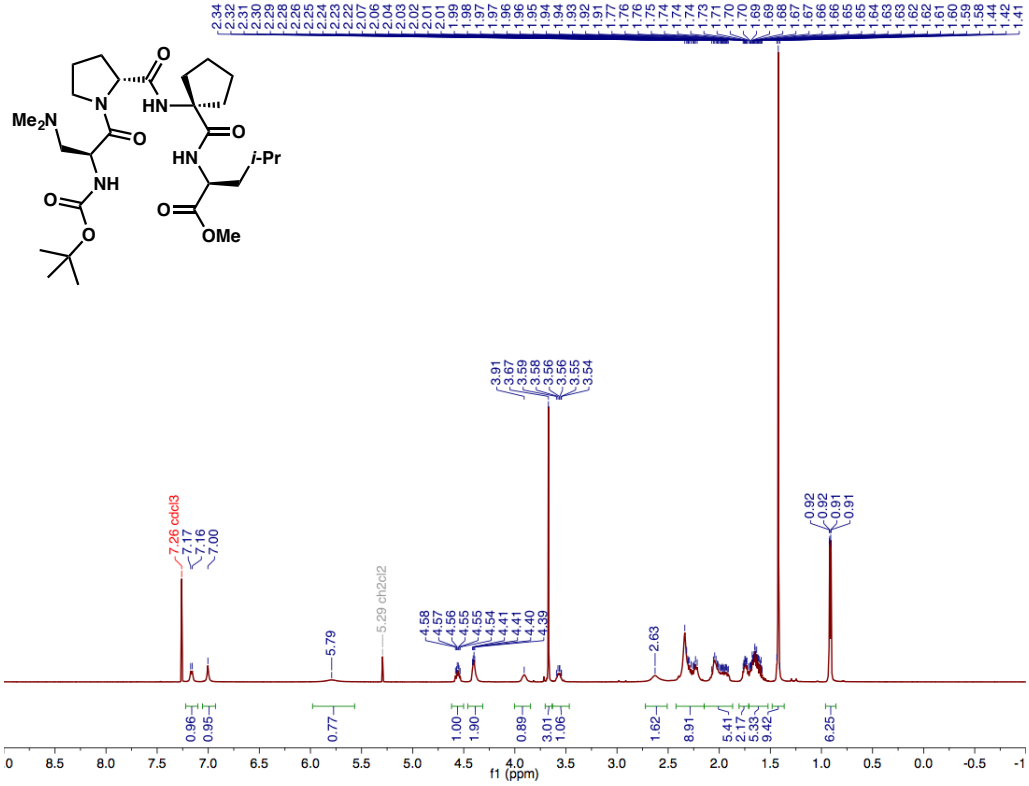

^{13}C-NMR (126 MHz, $CDCl_3$)

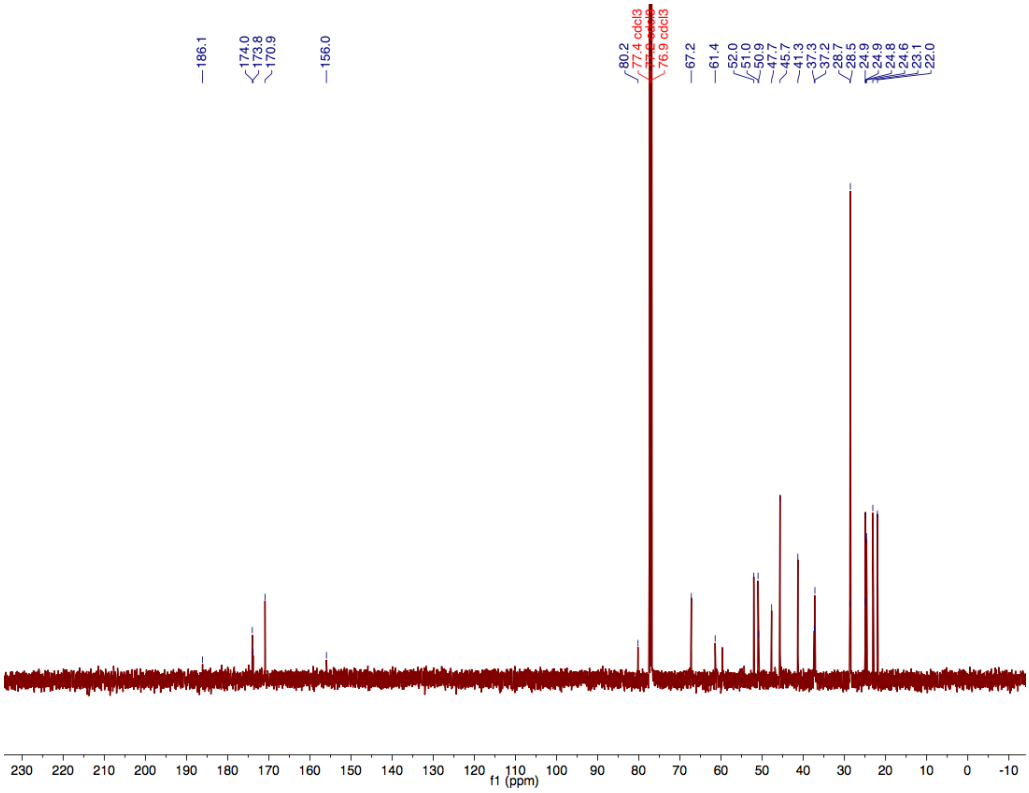

Peptide 19

^{1}H-NMR (500 MHz, $CDCl_3$)

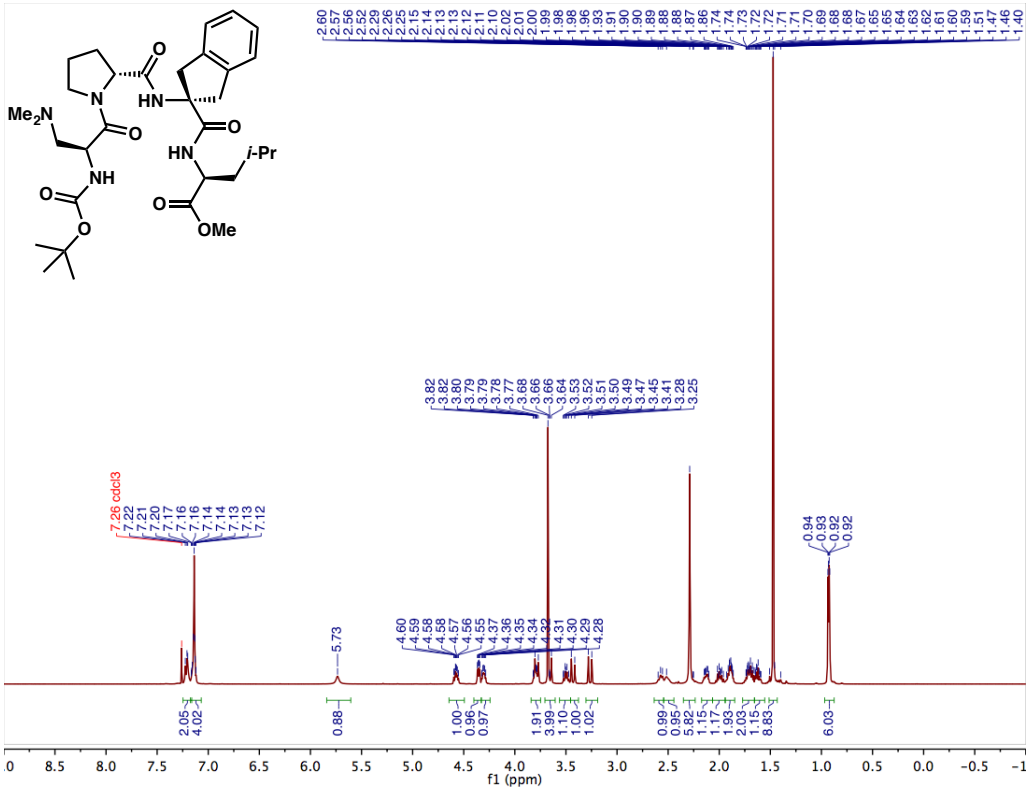

^{13}C-NMR (126 MHz, $CDCl_3$)

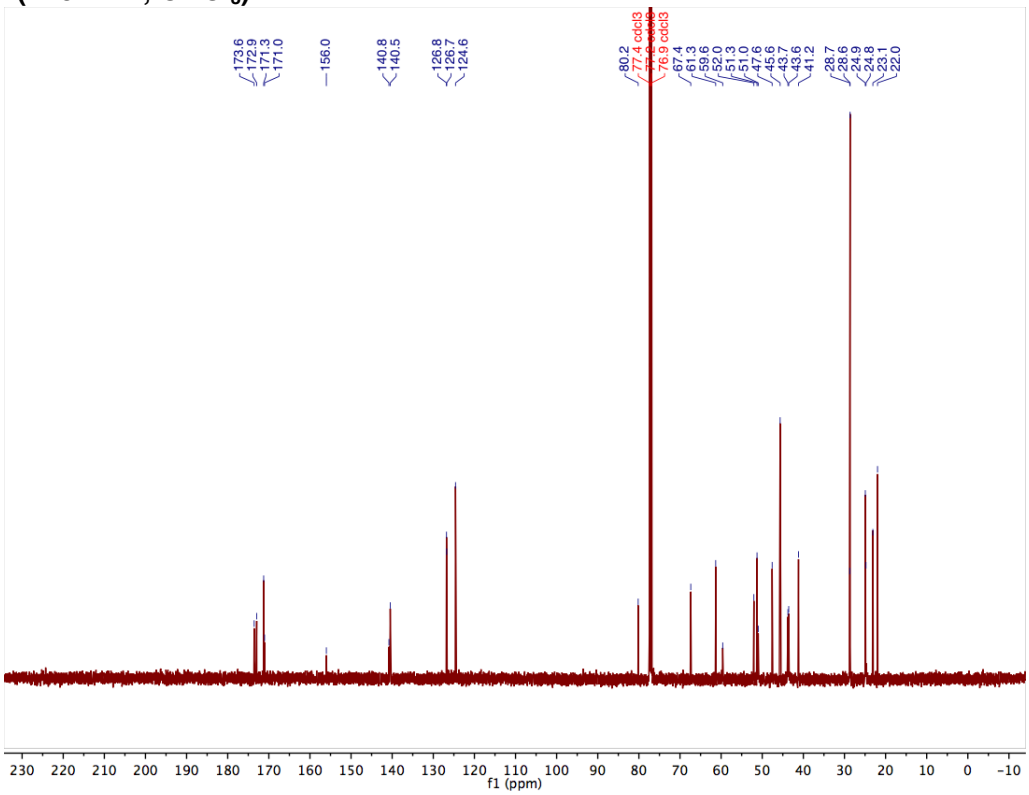

Peptide 20

^{1}H-NMR (500 MHz, $CDCl_3$)

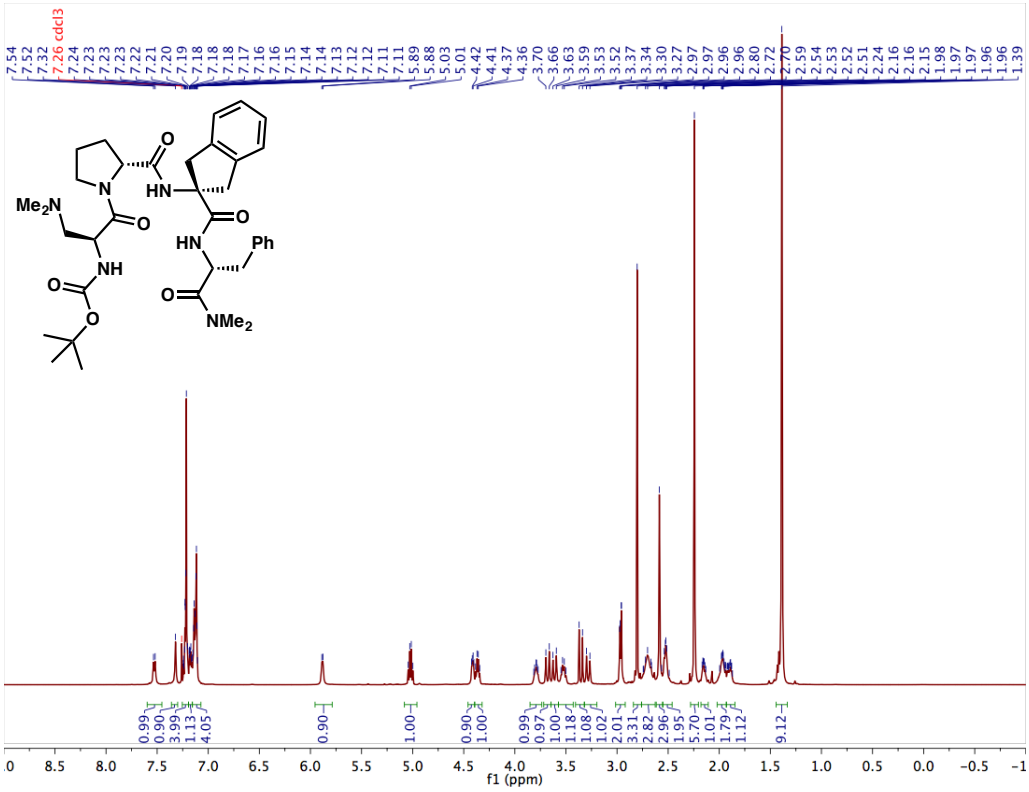

^{13}C-NMR (126 MHz, $CDCl_3$)

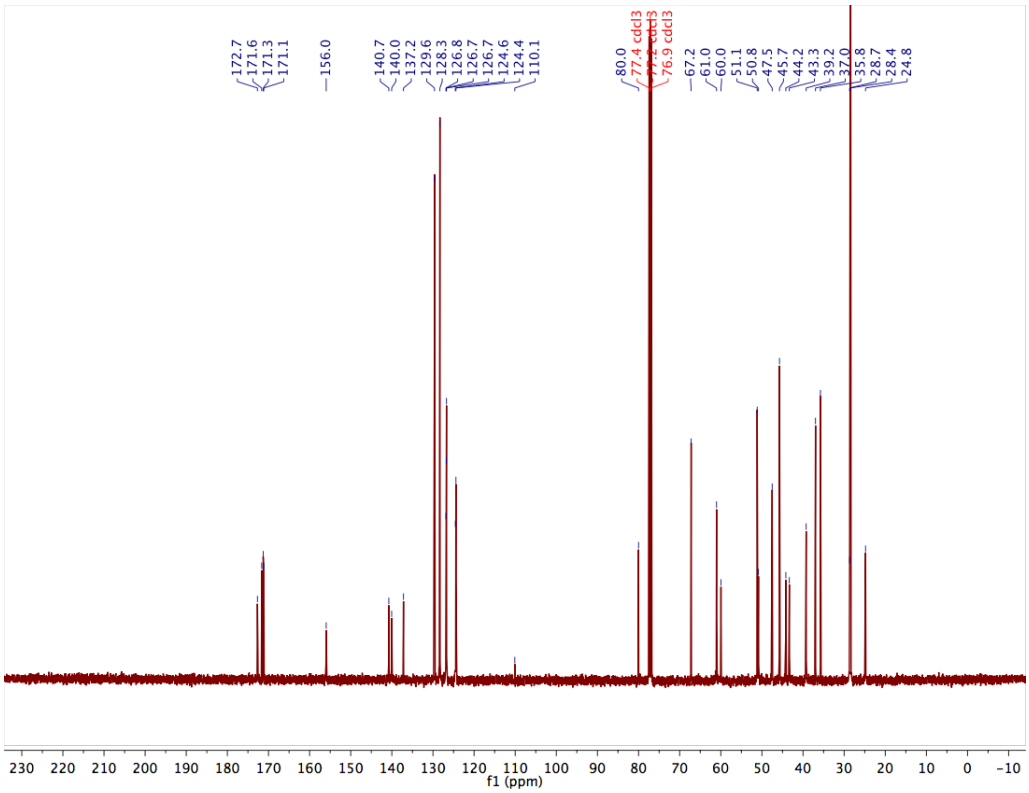

Peptide 21

^{1}H-NMR (500 MHz, $CDCl_3$)

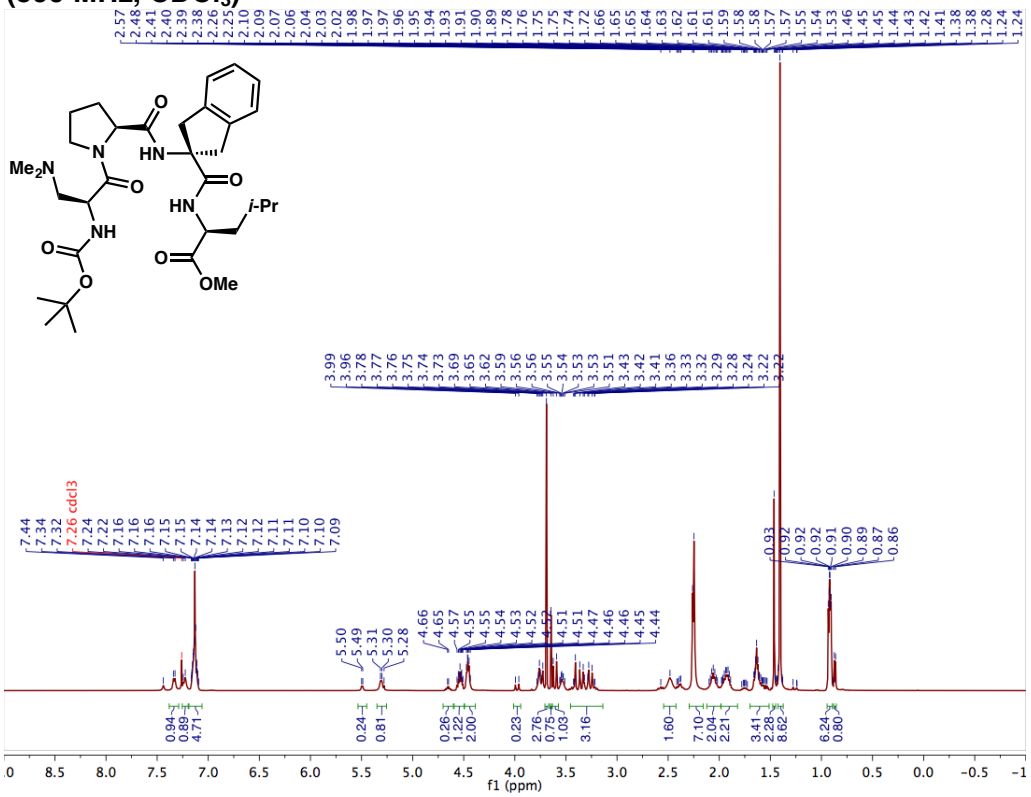

^{13}C-NMR (126 MHz, $CDCl_3$)

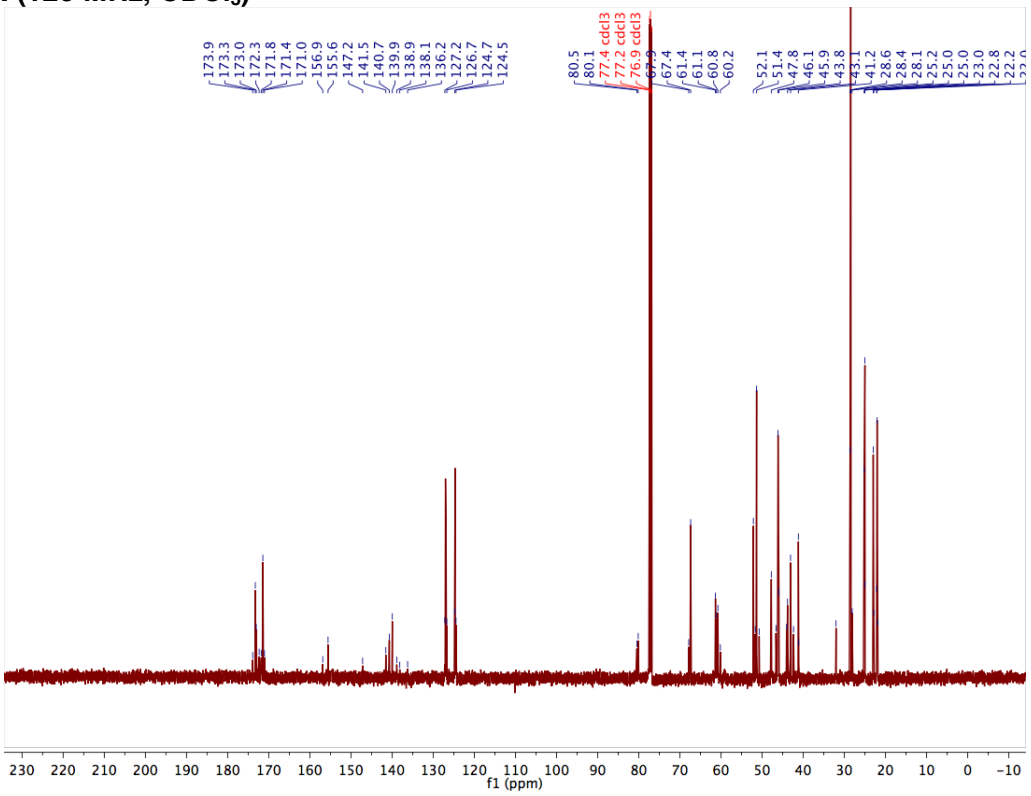

Peptide 22

^{1}H-NMR (500 MHz, $CDCl_3$)

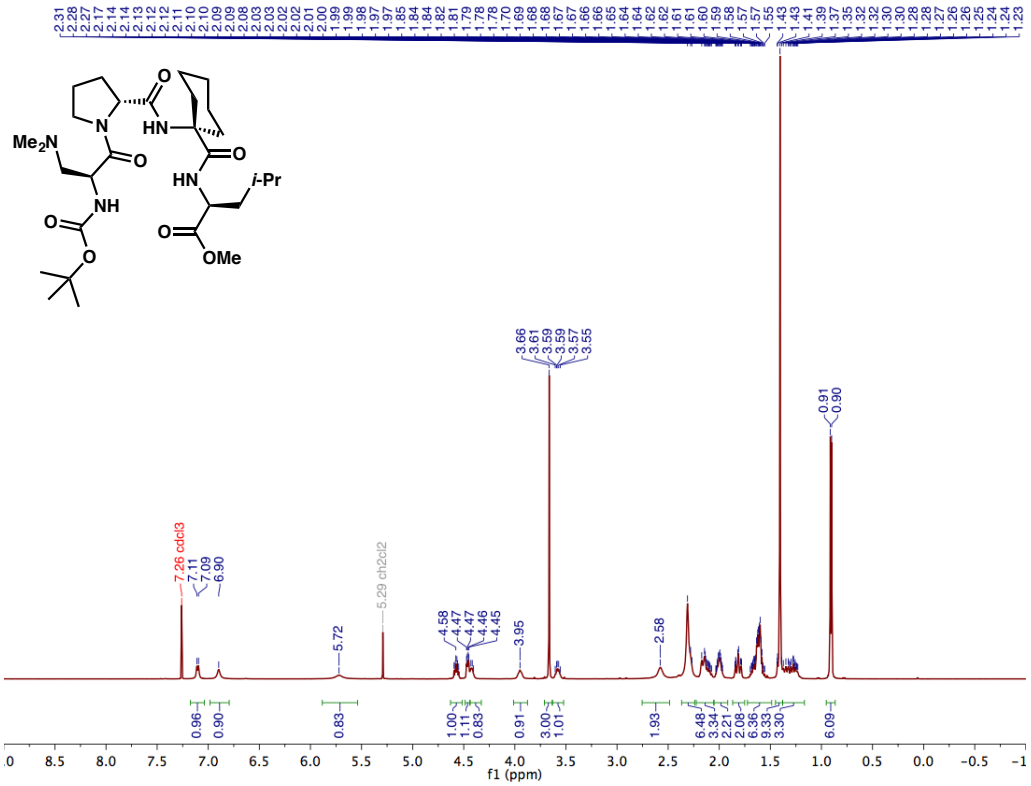

^{13}C-NMR (126 MHz, $CDCl_3$)

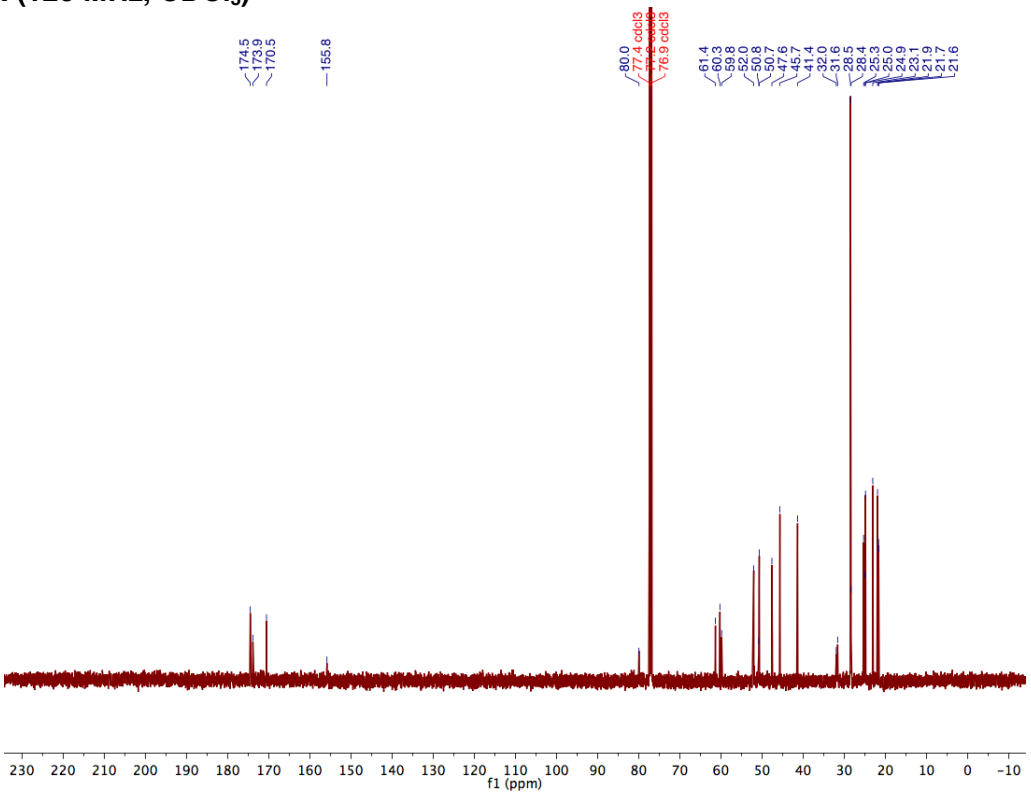

Peptide 23

^{1}H-NMR (500 MHz, $CDCl_3$)

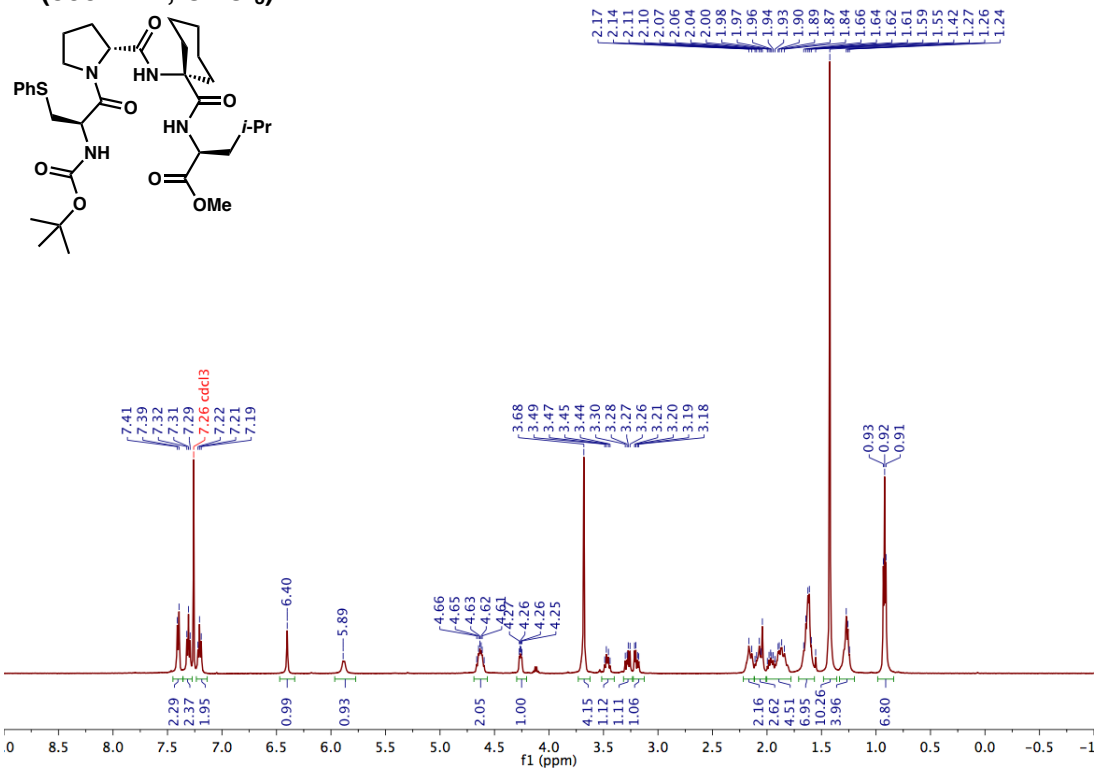

^{13}C-NMR (151 MHz, $CDCl_3$)

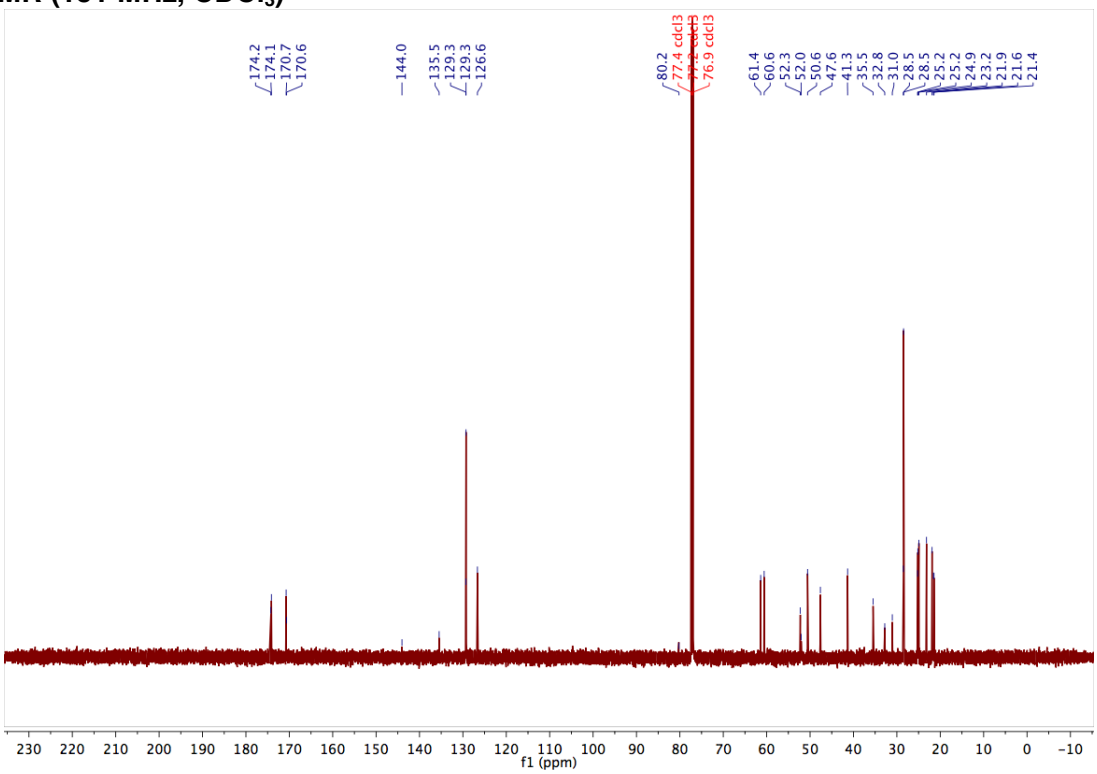

Peptide 24

^{1}H-NMR (500 MHz, $CDCl_3$)

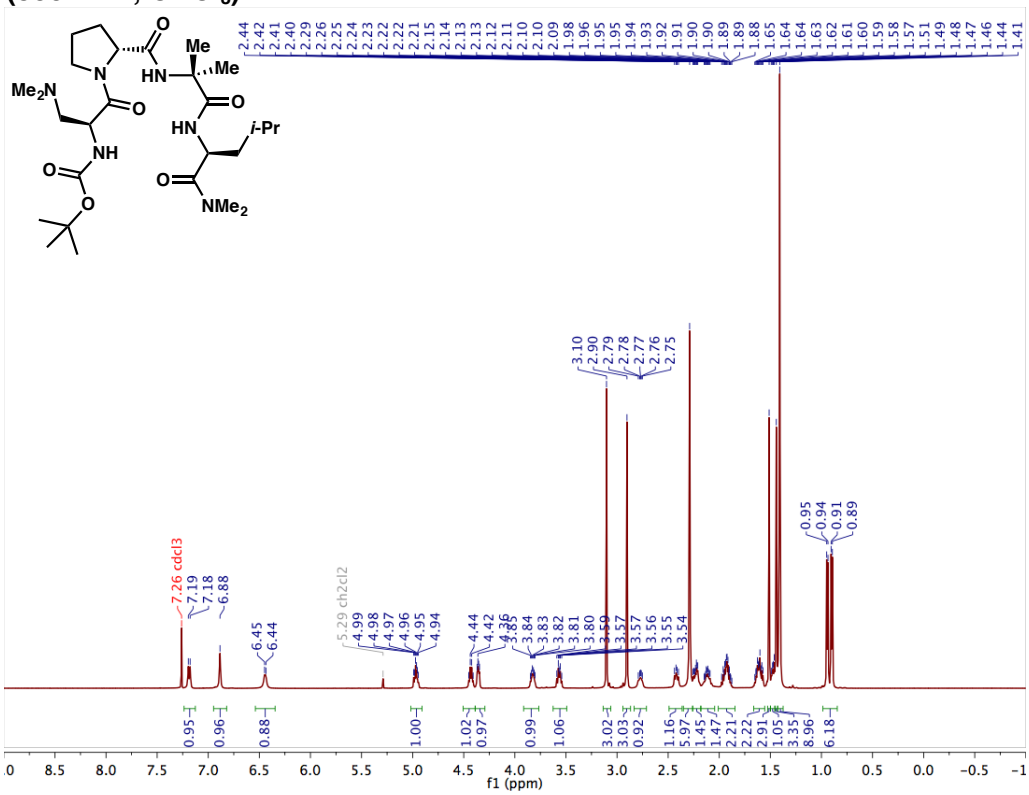

^{13}C-NMR (126 MHz, $CDCl_3$)

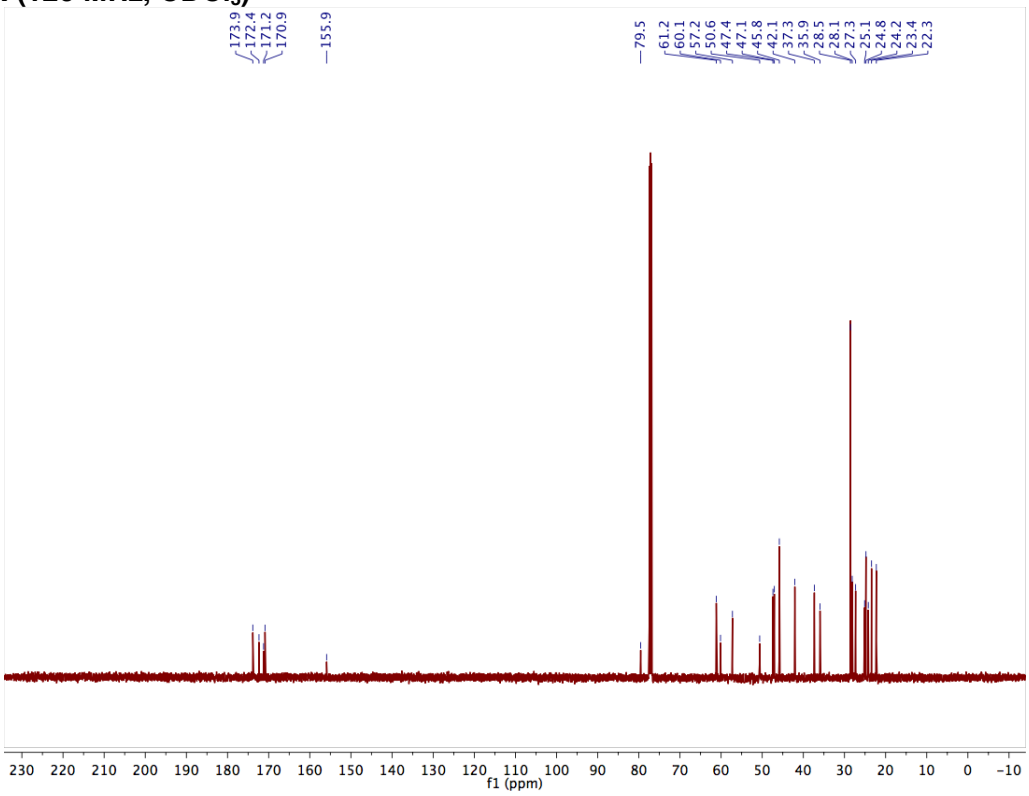

Peptide 25

^{1}H-NMR (500 MHz, $CDCl_3$)

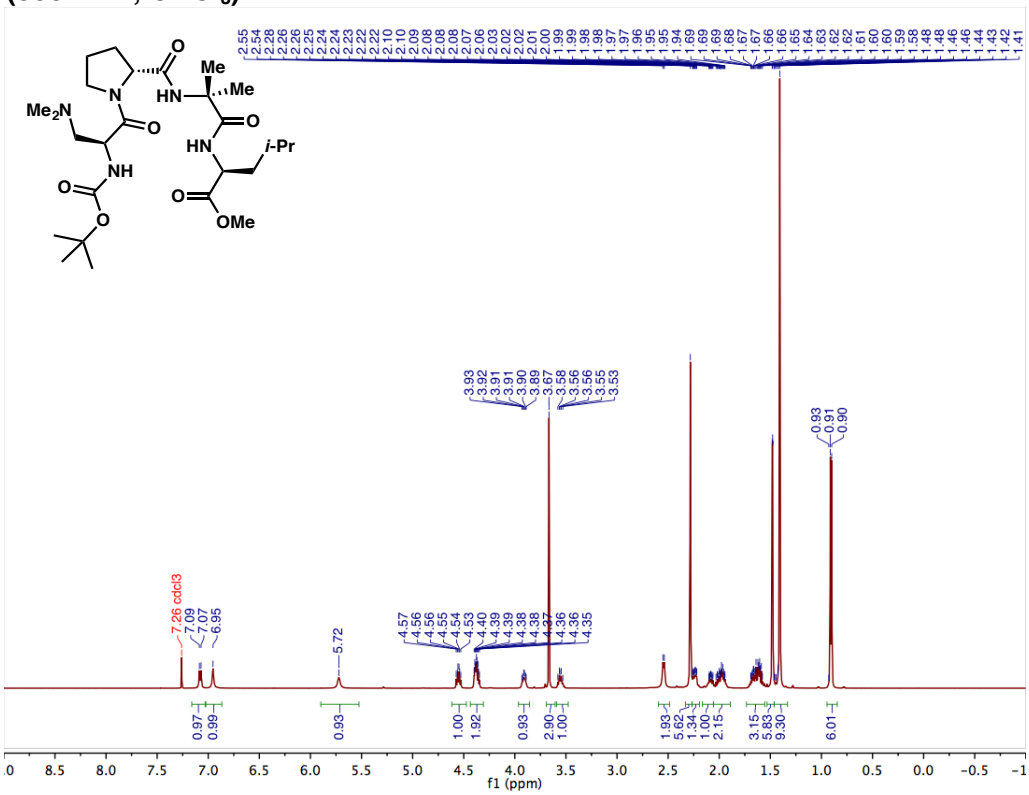

^{13}C-NMR (126 MHz, $CDCl_3$)

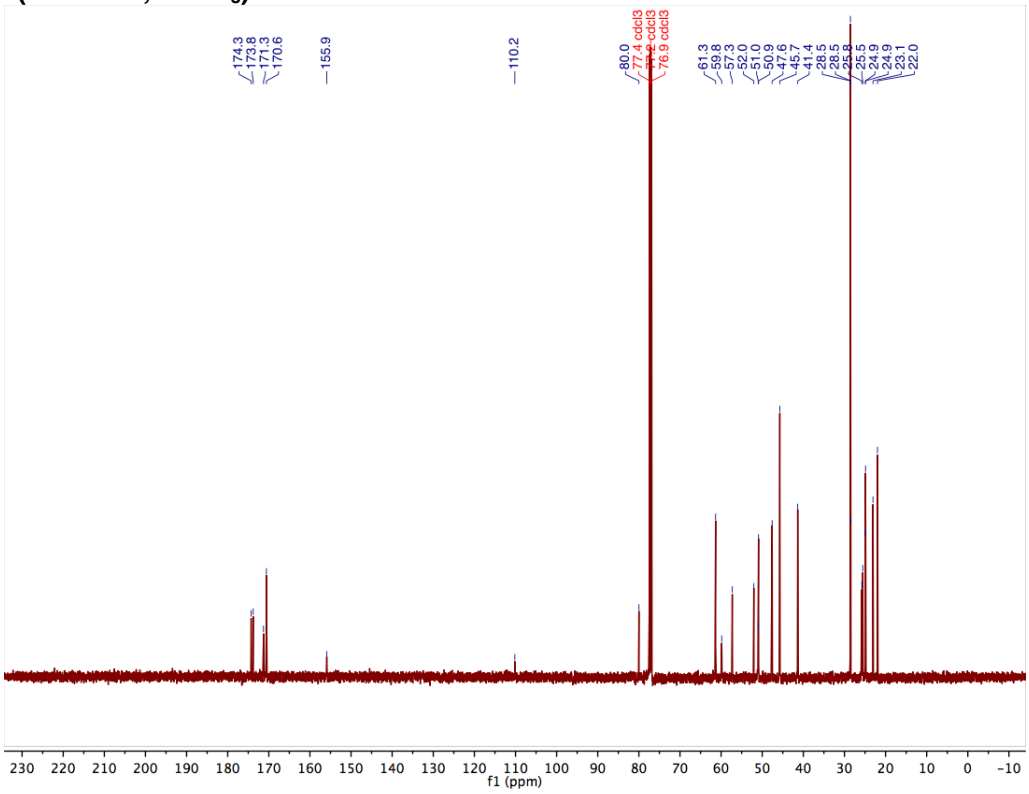

Peptide 26

^{1}H-NMR (500 MHz, $CDCl_3$)

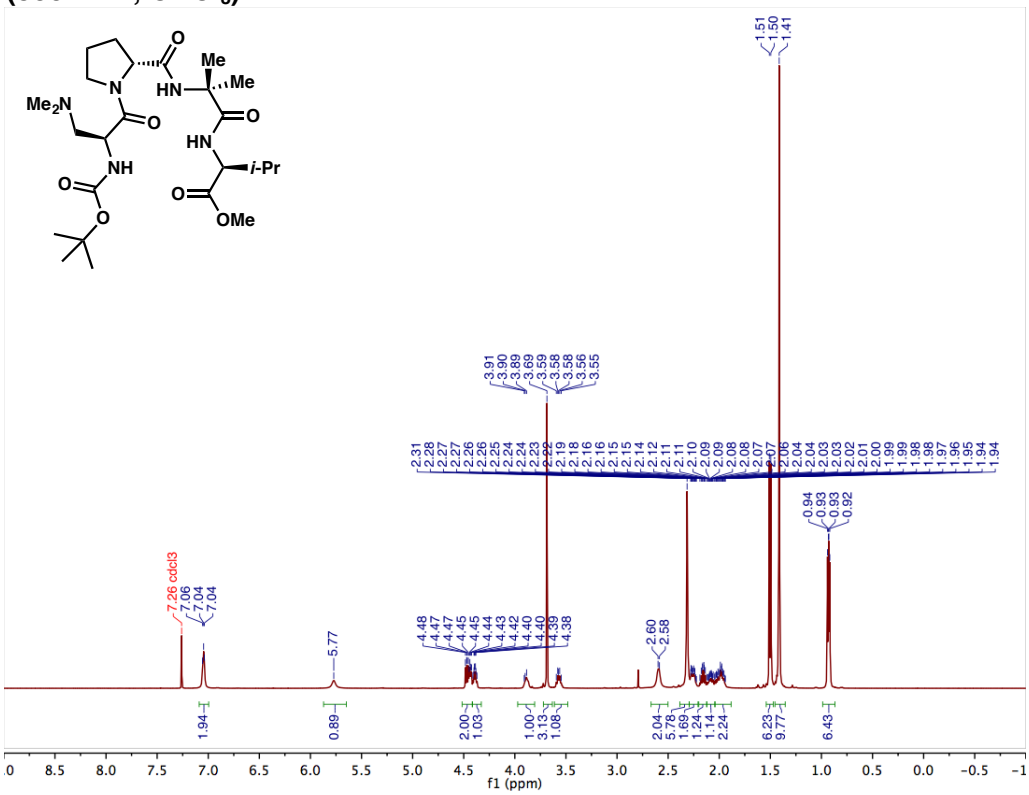

^{13}C-NMR (126 MHz, $CDCl_3$)

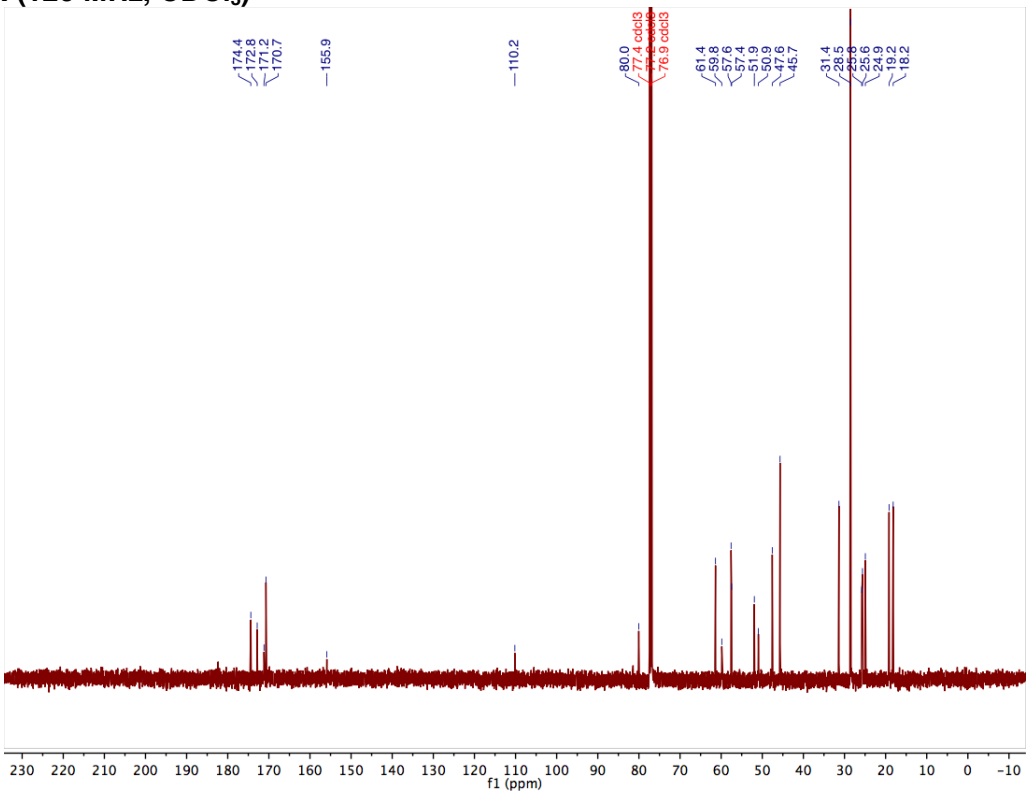

Peptide 27

^{1}H-NMR (600 MHz, $CDCl_3$)

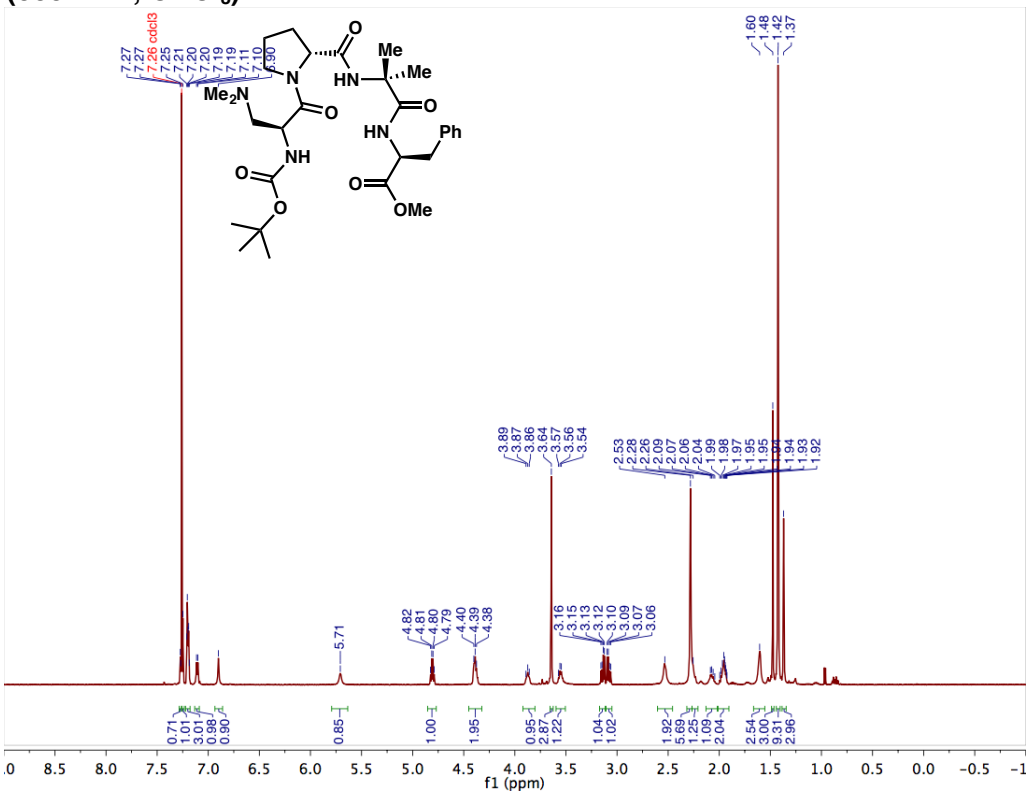

^{13}C-NMR (151 MHz, $CDCl_3$)

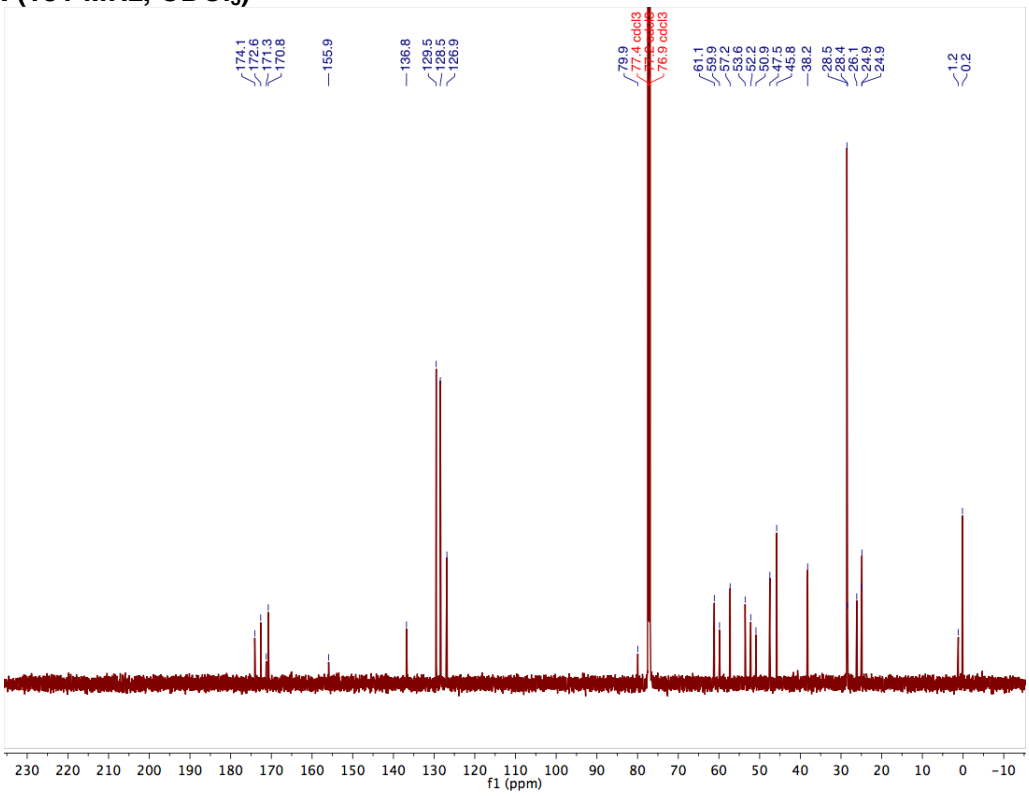

Peptide 28

^{1}H-NMR (500 MHz, $CDCl_3$)

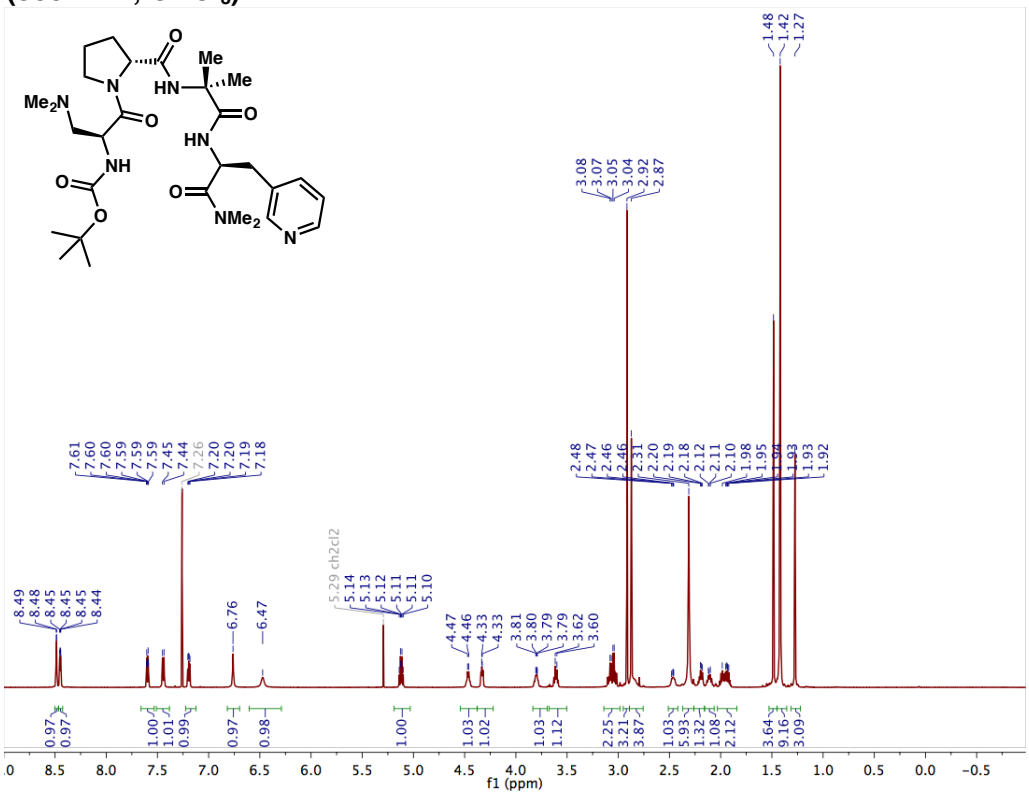

^{13}C-NMR (126 MHz, $CDCl_3$)

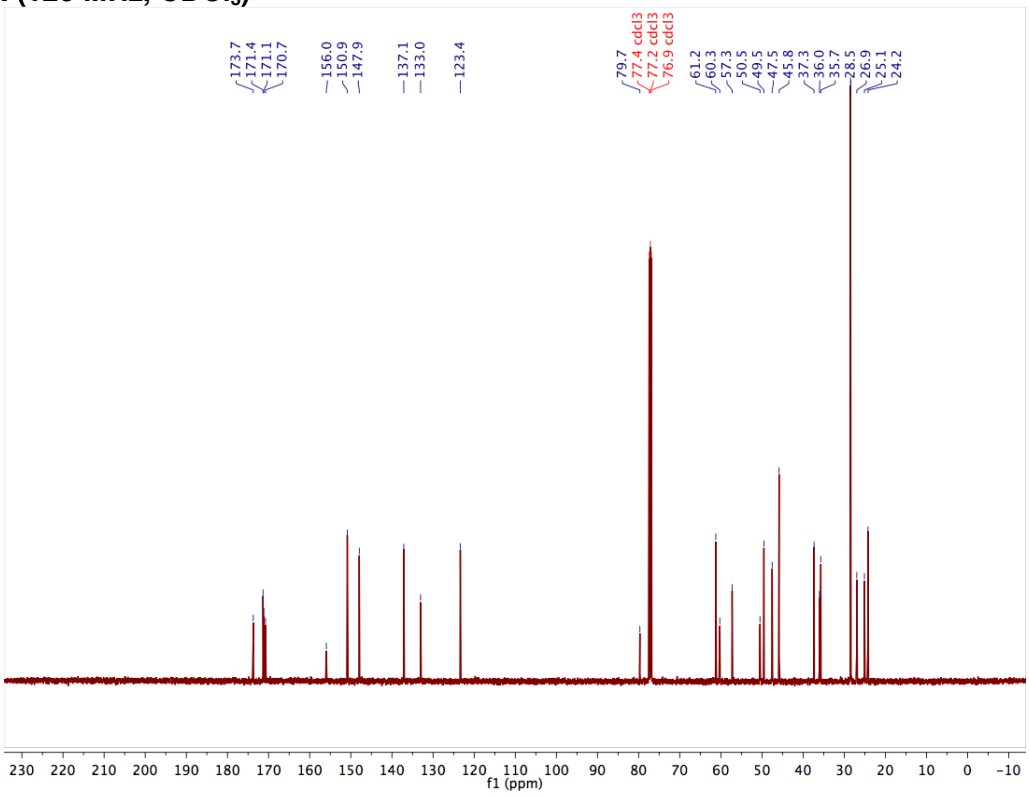

Peptide 29

^{1}H-NMR (500 MHz, $CDCl_3$)

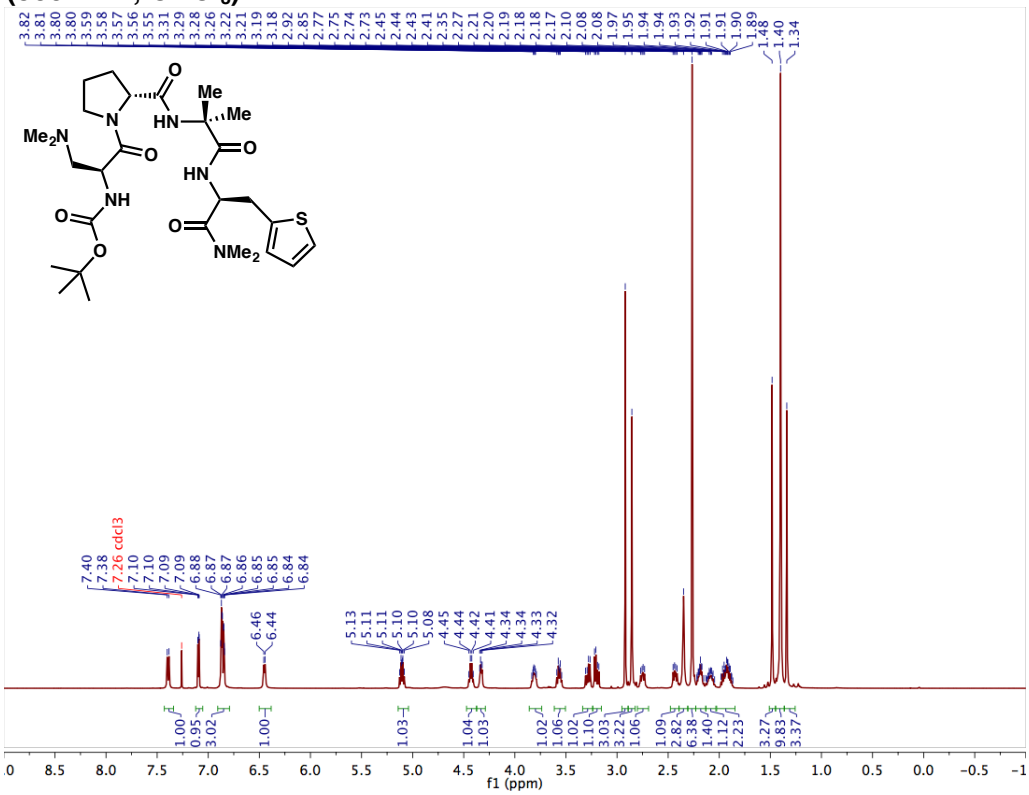

^{13}C-NMR (126 MHz, $CDCl_3$)

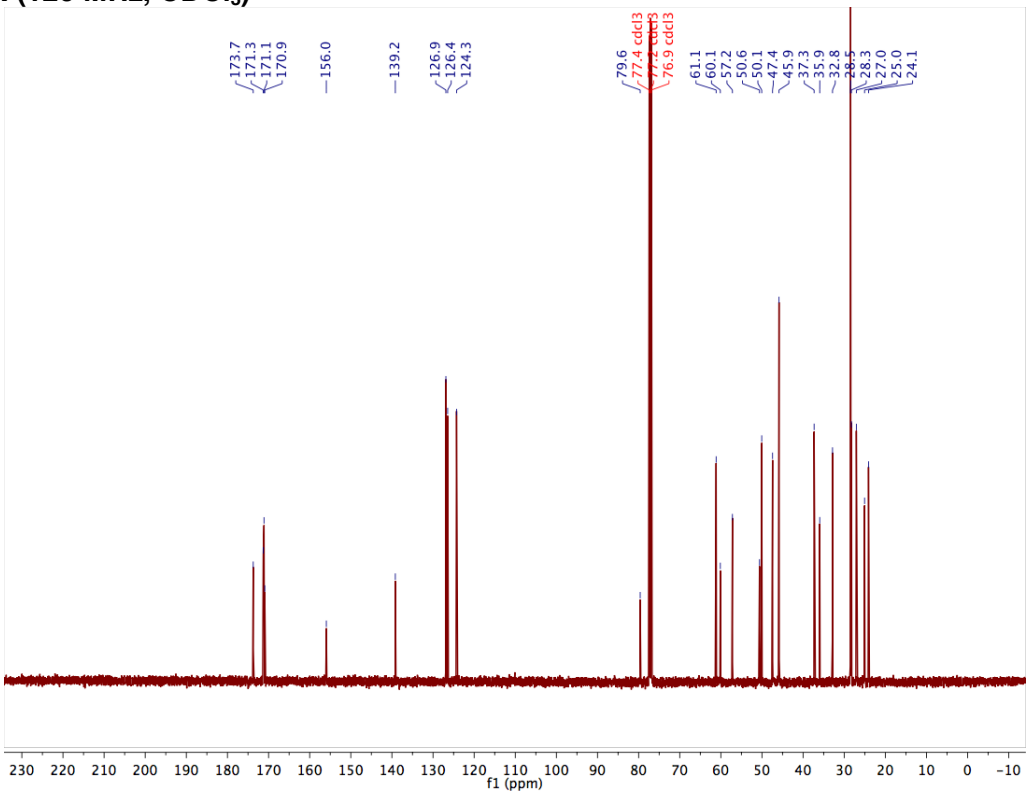

Peptide 30

^{1}H-NMR (500 MHz, $CDCl_3$)

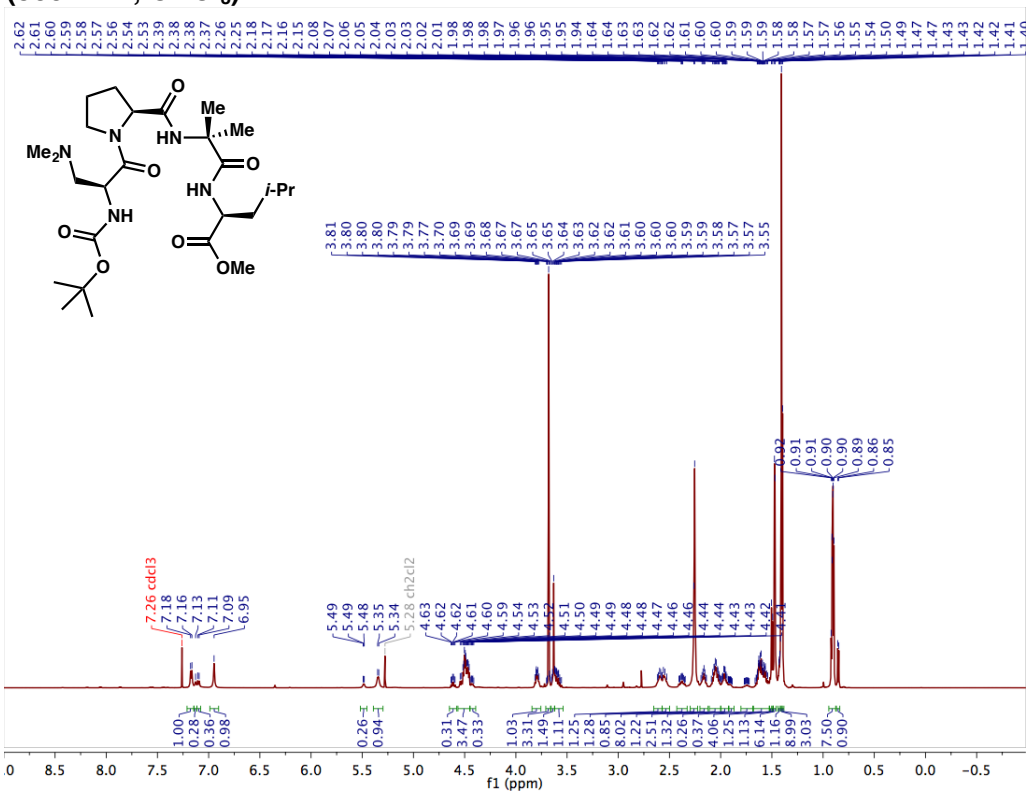

^{13}C-NMR (126 MHz, $CDCl_3$)

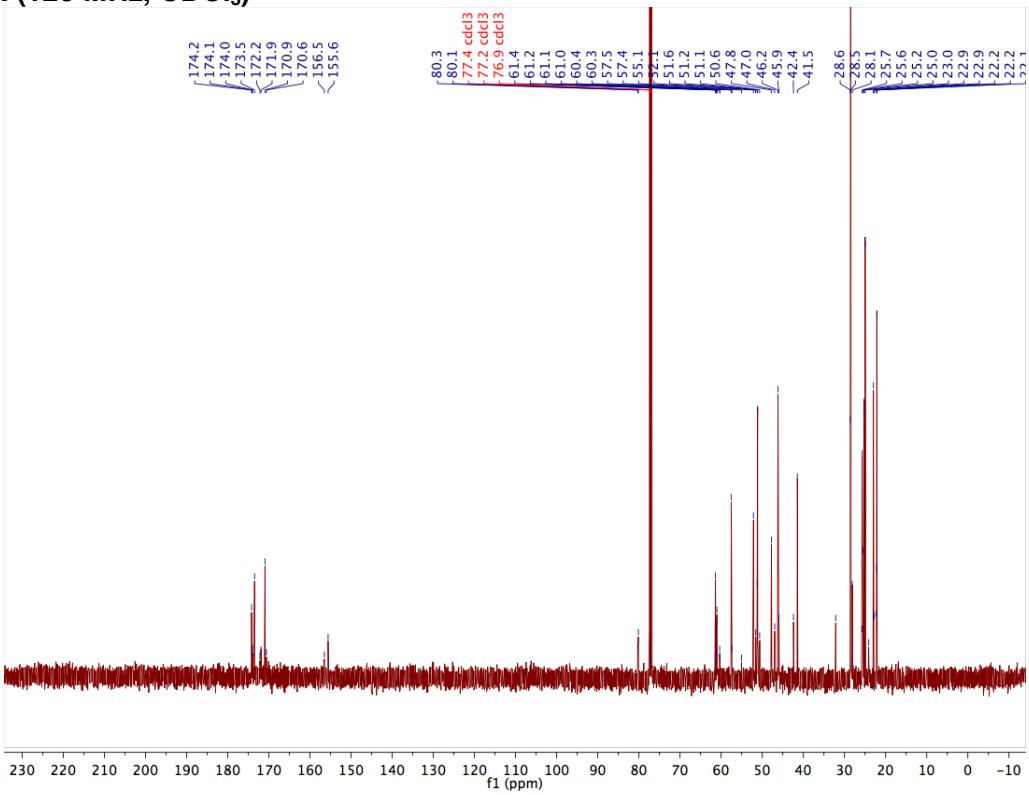

Peptide 31

^{1}H-NMR (600 MHz, $CDCl_3$)

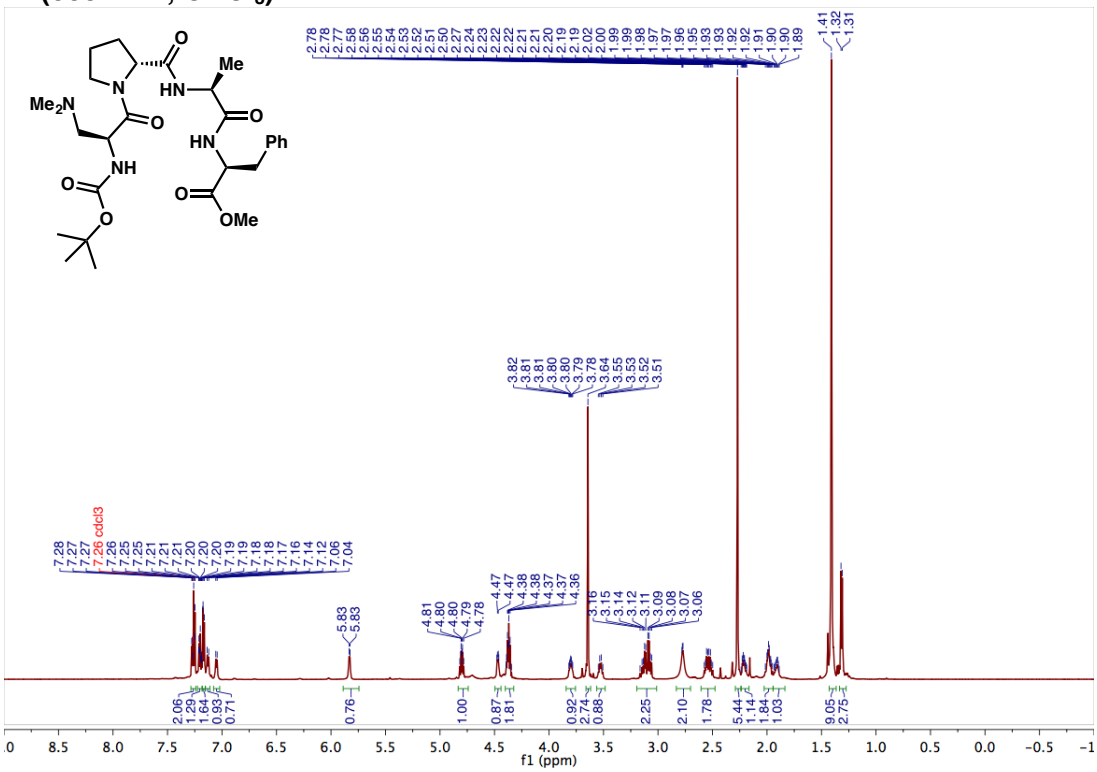

^{13}C-NMR (151 MHz, $CDCl_3$)

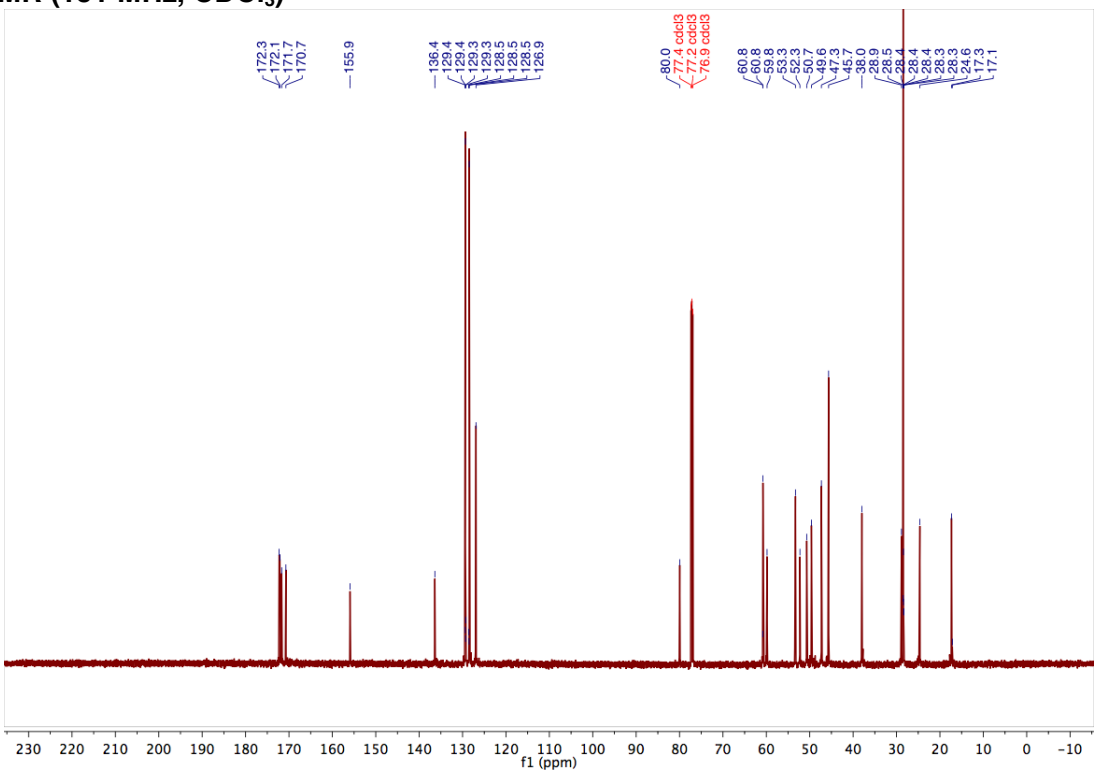

Peptide 32

^{1}H-NMR (500 MHz, $CDCl_3$)

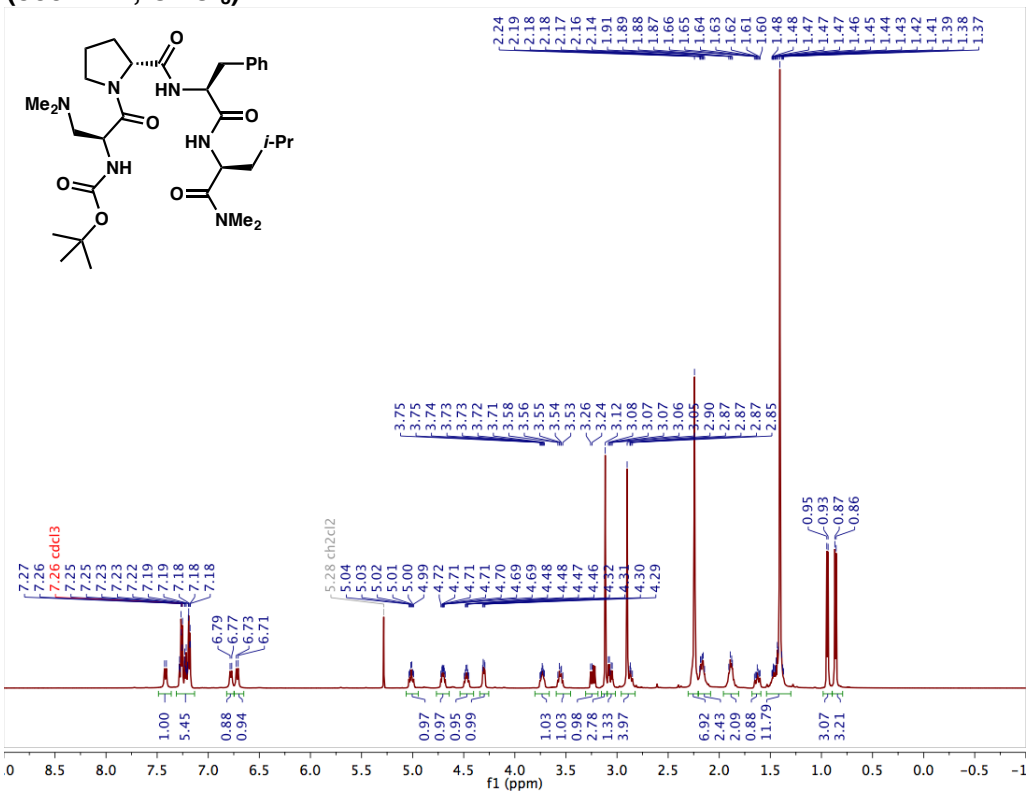

^{13}C-NMR (126 MHz, $CDCl_3$)

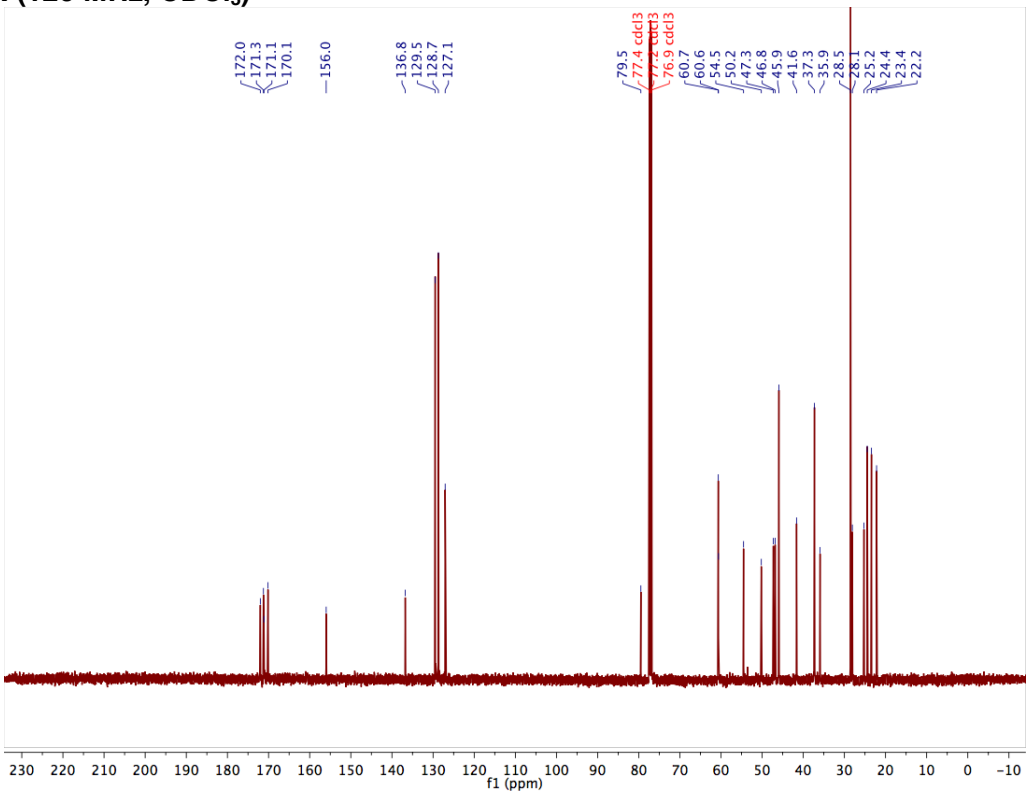

Peptide 33

^{1}H-NMR (500 MHz, $CDCl_3$)

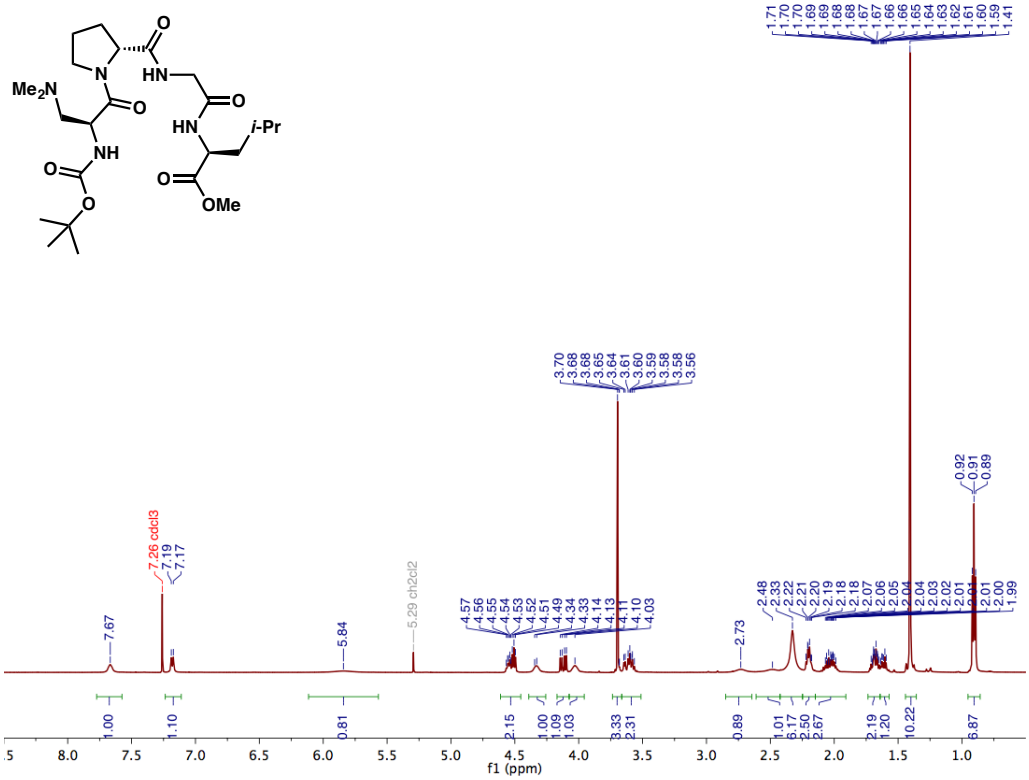

^{13}C-NMR (126 MHz, $CDCl_3$)

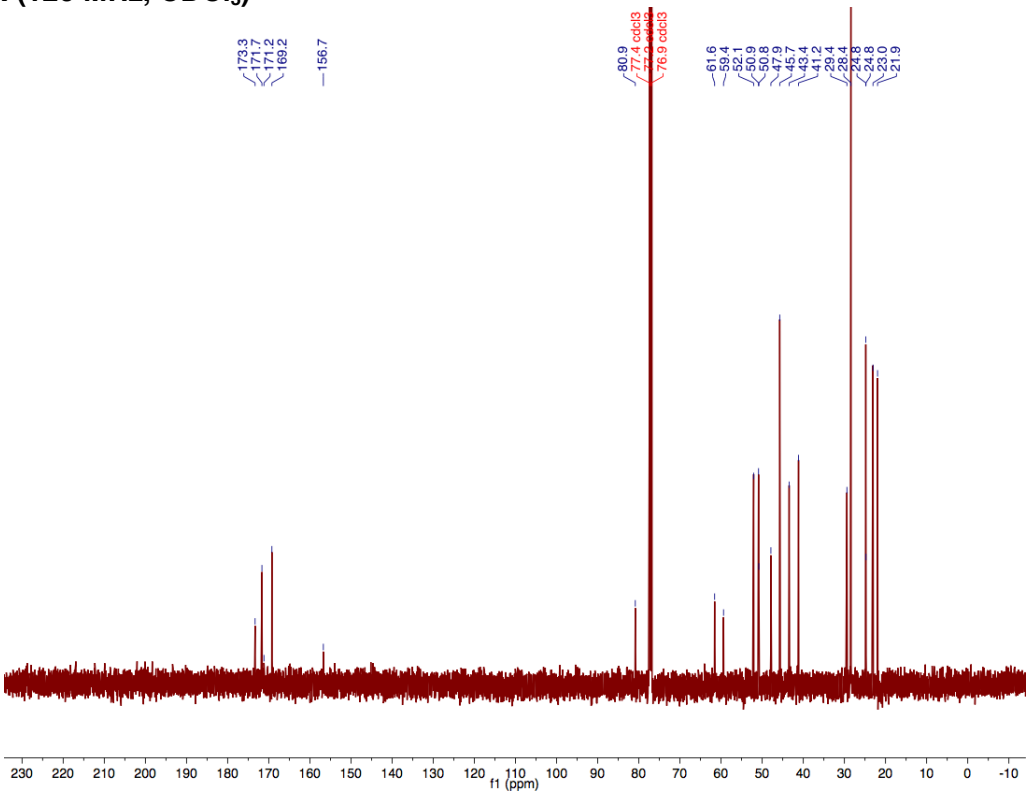

III. Crystallographic Information

A. Experimental

Low-temperature diffraction data (ω-scans) were collected on a Rigaku MicroMax-007HF diffractometer coupled to a Saturn994+ CCD detector with Cu Kα (λ = 1.54178 Å) for the structures of peptides **3**, **6**–**11**, **13**–**15**, **17**–**20**, **22**, **24**, **26**–**30**, and **33**. The diffraction images were processed and scaled using the Rigaku CrystalClear software.[12] For the structures of peptides **4**, **5**, **12**, **16**, **21**, **23**, **25**, **31**, and **32**, low-temperature diffraction data (ω-scans) were collected at the Advanced Light Source, Lawrence Berkeley National Laboratory on a Bruker D8 goniometer coupled to a PHOTON 100 detector with synchrotron radiation (λ = 0.7749 Å). The data were integrated with the APEX2 software package and absorption-corrected with SADABS.[13] All structures were solved with SHELXT and refined against F^2 on all data by full-matrix least squares with SHELXL.[14] All non-hydrogen atoms were refined anisotropically. Unless noted otherwise, hydrogen atoms were included in the model at geometrically calculated positions and refined using a riding model. The isotropic displacement parameters of all hydrogen atoms were fixed to 1.2 times the U-value of the atoms to which they are bonded (1.5 times for methyl groups). Full numbering schemes and additional refinement details for all of the peptides can be found in the crystallographic information files (.cif), which are provided as supplementary information. The CCDC numbers for all compounds are provided in Table S3.01, which are linked to the supplementary crystallographic data for this paper. These data can be obtained free of charge from The Cambridge Crystallographic Data Centre *via* the following web link: http://www.ccdc.cam.ac.uk/data_request/cif.

X-Ray crystal structures were rendered using CYLview,[15] and structure overlays were calculated and rendered using the "structure overlay" and "molecule overlay" features of Mercury 3.8.[16] Three different types of structure overlays are used throughout the manuscript–loop, backbone, and all-atom. Loop overlays were accomplished using the "structure overlay" feature specifying N(*i*+1)–Cα(*i*+1)–C′(*i*+1)–N(*i*+2)–Cα(*i*+2)–C′(*i*+2), the loop atoms, as the atoms to be overlaid. Backbone overlays were also accomplished using the "structure overlay" feature, specifying all of the backbone/main-chain atoms (excluding those on the *N*-terminal Boc-group and the *C*-terminal cap (methyl ester or *N,N*-dimethyl amide). All-atom overlays were accomplished using the "molecule overlay" feature. Overlays of all three types are reported with a corresponding RMSD value.

Table S3.01: Peptide Information

Peptide Sequence	#	MF	MW (g/mol)	Crystallization			Facility Code	CCDC #	β-Turn Motif
				Method	Sample Solvent	Temp			
Boc-Dmaa-D-Pro-Acpc-Leu-NMe_2	3a,b	$C_{27}H_{48}N_6O_6$	552.72	vapor diffusion	EtOAc/pentane	rt	007-15050	1412920	type II' hairpins
Boc-Dmaa-D-Pro-Acpc-Leu-NMe_2	3c	$C_{27}H_{48}N_6O_6$	552.72	vapor diffusion	EtOAc/pentane	rt	007-15126	1453125	type II' hairpin
Boc-Dmaa-D-Pro-Acpc-Leu-OMe	4a	$C_{26}H_{45}N_5O_7$	539.67	vapor diffusion	EtOAc/pentane	rt	007-15146	1453124	type I' pre-helical
Boc-Dmaa-D-Pro-Acpc-Leu-OMe	4b–e	$C_{26}H_{45}N_5O_7$	539.67	vapor diffusion	EtOAc/pentane	rt	ALS-16027	1510507	type I' pre-helical
Boc-Cys(Ph)-D-Pro-Acpc-Leu-OMe	5	$C_{30}H_{44}N_4O_7S$	604.76	vapor diffusion	EtOAc/pentane	rt	SJM-19	1510503	type I' pre-helical
Boc-Leu-D-Pro-Acpc-Leu-OMe	6	$C_{27}H_{46}N_4O_7$	538.69	vapor diffusion	THF/pentane	rt	007-16093	1510502	type II' hairpin
Boc-Dmaa-D-Pro-Acpc-Gly-OMe	7a,b	$C_{22}H_{37}N_5O_7$	483.57	vapor diffusion	EtOAc/pentane	rt	007-15028	1510506	types II'/I' pre-helical
Boc-Dmaa-D-Pro-Acpc-Nle-NMe_2	8	$C_{27}H_{48}N_6O_6$	552.72	vapor diffusion	EtOAc/pentane	rt	007-15071	1510504	type II' hairpin
Boc-Dmaa-D-Pro-Acpc-Val-NMe_2	9	$C_{26}H_{46}N_6O_6$	538.69	vapor diffusion	EtOAc/pentane	rt	007-15070	1510505	type II' hairpin
Boc-Dmaa-D-Pro-Acpc-Val-OMe	10	$C_{25}H_{43}N_5O_7$	525.65	vapor diffusion	EtOAc/pentane	rt	007-15121	1510508	type I' pre-helical
Boc-Dmaa-D-Pro-Acpc-Chg-NMe_2	11	$C_{29}H_{50}N_6O_6$	578.76	vapor diffusion	EtOAc/pentane	rt	007-15102	1510516	type II' hairpin
Boc-Dmaa-D-Pro-Acpc-Phe-NMe_2	12	$C_{30}H_{46}N_6O_6$	586.73	vapor diffusion	EtOAc/pentane	rt	SJM16	1510513	type I' pre-helical
Boc-Dmaa-D-Pro-Acpc-Phe-OMe	13	$C_{29}H_{43}N_5O_7$	573.69	vapor diffusion	EtOAc/hexanes	rt	007-15129	1510509	type II' hairpin
Boc-Dmaa-D-Pro-Acpc-D-Phe-NMe_2	14	$C_{30}H_{46}N_6O_6$	586.73	vapor diffusion	EtOAc/pentane	rt	007-15058	1510514	type II' hairpin
Boc-Dmaa-Pro-Acpc-Leu-OMe	15	$C_{26}H_{45}N_5O_7$	539.67	vapor diffusion	EtOAc/pentane	rt	007-15158	1510510	type II hairpin
Boc-Dmaa-D-Pro-Acbc-Leu-NMe_2	16a,b	$C_{28}H_{50}N_6O_6$	566.74	vapor diffusion	EtOAc/pentane	rt	007-16060	1510512	type II' hairpins
Boc-Dmaa-D-Pro-Acbc-Leu-NMe_2	16c	$C_{28}H_{50}N_6O_6$	566.74	vapor diffusion	EtOAc/pentane	rt	ALS-16026	1510511	type I' pre-helical
Boc-Dmaa-D-Pro-Acbc-Leu-OMe	17a,b	$C_{27}H_{47}N_5O_7$	553.70	vapor diffusion	EtOAc/pentane	rt	007-16055	1510515	type I' pre-helical
Boc-Dmaa-D-Pro-Cle-Leu-OMe	18a,b	$C_{28}H_{49}N_5O_7$	567.73	vapor diffusion	EtOAc/pentane	rt	007-16087	1510517	type I' pre-helical
Boc-Dmaa-D-Pro-Aic-Leu-OMe	19a,b	$C_{32}H_{49}N_5O_7$	615.77	vapor diffusion	THF/pentane	rt	007-16091	1510525	type I' pre-helical
Boc-Dmaa-D-Pro-Aic-D-Phe-NMe_2	20a,b	$C_{36}H_{50}N_6O_6$	662.83	vapor diffusion	EtOAc/pentane	rt	007-15115	1510518	type II'
Boc-Dmaa-Pro-Aic-Leu-OMe	21a,b	$C_{32}H_{49}N_5O_7$	615.77	vapor diffusion	EtOAc/pentane	rt	SJM15	1510519	type II
Boc-Dmaa-D-Pro-Achc-Leu-OMe	22a,b	$C_{29}H_{51}N_5O_7$	581.76	vapor diffusion	EtOAc/pentane	rt	007-16083	1510522	type I' pre-helical
Boc-Cys(Ph)-D-Pro-Achc-Leu-OMe	23	$C_{33}H_{50}N_4O_7S$	646.84	vapor diffusion	EtOAc/pentane	rt	SJM23	1510526	type I' pre-helical
Boc-Dmaa-D-Pro-Aib-Leu-NMe_2	24	$C_{27}H_{50}N_6O_6$	554.73	vapor diffusion	EtOAc/pentane	rt	007-16092	1510521	type II' hairpin
Boc-Dmaa-D-Pro-Aib-Leu-OMe	25	$C_{26}H_{47}N_5O_7$	541.69	vapor diffusion	EtOAc/pentane	rt	SJM17	1510520	type II' hairpin
Boc-Dmaa-D-Pro-Aib-Val-OMe	26	$C_{25}H_{45}N_5O_7$	527.66	vapor diffusion	EtOAc/pentane	rt	007-16004	1510524	type II' hairpin
Boc-Dmaa-D-Pro-Aib-Phe-OMe	27	$C_{29}H_{45}N_5O_7$	575.71	vapor diffusion	Et_2O/hexanes	rt	007-15168	1510523	type II' hairpin
Boc-Dmaa-D-Pro-Aib-3-Pal-NMe_2	28	$C_{29}H_{47}N_7O_6$	589.74	vapor diffusion	EtOAc/pentane	rt	007-15136	1510530	type II' hairpin
Boc-Dmaa-D-Pro-Aib-2-Thi-NMe_2	29a,b	$C_{28}H_{46}N_6O_6S$	594.77	vapor diffusion	EtOAc/pentane	rt	007-15145	1510527	type II' hairpins
Boc-Dmaa-Pro-Aib-Leu-OMe	30	$C_{26}H_{47}N_5O_7$	541.69	vapor diffusion	EtOAc/pentane	rt	007-15152	1510531	type II
Boc-Dmaa-D-Pro-Ala-Phe-OMe	31	$C_{28}H_{43}N_5O_7$	561.68	vapor diffusion	EtOAc/pentane	rt	SJM5	1510528	type II' hairpin
Boc-Dmaa-D-Pro-Phe-Leu-NMe_2	32a,b	$C_{32}H_{52}N_6O_6$	616.80	vapor diffusion	EtOAc/pentane	rt	SJM21	1510529	unfolded
Boc-Dmaa-D-Pro-Gly-Leu-OMe	33a,b	$C_{24}H_{43}N_5O_7$	513.64	vapor diffusion	PhMe/pentane	rt	007-16123	1510532	type I' pre-helical
Boc-Keto-D-Pro-Aib-Phe-NMe_2	34	$C_{30}H_{44}N_4O_8$	588.70	slow evaportation	$CHCl_3$	rt	JTB55t	604845	type II' hairpin
Boc-Phe-Pro-Aib-(*R*)-α-Mba	35	$C_{31}H_{42}N_4O_5$	550.70	slow evaportation	$CHCl_3$	–20 ºC	final	147004	type II
2-Msa-Pro-D-Val-(*R*)-α-Mba	36	$C_{22}H_{31}N_3O_5$	417.51	slow evaportation	CH_2Cl_2	rt	cj02	687520	type II
Boc-His(τ-Bn)-Pro-Aib-(*R*)-α-Mba	37	$C_{35}H_{46}N_6O_5$	630.79	slow evaportation	$CHCl_3$	rt	djg280t	147003	type I Pro-ASX

Table S3.02: Details of X-Ray Crystal Structures **3a–c**, **4a–e**, and **5**

Compound	3a,b[4,5]	3c[5]	4a[5]	4b–e	5
Data Code	007-15050	007-15126	007-15146	ALS-16027	SJM19
Empirical Formula	$C_{27}H_{49}N_6O_{6.5}$	$C_{27}H_{48}N_6O_6$	$C_{26}H_{45}N_5O_7$	$C_{26}H_{45}N_5O_7$	$C_{30}H_{44}N_4O_7S$
Temperature (K)	93(2)	93(2)	228(2)	100(2)	100(2) K
Wavelength (Å)	1.54187	1.54187	1.54187	0.7749	0.7749
FW	561.72	552.71	538.66	539.67	604.75
Crystal System	Monoclinic	Orthorhombic	Orthorhombic	Triclinic	Orthorhombic
Space Group	$P2_1$	$P2_12_12_1$	$P2_12_12_1$	$P1$	$P2_12_12_1$
a **(Å)**	16.1717(11)	11.7899(8)	11.9360(8)	11.9119(13)	14.0134(6)
b **(Å)**	9.364(6)	15.9908(11)	16.0501(11)	15.6190(17)	21.2939(9) Å
c **(Å)**	21.5606(15)	16.3363(11)	16.5597(12)	16.4598(17)	11.1225(4)
α (°)	90	90	90	86.532(2)	90
β (°)	104.7162(2)	90	90	89.527(2)	90
γ (°)	90	90	90	88.976(2)	90
V **(Å^3)**	3157.9(4)	3079.9(4)	3172.4(4)	3056.2(6)	3319.0(2) Å3
Z	4	4	4	4	4
ρ **(mg/m^3)**	1.181	1.192	1.128	1.173	1.210
μ **(mm^{-1})**	0.693	0.691	0.676	0.104	0.179
Flack Parameter	–0.04(15)	0.01(4)	–0.01(3)	–0.2(6)	0.09(3)
R**1, w*****R*****2 (I > 2σ(I))**	0.0651, 0.1665	0.0287, 0.0784	0.0504, 0.1454	0.0526, 0.1115	0.0416, 0.1062
R**1, *wR*2 (all data)**	0.0982, 0.1864	0.0307, 0.0792	0.0534, 0.1513	0.0810, 0.1219	0.0458, 0.1082
GOF	1.023	1.060	1.023	1.063	1.138
Largest Diff. Peak, Hole (e A^{-3})	0.760, 0.285	0.274, –0.166	0.280, –0.190	0.570, –0.241	0.362, –0.255

Table S3.03: Details of X-Ray Crystal Structures **6**–**7a,b** and **8**–**10**

Compound	**6**	**7a,b**	**8**	**9**	**10**
Data Code	007-16093	007-15028	007-15071	007-15070	007-15121
Empirical Formula	$C_{27}H_{46}N_4O_7$	$C_{22}H_{37}N_5O_7$	$C_{27}H_{48}N_6O_6$	$C_{26}H_{46}N_6O_6$	$C_{25}H_{43}N_5O_7$
Temperature (K)	93(2)	93(2)	93(2)	93(2)	93(2)
Wavelength (Å)	1.54178	1.54187	1.54187	1.54187	1.54187
FW	538.68	483.56	552.71	525.64	525.64
Crystal System	Monoclinic	Monoclinic	Orthorhombic	Orthorhombic	Orthorhombic
Space Group	$P2_1$	$P2_1$	$P2_12_12_1$	$P2_12_12_1$	$P2_12_12_1$
***a* (Å)**	12.0174(8)	9.8381(2)	9.7541(7)	9.4965(7)	11.7505(8)
***b* (Å)**	9.4647(7)	10.3396(2)	10.7355(8)	10.4398(7)	15.3610(11)
***c* (Å)**	13.6217(10)	25.5626(18)	29.430(2)	31.132(2)	16.1615(11)
α (°)	90	90	90	90	90
β (°)	106.691(3)	97.525(7)	90	90	90
γ (°)	90	90	90	90	90
***V* (Å^3)**	1484.07(18)	2577.9(2)	3081.7(4)	3086.5(4)	2917.1(4)
Z	2	4	4	4	4
ρ (mg/m^3)	1.205	1.246	1.191	1.159	1.197
μ (mm^{-1})	0.711	0.775	0.691	0.678	0.722
Flack Parameter	0.00(11)	–0.01(5)	0.02(2)	0.01(6)	0.01(2)
***R*1, w*R*2 ($I > 2\sigma(I)$)**	0.0387, 0.0848	0.0433, 0.1104	0.0239, 0.0667	0.0320, 0.0751	0.0244, 0.0630
***R*1, *wR*2 (all data)**	0.0518, 0.0918	0.0470, 0.1137	0.0255, 0.0737	0.0375, 0.0764	0.0251, 0.0635
GOF	1.020	1.047	1.148	1.025	1.043
Largest Diff. Peak, Hole (e A^{-3})	0.260, –0.159	0.257, –0.251	0.225, –0.258	0.277, –0.335	0.192, –0.138

Table S3.04: Details of X-Ray Crystal Structures **11–15**

Compound	**11**	**12**	**13**	**14**	**15**
Data Code	007-15102	SJM16	007-15129	007-15058	007-15158
Empirical Formula	$C_{29}H_{50}N_6O_6$	$C_{30}H_{46}N_6O_6$	$C_{29}H_{43}N_5O_7$	$C_{30}H_{46}N_6O_6$	$C_{26}H_{45}N_5O_7$
Temperature (K)	93(2)	100(2)	93(2)	93(2)	93(2)
Wavelength (Å)	1.54178	1.512	1.54178	1.54178	1.54178
FW	578.75	586.73	573.68	586.73	539.67
Crystal System	Orthorhombic	Orthorhombic	Monoclinic	Monoclinic	Monoclinic
Space Group	$P2_12_12_1$	$P2_12_12_1$	$P2_1$	$P2_1$	$P2_1$
***a* (Å)**	9.6852(7)	9.5116(4)	10.6027(7)	11.0991(3)	9.9289(7)
***b* (Å)**	10.7444(8)	10.8943(4)	8.8911(6)	9.2550(3)	14.2705(10)
***c* (Å)**	31.296(2)	30.9331(11)	15.9646(11)	16.0095(11)	11.0675(8)
α (°)	90	90	90	90	90
β (°)	90	90	97.122(2)	100.869(7)	98.876(7)
γ (°)	90	90	90	90	90
***V* (Å^3)**	3256.8(4)	3205.4(2)	1493.37(17)	1615.03(14)	1549.38(19)
Z	4	4	2	2	2
ρ (mg/m^3)	1.180	1.216	1.276	1.207	1.157
μ (mm^{-1})	0.676	0.632	0.754	0.692	0.692
Flack Parameter	0.18(6)	–0.03(4)	–0.07(4)	0.06(11)	0.03(9)
***R*1, w*R*2 (I > 2σ(I))**	0.0419, 0.0990	0.0309, 0.0777	0.0252, 0.0630	0.0441, 0.1039	0.0611, 0.1615
***R*1, *wR*2 (all data)**	0.0502, 0.1044	0.0317, 0.0782	0.0262, 0.0635	0.0507, 0.1137	0.0656, 0.1675
GOF	1.047	1.054	1.045	1.103	1.050
Largest Diff. Peak, Hole (e A^{-3})	0.359, –0.353	0.169, –0.207	0.103, –0.146	0.262, –0.246	0.623, –0.424

Table S3.05: Details of X-Ray Crystal Structures **16a–c**, **17a,b**, **18a,b**, and **19a,b**

Compound	16a,b	16c	17a,b	18a,b	19a,b
Data Code	007-16060	ALS-16026	007-16055	007-16087	007-16091
Empirical Formula	$C_{29.25}H_{54.50}ClN_6O_{6.25}$	$C_{28}H_{50}N_6O_6$	$C_{27}H_{47}N_5O_7$	$C_{28}H_{49}N_5O_7$	$C_{34}H_{53}N_5O_{7.50}$
Temperature (K)	93(2)	100(2)	93(2)	93(2)	93(2)
Wavelength (Å)	1.54178	0.7749	1.54178	1.54178	1.54178
FW	625.74	566.74	553.69	567.72	651.81
Crystal System	Monoclinic	Orthorhombic	Monoclinic	Monoclinic	Orthorhombic
Space Group	C_2	$P2_12_12_1$	$P2_1$	$P2_1$	$P2_12_12_1$
a **(Å)**	27.2814(19)	12.4001(19)	11.7452(8)	11.7165(8)	16.3898(11)
b **(Å)**	15.4659(11)	15.333(2)	16.8106(12)	16.9463(12)	18.3004(13)
c **(Å)**	17.7648(12)	16.440(2)	15.9153(11)	16.0776(11)	24.0255(17)
α (°)	90	90	90	90	90
β (°)	106.757(2)	90	91.065(2)	91.257(3)	90
γ (°)	90	90	90	90	90
V **(Å^3)**	7177.2(9)	3125.7(8)	3141.8(4)	3191.5(4)	7206.2(9)
Z	8	4	4	4	8
ρ (mg/m^3)	1.158	1.204	1.171	1.182	1.202
μ (mm^{-1})	1.320	0.104	0.694	0.695	0.692
Flack Parameter	0.035(2)	–0.9(8)	0.03(4)	0.07(7)	–0.08(7)
R**1, w*****R*****2 (I > 2σ(I))**	0.0392, 0.1146	0.0507, 0.1139	0.0342, 0.0925	0.0376, 0.0941	0.0445, 0.1004
R**1, *w*****R*****2 (all data)**	0.0401, 0.1154	0.0659, 0.1212	0.0361, 0.0944	0.0426, 0.0966	0.0731, 0.1180
GOF	1.042	1.065	1.026	1.046	1.010
Largest Diff. Peak, Hole (e A^{-3})	0.937, –0.527	0.354, –0.221	0.225, –0.186	0.400, –0.170	0.275, –0.265

Table S3.06: Details of X-Ray Crystal Structures **20a,b**, **21a,b**, **22a,b**, and **23**–**24**

Compound	20a,b	21a,b	22a,b	23	24
Data Code	007-15115	SJM15	007-16083	SJM23	007-16092
Empirical Formula	$C_{36}H_{50}N_6O_6$	$C_{32}H_{49}N_5O_7$	$C_{29}H_{51}N_5O_7$	$C_{33}H_{50}N_4O_7S$	$C_{27}H_{50}N_6O_6$
Temperature (K)	93(2)	100(2)	93(2)	100(2)	93(2)
Wavelength (Å)	1.54178	0.7749	1.54178	0.7749	1.54178
FW	662.82	615.76	581.74	646.83	554.73
Crystal System	Monoclinic	Triclinic	Monoclinic	Orthorhombic	Orthorhombic
Space Group	$P2_1$	$P1$	$P2_1$	$P2_12_12_1$	$P2_12_12_1$
a **(Å)**	18.9459(13)	5.8475(2)	11.5458(8)	11.8017(5)	9.6322(7)
b **(Å)**	10.2874(7)	11.4463(4)	16.5702(12)	15.0992(6)	10.7847(8)
c **(Å)**	20.3541(14)	26.2716(8)	16.8885(12)	19.6217(8)	30.960(2)
α (°)	90	83.314(2)	90	90	90
β (°)	114.654(2)	84.006(2)	92.912(2)	90	90
γ (°)	90	78.952(2)	90	90	90
V **(Å^3)**	3605.5(4)	1708.00(10)	3226.9(4)	3496.5(2)	3216.1(4)
Z	4	2	4	4	4
ρ **(mg/m^3)**	1.221	1.197	1.197	1.229	1.146
μ **(mm^{-1})**	0.680	0.102	0.698	0.175	0.662
Flack Parameter	–0.01(5)	–0.3(4)	0.00(2)	–0.002(11)	–0.01(7)
R**1, w*****R*****2 (I > 2σ(I))**	0.0350, 0.0900	0.0420, 0.0815	0.0258, 0.0657	0.0318, 0.0824	0.0466, 0.1179
R**1, *w*****R*****2 (all data)**	0.0375, 0.0918	0.0606, 0.0879	0.0261, 0.0659	0.0368, 0.0853	0.0511, 0.1207
GOF	1.024	1.017	1.015	1.037	1.204
Largest Diff. Peak, Hole (e A^{-3})	0.447, –0.284	0.175, –0.217	0.321, –0.130	0.362, –0.268	0.245, –0.163

Table S3.07: Details of X-Ray Crystal Structures **25–29a,b**

Compound	**25**	**26**	**27**	**28**	**29a,b**
Data Code	SJM17	007-16004	007-15168	007-15136	007-15145
Empirical Formula	$C_{26}H_{47}N_5O_7$	$C_{25}H_{45}N_5O_7$	$C_{29}H_{45}N_5O_7$	$C_{29}H_{53}N_7O_9$	$C_{28}H_{46}N_6O_6S$
Temperature (K)	100(2)	93(2)	93(2)	93(2)	93(2)
Wavelength (Å)	0.7749	1.54178	1.54178	1.54178	1.54178
FW	541.68	527.66	575.70	643.78	594.77
Crystal System	Orthorhombic	Orthorhombic	Orthorhombic	Monoclinic	Triclinic
Space Group	$P2_12_12_1$	$P2_12_12_1$	$P2_12_12_1$	$P2_1$	$P1$
***a* (Å)**	9.5263(3)	9.6442(7)	9.7528(7)	9.6527(7)	10.2959(7)
***b* (Å)**	10.9728(4)	10.6337(7)	10.8277(8)	18.7582(13)	10.4853(7)
***c* (Å)**	28.9779(10)	28.723(2)	29.439(2)	10.5398(7)	14.9355(10)
α (°)	90	90	90	90	94.868(2)
β (°)	90	90	90	115.399(2)	100.913(2)
γ (°)	90	90	90	90	90.106(3)
***V* (Å^3)**	3029.07(18)	2945.6(4)	3108.7(4)	1724.0(2)	1577.24(18)
Z	4	4	4	2	2
ρ (mg/m^3)	1.188	1.190	1.230	1.240	1.252
μ (mm^{-1})	0.104	0.716	0.724	0.764	1.316
Flack Parameter	–0.3(6)	0.00(3)	0.06(2)	0.03(6)	0.025(13)
***R*1, w*R*2 (I > 2σ(I))**	0.0383, 0.0893	0.0241, 0.0625	0.0232, 0.0571	0.0291, 0.0646	0.0628, 0.1551
***R*1, *wR*2 (all data)**	0.0479, 0.0943	0.0245, 0.0629	0.0235, 0.0573	0.0348, 0.0667	0.0751, 0.1684
GOF	1.020	1.048	1.052	1.038	1.017
Largest Diff. Peak, Hole (e A^{-3})	0.289, –0.251	0.137, –0.128	0.111, –0.137	0.139, -0.149	0.577, –0.419

Table S3.08: Details of X-Ray Crystal Structures **30–33a,b**

Compound	**30**	**31**	**32a,b**	**33a,b**
Data Code	007-15152	SJM5	SJM21	007-16123
Empirical Formula	$C_{26}H_{47}N_5O_7$	$C_{28}H_{43}N_5O_7$	$C_{32}H_{52}N_6O_6$	$C_{24}H_{43}N_5O_7$
Temperature (K)	93(2)	100(2)	100(2)	93(2)
Wavelength (Å)	1.54178	0.7749	0.7749	1.54178
FW	541.68	561.67	616.79	513.63
Crystal System	Monoclinic	Monoclinic	Orthorhombic	Orthorhombic
Space Group	$P2_1$	$P2_1$	$P2_12_12_1$	$P2_12_12_1$
***a* (Å)**	5.9090(4)	10.6617(4)	11.725(15)	16.1450(11)
***b* (Å)**	24.4001(17)	8.8095(4)	22.82(3)	16.2685(11)
***c* (Å)**	10.6197(7)	15.8579(7)	25.93(3)	21.7425(15)
α (°)	90	90	90	90
β (°)	102.609(3)	97.106(2)	90	90
γ (°)	90	90	90	90
***V* (Å^3)**	1494.22(18)	1478.00(11)	6937(16)	5710.8(7)
Z	2	2	8	8
ρ (0.75mg/m^3)	1.204	1.262	1.181	1.195
μ (mm^{-1})	0.718	0.110	0.100	0.725
Flack Parameter	–0.03(5)	0.1(2)	0.4(6)	0.09(10)
***R*1, w*R*2 (I > 2σ(I))**	0.0292, 0.0738	0.0434, 0.1043	0.0575, 0.1290	0.0592, 0.1260
***R*1, *wR*2 (all data)**	0.0303, 0.0743	0.0556, 0.1108	0.0773, 0.1385	0.1062, 0.1479
GOF	1.037	1.062	1.093	1.048
Largest Diff. Peak, Hole (e A^{-3})	0.123, –0.153	0.425, –0.246	0.742, –0.213	0.352, –0.265

Table S3.09: Details of X-Ray Crystal Structures **34**–**37** Reproduced from Previous References

Compound	**34**[8]	**35**[9]	**36**[10]	**37**[11]
CSD Refcode	WEDBUD	GOPDEU	COFXUR	LOHWOU
Empirical Formula	$C_{30}H_{44}N_4O_8$• 2($CHCl_3$)	$C_{31}H_{42}N_4O_5$	$C_{22}H_{31}N_3O_5$• CH_2Cl_2	$C_{35}H_{46}N_6O_5$
Temperature (K)	193	183	173	N/A
FW	588.70	550.70	417.51	630.79
Crystal System	Monoclinic	Orthorhombic	Orthorhombic	Orthorhombic
Space Group	$P2_1$	$P2_12_12_1$	$P2_12_12_1$	$P2_12_12_1$
***a* (Å)**	10.8964(7)	11.5439(1)	9.0028(18)	12.1058(7)
***b* (Å)**	11.0190(8)	27.4393(2)	11.376(2)	12.1453(7)
***c* (Å)**	17.9964(12)	9.8370(1)	26.325(5)	23.493(1)
α (°)	90	90	90	90
β (°)	102.471(2)	90	90	90
γ (°)	90	90	90	90
***V* (Å^3)**	2109.8	3115.9	2696.1	3454.1
Z	2	4	4	4
***R*1, w*R*2 (I > 2*σ*(I))**	0.0581	0.0756	0.0473	0.0639

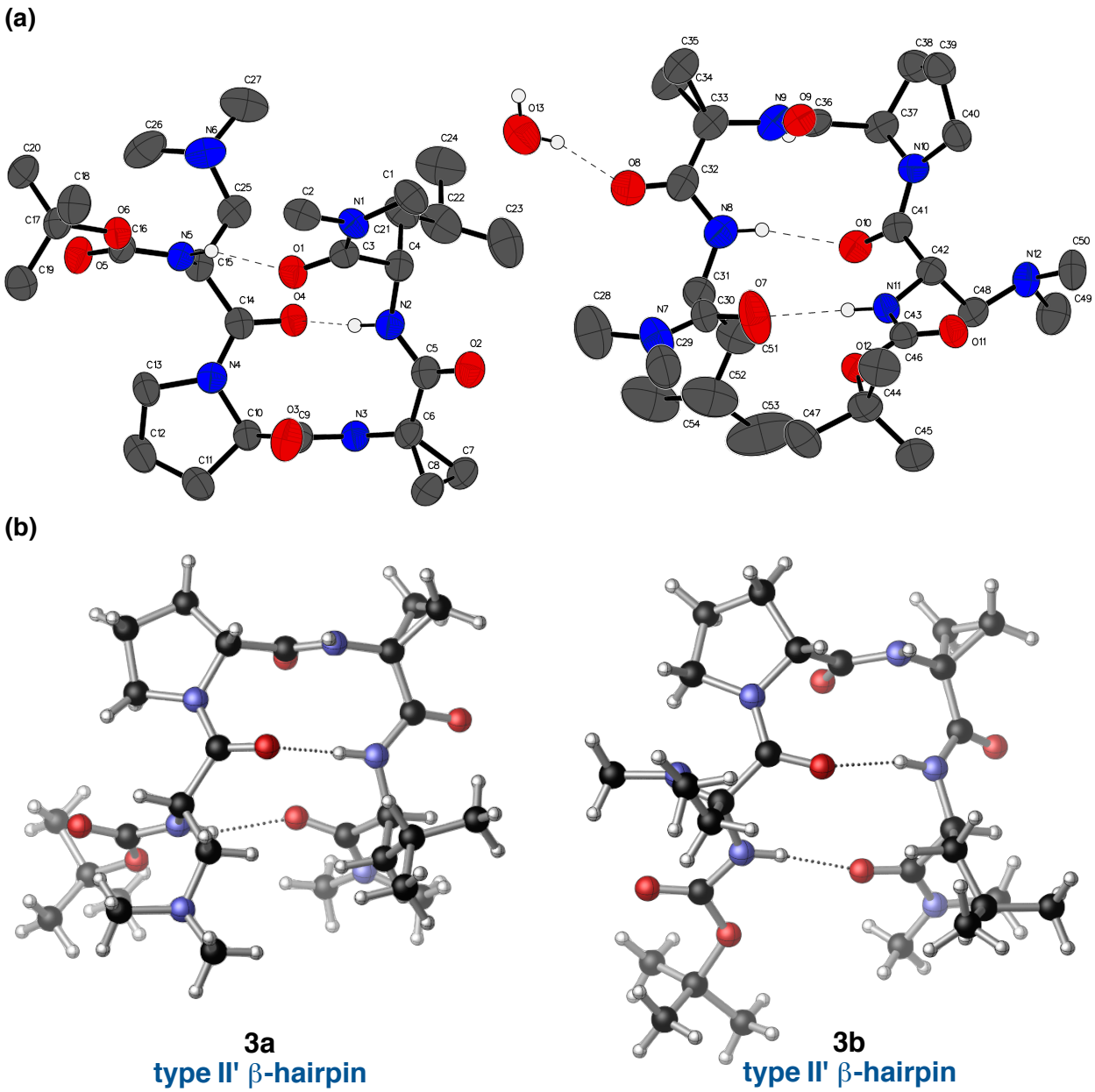

Figure S3.01: (a) The full numbering scheme of **3a,b** with 50% thermal ellipsoids. Most H-atoms have been omitted for clarity, while some are depicted as circles. Dashed lines highlight H-bonding interactions. **(b)** Images of **3a** and **3b** rendered separately using CYLview.

(a)

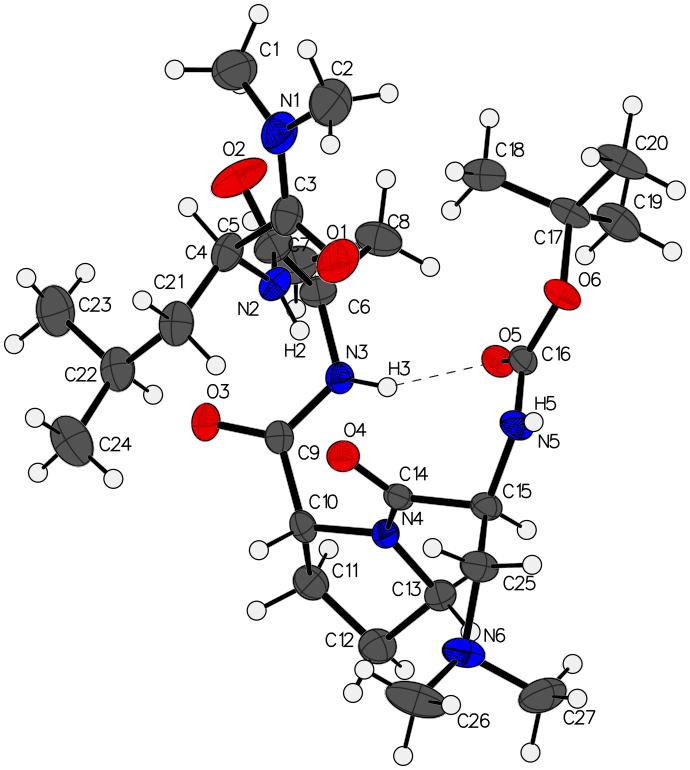

(b)

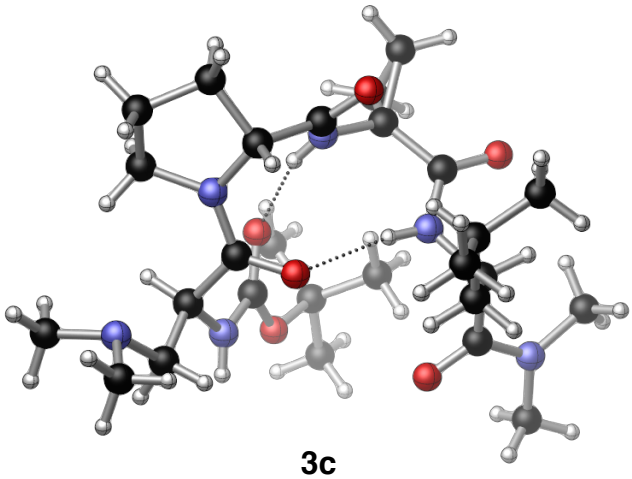

3c
type I' double β-turn

Figure S3.02: (a) The full numbering scheme of **3c** with 50% thermal ellipsoids. The H-atoms are shown as circles for clarity. Dashed lines highlight H-bonding interactions. **(b)** Image of **3c** rendered using CYLview.

(a)

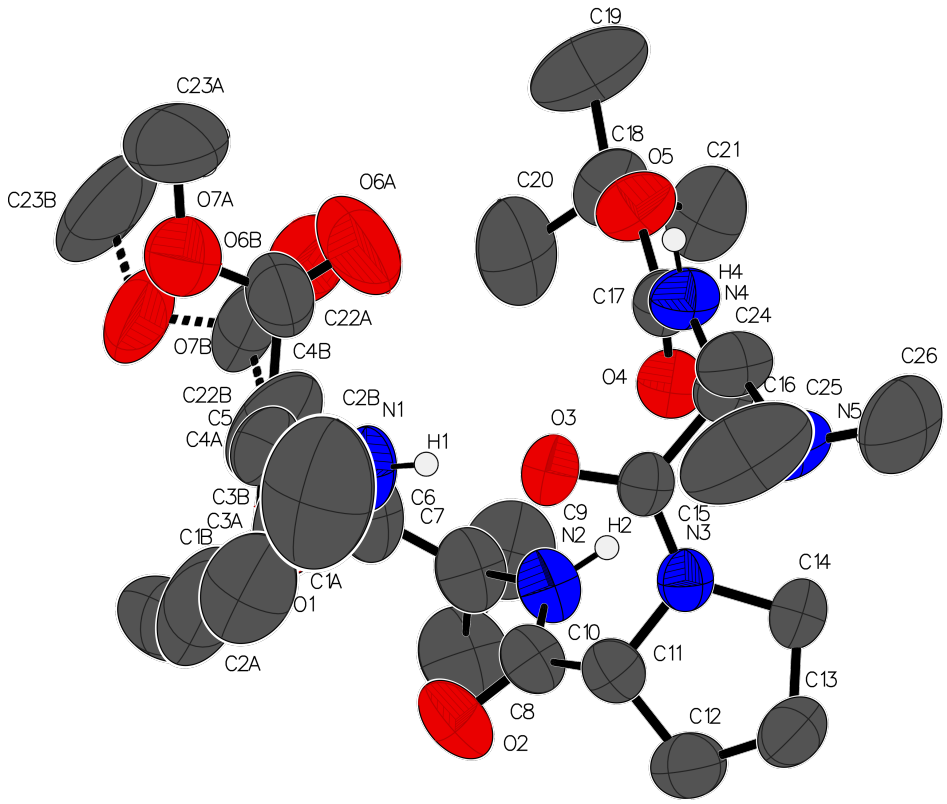

(b)

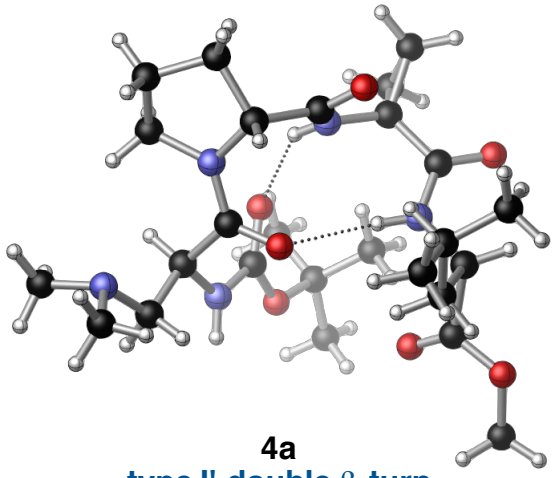

4a
type I' double β-turn

Figure S3.03: (a) The full numbering scheme of **4a** with 50% thermal ellipsoids. Most of the H-atoms have been omitted for clarity, while some are depicted as circles. Dashed bonds highlight disordered portions of the model. **(b)** Image of **4a** rendered using CYLview.

(a)

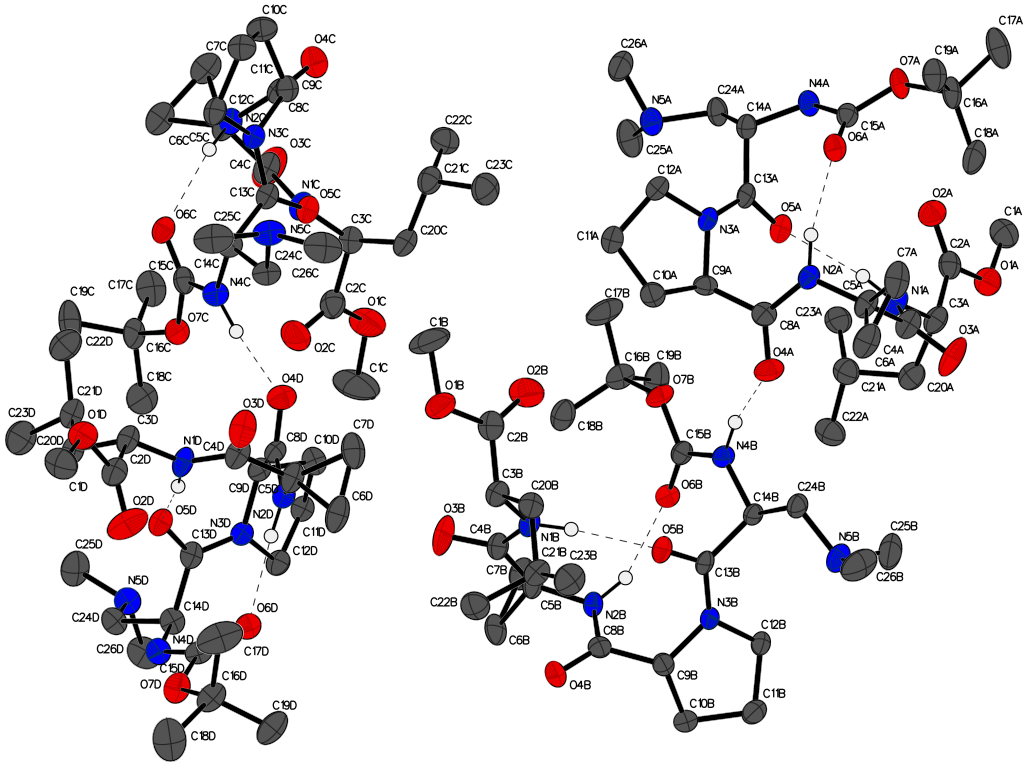

(b)

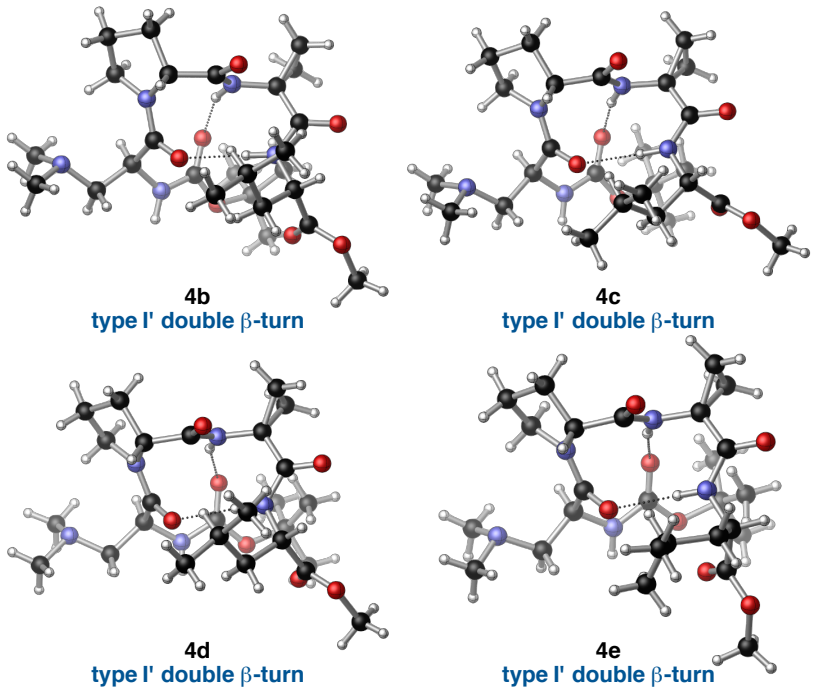

Figure S3.04: (a) The full numbering scheme of **4b–e** with 50% thermal ellipsoids. Most of the H-atoms have been omitted for clarity, while some are depicted as circles. Dashed lines highlight H-bonding interactions. **(b)** Images of **4b–e** rendered separately using CYLview.

(a)

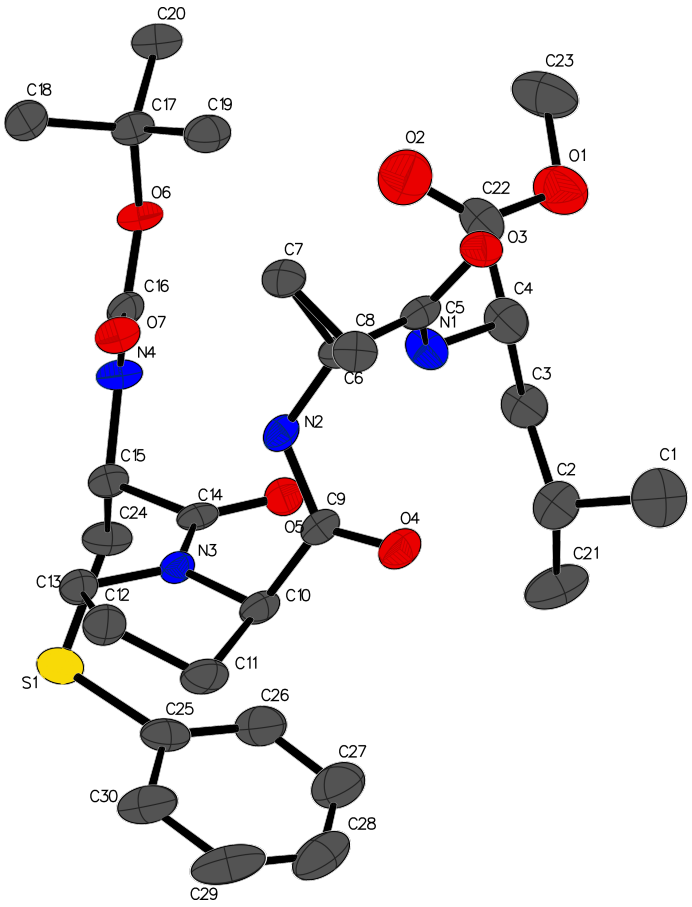

(b)

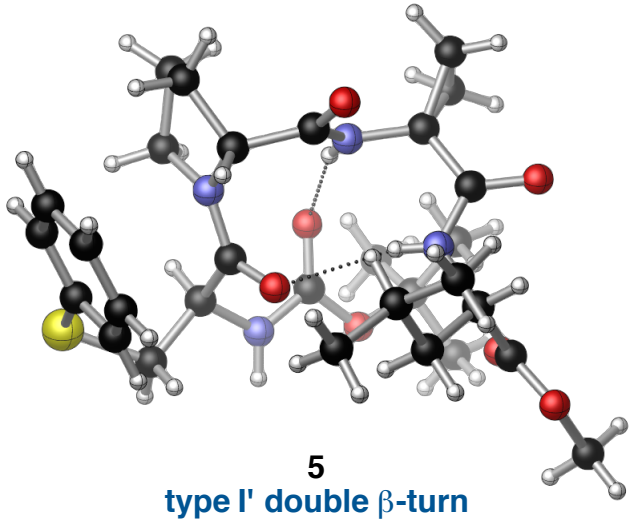

5
type I' double β-turn

Figure S3.05: (a) The full numbering scheme of **5** with 50% thermal ellipsoids. The H-atoms have been omitted for clarity. **(b)** Image of **5** rendered using CYLview.

(a)

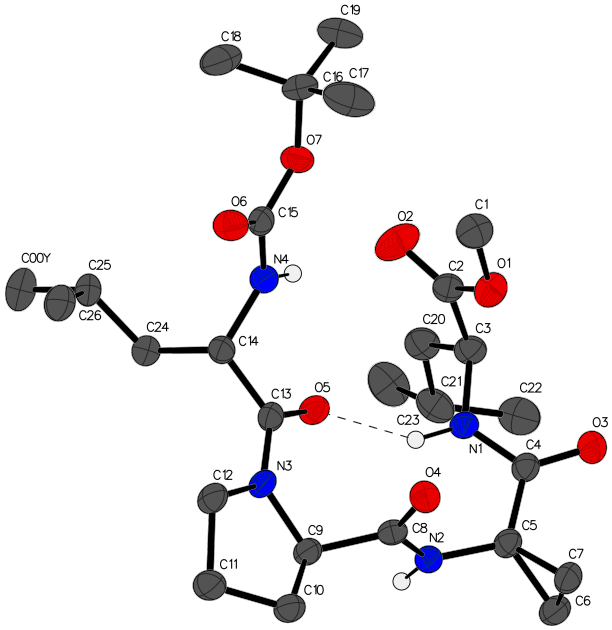

(b)

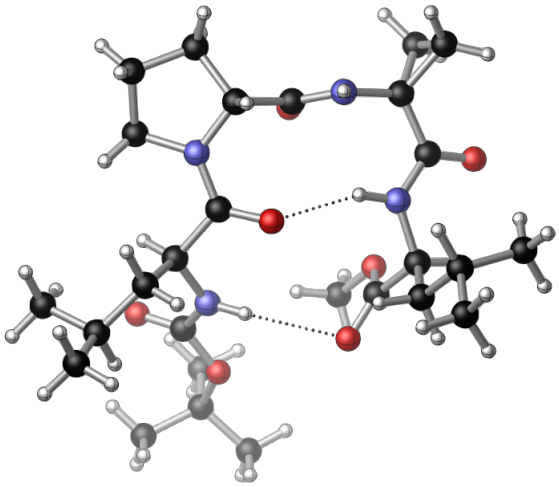

6

type II' β-hairpin

Figure S3.06: (a) The full numbering scheme of **6** with 50% thermal ellipsoids. Most of the H-atoms have been omitted for clarity, while some are shown as circles. Dashed lines highlight H-bonding interactions. **(b)** Image of **6** rendered using CYLview.

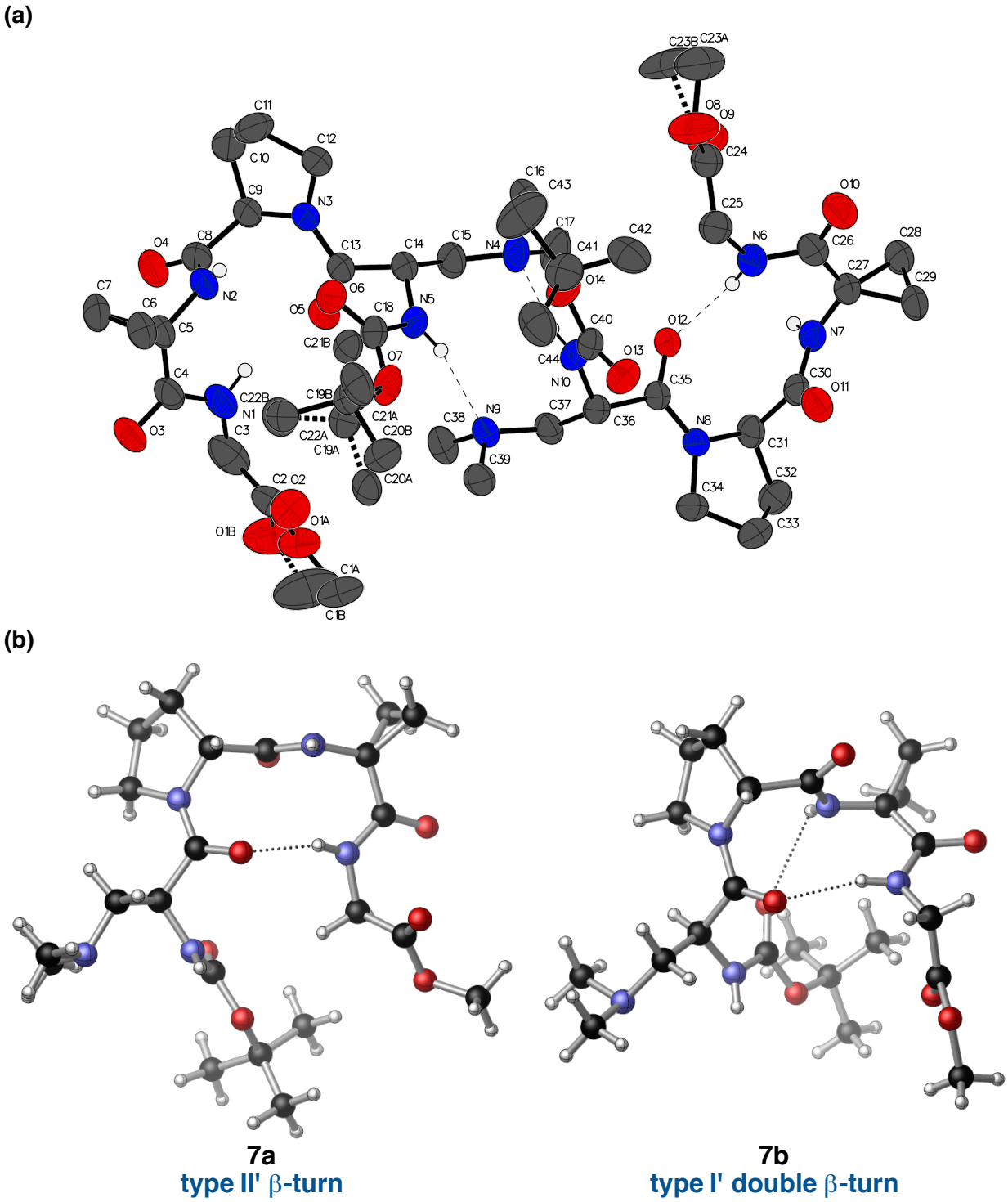

Figure S3.07: **(a)** The full numbering scheme of **7a,b** with 50% thermal ellipsoids. Most of the H-atoms have been omitted for clarity, while some are shown as circles. Dashed lines highlight H-bonding interactions. **(b)** Images of **7a** and **7b** rendered separately using CYLview.

(a)

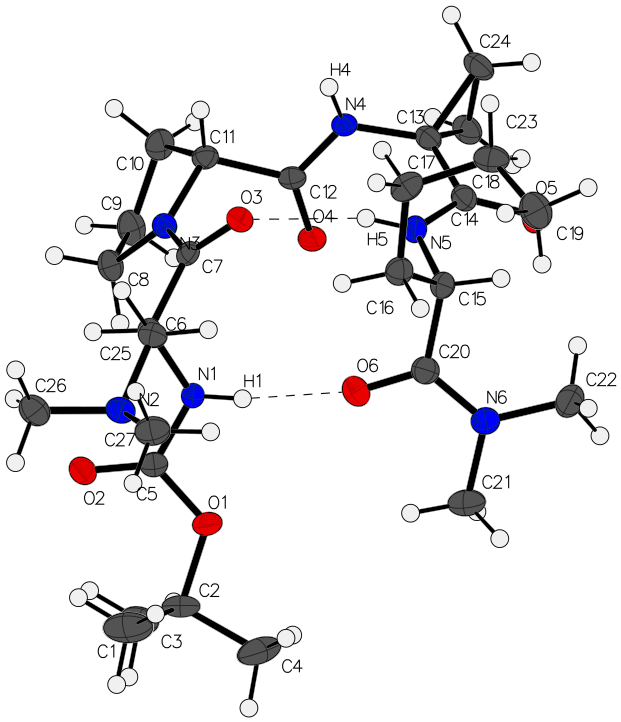

(b)

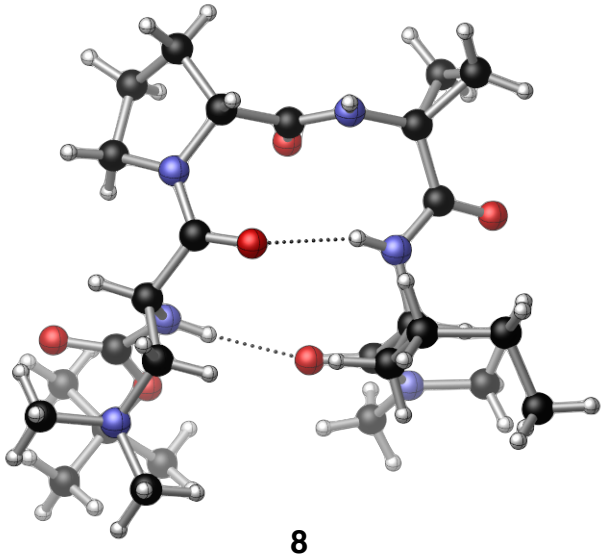

8

type II' β-hairpin

Figure S3.08: (a) The full numbering scheme of **8** with 50% thermal ellipsoids. The H-atoms are shown as circles for clarity. Dashed lines highlight H-bonding interactions. **(b)** Image of **8** rendered using CYLview.

(a)

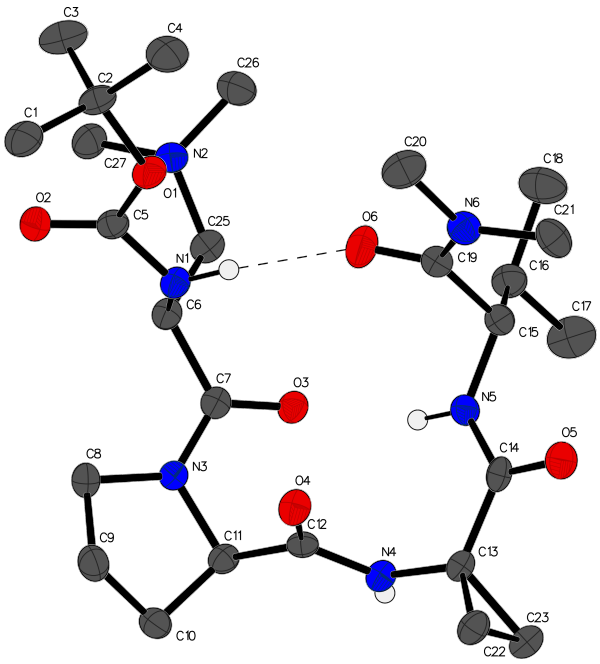

(b)

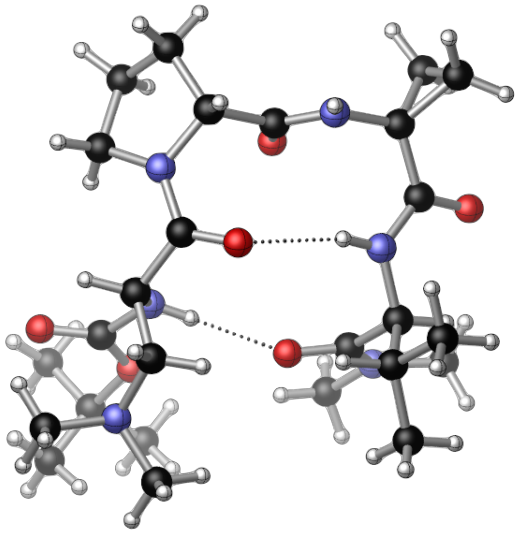

9

type II' β-hairpin

Figure S3.09: (a) The full numbering scheme of **9** with 50% thermal ellipsoids. Most of the H-atoms have been omitted for clarity, while some are shown as circles. Dashed lines highlight H-bonding interactions. **(b)** Image of **9** rendered using CYLview.

(a)

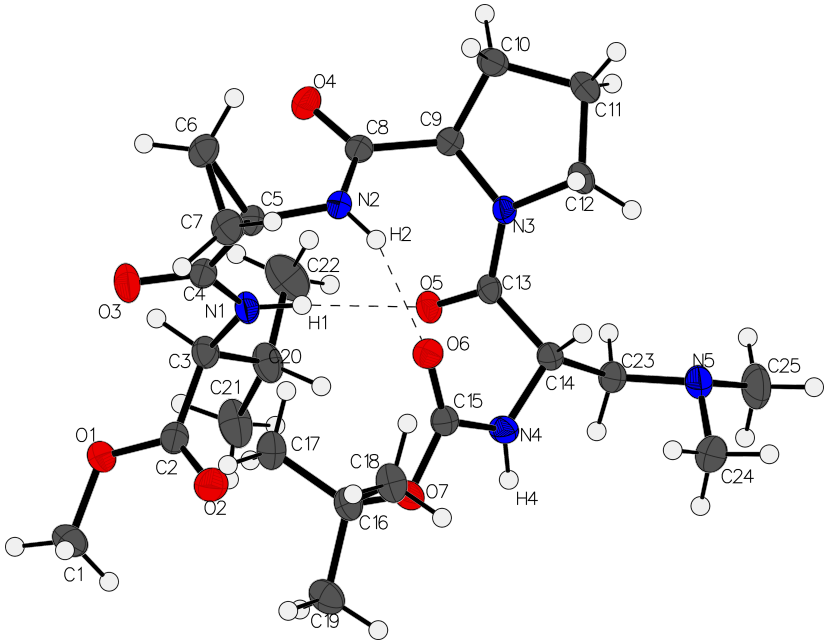

(b)

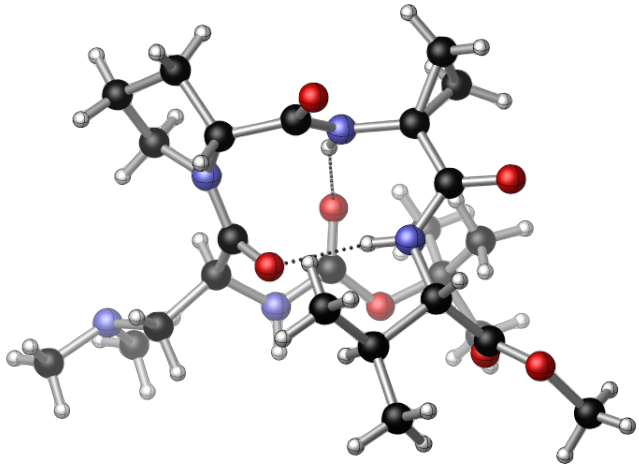

10
type I' double β-turn

Figure S3.10: (a) The full numbering scheme of **10** with 50% thermal ellipsoids. The H-atoms are shown as circles for clarity. Dashed lines highlight H-bonding interactions. **(b)** Image of **10** rendered using CYLview.

(a)

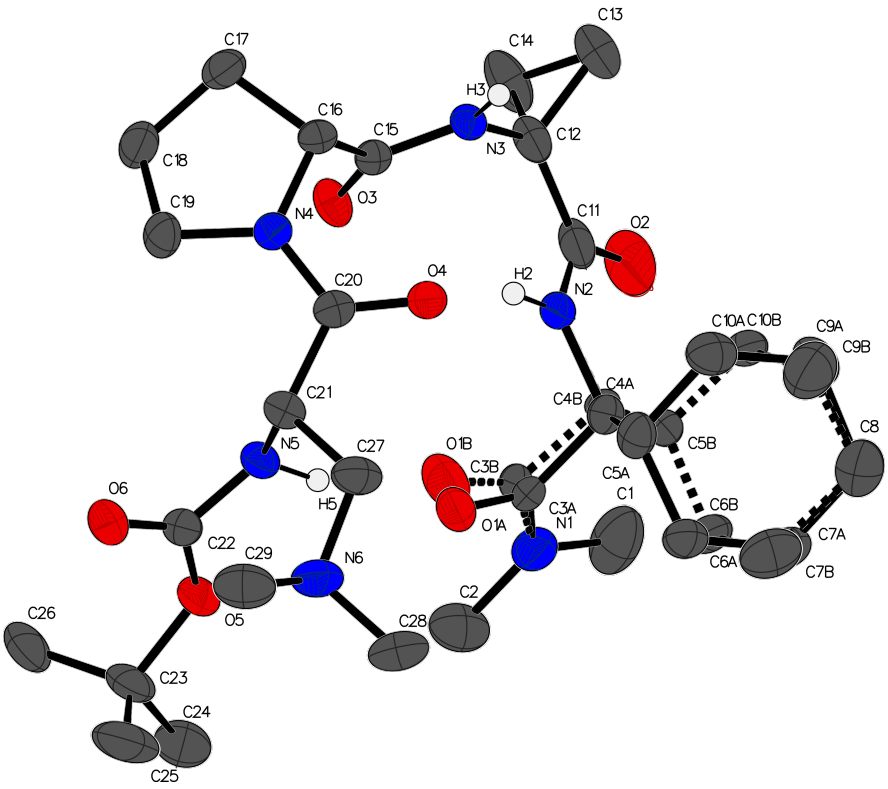

(b)

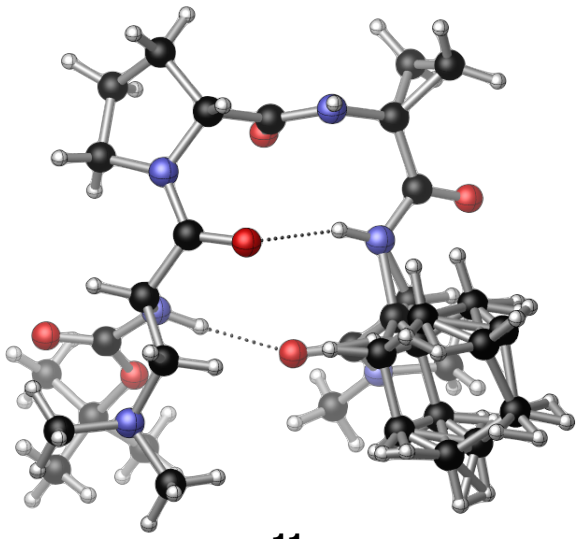

11

type II' β-hairpin

Figure S3.11: (a) The full numbering scheme of **11** with 50% thermal ellipsoids. Most of the H-atoms have been omitted for clarity, while some are depicted as circles. Dashed bonds highlight disordered portions of the model. **(b)** Image of **11** rendered using CYLview.

(a)

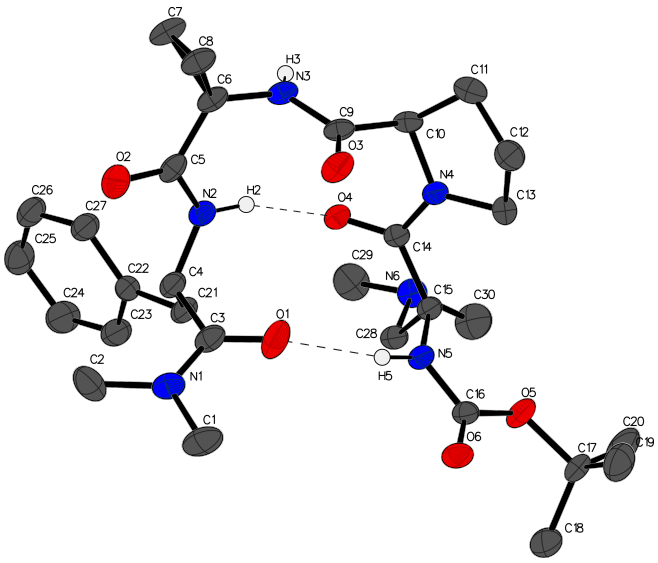

(b)

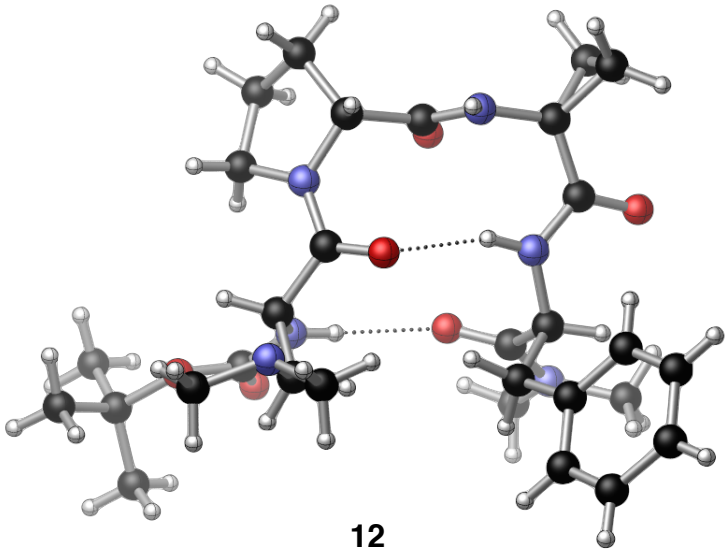

12

type II' β-hairpin

Figure S3.12: (a) The full numbering scheme of **12** with 50% thermal ellipsoids. Most of the H-atoms have been omitted for clarity, while some are depicted as circles. Dashed lines highlight H-bonding interactions. **(b)** Image of **12** rendered using CYLview.

(a)

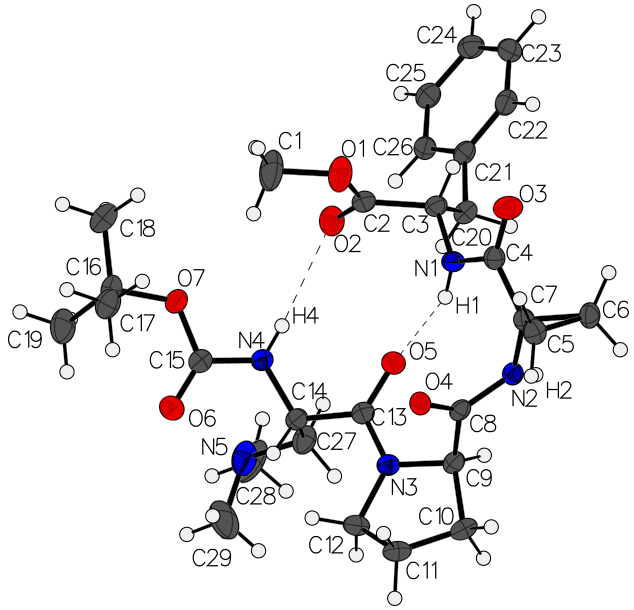

(b)

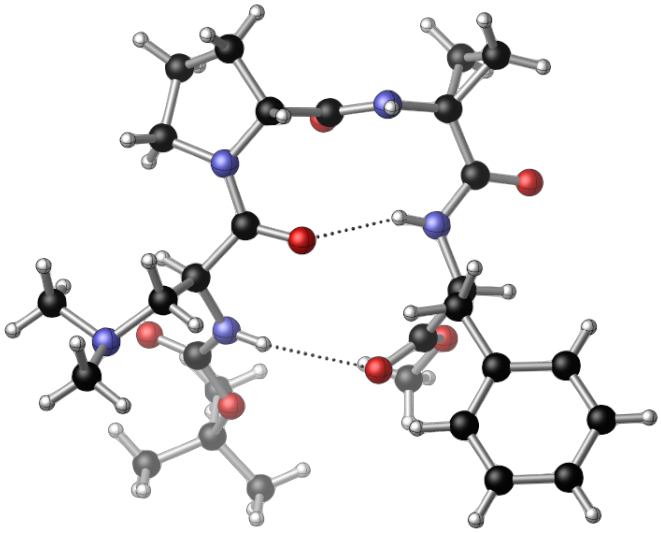

13
type II' β-hairpin

Figure S3.13: (a) The full numbering scheme of **13** with 50% thermal ellipsoids. The H-atoms are depicted as circles for clarity. Dashed lines highlight H-bonding interactions. **(b)** Image of **13** rendered using CYLview.

(a)

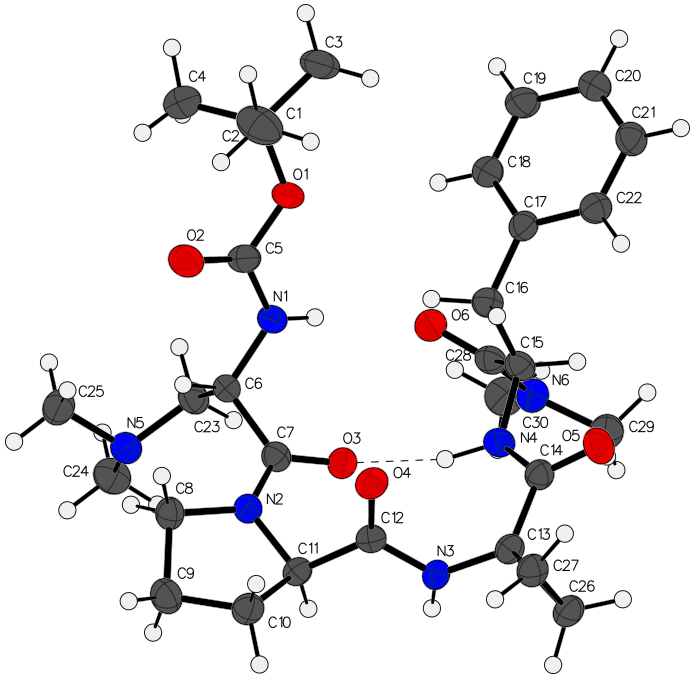

(b)

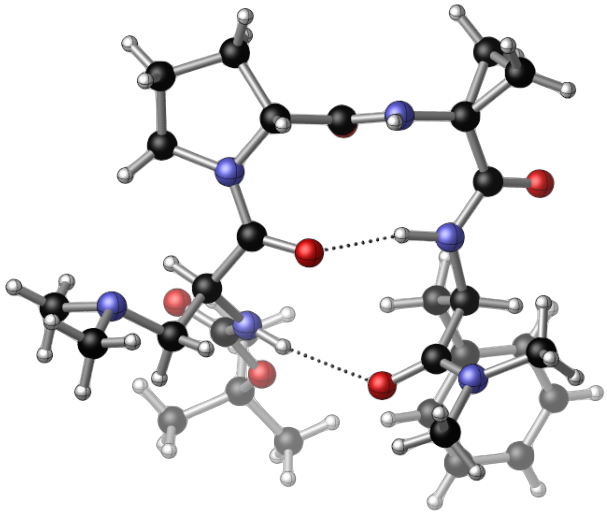

14

type II' β-hairpin

Figure S3.14: (a) The full numbering scheme of **14** with 50% thermal ellipsoids. The H-atoms are depicted as circles for clarity. Dashed lines highlight H-bonding interactions. **(b)** Image of **14** rendered using CYLview.

(a)

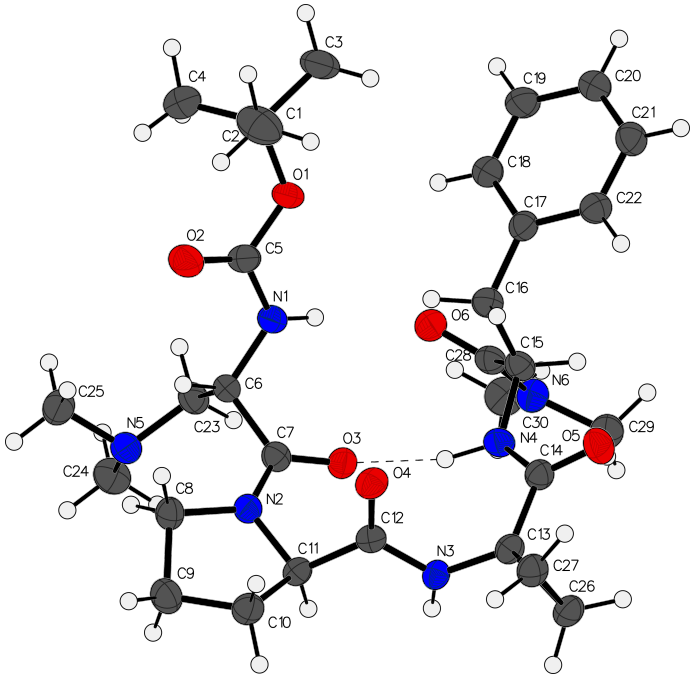

(b)

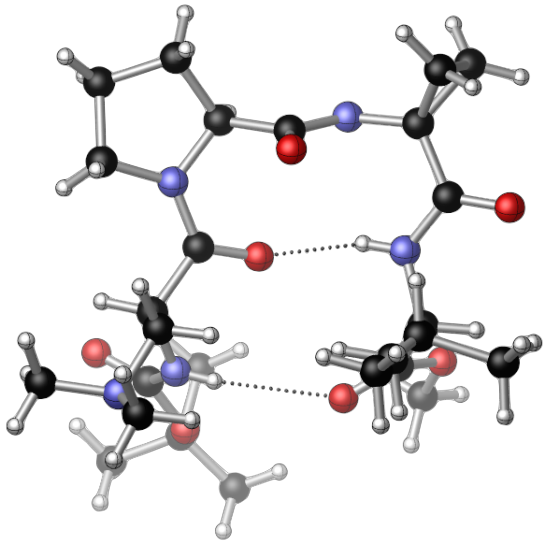

15
type II β-hairpin

Figure S3.15: (a) The full numbering scheme of **15** with 50% thermal ellipsoids. The H-atoms are depicted as circles for clarity. Dashed lines highlight H-bonding interactions. **(b)** Image of **15** rendered using CYLview.

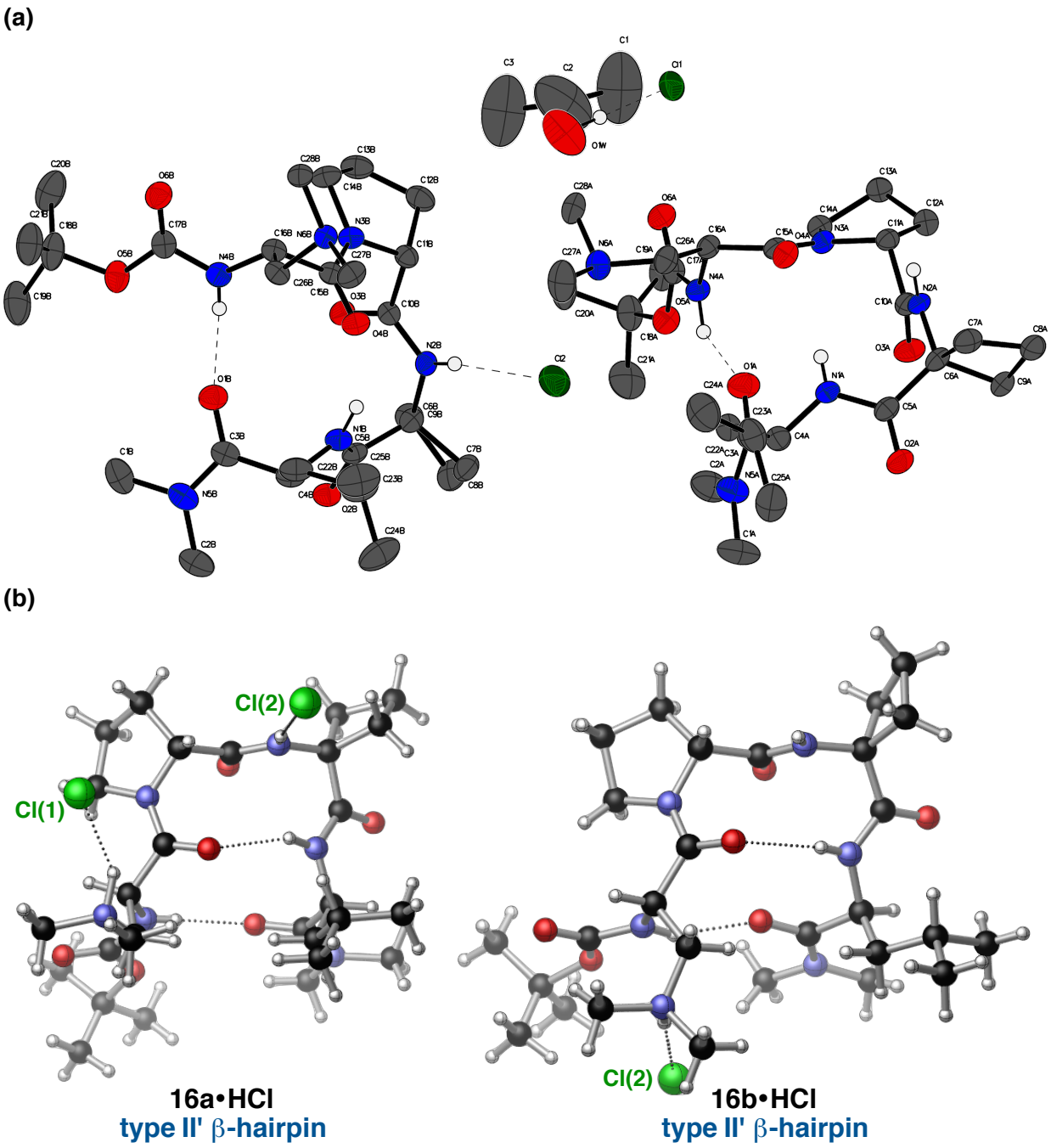

Figure S3.16: (a) The full numbering scheme of **16a,b•2HCl** with 50% thermal ellipsoids. Most of the H-atoms have been omitted for clarity, while some are depicted as circles. Dashed lines highlight H-bonding interactions. **(b)** Images of **16a•HCl** and **16b•HCl** rendered separately using CYLview.

(a)

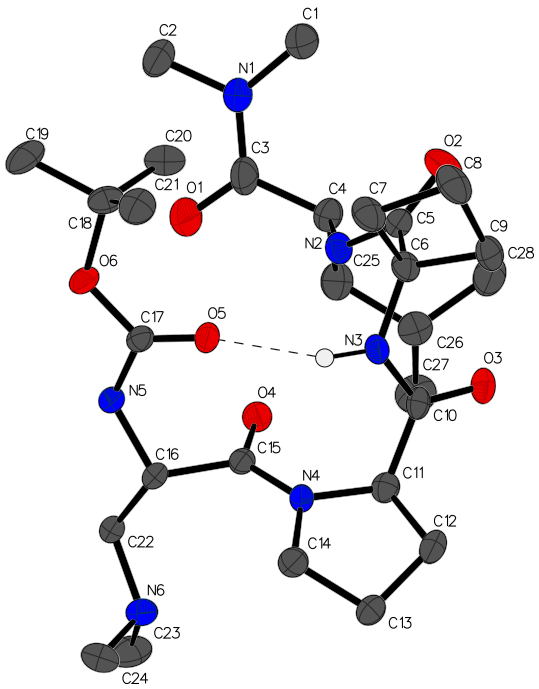

(b)

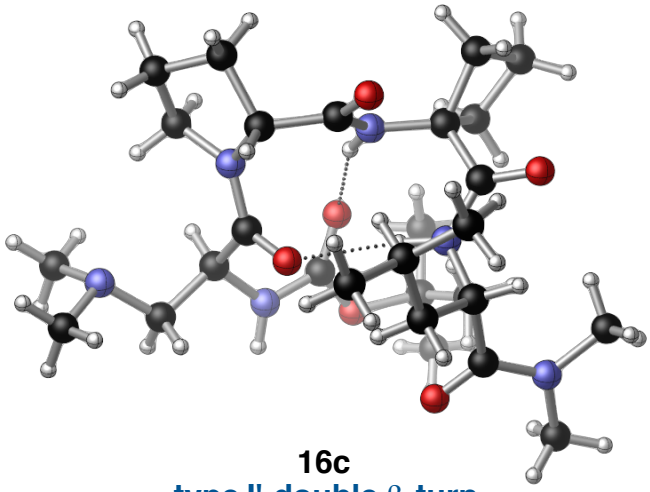

16c
type I' double β-turn

Figure S3.17: (a) The full numbering scheme of **16c** with 50% thermal ellipsoids. Most of the H-atoms have been omitted for clarity, while some are depicted as circles. Dashed lines highlight H-bonding interactions. **(b)** Image of **16c** rendered using CYLview.

(a)

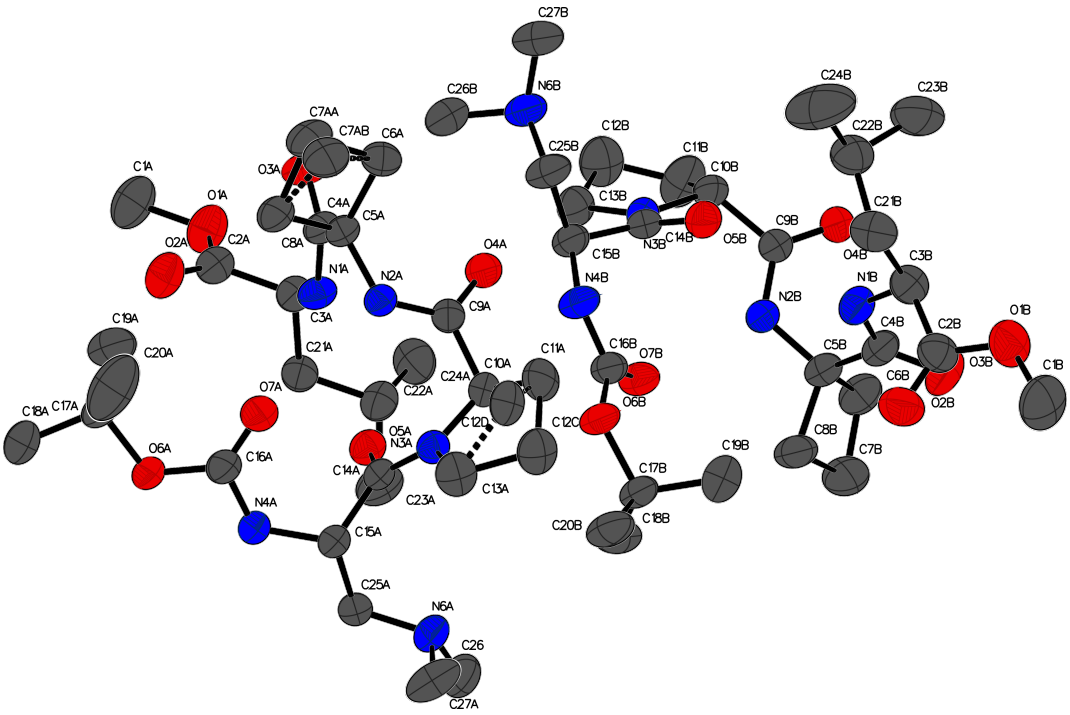

(b)

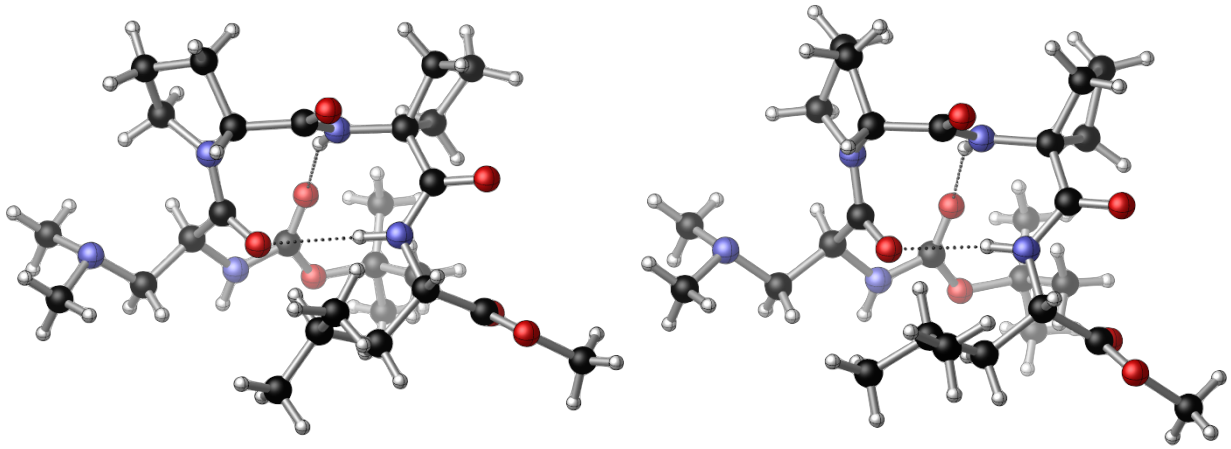

17a
type I' double β-turn

17b
type I' double β-turn

Figure S3.18: (a) The full numbering scheme of **17a,b** with 50% thermal ellipsoids. The H-atoms have been omitted for clarity. Dashed bonds highlight disordered portions of the model. **(b)** Images of **17a** and **17b** rendered separately using CYLview.

(a)

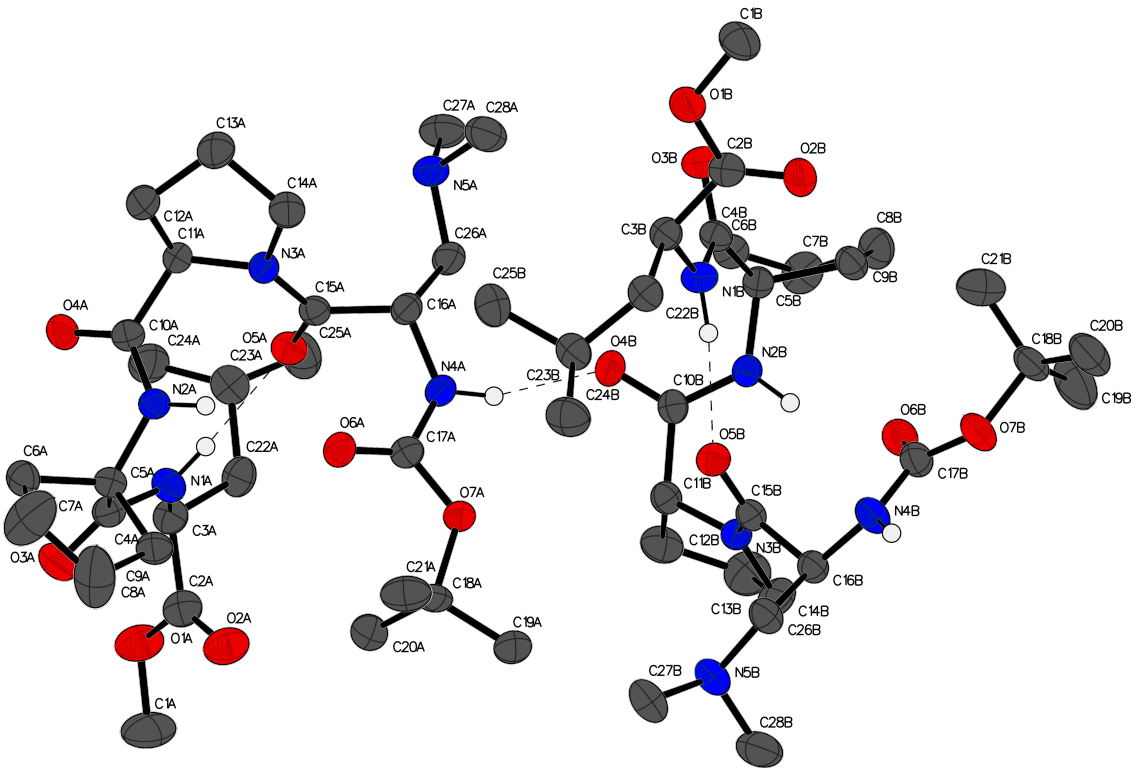

(b)

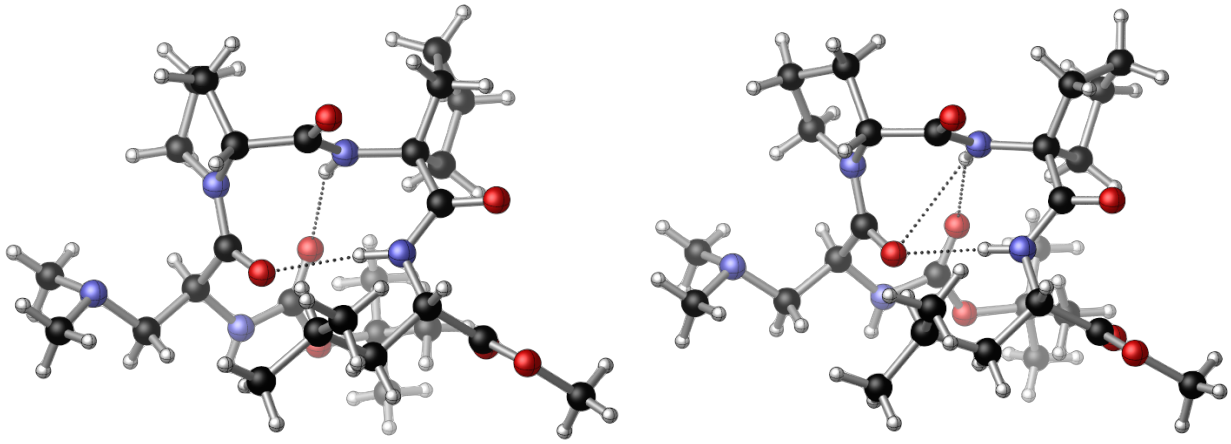

18a
type I' double β-turn

18b
type I' double β-turn

Figure S3.19: (a) The full numbering scheme of **18a,b** with 50% thermal ellipsoids. Most of the H-atoms have been omitted for clarity, while some are depicted as circles. Dashed lines highlight H-bonding interactions. **(b)** Images of **18a** and **18b** rendered separately using CYLview.

(a)

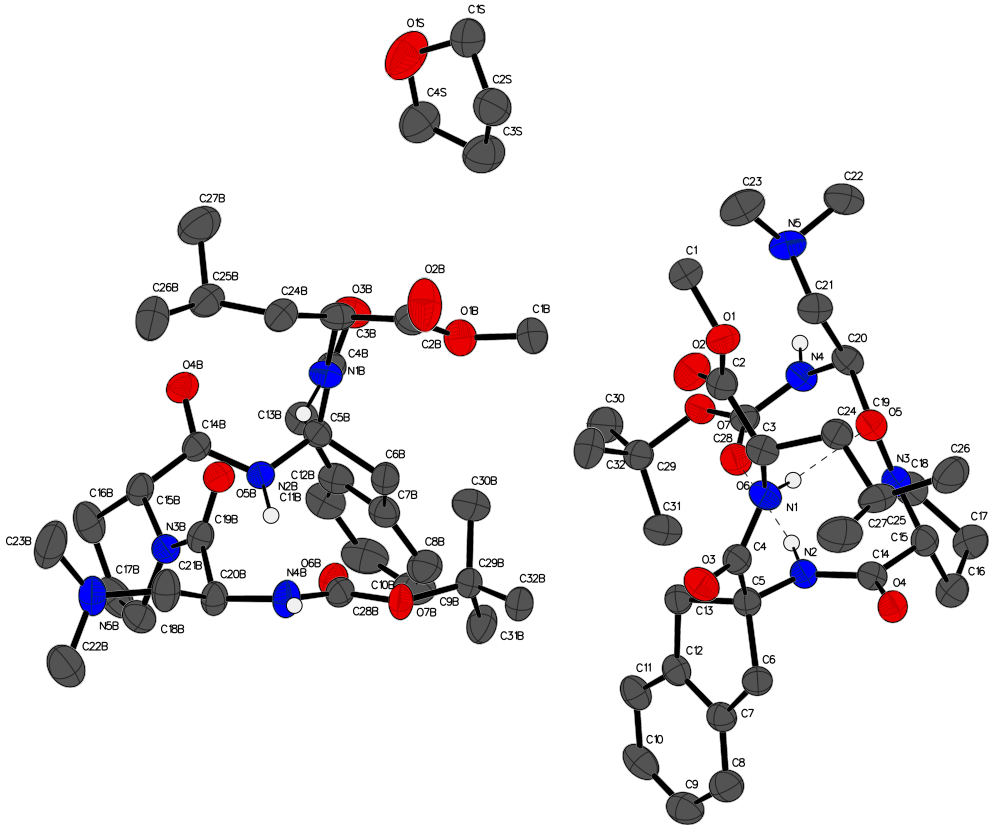

(b)

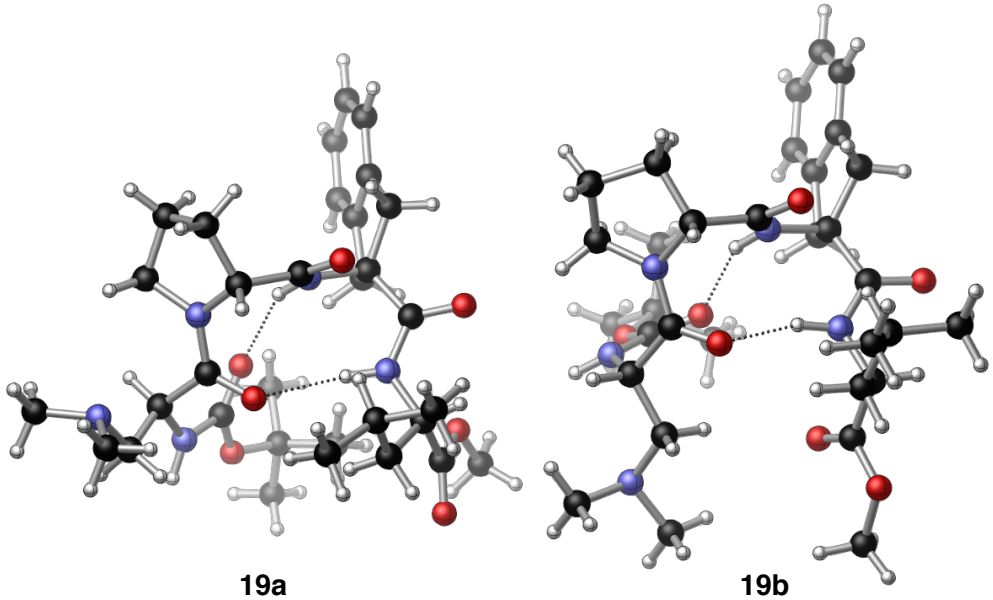

19a
type I' double β-turn

19b
type I' double β-turn

Figure S3.20: (a) The full numbering scheme of **19a,b** with 50% thermal ellipsoids. Most of the H-atoms have been omitted for clarity, while some are depicted as circles. Dashed lines highlight H-bonding interactions. **(b)** Images of **19a** and **19b** rendered separately using CYLview.

(a)

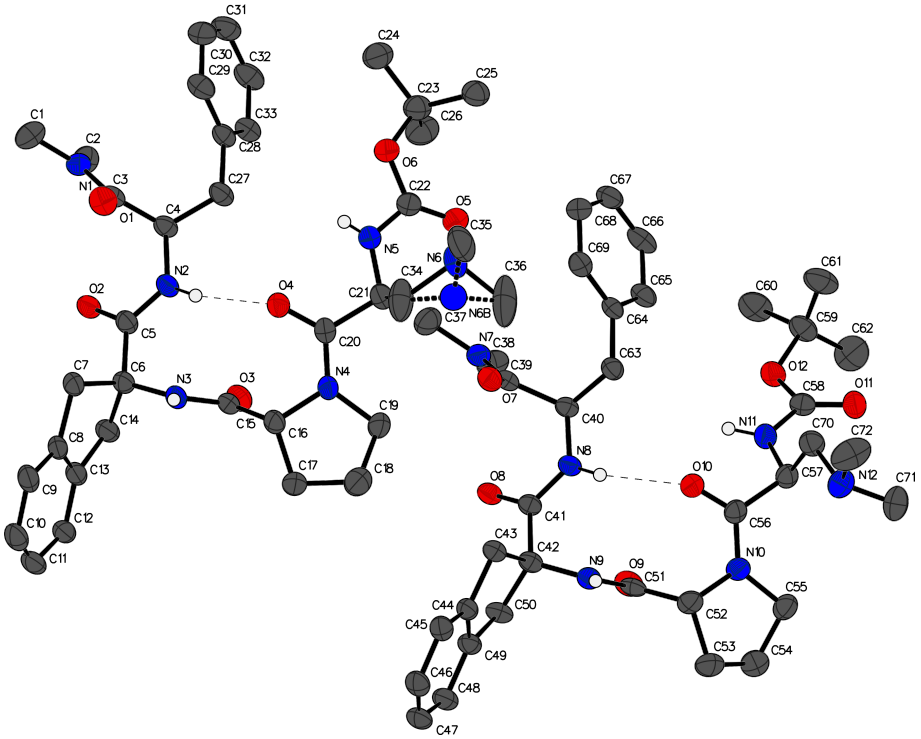

(b)

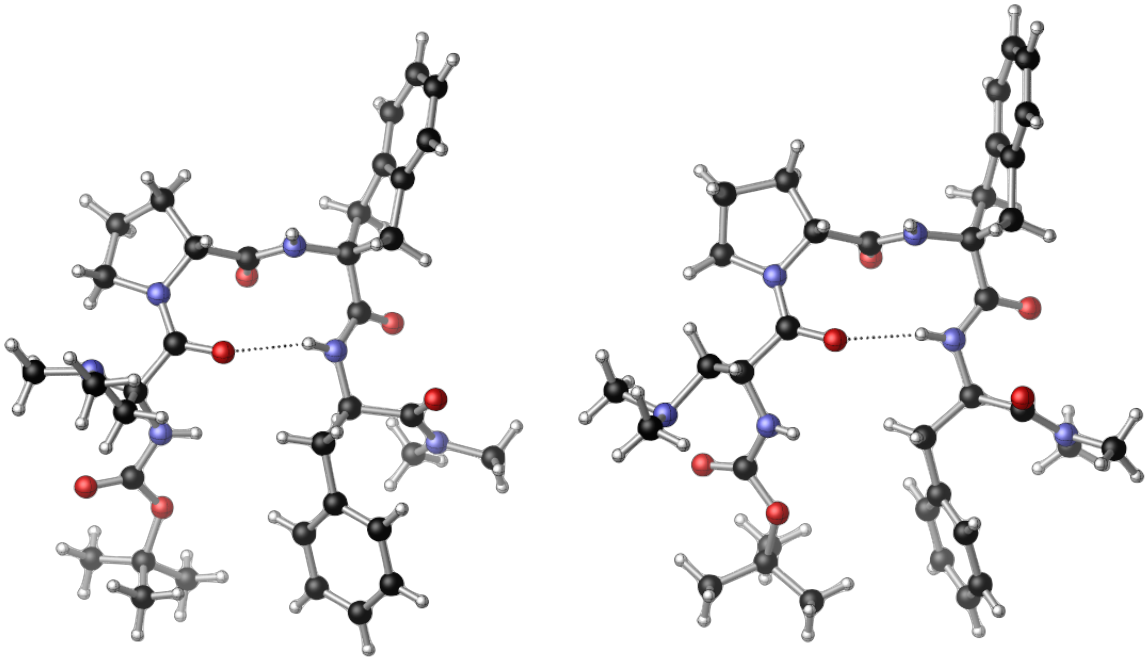

20a
type II' β-turn

20b
type II' β-turn

Figure S3.21: (a) The full numbering scheme of **20a,b** with 50% thermal ellipsoids. Most of the H-atoms have been omitted for clarity, while some are depicted as circles. Dashed lines highlight H-bonding interactions. **(b)** Images of **20a** and **20b** rendered separately using CYLview.

(a)

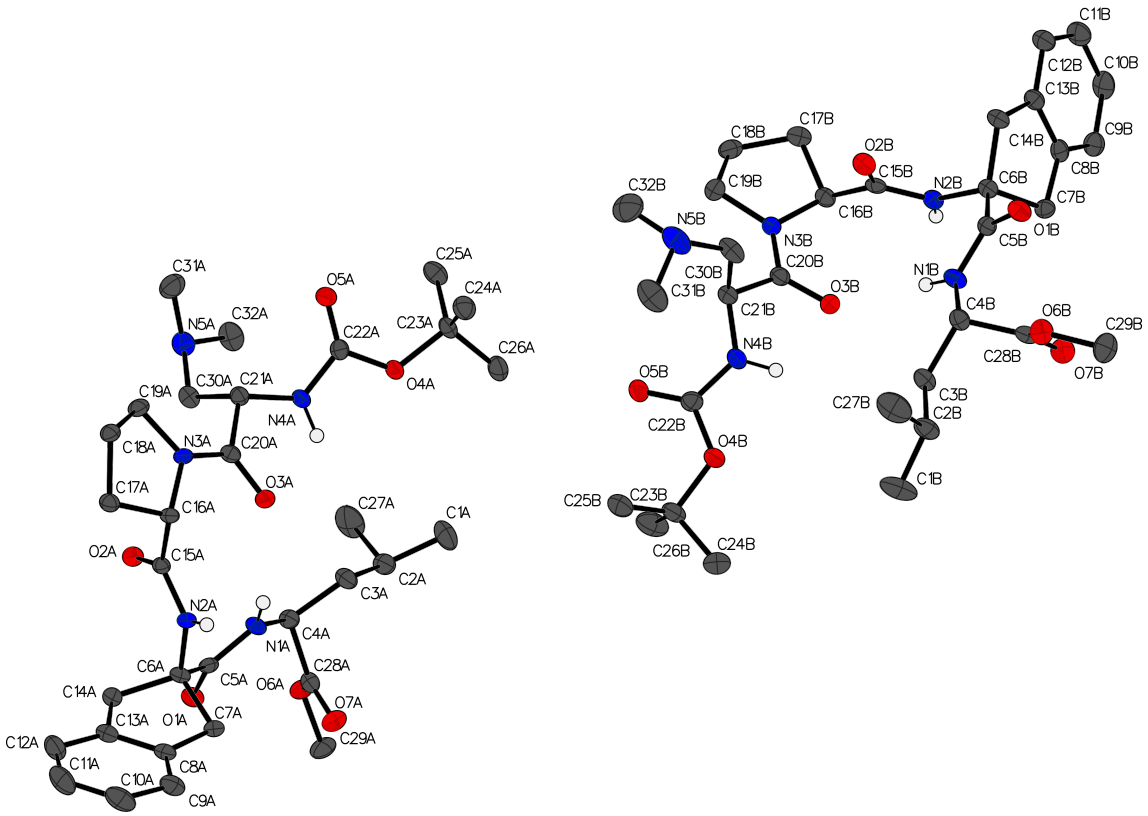

(b)

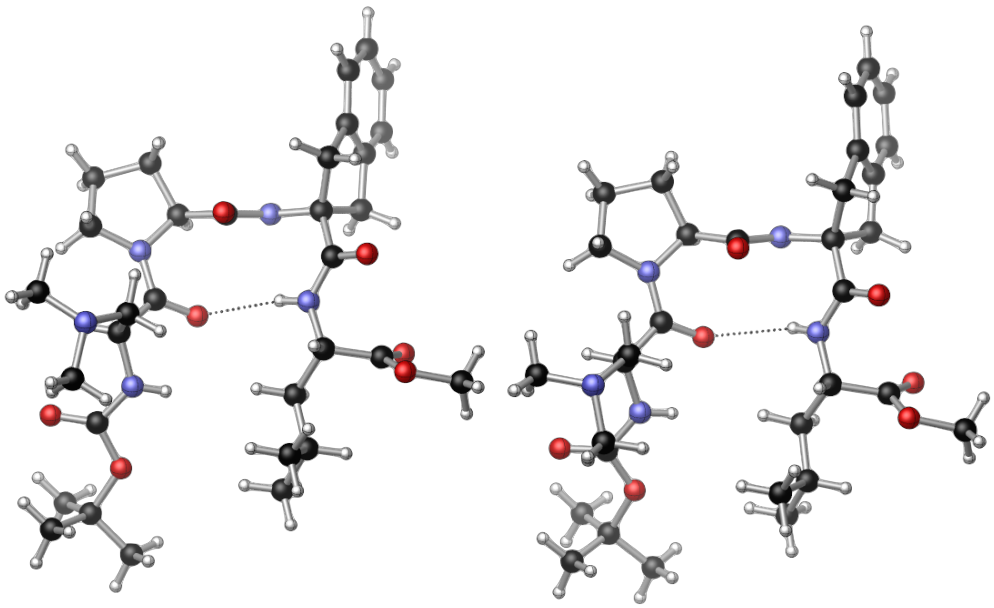

21a
type II β-turn

21b
type II β-turn

Figure S3.22: (a) The full numbering scheme of **21a,b** with 50% thermal ellipsoids. Most of the H-atoms have been omitted for clarity, while some are depicted as circles. **(b)** Images of **21a** and **21b** rendered separately using CYLview.

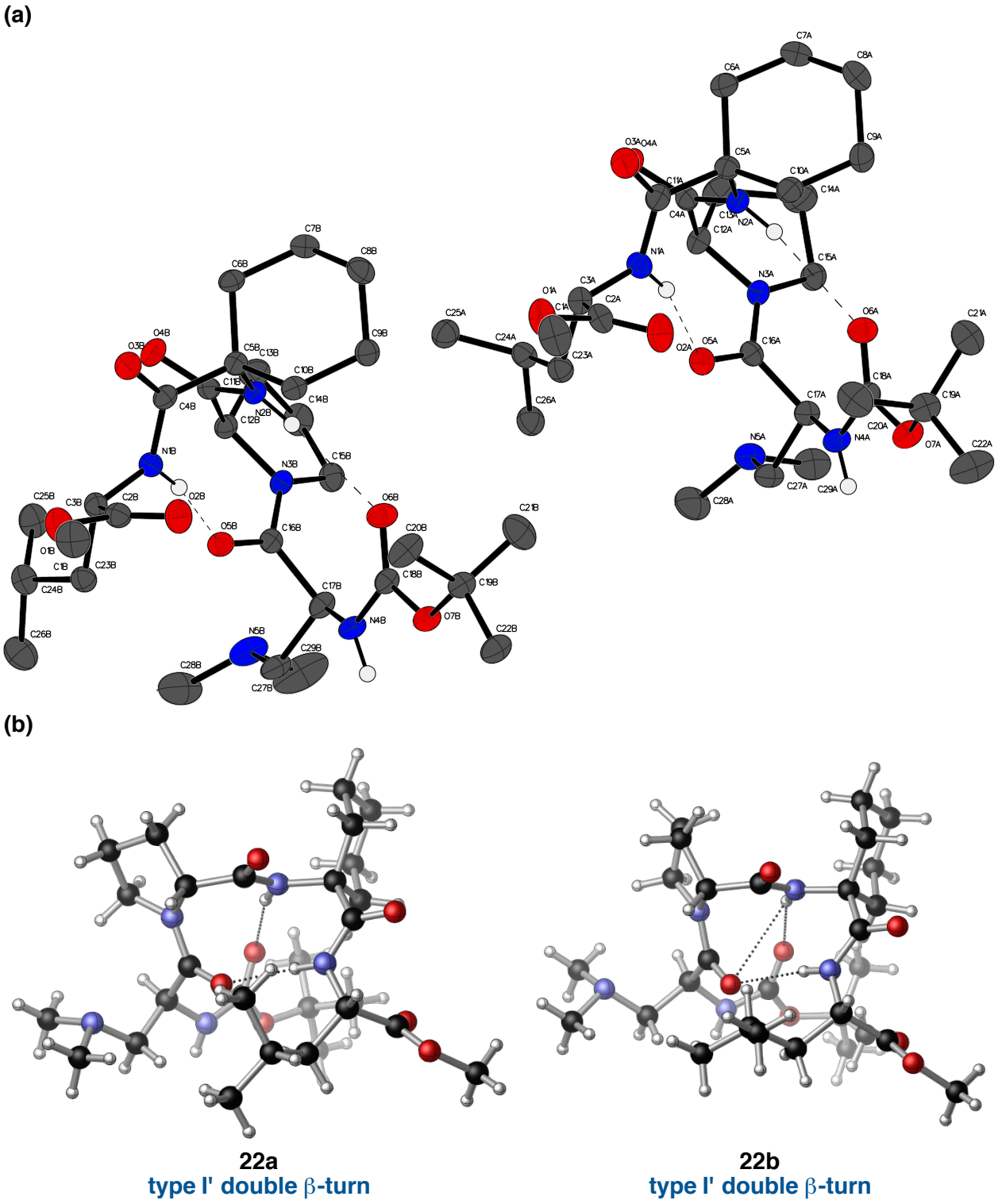

Figure S3.23: (a) The full numbering scheme of **22a,b** with 50% thermal ellipsoids. Most of the H-atoms have been omitted for clarity, while some are depicted as circles. Dashed lines highlight H-bonding interactions. **(b)** Images of **22a** and **22b** rendered separately using CYLview.

(a)

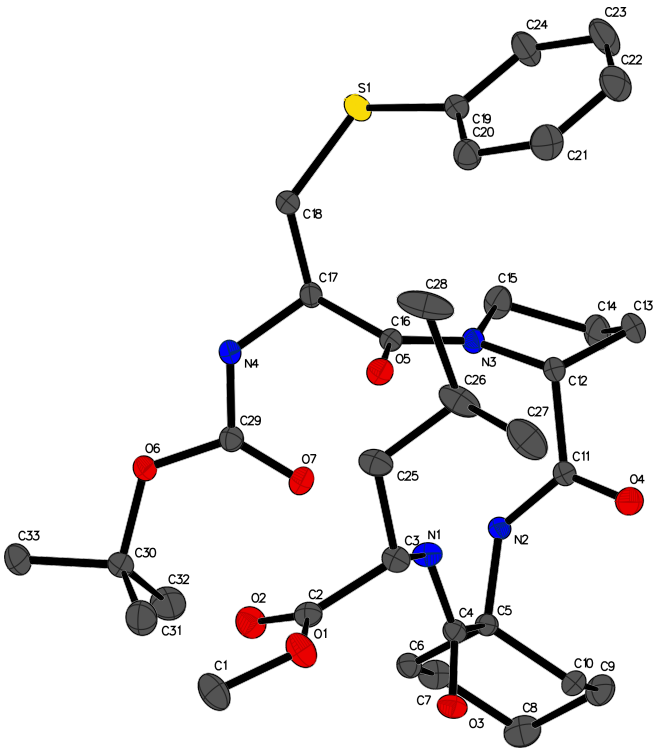

(b)

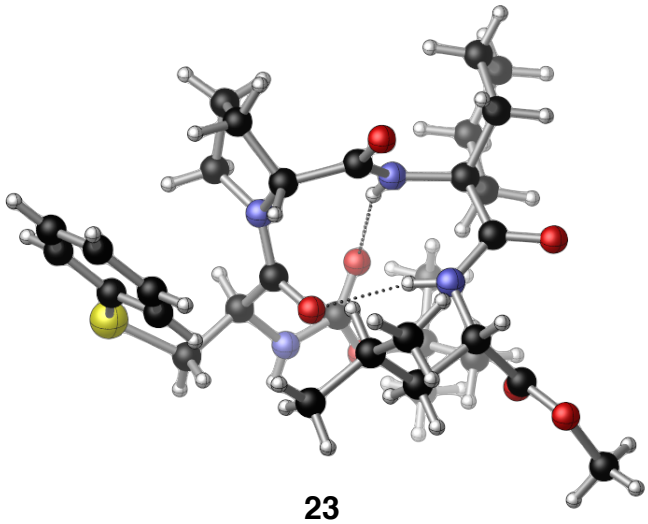

23

type I' double β-turn

Figure S3.24: (a) The full numbering scheme of **23** with 50% thermal ellipsoids. The H-atoms have been omitted for clarity. **(b)** Image of **23** rendered using CYLview.

(a)

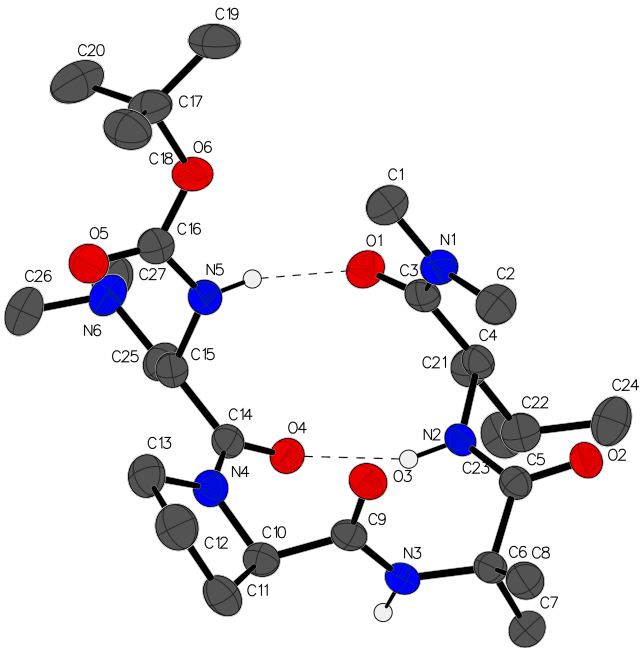

(b)

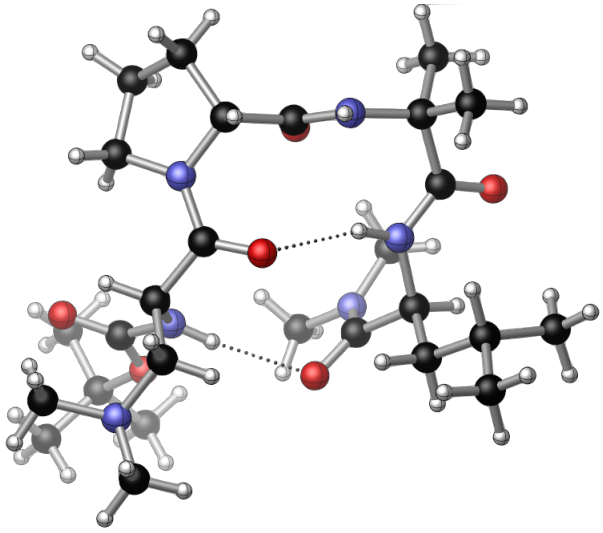

24
type II' β-hairpin

Figure S3.25: (a) The full numbering scheme of **24** with 50% thermal ellipsoids. Most of the H-atoms have been omitted for clarity, while some are depicted as circles. Dashed lines highlight H-bonding interactions. **(b)** Image of **24** rendered using CYLview.

(a)

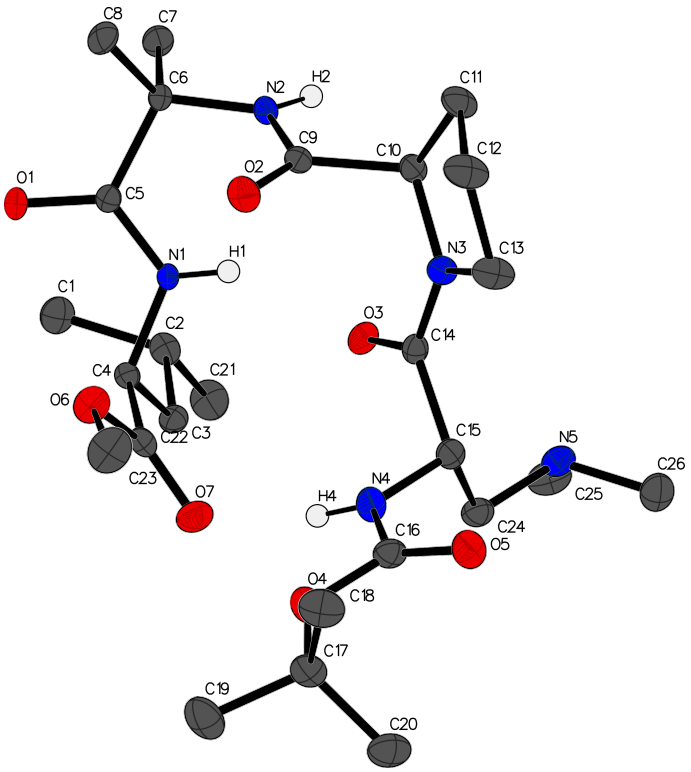

(b)

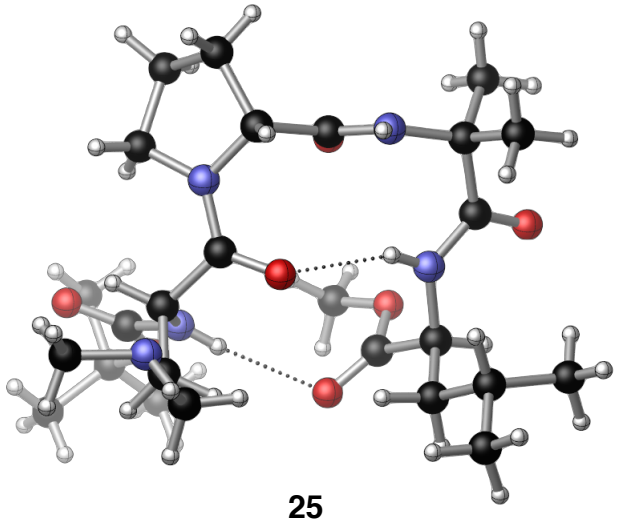

25

type II' β-hairpin

Figure S3.26: (a) The full numbering scheme of **25** with 50% thermal ellipsoids. Most of the H-atoms have been omitted for clarity, while some are depicted as circles. **(b)** Image of **25** rendered using CYLview.

(a)

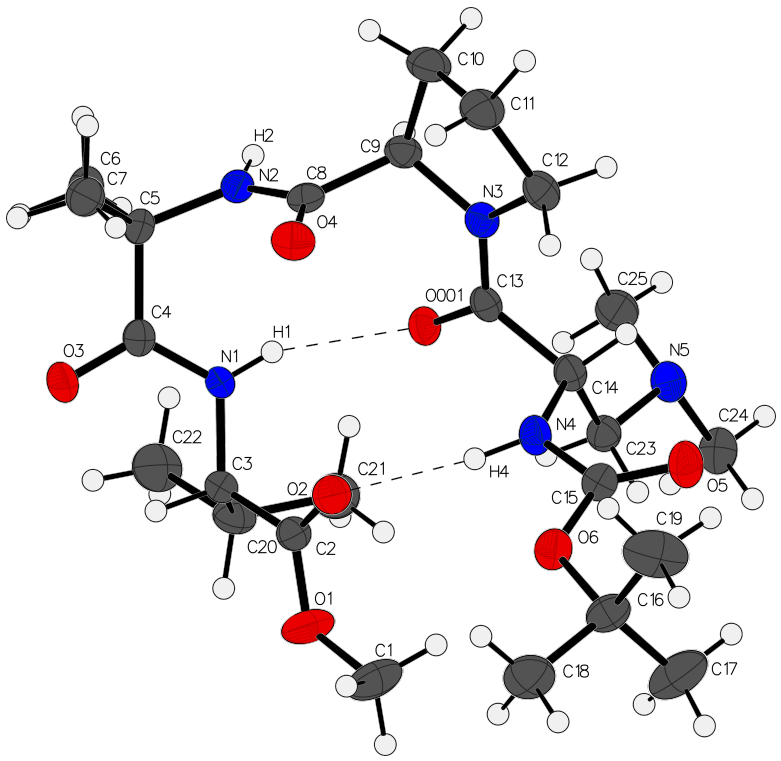

(b)

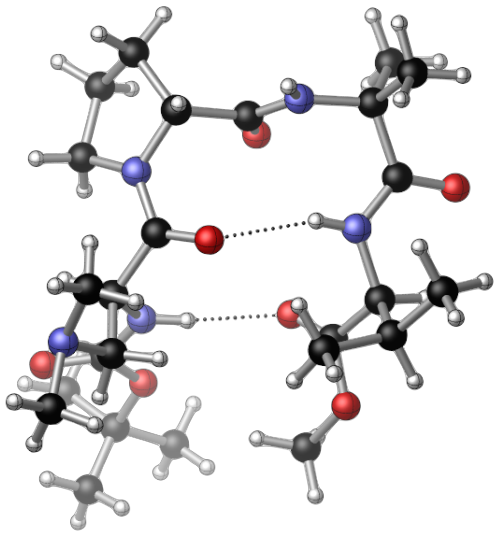

26
type II' β-hairpin

Figure S3.27: (a) The full numbering scheme of **26** with 50% thermal ellipsoids. The H-atoms are depicted as circles for clarity. Dashed lines highlight H-bonding interactions. **(b)** Image of **26** rendered using CYLview.

(a)

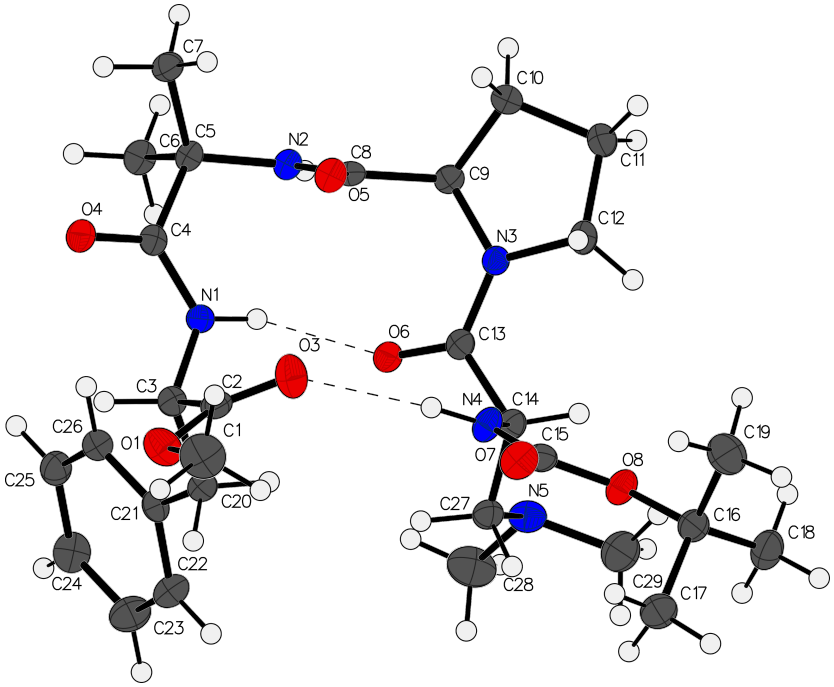

(b)

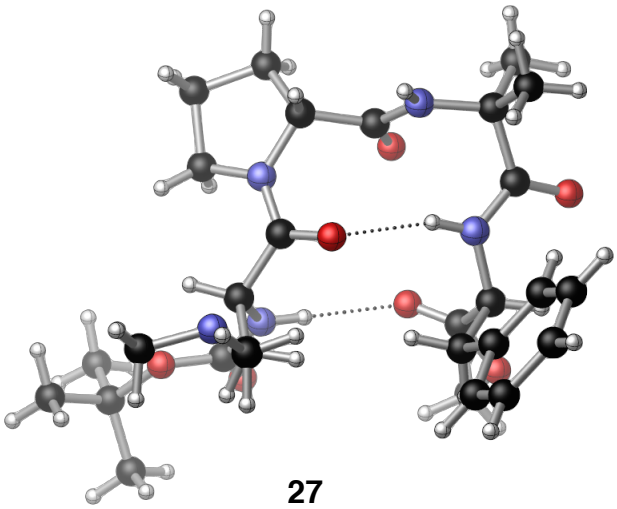

27
type II' β-hairpin

Figure S3.28: (a) The full numbering scheme of **27** with 50% thermal ellipsoids. The H-atoms are depicted as circles for clarity. Dashed lines highlight H-bonding interactions. **(b)** Image of **27** rendered using CYLview.

(a)

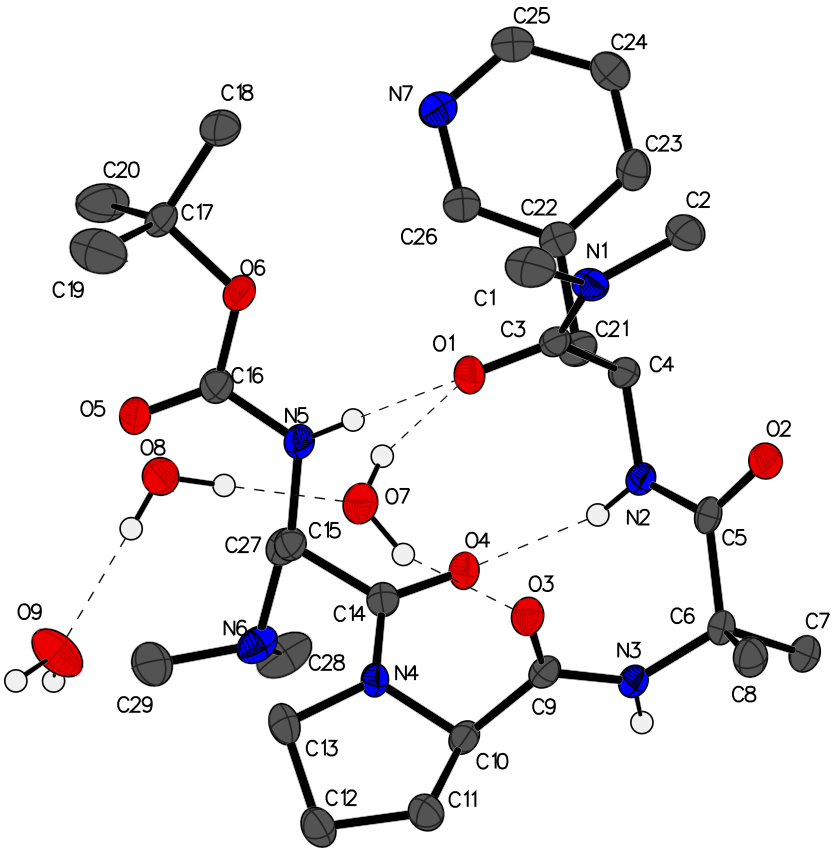

(b)

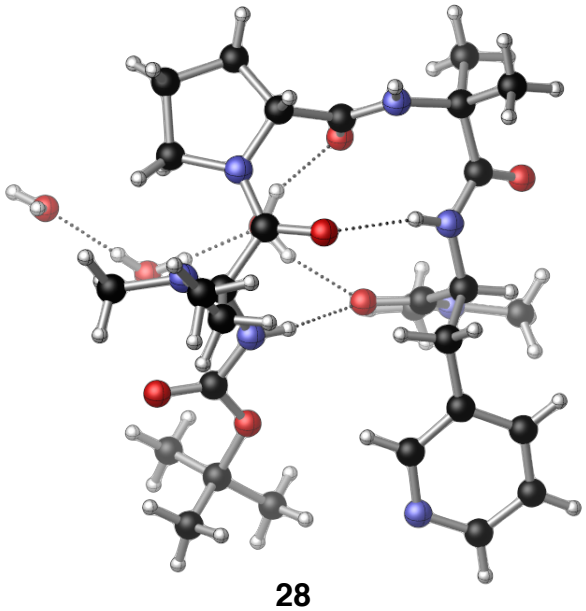

28

type II' β-hairpin

Figure S3.29: (a) The full numbering scheme of **28** with 50% thermal ellipsoids. Most of the H-atoms have been omitted for clarity, while some are depicted as circles. Dashed lines highlight H-bonding interactions. **(b)** Image of **28** rendered using CYLview.

(a)

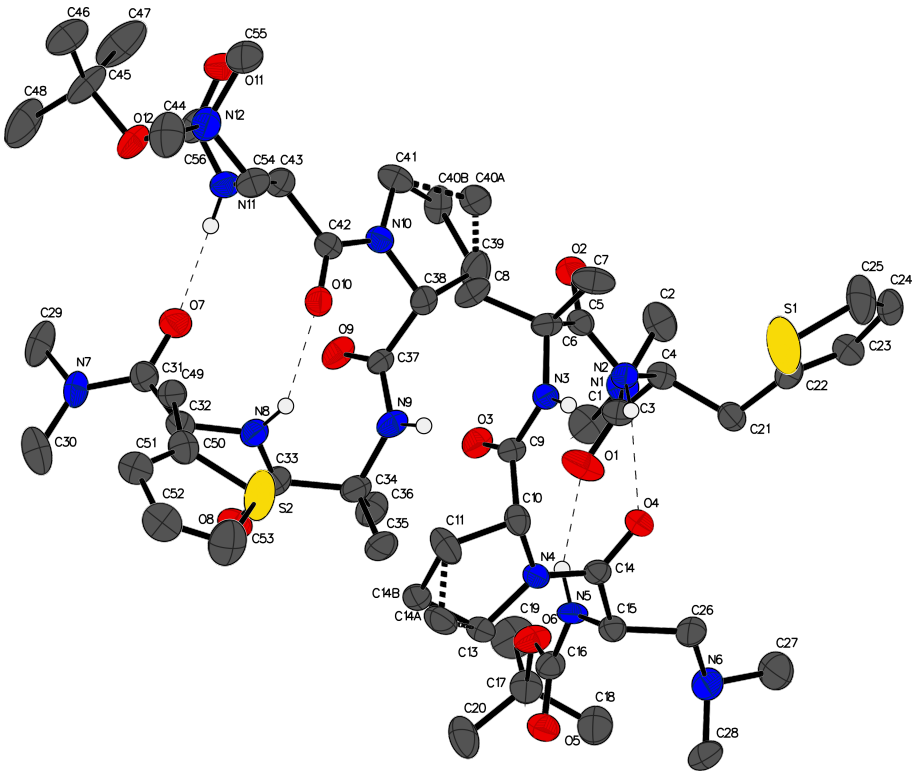

(b)

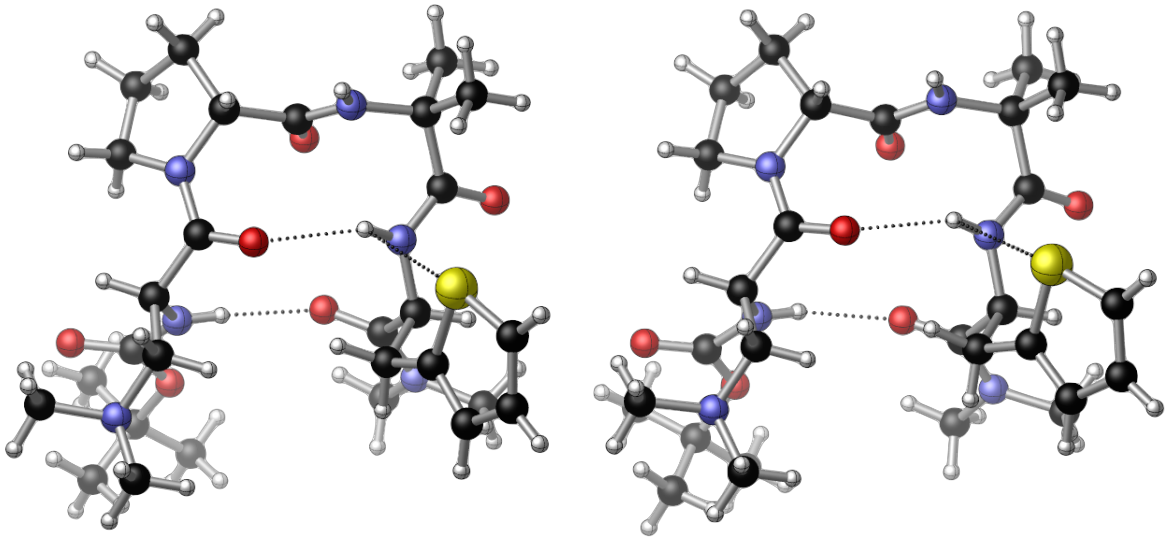

29a
type II' β-hairpin

29b
type II' β-hairpin

Figure S3.30: (a) The full numbering scheme of **29a,b** with 50% thermal ellipsoids. Most of the H-atoms have been omitted for clarity, while some are depicted as circles. Dashed lines highlight H-bonding interactions. **(b)** Images of **29a** and **29b** rendered separately using CYLview.

(a)

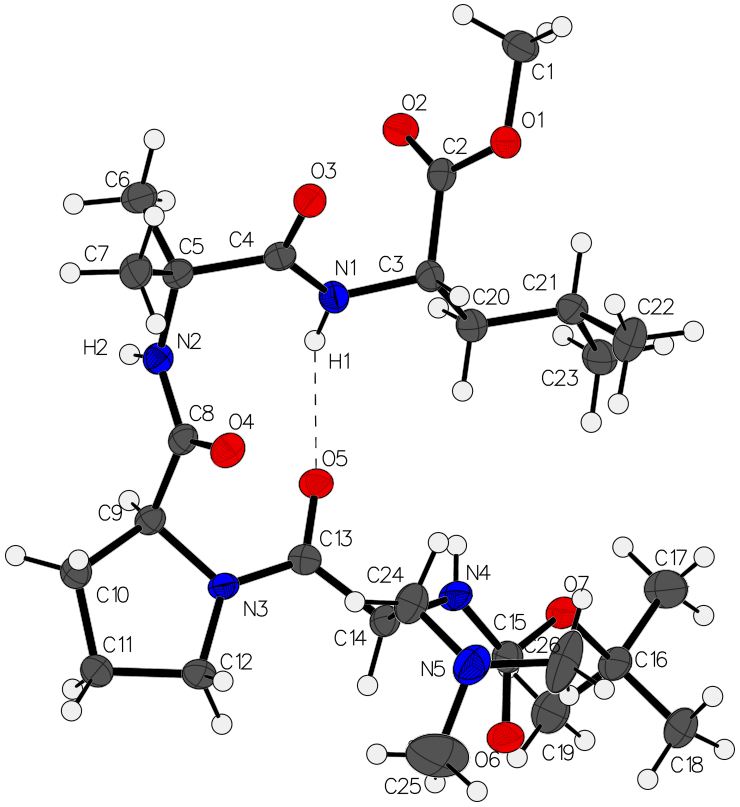

(b)

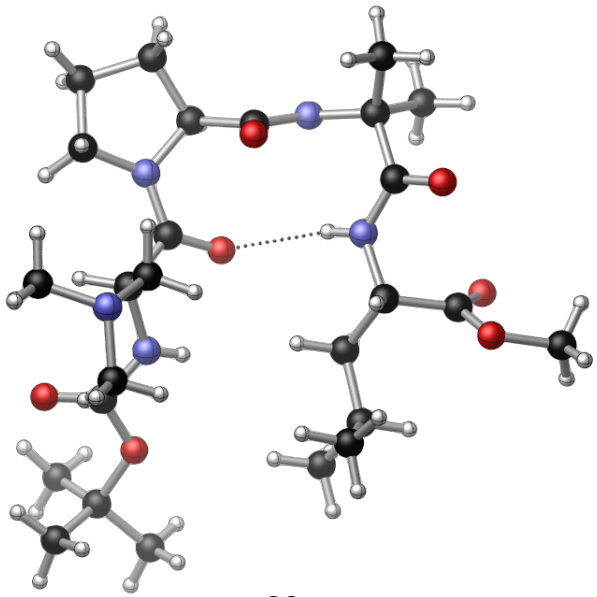

30
type II β-turn

Figure S3.31: (a) The full numbering scheme of **30** with 50% thermal ellipsoids. The H-atoms are depicted as circles for clarity. Dashed lines highlight H-bonding interactions. **(b)** Image of **30** rendered using CYLview.

(a)

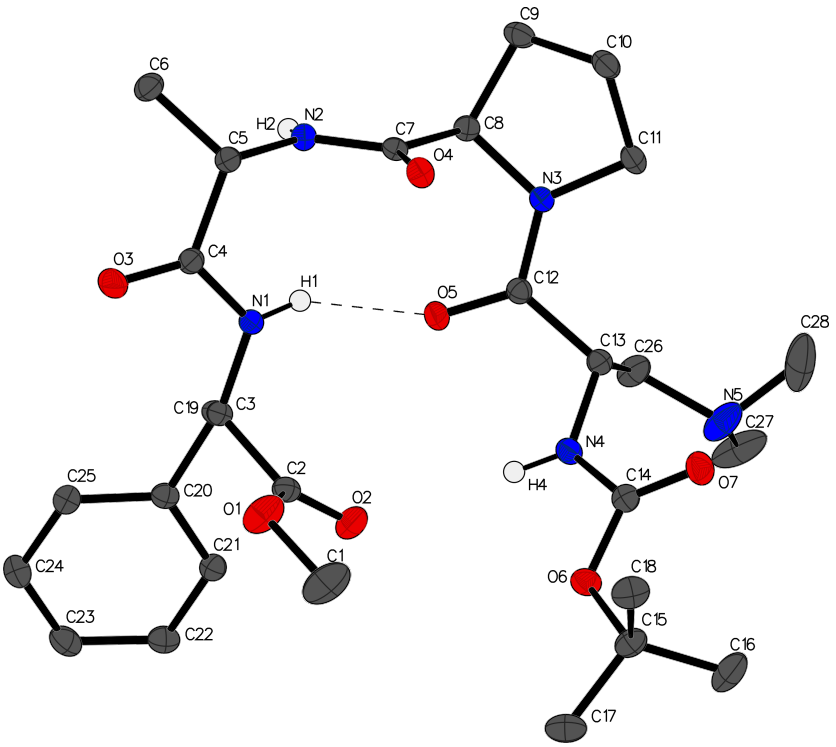

(b)

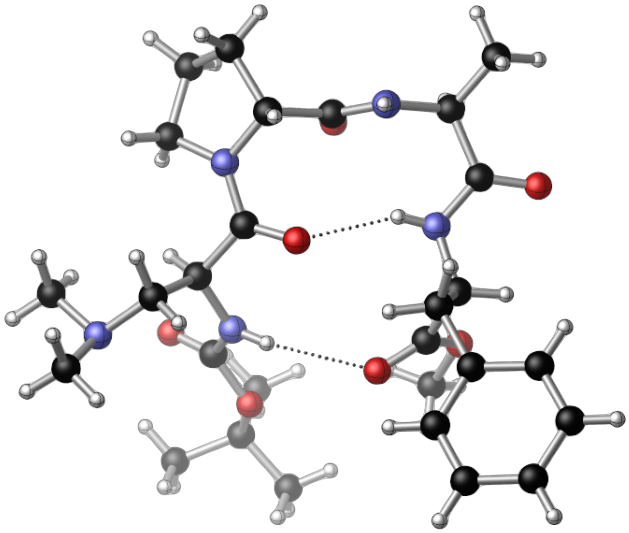

31
type II' β-hairpin

Figure S3.32: (a) The full numbering scheme of **31** with 50% thermal ellipsoids. Most of the H-atoms have been omitted for clarity, while some are depicted as circles. Dashed lines highlight H-bonding interactions. **(b)** Image of **31** rendered using CYLview.

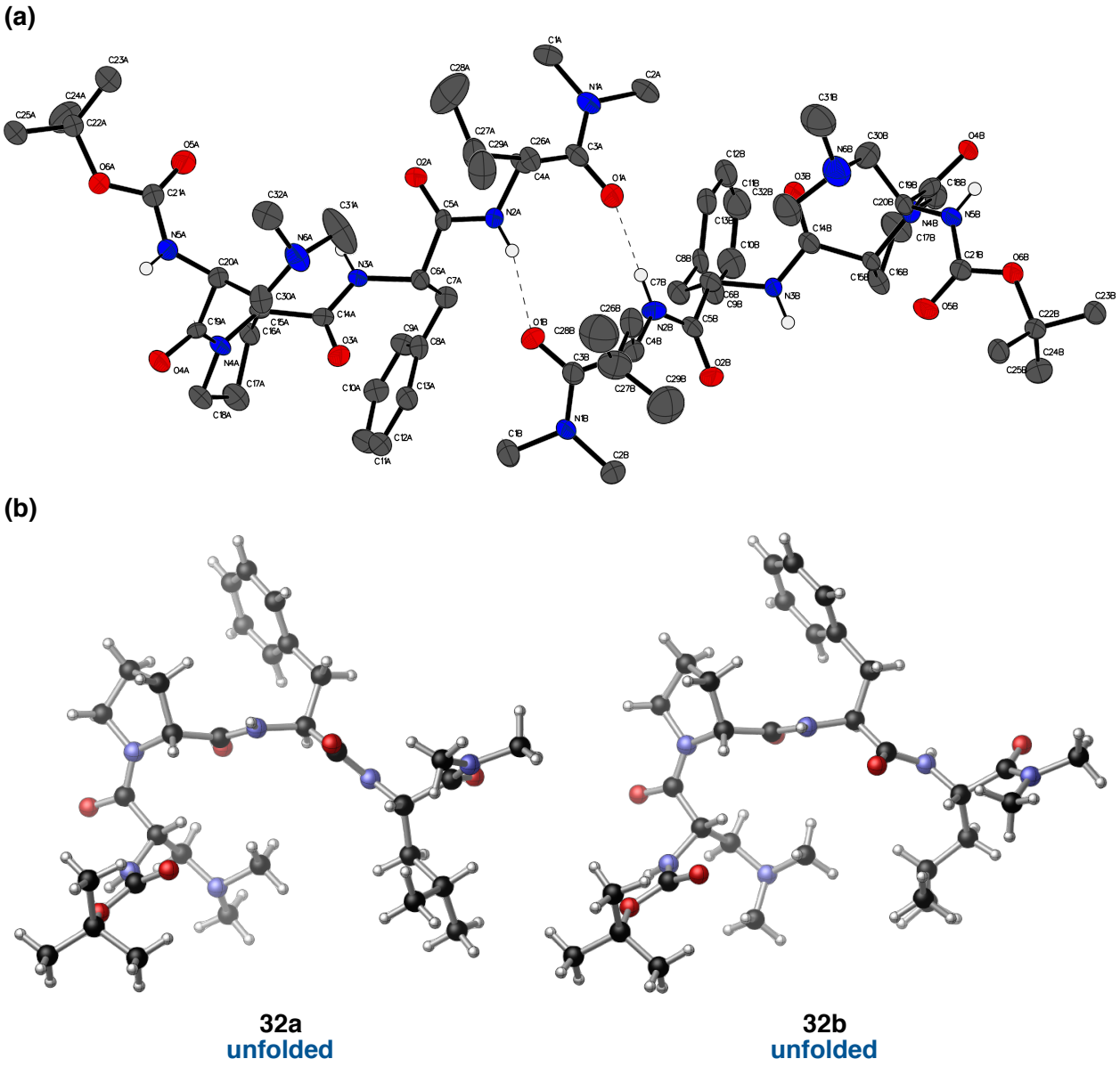

Figure S3.33: (a) The full numbering scheme of **32a,b** with 50% thermal ellipsoids. Most of the H-atoms have been omitted for clarity, while some are depicted as circles. Dashed lines highlight H-bonding interactions. **(b)** Images of **32a** and **32b** rendered separately using CYLview.

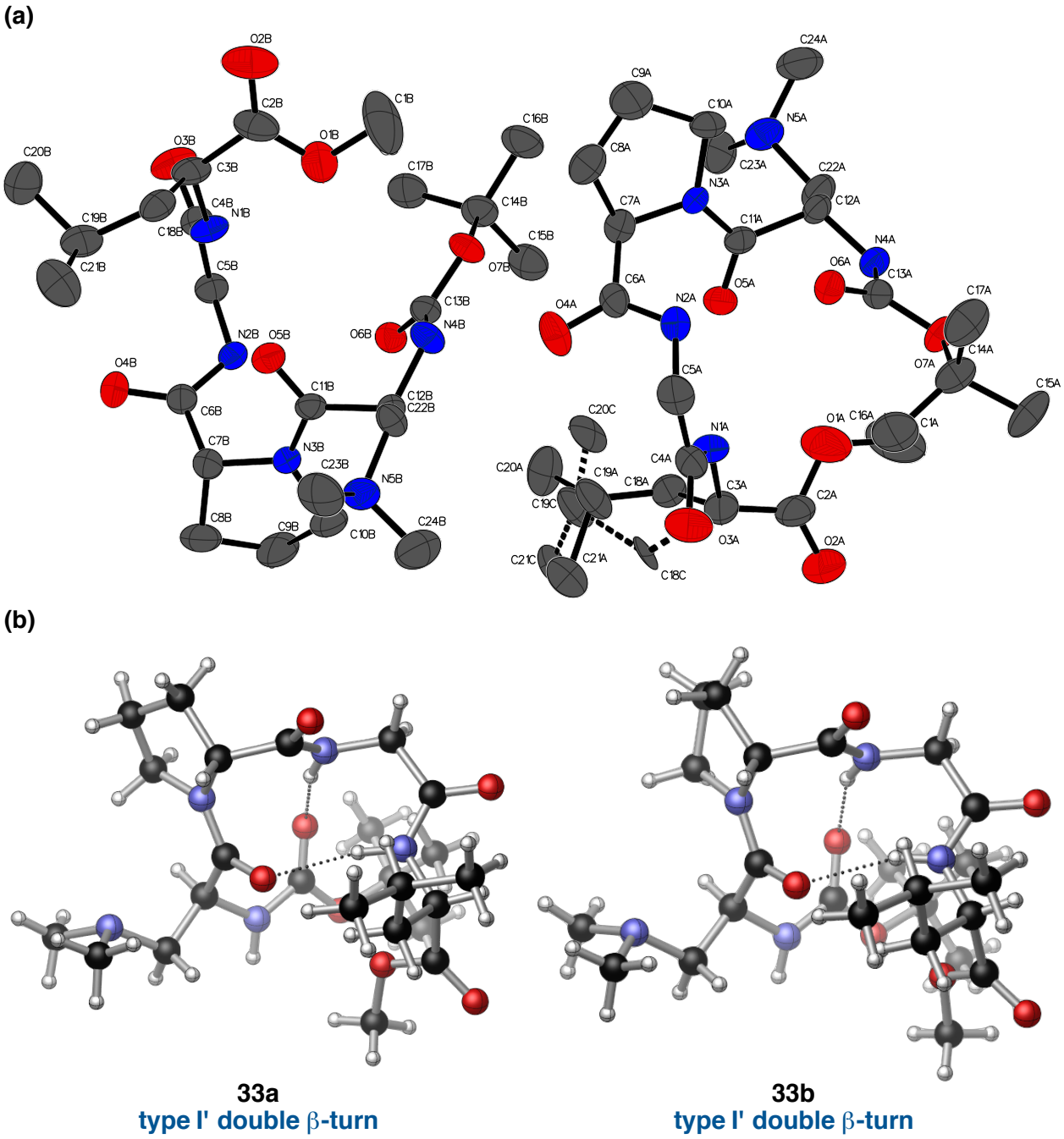

Figure S3.34: (a) The full numbering scheme of **33a,b** with 50% thermal ellipsoids. The H-atoms have been omitted for clarity. The dashed bonds highlight disordered positions. **(b)** Images of **33a** and **33b** rendered separately using CYLview.

(a)

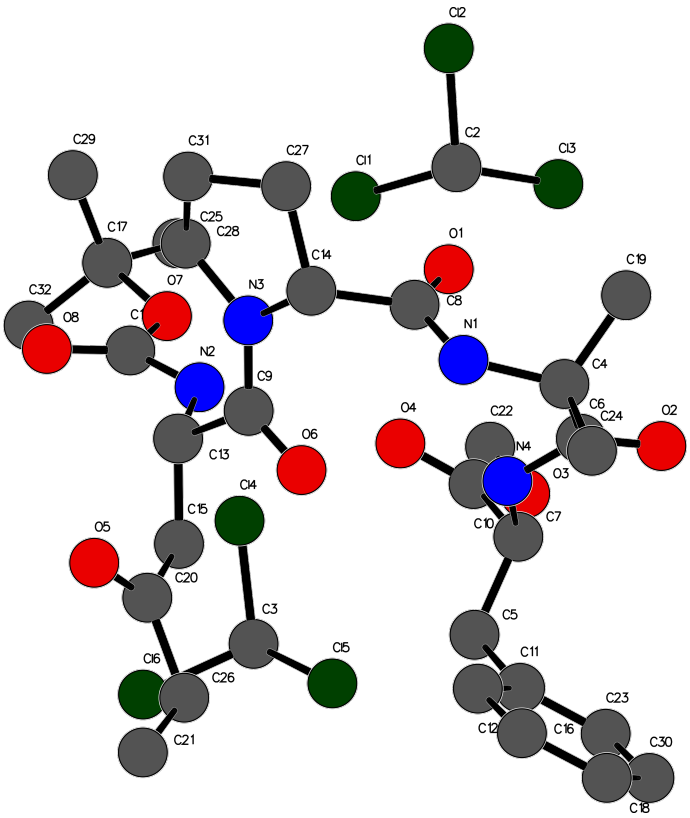

(b)

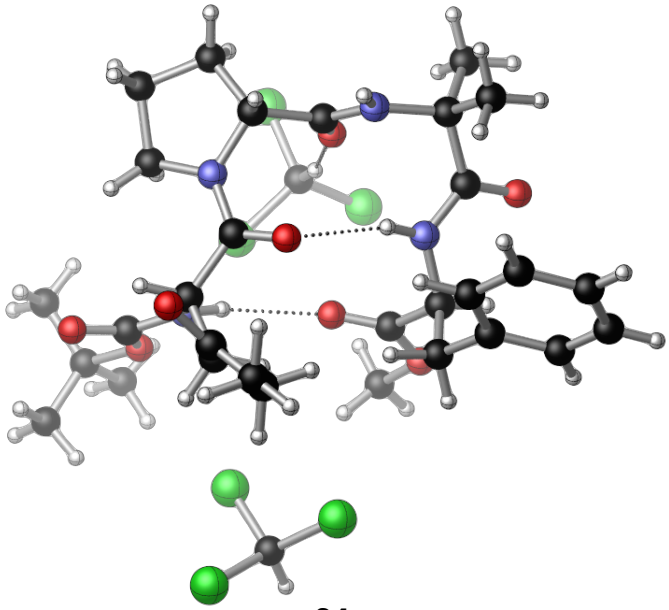

34

type II' β-hairpin

Figure S3.35: (a) The full numbering scheme of **34**.[8] The H-atoms have been omitted for clarity. **(b)** Image of **34** rendered using CYLview.

(a)

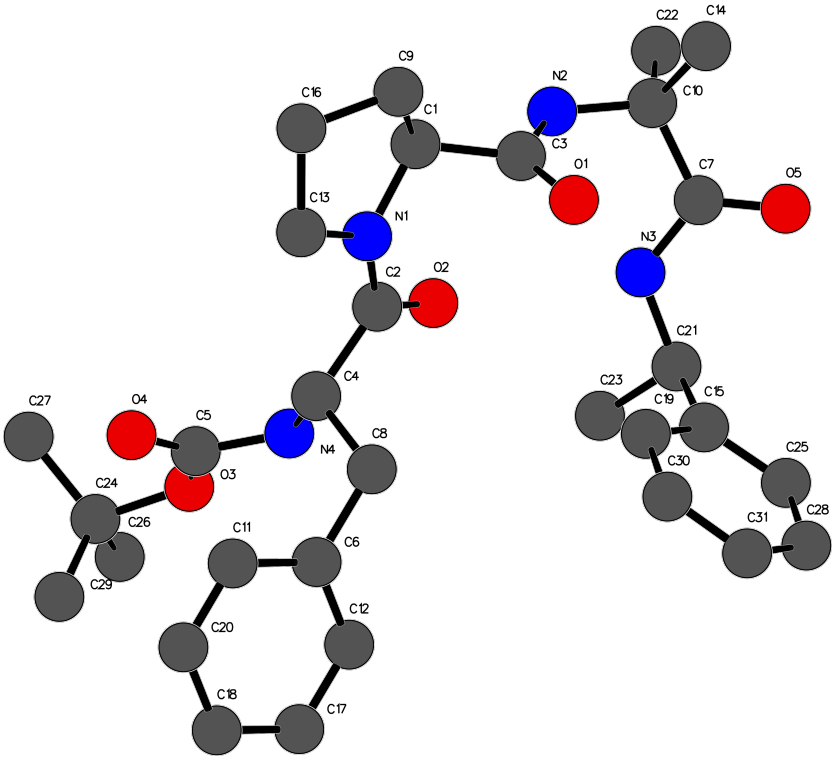

(b)

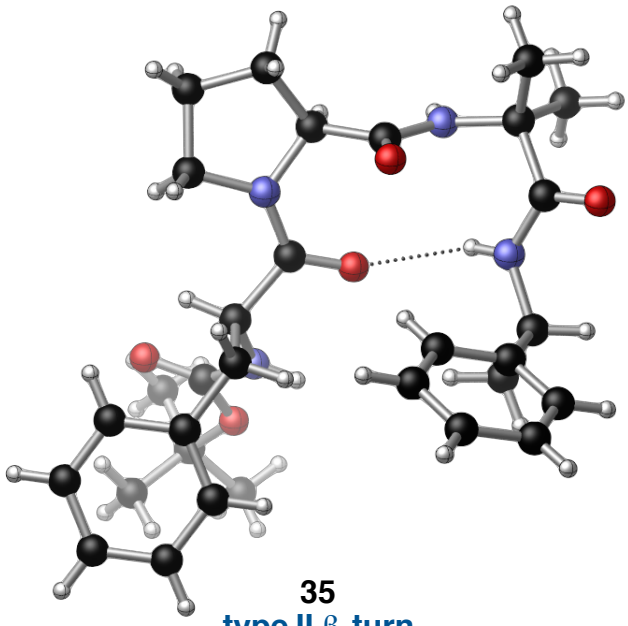

35
type II β-turn

Figure S3.36: (a) The full numbering scheme of **35**.[9] The H-atoms have been omitted for clarity. **(b)** Image of **35** rendered using CYLview.

(a)

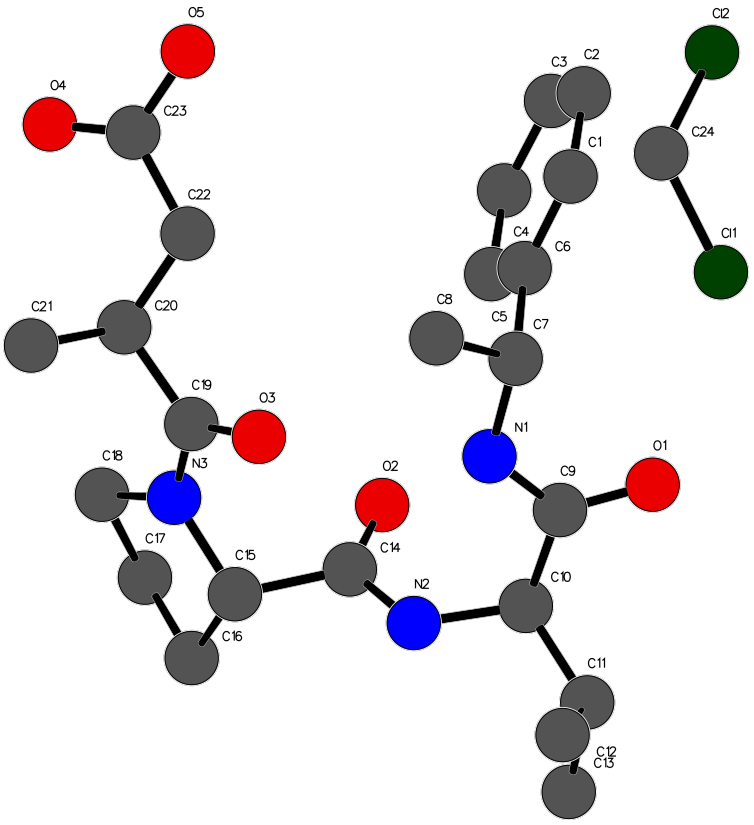

(b)

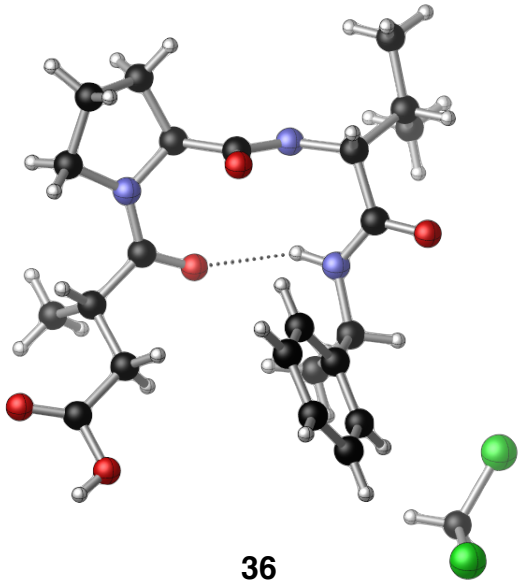

36
type II β-turn

Figure S3.37: (a) The full numbering scheme of **36**.[10] The H-atoms have been omitted for clarity. **(b)** Image of **36** rendered using CYLview.

(a)

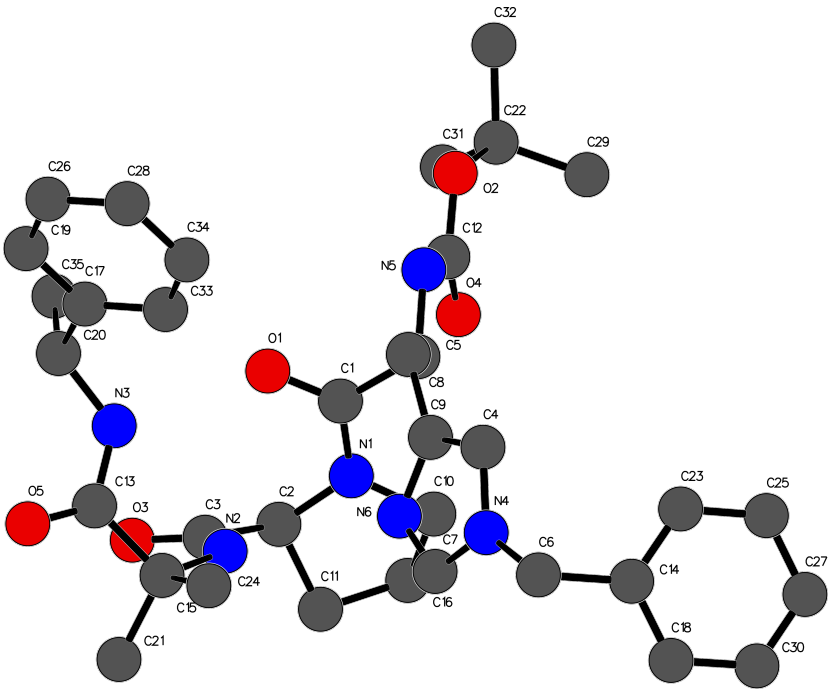

(b)

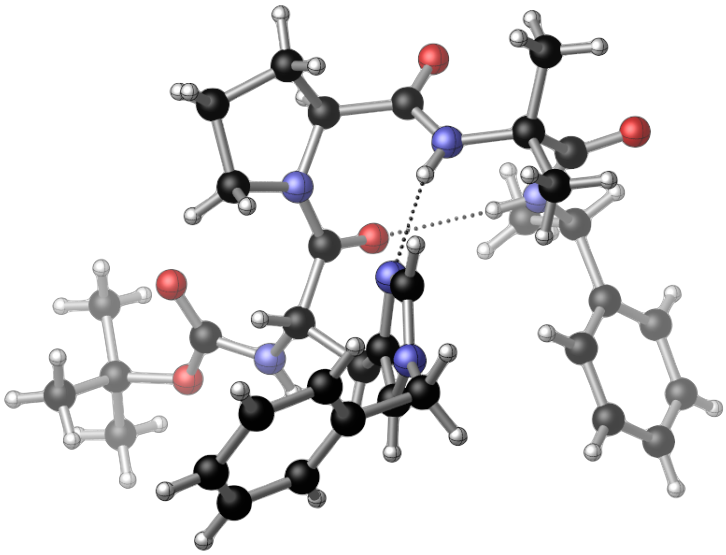

37

type I' ASX-Pro turn

Figure S3.38: (a) The full numbering scheme of **37**.[11] The H-atoms have been omitted for clarity. **(b)** Image of **37** rendered using CYLview.

IV. Analysis of X-Ray Crystal Structure Library

A. General Information

In this section, we provide the data that was used to analyze various structural features of our peptide crystal structure library. Measurements were extracted from the crystallographic information files (.cif) using Mercury 3.8[16] and were subsequently tabulated in Microsoft Excel® spreadsheets. We note that all measurements were rounded to the nearest pre-error digit, and the error values were not considered for the purposes of these whole-library analyses. Mean values are presented with standard deviations. The median and range were also determined for all average measurements. Publication-quality plots were constructed using Prism 7.0a.[17]

B. Analysis of Peptide Backbones

Table S4.01: ϕ,ψ Dihedrals of Type II′ β-Turns

Type II' β-Turns	$\phi(i)$	$\psi(i)$	$\phi(i+1)$	$\psi(i+1)$	$\phi(i+2)$	$\psi(i+2)$	$\phi(i+3)$	$\psi(i+3)$
Boc-Dmaa-D-Pro-Acpc-Leu-NMe_2 (**3a**)	-127.9	66.8	63.6	-113.0	-77.2	-3.7	-109.3	145.6
Boc-Dmaa-D-Pro-Acpc-Leu-NMe_2 (**3b**)	-158.2	134.0	62.9	-138.7	-78.1	-5.3	-96.2	126.6
Boc-Leu-D-Pro-Acpc-Leu-OMe (**6**)	-141.0	148.1	50.8	-134.1	-80.6	-5.9	-108.3	57.5
Boc-Dmaa-D-Pro-Acpc-Gly-OMe (**7a**)	-92.4	154.6	69.1	-123.1	-76.4	-3.0	71.5	-157.3
Boc-Dmaa-D-Pro-Acpc-Nle-NMe_2 (**8**)	-151.5	83.3	62.0	-130.1	-74.4	-5.5	-96.9	117.6
Boc-Dmaa-D-Pro-Acpc-Val-NMe_2 (**9**)	-156.4	79.9	58.0	-133.0	-70.5	-10.3	-101.3	112.9
Boc-Dmaa-D-Pro-Acpc-Chg-NMe_2 (**11**)	-153.4	82.1	61.6	-129.8	-75.5	-3.6	-131.2	139.6
Boc-Dmaa-D-Pro-Acpc-Phe-NMe_2 (**12**)	-152.5	77.2	63.6	-125.7	-72.0	-9.2	-90.8	135.5
Boc-Dmaa-D-Pro-Acpc-Phe-OMe (**13**)	-136.9	147.3	58.6	-136.9	-84.3	8.8	-129.0	81.9
Boc-Dmaa-D-Pro-Acpc-D-Phe-NMe_2 (**14**)	-130.4	132.9	52.7	-135.3	-70.5	-8.6	156.3	-77.8
Boc-Dmaa-D-Pro-Acbc-Leu-NMe_2 (**16a**)	-156.5	89.0	71.0	-128.0	-71.0	-20.6	-80.6	130.8
Boc-Dmaa-D-Pro-Acbc-Leu-NMe_2 (**16b**)	-126.3	52.2	67.9	-116.6	-66.8	-14.6	-121.3	141.7
Boc-Dmaa-D-Pro-Aic-D-Phe-NMe_2 (**20a**)	-171.1	127.1	57.6	-134.6	-59.0	-31.4	54.2	-131.6
Boc-Dmaa-D-Pro-Aic-D-Phe-NMe_2 (**20b**)	-146.8	156.9	59.4	-134.2	-64.3	-14.6	67.8	-134.9
Boc-Dmaa-D-Pro-Aib-Leu-NMe_2 (**24**)	-135.4	95.5	59.3	-129.9	-63.6	-14.7	-121.9	75.3
Boc-Dmaa-D-Pro-Aib-Leu-OMe (**25**)	-133.6	97.6	60.4	-136.0	-62.0	-21.3	-104.1	62.9
Boc-Dmaa-D-Pro-Aib-Val-OMe (**26**)	-159.2	90.1	63.1	-133.7	-68.1	-13.6	-118.5	-168.4
Boc-Dmaa-D-Pro-Aib-Phe-OMe (**27**)	-152.9	79.1	54.4	-127.3	-58.5	-26.2	-87.8	148.0
Boc-Dmaa-D-Pro-Aib-3-Pal-NMe_2 (**28**)	-162.9	122.8	52.6	-129.3	-59.9	-23.5	-81.9	112.4
Boc-Dmaa-D-Pro-Aib-2-Thi-NMe_2 (**29a**)	-149.6	84.3	60.8	-130.7	-61.0	-23.2	-85.3	145.8
Boc-Dmaa-D-Pro-Aib-2-Thi-NMe_2 (**29b**)	-150.5	77.1	61.7	-132.1	-60.3	-22.5	-89.4	144.4
Boc-Dmaa-D-Pro-Ala-Phe-OMe (**31**)	-136.5	147.7	60.1	-139.6	-93.4	22.5	-130.3	81.9
Boc-Keto-D-Pro-Aib-Phe-OMe (**34**)	-138.5	63.4	62.1	-123.7	-61.4	-19.7	-108.9	140.7
average	-144.4	103.9	60.6	-130.2	-69.9	-11.7	-71.4	62.2
st. dev.	16.5	33.0	5.0	6.6	9.1	12.0	78.0	110.2
median	-149.6	90.1	60.8	-130.7	-70.5	-13.6	-96.9	112.9
minimum	-171.1	52.2	50.8	-139.6	-93.4	-31.4	-131.2	-168.4
maximum	-92.4	156.9	71.0	-113.0	-58.5	22.5	156.3	148.0
count	23	23	23	23	23	23	23	23

Table S4.02: ϕ,ψ Dihedrals of Type II β-Turns

Type II β-Turns	ϕ(*i*)	ψ(*i*)	ϕ(*i*+1)	ψ(*i*+1)	ϕ(*i*+2)	ψ(*i*+2)	ϕ(*i*+3)	ψ(*i*+3)
Boc-Dmaa-Pro-Acpc-Leu-OMe (**15**)	-89.6	158.0	-51.0	132.3	76.8	-0.1	-142.5	81.6
Boc-Dmaa-Pro-Aic-Leu-OMe (**21a**)	-129.4	161.3	-51.3	137.4	62.5	26.8	-55.3	136.3
Boc-Dmaa-Pro-Aic-Leu-OMe (**21b**)	-139.2	165.1	-54.3	140.0	61.6	28.6	-53.4	137.7
Boc-Dmaa-Pro-Aib-Leu-OMe (**30**)	-138.7	159.8	-52.0	138.0	63.5	22.9	-55.1	136.6
Boc-Phe-Pro-Aib-(*R*)-α-Mba (**35**)	-127.2	144.5	-51.3	127.9	61.6	24.8	N/A	N/A
2-Msa-Pro-D-Val-(*R*)-α-Mba (**36**)	N/A	N/A	-60.6	139.1	79.8	3.6	N/A	N/A
average	-124.8	157.7	-53.4	135.8	67.6	17.8	-76.6	123.1
st. dev.	20.4	7.8	3.7	4.7	8.3	12.6	44.0	27.6
median	-129.4	159.8	-51.7	137.7	63.0	23.9	-55.2	136.5
minimum	-139.2	19.0	-60.6	127.9	7.3	-0.1	-142.5	-175.9
maximum	-89.6	165.1	-51.0	140.0	79.8	28.6	-53.4	137.7
count	5	5	6	6	6	6	4	4

Table S4.03: ϕ,ψ Dihedrals of Type I′ β-Turns

Type I' β-Turns	ϕ(*i*)	ψ(*i*)	ϕ(*i*+1)	ψ(*i*+1)	ϕ(*i*+2)	ψ(*i*+2)	ϕ(*i*+3)	ψ(*i*+3)
Boc-Dmaa-D-Pro-Acpc-Leu-NMe_2 (**3c**)	-56.8	132.6	64.3	15.2	71.9	14.9	-110.3	118.9
Boc-Dmaa-D-Pro-Acpc-Leu-OMe (**4a**)	-57.8	133.4	62.4	17.7	72.7	11.9	-119.3	171.1
Boc-Dmaa-D-Pro-Acpc-Leu-OMe (**4b**)	-59.4	135.2	61.1	21.8	71.0	11.4	-90.7	150.4
Boc-Dmaa-D-Pro-Acpc-Leu-OMe (**4c**)	-54.1	131.8	63.8	12.6	71.7	12.3	-65.1	152.2
Boc-Dmaa-D-Pro-Acpc-Leu-OMe (**4d**)	-58.9	137.7	61.6	19.3	73.0	10.9	-96.2	152.3
Boc-Dmaa-D-Pro-Acpc-Leu-OMe (**4e**)	-54.8	132.5	62.8	13.3	74.6	15.1	-135.7	178.3
Boc-Cys(Ph)-D-Pro-Acpc-Leu-OMe (**5**)	-58.3	128.5	69.5	13.7	75.1	6.9	-82.9	172.1
Boc-Dmaa-D-Pro-Acpc-Gly-OMe (**7b**)	-60.9	132.8	67.9	15.8	73.5	11.7	-104.1	-156.7
Boc-Dmaa-D-Pro-Acpc-Val-OMe (**10**)	-56.2	136.3	61.8	13.4	75.4	6.0	-74.3	144.4
Boc-Dmaa-D-Pro-Acbc-Leu-NMe_2 (**16c**)	-55.0	133.0	65.7	14.2	67.1	28.7	-120.0	97.6
Boc-Dmaa-D-Pro-Acbc-Leu-OMe (**17a**)	-51.7	133.3	63.6	14.6	65.0	26.1	-62.9	144.5
Boc-Dmaa-D-Pro-Acbc-Leu-OMe (**17b**)	-55.4	129.7	65.0	17.9	66.2	20.8	-63.1	147.1
Boc-Dmaa-D-Pro-Cle-Leu-OMe (**18a**)	-54.7	130.0	67.8	18.0	63.6	20.9	-63.0	147.8
Boc-Dmaa-D-Pro-Cle-Leu-OMe (**18b**)	-52.0	133.2	61.4	19.7	62.3	24.9	-61.8	144.0
Boc-Dmaa-D-Pro-Aic-Leu-OMe (**19a**)	-49.2	133.4	71.2	17.1	59.3	37.1	-99.8	41.1
Boc-Dmaa-D-Pro-Aic-Leu-OMe (**19b**)	50.3	46.3	62.4	29.0	67.3	17.1	-117.8	-175.9
Boc-Dmaa-D-Pro-Achc-Leu-OMe (**22a**)	-54.1	128.4	61.3	16.7	56.1	30.7	-62.6	155.2
Boc-Dmaa-D-Pro-Achc-Leu-OMe (**22b**)	-55.6	132.0	71.1	12.4	55.9	29.6	-70.6	150.0
Boc-Cys(Ph)-D-Pro-Achc-Leu-OMe (**23**)	-59.3	134.9	77.6	0.8	65.4	12.3	-65.7	154.3
Boc-Dmaa-D-Pro-Gly-Leu-OMe (**33a**)	-52.3	126.8	62.0	18.1	82.9	6.7	-120.8	-32.4
Boc-Dmaa-D-Pro-Gly-Leu-OMe (**33b**)	-53.5	125.5	66.7	14.8	81.1	4.1	-100.2	-28.7
average	-50.5	128.0	65.3	16.0	69.1	17.1	-89.9	96.6
st. dev.	23.3	19.0	4.3	5.1	7.3	9.3	24.5	105.6
median	-55.0	132.6	63.8	15.8	71.0	14.9	-90.7	147.1
minimum	-60.9	46.3	61.1	0.8	55.9	4.1	-135.7	-175.9
maximum	50.3	137.7	77.6	29.0	82.9	37.1	-61.8	178.3
count	21	21	21	21	21	21	21	21

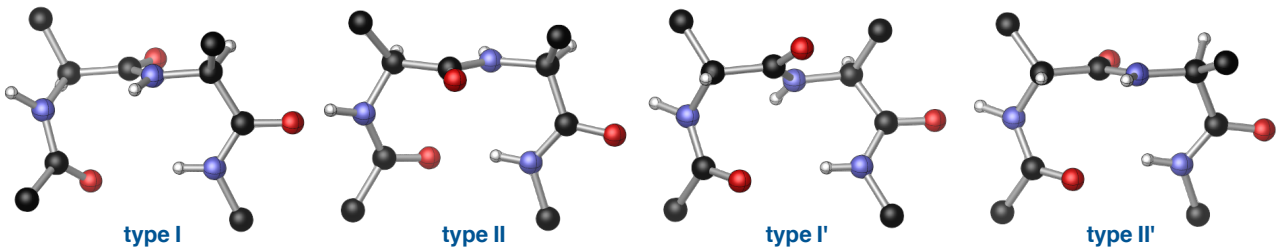

type I
$\phi_{(i+1)} = -60°$, $\psi_{(i+1)} = -30°$
$\phi_{(i+2)} = -90°$, $\psi_{(i+2)} = 0°$

type II
$\phi_{(i+1)} = -60°$, $\psi_{(i+1)} = 120°$
$\phi_{(i+2)} = 80°$, $\psi_{(i+2)} = 0°$

type I'
$\phi_{(i+1)} = 60°$, $\psi_{(i+1)} = 30°$
$\phi_{(i+2)} = 90°$, $\psi_{(i+2)} = 0°$

type II'
$\phi_{(i+1)} = 60°$, $\psi_{(i+1)} = -120°$
$\phi_{(i+2)} = -80°$, $\psi_{(i+2)} = 0°$

Figure S4.01: The canonical β-turn motifs loop and dihedrals describing them.[18]

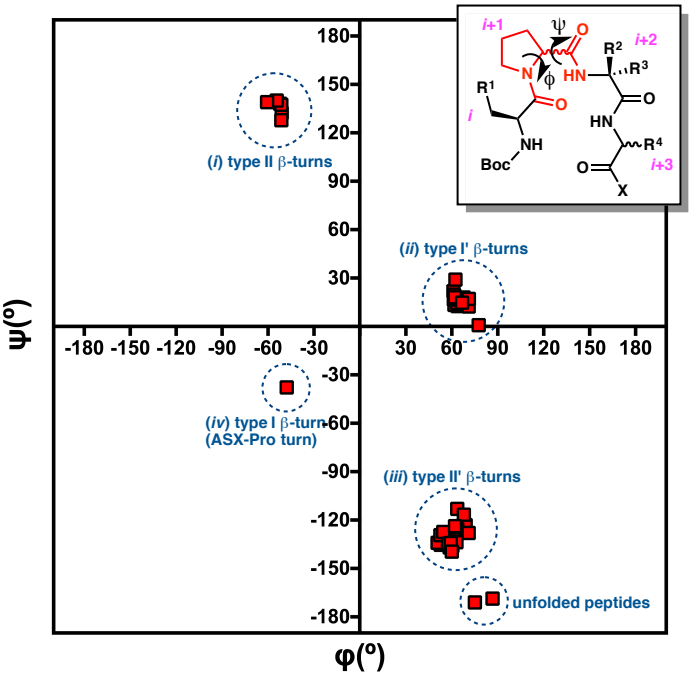

Figure S4.02: Ramachandran plot showing ϕ,ψ dihedrals of *i*+1 position for all 35 peptides (reproduced from Figure 11b in the manuscript).

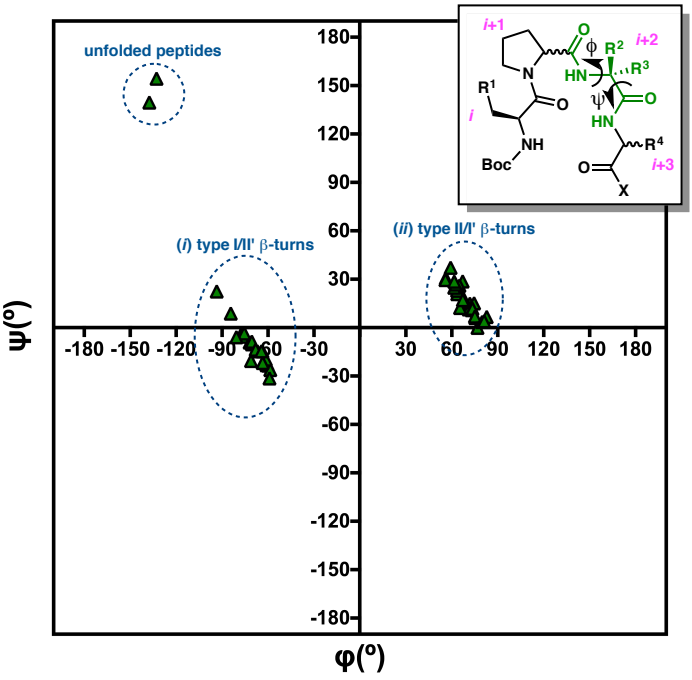

Figure S4.03: Ramachandran plot showing ϕ,ψ dihedrals of *i*+2 position for all 35 peptides (reproduced from Figure 11c in the manuscript).

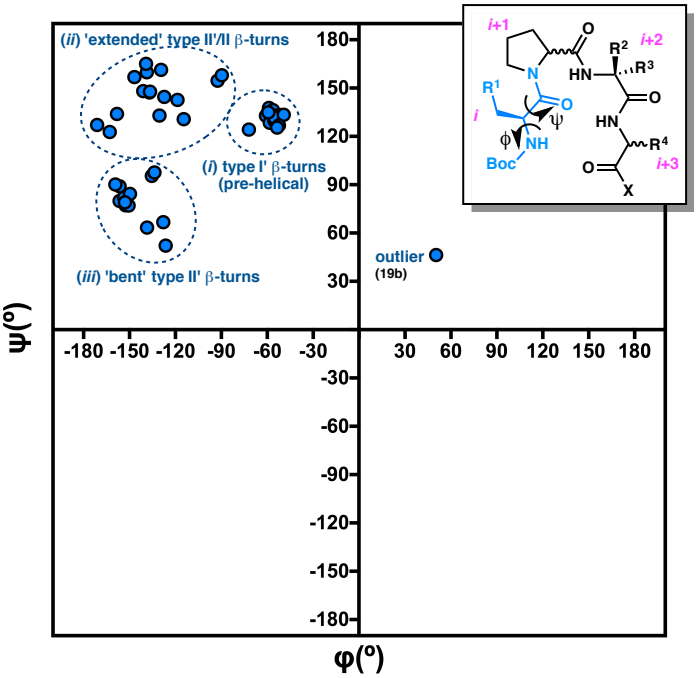

Figure S4.04: Ramachandran plot showing ϕ,ψ dihedrals of *i* position for all peptides except peptide **36**, which has a backbone-modified *i* residue (reproduced from Figure 11a in the manuscript).

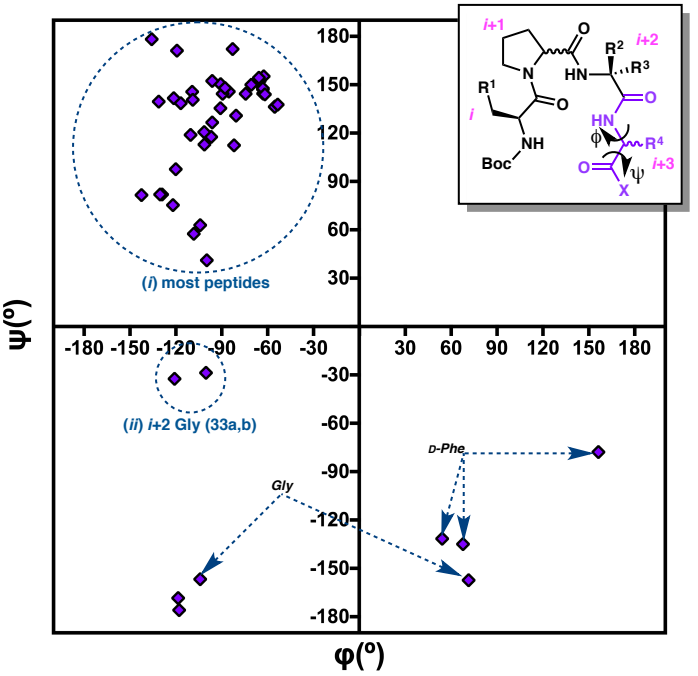

Figure S4.05: Ramachandran plot showing ϕ,ψ dihedrals of *i*+3 position for all peptides except **35**–**37**, those without *i*+3 residues (reproduced from Figure 11d in the manuscript).

Table S4.04: Deviation from 3_{10}-Helical Dihedrals (ϕ,ψ = 49°,26°) in Type I′ Loop Regions[19]

Deviation from 3_{10}-helix (loop region)	$\phi(i+1)$	$\Delta\phi(i+1)$	$\psi(i+1)$	$\Delta\psi(i+1)$	$\phi(i+2)$	$\Delta\phi(i+2)$	$\psi(i+2)$	$\Delta\psi(i+2)$
Boc-Dmaa-D-Pro-Acpc-Leu-NMe_2 (**3c**)	64.3	15.3	15.2	-10.8	71.9	22.9	14.9	-11.1
Boc-Dmaa-D-Pro-Acpc-Leu-OMe (**4a**)	62.4	13.4	17.7	-8.3	72.7	23.7	11.9	-14.1
Boc-Dmaa-D-Pro-Acpc-Leu-OMe (**4b**)	61.1	12.1	21.8	-4.2	71.0	22.0	11.4	-14.6
Boc-Dmaa-D-Pro-Acpc-Leu-OMe (**4c**)	63.8	14.8	12.6	-13.4	71.7	22.7	12.3	-13.7
Boc-Dmaa-D-Pro-Acpc-Leu-OMe (**4d**)	61.6	12.6	19.3	-6.7	73.0	24.0	10.9	-15.1
Boc-Dmaa-D-Pro-Acpc-Leu-OMe (**4e**)	62.8	13.8	13.3	-12.7	74.6	25.6	15.1	-10.9
Boc-Cys(Ph)-D-Pro-Acpc-Leu-OMe (**5**)	69.5	20.5	13.7	-12.3	75.1	26.1	6.9	-19.1
Boc-Dmaa-D-Pro-Acpc-Gly-OMe (**7b**)	67.9	18.9	15.8	-10.2	73.5	24.5	11.7	-14.3
Boc-Dmaa-D-Pro-Acpc-Val-OMe (**10**)	61.8	12.8	13.4	-12.6	75.4	26.4	6.0	-20.0
Boc-Dmaa-D-Pro-Acbc-Leu-NMe_2 (**16c**)	65.7	16.7	14.2	-11.8	67.1	18.1	28.7	2.7
Boc-Dmaa-D-Pro-Acbc-Leu-OMe (**17a**)	63.6	14.6	14.6	-11.4	65.0	16.0	26.1	0.1
Boc-Dmaa-D-Pro-Acbc-Leu-OMe (**17b**)	65.0	16.0	17.9	-8.1	66.2	17.2	20.8	-5.2
Boc-Dmaa-D-Pro-Cle-Leu-OMe (**18a**)	67.8	18.8	18.0	-8.0	63.6	14.6	20.9	-5.1
Boc-Dmaa-D-Pro-Cle-Leu-OMe (**18b**)	61.4	12.4	19.7	-6.3	62.3	13.3	24.9	-1.1
Boc-Dmaa-D-Pro-Aic-Leu-OMe (**19a**)	71.2	22.2	17.1	-8.9	59.3	10.3	37.1	11.1
Boc-Dmaa-D-Pro-Aic-Leu-OMe (**19b**)	62.4	13.4	29.0	3.0	67.3	18.3	17.1	-8.9
Boc-Dmaa-D-Pro-Achc-Leu-OMe (**22a**)	61.3	12.3	16.7	-9.3	56.1	7.1	30.7	4.7
Boc-Dmaa-D-Pro-Achc-Leu-OMe (**22b**)	71.1	22.1	12.4	-13.6	55.9	6.9	29.6	3.6
Boc-Cys(Ph)-D-Pro-Achc-Leu-OMe (**23**)	77.6	28.6	0.8	-25.2	65.4	16.4	12.3	-13.7
Boc-Dmaa-D-Pro-Gly-Leu-OMe (**33a**)	62.0	13.0	18.1	-7.9	82.9	33.9	6.7	-19.3
Boc-Dmaa-D-Pro-Gly-Leu-OMe (**33a**)	66.7	17.7	14.8	-11.2	81.1	32.1	4.1	-21.9
average	65.3		16.0		69.1		17.1	
st. dev.	4.3		5.1		7.3		9.3	
median	63.8	16.3	15.8	-10.0	71.0	20.1	14.9	-8.9
minimum	61.1		0.8		55.9		4.1	
maximum	77.6		29.0		82.9		37.1	
count	21		21		21		21	

Table S4.05: Deviation from 3_{10}-Helical Dihedrals (ϕ,ψ = 49°,26°) in Type I′ Flanking Residues[19]

Deviation from 3_{10}-helix (*i* and *i*+3)	$\phi(i)$	$\Delta\phi(i)$	$\psi(i)$	$\Delta\psi(i)$	$\phi(i+3)$	$\Delta\phi(i+3)$	$\psi(i+3)$	$\Delta\psi(i+3)$
Boc-Dmaa-D-Pro-Acpc-Leu-NMe_2 (**3c**)	-56.8	-105.8	132.6	106.6	-110.3	-159.3	118.9	92.9
Boc-Dmaa-D-Pro-Acpc-Leu-OMe (**4a**)	-57.8	-106.8	133.4	107.4	-119.3	-168.3	171.1	145.1
Boc-Dmaa-D-Pro-Acpc-Leu-OMe (**4b**)	-59.4	-108.4	135.2	109.2	-90.7	-139.7	150.4	124.4
Boc-Dmaa-D-Pro-Acpc-Leu-OMe (**4c**)	-54.1	-103.1	131.8	105.8	-65.1	-114.1	152.2	126.2
Boc-Dmaa-D-Pro-Acpc-Leu-OMe (**4d**)	-58.9	-107.9	137.7	111.7	152.3	103.3	-96.2	-122.2
Boc-Dmaa-D-Pro-Acpc-Leu-OMe (**4e**)	-54.8	-103.8	132.5	106.5	-135.7	-184.7	178.3	152.3
Boc-Cys(Ph)-D-Pro-Acpc-Leu-OMe (**5**)	-58.3	-107.3	128.5	102.5	-82.9	-131.9	172.1	146.1
Boc-Dmaa-D-Pro-Acpc-Gly-OMe (**7b**)	-60.9	-109.9	132.8	106.8	-104.1	-153.1	-156.7	-182.7
Boc-Dmaa-D-Pro-Acpc-Val-OMe (**10**)	-56.2	-105.2	136.3	110.3	-74.3	-123.3	144.4	118.4
Boc-Dmaa-D-Pro-Acbc-Leu-NMe_2 (**16c**)	-55.0	-104.0	133.0	107.0	-120.0	-169.0	97.6	71.6
Boc-Dmaa-D-Pro-Acbc-Leu-OMe (**17a**)	-51.7	-100.7	133.3	107.3	-62.9	-111.9	144.5	118.5
Boc-Dmaa-D-Pro-Acbc-Leu-OMe (**17b**)	-55.4	-104.4	129.7	103.7	-63.1	-112.1	147.1	121.1
Boc-Dmaa-D-Pro-Cle-Leu-OMe (**18a**)	-54.7	-103.7	130.0	104.0	-63.0	-112.0	147.8	121.8
Boc-Dmaa-D-Pro-Cle-Leu-OMe (**18b**)	-52.0	-101.0	133.2	107.2	-61.8	-110.8	144.0	118.0
Boc-Dmaa-D-Pro-Aic-Leu-OMe (**19a**)	-49.2	-98.2	133.4	107.4	-99.8	-148.8	41.1	15.1
Boc-Dmaa-D-Pro-Aic-Leu-OMe (**19b**)	50.3	1.3	46.3	20.3	-118	-166.8	-175.9	-201.9
Boc-Dmaa-D-Pro-Achc-Leu-OMe (**22a**)	-54.1	-103.1	128.4	102.4	-62.6	-111.6	155.2	129.2
Boc-Dmaa-D-Pro-Achc-Leu-OMe (**22b**)	-55.6	-104.6	132.0	106.0	-70.6	-119.6	150.0	124.0
Boc-Cys(Ph)-D-Pro-Achc-Leu-OMe (**23**)	-59.3	-108.3	134.9	108.9	-65.7	-114.7	154.3	128.3
Boc-Dmaa-D-Pro-Gly-Leu-OMe (**33a**)	-52.3	-101.3	126.8	100.8	-121	-169.8	-32.4	-58.4
Boc-Dmaa-D-Pro-Gly-Leu-OMe (**33a**)	-53.5	-102.5	125.5	99.5	-100	-149.2	-28.7	-54.7
average	-50.5		128.0		-78.0		84.7	
st. dev.	23.3		19.0		58.2		112.7	
median	-55.0	-99.5	132.6	102.0	-82.9	-127.0	144.5	58.7
minimum	-60.9		46.3		-135.7		-175.9	
maximum	50.3		137.7		152.3		178.3	
count	21		21		21		21	

Table S4.06: ϕ,ψ Dihedrals of *i* & *i*+3 Residues in Type I/I′ β-Turns

Type I/I' β-Turns	$\phi(i)$	$\psi(i)$	$\phi(i+3)$	$\psi(i+3)$
Boc-Dmaa-D-Pro-Acpc-Leu-NMe_2 (**3c**)	-56.8	132.6	-110.3	118.9
Boc-Dmaa-D-Pro-Acpc-Leu-OMe (**4a**)	-57.8	133.4	-119.3	171.1
Boc-Dmaa-D-Pro-Acpc-Leu-OMe (**4b**)	-59.4	135.2	-90.7	150.4
Boc-Dmaa-D-Pro-Acpc-Leu-OMe (**4c**)	-54.1	131.8	-65.1	152.2
Boc-Dmaa-D-Pro-Acpc-Leu-OMe (**4d**)	-58.9	137.7	-96.2	152.3
Boc-Dmaa-D-Pro-Acpc-Leu-OMe (**4e**)	-54.8	132.5	-135.7	178.3
Boc-Cys(Ph)-D-Pro-Acpc-Leu-OMe (**5**)	-58.3	128.5	-82.9	172.1
Boc-Dmaa-D-Pro-Acpc-Gly-OMe (**7b**)	-60.9	132.8	-104.1	-156.7
Boc-Dmaa-D-Pro-Acpc-Val-OMe (**10**)	-56.2	136.3	-74.3	144.4
Boc-Dmaa-D-Pro-Acbc-Leu-NMe_2 (**16c**)	-55.0	133.0	-120.0	97.6
Boc-Dmaa-D-Pro-Acbc-Leu-OMe (**17a**)	-51.7	133.3	-62.9	144.5
Boc-Dmaa-D-Pro-Acbc-Leu-OMe (**17b**)	-55.4	129.7	-63.1	147.1
Boc-Dmaa-D-Pro-Cle-Leu-OMe (**18a**)	-54.7	130.0	-63.0	147.8
Boc-Dmaa-D-Pro-Cle-Leu-OMe (**18b**)	-52.0	133.2	-61.8	144.0
Boc-Dmaa-D-Pro-Aic-Leu-OMe (**19a**)	-49.2	133.4	-99.8	41.1
Boc-Dmaa-D-Pro-Achc-Leu-OMe (**22a**)	-54.1	128.4	-62.6	155.2
Boc-Dmaa-D-Pro-Achc-Leu-OMe (**22b**)	-55.6	132.0	-70.6	150.0
Boc-Cys(Ph)-D-Pro-Achc-Leu-OMe (**23**)	-59.3	134.9	-65.7	154.3
Boc-Dmaa-D-Pro-Gly-Leu-OMe (**33a**)	-52.3	126.8	-120.8	-32.4
Boc-Dmaa-D-Pro-Gly-Leu-OMe (**33b**)	-53.5	125.5	-100.2	-28.7
Boc-His(τ-Bn)-Pro-Aib-(*R*)-α-Mba (**37**)	-72.0	124.3	N/A	N/A
average	-56.3	131.7	-88.5	110.2
st. dev.	4.6	3.5	24.3	87.4
median	-55.4	132.6	-86.8	147.5
minimum	-72.0	124.3	-135.7	-156.7
maximum	-49.2	137.7	-61.8	178.3
count	21	21	20	20

NOTE: The data presented in this table was used to calculate the average ϕ,ψ values for cluster (*i*) in Figure S4.04.

Table S4.07: ϕ,ψ Dihedrals of *i* & *i*+3 Residues in Extended Type II/II′ β-Turns

Type II/II' β-Turns (extended)	ϕ(*i*)	ψ(*i*)	ϕ(*i*+3)	ψ(*i*+3)
Boc-Dmaa-D-Pro-Acpc-Leu-NMe_2 (**3b**)	-158.2	134.0	-96.2	126.6
Boc-Leu-D-Pro-Acpc-Leu-OMe (**6**)	-141.0	148.1	-108.3	57.5
Boc-Dmaa-D-Pro-Acpc-Gly-OMe (**7a**)	-92.4	154.6	71.5	-157.3
Boc-Dmaa-D-Pro-Acpc-Phe-OMe (**13**)	-136.9	147.3	-129.0	81.9
Boc-Dmaa-D-Pro-Acpc-D-Phe-NMe_2 (**14**)	-130.4	132.9	156.3	-77.8
Boc-Dmaa-Pro-Acpc-Leu-OMe (**15**)	-89.6	158.0	-142.5	81.6
Boc-Dmaa-D-Pro-Aic-D-Phe-NMe_2 (**20a**)	-171.1	127.1	54.2	-131.6
Boc-Dmaa-D-Pro-Aic-D-Phe-NMe_2 (**20b**)	-146.8	156.9	67.8	-134.9
Boc-Dmaa-Pro-Aic-Leu-OMe (**21a**)	-129.4	161.3	-55.3	136.3
Boc-Dmaa-Pro-Aic-Leu-OMe (**21b**)	-139.2	165.1	-53.4	137.7
Boc-Dmaa-D-Pro-Aib-3-Pal-NMe_2 (**28**)	-162.9	122.8	-81.9	112.4
Boc-Dmaa-Pro-Aib-Leu-OMe (**30**)	-138.7	159.8	-55.1	136.6
Boc-Dmaa-D-Pro-Ala-Phe-OMe (**31**)	-136.5	147.7	-130.3	81.9
Boc-Dmaa-D-Pro-Phe-Leu-NMe_2 (**32a**)	-114.6	130.7	-101.5	120.6
Boc-Dmaa-D-Pro-Phe-Leu-NMe_2 (**32b**)	-118.6	142.7	-116.7	138.6
average	-133.8	145.9	-48.0	47.3
st. dev.	23.0	13.6	91.4	111.7
median	-136.9	147.7	-81.9	81.9
minimum	-171.1	122.8	-142.5	-157.3
maximum	-89.6	165.1	156.3	138.6
count	15	15	15	15

NOTE: The data presented in this table was used to calculate the average ϕ,ψ values for cluster (*ii*) in Figure S4.04.

Table S4.08: ϕ,ψ Dihedrals of *i* & *i*+3 Residues in Bent Type II′ β-Turns

Type II' β-Turns (bent)	ϕ(*i*)	ψ(*i*)	ϕ(*i*+3)	ψ(*i*+3)
Boc-Dmaa-D-Pro-Acpc-Leu-NMe_2 (**3a**)	-127.9	66.8	-109.3	145.6
Boc-Dmaa-D-Pro-Acpc-Nle-NMe_2 (**8**)	-151.5	83.3	-96.9	117.6
Boc-Dmaa-D-Pro-Acpc-Val-NMe_2 (**9**)	-156.4	79.9	-101.3	112.9
Boc-Dmaa-D-Pro-Acpc-Chg-NMe_2 (**11**)	-153.4	82.1	-131.2	139.6
Boc-Dmaa-D-Pro-Acpc-Phe-NMe_2 (**12**)	-152.5	77.2	-90.8	135.5
Boc-Dmaa-D-Pro-Acbc-Leu-NMe_2 (**16a**)	-156.5	89.0	-80.6	130.8
Boc-Dmaa-D-Pro-Acbc-Leu-NMe_2 (**16b**)	-126.3	52.2	-121.3	141.7
Boc-Dmaa-D-Pro-Aib-Leu-NMe_2 (**24**)	-135.4	95.5	-121.9	75.3
Boc-Dmaa-D-Pro-Aib-Leu-OMe (**25**)	-133.6	97.6	-104.1	62.9
Boc-Dmaa-D-Pro-Aib-Val-OMe (**26**)	-159.2	90.1	-118.5	-168.4
Boc-Dmaa-D-Pro-Aib-Phe-OMe (**27**)	-152.9	79.1	-87.8	148.0
Boc-Dmaa-D-Pro-Aib-2-Thi-NMe_2 (**29a**)	-149.6	84.3	-85.3	145.8
Boc-Dmaa-D-Pro-Aib-2-Thi-NMe_2 (**29b**)	-150.5	77.1	-89.4	144.4
Boc-Keto-D-Pro-Aib-Phe-OMe (**34**)	-138.5	63.4	-108.9	140.7
average	-146.0	79.8	-103.4	105.2
st. dev.	11.2	12.4	15.7	83.1
median	-151.0	81.0	-102.7	137.6
minimum	-159.2	52.2	-131.2	-168.4
maximum	-126.3	97.6	-80.6	148
count	14	14	14	14

NOTE: The data presented in this table was used to calculate the average ϕ,ψ values for cluster (*iii*) in Figure S4.04.

Table S4.09: ϕ,ψ Dihedrals of *i*+3 Residues

Peptide Sequence	$\phi(i+3)$	$\psi(i+3)$
Boc-Dmaa-D-Pro-Acpc-Leu-NMe_2 (**3a**)	-109.3	145.6
Boc-Dmaa-D-Pro-Acpc-Leu-NMe_2 (**3b**)	-96.2	126.6
Boc-Dmaa-D-Pro-Acpc-Leu-NMe_2 (**3c**)	-110.3	118.9
Boc-Dmaa-D-Pro-Acpc-Leu-OMe (**4a**)	-119.3	171.1
Boc-Dmaa-D-Pro-Acpc-Leu-OMe (**4b**)	-90.7	150.4
Boc-Dmaa-D-Pro-Acpc-Leu-OMe (**4c**)	-65.1	152.2
Boc-Dmaa-D-Pro-Acpc-Leu-OMe (**4d**)	-96.2	152.3
Boc-Dmaa-D-Pro-Acpc-Leu-OMe (**4e**)	-135.7	178.3
Boc-Cys(Ph)-D-Pro-Acpc-Leu-OMe (**5**)	-82.9	172.1
Boc-Leu-D-Pro-Acpc-Leu-OMe (**6**)	-108.3	57.5
Boc-Dmaa-D-Pro-Acpc-Nle-NMe_2 (**8**)	-96.9	117.6
Boc-Dmaa-D-Pro-Acpc-Val-NMe_2 (**9**)	-101.3	112.9
Boc-Dmaa-D-Pro-Acpc-Val-OMe (**10**)	-74.3	144.4
Boc-Dmaa-D-Pro-Acpc-Chg-NMe_2 (**11**)	-131.2	139.6
Boc-Dmaa-D-Pro-Acpc-Phe-NMe_2 (**12**)	-90.8	135.5
Boc-Dmaa-D-Pro-Acpc-Phe-OMe (**13**)	-129.0	81.9
Boc-Dmaa-Pro-Acpc-Leu-OMe (**15**)	-142.5	81.6
Boc-Dmaa-D-Pro-Acbc-Leu-NMe_2 (**16a**)	-80.6	130.8
Boc-Dmaa-D-Pro-Acbc-Leu-NMe_2 (**16b**)	-121.3	141.7
Boc-Dmaa-D-Pro-Acbc-Leu-NMe_2 (**16c**)	-120.0	97.6
Boc-Dmaa-D-Pro-Acbc-Leu-OMe (**17a**)	-62.9	144.5
Boc-Dmaa-D-Pro-Acbc-Leu-OMe (**17b**)	-63.1	147.1
Boc-Dmaa-D-Pro-Cle-Leu-OMe (**18a**)	-63.0	147.8
Boc-Dmaa-D-Pro-Cle-Leu-OMe (**18b**)	-61.8	144.0
Boc-Dmaa-D-Pro-Aic-Leu-OMe (**19a**)	-99.8	41.1
Boc-Dmaa-Pro-Aic-Leu-OMe (**21a**)	-55.3	136.3
Boc-Dmaa-Pro-Aic-Leu-OMe (**21b**)	-53.4	137.7
Boc-Dmaa-D-Pro-Achc-Leu-OMe (**22a**)	-62.6	155.2
Boc-Dmaa-D-Pro-Achc-Leu-OMe (**22b**)	-70.6	150.0
Boc-Cys(Ph)-D-Pro-Achc-Leu-OMe (**23**)	-65.7	154.3
Boc-Dmaa-D-Pro-Aib-Leu-NMe_2 (**24**)	-121.9	75.3
Boc-Dmaa-D-Pro-Aib-Leu-OMe (**25**)	-104.1	62.9
Boc-Dmaa-D-Pro-Aib-Phe-OMe (**27**)	-87.8	148.0
Boc-Dmaa-D-Pro-Aib-3-Pal-NMe_2 (**28**)	-81.9	112.4
Boc-Dmaa-D-Pro-Aib-2-Thi-NMe_2 (**29a**)	-85.3	145.8
Boc-Dmaa-D-Pro-Aib-2-Thi-NMe_2 (**29b**)	-89.4	144.4
Boc-Dmaa-Pro-Aib-Leu-OMe (**30**)	-55.1	136.6
Boc-Dmaa-D-Pro-Ala-Phe-OMe (**31**)	-130.3	81.9
Boc-Dmaa-D-Pro-Phe-Leu-NMe_2 (**32a**)	-101.5	120.6
Boc-Dmaa-D-Pro-Phe-Leu-NMe_2 (**32b**)	-116.7	138.6
Boc-Keto-D-Pro-Aib-Phe-OMe (**34**)	-108.9	140.7
average	-93.7	128.6
st. dev.	25.2	32.1
median	-96.2	139.6
minimum	-142.5	41.1
maximum	-53.4	178.3
count	41	41

NOTE: The data presented in this table was used to calculate the average ϕ,ψ values for cluster (*i*) in Figure S4.05.

Table S4.10: ω Dihedrals for All Peptides

Peptide Sequence	ω(*i*)	ω(*i*+1)	ω(*i*+2)	ω(*i*+3)
Boc-Dmaa-D-Pro-Acpc-Leu-NMe_2 (**3a**)	179.7	175.3	174.2	177.6
Boc-Dmaa-D-Pro-Acpc-Leu-NMe_2 (**3b**)	178.4	175.9	170.6	170.2
Boc-Dmaa-D-Pro-Acpc-Leu-NMe_2 (**3c**)	179.9	173.0	173.4	173.4
Boc-Dmaa-D-Pro-Acpc-Leu-OMe (**4a**)	179.5	177.3	172.5	178.0
Boc-Dmaa-D-Pro-Acpc-Leu-OMe (**4b**)	178.5	177.5	170.3	176.8
Boc-Dmaa-D-Pro-Acpc-Leu-OMe (**4c**)	177.7	173.5	178.9	173.2
Boc-Dmaa-D-Pro-Acpc-Leu-OMe (**4c**)	177.3	177.2	169.1	178.2
Boc-Dmaa-D-Pro-Acpc-Leu-OMe (**4e**)	178.9	175.8	179.5	178.7
Boc-Cys(Ph)-D-Pro-Acpc-Leu-OMe (**5**)	176.9	174.1	176.6	179.9
Boc-Leu-D-Pro-Acpc-Leu-OMe (**6**)	179.9	176.5	179.2	178.2
Boc-Dmaa-D-Pro-Acpc-Gly-OMe (**7a**)	172.5	170.6	176.6	165.0
Boc-Dmaa-D-Pro-Acpc-Gly-OMe (**7b**)	172.1	173.7	169.7	178.0
Boc-Dmaa-D-Pro-Acpc-Nle-NMe_2 (**8**)	173.6	176.7	177.5	175.5
Boc-Dmaa-D-Pro-Acpc-Val-NMe_2 (**9**)	170.9	179.2	178.8	177.4
Boc-Dmaa-D-Pro-Acpc-Val-OMe (**10**)	179.3	171.3	173.5	173.6
Boc-Dmaa-D-Pro-Acpc-Chg-NMe_2 (**11**)	173.0	177.1	176.2	170.7
Boc-Dmaa-D-Pro-Acpc-Phe-NMe_2 (**12**)	178.7	174.7	172.9	175.5
Boc-Dmaa-D-Pro-Acpc-Phe-OMe (**13**)	175.8	175.5	160.1	177.1
Boc-Dmaa-D-Pro-Acpc-D-Phe-NMe_2 (**14**)	174.8	179.9	173.7	175.5
Boc-Dmaa-Pro-Acpc-Leu-OMe (**15**)	173.9	179.1	172.2	179.7
Boc-Dmaa-D-Pro-Acbc-Leu-NMe_2 (**16a**)	178.6	176.9	171.4	176.4
Boc-Dmaa-D-Pro-Acbc-Leu-NMe_2 (**16b**)	176.7	179.8	172.5	175.2
Boc-Dmaa-D-Pro-Acbc-Leu-NMe_2 (**16c**)	178.6	176.1	176.7	176.4
Boc-Dmaa-D-Pro-Acbc-Leu-OMe (**17a**)	173.9	178.1	179.2	175.9
Boc-Dmaa-D-Pro-Acbc-Leu-OMe (**17b**)	171.8	177.7	177.3	177.0
Boc-Dmaa-D-Pro-Cle-Leu-OMe (**18a**)	167.7	175.6	174.9	178.6
Boc-Dmaa-D-Pro-Cle-Leu-OMe (**18b**)	170.5	177.4	176.3	177.1
Boc-Dmaa-D-Pro-Aic-Leu-OMe (**19a**)	168.1	177.2	179.4	174.4
Boc-Dmaa-D-Pro-Aic-Leu-OMe (**19b**)	175.4	175.9	177.6	179.7
Boc-Dmaa-D-Pro-Aic-D-Phe-NMe_2 (**20a**)	175.2	178.6	171.0	169.1
Boc-Dmaa-D-Pro-Aic-D-Phe-NMe_2 (**20b**)	168.6	177.2	173.2	178.1
Boc-Dmaa-Pro-Aic-Leu-OMe (**21a**)	164.8	176.6	171.9	178.1
Boc-Dmaa-Pro-Aic-Leu-OMe (**21b**)	170.7	176.0	174.0	177.4
Boc-Dmaa-D-Pro-Achc-Leu-OMe (**22a**)	168.9	172.6	164.7	176.8
Boc-Dmaa-D-Pro-Achc-Leu-OMe (**22b**)	166.4	173.9	173.3	178.0
Boc-Cys(Ph)-D-Pro-Achc-Leu-OMe (**23**)	170.1	163.6	179.3	170.3
Boc-Dmaa-D-Pro-Aib-Leu-NMe_2 (**24**)	177.6	180.0	174.6	179.7
Boc-Dmaa-D-Pro-Aib-Leu-OMe (**25**)	177.6	175.4	177.8	171.3
Boc-Dmaa-D-Pro-Aib-Val-OMe (**26**)	179.8	177.1	176.3	178.9
Boc-Dmaa-D-Pro-Aib-Phe-OMe (**27**)	178.1	178.8	179.7	177.7
Boc-Dmaa-D-Pro-Aib-3-Pal-NMe_2 (**28**)	175.7	177.6	178.9	170.7
Boc-Dmaa-D-Pro-Aib-2-Thi-NMe_2 (**29a**)	176.4	179.8	177.1	177.5
Boc-Dmaa-D-Pro-Aib-2-Thi-NMe_2 (**29b**)	176.6	179.5	176.6	173.6
Boc-Dmaa-Pro-Aib-Leu-OMe (**30**)	163.3	176.1	174.1	179.9
Boc-Dmaa-D-Pro-Ala-Phe-OMe (**31**)	177.3	176.4	167.3	177.1
Boc-Dmaa-D-Pro-Phe-Leu-NMe_2 (**32a**)	-7.8	176.0	179.9	169.7
Boc-Dmaa-D-Pro-Phe-Leu-NMe_2 (**32b**)	-14.8	170.2	178.7	172.8
Boc-Dmaa-D-Pro-Gly-Leu-OMe (**33a**)	177.1	177.3	175.3	172.0
Boc-Dmaa-D-Pro-Gly-Leu-OMe (**33b**)	174.5	173.4	174.5	173.4
Boc-Keto-D-Pro-Aib-Phe-OMe (**34**)	177.2	179.6	177.6	179.8
Boc-Phe-Pro-Aib-(*R*)-α-Mba (**35**)	173.5	172.2	174.2	N/A
2-Msa-Pro-D-Val-(*R*)-α-Mba (**36**)	176.8	179.6	174.6	N/A
Boc-His(τ-Bn)-Pro-Aib-(*R*)-α-Mba (**37**)	175.4	172.1	174.6	N/A
average	167.8	176.0	174.7	175.7
st. dev.	36.0	3.0	4.0	3.4
median	175.7	176.5	174.6	176.9
minimum	-14.8	163.6	160.1	165.0
maximum	179.9	180.0	179.9	179.9
count	53	53	53	50

All ω	All ω (w/o 32)
173.5	175.3
18.6	3.7
176.3	176.4
-14.8	160.1
180.0	180.0
209	201

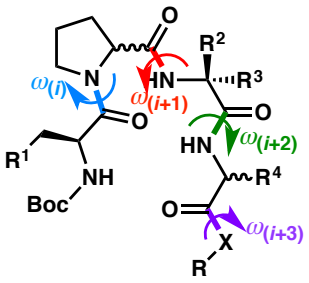

Table S4.11: Backbone Dihedrals in Unfolded Peptides **32a,b** (vs. Avg. Type II′ Potentials)

Unfolded Peptide	$\phi(i)$	$\psi(i)$	$\omega(i)$	$\phi(i+1)$	$\psi(i+1)$	$\omega(i+1)$	$\phi(i+2)$	$\psi(i+2)$	$\omega(i+2)$	$\phi(i+3)$	$\psi(i+3)$	$\omega(i+3)$
Boc-Dmaa-D-Pro-Phe-Leu-NMe_2 (**32a**)	-114.6	130.7	-7.8	75.1	-171.0	-176.0	-137.5	139.6	-179.9	-101.5	120.6	169.7
Boc-Dmaa-D-Pro-Phe-Leu-NMe_2 (**32b**)	-118.6	142.7	-14.8	86.6	-168.7	-170.2	-132.7	154.4	178.7	-116.7	138.6	172.8
average type II'	-144.4	103.9	175.0	60.6	-129.9	177.2	-69.9	-11.7	174.3	-71.4	62.2	175.7

NOTE: The ϕ,ψ presented in this table is labeled "unfolded peptide" in Figures S.02 and S.03.

Table S4.12: Degree of Backbone Bending in Type II/II′ β-Turns & Hairpins

Peptide Sequence	Bend
Boc-Dmaa-D-Pro-Acpc-Leu-NMe_2 (**3a**)	65.9
Boc-Dmaa-D-Pro-Acpc-Leu-NMe_2 (**3b**)	41.0
Boc-Leu-D-Pro-Acpc-Leu-OMe (**6**)	46.9
Boc-Dmaa-D-Pro-Acpc-Gly-OMe (**7a**)	26.9
Boc-Dmaa-D-Pro-Acpc-Nle-NMe_2 (**8**)	58.4
Boc-Dmaa-D-Pro-Acpc-Val-NMe_2 (**9**)	57.8
Boc-Dmaa-D-Pro-Acpc-Chg-NMe_2 (**11**)	50.6
Boc-Dmaa-D-Pro-Acpc-Phe-NMe_2 (**12**)	58.9
Boc-Dmaa-D-Pro-Acpc-Phe-OMe (**13**)	45.9
Boc-Dmaa-D-Pro-Acpc-D-Phe-NMe_2 (**14**)	43.4
Boc-Dmaa-Pro-Acpc-Leu-OMe (**15**)	64.8
Boc-Dmaa-D-Pro-Acbc-Leu-NMe_2 (**16a**)	57.4
Boc-Dmaa-D-Pro-Acbc-Leu-NMe_2 (**16b**)	64.9
Boc-Dmaa-D-Pro-Aic-D-Phe-NMe_2 (**20a**)	28.2
Boc-Dmaa-D-Pro-Aic-D-Phe-NMe_2 (**20b**)	13.7
Boc-Dmaa-Pro-Aic-Leu-OMe (**21a**)	34.4
Boc-Dmaa-Pro-Aic-Leu-OMe (**21b**)	34.4
Boc-Dmaa-D-Pro-Aib-Leu-NMe_2 (**24**)	60.3
Boc-Dmaa-D-Pro-Aib-Leu-OMe (**25**)	82.0
Boc-Dmaa-D-Pro-Aib-Val-OMe (**26**)	45.9
Boc-Dmaa-D-Pro-Aib-Phe-OMe (**27**)	56.3
Boc-Dmaa-D-Pro-Aib-3-Pal-NMe_2 (**28**)	50.0
Boc-Dmaa-D-Pro-Aib-2-Thi-NMe_2 (**29a**)	55.6
Boc-Dmaa-D-Pro-Aib-2-Thi-NMe_2 (**29b**)	54.8
Boc-Dmaa-Pro-Aib-Leu-OMe (**30**)	34.0
Boc-Dmaa-D-Pro-Ala-Phe-OMe (**31**)	48.0
Boc-Keto-D-Pro-Aib-Phe-OMe (**34**)	62.3
average	49.7
st. dev.	14.6
median	50.6
minimum	13.7
maximum	82.0
count	27

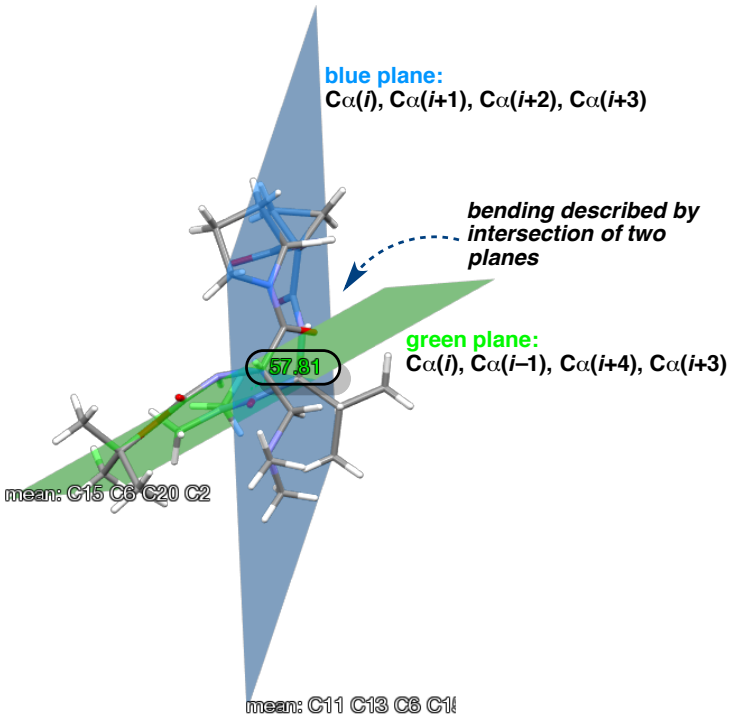

NOTE: Backbone bending is only defined for type II/II′ β-turn and β-hairpin structures.

Table S4.13: Backbone Bending as a Function of ϕ,ψ(*i*, *i*+3) Dihedrals in Type II/II′ β-Turns

Peptide Sequence	ϕ(*i*)	ψ(*i*)	ϕ(*i*+3)	ψ(*i*+3)	Bend (°)
Boc-Dmaa-D-Pro-Acpc-Leu-NMe_2 (**3a**)	-127.9	66.8	-109.3	145.6	65.9
Boc-Dmaa-D-Pro-Acpc-Leu-NMe_2 (**3b**)	-158.2	134.0	-96.2	126.6	41.0
Boc-Leu-D-Pro-Acpc-Leu-OMe (**6**)	-141.0	148.1	-108.3	57.5	46.9
Boc-Dmaa-D-Pro-Acpc-Gly-OMe (**7a**)	-92.4	154.6	71.5	-157.3	26.9
Boc-Dmaa-D-Pro-Acpc-Nle-NMe_2 (**8**)	-151.5	83.3	-96.9	117.6	58.4
Boc-Dmaa-D-Pro-Acpc-Val-NMe_2 (**9**)	-156.4	79.9	-101.3	112.9	57.8
Boc-Dmaa-D-Pro-Acpc-Chg-NMe_2 (**11**)	-153.4	82.1	-131.2	139.6	50.6
Boc-Dmaa-D-Pro-Acpc-Phe-NMe_2 (**12**)	-152.5	77.2	-90.8	135.5	58.9
Boc-Dmaa-D-Pro-Acpc-Phe-OMe (**13**)	-136.9	147.3	-129.0	81.9	45.9
Boc-Dmaa-D-Pro-Acpc-D-Phe-NMe_2 (**14**)	-130.4	132.9	156.3	-77.8	43.4
Boc-Dmaa-Pro-Acpc-Leu-OMe (**15**)	-89.6	158.0	-142.5	81.6	64.8
Boc-Dmaa-D-Pro-Acbc-Leu-NMe_2 (**16a**)	-156.5	89.0	-80.6	130.8	57.4
Boc-Dmaa-D-Pro-Acbc-Leu-NMe_2 (**16b**)	-126.3	52.2	-121.3	141.7	64.9
Boc-Dmaa-D-Pro-Aic-D-Phe-NMe_2 (**20a**)	-171.1	127.1	54.2	-131.6	28.2
Boc-Dmaa-D-Pro-Aic-D-Phe-NMe_2 (**20b**)	-146.8	156.9	67.8	-134.9	13.7
Boc-Dmaa-Pro-Aic-Leu-OMe (**21a**)	-129.4	161.3	-55.3	136.3	34.4
Boc-Dmaa-Pro-Aic-Leu-OMe (**21b**)	-139.2	165.1	-53.4	137.7	34.4
Boc-Dmaa-D-Pro-Aib-Leu-NMe_2 (**24**)	-135.4	95.5	-121.9	75.3	60.3
Boc-Dmaa-D-Pro-Aib-Leu-OMe (**25**)	-133.6	97.6	-104.1	62.9	82.0
Boc-Dmaa-D-Pro-Aib-Val-OMe (**26**)	-159.2	90.1	-118.5	-168.4	45.9
Boc-Dmaa-D-Pro-Aib-Phe-OMe (**27**)	-152.9	79.1	-87.8	148.0	56.3
Boc-Dmaa-D-Pro-Aib-3-Pal-NMe_2 (**28**)	-162.9	122.8	-81.9	112.4	50.0
Boc-Dmaa-D-Pro-Aib-2-Thi-NMe_2 (**29a**)	-149.6	84.3	-85.3	145.8	55.6
Boc-Dmaa-D-Pro-Aib-2-Thi-NMe_2 (**29b**)	-150.5	77.1	-89.4	144.4	54.8
Boc-Dmaa-Pro-Aib-Leu-OMe (**30**)	-138.7	159.8	-55.1	136.6	34.0
Boc-Dmaa-D-Pro-Ala-Phe-OMe (**31**)	-136.5	147.7	-130.3	81.9	48.0
Boc-Keto-D-Pro-Aib-Phe-OMe (**34**)	-138.5	63.4	-108.9	140.7	62.3
average	-141.381	112.34	-72.2	71.233	49.7
st. dev.	18.60356	36.723	73.31	104.17	14.6
median	-141	97.6	-96.2	117.6	50.6
minimum	-171.1	52.2	-142.5	-168.4	13.7
maximum	-89.6	165.1	156.3	148	82.0
count	27	27	27	27	27

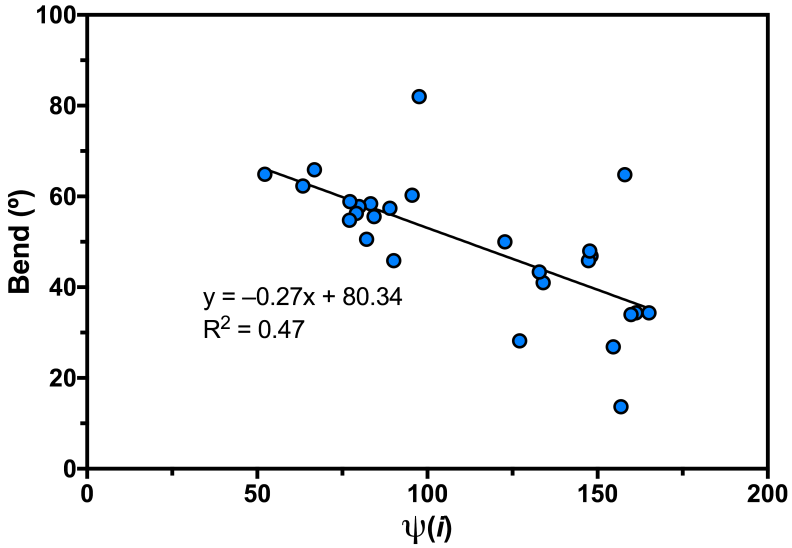

Figure S4.06: A plot of backbone bend (°) vs. ψ(*i*) shows a loose correlation.

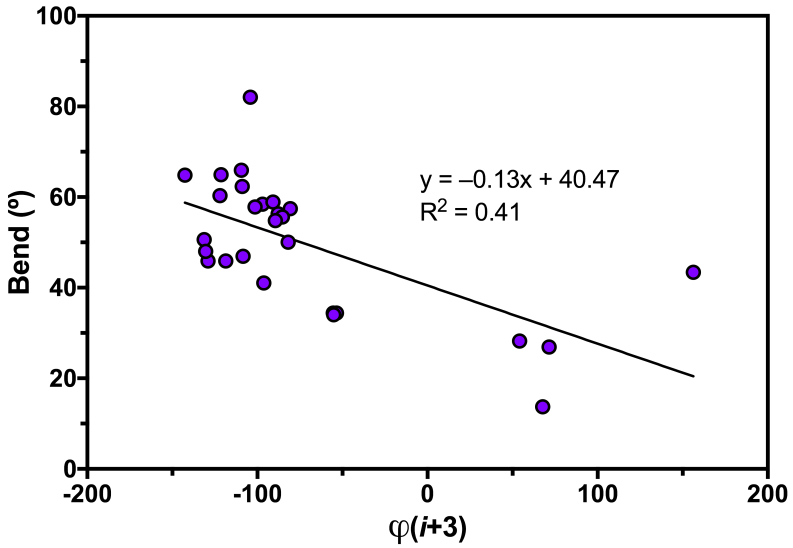

Figure S4.07: A plot of backbone bend (°) vs. ϕ(*i*+3) shows a loose correlation.

Table S4.14: Backbone Twisting (ϖ) in Type II′ β-Turns[20]

Type II' β-Turns	twist (ϖ)
Boc-Dmaa-D-Pro-Acpc-Leu-NMe_2 (**3a**)	9.38
Boc-Dmaa-D-Pro-Acpc-Leu-NMe_2 (**3b**)	-21.31
Boc-Leu-D-Pro-Acpc-Leu-OMe (**6**)	-20.63
Boc-Dmaa-D-Pro-Acpc-Gly-OMe (**7a**)	-0.78
Boc-Dmaa-D-Pro-Acpc-Nle-NMe_2 (**8**)	-9.42
Boc-Dmaa-D-Pro-Acpc-Val-NMe_2 (**9**)	-9.18
Boc-Dmaa-D-Pro-Acpc-Chg-NMe_2 (**11**)	-5.41
Boc-Dmaa-D-Pro-Acpc-Phe-NMe_2 (**12**)	-0.23
Boc-Dmaa-D-Pro-Acpc-Phe-OMe (**13**)	-24.78
Boc-Dmaa-D-Pro-Acpc-D-Phe-NMe_2 (**14**)	-8.51
Boc-Dmaa-D-Pro-Acbc-Leu-NMe_2 (**16a**)	-7.86
Boc-Dmaa-D-Pro-Acbc-Leu-NMe_2 (**16b**)	17.80
Boc-Dmaa-D-Pro-Aic-D-Phe-NMe_2 (**20a**)	-3.48
Boc-Dmaa-D-Pro-Aic-D-Phe-NMe_2 (**20b**)	3.91
Boc-Dmaa-D-Pro-Aib-Leu-NMe_2 (**24**)	2.16
Boc-Dmaa-D-Pro-Aib-Leu-OMe (**25**)	-6.53
Boc-Dmaa-D-Pro-Aib-Val-OMe (**26**)	-6.88
Boc-Dmaa-D-Pro-Aib-Phe-OMe (**27**)	4.82
Boc-Dmaa-D-Pro-Aib-3-Pal-NMe_2 (**28**)	6.85
Boc-Dmaa-D-Pro-Aib-2-Thi-NMe_2 (**29a**)	-1.29
Boc-Dmaa-D-Pro-Aib-2-Thi-NMe_2 (**29b**)	-0.07
Boc-Dmaa-D-Pro-Ala-Phe-OMe (**31**)	-30.17
Boc-Keto-D-Pro-Aib-Phe-OMe (**34**)	9.75
average	-4.43
st. dev.	11.65
median	-3.48
minimum	-30.17
maximum	17.80
count	23

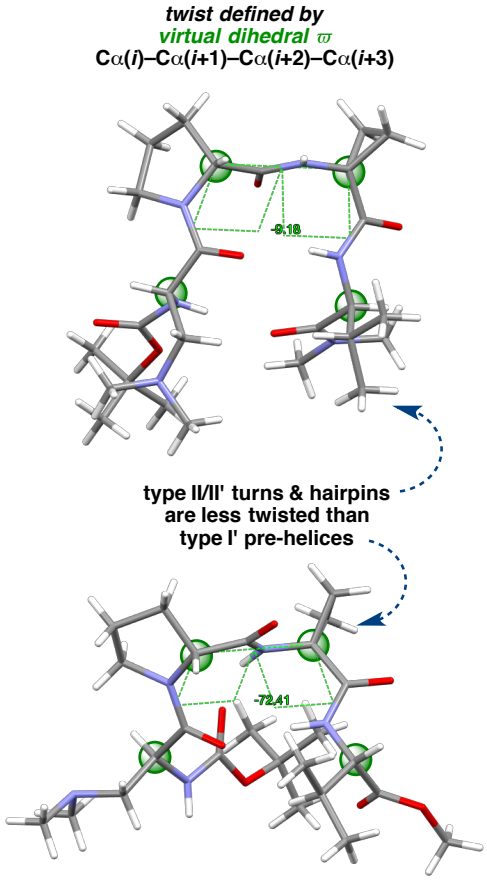

Table S4.15: Backbone Twisting (ϖ) in Type II β-Turns[20]

Type II β-Turns	twist (ϖ)
Boc-Dmaa-Pro-Acpc-Leu-OMe (**15**)	8.44
Boc-Dmaa-Pro-Aic-Leu-OMe (**19a**)	12.09
Boc-Dmaa-Pro-Aic-Leu-OMe (**19b**)	14.01
Boc-Dmaa-Pro-Aib-Leu-OMe (**30**)	13.88
Boc-Phe-Pro-Aib-(*R*)-α-Mba (**35**)	-7.38
2-Msa-Pro-D-Val-(*R*)-α-Mba (**36**)	16.15
average	9.53
st. dev.	8.68
median	12.99
minimum	-7.38
maximum	16.15
count	6

Table S4.16: Backbone Twisting (ϖ) in Type I′ β-Turns[20]

Type I' β-Turns	twist (ϖ)
Boc-Dmaa-D-Pro-Acpc-Leu-NMe_2 (**3c**)	-71.48
Boc-Dmaa-D-Pro-Acpc-Leu-OMe (**4a**)	-72.82
Boc-Dmaa-D-Pro-Acpc-Leu-OMe(**4b**)	-71.04
Boc-Dmaa-D-Pro-Acpc-Leu-OMe(**4c**)	-73.04
Boc-Dmaa-D-Pro-Acpc-Leu-OMe(**4d**)	-72.38
Boc-Dmaa-D-Pro-Acpc-Leu-OMe(**4e**)	-71.17
Boc-Cys(Ph)-D-Pro-Acpc-Leu-OMe (**5**)	-71.37
Boc-Dmaa-D-Pro-Acpc-Gly-OMe (**7b**)	-70.08
Boc-Dmaa-D-Pro-Acpc-Val-OMe (**9**)	-72.41
Boc-Dmaa-D-Pro-Acbc-Leu-NMe_2 (**16c**)	-72.39
Boc-Dmaa-D-Pro-Acbc-Leu-OMe (**17a**)	-76.16
Boc-Dmaa-D-Pro-Acbc-Leu-OMe (**17b**)	-71.27
Boc-Dmaa-D-Pro-Cle-Leu-OMe (**18a**)	-70.75
Boc-Dmaa-D-Pro-Cle-Leu-OMe (**18b**)	-72.21
Boc-Dmaa-D-Pro-Aic-Leu-OMe (**19a**)	-71.48
Boc-Dmaa-D-Pro-Aic-Leu-OMe (**19b**)	-59.96
Boc-Dmaa-D-Pro-Achc-Leu-OMe (**22a**)	-78.60
Boc-Dmaa-D-Pro-Achc-Leu-OMe (**22b**)	-71.50
Boc-Cys(Ph)-D-Pro-Achc-Leu-OMe (**23**)	-79.60
Boc-Dmaa-D-Pro-Gly-Leu-OMe (**33a**)	-63.05
Boc-Dmaa-D-Pro-Gly-Leu-OMe (**33b**)	-65.25
average	-71.33
st. dev.	4.42
median	-71.48
minimum	-79.60
maximum	-59.96
count	21

Table S4.17: Proline Cγ-Puckering[21]

Peptide Sequence	Proline Pucker Cα-Cβ-Cγ-Cδ (°)	Proline Pucker endo/exo
Boc-Dmaa-D-Pro-Acpc-Leu-NMe_2 (**3a**)	-41.5	endo
Boc-Dmaa-D-Pro-Acpc-Leu-NMe_2 (**3b**)	37.1	exo
Boc-Dmaa-D-Pro-Acpc-Leu-NMe_2 (**3c**)	-37.0	endo
Boc-Dmaa-D-Pro-Acpc-Leu-OMe (**4a**)	-36.2	endo
Boc-Dmaa-D-Pro-Acpc-Leu-OMe (**4b**)	-36.5	endo
Boc-Dmaa-D-Pro-Acpc-Leu-OMe (**4c**)	-39.0	endo
Boc-Dmaa-D-Pro-Acpc-Leu-OMe (**4d**)	-38.1	endo
Boc-Dmaa-D-Pro-Acpc-Leu-OMe (**4e**)	-39.0	endo
Boc-Cys(Ph)-D-Pro-Acpc-Leu-OMe (**5**)	39.3	exo
Boc-Leu-D-Pro-Acpc-Leu-OMe (**6**)	-39.7	endo
Boc-Dmaa-D-Pro-Acpc-Gly-OMe (**7a**)	36.2	exo
Boc-Dmaa-D-Pro-Acpc-Gly-OMe (**7b**)	37.6	exo
Boc-Dmaa-D-Pro-Acpc-Nle-NMe_2 (**8**)	37.4	exo
Boc-Dmaa-D-Pro-Acpc-Val-NMe_2 (**9**)	38.3	exo
Boc-Dmaa-D-Pro-Acpc-Val-OMe (**10**)	-39.3	endo
Boc-Dmaa-D-Pro-Acpc-Chg-NMe_2 (**11**)	37.2	exo
Boc-Dmaa-D-Pro-Acpc-Phe-NMe_2 (**12**)	37.3	exo
Boc-Dmaa-D-Pro-Acpc-Phe-OMe (**13**)	37.1	exo
Boc-Dmaa-D-Pro-Acpc-D-Phe-NMe_2 (**14**)	-41.4	endo
Boc-Dmaa-Pro-Acpc-Leu-OMe (**15**)	40.0	exo
Boc-Dmaa-D-Pro-Acbc-Leu-NMe_2 (**16a**)	37.7	exo
Boc-Dmaa-D-Pro-Acbc-Leu-NMe_2 (**16b**)	-37.8	endo
Boc-Dmaa-D-Pro-Acbc-Leu-NMe_2 (**16c**)	-36.3	endo
Boc-Dmaa-D-Pro-Acbc-Leu-OMe (**17a**)	-35.3	endo
Boc-Dmaa-D-Pro-Acbc-Leu-OMe (**17b**)	37.5	exo
Boc-Dmaa-D-Pro-Cle-Leu-OMe (**18a**)	38.6	exo
Boc-Dmaa-D-Pro-Cle-Leu-OMe (**18b**)	-38.6	endo
Boc-Dmaa-D-Pro-Aic-Leu-OMe (**19a**)	37.0	exo
Boc-Dmaa-D-Pro-Aic-Leu-OMe (**19b**)	-39.2	endo
Boc-Dmaa-D-Pro-Aic-D-Phe-NMe_2 (**20a**)	34.0	exo
Boc-Dmaa-D-Pro-Aic-D-Phe-NMe_2 (**20b**)	-42.1	endo
Boc-Dmaa-Pro-Aic-Leu-OMe (**21a**)	37.4	exo
Boc-Dmaa-Pro-Aic-Leu-OMe (**21b**)	37.3	exo
Boc-Dmaa-D-Pro-Achc-Leu-OMe (**22a**)	-34.7	endo
Boc-Dmaa-D-Pro-Achc-Leu-OMe (**22b**)	38.3	exo
Boc-Cys(Ph)-D-Pro-Achc-Leu-OMe (**23**)	41.9	exo
Boc-Dmaa-D-Pro-Aib-Leu-NMe_2 (**24**)	33.8	exo
Boc-Dmaa-D-Pro-Aib-Leu-OMe (**25**)	36.7	exo
Boc-Dmaa-D-Pro-Aib-Val-OMe (**26**)	37.4	exo
Boc-Dmaa-D-Pro-Aib-Phe-OMe (**27**)	-36.8	endo
Boc-Dmaa-D-Pro-Aib-3-Pal-NMe_2 (**28**)	-39.0	endo
Boc-Dmaa-D-Pro-Aib-2-Thi-NMe_2 (**29a**)	31.0	exo
Boc-Dmaa-D-Pro-Aib-2-Thi-NMe_2 (**29b**)	29.0	exo
Boc-Dmaa-Pro-Aib-Leu-OMe (**30**)	36.8	exo
Boc-Dmaa-D-Pro-Ala-Phe-OMe (**31**)	37.3	exo
Boc-Dmaa-D-Pro-Phe-Leu-NMe_2 (**32a**)	36.8	exo
Boc-Dmaa-D-Pro-Phe-Leu-NMe_2 (**32b**)	37.2	exo
Boc-Dmaa-D-Pro-Gly-Leu-OMe (**33a**)	-27.8	endo
Boc-Dmaa-D-Pro-Gly-Leu-OMe (**33b**)	38.8	exo
Boc-Keto-D-Pro-Aib-Phe-OMe (**34**)	-36.3	endo
Boc-Phe-Pro-Aib-(*R*)-α-Mba (**35**)	36.7	exo
2-Msa-Pro-D-Val-(*R*)-α-Mba (**36**)	-35.0	endo
Boc-His(τ-Bn)-Pro-Aib-(*R*)-α-Mba (**37**)	41.5	exo
average	6.1	***endo* count**
st. dev.	37.2	22
median	36.2	***exo* count**
minimum	-42.1	31
maximum	41.9	**total**
count	53	53

Table S4.18: Proline Cγ-*endo*-Puckering[21]

endo	Cα-Cβ-Cγ-Cδ (°)
Boc-Dmaa-D-Pro-Acpc-Leu-NMe_2 (**3a**)	-41.5
Boc-Dmaa-D-Pro-Acpc-Leu-NMe_2 (**3c**)	-37.0
Boc-Dmaa-D-Pro-Acpc-Leu-OMe (**4a**)	-36.2
Boc-Dmaa-D-Pro-Acpc-Leu-OMe (**4b**)	-36.5
Boc-Dmaa-D-Pro-Acpc-Leu-OMe (**4c**)	-39.0
Boc-Dmaa-D-Pro-Acpc-Leu-OMe (**4d**)	-38.1
Boc-Dmaa-D-Pro-Acpc-Leu-OMe (**4e**)	-39.0
Boc-Leu-D-Pro-Acpc-Leu-OMe (**6**)	-39.7
Boc-Dmaa-D-Pro-Acpc-Val-OMe (**10**)	-39.3
Boc-Dmaa-D-Pro-Acpc-D-Phe-NMe_2 (**14**)	-41.4
Boc-Dmaa-D-Pro-Acbc-Leu-NMe_2 (**16b**)	-37.8
Boc-Dmaa-D-Pro-Acbc-Leu-NMe_2 (**16c**)	-36.3
Boc-Dmaa-D-Pro-Acbc-Leu-OMe (**17a**)	-35.3
Boc-Dmaa-D-Pro-Cle-Leu-OMe (**18b**)	-38.6
Boc-Dmaa-D-Pro-Aic-Leu-OMe (**19b**)	-39.2
Boc-Dmaa-D-Pro-Aic-D-Phe-NMe_2 (**20b**)	-42.1
Boc-Dmaa-D-Pro-Achc-Leu-OMe (**22a**)	-34.7
Boc-Dmaa-D-Pro-Aib-Phe-OMe (**27**)	-36.8
Boc-Dmaa-D-Pro-Aib-3-Pal-NMe_2 (**28**)	-39.0
Boc-Dmaa-D-Pro-Gly-Leu-OMe (**33a**)	-27.8
Boc-Keto-D-Pro-Aib-Phe-OMe (**34**)	-36.3
2-Msa-Pro-D-Val-(*R*)-α-Mba (**36**)	-35.0
average	-37.6
st. dev.	3.0
median	-38.0
minimum	-42.1
maximum	-27.8
count	22

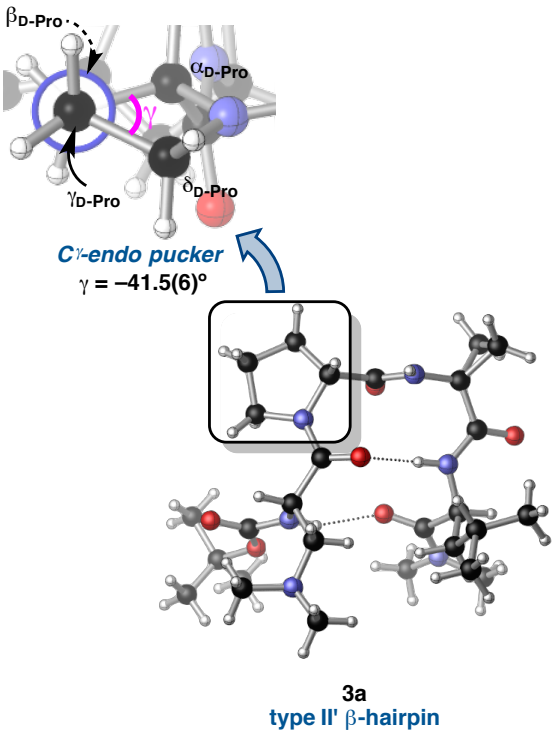

Table S4.19: Proline Cγ-*exo*-Puckering[21]

exo	Cα-Cβ-Cγ-Cδ (°)
Boc-Dmaa-D-Pro-Acpc-Leu-NMe_2 (**3b**)	37.1
Boc-Cys(Ph)-D-Pro-Acpc-Leu-OMe (**5**)	39.3
Boc-Dmaa-D-Pro-Acpc-Gly-OMe (**7a**)	36.2
Boc-Dmaa-D-Pro-Acpc-Gly-OMe (**7b**)	37.6
Boc-Dmaa-D-Pro-Acpc-Nle-NMe_2 (**8**)	37.4
Boc-Dmaa-D-Pro-Acpc-Val-NMe_2 (**9**)	38.3
Boc-Dmaa-D-Pro-Acpc-Chg-NMe_2 (**11**)	37.2
Boc-Dmaa-D-Pro-Acpc-Phe-NMe_2 (**12**)	37.3
Boc-Dmaa-D-Pro-Acpc-Phe-OMe (**13**)	37.1
Boc-Dmaa-Pro-Acpc-Leu-OMe (**15**)	40.0
Boc-Dmaa-D-Pro-Acbc-Leu-NMe_2 (**16a**)	37.7
Boc-Dmaa-D-Pro-Acbc-Leu-OMe (**17b**)	37.5
Boc-Dmaa-D-Pro-Cle-Leu-OMe (**18a**)	38.6
Boc-Dmaa-D-Pro-Aic-Leu-OMe (**19a**)	37.0
Boc-Dmaa-D-Pro-Aic-D-Phe-NMe_2 (**20a**)	34.0
Boc-Dmaa-Pro-Aic-Leu-OMe (**21a**)	37.4
Boc-Dmaa-Pro-Aic-Leu-OMe (**21b**)	37.3
Boc-Dmaa-D-Pro-Achc-Leu-OMe (**22b**)	38.3
Boc-Cys(Ph)-D-Pro-Achc-Leu-OMe (**23**)	41.9
Boc-Dmaa-D-Pro-Aib-Leu-NMe_2 (**24**)	33.8
Boc-Dmaa-D-Pro-Aib-Leu-OMe (**25**)	36.7
Boc-Dmaa-D-Pro-Aib-Val-OMe (**26**)	37.4
Boc-Dmaa-D-Pro-Aib-2-Thi-NMe_2 (**29a**)	31.0
Boc-Dmaa-D-Pro-Aib-2-Thi-NMe_2 (**29b**)	29.0
Boc-Dmaa-Pro-Aib-Leu-OMe (**30**)	36.8
Boc-Dmaa-D-Pro-Ala-Phe-OMe (**31**)	37.3
Boc-Dmaa-D-Pro-Phe-Leu-NMe_2 (**32a**)	36.8
Boc-Dmaa-D-Pro-Phe-Leu-NMe_2 (**32b**)	37.2
Boc-Dmaa-D-Pro-Gly-Leu-OMe (**33b**)	38.8
Boc-Phe-Pro-Aib-(*R*)-α-Mba (**35**)	36.7
Boc-His(τ-Bn)-Pro-Aib-(*R*)-α-Mba (**37**)	41.5
average	37.1
st. dev.	2.5
median	37.3
minimum	29.0
maximum	41.9
count	31

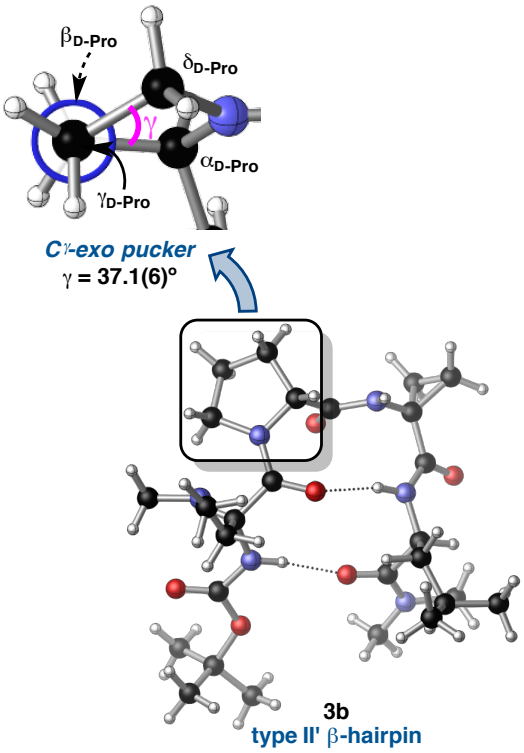

Table S4.20: Effect of Proline Cγ-Puckering on Backbone ϕ,ψ Dihedrals in Type II′ β-Turns

Type II' β-Turns	*i*+1		*i*+2		Proline Pucker		
	ϕ(*i*+1)	ψ(*i*+1)	ϕ(*i*+2)	ψ(*i*+2)	Cα-Cβ-Cγ-Cδ (°)	endo/exo	
Boc-Dmaa-D-Pro-Acpc-Leu-NMe_2 (**3a**)	63.6	-113.0	-77.2	-3.7	-41.5	endo	
Boc-Dmaa-D-Pro-Acpc-Leu-NMe_2 (**3b**)	62.9	-132.0	-78.1	-5.3	37.1	exo	
Boc-Leu-D-Pro-Acpc-Leu-OMe (**6**)	50.8	-134.1	-80.6	-5.9	-39.7	endo	
Boc-Dmaa-D-Pro-Acpc-Gly-OMe (**7a**)	69.1	-123.1	-76.4	-3.0	36.2	exo	
Boc-Dmaa-D-Pro-Acpc-Nle-NMe_2 (**8**)	62.0	-130.1	-74.4	-5.5	37.4	exo	
Boc-Dmaa-D-Pro-Acpc-Val-NMe_2 (**9**)	58.0	-133.0	-70.5	-10.3	38.3	exo	
Boc-Dmaa-D-Pro-Acpc-Chg-NMe_2 (**11**)	61.6	-129.8	-75.5	-3.6	37.2	exo	
Boc-Dmaa-D-Pro-Acpc-Phe-NMe_2 (**12**)	63.6	-125.7	-72.0	-9.2	37.3	exo	
Boc-Dmaa-D-Pro-Acpc-Phe-OMe (**13**)	58.6	-136.9	-84.3	8.8	37.1	exo	
Boc-Dmaa-D-Pro-Acpc-D-Phe-NMe_2 (**14**)	52.7	-135.3	-70.5	-8.6	-41.4	endo	
Boc-Dmaa-D-Pro-Acbc-Leu-NMe_2 (**16a**)	71.0	-128.0	-71.0	-20.6	37.7	exo	
Boc-Dmaa-D-Pro-Acbc-Leu-NMe_2 (**16b**)	67.9	-116.6	-66.8	-14.6	-37.8	endo	
Boc-Dmaa-D-Pro-Aic-D-Phe-NMe_2 (**20a**)	57.6	-134.6	-59.0	-31.4	34.0	exo	
Boc-Dmaa-D-Pro-Aic-D-Phe-NMe_2 (**20b**)	59.4	-134.2	-64.3	-14.6	-42.1	endo	
Boc-Dmaa-D-Pro-Aib-Leu-NMe_2 (**24**)	59.3	-129.9	-63.6	-14.7	33.8	exo	
Boc-Dmaa-D-Pro-Aib-Leu-OMe (**25**)	60.4	-136.0	-62.0	-21.3	36.7	exo	
Boc-Dmaa-D-Pro-Aib-Val-OMe (**26**)	63.1	-133.7	-68.1	-13.6	37.4	exo	
Boc-Dmaa-D-Pro-Aib-Phe-OMe (**27**)	54.4	-127.3	-58.5	-26.2	-36.8	endo	
Boc-Dmaa-D-Pro-Aib-3-Pal-NMe_2 (**28**)	52.6	-129.3	-59.9	-23.5	-39.0	endo	
Boc-Dmaa-D-Pro-Aib-2-Thi-NMe_2 (**29a**)	60.8	-130.7	-61.0	-23.2	31.0	exo	
Boc-Dmaa-D-Pro-Aib-2-Thi-NMe_2 (**29b**)	61.7	-132.1	-60.3	-22.5	29.0	exo	
Boc-Dmaa-D-Pro-Ala-Phe-OMe (**31**)	60.1	-139.6	-93.4	22.5	37.3	exo	
Boc-Keto-D-Pro-Aib-Phe-OMe (**34**)	62.1	-123.7	-61.4	-19.7	-36.3	endo	
average	60.6	-129.9	-69.9	-11.7	9.7	**endo count**	**% endo**
st. dev.	5.0	6.3	9.1	12.0	36.7	8	34.8
median	60.8	-130.7	-70.5	-13.6	34.0	**exo count**	**% exo**
minimum	50.8	-139.6	-93.4	-31.4	-42.1	15	65.2
maximum	71.0	-113.0	-58.5	22.5	38.3	**total**	**total**
count	23	23	23	23	23	23	100.0

Type II' β-Turns, *endo*	*i*+1		*i*+2		Proline Pucker		
	ϕ(*i*+1)	ψ(*i*+1)	ϕ(*i*+2)	ψ(*i*+2)	Cα-Cβ-Cγ-Cδ (°)	endo/exo	
Boc-Dmaa-D-Pro-Acpc-Leu-NMe_2 (**3a**)	63.6	-113.0	-77.2	-3.7	-41.5	endo	
Boc-Leu-D-Pro-Acpc-Leu-OMe (**6**)	50.8	-134.1	-80.6	-5.9	-39.7	endo	
Boc-Dmaa-D-Pro-Acpc-D-Phe-NMe_2 (**14**)	52.7	-135.3	-70.5	-8.6	-41.4	endo	
Boc-Dmaa-D-Pro-Acbc-Leu-NMe_2 (**16b**)	67.9	-116.6	-66.8	-14.6	-37.8	endo	
Boc-Dmaa-D-Pro-Aic-D-Phe-NMe_2 (**20b**)	59.4	-134.2	-64.3	-14.6	-42.1	endo	
Boc-Dmaa-D-Pro-Aib-Phe-OMe (**27**)	54.4	-127.3	-58.5	-26.2	-36.8	endo	
Boc-Dmaa-D-Pro-Aib-3-Pal-NMe_2 (**28**)	52.6	-129.3	-59.9	-23.5	-39.0	endo	
Boc-Keto-D-Pro-Aib-Phe-OMe (**34**)	62.1	-123.7	-61.4	-19.7	-36.3	endo	
average	57.9	-126.7	-67.4	-14.6	-39.3	**endo count**	**% endo**
st. dev.	6.2	8.4	8.1	8.2	2.2	8	100.0
median	56.9	-128.3	-65.6	-14.6	-39.4	**exo count**	**% exo**
minimum	50.8	-135.3	-80.6	-26.2	-42.1	0	0.0
maximum	67.9	-113.0	-58.5	-3.7	-36.3	**total**	**total**
count	8	8	8	8	8	8	100.0

Type II' β-Turns, *exo*	*i*+1		*i*+2		Proline Pucker		
	ϕ(*i*+1)	ψ(*i*+1)	ϕ(*i*+2)	ψ(*i*+2)	Cα-Cβ-Cγ-Cδ (°)	endo/exo	
Boc-Dmaa-D-Pro-Acpc-Leu-NMe_2 (**3b**)	62.9	-132.0	-78.1	-5.3	37.1	exo	
Boc-Dmaa-D-Pro-Acpc-Gly-OMe (**7a**)	69.1	-123.1	-76.4	-3.0	36.2	exo	
Boc-Dmaa-D-Pro-Acpc-Nle-NMe_2 (**8**)	62.0	-130.1	-74.4	-5.5	37.4	exo	
Boc-Dmaa-D-Pro-Acpc-Val-NMe_2 (**9**)	58.0	-133.0	-70.5	-10.3	38.3	exo	
Boc-Dmaa-D-Pro-Acpc-Chg-NMe_2 (**11**)	61.6	-129.8	-75.5	-3.6	37.2	exo	
Boc-Dmaa-D-Pro-Acpc-Phe-NMe_2 (**12**)	63.6	-125.7	-72.0	-9.2	37.3	exo	
Boc-Dmaa-D-Pro-Acpc-Phe-OMe (**13**)	58.6	-136.9	-84.3	8.8	37.1	exo	
Boc-Dmaa-D-Pro-Acbc-Leu-NMe_2 (**16a**)	71.0	-128.0	-71.0	-20.6	37.7	exo	
Boc-Dmaa-D-Pro-Aic-D-Phe-NMe_2 (**20a**)	57.6	-134.6	-59.0	-31.4	34.0	exo	
Boc-Dmaa-D-Pro-Aib-Leu-NMe_2 (**24**)	59.3	-129.9	-63.6	-14.7	33.8	exo	
Boc-Dmaa-D-Pro-Aib-Leu-OMe (**25**)	60.4	-136.0	-62.0	-21.3	36.7	exo	
Boc-Dmaa-D-Pro-Aib-Val-OMe (**26**)	63.1	-133.7	-68.1	-13.6	37.4	exo	
Boc-Dmaa-D-Pro-Aib-2-Thi-NMe_2 (**29a**)	60.8	-130.7	-61.0	-23.2	31.0	exo	
Boc-Dmaa-D-Pro-Aib-2-Thi-NMe_2 (**29b**)	61.7	-132.1	-60.3	-22.5	29.0	exo	
Boc-Dmaa-D-Pro-Ala-Phe-OMe (**31**)	60.1	-139.6	-93.4	22.5	37.3	exo	
average	62.0	-131.7	-71.3	-10.2	35.8	**endo count**	**% endo**
st. dev.	3.8	4.3	9.6	13.6	2.7	0	0.0
median	61.6	-132.0	-71.0	-10.3	37.1	**exo count**	**% exo**
minimum	57.6	-139.6	-93.4	-31.4	29.0	17	100.0
maximum	71.0	-123.1	-59.0	22.5	38.3	**total**	**total**
count	15	15	15	15	15	17	100.0

Table S4.21: Effect of Proline Cγ-Puckering on Backbone ϕ,ψ Dihedrals in Type I′ β-Turns

Type I' β-Turns	*i*+1		*i*+2		Proline Pucker		
	ϕ(*i*+1)	ψ(*i*+1)	ϕ(*i*+2)	ψ(*i*+2)	Cα-Cβ-Cγ-Cδ (°)	endo/exo	
Boc-Dmaa-D-Pro-Acpc-Leu-NMe_2 (**3c**)	64.3	15.2	71.9	14.9	-37.0	endo	
Boc-Dmaa-D-Pro-Acpc-Leu-OMe (**4a**)	62.4	17.7	72.7	11.9	-36.2	endo	
Boc-Dmaa-D-Pro-Acpc-Leu-OMe (**4b**)	61.1	21.8	71.0	11.4	-36.5	endo	
Boc-Dmaa-D-Pro-Acpc-Leu-OMe (**4c**)	63.8	12.6	71.7	12.3	-39.0	endo	
Boc-Dmaa-D-Pro-Acpc-Leu-OMe (**4d**)	61.6	19.3	73.0	10.9	-38.1	endo	
Boc-Dmaa-D-Pro-Acpc-Leu-OMe (**4e**)	62.8	13.3	74.6	15.1	-39.0	endo	
Boc-Cys(Ph)-D-Pro-Acpc-Leu-OMe (**5**)	69.5	13.7	75.1	6.9	39.3	exo	
Boc-Dmaa-D-Pro-Acpc-Gly-OMe (**7b**)	67.9	15.8	73.5	11.7	37.6	exo	
Boc-Dmaa-D-Pro-Acpc-Val-OMe (**10**)	61.8	13.4	75.4	6.0	-39.3	endo	
Boc-Dmaa-D-Pro-Acbc-Leu-NMe_2 (**16c**)	65.7	14.2	67.1	28.7	-36.3	endo	
Boc-Dmaa-D-Pro-Acbc-Leu-OMe (**17a**)	63.6	14.6	65.0	26.1	-35.3	endo	
Boc-Dmaa-D-Pro-Acbc-Leu-OMe (**17b**)	65.0	17.9	66.2	20.8	37.5	exo	
Boc-Dmaa-D-Pro-Cle-Leu-OMe (**18a**)	67.8	18.0	63.6	20.9	38.6	exo	
Boc-Dmaa-D-Pro-Cle-Leu-OMe (**18b**)	61.4	19.7	62.3	24.9	-38.6	endo	
Boc-Dmaa-D-Pro-Aic-Leu-OMe (**19a**)	71.2	17.1	59.3	37.1	37.0	exo	
Boc-Dmaa-D-Pro-Aic-Leu-OMe (**19b**)	62.4	29.0	67.3	17.1	-39.2	endo	
Boc-Dmaa-D-Pro-Achc-Leu-OMe (**22a**)	61.3	16.7	56.1	30.7	-34.7	endo	
Boc-Dmaa-D-Pro-Achc-Leu-OMe (**22b**)	71.1	12.4	55.9	29.6	38.3	exo	
Boc-Cys(Ph)-D-Pro-Achc-Leu-OMe (**23**)	77.6	0.8	65.4	12.3	41.9	exo	
Boc-Dmaa-D-Pro-Gly-Leu-OMe (**33a**)	62.0	18.1	82.9	6.7	-27.8	endo	
Boc-Dmaa-D-Pro-Gly-Leu-OMe (**33b**)	66.7	14.8	81.1	4.1	38.8	exo	
average	65.3	16.0	69.1	17.1	-8.0	**endo count**	**% endo**
st. dev.	4.3	5.1	7.3	9.3	37.6	13	61.9
median	63.8	15.8	71.0	14.9	-35.3	**exo count**	**% exo**
minimum	61.1	0.8	55.9	4.1	-39.3	8	38.1
maximum	77.6	29.0	82.9	37.1	41.9	**total**	**total**
count	21	21	21	21	21	21	100.0

Type I' β-Turns, *endo*	*i*+1		*i*+2		Proline Pucker		
	ϕ(*i*+1)	ψ(*i*+1)	ϕ(*i*+2)	ψ(*i*+2)	Cα-Cβ-Cγ-Cδ (°)	endo/exo	
Boc-Dmaa-D-Pro-Acpc-Leu-NMe_2 (**3c**)	64.3	15.2	71.9	14.9	-37.0	endo	
Boc-Dmaa-D-Pro-Acpc-Leu-OMe (**4a**)	62.4	17.7	72.7	11.9	-36.2	endo	
Boc-Dmaa-D-Pro-Acpc-Leu-OMe (**4b**)	61.1	21.8	71.0	11.4	-36.5	endo	
Boc-Dmaa-D-Pro-Acpc-Leu-OMe (**4c**)	63.8	12.6	71.7	12.3	-39.0	endo	
Boc-Dmaa-D-Pro-Acpc-Leu-OMe (**4d**)	61.6	19.3	73.0	10.9	-38.1	endo	
Boc-Dmaa-D-Pro-Acpc-Leu-OMe (**4e**)	62.8	13.3	74.6	15.1	-39.0	endo	
Boc-Dmaa-D-Pro-Acpc-Val-OMe (**10**)	61.8	13.4	75.4	6.0	-39.3	endo	
Boc-Dmaa-D-Pro-Acbc-Leu-NMe_2 (**16c**)	65.7	14.2	67.1	28.7	-36.3	endo	
Boc-Dmaa-D-Pro-Acbc-Leu-OMe (**17a**)	63.6	14.6	65.0	26.1	-35.3	endo	
Boc-Dmaa-D-Pro-Cle-Leu-OMe (**18b**)	61.4	19.7	62.3	24.9	-38.6	endo	
Boc-Dmaa-D-Pro-Aic-Leu-OMe (**19b**)	62.4	29.0	67.3	17.1	-39.2	endo	
Boc-Dmaa-D-Pro-Achc-Leu-OMe (**22a**)	61.3	16.7	56.1	30.7	-34.7	endo	
Boc-Dmaa-D-Pro-Gly-Leu-OMe (**33a**)	62.0	18.1	82.9	6.7	-27.8	endo	
average	62.6	17.4	70.1	16.7	-36.7	**endo count**	**% endo**
st. dev.	1.4	4.5	6.7	8.3	3.1	13	100.0
median	62.4	16.7	71.7	14.9	-37.0	**exo count**	**% exo**
minimum	61.1	12.6	56.1	6.0	-39.3	0	0.0
maximum	65.7	29.0	82.9	30.7	-27.8	**total**	**total**
count	13	13	13	13	13	13	100.0

Type I' β-Turns, *exo*	*i*+1		*i*+2		Proline Pucker		
	ϕ(*i*+1)	ψ(*i*+1)	ϕ(*i*+2)	ψ(*i*+2)	Cα-Cβ-Cγ-Cδ (°)	endo/exo	
Boc-Cys(Ph)-D-Pro-Acpc-Leu-OMe (**5**)	69.5	13.7	75.1	6.9	39.3	exo	
Boc-Dmaa-D-Pro-Acpc-Gly-OMe (**7b**)	67.9	15.8	73.5	11.7	37.6	exo	
Boc-Dmaa-D-Pro-Acbc-Leu-OMe (**17b**)	65.0	17.9	66.2	20.8	37.5	exo	
Boc-Dmaa-D-Pro-Cle-Leu-OMe (**18a**)	67.8	18.0	63.6	20.9	38.6	exo	
Boc-Dmaa-D-Pro-Aic-Leu-OMe (**19a**)	71.2	17.1	59.3	37.1	37.0	exo	
Boc-Dmaa-D-Pro-Achc-Leu-OMe (**22b**)	71.1	12.4	55.9	29.6	38.3	exo	
Boc-Cys(Ph)-D-Pro-Achc-Leu-OMe (**23**)	77.6	0.8	65.4	12.3	41.9	exo	
Boc-Dmaa-D-Pro-Gly-Leu-OMe (**33b**)	66.7	14.8	81.1	4.1	38.8	exo	
average	69.6	13.8	67.5	17.9	38.6	**endo count**	**% endo**
st. dev.	3.9	5.6	8.5	11.4	1.5	0	0.0
median	68.7	15.3	65.8	16.6	38.5	**exo count**	**% exo**
minimum	65.0	0.8	55.9	4.1	37.0	8	100.0
maximum	77.6	18.0	81.1	37.1	41.9	**total**	**total**
count	8	8	8	8	8	8	100.0

Table S4.22: Effect of Proline Cγ-Puckering on Backbone ϕ,ψ Dihedrals in Type II β-Turns

Type II β-Turns	*i*+1		*i*+2		Proline Pucker		
	ϕ(*i*+1)	ψ(*i*+1)	ϕ(*i*+2)	ψ(*i*+2)	Cα-Cβ-Cγ-Cδ (°)	endo/exo	
Boc-Dmaa-Pro-Acpc-Leu-OMe (**15**)	-51.0	132.3	76.8	-0.1	40.0	exo	
Boc-Dmaa-Pro-Aic-Leu-OMe (**21a**)	-51.3	137.4	62.5	26.8	37.4	exo	
Boc-Dmaa-Pro-Aic-Leu-OMe (**21b**)	-54.3	140.0	61.6	28.6	37.3	exo	
Boc-Dmaa-Pro-Aib-Leu-OMe (**30**)	-52.0	138.0	63.5	22.9	36.8	exo	
Boc-Phe-Pro-Aib-(*R*)-α-Mba (**35**)	-51.3	127.9	61.6	24.8	36.7	exo	
2-Msa-Pro-D-Val-(*R*)-α-Mba (**36**)	-60.6	139.1	79.8	3.6	-35.0	endo	
average	-53.4	135.8	67.6	17.8	25.5	**endo count**	**% endo**
st. dev.	3.7	4.7	8.3	12.6	29.7	1	16.7
median	-51.7	137.7	63.0	23.9	37.1	**exo count**	**% exo**
minimum	-60.6	127.9	61.6	-0.1	-35.0	5	83.3
maximum	-51.0	140.0	79.8	28.6	40.0	**total**	**total**
count	6	6	6	6	6	6	100.0
Type II β-Turns	*i*+1		*i*+2		Proline Pucker		
	ϕ(*i*+1)	ψ(*i*+1)	ϕ(*i*+2)	ψ(*i*+2)	Cα-Cβ-Cγ-Cδ (°)	endo/exo	
Boc-Dmaa-Pro-Acpc-Leu-OMe (**15**)	-51.0	132.3	76.8	-0.1	40.0	exo	
Boc-Dmaa-Pro-Aic-Leu-OMe (**21a**)	-51.3	137.4	62.5	26.8	37.4	exo	
Boc-Dmaa-Pro-Aic-Leu-OMe (**21b**)	-54.3	140.0	61.6	28.6	37.3	exo	
Boc-Dmaa-Pro-Aib-Leu-OMe (**30**)	-52.0	138.0	63.5	22.9	36.8	exo	
Boc-Phe-Pro-Aib-(*R*)-α-Mba (**35**)	-51.3	127.9	61.6	24.8	36.7	exo	
average	-52.0	135.1	65.2	20.6	37.6	**endo count**	**% endo**
st. dev.	1.3	4.9	6.5	11.8	1.4	0	0.0
median	-51.3	137.4	62.5	24.8	37.3	**exo count**	**% exo**
minimum	-54.3	127.9	61.6	-0.1	36.7	5	100.0
maximum	-51.0	140.0	76.8	28.6	40.0	**total**	**total**
count	5	5	5	5	5	5	100.0

Table S4.23: Summary of Proline Cγ-Puckering Across Canonical β-Turn Types

all peptides		type II'		type I'		type II		type I	
% endo	*% exo*	*% endo*	*% exo*	*% endo*	*% exo*	*% endo*	*% exo*	*% endo*	*% exo*
41.5	58.5	34.8	65.2	61.9	38.1	83.3	16.7	0.0	100.0

Table S4.24: Summary of the Effect of Proline Cγ-Puckering on Backbone ϕ,ψ Dihedrals

	type II'			
	ϕ(*i*+1)	ψ(*i*+1)	ϕ(*i*+2)	ψ(*i*+2)
average	60.5 ± 5.0°	–129.9 ± 6.3°	–69.9 ± 9.1°	–11.7 ± 12.0°
endo pucker	57.9 ± 6.2°	–126.7 ± 8.4°	–67.4 ± 8.1°	–14.6 ± 8.2°
exo pucker	62.0 ± 3.8°	–131.7 ± 4.3°	–71.3 ± 9.6°	–10.2 ± 13.6°
	type I'			
	ϕ(*i*+1)	ψ(*i*+1)	ϕ(*i*+2)	ψ(*i*+2)
average	65.3 ± 4.3°	16.0 ± 5.1°	–69.1 ± 7.3°	17.1 ± 9.3°
endo pucker	62.6 ± 1.4°	17.4 ± 4.5°	70.1 ± 6.7°	16.7 ± 8.3°
exo pucker	69.6 ± 3.8°	13.8 ± 5.6°	67.5 ± 8.5°	17.9 ± 11.4°
	type II			
	ϕ(*i*+1)	ψ(*i*+1)	ϕ(*i*+2)	ψ(*i*+2)
average	–53.4 ± 3.7°	135.8 ± 4.7°	67.6 ± 8.3°	17.8 ± 12.6°
endo pucker	–60.6°	139.1°	79.8°	3.6°
exo pucker	–52.0 ± 1.3°	135.1 ± 4.9°	65.2 ± 6.5°	20.6 ± 11.7°

Table S4.25: Main-Chain Angles (τ)[22]

Peptide Sequence	τ(*i*) (°)	τ(*i*+1) (°)	τ(*i*+2) (°)	τ(*i*+3) (°)
Boc-Dmaa-D-Pro-Acpc-Leu-NMe_2 (**3a**)	109.4	111.9	118.1	108.0
Boc-Dmaa-D-Pro-Acpc-Leu-NMe_2 (**3b**)	108.2	110.0	116.5	111.0
Boc-Dmaa-D-Pro-Acpc-Leu-NMe_2 (**3c**)	110.3	114.3	117.4	110.5
Boc-Dmaa-D-Pro-Acpc-Leu-OMe (**4a**)	110.1	114.6	117.0	112.2
Boc-Dmaa-D-Pro-Acpc-Leu-OMe (**4b**)	109.6	114.3	117.7	112.6
Boc-Dmaa-D-Pro-Acpc-Leu-OMe (**4c**)	111.0	115.1	117.0	111.7
Boc-Dmaa-D-Pro-Acpc-Leu-OMe (**4d**)	109.4	113.6	117.3	112.7
Boc-Dmaa-D-Pro-Acpc-Leu-OMe (**4e**)	110.8	115.0	118.0	110.4
Boc-Cys(Ph)-D-Pro-Acpc-Leu-OMe (**5**)	109.3	113.4	116.5	110.7
Boc-Leu-D-Pro-Acpc-Leu-OMe (**6**)	108.7	110.8	117.0	110.0
Boc-Dmaa-D-Pro-Acpc-Gly-OMe (**7a**)	110.9	108.9	117.0	112.7
Boc-Dmaa-D-Pro-Acpc-Gly-OMe (**7b**)	111.1	113.4	115.7	114.6
Boc-Dmaa-D-Pro-Acpc-Nle-NMe_2 (**8**)	107.0	109.4	117.4	109.8
Boc-Dmaa-D-Pro-Acpc-Val-NMe_2 (**9**)	106.8	109.3	117.7	109.1
Boc-Dmaa-D-Pro-Acpc-Val-OMe (**10**)	109.8	114.8	117.2	111.5
Boc-Dmaa-D-Pro-Acpc-Chg-NMe_2 (**11**)	107.0	109.3	117.4	109.3
Boc-Dmaa-D-Pro-Acpc-Phe-NMe_2 (**12**)	108.2	110.1	116.9	110.1
Boc-Dmaa-D-Pro-Acpc-Phe-OMe (**13**)	110.7	109.9	116.9	108.8
Boc-Dmaa-D-Pro-Acpc-D-Phe-NMe_2 (**14**)	108.9	109.6	117.7	106.9
Boc-Dmaa-Pro-Acpc-Leu-OMe (**15**)	109.8	109.9	117.8	107.3
Boc-Dmaa-D-Pro-Acbc-Leu-NMe_2 (**16a**)	108.1	107.9	111.8	110.4
Boc-Dmaa-D-Pro-Acbc-Leu-NMe_2 (**16b**)	113.4	109.9	114.4	108.5
Boc-Dmaa-D-Pro-Acbc-Leu-NMe_2 (**16c**)	110.1	115.4	112.5	110.5
Boc-Dmaa-D-Pro-Acbc-Leu-OMe (**17a**)	110.8	115.8	112.3	110.9
Boc-Dmaa-D-Pro-Acbc-Leu-OMe (**17b**)	110.8	115.3	112.3	110.9
Boc-Dmaa-D-Pro-Cle-Leu-OMe (**18a**)	111.0	114.8	111.7	110.2
Boc-Dmaa-D-Pro-Cle-Leu-OMe (**18b**)	110.8	116.4	111.3	110.3
Boc-Dmaa-D-Pro-Aic-Leu-OMe (**19a**)	111.4	114.6	110.6	111.6
Boc-Dmaa-D-Pro-Aic-Leu-OMe (**19b**)	113.5	114.5	112.6	110.0
Boc-Dmaa-D-Pro-Aic-D-Phe-NMe_2 (**20a**)	107.3	110.6	112.2	109.9
Boc-Dmaa-D-Pro-Aic-D-Phe-NMe_2 (**20b**)	107.5	111.6	112.4	108.5
Boc-Dmaa-Pro-Aic-Leu-OMe (**21a**)	108.5	109.5	112.2	108.7
Boc-Dmaa-Pro-Aic-Leu-OMe (**21b**)	107.3	109.7	111.8	108.6
Boc-Dmaa-D-Pro-Achc-Leu-OMe (**22a**)	111.9	117.4	110.8	109.4
Boc-Dmaa-D-Pro-Achc-Leu-OMe (**22b**)	112.0	115.2	109.8	110.0
Boc-Cys(Ph)-D-Pro-Achc-Leu-OMe (**23**)	110.3	115.2	110.2	111.0
Boc-Dmaa-D-Pro-Aib-Leu-NMe_2 (**24**)	109.7	111.0	112.0	109.6
Boc-Dmaa-D-Pro-Aib-Leu-OMe (**25**)	109.6	110.1	111.7	107.8
Boc-Dmaa-D-Pro-Aib-Val-OMe (**26**)	105.9	109.8	112.0	110.1
Boc-Dmaa-D-Pro-Aib-Phe-OMe (**27**)	107.0	111.4	111.0	110.1
Boc-Dmaa-D-Pro-Aib-3-Pal-NMe_2 (**28**)	108.5	111.3	112.3	108.2
Boc-Dmaa-D-Pro-Aib-2-Thi-NMe_2 (**29a**)	108.4	111.1	110.9	110.9
Boc-Dmaa-D-Pro-Aib-2-Thi-NMe_2 (**29b**)	108.0	110.2	111.6	111.1
Boc-Dmaa-Pro-Aib-Leu-OMe (**30**)	108.0	109.1	111.8	109.0
Boc-Dmaa-D-Pro-Ala-Phe-OMe (**31**)	110.6	109.3	111.8	108.6
Boc-Dmaa-D-Pro-Phe-Leu-NMe_2 (**32a**)	109.0	110.2	107.2	109.8
Boc-Dmaa-D-Pro-Phe-Leu-NMe_2 (**32b**)	107.0	111.4	109.5	110.8
Boc-Dmaa-D-Pro-Gly-Leu-OMe (**33a**)	111.1	115.5	115.6	115.3
Boc-Dmaa-D-Pro-Gly-Leu-OMe (**33b**)	109.9	113.8	115.4	113.9
Boc-Keto-D-Pro-Aib-Phe-OMe (**34**)	110.3	110.6	111.1	109.5
Boc-Phe-Pro-Aib-(*R*)-α-Mba (**35**)	108.9	112.3	112.3	N/A
2-Msa-Pro-D-Val-(*R*)-α-Mba (**36**)	N/A	109.7	113.1	N/A
Boc-His(τ-Bn)-Pro-Aib-(*R*)-α-Mba (**37**)	109.4	116.0	112.6	113.9
average	109.5	112.2	113.9	110.4
st. dev.	1.7	2.5	2.9	1.8
median	109.6	111.4	112.5	110.1
minimum	105.9	107.9	107.2	106.9
maximum	113.5	117.4	118.1	115.3
count	52	53	53	51

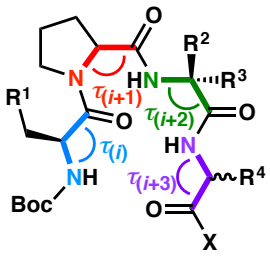

Table S4.26: Positional Distribution of Main-Chain Angles (τ)[22]

Bin	τ (°) Count	τ(*i*) (°) Count	τ(*i*+1) (°) Count	τ(*i*+2) (°) Count	τ(*i*+3) (°) Count
100-102	0	0	0	0	0
103-104	0	0	0	0	0
105-106	3	2	0	0	1
107-108	31	18	2	1	10
109-110	76	23	21	6	26
111-112	47	7	8	22	10
113-114	17	2	11	2	2
115-116	18	0	10	7	1
117-118	16	0	1	15	0
119-120	0	0	0	0	0
sum	208	52	53	53	50
average	111.5	109.5	112.2	113.9	110.3
st. dev.	2.8	1.7	2.5	2.9	1.7
median	110.8	109.6	111.4	112.5	110.1
minimum	105.9	105.9	107.9	107.2	106.9
maximum	118.1	113.5	117.4	118.1	115.3
count	208	52	53	53	50

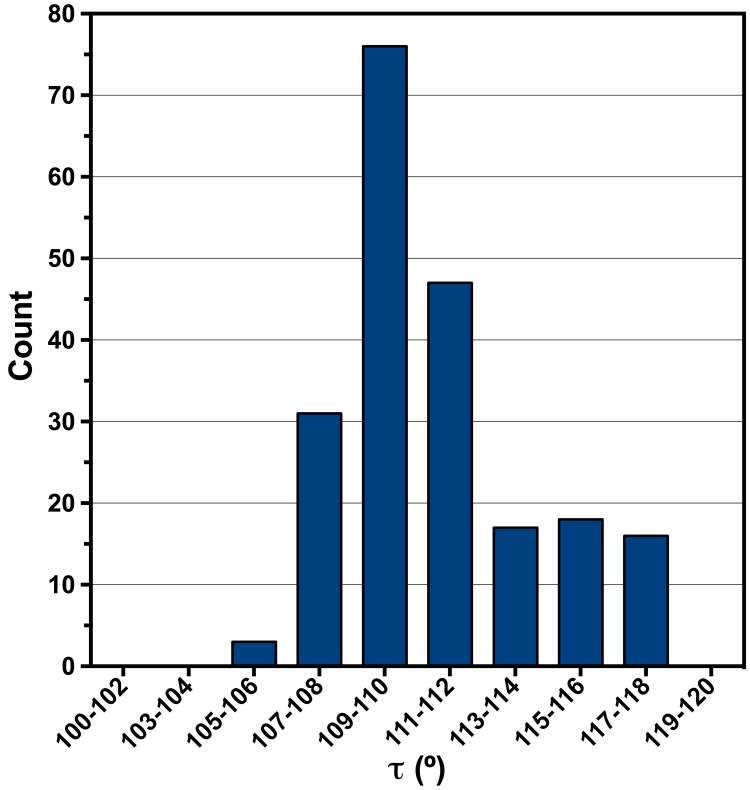

Figure S4.08: Histogram showing the distribution of τ angles across all peptides.

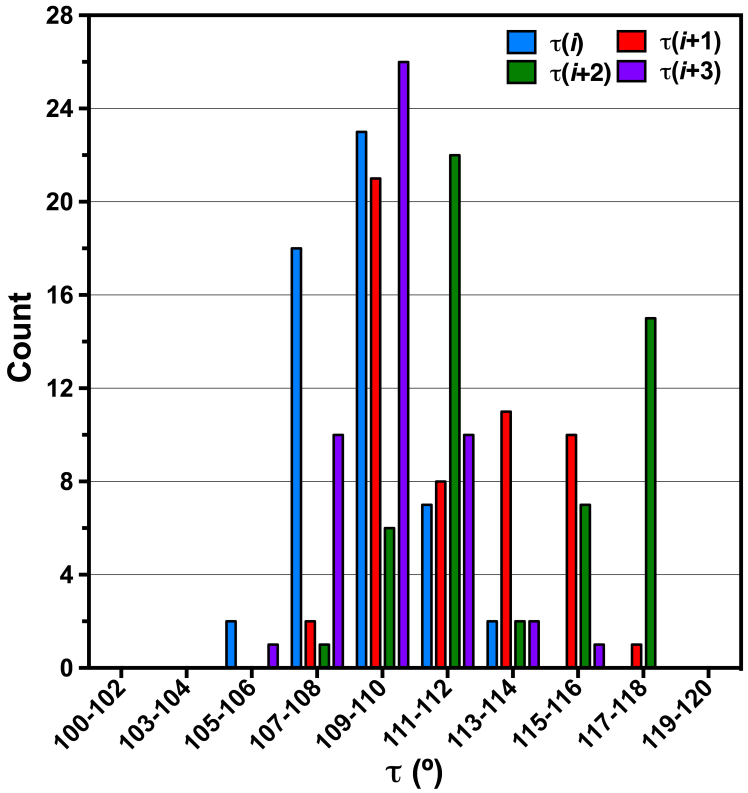

Figure S4.09: Histogram showing the positional distribution of τ angles across all peptides.

Table S4.27: Main-Chain Angles (τ) in Types II/II′ β-Turns

Type II/II' β-Turns	τ(*i*) (°)	τ(*i*+1) (°)	τ(*i*+2) (°)	τ(*i*+3) (°)	
Boc-Dmaa-D-Pro-Acpc-Leu-NMe_2 (**3a**)	109.4	111.9	118.1	108.0	
Boc-Dmaa-D-Pro-Acpc-Leu-NMe_2 (**3b**)	108.2	110.0	116.5	111.0	
Boc-Leu-D-Pro-Acpc-Leu-OMe (**6**)	108.7	110.8	117.0	110.0	
Boc-Dmaa-D-Pro-Acpc-Gly-OMe (**7a**)	110.9	108.9	117.0	112.7	
Boc-Dmaa-D-Pro-Acpc-Nle-NMe_2 (**8**)	107.0	109.4	117.4	109.8	
Boc-Dmaa-D-Pro-Acpc-Val-NMe_2 (**9**)	108.2	110.1	116.9	110.1	
Boc-Dmaa-D-Pro-Acpc-Chg-NMe_2 (**11**)	107.0	109.3	117.4	109.3	
Boc-Dmaa-D-Pro-Acpc-Phe-NMe_2 (**12**)	108.2	110.1	116.9	110.1	
Boc-Dmaa-D-Pro-Acpc-Phe-OMe (**13**)	110.7	109.9	116.9	108.8	
Boc-Dmaa-D-Pro-Acpc-D-Phe-NMe_2 (**14**)	108.9	109.6	117.7	106.9	
Boc-Dmaa-Pro-Acpc-Leu-OMe (**15**)	109.8	109.9	117.8	107.3	
Boc-Dmaa-D-Pro-Acbc-Leu-NMe_2 (**16a**)	108.1	107.9	111.8	110.4	
Boc-Dmaa-D-Pro-Acbc-Leu-NMe_2 (**16b**)	113.4	109.9	114.4	108.5	
Boc-Dmaa-D-Pro-Aic-D-Phe-NMe_2 (**20a**)	107.3	110.6	112.2	109.9	
Boc-Dmaa-D-Pro-Aic-D-Phe-NMe_2 (**20b**)	107.5	111.6	112.4	108.5	
Boc-Dmaa-Pro-Aic-Leu-OMe (**21a**)	108.5	109.5	112.2	108.7	
Boc-Dmaa-Pro-Aic-Leu-OMe (**21b**)	107.3	109.7	111.8	108.6	
Boc-Dmaa-D-Pro-Aib-Leu-NMe_2 (**24**)	109.7	111.0	112.0	109.6	
Boc-Dmaa-D-Pro-Aib-Leu-OMe (**25**)	109.6	110.1	111.7	107.8	
Boc-Dmaa-D-Pro-Aib-Val-OMe (**26**)	108.0	110.2	111.6	111.1	
Boc-Dmaa-D-Pro-Aib-Phe-OMe (**27**)	107.0	111.4	111.0	110.1	
Boc-Dmaa-D-Pro-Aib-3-Pal-NMe_2 (**28**)	108.5	111.3	112.3	108.2	
Boc-Dmaa-D-Pro-Aib-2-Thi-NMe_2 (**29a**)	108.4	111.1	110.9	110.9	
Boc-Dmaa-D-Pro-Aib-2-Thi-NMe_2 (**29b**)	108.0	110.2	111.6	111.1	
Boc-Dmaa-Pro-Aib-Leu-OMe (**30**)	108.0	109.1	111.8	109.0	
Boc-Dmaa-D-Pro-Ala-Phe-OMe (**31**)	110.6	109.3	111.8	108.6	
Boc-Keto-D-Pro-Aib-Phe-OMe (**34**)	110.3	110.6	111.1	109.5	
Boc-Phe-Pro-Aib-(*R*)-α-Mba (**35**)	108.9	112.3	112.3	N/A	
2-Msa-Pro-D-Val-(*R*)-α-Mba (**36**)	N/A	109.7	113.1	N/A	**All Type II/II'**
average	108.8	110.2	114.0	109.4	110.6
st. dev.	1.5	1.0	2.7	1.3	2.7
median	108.5	110.1	112.3	109.5	110.1
minimum	107.0	107.9	110.9	106.9	106.9
maximum	113.4	112.3	118.1	112.7	118.1
count	28	29	29	27	113.0

Table S4.28: Positional Distribution of Main-Chain Angles (τ) in Types II/II′ β-Turns

bin	τ(*i*) (°) Count	τ(*i*+1) (°) Count	τ(*i*+2) (°) Count	τ(*i*+3) (°) Count
100-102	0	0	0	0
103-104	0	0	0	0
105-106	0	0	0	1
107-108	19	2	0	10
109-110	8	20	1	12
111-112	0	7	15	4
113-114	1	0	2	0
115-116	0	0	4	0
117-118	0	0	7	0
119-120	0	0	0	0
sum	28	29	29	27
average	108.7	110.1	114.0	109.4
st. dev.	1.6	1.0	2.7	1.3
median	108.5	109.9	112.3	109.3
minimum	105.9	107.9	110.9	106.9
maximum	113.4	112.3	118.1	112.7
count	28	29	29	27

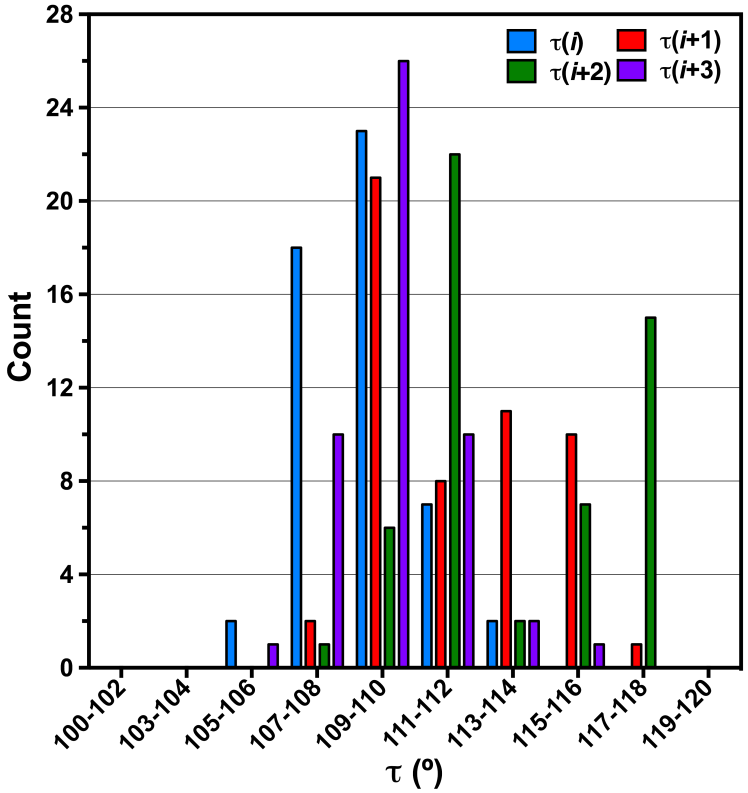

Figure S4.10: Histogram showing the distribution of τ angles in type II/II′ β-turns (reproduced from Figure 11h in the manuscript).

Table S4.29: Main-Chain Angles (τ) in Types I/I′ β-Turns

Type I/I' β-Turns	τ(*i*) (°)	τ(*i*+1) (°)	τ(*i*+2) (°)	τ(*i*+3) (°)	
Boc-Dmaa-D-Pro-Acpc-Leu-NMe_2 (**3c**)	110.3	114.3	117.4	110.5	
Boc-Dmaa-D-Pro-Acpc-Leu-OMe (**4a**)	110.1	114.6	117.0	112.2	
Boc-Dmaa-D-Pro-Acpc-Leu-OMe (**4b**)	109.6	114.3	117.7	112.6	
Boc-Dmaa-D-Pro-Acpc-Leu-OMe (**4c**)	111.0	115.1	117.0	111.7	
Boc-Dmaa-D-Pro-Acpc-Leu-OMe (**4d**)	109.4	113.6	117.3	112.7	
Boc-Dmaa-D-Pro-Acpc-Leu-OMe (**4e**)	110.8	115.0	118.0	110.4	
Boc-Cys(Ph)-D-Pro-Acpc-Leu-OMe (**5**)	109.3	113.4	116.5	110.7	
Boc-Dmaa-D-Pro-Acpc-Gly-OMe (**7b**)	111.1	113.4	115.7	114.6	
Boc-Dmaa-D-Pro-Acpc-Val-OMe (**10**)	109.8	114.8	117.2	111.5	
Boc-Dmaa-D-Pro-Acbc-Leu-NMe_2 (**16c**)	110.1	115.4	112.5	110.5	
Boc-Dmaa-D-Pro-Acbc-Leu-OMe (**17a**)	110.8	115.8	112.3	110.9	
Boc-Dmaa-D-Pro-Acbc-Leu-OMe (**17b**)	110.8	115.3	112.3	110.9	
Boc-Dmaa-D-Pro-Cle-Leu-OMe (**18a**)	111.0	114.8	111.7	110.2	
Boc-Dmaa-D-Pro-Cle-Leu-OMe (**18b**)	110.8	116.4	111.3	110.3	
Boc-Dmaa-D-Pro-Aic-Leu-OMe (**19a**)	111.4	114.6	110.6	111.6	
Boc-Dmaa-D-Pro-Aic-Leu-OMe (**19b**)	113.5	114.5	112.6	110.0	
Boc-Dmaa-D-Pro-Achc-Leu-OMe (**22a**)	111.9	117.4	110.8	109.4	
Boc-Dmaa-D-Pro-Achc-Leu-OMe (**22b**)	112.0	115.2	109.8	110.0	
Boc-Cys(Ph)-D-Pro-Achc-Leu-OMe (**23**)	110.3	115.2	110.2	111.0	
Boc-Dmaa-D-Pro-Gly-Leu-OMe (**33a**)	111.1	115.5	115.6	115.3	
Boc-Dmaa-D-Pro-Gly-Leu-OMe (**33b**)	109.9	113.8	115.4	113.9	
Boc-His(τ-Bn)-Pro-Aib-(*R*)-α-Mba	109.4	116.0	112.6	N/A	**All Type I'**
average	110.7	114.9	114.2	111.5	112.8
st. dev.	1.0	1.0	2.9	1.6	2.5
median	110.8	114.9	114.0	110.9	112.3
minimum	109.3	113.4	109.8	109.4	109.3
maximum	113.5	117.4	118.0	115.3	118.0
count	22	22	22	21	87.0

Table S4.30: Positional Distribution of Main-Chain Angles (τ) in Types I/I′ β-Turns

bin	τ(*i*) (°) Count	τ(*i*+1) (°) Count	τ(*i*+2) (°) Count	τ(*i*+3) (°) Count
100-102	0	0	0	0
103-104	0	0	0	0
105-106	0	0	0	0
107-108	0	0	0	0
109-110	14	0	4	11
111-112	7	0	7	7
113-114	1	11	0	2
115-116	0	10	4	1
117-118	0	1	7	0
119-120	0	0	0	0
sum	22	22	22	21
average	110.7	114.9	114.2	111.5
st. dev.	1.0	1.0	2.9	1.6
median	110.8	114.9	114.0	110.9
minimum	109.3	113.4	109.8	109.4
maximum	113.5	117.4	118.0	115.3
count	22	22	22	21

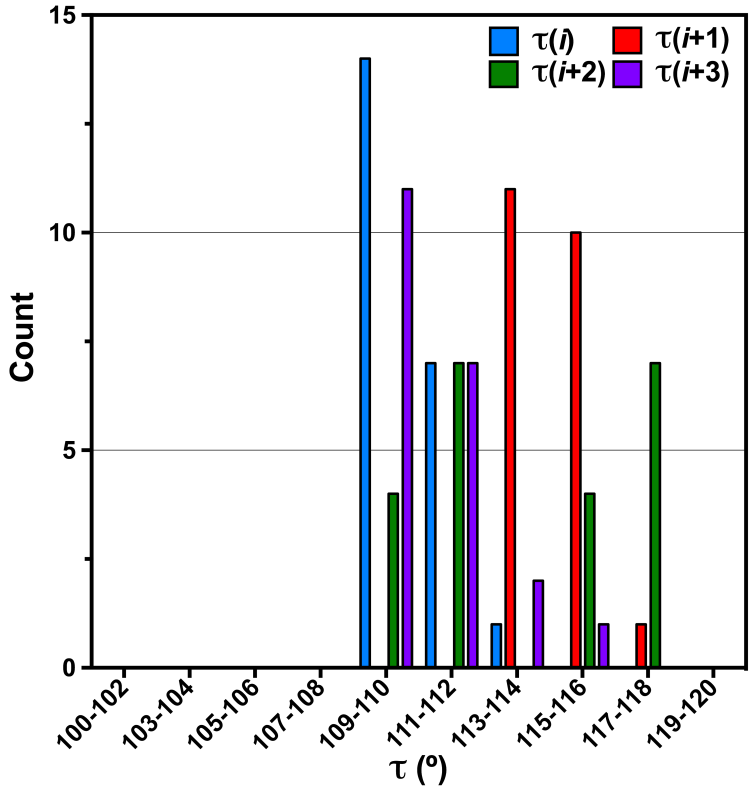

Figure S4.11: Histogram showing the distribution of τ angles in type I/I′ β-turns (reproduced from Figure 11i in the manuscript).

Table S4.31: Interstrand Distances[18]

Peptide Sequence	Cα(*i*)–Cα(*i*+3)	Cβ(*i*)–Cβ(*i*+3)
Boc-Dmaa-D-Pro-Acpc-Leu-NMe_2 (**3a**)	4.937	4.100
Boc-Dmaa-D-Pro-Acpc-Leu-NMe_2 (**3b**)	5.389	5.530
Boc-Dmaa-D-Pro-Acpc-Leu-NMe_2 (**3c**)	5.766	6.160
Boc-Dmaa-D-Pro-Acpc-Leu-OMe (**4a**)	5.912	6.160
Boc-Dmaa-D-Pro-Acpc-Leu-OMe (**4b**)	5.785	6.030
Boc-Dmaa-D-Pro-Acpc-Leu-OMe (**4c**)	5.914	5.706
Boc-Dmaa-D-Pro-Acpc-Leu-OMe (**4d**)	5.808	6.187
Boc-Dmaa-D-Pro-Acpc-Leu-OMe (**4e**)	5.961	7.168
Boc-Cys(Ph)-D-Pro-Acpc-Leu-OMe (**5**)	5.813	5.998
Boc-Leu-D-Pro-Acpc-Leu-OMe (**6**)	5.407	6.085
Boc-Dmaa-D-Pro-Acpc-Gly-OMe (**7a**)	4.782	N/A
Boc-Dmaa-D-Pro-Acpc-Gly-OMe (**7b**)	5.727	N/A
Boc-Dmaa-D-Pro-Acpc-Nle-NMe_2 (**8**)	5.052	4.326
Boc-Dmaa-D-Pro-Acpc-Val-NMe_2 (**9**)	5.126	4.617
Boc-Dmaa-D-Pro-Acpc-Val-OMe (**10**)	5.808	5.825
Boc-Dmaa-D-Pro-Acpc-Chg-NMe_2 (**11**)	5.324	4.970
Boc-Dmaa-D-Pro-Acpc-Phe-NMe_2 (**12**)	4.960	4.077
Boc-Dmaa-D-Pro-Acpc-Phe-OMe (**13**)	5.488	5.999
Boc-Dmaa-D-Pro-Acpc-D-Phe-NMe_2 (**14**)	5.133	6.000
Boc-Dmaa-Pro-Acpc-Leu-OMe (**15**)	5.097	4.363
Boc-Dmaa-D-Pro-Acbc-Leu-NMe_2 (**16a**)	5.045	4.437
Boc-Dmaa-D-Pro-Acbc-Leu-NMe_2 (**16b**)	5.389	5.530
Boc-Dmaa-D-Pro-Acbc-Leu-NMe_2 (**16c**)	5.876	6.209
Boc-Dmaa-D-Pro-Acbc-Leu-OMe (**17a**)	6.161	6.012
Boc-Dmaa-D-Pro-Acbc-Leu-OMe (**17b**)	5.951	5.651
Boc-Dmaa-D-Pro-Cle-Leu-OMe (**18a**)	5.957	5.640
Boc-Dmaa-D-Pro-Cle-Leu-OMe (**18b**)	6.053	5.742
Boc-Dmaa-D-Pro-Aic-Leu-OMe (**19a**)	5.982	5.833
Boc-Dmaa-D-Pro-Aic-Leu-OMe (**19b**)	5.307	4.913
Boc-Dmaa-D-Pro-Aic-D-Phe-NMe_2 (**20a**)	5.339	4.980
Boc-Dmaa-D-Pro-Aic-D-Phe-NMe_2 (**20b**)	5.632	5.740
Boc-Dmaa-Pro-Aic-Leu-OMe (**21a**)	5.277	5.029
Boc-Dmaa-Pro-Aic-Leu-OMe (**21b**)	5.303	5.230
Boc-Dmaa-D-Pro-Achc-Leu-OMe (**22a**)	5.960	5.377
Boc-Dmaa-D-Pro-Achc-Leu-OMe (**22b**)	6.156	5.861
Boc-Cys(Ph)-D-Pro-Achc-Leu-OMe (**23**)	5.963	5.842
Boc-Dmaa-D-Pro-Aib-Leu-NMe_2 (**24**)	5.808	5.825
Boc-Dmaa-D-Pro-Aib-Leu-OMe (**25**)	5.054	4.885
Boc-Dmaa-D-Pro-Aib-Val-OMe (**26**)	5.199	5.425
Boc-Dmaa-D-Pro-Aib-Phe-OMe (**27**)	4.968	4.189
Boc-Dmaa-D-Pro-Aib-3-Pal-NMe_2 (**28**)	5.170	4.938
Boc-Dmaa-D-Pro-Aib-2-Thi-NMe_2 (**29a**)	4.988	4.302
Boc-Dmaa-D-Pro-Aib-2-Thi-NMe_2 (**29b**)	4.990	4.182
Boc-Dmaa-Pro-Aib-Leu-OMe (**30**)	5.183	4.752
Boc-Dmaa-D-Pro-Ala-Phe-OMe (**31**)	5.463	5.955
Boc-Dmaa-D-Pro-Phe-Leu-NMe_2 (**32a**)	7.199	6.940
Boc-Dmaa-D-Pro-Phe-Leu-NMe_2 (**32b**)	7.637	7.101
Boc-Dmaa-D-Pro-Gly-Leu-OMe (**33a**)	5.665	6.043
Boc-Dmaa-D-Pro-Gly-Leu-OMe (**33b**)	5.634	5.791
Boc-Keto-D-Pro-Aib-Phe-OMe (**34**)	4.989	4.359
Boc-Phe-Pro-Aib-(*R*)-α-Mba (**35**)	5.567	5.082
2-Msa-Pro-D-Val-(*R*)-α-Mba (**36**)	5.389	4.386
Boc-His(τ-Bn)-Pro-Aib-(*R*)-α-Mba (**37**)	5.867	5.313
average	5.572	5.427
st. dev.	0.531	0.783
median	5.488	5.640
minimum	4.782	4.077
maximum	7.637	7.168
count	53	51

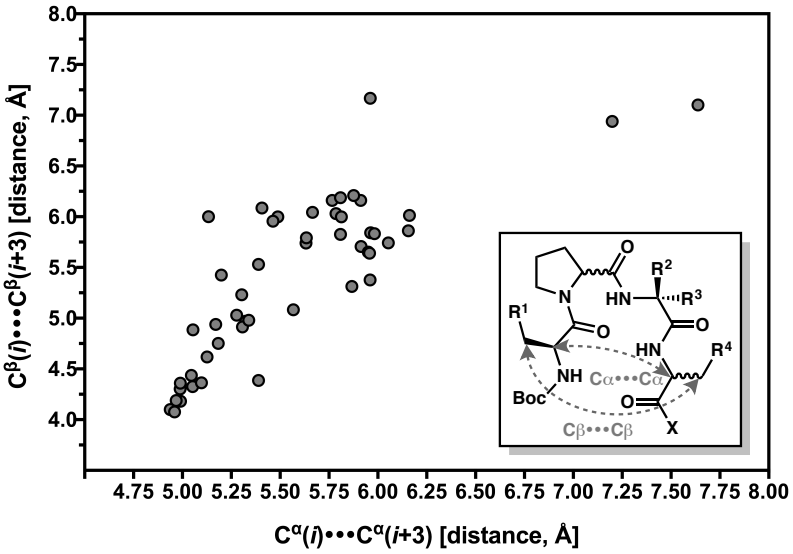

Figure S4.12: A plot of Cβ–Cβ distance vs. Cα–Cα shows a loose trend; larger Cα–Cα distances tend to correlate with longer Cβ–Cβ distances.

C. Side-chain (χ_1) Dihedrals

Table S4.32: Side-chain χ_1 Dihedrals for All Peptides[23]

Peptide Sequence	$\chi_1(i)$	$\chi_1(i+3)$
Boc-Dmaa-D-Pro-Acpc-Leu-NMe_2 (**3a**)	-51.7	-44.9
Boc-Dmaa-D-Pro-Acpc-Leu-NMe_2 (**3b**)	-168.6	-168.3
Boc-Dmaa-D-Pro-Acpc-Leu-NMe_2 (**3c**)	-169.9	-55.8
Boc-Dmaa-D-Pro-Acpc-Leu-OMe (**4a**)	-170.8	-66.0
Boc-Dmaa-D-Pro-Acpc-Leu-OMe (**4b**)	-167.2	-59.3
Boc-Dmaa-D-Pro-Acpc-Leu-OMe (**4c**)	-169.9	-67.2
Boc-Dmaa-D-Pro-Acpc-Leu-OMe (**4d**)	-164.5	-58.3
Boc-Dmaa-D-Pro-Acpc-Leu-OMe (**4e**)	-167.8	57.3
Boc-Cys(Ph)-D-Pro-Acpc-Leu-OMe (**5**)	-164.2	-60.6
Boc-Leu-D-Pro-Acpc-Leu-OMe (**6**)	-64.1	-53.5
Boc-Dmaa-D-Pro-Acpc-Gly-OMe (**7a**)	-49.2	N/A
Boc-Dmaa-D-Pro-Acpc-Gly-OMe (**7b**)	-63.1	N/A
Boc-Dmaa-D-Pro-Acpc-Nle-NMe_2 (**8**)	-57.7	-56.4
Boc-Dmaa-D-Pro-Acpc-Val-NMe_2 (**9**)	-52.3	N/A
Boc-Dmaa-D-Pro-Acpc-Val-OMe (**10**)	-103.0	N/A
Boc-Dmaa-D-Pro-Acpc-Chg-NMe_2 (**11**)	-53.0	-66.9
Boc-Dmaa-D-Pro-Acpc-Phe-NMe_2 (**12**)	-171.7	-86.6
Boc-Dmaa-D-Pro-Acpc-Phe-OMe (**13**)	-68.5	-167.2
Boc-Dmaa-D-Pro-Acpc-D-Phe-NMe_2 (**14**)	-158.1	166.4
Boc-Dmaa-Pro-Acpc-Leu-OMe (**15**)	-57.0	-68.8
Boc-Dmaa-D-Pro-Acbc-Leu-NMe_2 (**16a**)	-167.2	-56.5
Boc-Dmaa-D-Pro-Acbc-Leu-NMe_2 (**16b**)	-51.1	-64.7
Boc-Dmaa-D-Pro-Acbc-Leu-NMe_2 (**16c**)	-168.8	-55.2
Boc-Dmaa-D-Pro-Acbc-Leu-OMe (**17a**)	-169.9	-65.5
Boc-Dmaa-D-Pro-Acbc-Leu-OMe (**17b**)	-170.0	-73.3
Boc-Dmaa-D-Pro-Cle-Leu-OMe (**18a**)	-172.4	-68.3
Boc-Dmaa-D-Pro-Cle-Leu-OMe (**18b**)	-168.3	-65.3
Boc-Dmaa-D-Pro-Aic-Leu-OMe (**19a**)	-175.0	-64.4
Boc-Dmaa-D-Pro-Aic-Leu-OMe (**19b**)	-51.3	-63.9
Boc-Dmaa-D-Pro-Aic-D-Phe-NMe_2 (**20a**)	-171.5	178.0
Boc-Dmaa-D-Pro-Aic-D-Phe-NMe_2 (**20b**)	-57.9	172.4
Boc-Dmaa-Pro-Aic-Leu-OMe (**21a**)	-84.9	178.0
Boc-Dmaa-Pro-Aic-Leu-OMe (**21b**)	-68.5	-176.8
Boc-Dmaa-D-Pro-Achc-Leu-OMe (**22a**)	-174.9	-91.8
Boc-Dmaa-D-Pro-Achc-Leu-OMe (**22b**)	-168.8	-71.0
Boc-Cys(Ph)-D-Pro-Achc-Leu-OMe (**23**)	-156.7	-67.5
Boc-Dmaa-D-Pro-Aib-Leu-NMe_2 (**24**)	-59.5	-57.0
Boc-Dmaa-D-Pro-Aib-Leu-OMe (**25**)	-179.2	-54.0
Boc-Dmaa-D-Pro-Aib-Val-OMe (**26**)	-160.4	N/A
Boc-Dmaa-D-Pro-Aib-Phe-OMe (**27**)	-170.1	-68.9
Boc-Dmaa-D-Pro-Aib-3-Pal-NMe_2 (**28**)	-170.1	179.5
Boc-Dmaa-D-Pro-Aib-2-Thi-NMe_2 (**29a**)	-58.9	-77.6
Boc-Dmaa-D-Pro-Aib-2-Thi-NMe_2 (**29b**)	-58.6	-80.0
Boc-Dmaa-Pro-Aib-Leu-OMe (**30**)	-76.6	177.5
Boc-Dmaa-D-Pro-Ala-Phe-OMe (**31**)	-70.3	-166.9
Boc-Dmaa-D-Pro-Phe-Leu-NMe_2 (**32a**)	-67.1	-175.8
Boc-Dmaa-D-Pro-Phe-Leu-NMe_2 (**32b**)	-75.5	-68.5
Boc-Dmaa-D-Pro-Gly-Leu-OMe (**33a**)	-175.6	-69.0
Boc-Dmaa-D-Pro-Gly-Leu-OMe (**33b**)	-175.3	-67.3
Boc-Keto-D-Pro-Aib-Phe-OMe (**34**)	-174.3	-59.1
Boc-Phe-Pro-Aib-(*R*)-α-Mba (**35**)	-55.7	N/A
2-Msa-Pro-D-Val-(*R*)-α-Mba (**36**)	N/A	N/A
Boc-His(τ-Bn)-Pro-Aib-(*R*)-α-Mba (**37**)	-160.9	N/A
average	-122.3	-42.2
st. dev.	53.8	95.0
median	-160.7	-65.3
minimum	-179.2	-176.8
maximum	-49.2	179.5
count	52	45

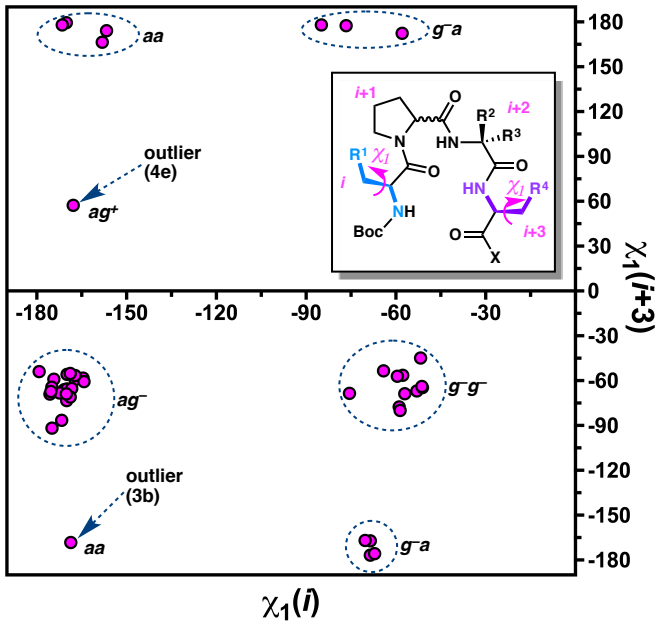

Figure S4.13: Plot of $\chi_1(i+3)$ vs. $\chi_1(i+1)$ shows clustering of peptides with similar side-chain dihedrals (reproduced from Figure 11e in the manuscript).

Table S4.33: Side-chain χ_1 Dihedrals for *ag*⁻ Cluster in Figure S4.13

ag⁻	$\chi_1(i)$	$\chi_1(i+3)$	Turn Type
Boc-Dmaa-D-Pro-Acpc-Leu-NMe_2 (**3c**)	-169.9	-55.8	I'
Boc-Dmaa-D-Pro-Acpc-Leu-OMe (**4a**)	-170.8	-66.0	I'
Boc-Dmaa-D-Pro-Acpc-Leu-OMe (**4b**)	-167.2	-59.3	I'
Boc-Dmaa-D-Pro-Acpc-Leu-OMe (**4c**)	-169.9	-67.2	I'
Boc-Dmaa-D-Pro-Acpc-Leu-OMe (**4d**)	-164.5	-58.3	I'
Boc-Cys(Ph)-D-Pro-Acpc-Leu-OMe (**5**)	-164.2	-60.6	I'
Boc-Dmaa-D-Pro-Acpc-Phe-NMe_2 (**12**)	-171.7	-86.6	II'
Boc-Dmaa-D-Pro-Acbc-Leu-NMe_2 (**16a**)	-167.2	-56.5	II'
Boc-Dmaa-D-Pro-Acbc-Leu-NMe_2 (**16c**)	-168.8	-55.2	I'
Boc-Dmaa-D-Pro-Acbc-Leu-OMe (**17a**)	-169.9	-65.5	I'
Boc-Dmaa-D-Pro-Acbc-Leu-OMe (**17b**)	-170.0	-73.3	I'
Boc-Dmaa-D-Pro-Cle-Leu-OMe (**18a**)	-172.4	-68.3	I'
Boc-Dmaa-D-Pro-Cle-Leu-OMe (**18b**)	-168.3	-65.3	I'
Boc-Dmaa-D-Pro-Aic-Leu-OMe (**19a**)	-175.0	-64.4	I'
Boc-Dmaa-D-Pro-Achc-Leu-OMe (**22a**)	-174.9	-91.8	I'
Boc-Dmaa-D-Pro-Achc-Leu-OMe (**22b**)	-168.8	-71.0	I'
Boc-Cys(Ph)-D-Pro-Achc-Leu-OMe (**23**)	-156.7	-67.5	I'
Boc-Dmaa-D-Pro-Aib-Leu-NMe_2 (**24**)	-59.5	-57.0	II'
Boc-Dmaa-D-Pro-Aib-Phe-OMe (**27**)	-170.1	-68.9	II'
Boc-Dmaa-D-Pro-Gly-Leu-OMe (**33a**)	-175.6	-69.0	I'
Boc-Dmaa-D-Pro-Gly-Leu-OMe (**33b**)	-175.3	-67.3	I'
Boc-Keto-D-Pro-Aib-Phe-OMe (**34**)	-174.3	-59.1	II'
average	-164.8	-66.1	total I/I'
st. dev.	23.9	9.2	17
median	-169.9	-65.8	total II/II'
minimum	-175.6	-91.8	5
maximum	-59.5	-55.2	
count	22	22	

Table S4.34: Side-chain χ_1 Dihedrals for g^-g^- Cluster in Figure S4.13

g^-g^-	$\chi_1(i)$	$\chi_1(i+3)$	Turn Type
Boc-Dmaa-D-Pro-Acpc-Leu-NMe_2 (**3a**)	-51.7	-44.9	II'
Boc-Leu-D-Pro-Acpc-Leu-OMe (**6**)	-64.1	-53.5	II'
Boc-Dmaa-D-Pro-Acpc-Nle-NMe_2 (**8**)	-57.7	-56.4	II'
Boc-Dmaa-D-Pro-Acpc-Chg-NMe_2 (**11**)	-53.0	-66.9	II'
Boc-Dmaa-Pro-Acpc-Leu-OMe (**15**)	-57.0	-68.8	II
Boc-Dmaa-D-Pro-Acbc-Leu-NMe_2 (**16b**)	-51.1	-64.7	II'
Boc-Dmaa-D-Pro-Aic-Leu-OMe (**19b**)	-51.3	-63.9	I'
Boc-Dmaa-D-Pro-Aib-Leu-NMe_2 (**24**)	-59.5	-57.0	II'
Boc-Dmaa-D-Pro-Aib-2-Thi-NMe_2 (**29a**)	-58.9	-77.6	II'
Boc-Dmaa-D-Pro-Aib-2-Thi-NMe_2 (**29b**)	-58.6	-80.0	II'
Boc-Dmaa-D-Pro-Phe-Leu-NMe_2 (**32b**)	-75.5	-68.5	N/A
average	-58.0	-63.8	total II/II'
st. dev.	7.1	10.4	9
median	-57.7	-64.7	total I/I'
minimum	-75.5	-80.0	1
maximum	-51.1	-44.9	
count	11	11	

Table S4.35: Side-chain χ_1 Dihedrals for g^-a^- Cluster in Figure S4.13

g^-a^-	$\chi_1(i)$	$\chi_1(i+3)$	Turn Type
Boc-Dmaa-D-Pro-Acpc-Phe-OMe (**13**)	-68.5	-167.2	II'
Boc-Dmaa-Pro-Aic-Leu-OMe (**21b**)	-68.5	-176.8	II
Boc-Dmaa-D-Pro-Ala-Phe-OMe (**31**)	-70.3	-166.9	II'
Boc-Dmaa-D-Pro-Phe-Leu-NMe_2 (**32a**)	-67.1	-175.8	N/A
average	-68.6	-171.7	total II/II'
st. dev.	1.3	5.4	3
median	-68.5	-171.5	total I/I'
minimum	-70.3	-176.8	0
maximum	-67.1	-166.9	
count	4	4	

Table S4.36: Side-chain χ_1 Dihedrals for g^-a Cluster in Figure S4.13

g^-a	$\chi_1(i)$	$\chi_1(i+3)$	Turn Type
Boc-Dmaa-Pro-Aib-Leu-OMe (**30**)	-76.6	177.5	II
Boc-Dmaa-Pro-Aic-Leu-OMe (**21a**)	-84.9	178.0	II
Boc-Dmaa-D-Pro-Aic-D-Phe-NMe_2 (**20b**)	-57.9	172.4	II'
average	-73.1	176.0	total II/II'
st. dev.	13.8	3.1	3
median	-76.6	177.5	total I/I'
minimum	-84.9	172.4	0
maximum	-57.9	178.0	
count	3	3	

Table S4.37: Side-chain χ_1 Dihedrals for *aa* Cluster in Figure S4.13

aa	$\chi_1(i)$	$\chi_1(i+3)$	Turn Type
Boc-Dmaa-D-Pro-Acpc-D-Phe-NMe_2 (**14**)	-158.1	166.4	II'
Boc-Dmaa-D-Pro-Aic-D-Phe-NMe_2 (**20a**)	-171.5	178.0	II'
Boc-Dmaa-D-Pro-Aib-3-Pal-NMe_2 (**28**)	-170.1	179.5	II'
average	-166.6	174.6	total II/II'
st. dev.	7.4	7.2	3
median	-170.1	178.0	total I/I'
minimum	-171.5	166.4	0
maximum	-158.1	179.5	
count	3	3	

Table S4.38: Summary of *gauche* & *anti* χ_1 Values in Figure S4.13

Turn Motif	total	*a*(*i*)	*g*(*i*)	*a*(*i*+3)	*g*(*i*+3)
type I/I'	19	18 94.7%	1 5.3%	0 0.0%	19 100.0%
type II/II'	23	8 34.8%	15 65.2%	9 39.1%	14 60.9%

D. Hydrogen Bonding[24]

Table S4.39: H-Bond Lengths (*r*) & Angles (θ) for All Peptides

Peptide Sequence	NH(*i*+3)•••O(*i*) [Central β-Turn]		NH(*i*)•••O(*i*+3) [β-Hairpin]		NH(*i*+2)•••O(*i*) [γ-Turn]		NH(*i*+2)•••O(*i*–1) [*N*-Terminal β-Turn]	
	r (Å)	θ (°)	*r* (Å)	θ (°)	*r* (Å)	θ (°)	*r* (Å)	θ (°)
Boc-Dmaa-D-Pro-Acpc-Leu-NMe_2 (**3a**)	2.952	156	2.906	158	3.029	96		
Boc-Dmaa-D-Pro-Acpc-Leu-NMe_2 (**3b**)	2.968	167	2.937	168	3.334	87		
Boc-Dmaa-D-Pro-Acpc-Leu-NMe_2 (**3c**)	3.022	167					2.871	158
Boc-Dmaa-D-Pro-Acpc-Leu-OMe (**4a**)	3.096	165					2.964	145
Boc-Dmaa-D-Pro-Acpc-Leu-OMe (**4b**)	3.046	168					2.958	157
Boc-Dmaa-D-Pro-Acpc-Leu-OMe (**4c**)	3.008	168					2.963	166
Boc-Dmaa-D-Pro-Acpc-Leu-OMe (**4d**)	3.059	174					2.915	154
Boc-Dmaa-D-Pro-Acpc-Leu-OMe (**4e**)	3.093	170					2.899	167
Boc-Cys(Ph)-D-Pro-Acpc-Leu-OMe (**5**)	3.099	165					3.005	162
Boc-Leu-D-Pro-Acpc-Leu-OMe (**6**)	2.875	149	3.260	160	3.281	75		
Boc-Dmaa-D-Pro-Acpc-Gly-OMe (**7a**)	2.804	157			3.172	90		
Boc-Dmaa-D-Pro-Acpc-Gly-OMe (**7b**)	3.006	162			3.128	64	3.256	127
Boc-Dmaa-D-Pro-Acpc-Nle-NMe_2 (**8**)	2.986	162	2.858	173	3.239	86		
Boc-Dmaa-D-Pro-Acpc-Val-NMe_2 (**9**)	3.038	165	2.856	161	3.222	85		
Boc-Dmaa-D-Pro-Acpc-Val-OMe (**10**)	2.927	171	2.954	159	3.011	97		
Boc-Dmaa-D-Pro-Acpc-Chg-NMe_2 (**11**)	2.994	161	2.833	162	3.214	85		
Boc-Dmaa-D-Pro-Acpc-Phe-NMe_2 (**12**)	2.887	159	2.926	164	3.206	91		
Boc-Dmaa-D-Pro-Acpc-Phe-OMe (**13**)	2.904	156	3.274	162	3.301	81		
Boc-Dmaa-D-Pro-Acpc-D-Phe-NMe_2 (**14**)	2.895	165	3.122	171	3.213	81		
Boc-Dmaa-Pro-Acpc-Leu-OMe (**15**)	2.856	163	3.243	165	3.163	81		
Boc-Dmaa-D-Pro-Acbc-Leu-NMe_2 (**16a**)	2.995	154	2.859	175	3.276	84		
Boc-Dmaa-D-Pro-Acbc-Leu-NMe_2 (**16b**)	3.190	172	2.805	137	3.055	96		
Boc-Dmaa-D-Pro-Acbc-Leu-NMe_2 (**16c**)	3.106	160					2.891	159
Boc-Dmaa-D-Pro-Acbc-Leu-OMe (**17a**)	3.141	160					3.046	170
Boc-Dmaa-D-Pro-Acbc-Leu-OMe (**17b**)	3.045	163					3.093	156
Boc-Dmaa-D-Pro-Cle-Leu-OMe (**18a**)	3.031	169			3.109	98	3.236	156
Boc-Dmaa-D-Pro-Cle-Leu-OMe (**18b**)	3.030	173			3.011	99	3.179	158
Boc-Dmaa-D-Pro-Aic-Leu-OMe (**19a**)	3.192	157			3.157	100	3.198	153
Boc-Dmaa-D-Pro-Aic-Leu-OMe (**19b**)	2.897	154			3.160	91	2.926	152
Boc-Dmaa-D-Pro-Aic-D-Phe-NMe_2 (**20a**)	2.926	150			3.227	76		
Boc-Dmaa-D-Pro-Aic-D-Phe-NMe_2 (**20b**)	3.034	163			3.237	80		
Boc-Dmaa-Pro-Aic-Leu-OMe (**21a**)	3.057	154			3.283	79		
Boc-Dmaa-Pro-Aic-Leu-OMe (**21b**)	3.062	146			3.273	71		
Boc-Dmaa-D-Pro-Achc-Leu-OMe (**22a**)	2.919	167			2.970	101	3.297	165
Boc-Dmaa-D-Pro-Achc-Leu-OMe (**22b**)	3.115	164			3.108	102	3.358	161
Boc-Cys(Ph)-D-Pro-Achc-Leu-OMe (**23**)	2.980	167			3.181	107	3.218	160
Boc-Dmaa-D-Pro-Aib-Leu-NMe_2 (**24**)	2.895	157	2.998	162	3.181	83		
Boc-Dmaa-D-Pro-Aib-Leu-OMe (**25**)	2.813	149	3.027	165	3.303	82		
Boc-Dmaa-D-Pro-Aib-Val-OMe (**26**)	2.929	159	2.946	170	3.282	79		
Boc-Dmaa-D-Pro-Aib-Phe-OMe (**27**)	2.861	159	2.959	163	3.181	83		
Boc-Dmaa-D-Pro-Aib-3-Pal-NMe_2 (**28**)	2.887	164	2.974	163	3.134	72		
Boc-Dmaa-D-Pro-Aib-2-Thi-NMe_2 (**29a**)	2.950	150	2.892	173	3.237	78		
Boc-Dmaa-D-Pro-Aib-2-Thi-NMe_2 (**29b**)	2.955	149	2.868	156	3.264	78		
Boc-Dmaa-Pro-Aib-Leu-OMe (**30**)	3.054	153			3.290	73		
Boc-Dmaa-D-Pro-Ala-Phe-OMe (**31**)	2.904	153	3.249	164	3.339	79		
Boc-Dmaa-D-Pro-Phe-Leu-NMe_2 (**32a**)								
Boc-Dmaa-D-Pro-Phe-Leu-NMe_2 (**32b**)								
Boc-Dmaa-D-Pro-Gly-Leu-OMe (**33a**)	3.037	169					2.884	164
Boc-Dmaa-D-Pro-Gly-Leu-OMe (**33b**)	2.978	163					2.931	159
Boc-Keto-D-Pro-Aib-Phe-OMe (**34**)	2.955	161	2.938	143	3.139	83		
Boc-Phe-Pro-Aib-(*R*)-α-Mba (**35**)	3.038	150			3.153	94		
2-Msa-Pro-D-Val-(*R*)-α-Mba (**36**)	2.996	151			3.396	108		
Boc-His(τ-Bn)-Pro-Aib-(*R*)-α-Mba (**37**)	3.129	166					3.074	166
average	2.992	161	2.986	162	3.196	86	3.055	158
st. dev.	0.092	7	0.148	9	0.098	11	0.155	9
median	2.995	162	2.942	163	3.210	84	3.005	159
minimum	2.804	146	2.805	137	2.970	64	2.871	127
maximum	3.192	174	3.274	175	3.396	108	3.358	170
count	51	51	22	22	38	38	21	21

Table S4.40: Distribution of H-Bond Lengths (*r*) & Angles (θ) Across All Peptides

r **(N•••O) (Å)**		**θ (N–H•••O) (º)**	
Bins	**Count**	**Bins**	**Count**
2.40–2.79	0	120–124	0
2.80–2.84	4	125–129	1
2.85–2.89	17	130–134	0
2.90–2.94	14	135–139	1
2.95–2.99	18	140–144	2
3.00–3.04	14	145–149	5
3.05–3.09	9	150–154	11
3.10–3.14	5	155–159	18
3.15–3.19	4	160–164	26
3.20–3.24	4	165–169	19
3.25–3.29	4	170–174	10
3.30–3.34	0	175–180	1
3.35–3.40	1		
3.41–4.00	0		
average	3.005	**average**	160
st. dev.	0.124	**st. dev.**	8
median	2.979	**median**	162
minimum	2.804	**minimum**	127
maximum	3.358	**maximum**	175
count	94	**count**	94

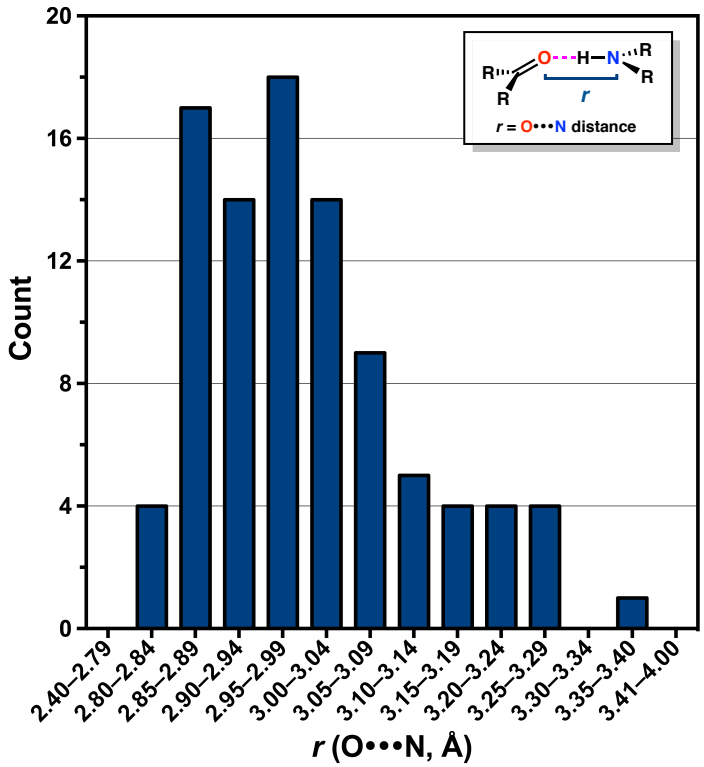

Figure S4.14: Histogram showing the distribution of H-bond lengths (*r*) across all peptides (reproduced from Figure 11f in the manuscript).

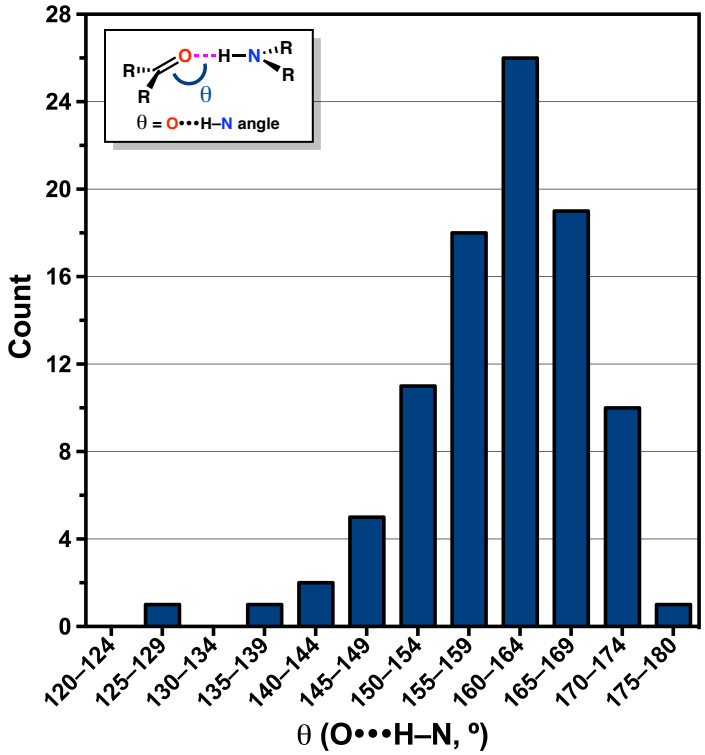

Figure S4.15: Histogram showing the distribution of H-bond angles (θ) across all peptides (reproduced from Figure 11g in the manuscript).

Table S4.41: Intermolecular H-Bond Lengths (*r*) & Angles (θ) for All Peptides[24]

Peptide Sequence	*i* N–H		*i*+1 C=O		*i*+2 N–H		*i*+2 C=O	
	r (Å)	θ (°)	*r* (Å)	θ (°)	*r* (Å)	θ (°)	*r* (Å)	θ (°)
Boc-Dmaa-D-Pro-Acpc-Leu-NMe_2 (**3a**)			2.765	152	2.765	152		
Boc-Dmaa-D-Pro-Acpc-Leu-NMe_2 (**3b**)			2.917	149	2.917	149	2.811	161
Boc-Dmaa-D-Pro-Acpc-Leu-NMe_2 (**3c**)	2.872	168	2.872	168				
Boc-Dmaa-D-Pro-Acpc-Leu-OMe (**4a**)	2.857	163	2.857	163				
Boc-Dmaa-D-Pro-Acpc-Leu-OMe (**4b**)	2.786	165	2.871	165				
Boc-Dmaa-D-Pro-Acpc-Leu-OMe (**4c**)	2.818	162	2.805	160				
Boc-Dmaa-D-Pro-Acpc-Leu-OMe (**4d**)	2.805	160	2.818	162				
Boc-Dmaa-D-Pro-Acpc-Leu-OMe (**4e**)	2.871	165	2.786	165				
Boc-Cys(Ph)-D-Pro-Acpc-Leu-OMe (**5**)	2.807	170					2.807	170
Boc-Leu-D-Pro-Acpc-Leu-OMe (**6**)			2.834	152	2.834	152		
Boc-Dmaa-D-Pro-Acpc-Gly-OMe (**7a**)	2.951	166			2.908	167	2.908	167
Boc-Dmaa-D-Pro-Acpc-Gly-OMe (**7b**)	3.067	165						
Boc-Dmaa-D-Pro-Acpc-Nle-NMe_2 (**8**)			2.929	176	2.929	176		
Boc-Dmaa-D-Pro-Acpc-Val-NMe_2 (**9**)			2.870	171	2.87	171		
Boc-Dmaa-D-Pro-Acpc-Val-OMe (**10**)	2.817	167	2.817	167				
Boc-Dmaa-D-Pro-Acpc-Chg-NMe_2 (**11**)			2.916	174	2.916	174		
Boc-Dmaa-D-Pro-Acpc-Phe-NMe_2 (**12**)			2.803	162	2.803	162		
Boc-Dmaa-D-Pro-Acpc-Phe-OMe (**13**)			2.814	135	2.814	135		
Boc-Dmaa-D-Pro-Acpc-D-Phe-NMe_2 (**14**)			2.768	173	2.768	173		
Boc-Dmaa-Pro-Acpc-Leu-OMe (**15**)					3.100	161		
Boc-Dmaa-D-Pro-Acbc-Leu-NMe_2 (**16a**)					3.009	161	2.847	167
Boc-Dmaa-D-Pro-Acbc-Leu-NMe_2 (**16b**)					2.847	167		
Boc-Dmaa-D-Pro-Acbc-Leu-NMe_2 (**16c**)	2.840	166	2.840	166				
Boc-Dmaa-D-Pro-Acbc-Leu-OMe (**17a**)	2.933	167	2.999	157				
Boc-Dmaa-D-Pro-Acbc-Leu-OMe (**17b**)	2.999	157	2.933	167				
Boc-Dmaa-D-Pro-Cle-Leu-OMe (**18a**)	2.885	160	2.915	158				
Boc-Dmaa-D-Pro-Cle-Leu-OMe (**18b**)	2.915	158	2.885	160				
Boc-Dmaa-D-Pro-Aic-Leu-OMe (**19a**)	2.812	165	2.812	165				
Boc-Dmaa-D-Pro-Aic-Leu-OMe (**19b**)	2.874	167	2.874	167				
Boc-Dmaa-D-Pro-Aic-D-Phe-NMe_2 (**20a**)					2.844	169	2.844	169
Boc-Dmaa-D-Pro-Aic-D-Phe-NMe_2 (**20b**)					2.823	174	2.823	174
Boc-Dmaa-Pro-Aic-Leu-OMe (**21a**)					2.905	172	2.905	172
Boc-Dmaa-Pro-Aic-Leu-OMe (**21b**)					2.859	175	2.859	175
Boc-Dmaa-D-Pro-Achc-Leu-OMe (**22a**)	2.877	157	2.887	157				
Boc-Dmaa-D-Pro-Achc-Leu-OMe (**22b**)	2.994	167	2.994	167				
Boc-Cys(Ph)-D-Pro-Achc-Leu-OMe (**23**)	2.844	171					2.844	171
Boc-Dmaa-D-Pro-Aib-Leu-NMe_2 (**24**)					2.95	173	2.95	173
Boc-Dmaa-D-Pro-Aib-Leu-OMe (**25**)					2.837	174	2.837	174
Boc-Dmaa-D-Pro-Aib-Val-OMe (**26**)					2.853	171	2.853	171
Boc-Dmaa-D-Pro-Aib-Phe-OMe (**27**)			2.917	170	2.917	170		
Boc-Dmaa-D-Pro-Aib-3-Pal-NMe_2 (**28**)			2.812	174	2.877	174	2.847	137
Boc-Dmaa-D-Pro-Aib-2-Thi-NMe_2 (**29a**)			3.190	162				
Boc-Dmaa-D-Pro-Aib-2-Thi-NMe_2 (**29b**)					3.190	162		
Boc-Dmaa-Pro-Aib-Leu-OMe (**30**)					2.906	176	2.906	176
Boc-Dmaa-D-Pro-Ala-Phe-OMe (**31**)			2.867	135	2.867	135		
Boc-Dmaa-D-Pro-Phe-Leu-NMe_2 (**32a**)								
Boc-Dmaa-D-Pro-Phe-Leu-NMe_2 (**32b**)								
Boc-Dmaa-D-Pro-Gly-Leu-OMe (**33a**)	2.939	158	2.873	160				
Boc-Dmaa-D-Pro-Gly-Leu-OMe (**33b**)	2.873	160	2.939	158				
Boc-Keto-D-Pro-Aib-Phe-OMe (**34**)					2.797	168	2.797	168
Boc-Phe-Pro-Aib-(*R*)-α-Mba (**35**)			3.036	164	3.036	164		
2-Msa-Pro-D-Val-(*R*)-α-Mba (**36**)			2.655	172	2.904	167	2.904	167
Boc-His(τ-Bn)-Pro-Aib-(*R*)-α-Mba (**37**)	2.975	130	2.975	130				
average	2.887	162	2.878	161	2.894	165	2.859	168
st. dev.	0.073	8	0.094	11	0.096	11	0.044	9
median	2.873	165	2.872	164	2.874	169	2.847	171
minimum	2.786	130	2.655	130	2.765	135	2.797	137
maximum	3.067	171	3.190	176	3.190	176	2.950	176
count	23	23	34	34	28	28	16	16

Table S4.42: Distribution of Intermolecular H-Bond Lengths (*r*) & Angles (θ) Across All Peptides

r **(N•••O) (Å)**		**θ (N–H•••O) (°)**	
Bins	**Count**	**Bins**	**Count**
2.40–2.79	9	120–124	0
2.80–2.84	31	125–129	0
2.85–2.89	23	130–134	2
2.90–2.94	22	135–139	5
2.95–2.99	10	140–144	1
3.00–3.04	5	145–149	2
3.05–3.09	2	150–154	4
3.10–3.14	2	155–159	8
3.15–3.19	2	160–164	21
3.20–3.24	0	165–169	32
3.25–3.29	0	170–174	25
3.30–3.34	0	175–180	6
3.35–3.40	0		
3.41–4.00	0		
average	2.888	**average**	163
st. dev.	0.088	**st. dev.**	10
median	2.872	**median**	166
minimum	2.655	**minimum**	130
maximum	3.190	**maximum**	176
count	106	**count**	106

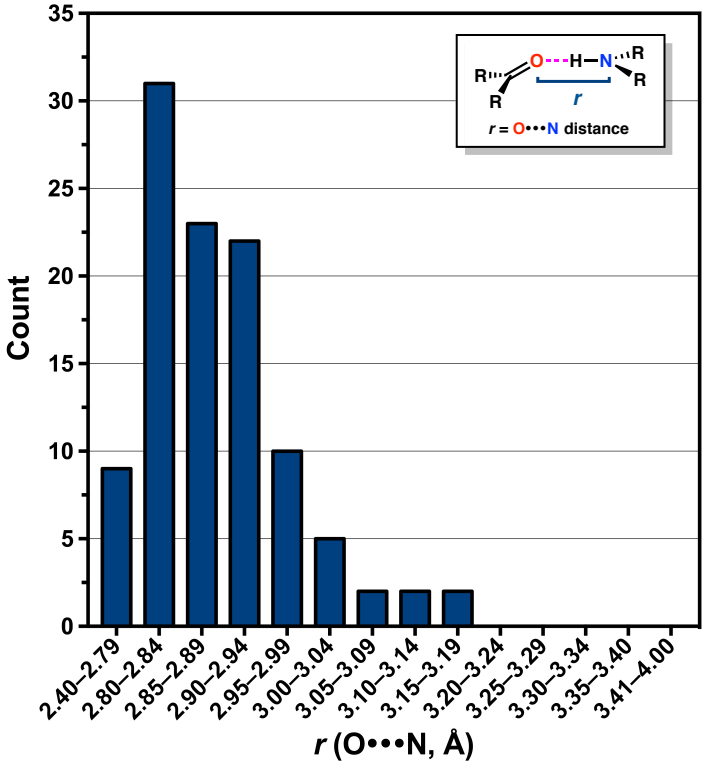

Figure S4.16: Histogram showing the distribution of intermolecular H-bond lengths (*r*) across all peptides.

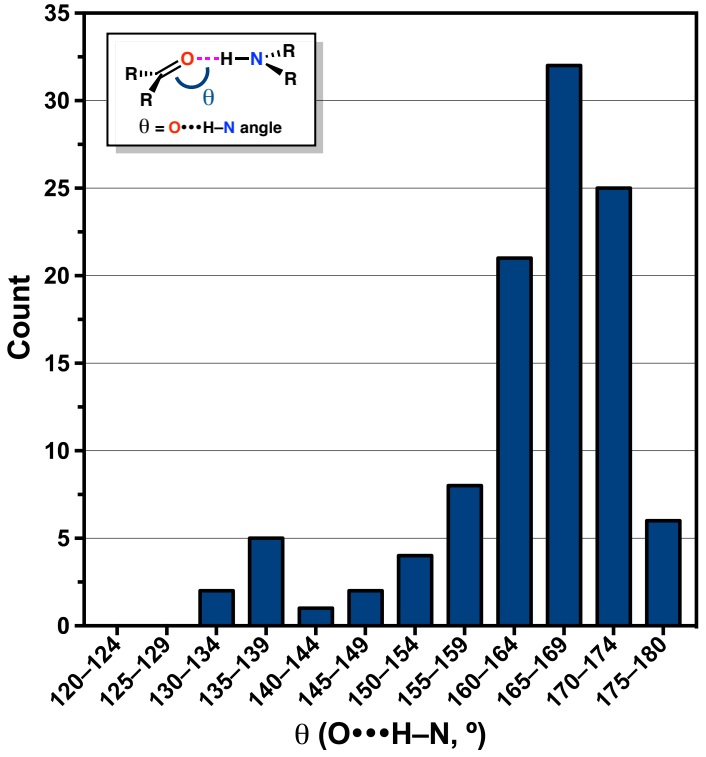

Figure S4.17: Histogram showing the distribution of intermolecular H-bond angles (θ) across all peptides.

Table S4.43: Summary of Intermolecular H-Bonds Donated From/Accepted to Various Positions Across the Canonical Turn Motifs

Turn Motif	donating H-bonds from N–H (*i*)		accepting H-bonds to NMe_2 (*i*)		accepting H-bonds to C=O (*i*+1)		donating H-bonds from N–H (*i*+2)		accepting H-bonds to C=O (*i*+2)	
types II/II'	1	3.4%	4	13.8%	16	55.2%	28	96.6%	14	48.3%
types I/I'	22	100.0%	1	4.5%	19	86.4%	0	0.0%	2	9.1%

E. Turn-Stabilizing $n \rightarrow \pi^*$ Stereoelectronic Effect[25]

Table S4.44: Summary of $n \rightarrow \pi^*$ Geometry in All peptides

Peptide Sequence	$n_O \rightarrow \pi^*_{C=O}$ (*i*+1)		$r_{C=O}$ (Å)	Δ_C (Å)
	r (Å)	θ (°)		
Boc-Dmaa-D-Pro-Acpc-Leu-NMe_2 (**3a**)	2.959	121.0	1.225	0.007
Boc-Dmaa-D-Pro-Acpc-Leu-NMe_2 (**3b**)	2.844	100.9	1.232	0.002
Boc-Dmaa-D-Pro-Acpc-Leu-NMe_2 (**3c**)	2.992	126.0	1.232	0.014
Boc-Dmaa-D-Pro-Acpc-Leu-OMe (**4a**)	2.940	124.8	1.228	0.017
Boc-Dmaa-D-Pro-Acpc-Leu-OMe (**4b**)	2.895	121.6	1.232	0.024
Boc-Dmaa-D-Pro-Acpc-Leu-OMe (**4c**)	2.949	128.3	1.225	0.015
Boc-Dmaa-D-Pro-Acpc-Leu-OMe (**4d**)	2.900	123.4	1.230	0.000
Boc-Dmaa-D-Pro-Acpc-Leu-OMe (**4e**)	2.947	128.0	1.227	0.014
Boc-Cys(Ph)-D-Pro-Acpc-Leu-OMe (**5**)	3.045	126.7	1.223	0.016
Boc-Leu-D-Pro-Acpc-Leu-OMe (**6**)	2.790	98.4	1.226	0.015
Boc-Dmaa-D-Pro-Acpc-Gly-OMe (**7a**)	2.955	116.4	1.222	0.000
Boc-Dmaa-D-Pro-Acpc-Gly-OMe (**7b**)	3.018	122.5	1.209	0.007
Boc-Dmaa-D-Pro-Acpc-Nle-NMe_2 (**8**)	2.903	108.8	1.228	0.001
Boc-Dmaa-D-Pro-Acpc-Val-NMe_2 (**9**)	2.827	105.6	1.232	0.005
Boc-Dmaa-D-Pro-Acpc-Val-OMe (**10**)	2.979	126.8	1.231	0.002
Boc-Dmaa-D-Pro-Acpc-Chg-NMe_2 (**11**)	2.888	109.2	1.229	0.001
Boc-Dmaa-D-Pro-Acpc-Phe-NMe_2 (**12**)	2.927	111.7	1.232	0.000
Boc-Dmaa-D-Pro-Acpc-Phe-OMe (**13**)	2.814	100.9	1.229	0.012
Boc-Dmaa-D-Pro-Acpc-D-Phe-NMe_2 (**14**)	2.732	99.4	1.240	0.012
Boc-Dmaa-Pro-Acpc-Leu-OMe (**15**)	2.716	99.5	1.222	0.007
Boc-Dmaa-D-Pro-Acbc-Leu-NMe_2 (**16a**)	2.983	112.0	1.228	0.006
Boc-Dmaa-D-Pro-Acbc-Leu-NMe_2 (**16b**)	2.965	122.6	1.214	0.007
Boc-Dmaa-D-Pro-Acbc-Leu-NMe_2 (**16c**)	3.006	126.9	1.229	0.017
Boc-Dmaa-D-Pro-Acbc-Leu-OMe (**17a**)	2.966	128.2	1.226	0.019
Boc-Dmaa-D-Pro-Acbc-Leu-OMe (**17b**)	2.950	125.0	1.233	0.023
Boc-Dmaa-D-Pro-Cle-Leu-OMe (**18a**)	2.971	123.7	1.237	0.017
Boc-Dmaa-D-Pro-Cle-Leu-OMe (**18b**)	2.915	124.9	1.234	0.023
Boc-Dmaa-D-Pro-Aic-Leu-OMe (**19a**)	2.874	114.6	1.228	0.006
Boc-Dmaa-D-Pro-Aic-Leu-OMe (**19b**)	2.988	122.2	1.231	0.017
Boc-Dmaa-D-Pro-Aic-D-Phe-NMe_2 (**20a**)	2.772	100.3	1.220	0.001
Boc-Dmaa-D-Pro-Aic-D-Phe-NMe_2 (**20b**)	2.797	103.6	1.225	0.022
Boc-Dmaa-Pro-Aic-Leu-OMe (**21a**)	2.743	97.6	1.224	0.010
Boc-Dmaa-Pro-Aic-Leu-OMe (**21b**)	2.778	98.2	1.227	0.008
Boc-Dmaa-D-Pro-Achc-Leu-OMe (**22a**)	3.048	126.9	1.231	0.004
Boc-Dmaa-D-Pro-Achc-Leu-OMe (**22b**)	2.917	126.7	1.228	0.015
Boc-Cys(Ph)-D-Pro-Achc-Leu-OMe (**23**)	3.185	132.3	1.226	0.013
Boc-Dmaa-D-Pro-Aib-Leu-NMe_2 (**24**)	2.821	106.0	1.225	0.007
Boc-Dmaa-D-Pro-Aib-Leu-OMe (**25**)	2.845	101.3	1.224	0.002
Boc-Dmaa-D-Pro-Aib-Val-OMe (**26**)	2.884	105.1	1.222	0.000
Boc-Dmaa-D-Pro-Aib-Phe-OMe (**27**)	2.820	105.5	1.234	0.012
Boc-Dmaa-D-Pro-Aib-3-Pal-NMe_2 (**28**)	2.733	102.2	1.236	0.011
Boc-Dmaa-D-Pro-Aib-2-Thi-NMe_2 (**29a**)	2.879	107.1	1.229	0.012
Boc-Dmaa-D-Pro-Aib-2-Thi-NMe_2 (**29b**)	2.865	106.4	1.230	0.003
Boc-Dmaa-Pro-Aib-Leu-OMe (**30**)	2.782	97.7	1.223	0.005
Boc-Dmaa-D-Pro-Ala-Phe-OMe (**31**)	2.822	100.1	1.233	0.013
Boc-Dmaa-D-Pro-Phe-Leu-NMe_2 (**32a**)	N/A	N/A	1.218	N/A
Boc-Dmaa-D-Pro-Phe-Leu-NMe_2 (**32b**)	N/A	N/A	1.238	N/A
Boc-Dmaa-D-Pro-Gly-Leu-OMe (**33a**)	2.972	124.5	1.226	0.015
Boc-Dmaa-D-Pro-Gly-Leu-OMe (**33b**)	2.995	125.2	1.235	0.007
Boc-Keto-D-Pro-Aib-Phe-OMe (**34**)	2.895	111.4	1.217	0.004
Boc-Phe-Pro-Aib-(*R*)-α-Mba (**35**)	2.758	101.3	1.236	0.019
2-Msa-Pro-D-Val-(*R*)-α-Mba (**36**)	2.802	100.6	1.243	0.012
Boc-His(τ-Bn)-Pro-Aib-(*R*)-α-Mba (**37**)	2.805	114.2	1.221	0.033
average	2.893	113.6	1.228	0.010
st. dev.	0.098	11.3	0.006	0.008
median	2.895	112.0	1.228	0.011
minimum	2.716	97.6	1.209	0.000
maximum	3.185	132.3	1.243	0.033
count	51	51	53	51

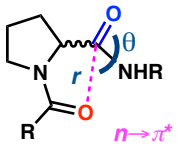

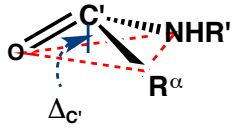

distance from C' to plane defined by substituents

Table S4.45: $n \rightarrow \pi^*$ Geometry in Type II β-Turns

Type II β-Turns	$n_O \rightarrow \pi^*_{C=O}$ (*i*+1)		$r_{C=O}$ (Å)	Δ_C (Å)	Pro Cγ-Pucker
	r (Å)	θ (°)			
Boc-Dmaa-Pro-Acpc-Leu-OMe (**15**)	2.716	99.5	1.222	0.007	exo
Boc-Dmaa-Pro-Aic-Leu-OMe (**21a**)	2.743	97.6	1.224	0.010	exo
Boc-Dmaa-Pro-Aic-Leu-OMe (**21b**)	2.778	98.2	1.227	0.008	exo
Boc-Dmaa-Pro-Aib-Leu-OMe (**30**)	2.782	97.7	1.223	0.005	exo
Boc-Phe-Pro-Aib-(*R*)-α-Mba (**35**)	2.758	101.3	1.236	0.019	exo
2-Msa-Pro-D-Val-(*R*)-α-Mba (**36**)	2.802	100.6	1.243	0.012	endo
average	2.763	99.2	1.229	0.010	**endo count**
st. dev.	0.031	1.6	0.008	0.005	1
median	2.768	98.9	1.226	0.009	**exo count**
minimum	2.716	97.6	1.222	0.005	5
maximum	2.802	101.3	1.243	0.019	**total**
count	6	6	6	6	6

Table S4.46: $n \rightarrow \pi^*$ Geometry in Type II′ β-Turns

Type II' β-Turns	$n_O \rightarrow \pi^*_{C=O}$ (*i*+1)		$r_{C=O}$ (Å)	Δ_C (Å)	Pro Cγ-Pucker
	r (Å)	θ (°)			
Boc-Dmaa-D-Pro-Acpc-Leu-NMe_2 (**3a**)	2.959	121.0	1.225	0.007	endo
Boc-Dmaa-D-Pro-Acpc-Leu-NMe_2 (**3b**)	2.844	100.9	1.232	0.002	exo
Boc-Leu-D-Pro-Acpc-Leu-OMe (**6**)	2.790	98.4	1.226	0.015	endo
Boc-Dmaa-D-Pro-Acpc-Gly-OMe (**7a**)	2.955	116.4	1.222	0.000	exo
Boc-Dmaa-D-Pro-Acpc-Nle-NMe_2 (**8**)	2.903	108.8	1.228	0.001	exo
Boc-Dmaa-D-Pro-Acpc-Val-NMe_2 (**9**)	2.927	111.7	1.232	0.000	exo
Boc-Dmaa-D-Pro-Acpc-Chg-NMe_2 (**11**)	2.888	109.2	1.229	0.001	exo
Boc-Dmaa-D-Pro-Acpc-Phe-NMe_2 (**12**)	2.927	111.7	1.232	0.000	exo
Boc-Dmaa-D-Pro-Acpc-Phe-OMe (**13**)	2.814	100.9	1.229	0.012	exo
Boc-Dmaa-D-Pro-Acpc-D-Phe-NMe_2 (**14**)	2.732	99.4	1.240	0.012	endo
Boc-Dmaa-D-Pro-Acbc-Leu-NMe_2 (**16a**)	2.983	112.0	1.228	0.006	exo
Boc-Dmaa-D-Pro-Acbc-Leu-NMe_2 (**16b**)	2.965	122.6	1.214	0.007	endo
Boc-Dmaa-D-Pro-Aic-D-Phe-NMe_2 (**20a**)	2.772	100.3	1.220	0.001	exo
Boc-Dmaa-D-Pro-Aic-D-Phe-NMe_2 (**20b**)	2.797	103.6	1.225	0.022	endo
Boc-Dmaa-D-Pro-Aib-Leu-NMe_2 (**24**)	2.821	106.0	1.225	0.007	exo
Boc-Dmaa-D-Pro-Aib-Leu-OMe (**25**)	2.845	101.3	1.224	0.002	exo
Boc-Dmaa-D-Pro-Aib-Val-OMe (**26**)	2.884	105.1	1.222	0.000	exo
Boc-Dmaa-D-Pro-Aib-Phe-OMe (**27**)	2.820	105.5	1.234	0.012	endo
Boc-Dmaa-D-Pro-Aib-3-Pal-NMe_2 (**28**)	2.733	102.2	1.236	0.011	endo
Boc-Dmaa-D-Pro-Aib-2-Thi-NMe_2 (**29a**)	2.879	107.1	1.229	0.012	exo
Boc-Dmaa-D-Pro-Aib-2-Thi-NMe_2 (**29b**)	2.865	106.4	1.230	0.003	exo
Boc-Dmaa-D-Pro-Ala-Phe-OMe (**31**)	2.822	100.1	1.233	0.013	exo
Boc-Keto-D-Pro-Aib-Phe-OMe (**34**)	2.895	111.4	1.217	0.004	endo
average	2.862	107.0	1.227	0.007	**endo count**
st. dev.	0.072	6.7	0.006	0.006	8
median	2.865	106.0	1.228	0.006	**exo count**
minimum	2.732	98.4	1.214	0.000	15
maximum	2.983	122.6	1.240	0.022	**total**
count	23	23	23	23	23

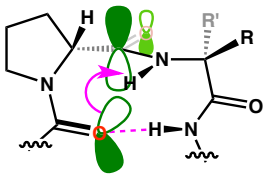

type II' β-turn

• $n \rightarrow \pi^*$ near Bürgi-Dunitz trajectory

Table S4.47: $n \rightarrow \pi^*$ Geometry in Type I′ β-Turns

Type I' β-Turns	$n_O \rightarrow \pi^*_{C=O}$ (i+1)		$r_{C=O}$ (Å)	Δ_C (Å)	Pro Cγ-Pucker
	r (Å)	θ (°)			
Boc-Dmaa-D-Pro-Acpc-Leu-NMe_2 (**3c**)	2.992	126.0	1.232	0.014	endo
Boc-Dmaa-D-Pro-Acpc-Leu-OMe (**4a**)	2.940	124.8	1.228	0.017	endo
Boc-Dmaa-D-Pro-Acpc-Leu-OMe (**4b**)	2.895	121.6	1.232	0.024	endo
Boc-Dmaa-D-Pro-Acpc-Leu-OMe (**4c**)	2.949	128.3	1.225	0.015	endo
Boc-Dmaa-D-Pro-Acpc-Leu-OMe (**4d**)	2.900	123.4	1.230	0.000	endo
Boc-Dmaa-D-Pro-Acpc-Leu-OMe (**4e**)	2.947	128.0	1.227	0.014	endo
Boc-Cys(Ph)-D-Pro-Acpc-Leu-OMe (**5**)	3.045	126.7	1.223	0.016	exo
Boc-Dmaa-D-Pro-Acpc-Gly-OMe (**7b**)	3.018	122.5	1.209	0.007	exo
Boc-Dmaa-D-Pro-Acpc-Val-OMe (**10**)	2.979	126.8	1.231	0.002	endo
Boc-Dmaa-D-Pro-Acbc-Leu-NMe_2 (**16c**)	3.006	126.9	1.229	0.017	endo
Boc-Dmaa-D-Pro-Acbc-Leu-OMe (**17a**)	2.966	128.2	1.226	0.019	endo
Boc-Dmaa-D-Pro-Acbc-Leu-OMe (**17b**)	2.950	125.0	1.233	0.023	exo
Boc-Dmaa-D-Pro-Cle-Leu-OMe (**18a**)	2.971	123.7	1.237	0.017	exo
Boc-Dmaa-D-Pro-Cle-Leu-OMe (**18b**)	2.915	124.9	1.234	0.023	endo
Boc-Dmaa-D-Pro-Aic-Leu-OMe (**19a**)	2.874	114.6	1.228	0.006	exo
Boc-Dmaa-D-Pro-Aic-Leu-OMe (**19b**)	2.988	122.2	1.231	0.017	endo
Boc-Dmaa-D-Pro-Achc-Leu-OMe (**22a**)	3.048	126.9	1.231	0.004	endo
Boc-Dmaa-D-Pro-Achc-Leu-OMe (**22b**)	2.917	126.7	1.228	0.015	exo
Boc-Cys(Ph)-D-Pro-Achc-Leu-OMe (**23**)	3.185	132.3	1.226	0.013	exo
Boc-Dmaa-D-Pro-Gly-Leu-OMe (**33a**)	2.972	124.5	1.226	0.015	endo
Boc-Dmaa-D-Pro-Gly-Leu-OMe (**33b**)	2.995	125.2	1.235	0.007	exo
average	2.974	125.2	1.229	0.014	**endo count**
st. dev.	0.067	3.5	0.006	0.007	13
median	2.971	125.2	1.229	0.015	**exo count**
minimum	2.874	114.6	1.209	0.000	8
maximum	3.185	132.3	1.237	0.024	**total**
count	21	21	21	21	21

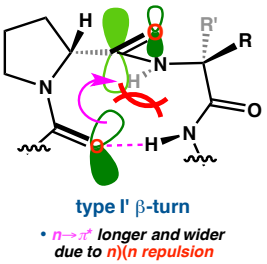

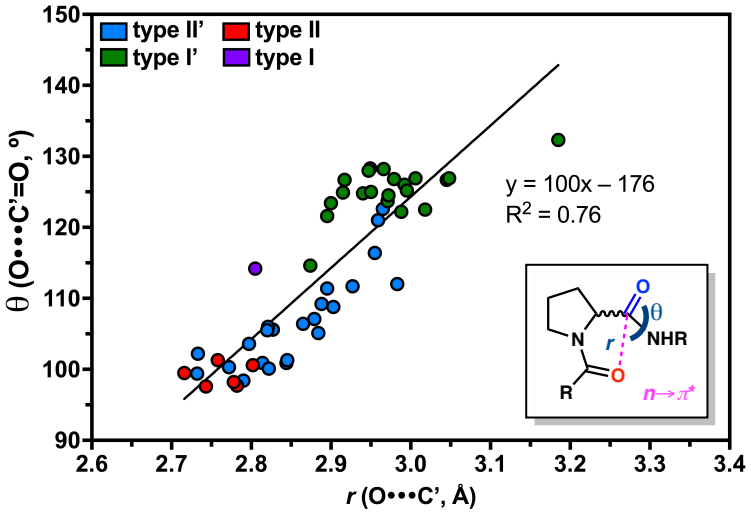

Figure S4.18: A plot of O•••C′=O angle vs. O•••C′ distance shows a loose correlation, as well as clustering by canonical turn types (reproduced from Figure 11j in the manuscript).

F. Amide N-Pyramidalization (Δ_N)[26]

Table S4.48: Amide Pyramidalization (Δ_N) Across All Peptides

Peptide Sequence	$\Delta_N(i)$	$\Delta_N(i+1)$	$\Delta_N(i+2)$	$\Delta_N(i+3)$	Δ_N(Dmaa)
Boc-Dmaa-D-Pro-Acpc-Leu-NMe_2 (**3a**)	0.059	0.064	0.043	0.096	0.438
Boc-Dmaa-D-Pro-Acpc-Leu-NMe_2 (**3b**)	0.028	0.055	0.123	0.077	0.462
Boc-Dmaa-D-Pro-Acpc-Leu-NMe_2 (**3c**)	0.032	0.076	0.108	0.041	0.456
Boc-Dmaa-D-Pro-Acpc-Leu-OMe (**4a**)	0.000	0.065	0.000	0.000	0.456
Boc-Dmaa-D-Pro-Acpc-Leu-OMe (**4b**)	0.012	0.052	0.125	0.034	0.455
Boc-Dmaa-D-Pro-Acpc-Leu-OMe (**4c**)	0.027	0.093	0.133	0.000	0.457
Boc-Dmaa-D-Pro-Acpc-Leu-OMe (**4d**)	0.090	0.068	0.116	0.045	0.468
Boc-Dmaa-D-Pro-Acpc-Leu-OMe (**4e**)	0.074	0.079	0.105	0.006	0.473
Boc-Cys(Ph)-D-Pro-Acpc-Leu-OMe (**5**)	0.008	0.018	0.054	0.011	
Boc-Leu-D-Pro-Acpc-Leu-OMe (**6**)	0.002	0.016	0.063	0.061	
Boc-Dmaa-D-Pro-Acpc-Gly-OMe (**7a**)	0.003	0.002	0.098	0.039	0.461
Boc-Dmaa-D-Pro-Acpc-Gly-OMe (**7b**)	0.068	0.012	0.140	0.089	0.480
Boc-Dmaa-D-Pro-Acpc-Nle-NMe_2 (**8**)	0.213	0.082	0.063	0.017	0.433
Boc-Dmaa-D-Pro-Acpc-Val-NMe_2 (**9**)	0.258	0.089	0.061	0.041	0.414
Boc-Dmaa-D-Pro-Acpc-Val-OMe (**10**)	0.049	0.077	0.076	0.005	0.457
Boc-Dmaa-D-Pro-Acpc-Chg-NMe_2 (**11**)	0.261	0.086	0.061	0.080	0.418
Boc-Dmaa-D-Pro-Acpc-Phe-NMe_2 (**12**)	0.085	0.021	0.085	0.092	0.426
Boc-Dmaa-D-Pro-Acpc-Phe-OMe (**13**)	0.003	0.046	0.104	0.110	0.473
Boc-Dmaa-D-Pro-Acpc-D-Phe-NMe_2 (**14**)	0.046	0.013	0.085	0.129	0.464
Boc-Dmaa-Pro-Acpc-Leu-OMe (**15**)	0.195	0.021	0.094	0.111	0.468
Boc-Dmaa-D-Pro-Acbc-Leu-NMe_2 (**16a**)	0.088	0.027	0.012	0.022	0.453
Boc-Dmaa-D-Pro-Acbc-Leu-NMe_2 (**16b**)	0.045	0.063	0.026	0.042	0.450
Boc-Dmaa-D-Pro-Acbc-Leu-NMe_2 (**16c**)	0.044	0.080	0.090	0.082	0.472
Boc-Dmaa-D-Pro-Acbc-Leu-OMe (**17a**)	0.081	0.110	0.077	0.032	0.472
Boc-Dmaa-D-Pro-Acbc-Leu-OMe (**17b**)	0.135	0.063	0.060	0.017	0.473
Boc-Dmaa-D-Pro-Cle-Leu-OMe (**18a**)	0.116	0.116	0.082	0.027	0.483
Boc-Dmaa-D-Pro-Cle-Leu-OMe (**18b**)	0.125	0.053	0.081	0.001	0.473
Boc-Dmaa-D-Pro-Aic-Leu-OMe (**19a**)	0.011	0.074	0.096	0.084	0.458
Boc-Dmaa-D-Pro-Aic-Leu-OMe (**19b**)	0.160	0.085	0.102	0.045	0.455
Boc-Dmaa-D-Pro-Aic-D-Phe-NMe_2 (**20a**)	0.044	0.018	0.014	0.043	0.472
Boc-Dmaa-D-Pro-Aic-D-Phe-NMe_2 (**20b**)	0.059	0.042	0.026	0.012	0.510
Boc-Dmaa-Pro-Aic-Leu-OMe (**21a**)	0.121	0.050	0.020	0.071	0.389
Boc-Dmaa-Pro-Aic-Leu-OMe (**21b**)	0.121	0.021	0.011	0.045	0.368
Boc-Dmaa-D-Pro-Achc-Leu-OMe (**22a**)	0.190	0.134	0.101	0.055	0.471
Boc-Dmaa-D-Pro-Achc-Leu-OMe (**22b**)	0.134	0.087	0.082	0.025	0.480
Boc-Cys(Ph)-D-Pro-Achc-Leu-OMe (**23**)	0.114	0.067	0.106	0.051	
Boc-Dmaa-D-Pro-Aib-Leu-NMe_2 (**24**)	0.111	0.019	0.054	0.001	0.454
Boc-Dmaa-D-Pro-Aib-Leu-OMe (**25**)	0.096	0.034	0.077	0.067	0.447
Boc-Dmaa-D-Pro-Aib-Val-OMe (**26**)	0.126	0.060	0.024	0.030	0.461
Boc-Dmaa-D-Pro-Aib-Phe-OMe (**27**)	0.041	0.024	0.046	0.099	0.427
Boc-Dmaa-D-Pro-Aib-3-Pal-NMe_2 (**28**)	0.045	0.015	0.025	0.101	0.461
Boc-Dmaa-D-Pro-Aib-2-Thi-NMe_2 (**29a**)	0.000	0.022	0.000	0.000	0.457
Boc-Dmaa-D-Pro-Aib-2-Thi-NMe_2 (**29b**)	0.001	0.015	0.000	0.001	0.441
Boc-Dmaa-Pro-Aib-Leu-OMe (**30**)	0.096	0.034	0.077	0.067	0.447
Boc-Dmaa-D-Pro-Ala-Phe-OMe (**31**)	0.019	0.053	0.086	0.128	0.475
Boc-Dmaa-D-Pro-Phe-Leu-NMe_2 (**32a**)	0.001	0.061	0.000	0.000	0.442
Boc-Dmaa-D-Pro-Phe-Leu-NMe_2 (**32b**)	0.001	0.087	0.000	0.000	0.376
Boc-Dmaa-D-Pro-Gly-Leu-OMe (**33a**)	0.123	0.059	0.128	0.077	0.433
Boc-Dmaa-D-Pro-Gly-Leu-OMe (**33b**)	0.157	0.023	0.069	0.041	0.429
Boc-Keto-D-Pro-Aib-Phe-OMe (**34**)	0.000	0.031	0.000	0.000	
Boc-Phe-Pro-Aib-(*R*)-α-Mba (**35**)	0.000	0.057	0.000	0.000	
2-Msa-Pro-D-Val-(*R*)-α-Mba (**36**)		0.013	0.048	0.068	
Boc-His(τ-Bn)-Pro-Aib-(*R*)-α-Mba (**37**)	0.000	0.042	0.001	0.001	
average	0.075	0.052	0.063	0.046	0.452
st. dev.	0.069	0.031	0.042	0.038	0.027
median	0.059	0.053	0.069	0.041	0.457
minimum	0.000	0.002	0.000	0.000	0.368
maximum	0.261	0.134	0.140	0.129	0.510
count	52	53	53	53	46

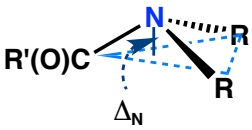

distance from N to plane defined by amide substituents

G. Symmetry-Independent Molecules[27]

Table S4.49: RMSD Values for Symmetry-Independent Molecules

Symmetry-Independent Conformers	ID	Backbone RMSD (Å)	Loop RMSD (Å)	All Atom RMSD (Å)
Boc-Dmaa-D-Pro-Acpc-Leu-NMe_2	3a,b	0.43	0.14	1.45
Boc-Dmaa-D-Pro-Acpc-Leu-OMe	4b–e	*vide infra*	*vide infra*	*vide infra*
Boc-Dmaa-D-Pro-Acpc-Gly-OMe	7a,b	1.23	0.72	1.51
Boc-Dmaa-D-Pro-Acbc-Leu-NMe_2	16a,b	0.52	0.11	1.10
Boc-Dmaa-D-Pro-Acbc-Leu-OMe	17a,b	0.13	0.03	0.32
Boc-Dmaa-D-Pro-Cle-Leu-OMe	18a,b	0.10	0.03	0.32
Boc-Dmaa-D-Pro-Aic-Leu-OMe	19a,b	1.04	0.12	1.87
Boc-Dmaa-D-Pro-Aic-D-Phe-NMe_2	20a,b	0.33	0.05	0.97
Boc-Dmaa-Pro-Aic-Leu-OMe	21a,b	0.13	0.02	0.26
Boc-Dmaa-D-Pro-Achc-Leu-OMe	22a,b	0.16	0.04	0.49
Boc-Dmaa-D-Pro-Aib-2-Thi-NMe_2	29a,b	0.11	0.01	0.21
Boc-Dmaa-D-Pro-Phe-Leu-NMe_2	32a,b	0.37	0.05	0.78
Boc-Dmaa-D-Pro-Gly-Leu-OMe	33a,b	0.17	0.03	0.34
average		0.39	0.11	0.80
st. dev.		0.38	0.20	0.57
median		0.25	0.05	0.64
minimum		0.10	0.01	0.21
maximum		1.23	0.72	1.87
count		13	13	13

Table S4.50: RMSD Values for Symmetry-Independent Molecules of Peptide **4b–e** (Z' = 4)

Boc-Dmaa-D-Pro-Acpc-Leu-OMe	Backbone RMSD (Å)	Loop RMSD (Å)	All Atom RMSD (Å)
4b/4b	N/A	N/A	N/A
4b/4c	0.27	0.04	0.54
4b/4d	0.05	0.01	0.13
4b/4e	0.34	0.03	0.66
4c/4b	N/A	N/A	N/A
4c/4c	N/A	N/A	N/A
4c/4d	0.32	0.03	0.64
4c/4e	0.47	0.03	0.79
4d/4b	N/A	N/A	N/A
4d/4c	N/A	N/A	N/A
4d/4d	N/A	N/A	N/A
4d/4e	0.34	0.03	0.67
4e/4b	N/A	N/A	N/A
4e/4c	N/A	N/A	N/A
4e/4d	N/A	N/A	N/A
4e/4e	N/A	N/A	N/A

H. Turn-Type Distributions[18]

Table S4.51: Distribution of Canonical Turn Types as a Function of *i*+2 Residue Across All Peptides (Except Unfolded **32a**,**b**)

i+2 Residue	Type II'	Type II	Type I'	Type I
Gly	0	0	2	0
Ala/D-Val	1	1	0	0
Aib	8	2	0	1
Acpc	10	1	9	0
Acbc	2	0	3	0
Cle	0	0	2	0
Aic	2	2	2	0
Achc	0	0	3	0
			Sum	**51**

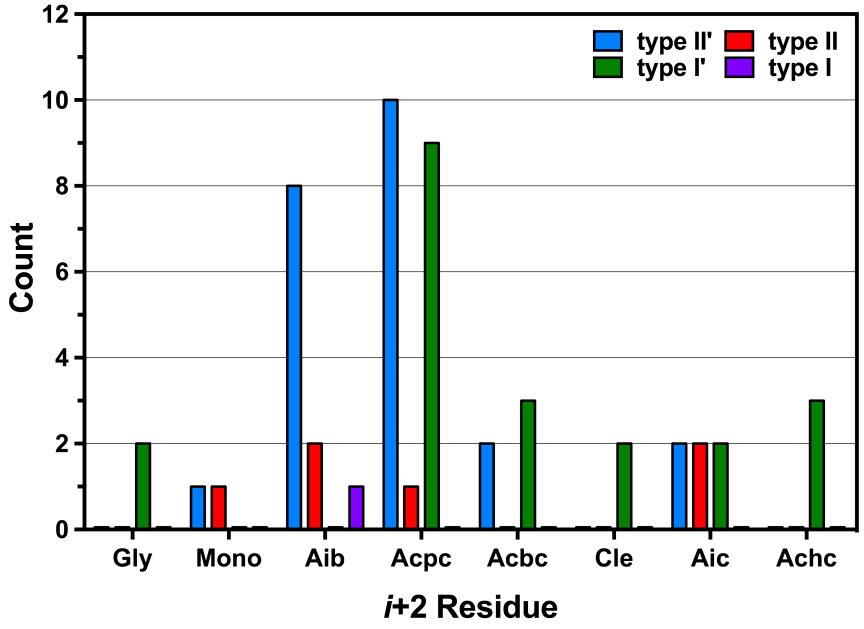

Figure S4.19: Chart showing the distribution of turn types as a function of *i*+2 residue (reproduced from Figure 14 in the manuscript). The symmetry-independent conformers of unfolded peptide **32** were excluded from this analysis.

Table S4.52: Distribution of Canonical Turn Types as a Function of *C*-Terminal Cap Across All Peptides (Except Unfolded **32a**,**b** and **35**–**37**)

C-Terminal Cap	Type II'	Type II	Type I'	Type I
methyl ester	8	4	19	0
dimethyl amide	15	0	2	0
			Sum	48

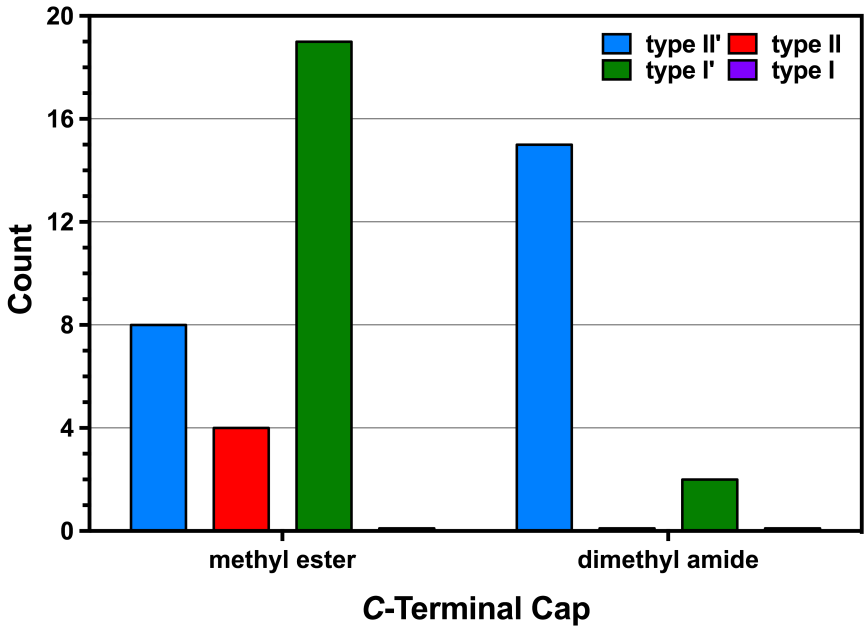

Figure S4.20: Chart showing the distribution of turn types as a function of *i*+2 residue (reproduced from Figure 17 in the manuscript). The symmetry-independent conformers of unfolded peptide **32** and the (*R*)-α-Mba-capped peptides **35**–**37** were excluded from this analysis.

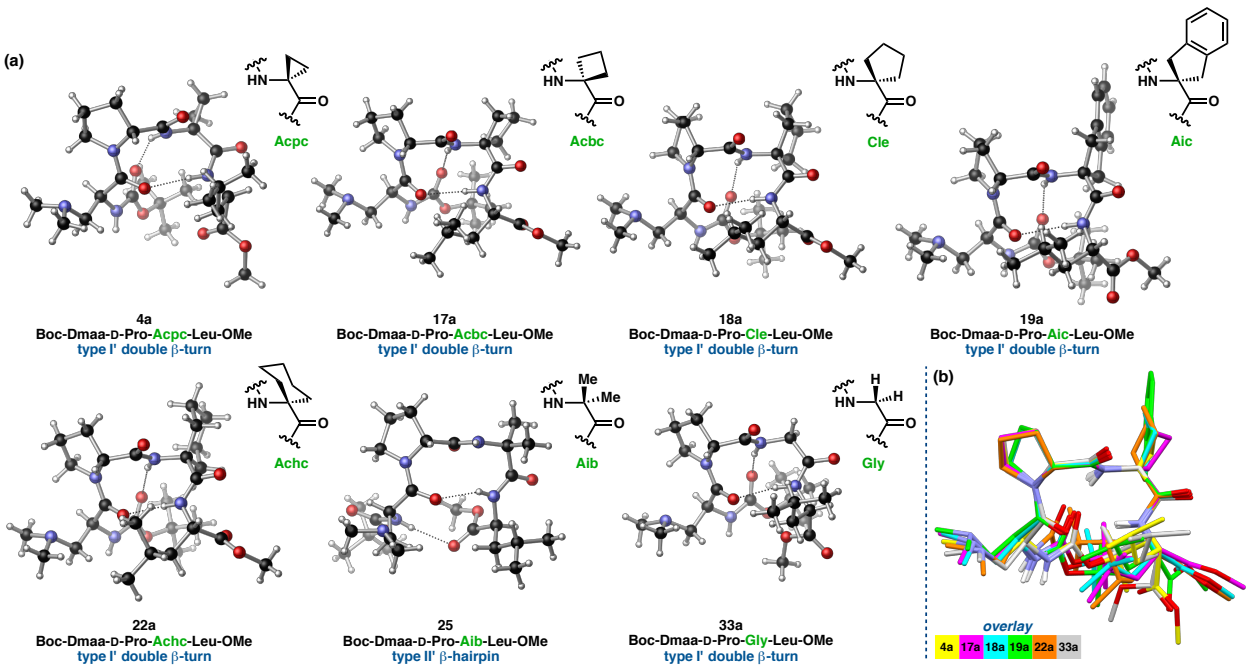

	Loop Dihedrals				Loop Angles		H-Bond Lengths		
	φ(*i*+1)	ψ(*i*+1)	φ(*i*+2)	ψ(*i*+2)	τ(*i*+1)	τ(*i*+2)	N(*i*+3)···O(*i*)	N(*i*)···O(*i*+3)	N(*i*+2)···O(*i*–1)
4a	62.4(3)°	17.7(3)°	72.7(4)°	11.9(5)°	114.6(2)°	117.0(3)°	3.096(3) Å	n/o	2.964(3) Å
17a	63.6(3)°	14.6(3)°	65.0(3)°	26.1(3)	115.3(2)°	112.3(2)°	3.141(3) Å	n/o	3.046(3) Å
18a	67.8(3)°	18.0(3)°	63.6(3)°	20.9(3)°	114.8(2)°	111.7(2)°	3.031(3) Å	n/o	3.236(3) Å
19a	71.2(4)°	17.1(5)°	59.3(4)°	37.1(4)°	114.6(3)°	110.6(3)°	3.192(4) Å	n/o	3.198(4) Å
22a	61.3(2)°	16.7(2)°	56.1(2)°	30.7(2)°	117.4(1)°	110.8(1)°	2.919(2) Å	n/o	3.297(2) Å
25	60.4(2)°	–136.0(1)°	–62.0(2)°	–21.3(2)°	110.1(1)°	111.7(1)°	2.813(1) Å	3.027(2) Å	n/o
33a	62.0(6)°	18.1(6)°	82.9(7)°	6.7(8)°	115.5(4)°	115.6(5)°	3.037(5) Å	n/o	2.884(6) Å

RMSD (4/17a) = 0.063 Å
(4/18a) = 0.057 Å
(4/19a) = 0.091 Å
(4/22a) = 0.105 Å
(4/33a) = 0.068 Å

Figure S4.21: Structural comparison of *i*+2 homologous series reproduced from Figure 15 in the manuscript. **(a)** A homologous series of peptides differing from one another only in the *i*+2 residue. For sequences with Z' > 1, only one structure is shown. The table highlights important structural differences among the members of the series. **(b)** An overlay of the type I′ β-turns from the homologous series shows tight overlap in the loop region and more deviations at the peripheral residues. All loop RMSDs are less than 0.11 Å.

V. Solution-Phase NMR Studies

A. NMR Methods

To fully characterize peptides in solution, one-dimensional ^{1}H and two-dimensional gCOSY and ^{1}H–^{1}H-NOESY experiments were carried out for each compound. All data were collected on Varian Inova 600 MHz spectrometers that were equipped with VnmrJ, version 4.2, revision A. Varian provided the pulse sequences for all experiments. All samples were prepared in C_6D_6 (referenced to residual C_6H_6 at 7.16 ppm)[1] at a concentration of 0.01 M, which was demonstrated to be below the aggregation limit for these peptides.

All NOESY spectra were acquired at 20–25 °C (specific temperatures are noted with spectra, *vide infra*). The NOESY data for each peptide were collected with a mixing time of 300 ms, a spectral width of 9615.4 Hz, and a d1 time of 3 s. The data were acquired with a total of 256 transients, 1442 points in the f2 dimension, and 256 points in the f1 dimension. The spectra were processed using MestReNova, version 9.0.0–12821. Zero-filling sized the spectra to 2048, 2048. Automatic phasing was used in conjunction with manual adjustments. Additionally, apodization was accomplished with a sine square function (90º) in both dimensions.[27] Each spectrum was automatically baseline corrected in each dimension using the Bernstein third order polynomial fit and treated with COSY-like symmetrization. The NOESY spectra were inspected before and after symmetrization, and peaks deemed to be artifacts were discarded. Further refinement included treatment of the spectrum to reduce t1 noise.

The NOESY spectra were integrated to extract distances from observed through-space interactions between protons. After integrating NOESY cross-peaks, the peak volumes were converted to distances using equation S1,[28] where r_{ij} is the calculated distance, r_{ref} is a reference distance, v_{ref} is the volume of a reference peak, and v_{ij} is the volume of the cross-peak in question. Reference peaks were chosen to be those that corresponded to interactions between the δ-protons of the respective D-Pro or L-Pro residues. Reference distances that corresponded to these volumes were extracted from the appropriate peptide crystal structure.

$$r_{ij} = r_{ref} \sqrt[6]{\left(\frac{v_{ref}}{v_{ij}} \right)} \tag{S1}$$

Integrated volumes were corrected using equation S2,[29] where v is the volume corresponding to either the reference or the peak in question from equation S1, v_{raw} is the uncorrected volume of a peak in question, and v_{diag1} and v_{diag2} correspond to the volumes of the diagonal peaks for each respective interacting proton.

$$v = \frac{2v_{raw}}{\left(v_{diag1} + v_{diag2} \right)} \tag{S2}$$

B. Characterization, Assignment, & Through-Space Interactions of Peptides in C_6D_6

General Information:

The notation used below is as follows. Each proton is designated by the three- of four-letter code of its amino acid residue.[30] Protons on the *tert*-butoxycarbonyl (Boc) *N*-terminal cap are called DmaaBoc protons. Additional notation equates the following: α = A, β = B, γ = G, and δ = D. Finally, for protons that are on the same carbon but are NMR-distinct, "2" is attributed to the more downfield proton and "1" to the more upfield proton. To further differentiate protons on the same sample, a, b, c, etc. are added, the more upfield shift having the earlier alphabetical identifier. For example, AcpcHB1a is the notation for the most upfield β-proton of the Acpc residue in our peptide.

The NOESY spectrum and nOe-map for each peptide is shown below. Each nOe map is accompanied by a legend that color-codes the distance between the protons whose through-space interactions were detected by our NOESY experiments. Additional contacts are noted on the nOe-maps of analyzed peptides that correspond to NOESY cross-peaks that were somehow compromised in resolution from another peak or high-noise areas. These contacts appear in purple and informed our overall conformational assessment of peptides, but were not quantitatively analyzed.

Peptide 3

^{1}H-NMR (600 MHz, 0.01 M in C_6D_6, 25 °C)

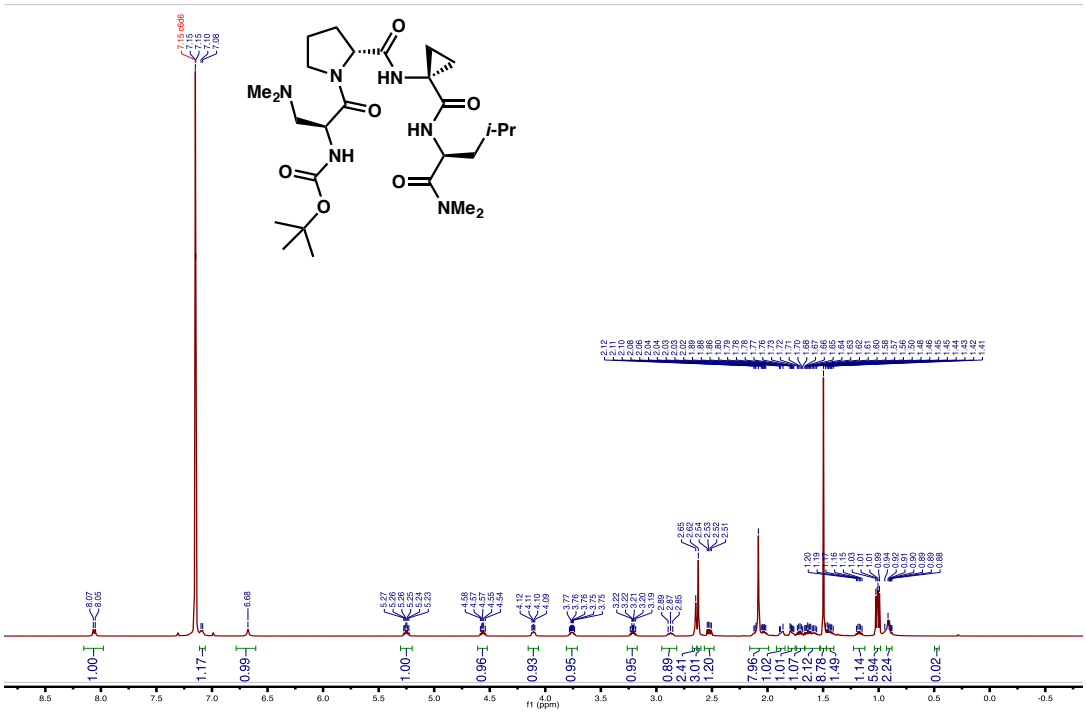

COSY (600 MHz, 0.01 M in C_6D_6, 25 °C)

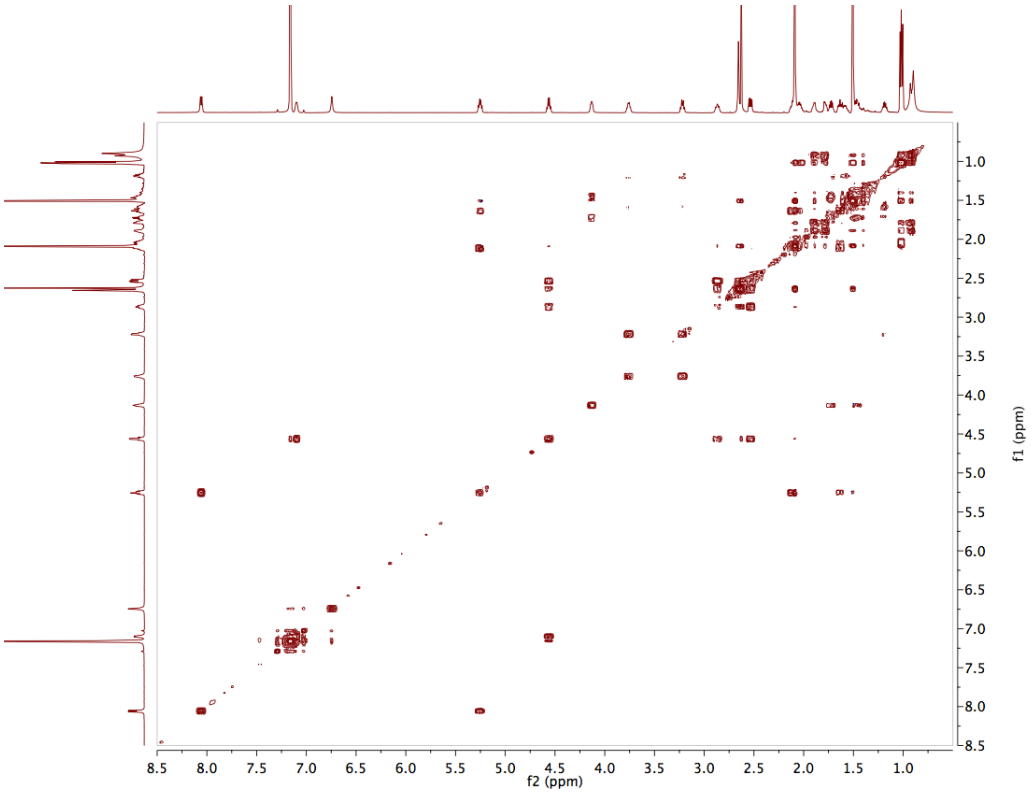

Table S5.01: Peak Assignments for Peptide **3**

Assignment (splitting)	Shift (ppm)	Range (ppm)	H's	*J*'s (Hz)
LeuNMe (m)	2.64	2.69–2.61	6	
LeuNH (d)	8.07	8.17–7.98	1	8.68
LeuHD (dd)	1.02	1.13–0.83	6	6.53, 10.01
LeuHG (m)	2.04	2.07–1.98	1	
LeuHB1 (ddd)	1.65	1.68–1.61	1	4.93, 8.47, 13.36
LeuHA (td)	5.26	5.58–5.19	1	4.91, 9.16
DProHG2 (m)	1.59	1.61–1.54	1	
DProHG1 (dt)	1.18	1.24–1.10	1	6.35, 12.57
DProHD2 (m)	3.77	3.81–3.73	1	
DProHD1 (dt)	3.22	3.33–3.09	1	7.10, 9.98
DProHB2 (m)	1.72	1.75–1.68	1	
DProHB1 (m)	1.45	1.48–1.40	1	
DProHA (dd)	4.12	4.19–4.00	1	4.97, 8.33
DmaaNH (d)	7.1	7.12–7.07	1	7.63
$DmaaNMe_2$, LeuHB2 (s)	2.09	2.22–1.90	7	
DmaaHB2 (t)	2.88	2.99–2.79	1	10.47
DmaaHB1 (dd)	2.53	2.56–2.44	1	6.20, 12.25
DmaaHA (m)	4.57	4.61–4.52	1	
DmaaBoc (s)	1.51	1.67–1.48	9	
AcpcNH (s)	6.69	6.91–6.50	1	
AcpcHB2b (d)	1.89	1.92–1.84	1	15.8
AcpcHB2a (m)	1.79	1.85–1.75	1	
AcpcHB1 (m)	0.92	0.96–0.83	2	

NOESY (600 MHz, 0.01 M in C_6D_6, 25 °C)

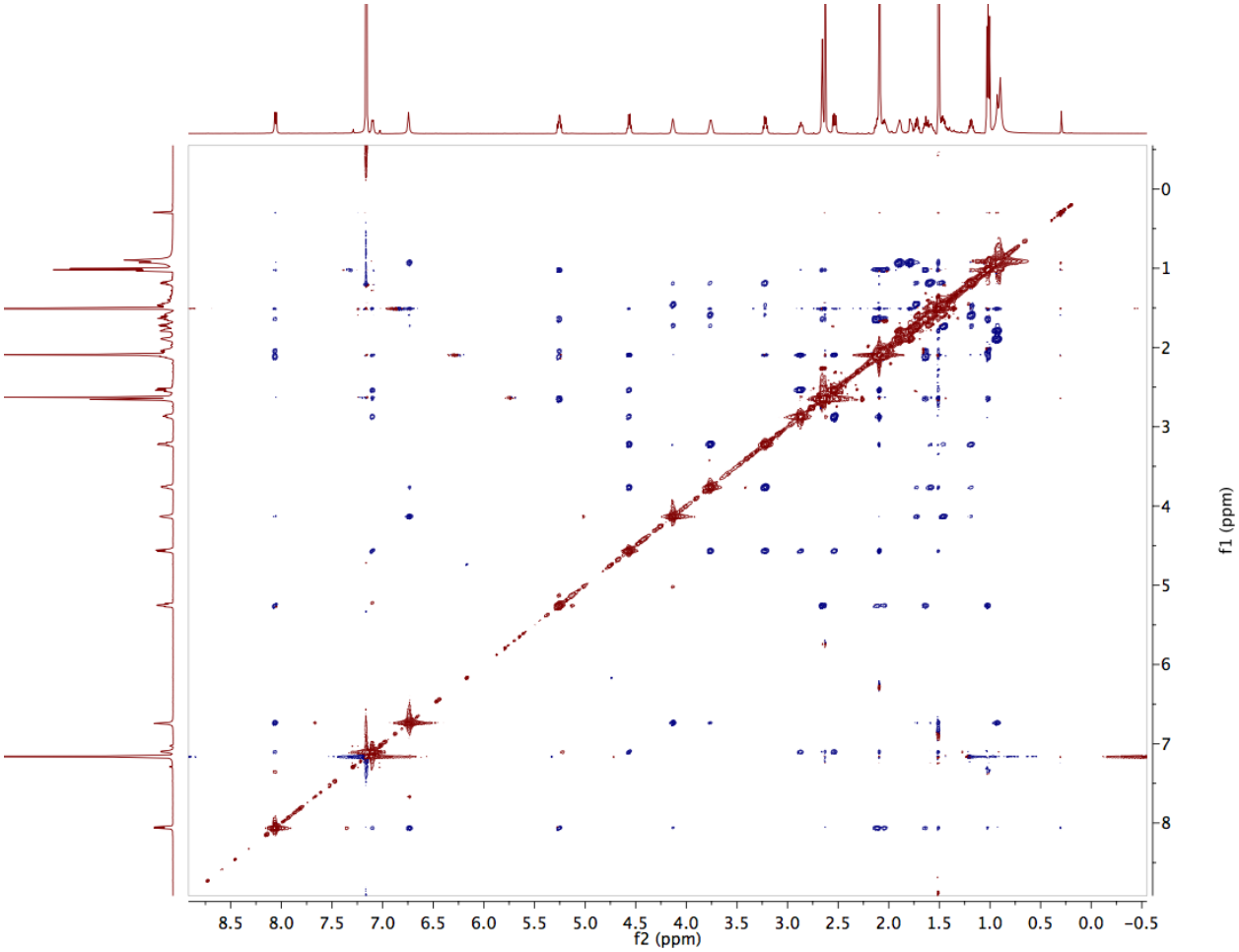

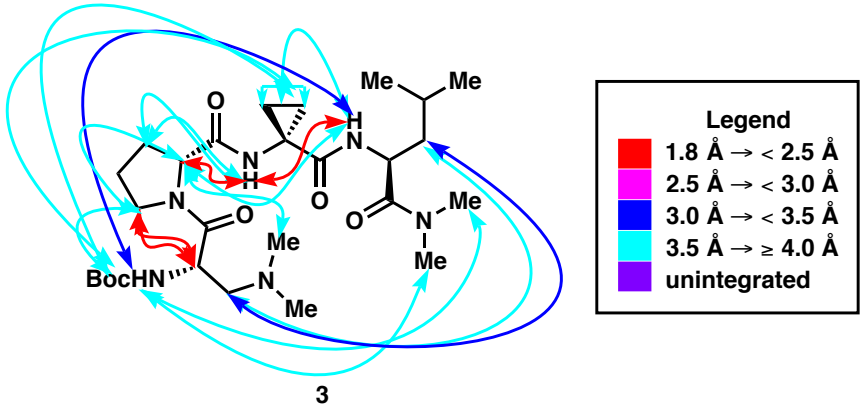

3

Figure S5.01: Inter-residue nOe Map for Peptide **3**

Table S5.02: Integrated NOESY Cross-peaks for Peptide **3**

	f2	f1	Normalized	Absolute	Assignment	Corrected Distances (Normalized)
1	8.06 1.02	1.04 8.06	–0.54 –0.64	–0.29 –0.34	LeuNH-LeuHD	4.29
2	8.06 0.91	0.92 8.07	–0.48 –0.52	–0.26 –0.28	LeuNH-AcpcHB1	3.66
3	8.06 7.11	7.11 8.08	–1 –0.97	–0.53 –0.52	LeuNH-DmaaNH	3.26
4	8.06 6.73	6.75 8.08	–5.67 –5.58	–3.02 –2.97	LeuNH-AcpcNH	2.42
5	8.06 2.03	2.04 8.06	–1.78 –1.7	–0.95 –0.91	LeuNH-LeuHG	3.00
6	8.06 2.11	2.11 8.06	–4.37 –4.59	–2.32 –2.44	LeuNH-LeuHB1	2.39
7	8.05 4.12	4.14 8.06	–0.4 –0.36	–0.21 –0.19	LeuNH-DProHA	3.89
8	8.05 1.64	1.65 8.07	–1.09 –1.04	–0.58 –0.56	LeuNH-LeuHB2	3.20
9	8.05 2.65	2.66 8.06	–0.1 –0.11	–0.05 –0.06	LeuNH-LeuNMe2	4.96
10	8.05 2.63	2.63 8.06	–0.08 –0.09	–0.04 –0.05	LeuNH-LeuNMe1	5.27
11	7.1 2.09	2.09 7.1	–0.81 –0.74	–0.43 –0.39	DmaaNH-DmaaNMe$_2$	4.02
12	7.1 2.87	2.89 7.11	–2.51 –2.57	–1.33 –1.37	DmaaNH-DmaaHB2	2.78
13	7.1 2.66	2.66 7.1	–0.21 –0.17	–0.11 –0.09	DmaaNH-LeuNMe2	4.53
14	7.1 2.53	2.54 7.1	–2.56 –2.69	–1.36 –1.43	DmaaNH-DmaaHB1	2.80
15	7.1 2.63	2.63 7.1	–0.57 –0.56	–0.3 –0.3	DmaaNH-LeuNMe1	3.87
16	6.73 0.93	0.93 6.75	–5.4 –5.35	–2.87 –2.85	AcpcNH-AcpcHB1	2.48
17	6.73 3.76	3.77 6.74	–0.93 –0.94	–0.49 –0.5	AcpcNH-DProHD2	3.29
18	6.73 1.58	1.61 6.74	–0.44 –0.49	–0.23 –0.26	AcpcNH-DProHB1	3.68
19	6.73 1.72	1.73 6.74	–0.52 –0.44	–0.27 –0.23	AcpcNH-DProHB2	3.73
20	6.73 4.11	4.14 6.75	–7.81 –7.78	–4.16 –4.14	AcpcNH-DProHA	2.36
21	5.25 2.63	2.63 5.26	–2.6 –3.14	–1.38 –1.67	LeuHA-LeuNMe1	3.00
22	5.25 1.02	1.02 5.26	–8.02 –7.98	–4.27 –4.24	LeuHA-LeuHD	2.81
23	5.25 2.67	2.67 5.26	–8.26 –8.25	–4.39 –4.39	LeuHA-LeuNMe2	3.43
24	5.25 2.04	2.04 5.26	–2.02 –2.04	–1.07 –1.09	LeuHA-LeuHG	3.02
25	4.57 3.22	3.22 4.57	–9.7 –9.66	–5.16 –5.14	DmaaHA-DProHD1	2.26
26	4.56 3.76	3.76 4.57	–8.64 –8.65	–4.6 –4.6	DmaaHA-DProHD2	2.31
27	4.56 2.09	2.1 4.58	–7.21 –7.17	–3.83 –3.81	DmaaHA-DmaaNMe$_2$	2.78
28	4.13 3.22	3.23 4.13	–0.52 –0.54	–0.28 –0.29	DProHA-DProHD1	3.70
29	4.13 1.19	1.2 4.14	–0.79 –0.85	–0.42 –0.45	DProHA-DProHG1	3.50
30	4.13 2.09	2.1 4.14	–0.25 –0.2	–0.13 –0.1	DProHA-DmaaNMe$_2$	4.97
31	3.76 1.72	1.73 3.76	–1.12 –1.13	–0.6 –0.6	DProHD2-DProHB2	3.50

32	3.76 1.51	1.51 3.76	–0.73 –0.73	–0.39 –0.39	DProHD2-DmaaBoc	4.30
33	3.22 1.46	1.46 3.22	–1.25 –1.25	–0.66 –0.66	DProHD1-DProHB1	3.18
34	2.88 1.64	1.64 2.87	–0.29 –0.33	–0.15 –0.17	DmaaHB2-LeuHB2	3.93
35	2.87 2.09	2.1 2.87	–8.64 –8.47	–4.59 –4.51	DmaaHB2-DmaaNMe$_2$	2.68
36	2.66 1.64	1.63 2.66	–1.57 –1.47	–0.84 –0.78	LeuNMe2-LeuHB2	3.20
37	2.65 1.01	1.02 2.66	–1.31 –1.26	–0.69 –0.67	LeuNMe2-LeuHD	4.10
38	2.62 1.02	1.02 2.63	–0.43 –0.52	–0.23 –0.28	LeuNMe1-LeuHD	4.59
39	2.54 2.09	2.1 2.53	–7.49 –7.55	–3.98 –4.02	DmaaHB1-LeuHB2	2.93
40	1.64 1.02	1.02 1.64	–7.41 –7.67	–3.94 –4.08	LeuHB2-LeuHD	2.82
41	1.51 1.79	1.79 1.51	–1.53 –1.55	–0.75 –0.76	DmaaBoc-AcpcHB	3.79
42	1.51 0.93	0.92 1.5	–1.13 –1.15	–0.56 –0.56	DmaaBoc-AcpcHB	4.00
43	3.77 3.22	3.23 3.79	–35.57 –35.4	–18.91 –18.82	DProHD1-DProHD2	1.80

Peptide 4

^{1}H-NMR (600 MHz, 0.01 M in C_6D_6, 20 °C)

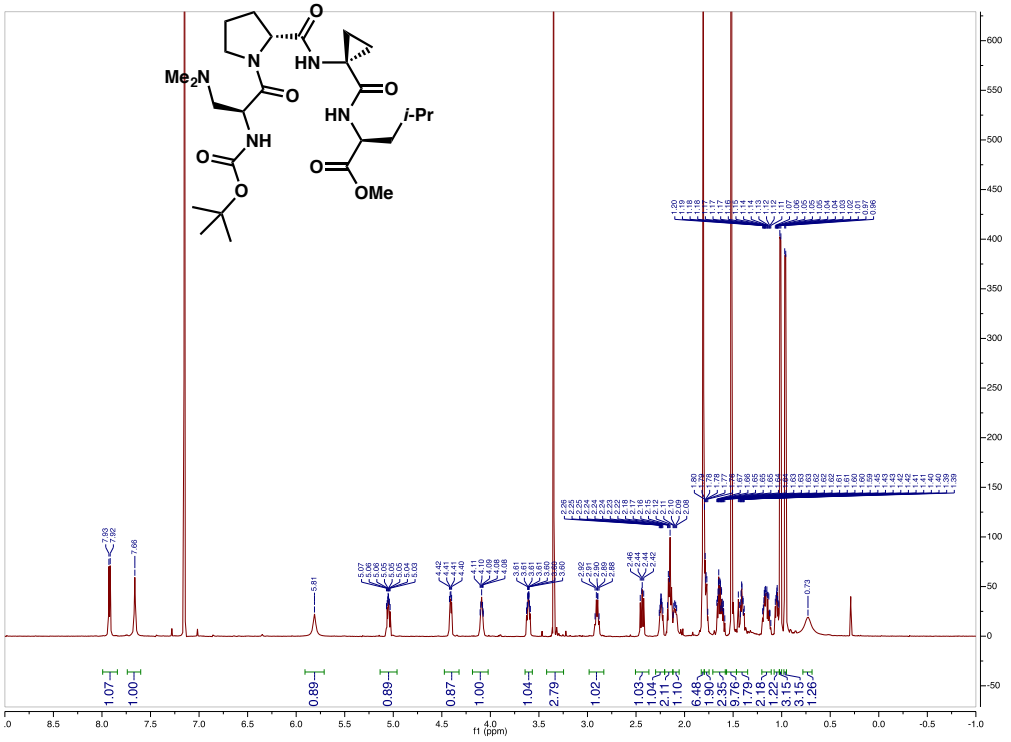

COSY (600 MHz, 0.01 M in C_6D_6, 25 °C)

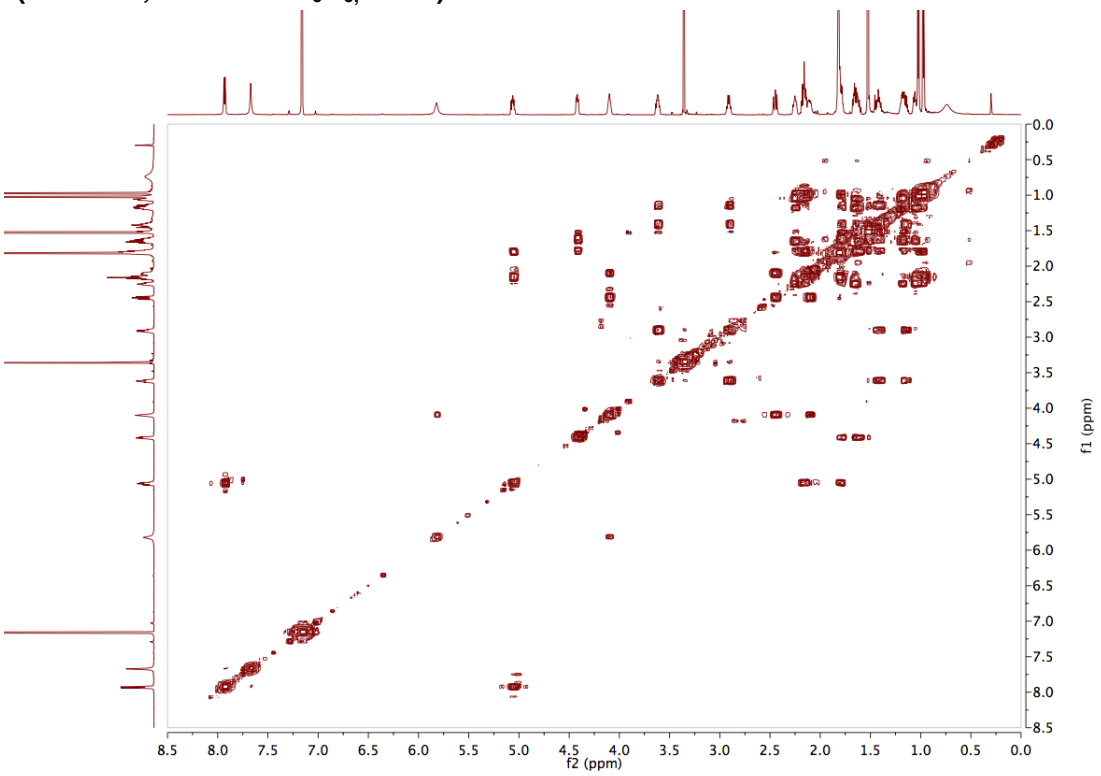

Table 5.03: Peak Assignments for Peptide **4**

Assignment (splitting)	Shift (ppm)	Range (ppm)	H's	*J*'s (Hz)
LeuOMe (s)	3.36	3.36–3.34	3	
LeuNH (d)	7.93	7.99–7.86	1	7.78
LeuHD (dd)	1	1.04–0.95	6	6.34, 30.02
LeuHB2, DProHB2 (m)	2.17	2.19–2.13	2	
LeuHB1 (m)	1.79	1.81–1.76	1	
LeuHA (ddd)	5.06	5.12–5.00	1	4.57, 7.77, 10.05
DProHG2 (m)	1.42	1.46–1.38	1	
DProHG1 (m)	1.14	1.16–1.11	1	
DProHD2 (td)	3.62	3.65–3.58	1	4.96, 8.58
DProHD1 (q)	2.91	2.94–2.88	1	8.29
DProHB1 (m)	1.62	1.65–1.59	1	
DProHA (dd)	4.42	4.45–4.39	1	4.40, 8.70
DmaaNH (s)	5.82	5.88–5.77	1	
$DmaaNMe_2$, LeuHG (s)	1.82	1.83–1.81	7	
DmaaHB2 (dd)	2.45	2.47–2.42	1	9.03, 12.18
DmaaHB1 (m)	2.11	2.13–2.07	1	
DmaaHA (m)	4.1	4.13–4.07	1	
DmaaBoc (s)	1.53	1.53–1.51	9	
AcpcNH (s)	7.67	7.70–7.63	1	
AcpcHB2b (m)	2.25	2.28–2.22	1	
AcpcHB2a (m)	1.66	1.68–1.65	1	
AcpcHB1b (m)	1.19	1.22–1.17	1	
AcpcHB1a (m)	1.06	1.09–1.03	1	

NOESY (600 MHz, 0.01 M in C_6D_6, 25 °C)

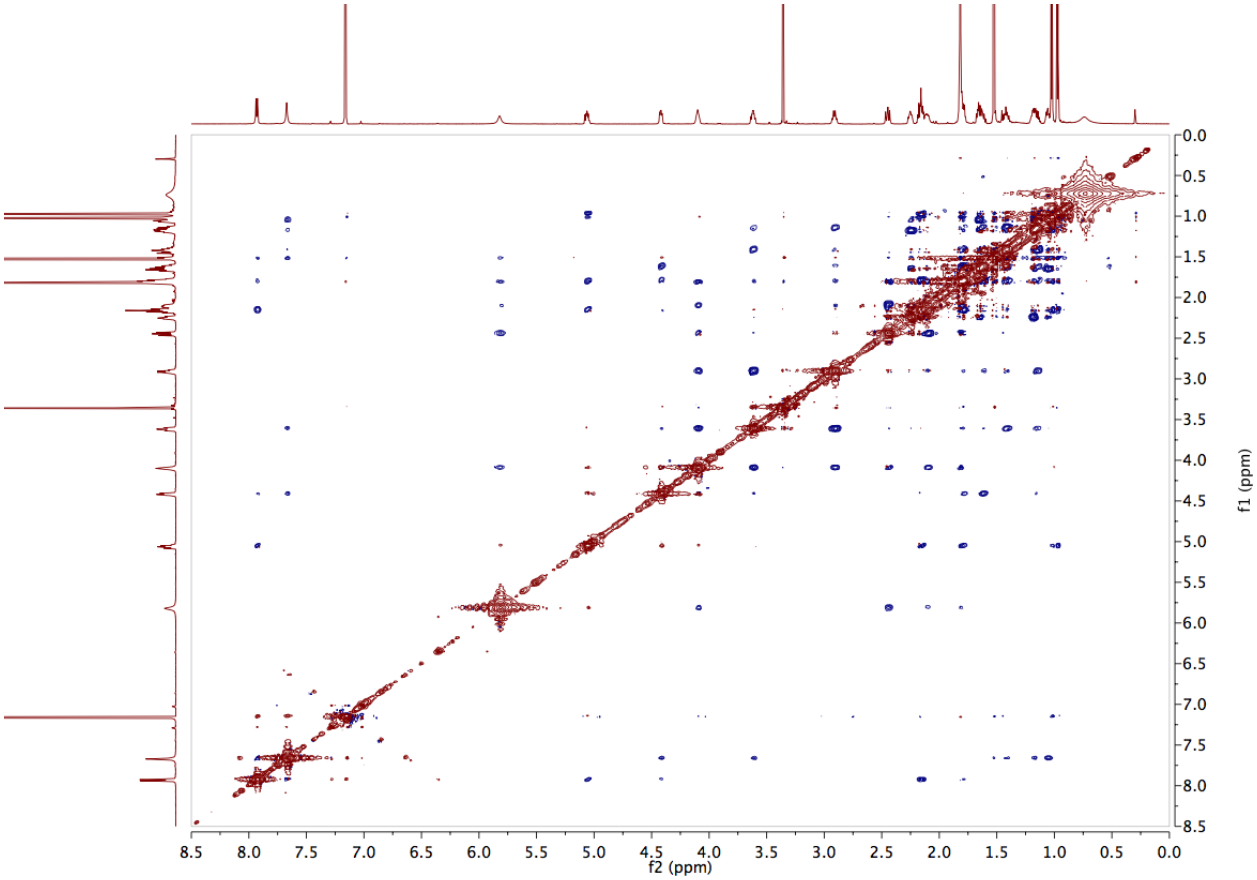

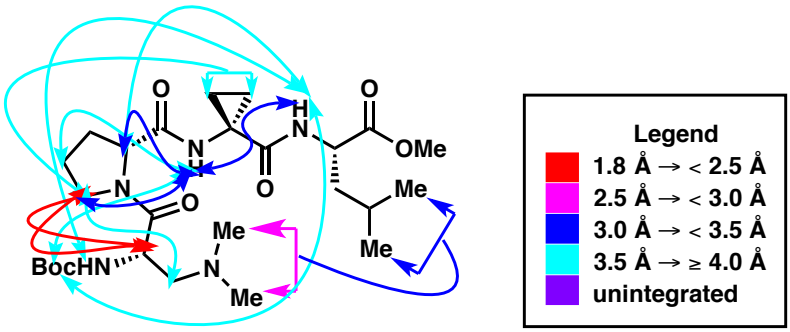

4

Figure S5.02: Inter-residue nOe Map for Peptide **4**

Table S5.04: Integrated NOESY Cross-peaks for Peptide **4**

	f2	f1	Normalized	Absolute	Assignment	Corrected Distances (Normalized)
1	7.93 5.81	5.81 7.94	–0.24 –0.24	–0.03 –0.03	LeuNH-DmaaNH	4.21
2	7.93 7.67	7.67 7.93	–1.27 –1.26	–0.18 –0.18	LeuNH-AcpcNH	3.19
3	7.93 1.53	1.53 7.93	–0.72 –0.7	–0.1 –0.1	LeuNH-DmaaBoc	4.31
4	7.93 4.42	4.42 7.93	–0.55 –0.58	–0.08 –0.08	LeuNH-DProHA	3.70
5	7.67 1.53	1.53 7.67	–1.75 –1.75	–0.25 –0.25	AcpcNH-DmaaBoc	3.70
6	7.67 1.42	1.42 7.67	–0.95 –0.9	–0.14 –0.13	AcpcNH-DProHG2	3.60
7	7.67 1.05	1.06 7.67	–4.47 –4.48	–0.64 –0.64	AcpcNH-AcpcHB1a	2.55
8	7.67 4.42	4.42 7.67	–1.76 –1.76	–0.25 –0.25	AcpcNH-DProHA	3.03
9	7.67 3.62	3.62 7.67	–1.63 –1.63	–0.23 –0.23	AcpcNH-DProHD2	3.04
10	7.67 1.18	1.18 7.67	–1.09 –1.11	–0.16 –0.16	AcpcNH-AcpcHB1b	3.32
11	7.67 1.66	1.66 7.67	–0.28 –0.28	–0.04 –0.04	AcpcNH-AcpcHB2a	4.18
12	5.82 2.45	2.45 5.83	–5.57 –5.55	–0.8 –0.8	DmaaNH-DmaaHB2	2.51
13	5.82 1.53	1.53 5.82	–0.91 –0.9	–0.13 –0.13	DmaaNH-DmaaBoc	4.13
14	5.81 2.1	2.1 5.82	–1.35 –1.31	–0.19 –0.19	DmaaNH-DmaaHB1	3.15
16	5.06 0.99	0.99 5.06	–6.49 –6.57	–0.93 –0.94	LeuHA-LeuHD	2.73
17	4.1 3.62	3.62 4.1	–13.32 –13.33	–1.92 –1.92	DmaaHA-DProHD2	2.18
18	4.42 1.41	1.42 4.42	–0.19 –0.18	–0.03 –0.03	DProHA-DProHG2	4.62
19	4.1 2.91	2.91 4.1	–10.44 –10.38	–1.5 –1.49	DmaaHA-DProHD1	2.28
20	4.1 1.82	1.82 4.11	–7.1 –7.11	–1.02 –1.02	DmaaHA-DmaaNMe$_2$	2.87
21	3.61 1.06	1.06 3.62	–0.27 –0.27	–0.04 –0.04	DProHD2-AcpcHB1a	4.10
23	2.91 1.61	1.62 2.91	–0.9 –0.96	–0.13 –0.14	DProHD1-DProHB1	3.31
24	2.91 2.11	2.11 2.91	–0.65 –0.64	–0.09 –0.09	DProHD1-DmaaHB1	3.60
25	2.44 1.82	1.82 2.44	–5.64 –5.64	–0.81 –0.81	DmaaHB2-DmaaNMe$_2$	2.99
26	1.81 1.02	1.02 1.82	–6.61 –6.59	–0.95 –0.95	LeuHD(downfield)-DmaaNMe$_2$	3.04
27	3.62 2.91	2.91 3.61	–40.93 –40.67	–5.89 –5.85	DProHD2-DProHD1	1.80

Peptide 7

^{1}H-NMR (600 MHz, 0.01 M in C_6D_6, 25 °C)

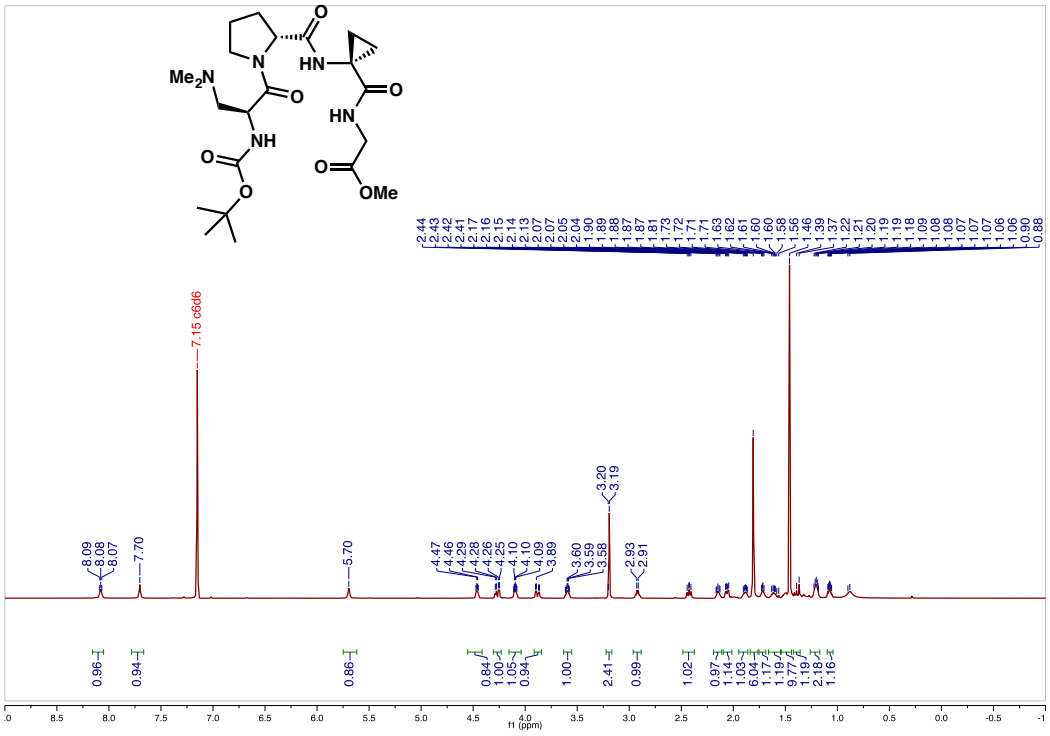

COSY (600 MHz, 0.01 M in C_6D_6, 25 °C)

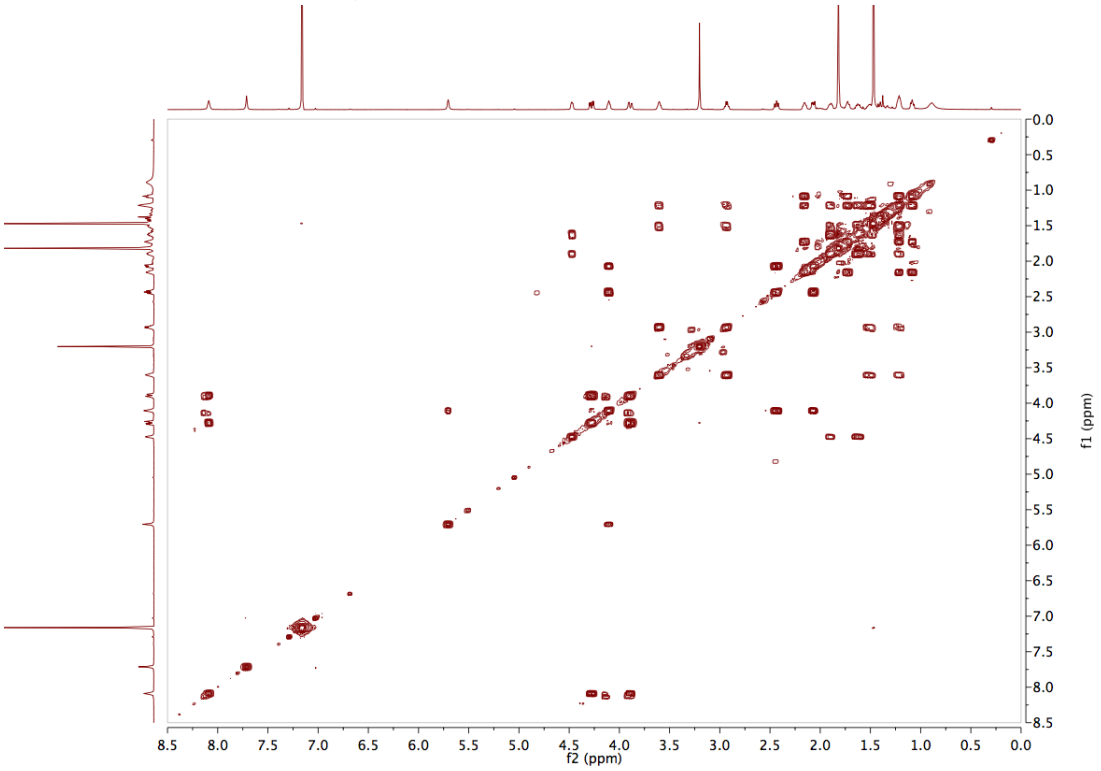

Table 5.05: Peak Assignments for Peptide **7**

Name	Shift (ppm)	Range (ppm)	H's	*J*'s (Hz)
GlyOMe (s)	3.20	3.31–3.15	2	
GlyNH (t)	8.09	8.12–8.06	1	6.01
GlyHA1 (dd)	3.89	4.01–3.81	1	5.21, 17.58
GlyHA2 (dd)	4.28	4.37–4.21	1	6.24, 17.54
DProHG2 (m)	1.53	1.59–1.49	1	
DProHD1 (d)	2.93	3.04–2.84	1	8.21
DProHD2 (m)	3.60	3.69–3.53	1	
DProHB1 (dd)	1.62	1.68–1.58	1	15.66, 8.02
DProHB2 (m)	1.90	1.93–1.86	1	
DProHA (dd)	4.47	4.53–4.41	1	8.77, 4.12
DmaaNMe$_2$ (s)	1.82	1.84–1.80	6	
DmaaNH (s)	5.71	5.77–5.65	1	
AcpcHB1a (ddd)	1.08	1.18–1.02	1	4.03, 7.60, 9.85
DmaaHB1 (dd)	2.07	2.12–2.02	1	5.85, 12.42
DmaaHB2 (dd)	2.44	2.49–2.39	1	9.27, 12.26
DmaaHA (dd)	4.11	4.14–4.07	1	9.49, 4.58
DmaaBoc (s)	1.47	1.56–1.36	9	
AcpcNH (s)	7.71	7.76–7.68	1	
AcpcHB1b, DProHG2 (m)	1.21	1.26–1.17	2	
AcpcHB2a (m)	1.73	1.76–1.69	1	
AcpcHB2b (m)	2.15	2.19–2.05	1	

NOESY (600 MHz, 0.01 M in C_6D_6, 25 °C)

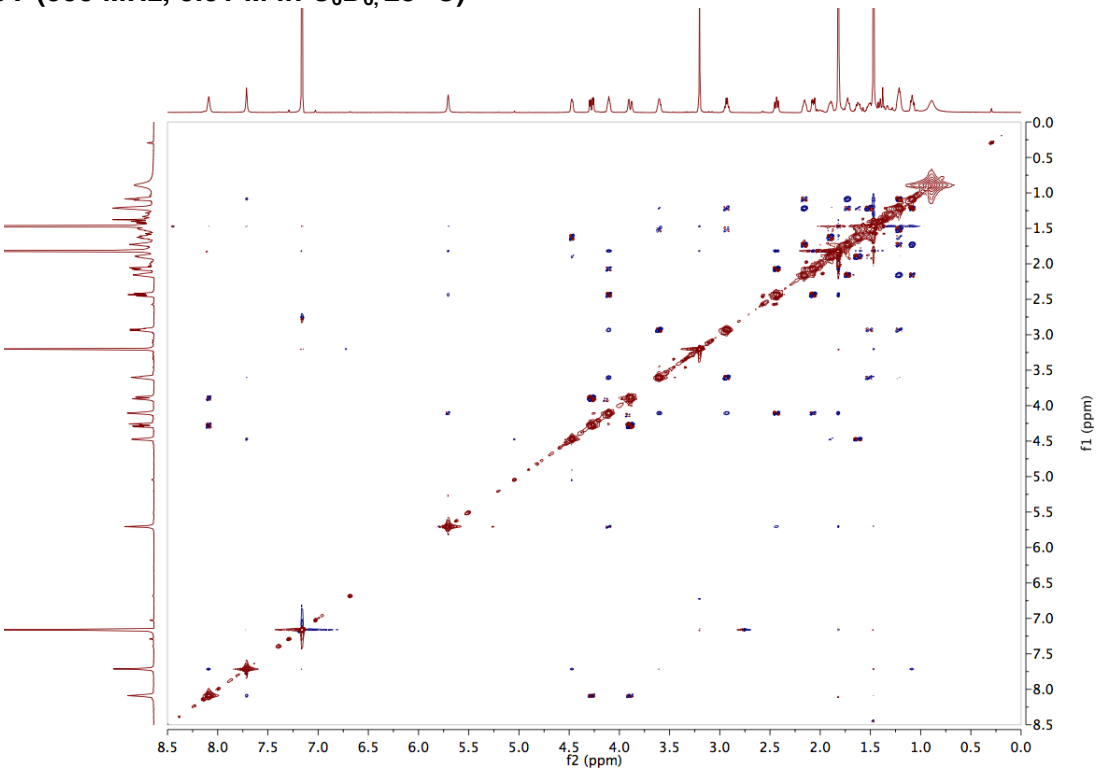

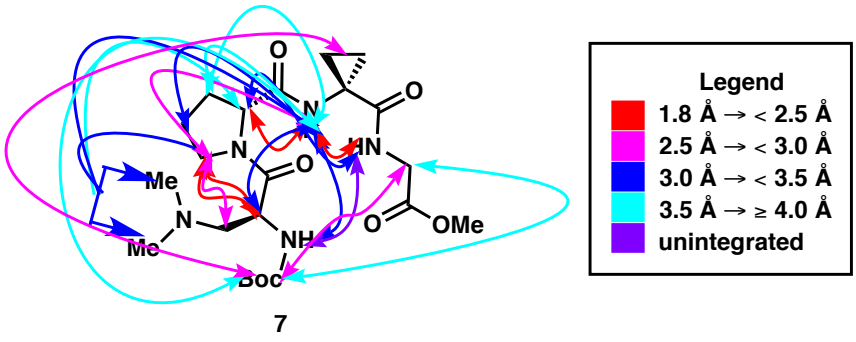

7

Figure S5.03: Inter-residue nOe Map for Peptide **7**

Table S5.06: Integrated NOESY Cross-peaks for Peptide **7**

	f2	f1	Normalized	Absolute	Assignment	Normalized Average Volume	Corrected Distances (Normalized)
1	8.09	7.71	-1.03	-0.66	GlyNH-AcpcNH	-1.03	2.21
	7.71	8.09	-1.03	-0.66			
2	8.09	4.47	-0.12	-0.08	GlyNH-DProHA	-0.12	3.23
	4.47	8.09	-0.12	-0.08			
3	7.72	5.7	-0.02	-0.01	AcpcNH-DmaaNH	-0.025	4.13
	5.7	7.71	-0.03	-0.02			
4	7.71	4.47	-0.86	-0.55	AcpcNH-DProHA	-0.86	2.31
	4.47	7.71	-0.86	-0.55			
5	7.71	4.11	-0.09	-0.06	AcpcNH-DmaaHA	-0.085	3.42
	4.1	7.71	-0.08	-0.05			
6	7.71	3.6	-0.48	-0.31	AcpcNH-DProHD	-0.485	2.55
	3.6	7.71	-0.49	-0.32			
7	7.71	2.16	-0.03	-0.02	AcpcNH-AcpcHB2b	-0.03	4.04
	2.16	7.71	-0.03	-0.02			
8	7.71	1.9	-0.14	-0.09	AcpcNH-DProHB2	-0.135	3.80
	1.89	7.71	-0.13	-0.09			
9	7.71	1.72	-0.04	-0.02	AcpcNH-DProHB1	-0.045	3.81
	1.72	7.71	-0.05	-0.03			
10	7.71	1.09	-0.85	-0.55	AcpcNH-AcpcHB2a	-0.86	2.32
	1.09	7.71	-0.87	-0.56			
11	7.71	1.51	-0.13	-0.08	AcpcNH-DProHG	-0.13	3.07
	1.51	7.71	-0.13	-0.09			
12	5.7	2.43	-1.01	-0.65	AcpcNH-AcpcHB1a	-1.01	2.26
	2.43	5.7	-1.01	-0.65			
13	5.7	2.07	-0.29	-0.19	DmaaNH-DmaaHB1	-0.295	2.81
	2.07	5.71	-0.3	-0.19			
14	5.7	1.82	-0.31	-0.2	AcpcNH-DmaaNMe$_2$	-0.315	3.31
	1.82	5.7	-0.32	-0.21			
15	5.71	1.47	-0.26	-0.17	AcpcNH-DmaaBoc	-0.26	3.66
	1.47	5.7	-0.26	-0.17			
16	4.47	2.94	-0.13	-0.09	DProHA-DProHD1	-0.135	3.21
	2.94	4.47	-0.14	-0.09			
17	4.48	1.82	-0.11	-0.07	DProHA-DmaaNMe$_2$	-0.115	3.93
	1.82	4.48	-0.12	-0.08			
18	4.27	1.47	-0.29	-0.18	GlyHA2-DmaaBoc	-0.305	3.58
	1.47	4.28	-0.32	-0.21			

19	4.1 3.6	3.6 4.11	-3.04 -3.09	-1.95 -1.98	DmaaHA-DProHD2	-3.065	1.91
20	4.1 2.93	2.93 4.11	-2.41 -2.45	-1.55 -1.57	DmaaHA-DProHD1	-2.43	1.99
21	4.09 1.82	1.82 4.09	-2.03 -2.03	-1.3 -1.3	DmaaHA-DmaaNMe$_2$	-2.03	2.44
22	4.11 1.47	1.47 4.11	-0.21 -0.21	-0.14 -0.14	DmaaHA-DmaaBoc	-0.21	3.81
23	3.89 1.47	1.47 3.89	-0.25 -0.26	-0.16 -0.17	GlyHA1-DmaaBoc	-0.255	2.90
24	3.61 1.9	1.9 3.61	-0.17 -0.17	-0.11 -0.11	DProHD2-DProHB2	-0.17	3.09
25	2.93 2.06	2.07 2.93	-0.31 -0.33	-0.2 -0.21	DProHD1-DmaaHB1	-0.32	2.80
26	2.93 1.82	1.82 2.93	-0.3 -0.3	-0.19 -0.19	DProHD1-DmaaNMe$_2$	-0.3	3.35
27	2.93 1.62	1.62 2.93	-0.38 -0.36	-0.24 -0.23	DProHD1-DProHB1	-0.37	2.71
28	2.43 1.82	1.82 2.43	-1.21 -1.23	-0.78 -0.79	DmaaHB2-DmaaNMe$_2$	-1.22	2.65
29	1.47 1.09	1.09 1.47	-1.67 -1.7	-1.07 -1.09	DmaaBoc-AcpcHB1a	-1.685	2.69
31	2.93 3.6	1.82 2.93	-0.3 -8.34	-0.19 -5.36	DProHD1-DProHD2	-4.32	2.21

Peptide 15

^{1}H-NMR (600 MHz, 0.01 M in C_6D_6, 20 °C)

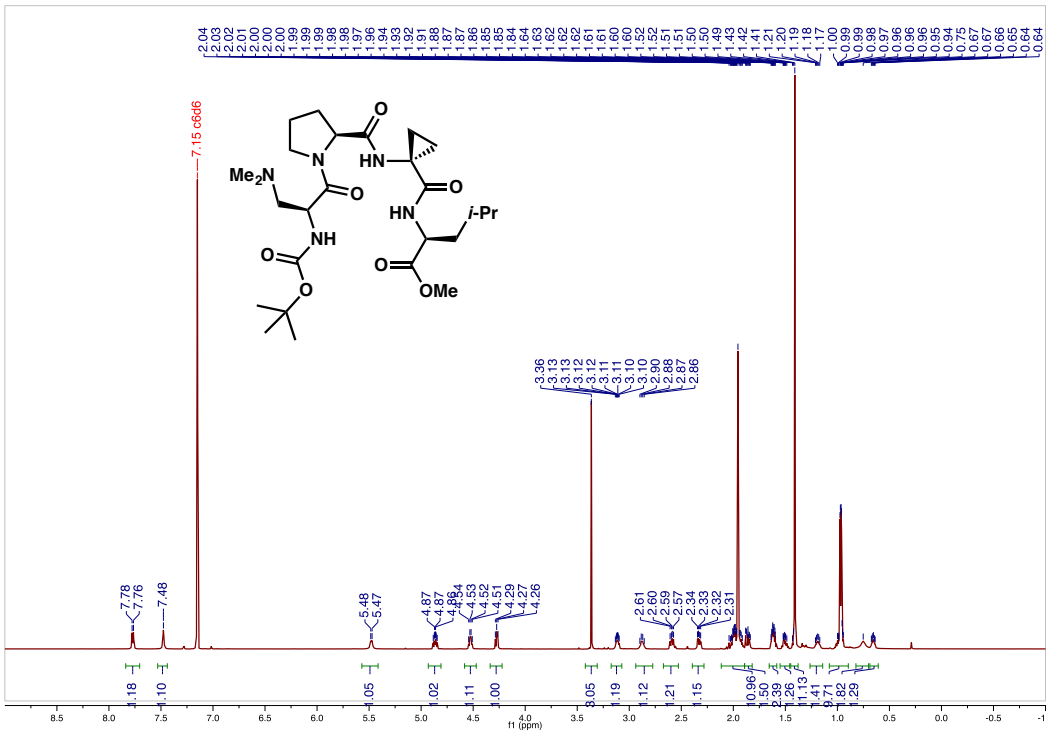

COSY (600 MHz, 0.01 M in C_6D_6, 20 °C)

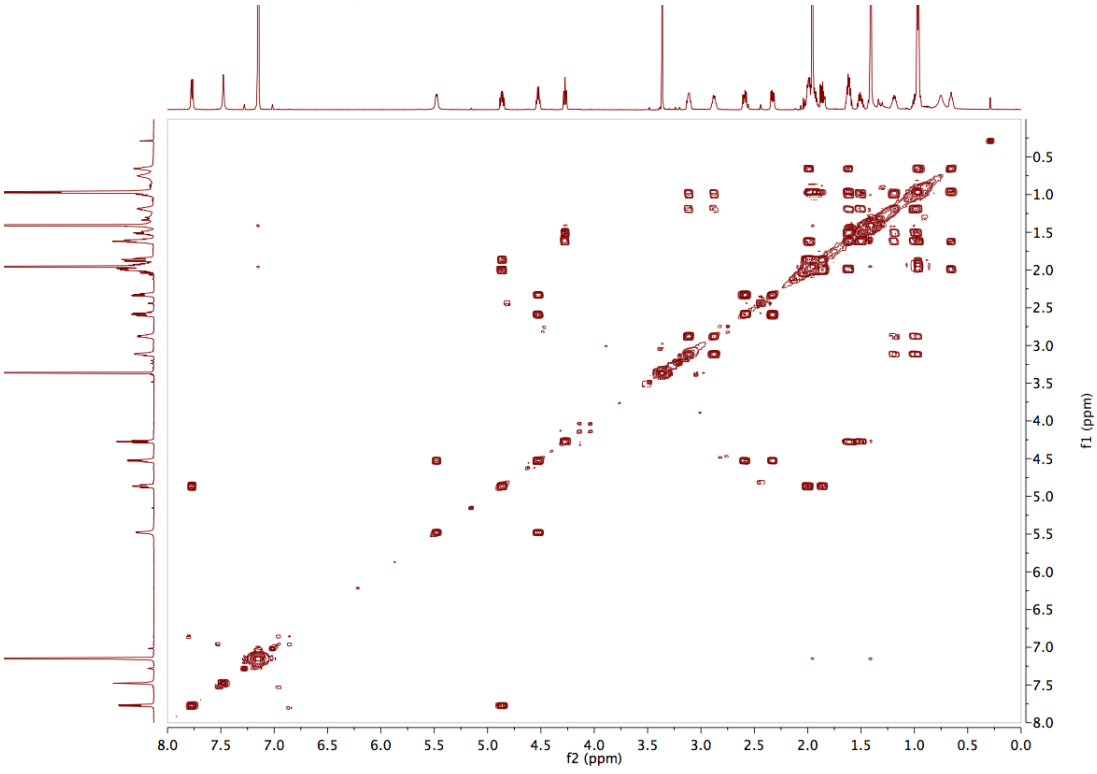

Table 5.07: Peak Assignments for Peptide **15**

Assignment (splitting)	Shift (ppm)	Range (ppm)	H's	*J*'s (Hz)
LeuOMe (s)	3.36	3.38–3.35	3	
LeuNH (d)	7.77	7.79–7.75	1	7.87
LeuHB2, AcpcHB2b (m)	2.01	2.05–1.97	2	
LeuHB1 (m)	1.86	1.90–1.82	1	
LeuHA (ddd)	4.86	4.90–4.83	1	5.45, 7.84, 9.35
DProHG2 (m)	1.18	1.23–1.14	1	
DProHD2 (m)	3.12	3.15–3.08	1	
DProHD1 (q)	2.88	2.91–2.84	1	7.44
DProHB2, AcpcHB2a (m)	1.61	1.65–1.57	2	
DProHB1 (m)	1.51	1.55–1.46	1	
DProHA (t)	4.27	4.30–4.24	1	7.56, 7.56
DmaaNH (d)	5.48	5.50–5.45	1	7.56
$DmaaNMe_2$ (s)	1.96	1.97–1.91	6	
DmaaHB2 (dd)	2.59	2.62–2.54	1	7.42, 12.33
DmaaHB1 (dd)	2.33	2.36–2.30	1	5.78, 12.32
DmaaHA (q)	4.53	4.56–4.49	1	7.21
DmaaBoc (s)	1.41	1.43–1.39	9	
AcpcNH (s)	7.48	7.49–7.46	1	
AcpcHB1b, LeuHD, DProHG1 (m)	0.97	1.04–0.93	8	
AcpcHB1a (m)	0.66	0.69–0.62	1	

NOESY (600 MHz, 0.01 M in C_6D_6, 20 °C)

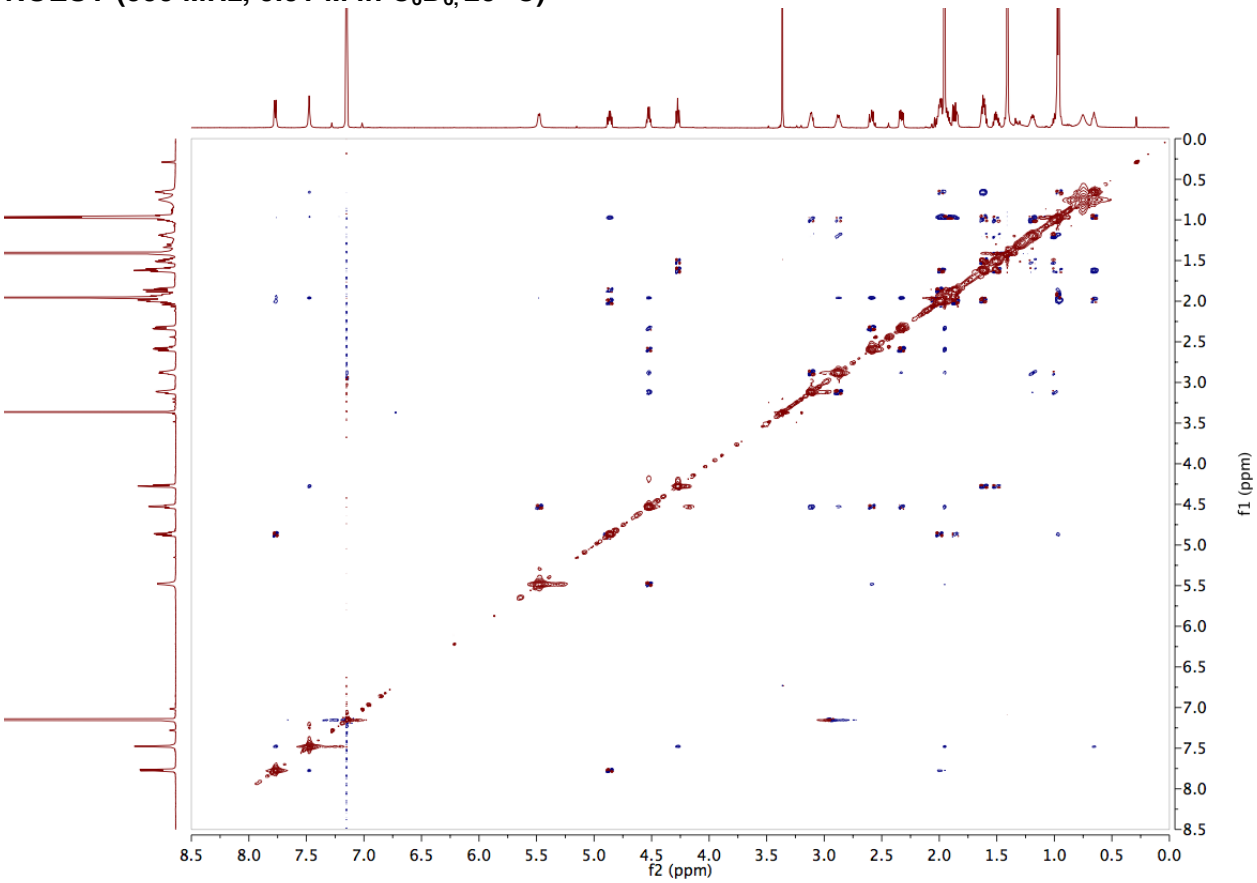

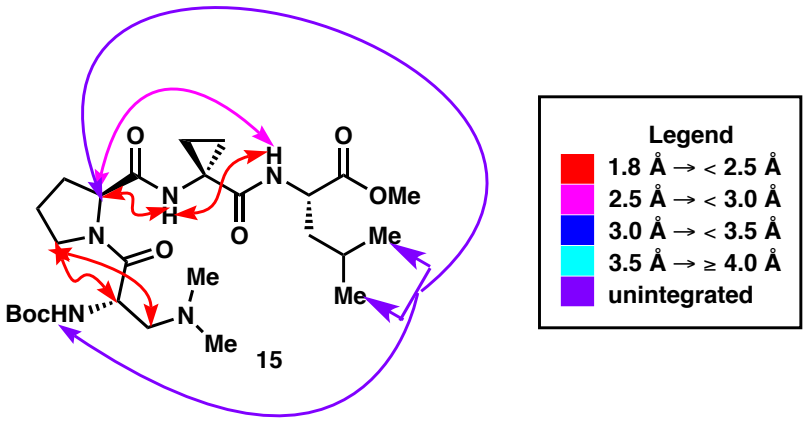

Figure S5.04: Inter-residue nOe Map for Peptide **15**

Table S5.08: Integrated NOESY Cross-peaks for Peptide **15**

	f2	f1	Normalized	Absolute	Assignment	Corrected Distances (Normalized)
1	7.77	1.86	–0.28	–202.4	LeuNH-LeuHB1	2.75
	1.85	7.77	–0.25	–177.35		
2	7.76	7.47	–1	–715.71	LeuNH-AcpcNH	2.16
	7.47	7.77	–0.85	–605.17		
3	7.75	4.27	–0.17	–124.61	LeuNH-DProHA	2.93
	4.26	7.77	–0.21	–151.7		
4	7.47	0.65	–0.57	–405.17	AcpcNH-AcpcHB1a	2.31
	0.65	7.48	–0.65	–468.61		
5	7.46	4.28	–0.94	–674.7	AcpcNH-DProHA	2.09
	4.27	7.47	–1.25	–896.5		
6	5.46	2.32	–0.22	–155.92	DmaaNH-DmaaHB1	2.66
	2.32	5.47	–0.39	–276.2		
7	5.46	2.58	–0.58	–411.74	DmaaNH-DmaaHB2	2.29
	2.58	5.48	–0.88	–632.26		
8	4.52	2.87	–1.42	–1017.38	DmaaHA-DProHD1	2.09
	2.86	4.53	–1.32	–943.21		
9	4.51	3.1	–3.75	–2681.45	DmaaHA-DProHD2	1.79
	3.1	4.49	–3.28	–2347.96		
10	2.87	2.33	–0.81	–578.27	DProHD1-DmaaHB1	2.25
	2.31	2.89	–0.88	–631.7		
11	2.87	3.12	–3.21	–2297.54	DProHD1-DProHD2	1.80
	3.11	2.87	–2.92	–2088.06		

Table S5.09: Unintegrated NOESY Cross-peaks for Peptide **15**

LeuNH-LeuHD
DmaaNH-LeuHD
DmaaNH-DmaaBoc
ProHA-LeuHD
ProHD-ProHB

Peptide 16

^{1}H-NMR (600 MHz, 0.01 M in C_6D_6, 20 °C)

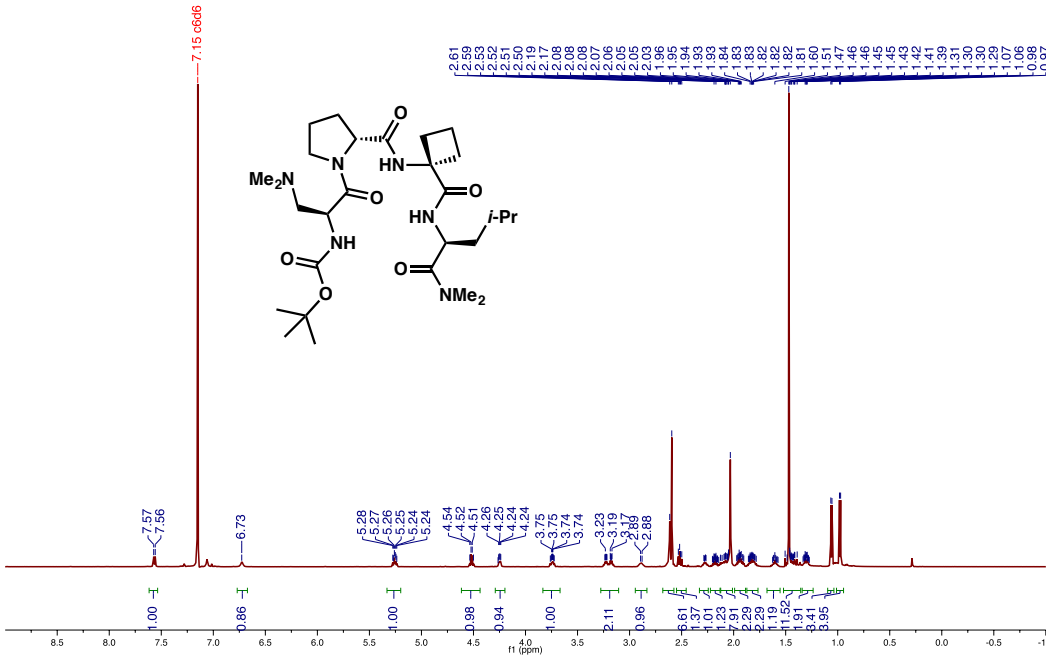

COSY (600 MHz, 0.01 M in C_6D_6, 20 °C)

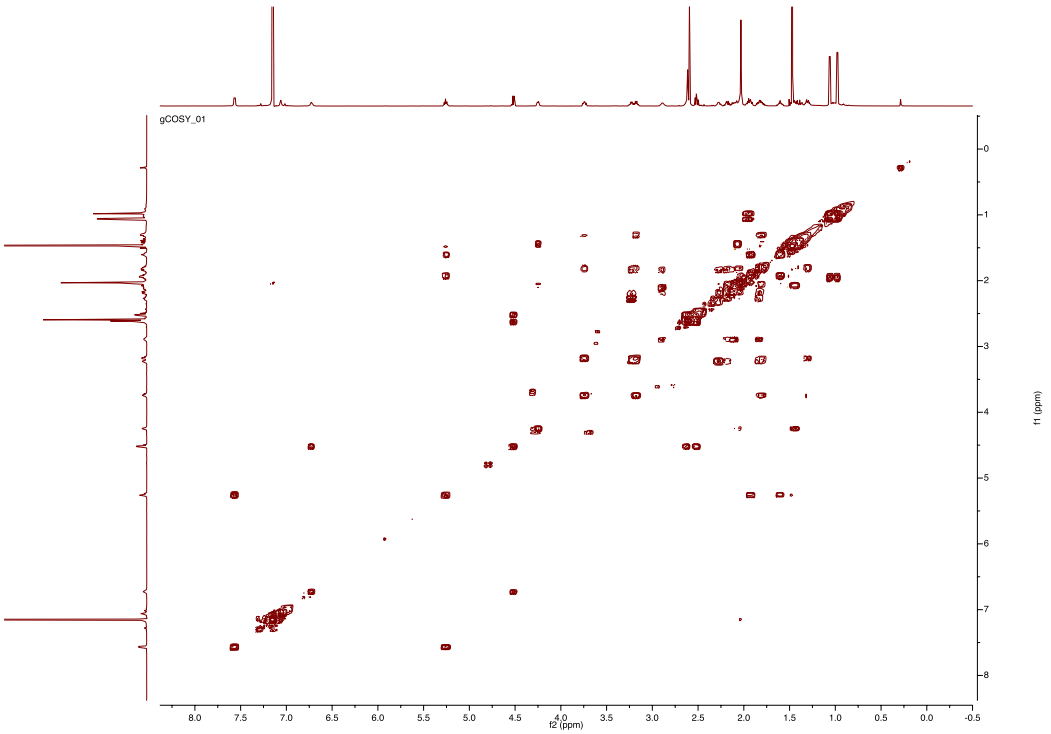

Table 5.10: Peak Assignments for Peptide **16**

Assignment (splitting)	Shift (ppm)	Range (ppm)	H's	J's (Hz)
LeuNH (d)	7.57	7.59–7.54	1	8.9
LeuHD2 (d)	1.06	1.09–1.02	3	6.4
LeuHD1 (d)	0.98	1.05–0.96	3	6.5
LeuHB2, LeuHG (m)	1.94	2.01–1.89	2	
LeuHB1 (m)	1.6	1.66–1.55	1	
LeuHA (dd)	5.26	5.29–5.22	1	9.0, 4.9
DProHG1 (m)	1.3	1.35–1.26	1	
DProHD2 (m)	3.74	3.78–3.71	1	
DProHD1 (d)	3.18	3.20–3.14	1	7.5
DProHB2, DmaaNMe$_2$ (s)	2.03	2.07–2.02	7	
DProHA (dd)	4.25	4.27–4.22	1	3.8, 8.3
DmaaNH (s)	6.73	6.74–6.71	1	
DmaaHB2, LeuNMe (m)	2.6	2.67–2.56	7	
DmaaHB1 (dd)	2.51	2.56–2.45	1	7.4, 12.4
DmaaHA (d)	4.52	4.55–4.48	1	7.1
DmaaBoc (s)	1.47	1.49–1.46	9	
AcbcNH (s)	7.06	7.08–7.04	1	
AcbcHG2 (m)	2.11	2.16–2.08	1	
AcbcHG1, DProHG2 (m)	1.82	1.88–1.75	2	
AcbcHB2b (m)	2.28	2.32–2.24	1	
AcbcHB2a (m)	2.18	2.23–2.15	1	
AcbcHB1b (m)	2.89	2.91–2.86	1	
AcbcHB1a (s)	3.23	3.27–3.20	1	

NOESY (600 MHz, 0.01 M in C_6D_6, 20 °C)

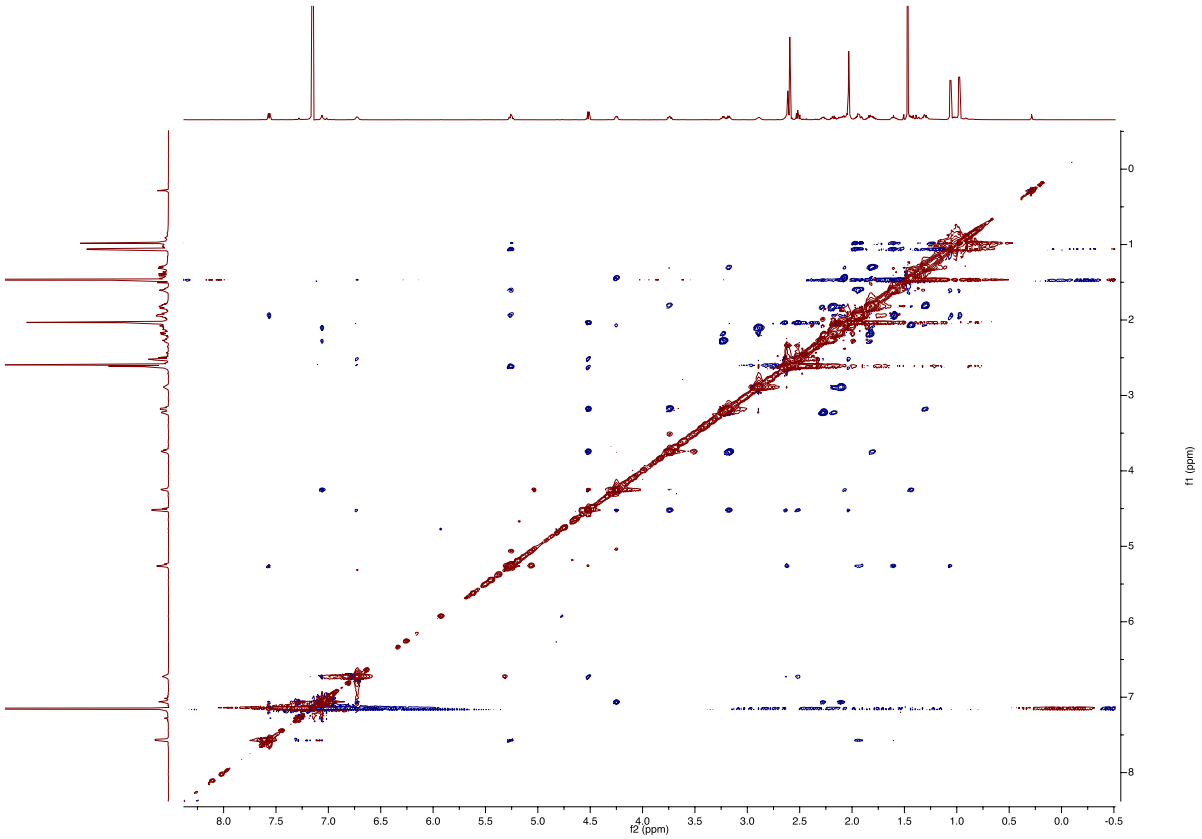

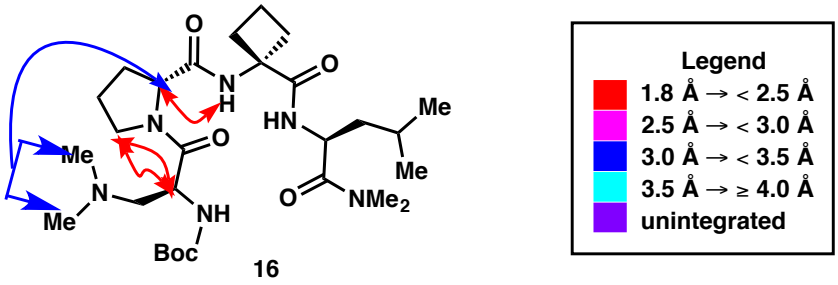

16

Figure S5.05: Inter-residue nOe Map for Peptide **16**

Table S5.11: Integrated NOESY Cross-peaks for Peptide **16**

	f2	f1	Normalized	Absolute	Assignment	Corrected Distances (Normalized)
1	7.57	1.61	0.26	247.93	LeuNH-LeuHB1	3.11
	1.62	7.55	0.25	239.25		
2	7.56	1.93	1	962.38	LeuNH-LeuHB2	2.65
	1.94	7.55	1	960.42		
3	7.07	4.23	1.13	1083.77	AcbcNH-DProHA	2.34
	4.24	7.06	1.51	1456.87		
4	7.06	2.09	0.83	795.97	AcbcNH-AcbcHG2	2.53
	2.1	7.06	1.18	1136.06		
5	7.05	2.28	0.46	440.42	AcbcNH-AcbcHB2b	2.69
	2.27	7.06	0.62	593.99		
6	6.72	2.61	0.41	398.9	DmaaNH-DmaaHB2	3.36
	2.64	6.71	0.24	235.5		
7	6.71	2.49	0.54	514.93	DmaaNH-DmaaHB1	2.81
	2.52	6.74	0.43	412.88		
8	5.26	1.93	0.81	778.96	LeuHA-LeuHG	2.80
	1.92	5.24	0.81	782.08		
9	5.25	1.05	1.23	1185.66	LeuHA-LeuNMe2	2.62
	1.06	5.25	0.37	354.23		
10	5.25	2.61	1.97	1892.08	LeuHA-LeuNMe1	2.64
	2.62	5.27	0.96	927		
11	5.25	0.96	0.31	295.97	LeuHA-LeuHMe1	3.29
	0.99	5.25	0.11	104.47		
12	4.52	3.74	1.92	1843.36	DmaaHA-DProHD2	2.28
	3.75	4.51	2.23	2144.73		
13	4.5	3.17	1.83	1765.22	DmaaHA-DProHD1	2.31
	3.18	4.51	1.83	1757.54		
14	4.25	2.04	0.49	470.01	DProHA-DmaaNMe$_2$	3.15
	2.07	4.25	0.37	353.02		
15	3.76	3.16	8.98	8642.74	DProHD2-DProHD1	1.80
	3.16	3.75	7.6	7315.56		

Table S5.12: Unintegrated NOESY Cross-peaks for Peptide **16**

DmaaNH-DmaaNMe$_2$
DmaaHB1-DmaaNMe$_2$
DmaaHB2-DmaaNMe$_2$
LeuHB1-LeuHD1
LeuHB1-LeuHD2

Peptide 17

^{1}H-NMR (600 MHz, 0.01 M in C_6D_6, 20 °C)

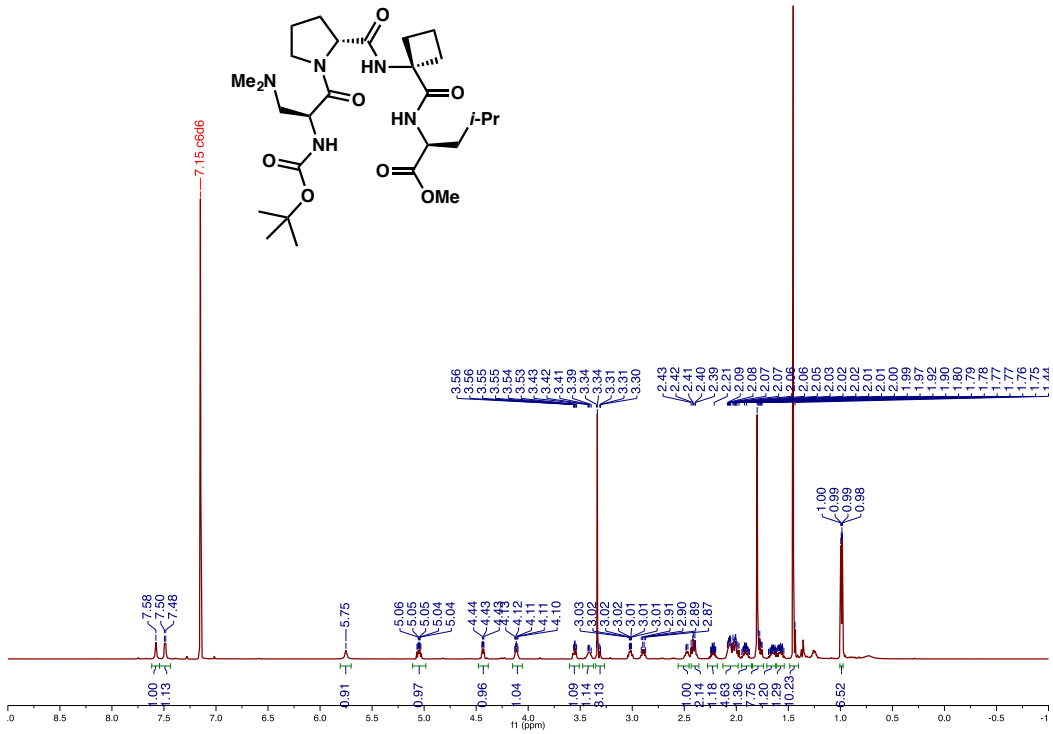

COSY (600 MHz, 0.01 M in C_6D_6, 20 °C)

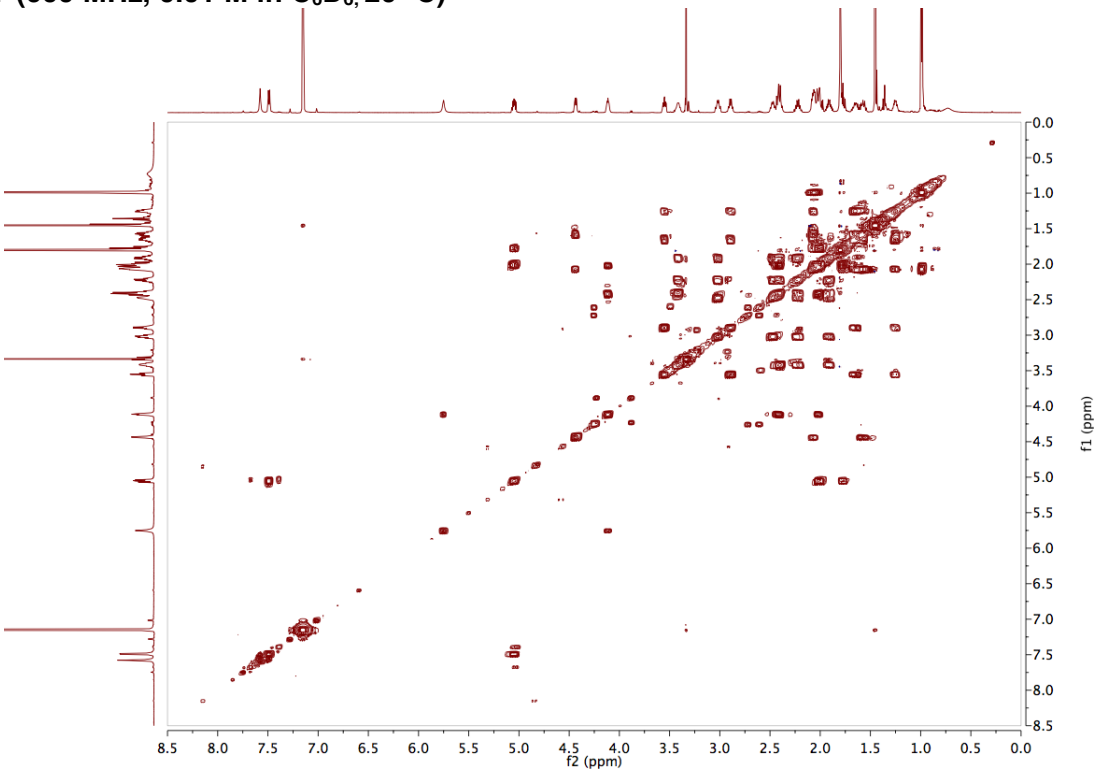

Table S5.13: Peak Assignments for Peptide **17**

Assignment (splitting)	Shift (ppm)	Range (ppm)	H's	*J*'s (Hz)
LeuOMe (s)	3.34	3.35–3.32	3	
LeuNH (d)	7.49	7.51–7.47	1	7.79
LeuHD (dd)	0.99	1.02–0.94	6	2.70, 6.53
LeuHG (m)	1.77	1.81–1.73	1	
LeuHB2, DmaaHB1 (m)	2	2.04–1.96	2	
LeuHA (ddd)	5.05	5.09–5.01	1	4.76, 7.76, 9.92
DProHG2 (m)	1.65	1.71–1.61	1	
DProHG1 (m)	1.25	1.30–1.21	1	
DProHD2 (m)	3.55	3.59–3.52	1	
DProHD1 (q)	2.89	2.93–2.86	1	8.39
DProHB2 (m)	2.07	2.12–2.04	1	
DProHB1 (m)	1.58	1.61–1.53	1	
DProHA (dd)	4.44	4.46–4.41	1	3.31, 8.47
DmaaNH (s)	5.75	5.77–5.73	1	
$DmaaNMe_2$, LeuHB1 (s)	1.8	1.82–1.78	7	
DmaaHB2, AcbcHB1a (m)	2.41	2.44–2.36	2	
DmaaHA (dt)	4.11	4.15–4.08	1	4.54, 9.41
DmaaBoc (s)	1.45	1.47–1.44	9	
AcbcNH (s)	7.58	7.59–7.56	1	
AcbcHG2 (dtt)	2.22	2.28–2.17	1	6.99, 9.32,10.93
AcbcHG1 (m)	1.91	1.95–1.86	1	
AcbcHB2b (m)	3.41	3.46–3.37	1	
AcbcHB2a (m)	3.02	3.06–2.97	1	
AcbcHB1b (m)	2.47	2.51–2.44	1	

NOESY (600 MHz, 0.01 M in C_6D_6, 20 °C)

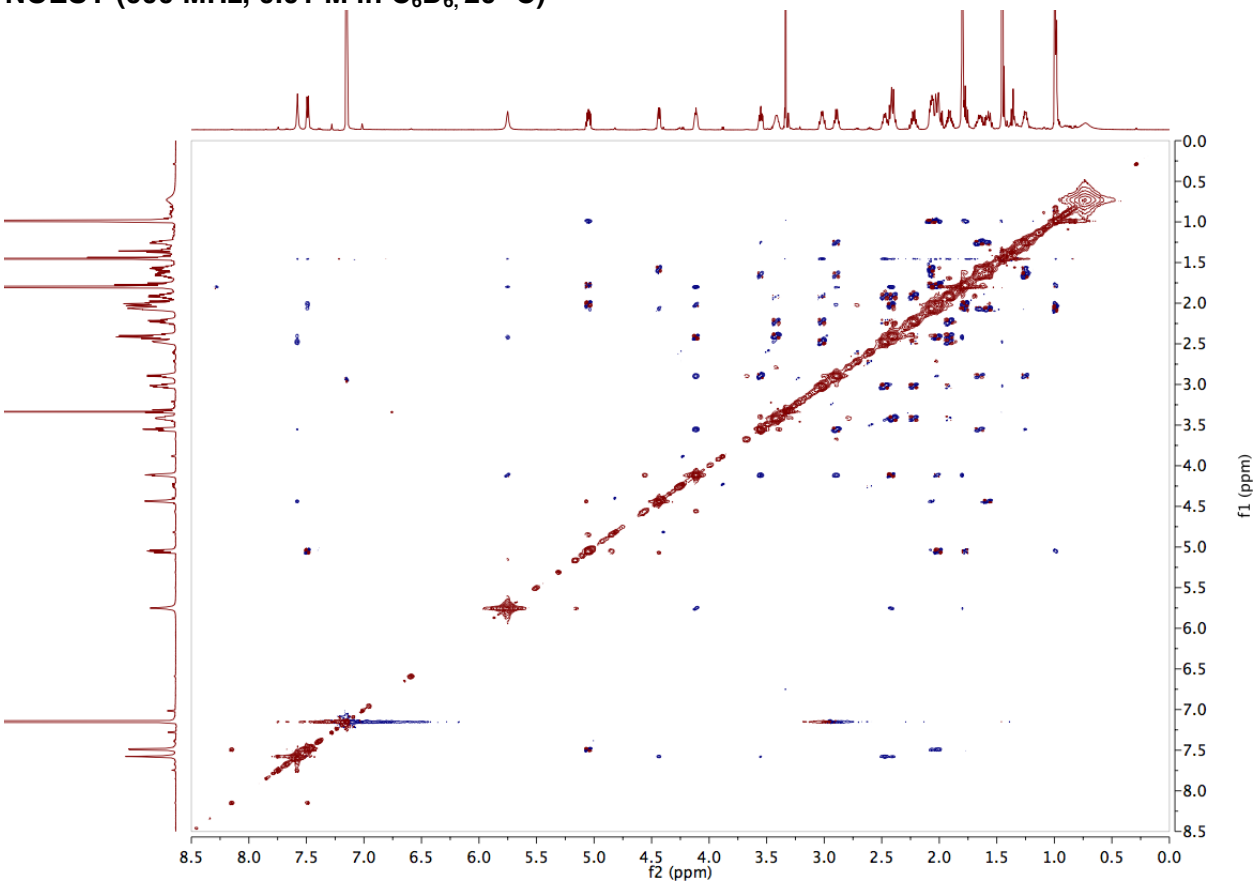

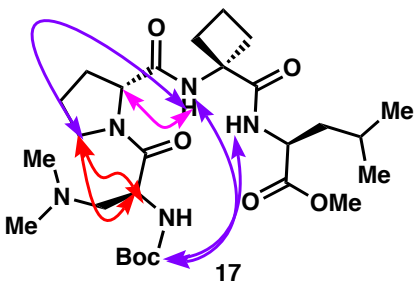

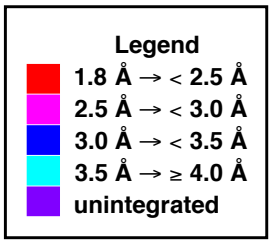

Figure S5.06: Inter-residue nOe Map for Peptide **17**

Table S5.14: Integrated NOESY Cross-peaks for Peptide **17**

	f2	f1	Normalized	Absolute	Assignment	Corrected Distances (Absolute)
1	7.58	2.48	–0.02	–1233.27	AcbcNH-AcbcHB1b	2.39
	2.48	7.57	–0.02	–1528.62		
2	7.58	2.4	–0.01	–422.27	AcbcNH-AcbcHG1	3.08
	2.39	7.58	–0.01	–432.76		
3	7.58	4.43	–0.01	–521.39	AcbcNH-DProHA	2.76
	4.43	7.58	–0.01	–582.74		
4	7.48	2.06	–0.01	–543.17	LeuNH-LeuHB2	3.01
	2.08	7.49	–0.01	–435.53		
5	7.48	1.99	–0.01	–617.03	LeuNH-LeuHD	2.75
	2	7.49	–0.02	–1079.18		
6	5.75	1.79	0	–298.27	DmaaNH-$DmaaNMe_2$	2.96
	1.79	5.75	0	–207.84		
7	5.74	2.41	–0.01	–681.6	DmaaNH-DmaaHB2	2.87
	2.41	5.75	–0.01	–737.49		
8	5.05	0.98	–0.03	–1696.58	LeuHA-LeuHD	2.75
	0.98	5.04	–0.01	–748.87		
9	4.11	2.02	–0.01	–876.01	DmaaHA-DmaaHB1	2.84
	2.01	4.1	–0.01	–723.58		
10	4.1	3.55	–0.04	–2620.33	DmaaHA-DProHD2	2.20
	3.55	4.11	–0.04	–2521.79		
11	4.12	2.9	–0.03	–1969.11	DmaaHA-DProHD1	2.31
	2.89	4.12	–0.03	–1872.56		
12	3.55	2.91	–0.12	–7821.48	DProHD1-DProHD2	1.80
	2.89	3.55	–0.12	–7844.24		

Table S5.15: Unintegrated NOESY Cross-peaks for Peptide **17**
AcbcNH-DProHD
AcbcNH-DmaaBoc
LeuNH-DmaaBoc
DmaaNH-DmaaHB
DmaaNH-$DmaaNMe_2$
LeuHA-LeuHD
DmaaHA-$DmaaNMe_2$
DmaaHA-DmaaBoc

Peptide 18

^{1}H-NMR (600 MHz, 0.01 M in C_6D_6, 20 °C)

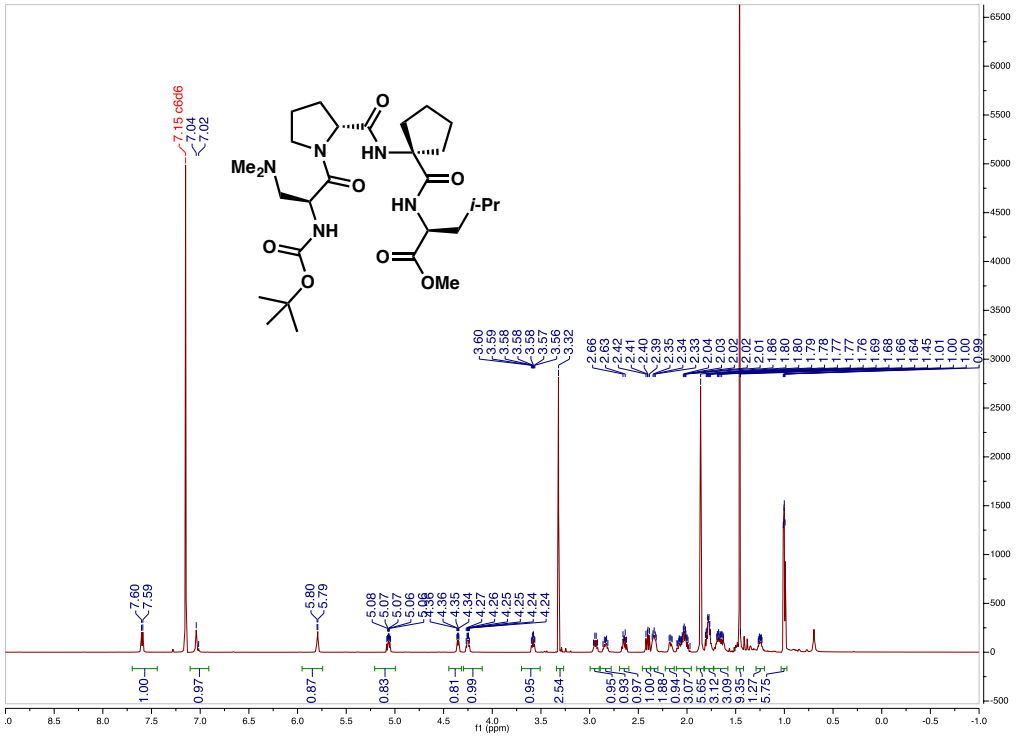

COSY (600 MHz, 0.01 M in C_6D_6, 20 °C)

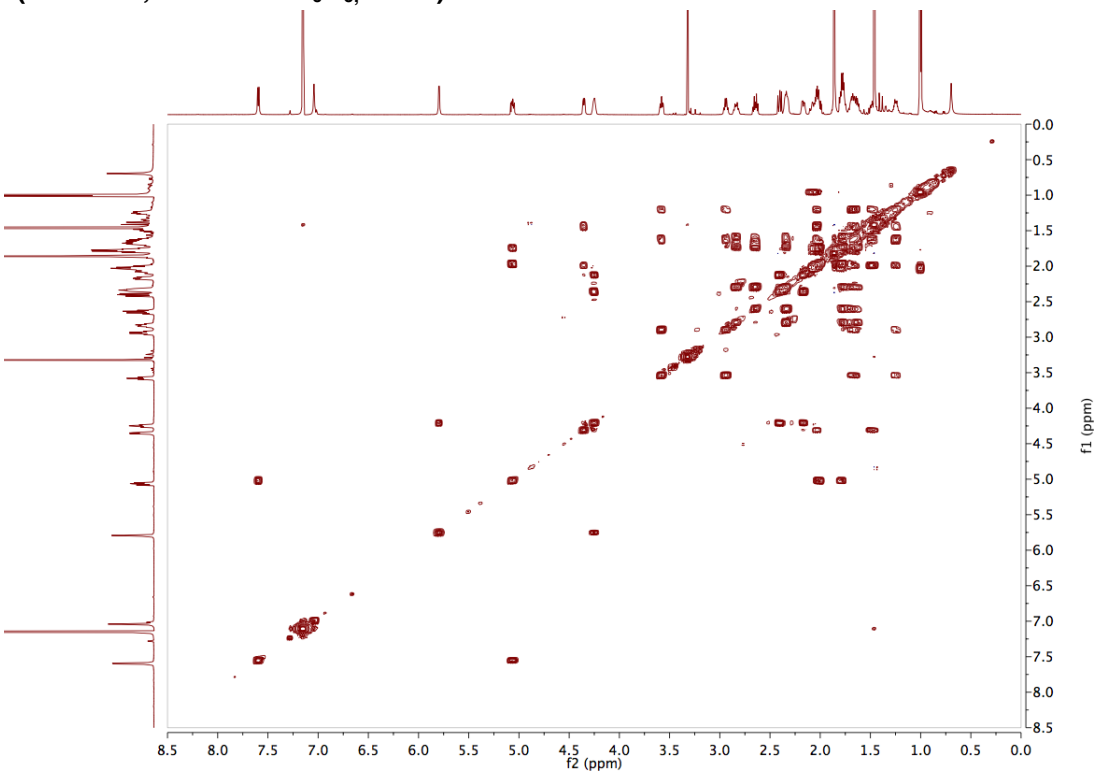

Table S5.16: Peak Assignments for Peptide **18**

Assignment (splitting)	Shift (ppm)	Range (ppm)	H's	*J*'s (Hz)
DmaaBoc (s)	1.46	1.48–1.44	9	
LeuOMe (s)	3.32	3.34–3.30	3	
LeuNH (d)	7.6	7.62–7.57	1	7.99
LeuHD (dd)	1	1.03–0.98	6	4.61, 6.55
LeuHB1, LeuHG, CleHG2b (m)	1.78	1.83–1.74	3	
LeuHA (ddd)	5.06	5.10–5.03	1	4.80, 7.98, 9.99
DProHG1 (m)	1.25	1.28–1.21	1	
DProHD2 (m)	3.58	3.61–3.55	1	
DProHD1 (q)	2.94	2.98–2.90	1	8.51
DProHB2, LeuHB2 (m)	2.03	2.12–1.97	2	
DProHB1 (m)	1.5	1.54–1.47	1	
DProHA (dd)	4.35	4.38–4.33	1	3.09, 8.68
DmaaNH (d)	5.8	5.82–5.78	1	4.62
$DmaaNMe_2$ (s)	1.86	1.88–1.84	6	
DmaaHB2 (dd)	2.4	2.44–2.37	1	8.78, 12.32
DmaaHB1 (dd)	2.17	2.20–2.14	1	5.96, 12.38
DmaaHA (dt)	4.25	4.28–4.22	1	5.42, 9.03
CleNH (s)	7.04	7.06–7.02	1	
CleHG2a, DProHG2 (m)	1.65	1.71–1.60	2	
CleHG1 (m)	1.37	1.43–1.29	2	
CleHB2b (dt)	2.84	2.88–2.80	1	7.98, 13.95
CleHB2a (dt)	2.65	2.69–2.60	1	8.20, 13.59
CleHB1 (m)	2.34	2.37–2.30	2	

NOESY (600 MHz, 0.01 M in C_6D_6, 20 °C)

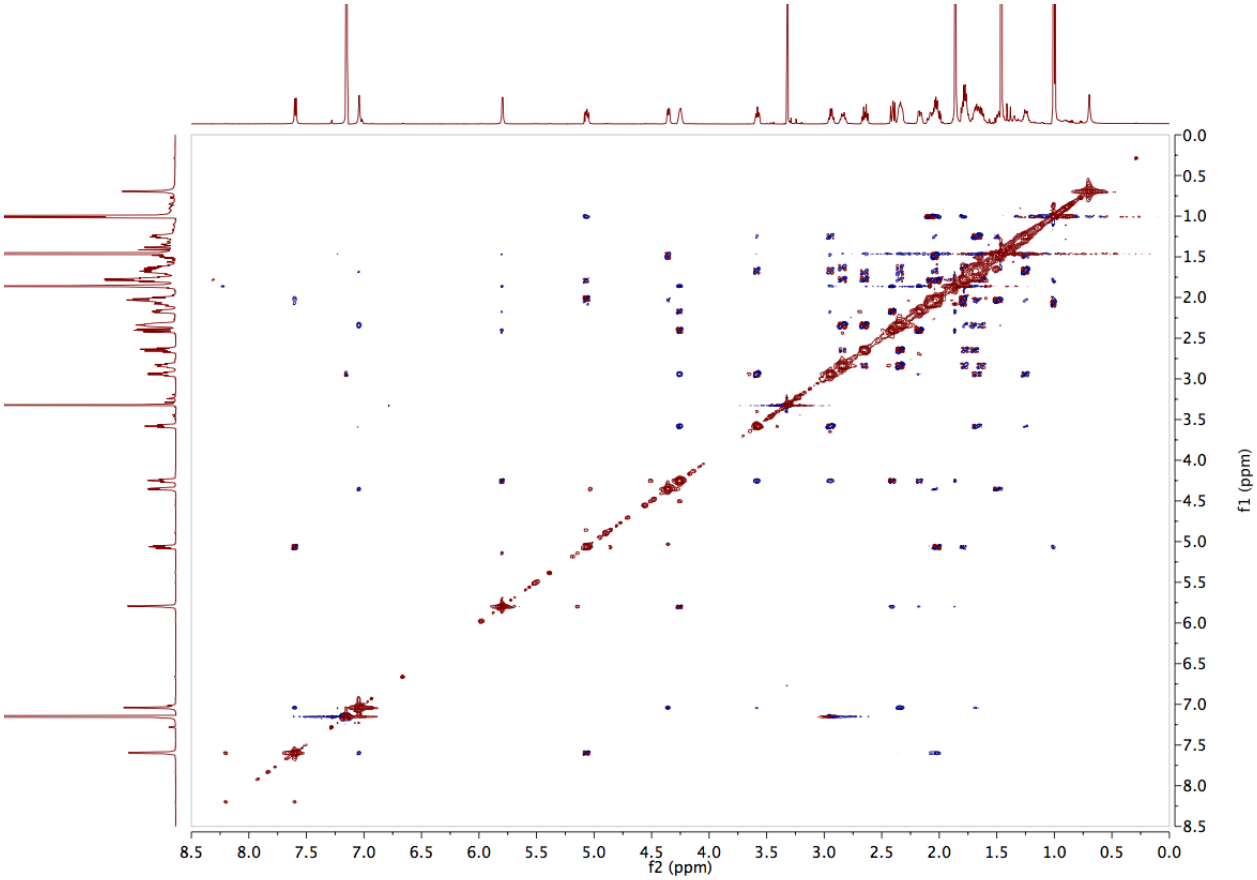

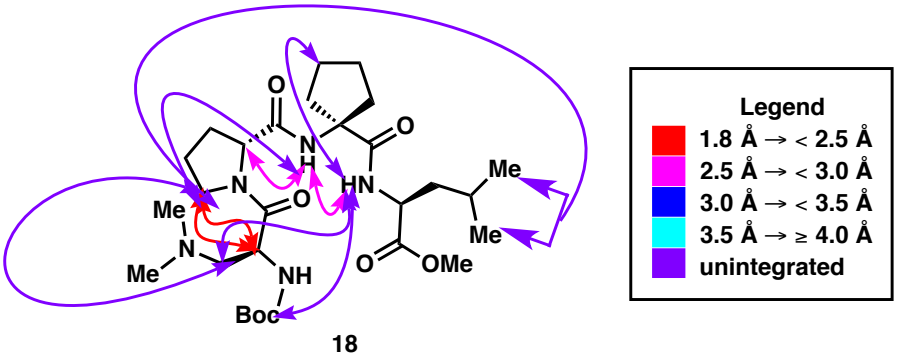

18

Figure S5.07: Inter-residue nOe Map for Peptide **18**

Table S5.17: Integrated NOESY Cross-peaks for Peptide **18**

	f2	f1	Normalized	Absolute	Assignment	Corrected Distances (Absolute)
1	7.6	2.01	–0.01	–899.36	LeuNH-LeuHB2	2.71
	2.02	7.59	–0.02	–1383.55		
2	7.6	7.04	–0.01	–769.25	LeuNH-CleNH	2.54
	7.04	7.59	–0.01	–767.51		
3	7.04	4.35	–0.01	–820.35	CleNH-DProHA	2.54
	4.35	7.04	–0.01	–1112.22		
4	7.03	2.33	–0.03	–2254.34	CleNH-CleHB1	2.35
	2.33	7.04	–0.03	–2610.85		
5	5.8	2.4	–0.01	–722.25	DmaaNH-DmaaHB2	2.67
	2.41	5.79	–0.01	–718.23		
6	5.8	2.16	0	–248.57	DmaaNH-DmaaHB1	3.22
	2.17	5.78	0	–247.54		
7	5.8	1.86	0	–303.88	DmaaNH-$DmaaNMe_2$	3.48
	1.86	5.79	0	–138.03		
8	5.07	0.99	–0.02	–1847.05	LeuHA-LeuHD	2.73
	1	5.06	–0.01	–588.97		
9	4.25	2.93	–0.03	–2260.02	DmaaHA-DProHD1	2.34
	2.93	4.25	–0.03	–2042.58		
10	4.25	1.85	–0.02	–1759.36	DmaaHA-$DmaaNMe_2$	2.69
	1.86	4.24	–0.01	–671.24		
11	4.24	3.58	–0.04	–3141.27	DmaaHA-DProHD2	2.21
	3.58	4.24	–0.04	–2950.44		
12	3.58	2.94	–0.12	–9240.91	DProHD1-DProHD2	1.80
	2.94	3.58	–0.12	–8966.64		

Table S5.18: Unintegrated NOESY Cross-peaks for Peptide **18**

LeuNH-CleHB
LeuNH-DmaaHB
LeuNH-CleHG
LeuNH-DmaaBoc
LeuNH-LeuHD
CleuNH-DProHD
DProHD-DProHB
DProHD-DmaaHB
DProHD-$DmaaNMe_2$

Peptide 19

^{1}H-NMR (600 MHz, 0.01 M in C_6D_6, 20 °C)

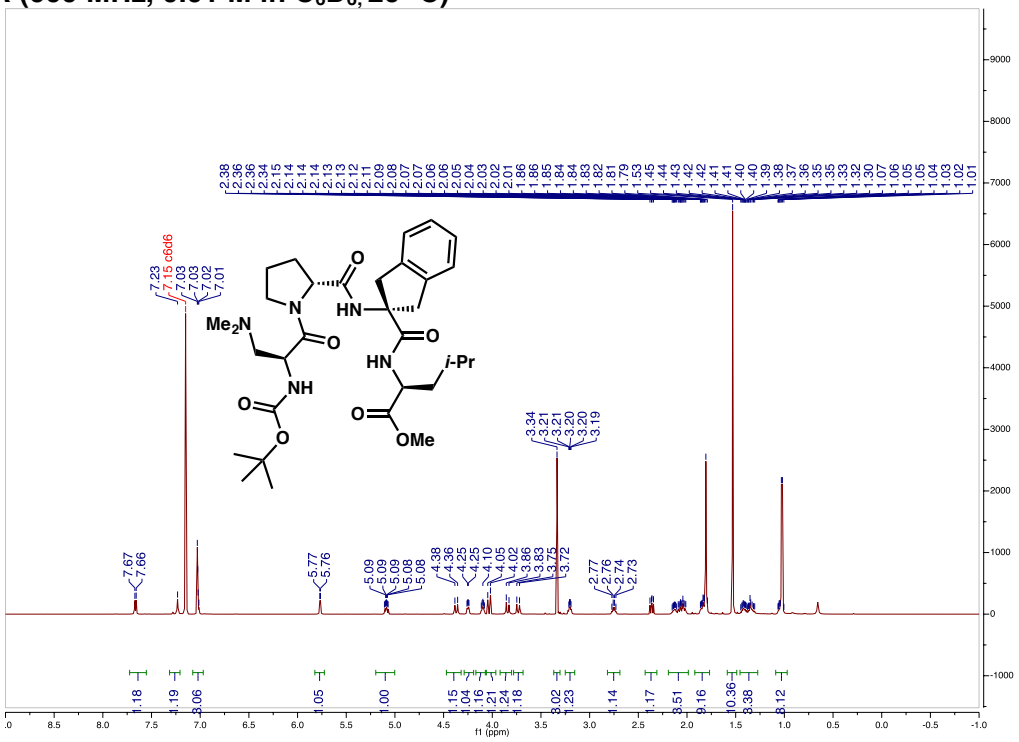

COSY (600 MHz, 0.01 M in C_6D_6, 20 °C)

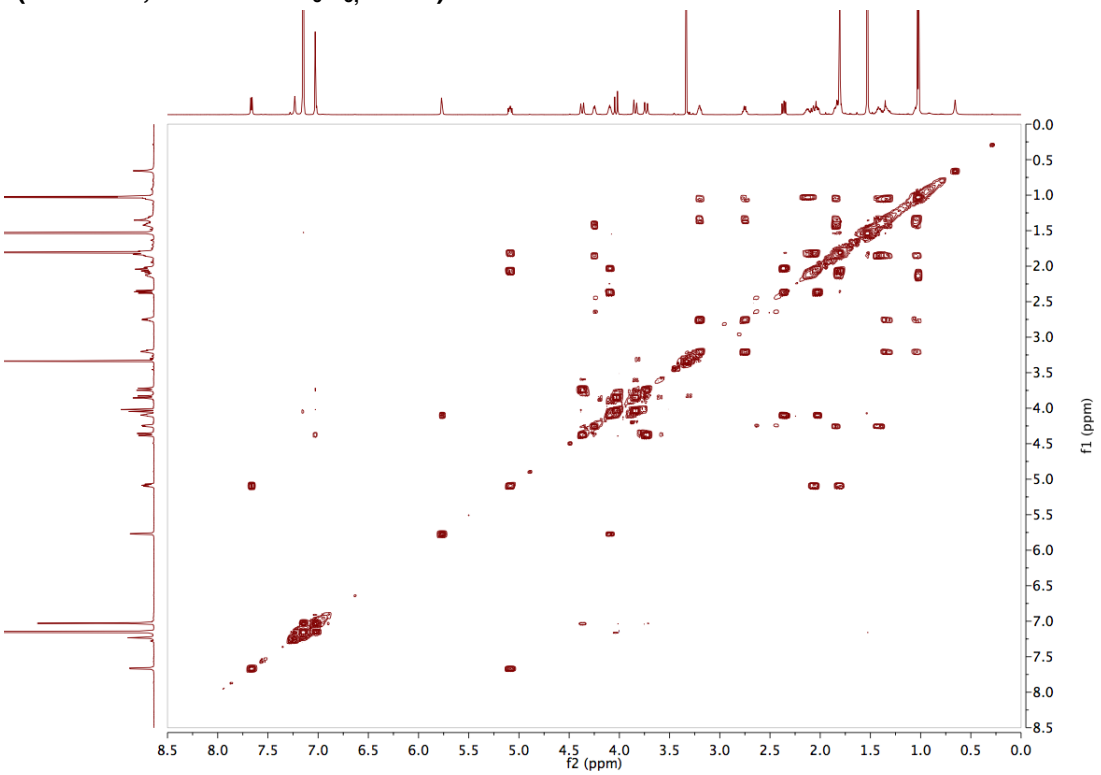

Table S5.19: Peak Assignments for Peptide **19**

Assignment (splitting)	Shift (ppm)	Range (ppm)	H's	*J*'s (Hz)
LeuOMe (s)	3.34	3.35–3.32	3	
LeuNH (d)	7.66	7.69–7.64	1	7.84
LeuHG (m)	2.12	2.17–2.08	1	
LeuHB2 (m)	2.04	2.08–2.00	2	
LeuHA (ddd)	5.09	5.12–5.05	1	4.66, 7.83, 10.09
DProHG2 (m)	1.34	1.38–1.29	1	
DProHG1, LeuHD (d)	1.03	1.09–1.00	7	6.51
DProHD2 (m)	3.2	3.24–3.17	1	
DProHD1 (q)	2.75	2.79–2.71	1	8.20
DProHB1 (m)	1.41	1.46–1.35	1	
DProHA (dd)	4.25	4.28–4.22	1	3.71, 8.37
DmaaNH (d)	5.77	5.79–5.75	1	3.92
$DmaaNMe_2$, LeuHB1 (s)	1.81	1.82–1.79	7	
DmaaHB2 (dd)	2.36	2.40–2.33	1	9.31, 12.35
DmaaHB1 (m)	1.83	1.89–1.77	1	
DmaaHA (dt)	4.10	4.13–4.06	1	4.80, 9.53
DmaaBoc (s)	1.53	1.55–1.51	9	
AicNH (s)	7.23	7.25–7.21	1	
AicHB2b (d)	4.37	4.40–4.34	1	16.78
AicHB2a (d)	4.03	4.06–4.00	1	16.64
AicHB1b (d)	3.84	3.87–3.81	1	16.66
AicHB1a (d)	3.73	3.76–3.70	1	16.75
AicAr (m)	7.03	7.05–7.00	4	

NOESY (600 MHz, 0.01 M in C_6D_6, 20 °C)

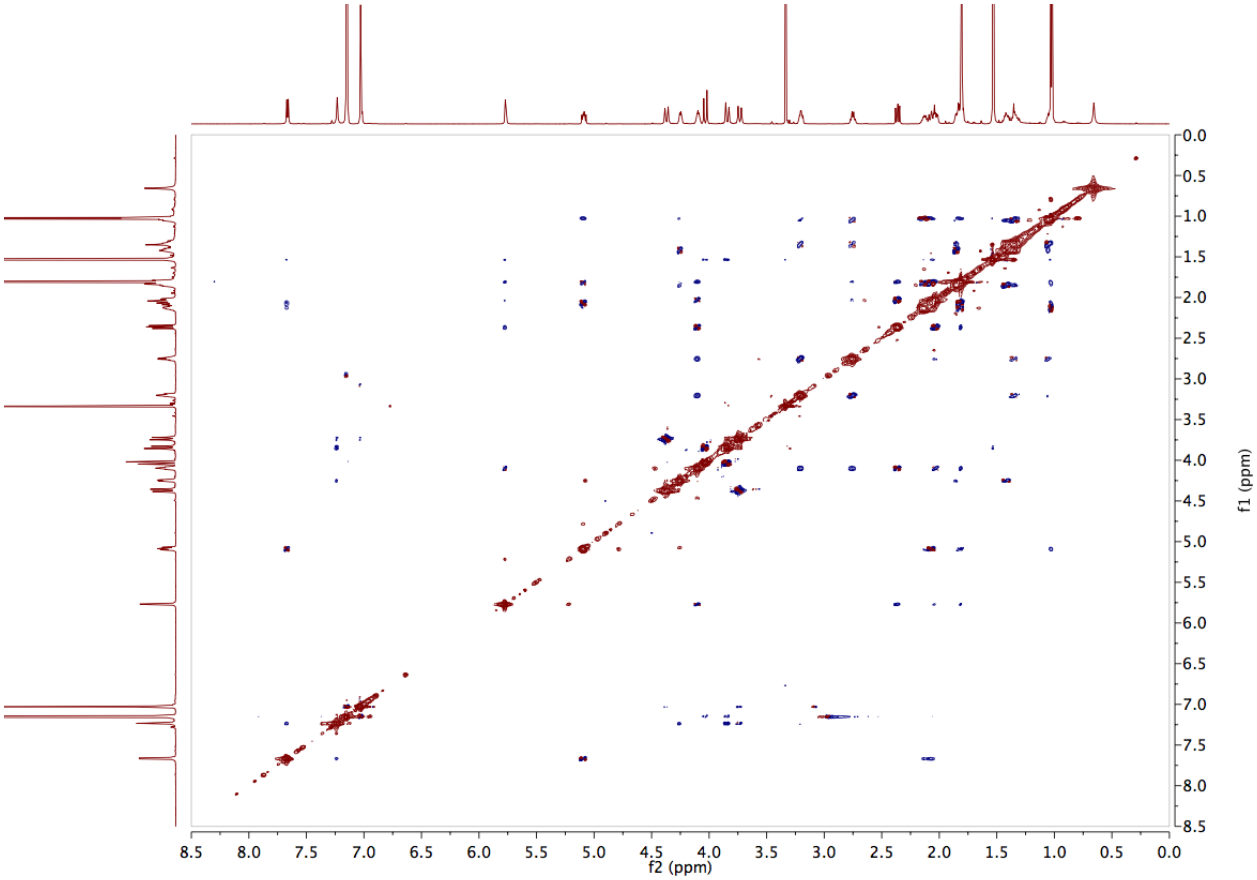

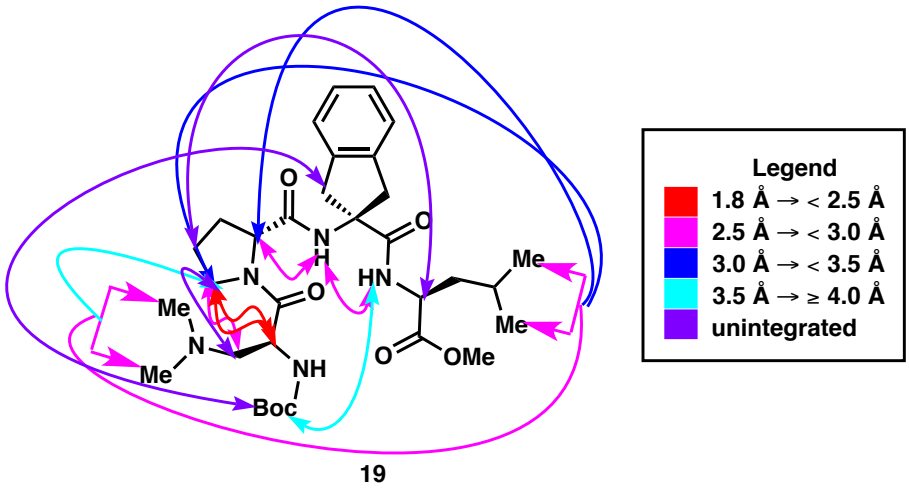

19

Figure S5.08: Inter-residue nOe Map for Peptide **19**

Table S5.20: Integrated NOESY Cross-peaks for Peptide **19**

	f2	f1	Normalized	Absolute	Assignment	Corrected Distances (Normalized)
1	7.67	1.82	–0.18	–134.35	LeuNH-LeuHB1	3.92
	1.83	7.67	–0.15	–110.15		
2	7.67	2.04	–0.99	–738.86	LeuNH-LeuHB2	2.43
	2.04	7.67	–1.78	–1322.29		
3	7.67	7.23	–1	–744.34	LeuNH-AicNH	2.52
	7.24	7.67	–0.76	–563.35		
4	7.66	1.51	–0.23	–167.79	LeuNH-DmaaBoc	3.73
	1.53	7.67	–0.11	–80.38		
5	7.66	2.14	–0.67	–498.32	LeuNH-LeuHG	2.82
	2.15	7.67	–0.85	–630.76		
6	7.24	4.24	–0.72	–532.75	AicNH-DProHA	2.58
	4.25	7.23	–1.13	–844.49		
7	7.23	3.84	–1.55	–1150.88	AicNH-AicHB2a	2.15
	3.84	7.23	–2.53	–1883.69		
8	7.23	3.72	–0.56	–419.15	AicNH-AicHB2b	2.60
	3.73	7.23	–0.92	–686.09		
9	7.15	3.84	–0.2	–149.27	AicArH-AicHB2a	3.42
	3.85	7.14	–0.54	–400.49		
10	7.14	4.02	–0.15	–111.92	AicArH-AicHB1b	3.62
	4.03	7.14	–0.36	–267.63		
11	7.03	3.73	–0.37	–274.37	AicArH-AicHB2b	3.15
	3.74	7.03	–0.56	–419.61		
12	7.03	4.36	–0.1	–76.57	AicArH-AicHB1a	3.89
	4.38	7.02	–0.16	–119.1		
13	5.77	1.53	–0.32	–236.4	DmaaNH-DmaaBoc	3.55
	1.54	5.77	–0.15	–108.06		
14	5.77	2.36	–1.08	–803.32	DmaaNH-DmaaHB2	2.55
	2.36	5.75	–1.25	–931.52		
15	5.77	2.02	–0.37	–278.75	DmaaNH-DmaaHB1	3.00
	2.04	5.79	–0.45	–335.44		
16	5.76	1.82	–0.57	–425.88	DmaaNH-$DmaaNMe_2$	3.32
	1.8	5.8	–0.34	–255.79		
17	5.09	1.02	–2.35	–1752.58	LeuHA-LeuHD	2.67
	1.02	5.09	–1.13	–837.82		
18	4.26	1.02	–0.51	–377.43	DProHA-LeuHD	3.35
	1.04	4.24	–0.32	–239.36		
19	4.1	1.81	–2.11	–1573.52	DmaaHA-$DmaaNMe_2$	2.72
	1.81	4.1	–1.17	–870.15		
20	4.09	3.17	–3.54	–2632.98	DmaaHA-DProHD2	2.19
	3.2	4.07	–3.88	–2887.86		
21	4.09	2.75	–2.8	–2081.09	DmaaHA-DProHD1	2.26
	2.75	4.1	–2.84	–2114.8		
22	3.2	1.02	–0.58	–431.11	DProHD2-LeuHD	3.25
	1.04	3.19	–0.43	–322.18		

23	2.76 2.02	2.01 2.75	–0.71 –0.7	–526.1 –524.28	DProHD1-DmaaHB1	2.77
24	2.76 1.8	1.79 2.75	–0.37 –0.21	–276.33 –156.26	DProHD1-DmaaNMe$_2$	3.60
25	2.36 1.81	1.79 2.36	–2.77 –1.36	–2063.39 –1015.91	DmaaHB2-DmaaNMe$_2$	2.59
26	1.8 1.03	1.01 1.82	–1.7 –1.6	–1265.07 –1188.4	DmaaNMe$_2$-LeuHD	2.83
27	3.21 2.75	2.75 3.2	–11.34 –10.68	–8438.15 –7948.53	DProHD1-DProHD2	1.80

Table S5.21: Unintegrated NOESY Cross-peaks for Peptide **19**
LeuHA-DProHG
DProHA-DProHG
AicHB-DmaaBoc
DProHD-DmaaHB

Peptide 21

^{1}H-NMR (600 MHz, 0.01 M in C_6D_6, 24 °C)

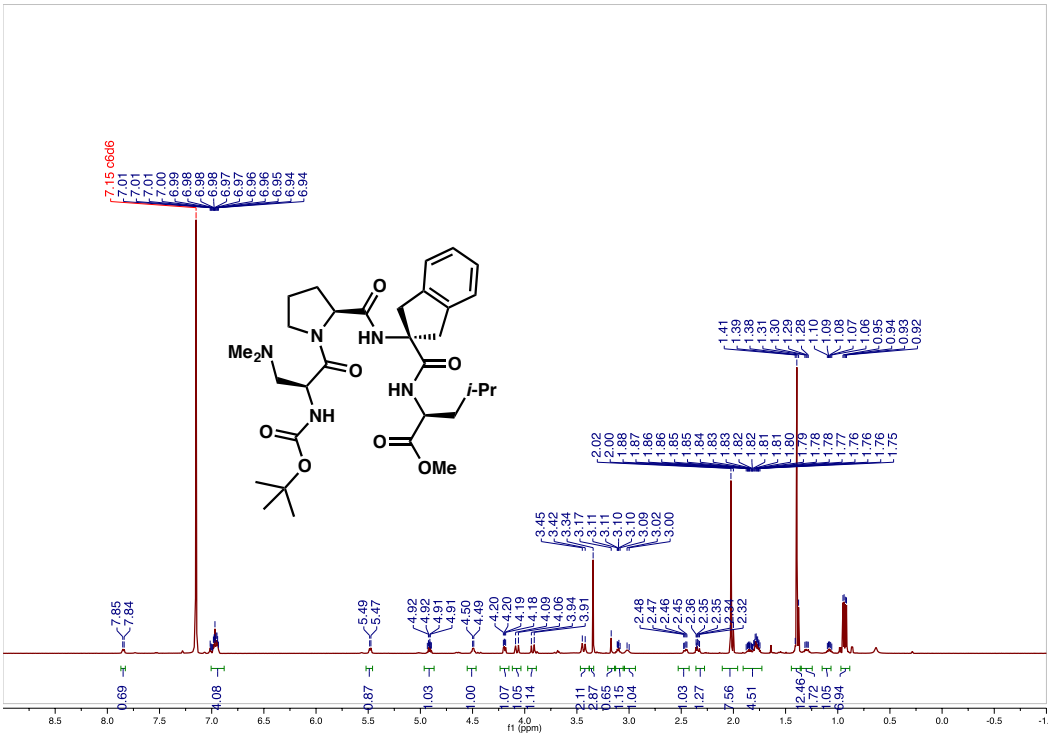

COSY (600 MHz, 0.01 M in C_6D_6, 24 °C)

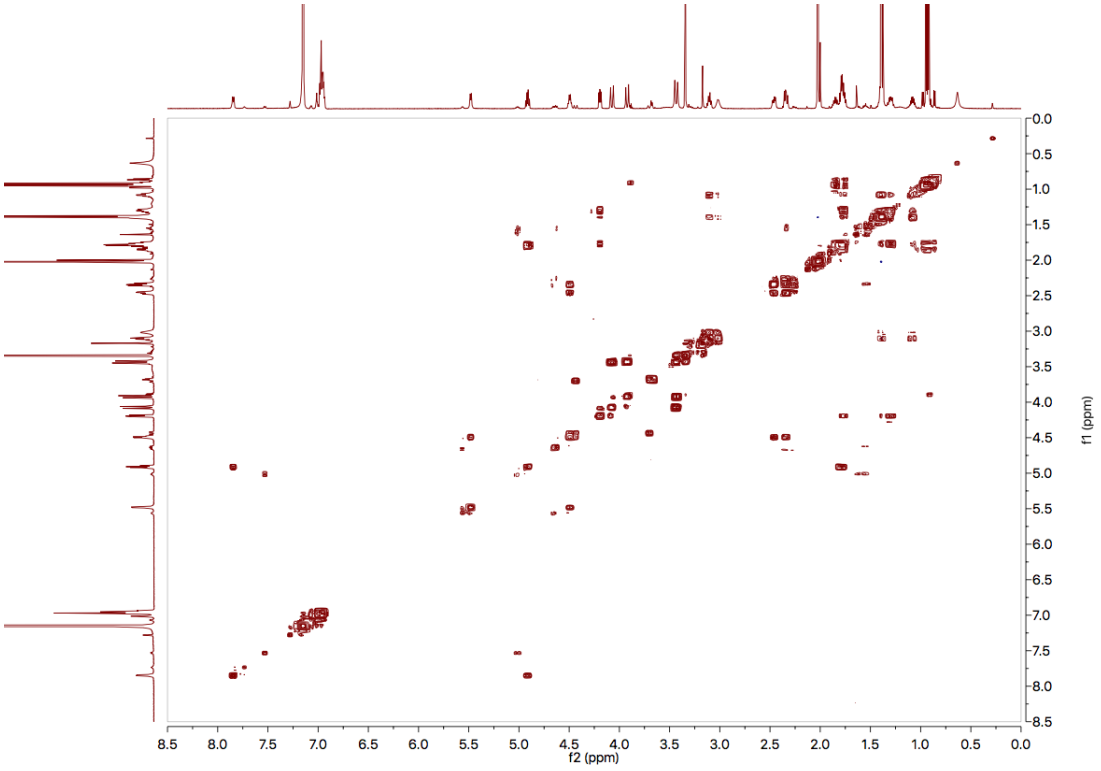

Table S5.22: Peak Assignments for Peptide **21**

Assignment (splitting)	Shift (ppm)	Range (ppm)	H's	*J*'s (Hz)
ProHG1 (m)	1.09	1.14–1.04	1	
ProHD1 (dt)	3.11	3.14–3.07	1	7.17, 9.60
ProHD1 (d)	3.01	3.04–2.98	1	11.72
ProHB1 (m)	1.3	1.35–1.25	1	
ProHA (dd)	4.19	4.22–4.17	1	4.96, 8.02
LeuOMe (s)	3.34	3.36–3.33	3	
LeuNH (d)	7.85	7.87–7.82	1	7.98
LeuHD, AicHB2b (m)	0.92	1.00–0.84	7	
LeuHB2 (m)	1.84	1.89–1.78	1	
LeuHB1, ProHB2 (m)	1.77	1.81–1.73	2	
LeuHA (m)	4.91	4.95–4.88	1	
DmaaNH (d)	5.48	5.50–5.46	1	7.14
DmaaNMe$_2$ (d)	2.01	2.04–1.98	6	14.2
DmaaHB2 (dd)	2.46	2.49–2.43	1	6.00, 12.64
DmaaHB1 (dd)	2.34	2.37–2.31	1	7.25, 12.51
DmaaHA (q)	4.49	4.53–4.47	1	6.76
DmaaBoc, ProHG2 (s)	1.39	1.45–1.35	10	
AicNH, AicAr (m)	6.97	7.09–6.92	5	
AicHB2b (d)	4.07	4.10–4.04	1	16.62
AicHB2a (d)	3.92	3.95–3.88	1	16.54
AicHB1b (d)	3.43	3.46–3.40	1	16.54

NOESY (600 MHz, 0.01 M in C_6D_6, 24 °C)

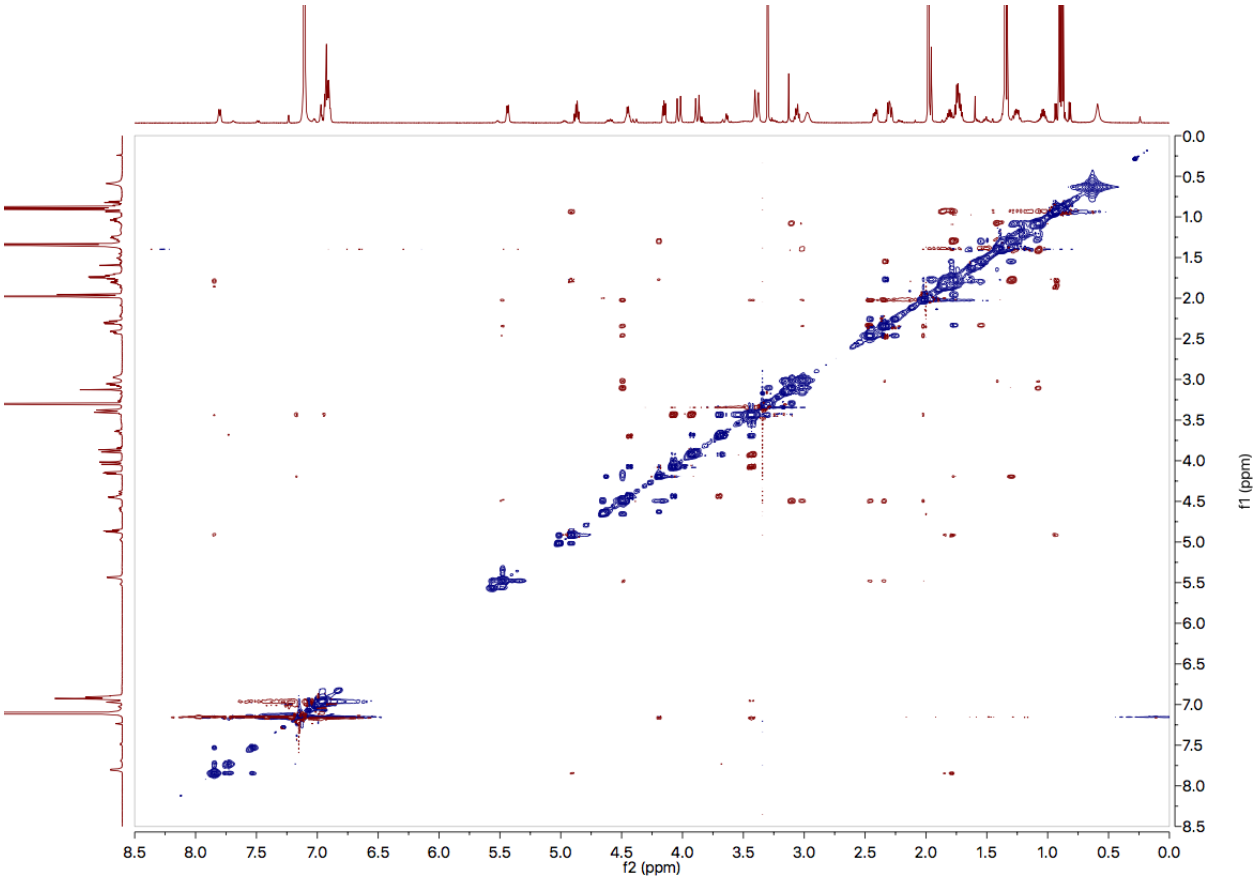

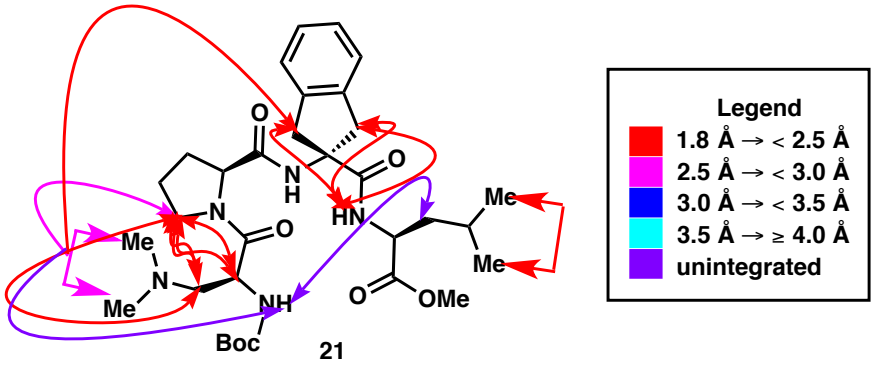

21

Figure S5.09: Inter-residue nOe Map for Peptide **21**

Table S5.23: Integrated NOESY Cross-peaks for Peptide **21**

	f2	f1	Normalized	Absolute	Assignment	Corrected Distances (Absolute)
1	7.85	3.92	0	74.44	LeuNH-AicHB1b	2.30
	3.92	7.85	0	50.54		
2	7.84	4.07	0	44.75	LeuNH-AicHB1a	2.47
	4.07	7.84	0	33.8		
3	7.84	3.44	0	89.81	LeuNH-AicHB2a	2.31
	3.43	7.85	0	66.85		
4	6.95	3.43	0.01	180.68	AicNH-AicHB2a	2.22
	3.43	6.97	0.01	208.48		
5	5.48	2.48	0.01	123.01	DmaaNH-DmaaHB2	2.07
	2.47	5.47	0.01	183.76		
6	5.48	2	0	91.82	DmaaNH-DmaaNMe$_2$	2.54
	2.02	5.47	0	49.54		
7	5.48	2.32	0.01	153.2	DmaaNH-DmaaHB1	2.06
	2.34	5.46	0.01	198.76		
8	4.91	0.94	0.03	585.56	LeuHA-LeuHD	2.03
	0.93	4.9	0.01	305.79		
9	4.5	2.99	0.02	552.94	DmaaHA-ProHD1	1.70
	3.01	4.49	0.02	475.56		
10	4.48	3.1	0.05	1149.77	DmaaHA-ProHD2	1.52
	3.1	4.49	0.05	1134.22		
11	4.48	2.03	0.02	439.94	DmaaHA-DmaaNMe$_2$	2.05
	2.02	4.47	0.01	148.24		
12	3.43	2.02	0.01	131.83	AicHB2a-DmaaNMe$_2$	2.41
	2.02	3.42	0	90.86		
13	3.1	2.33	0.01	125.09	ProHD2-DmaaHB1	2.25
	2.34	3.1	0	115.76		
14	3.02	1.77	0	57.79	ProHD1-ProHB1	2.73
	1.77	3.03	0	57.72		
15	3.02	2.02	0	71.18	ProHD1-DmaaNMe$_2$	2.67
	2.02	3.01	0	34.99		
16	3.01	2.33	0.01	157.16	ProHD1-DmaaHB1	2.10
	2.34	3	0.01	165.89		
17	3.01	2.46	0	87.75	ProHD1-DmaaHB2	2.22
	2.46	3.02	0	115.81		
18	2.47	2.32	0.03	694.61	DmaaHB2-DmaaHB1	1.80
	2.33	2.47	0.01	243.41		

Table S5.24: Unintegrated NOESY Cross-peaks for Peptide **21**
LeuHA-LeuHB
DmaaNH-LeuHB
DmaaNH-LeuHD

Peptide 22

^{1}H-NMR (600 MHz, 0.01 M in C_6D_6, 20 °C)

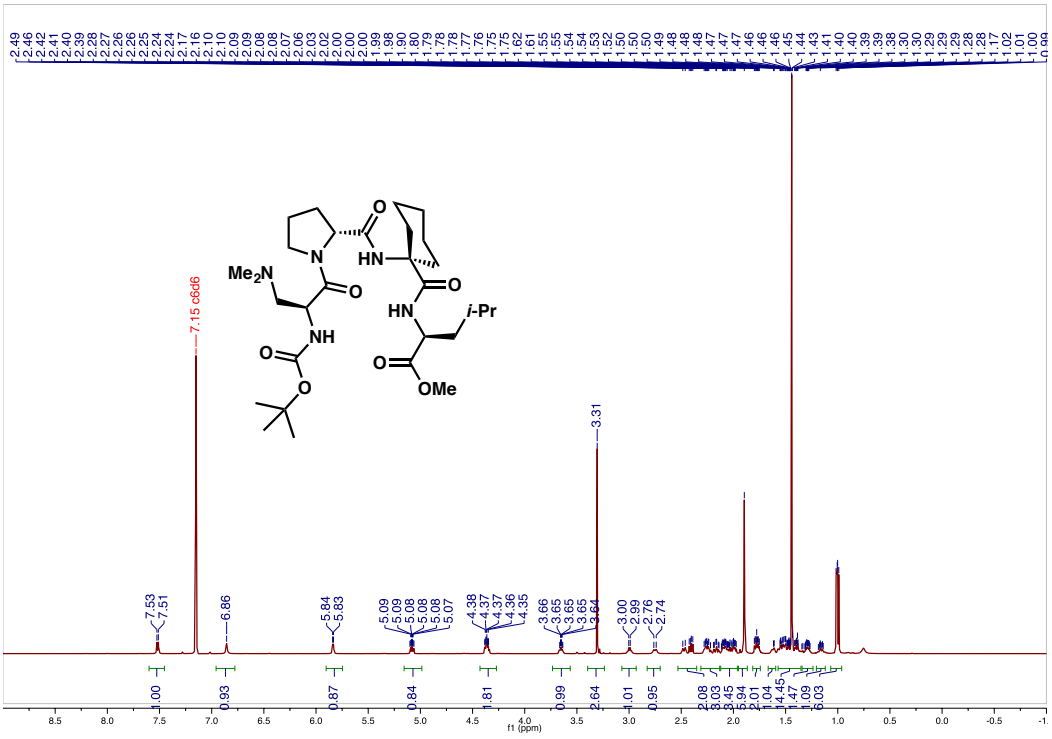

COSY (600 MHz, 0.01 M in C_6D_6, 20 °C)

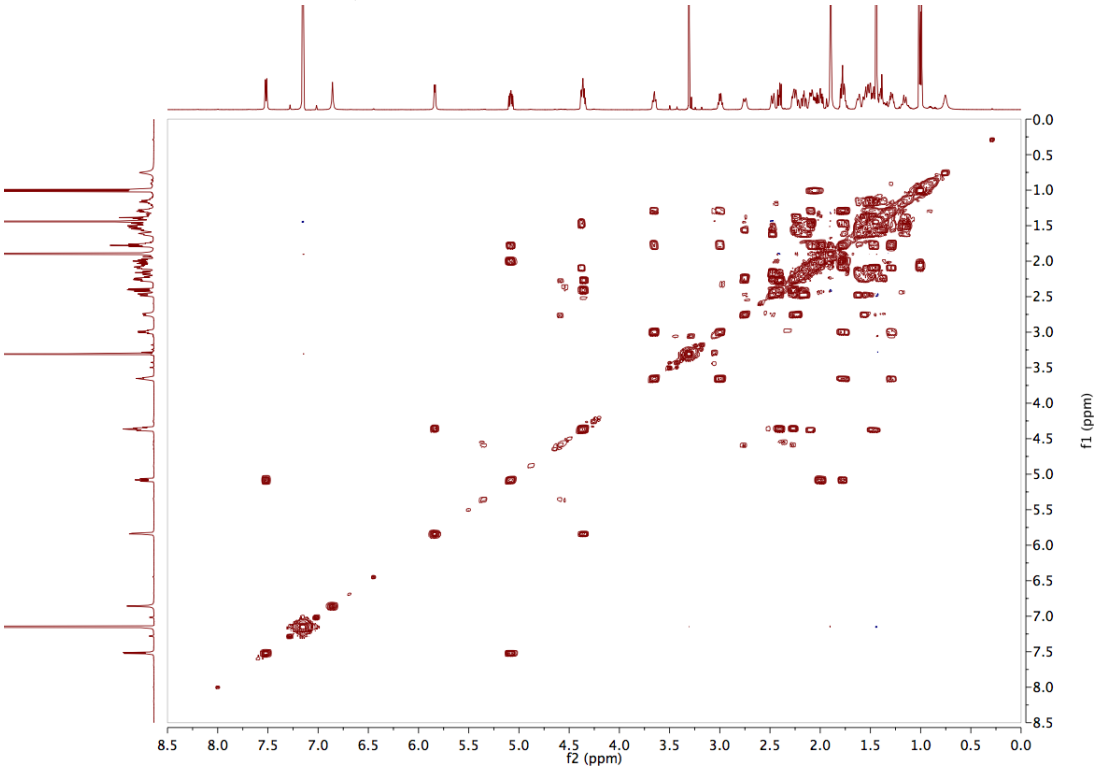

Table S5.25: Peak Assignments for Peptide **22**

Assignment (splitting)	Shift (ppm)	Range (ppm)	H's	J's (Hz)
LeuOMe (s)	3.31	3.32–3.29	3	
LeuNH (d)	7.52	7.54–7.49	1	8.23
LeuHD (dd)	1	1.03–0.97	6	6.52, 8.86
DProHG2 (m)	1.77	1.83–1.71	1	
DProHG1 (m)	1.29	1.33–1.24	1	
DProHD2 (m)	3.65	3.69–3.62	1	
DProHD1 (q)	3	3.03–2.96	1	8.71
DProHB (m)	2.04	2.13–1.96	2	
DProHA, DmaaHA (m)	4.36	4.40–4.32	2	
DmaaNH (d)	5.84	5.86–5.82	1	5.26
$DmaaNMe_2$ (s)	1.9	1.91–1.88	6	
DmaaHB2 (dd)	2.41	2.44–2.37	1	8.29, 12.31
DmaaHB1, AchcHB1b, AchcHB1a (m)	2.21	2.30–2.13	3	
DmaaBoc (s)	1.44	1.46–1.42	9	
AchcNH (s)	6.86	6.87–6.84	1	
AchcHG2b (m)	1.62	1.65–1.59	1	
AchcHG1 (m)	1.51	1.59–1.45	2	
AchcHD2 (m)	1.4	1.43–1.33	1	
AchcHD1 (m)	1.16	1.21–1.10	1	
AchcHB2b (d)	2.75	2.78–2.72	1	13.86
AchcHB2a (d)	2.47	2.50–2.44	1	14.12

NOESY (600 MHz, 0.01 M in C_6D_6, 20 °C)

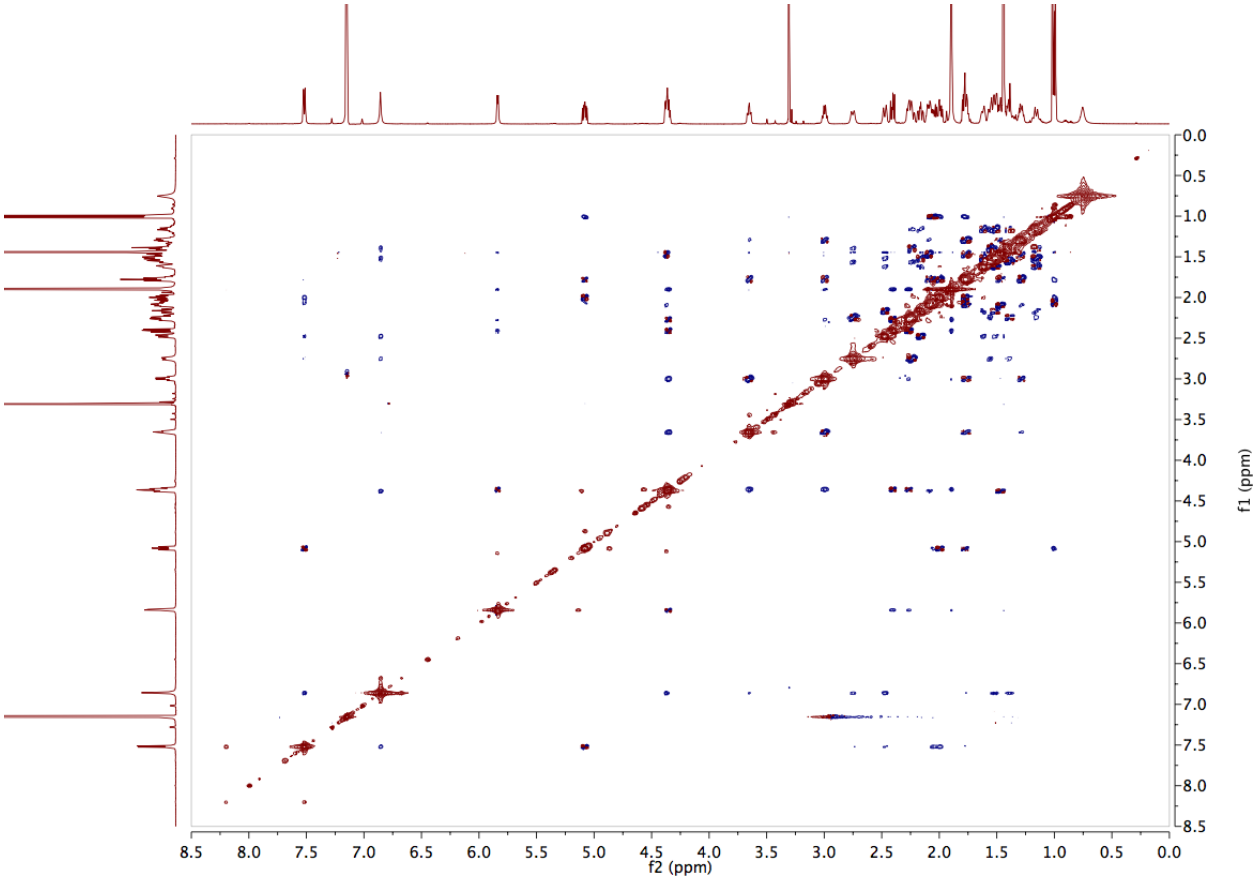

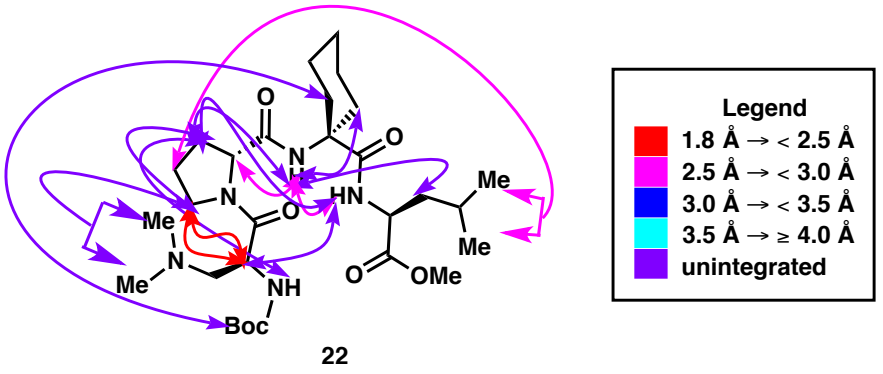

22

Figure S5.10: Inter-residue nOe Map for Peptide **22**

Table S5.26: Integrated NOESY Cross-peaks for Peptide **22**

	f2	f1	Normalized	Absolute	Assignment	Corrected Distances (Normalized)
1	7.51	1.98	–1	–1033.23	LeuNH-LeuHB2	2.52
	1.98	7.51	–0.82	–848.76		
2	7.51	6.86	–0.78	–802.01	LeuNH-AchcNH	2.52
	6.84	7.52	–0.78	–800.57		
3	6.85	2.47	–0.83	–857.38	AchcNH-AchcHB2a	2.43
	2.47	6.86	–0.92	–945.55		
4	6.84	4.38	–0.86	–881.72	AchcNH-DProHA	2.67
	4.36	6.85	–0.91	–933.27		
5	5.08	1.01	–1.78	–1835.88	LeuHA-LeuHD	2.77
	1	5.08	–0.93	–956.98		
6	4.35	1.9	–1.57	–1620.28	DmaaHA-DmaaNMe$_2$	2.72
	1.89	4.35	–0.85	–877.4		
7	4.34	3.65	–2.44	–2514.44	DmaaHA-DProHD2	2.28
	3.64	4.35	–2.83	–2918.57		
8	4.34	3	–1.83	–1885.67	DmaaHA-DProHD1	2.40
	2.99	4.35	–2.08	–2145.01		
9	2.4	1.89	–2.04	–2101.45	DmaaHB2-DmaaNMe$_2$	2.52
	1.89	2.4	–1.01	–1039.65		
10	2.25	1.9	–1.79	–1848.67	DmaaHB1-DmaaNMe$_2$	2.61
	1.89	2.27	–0.96	–984.04		
11	1.77	1	–1.73	–1781.7	DProHG1-LeuHD	2.83
	0.99	1.77	–1.09	–1118.4		
12	3.65	3	–8.14	–8387.59	DProHD1-DProHD2	1.80
	2.99	3.65	–8.05	–8294.98		

Table S5.27: Unintegrated NOESY Cross-peaks for Peptide **22**

LeuNH-DmaaHA
LeuNH-AchcHB
LeuNH-DProHB
LeuNH-LeuHD
AchcNH-AchcHB
AchcNH-DProHB
DmaaNH-DmaaNMe$_2$
DmaaNH-DProHB
DProHD-DmaaNMe$_2$
AchcHB-DmaaBoc

Peptide 25

^{1}H-NMR (600 MHz, 0.01 M in C_6D_6, 20 °C)

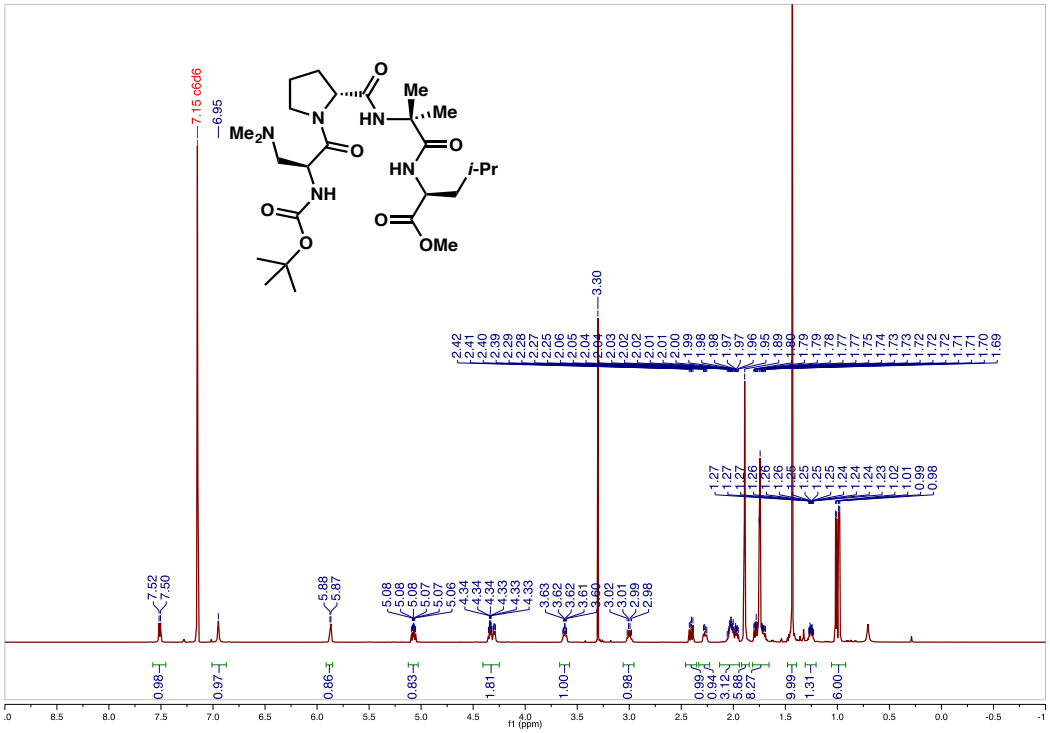

COSY (600 MHz, 0.01 M in C_6D_6, 20 °C)

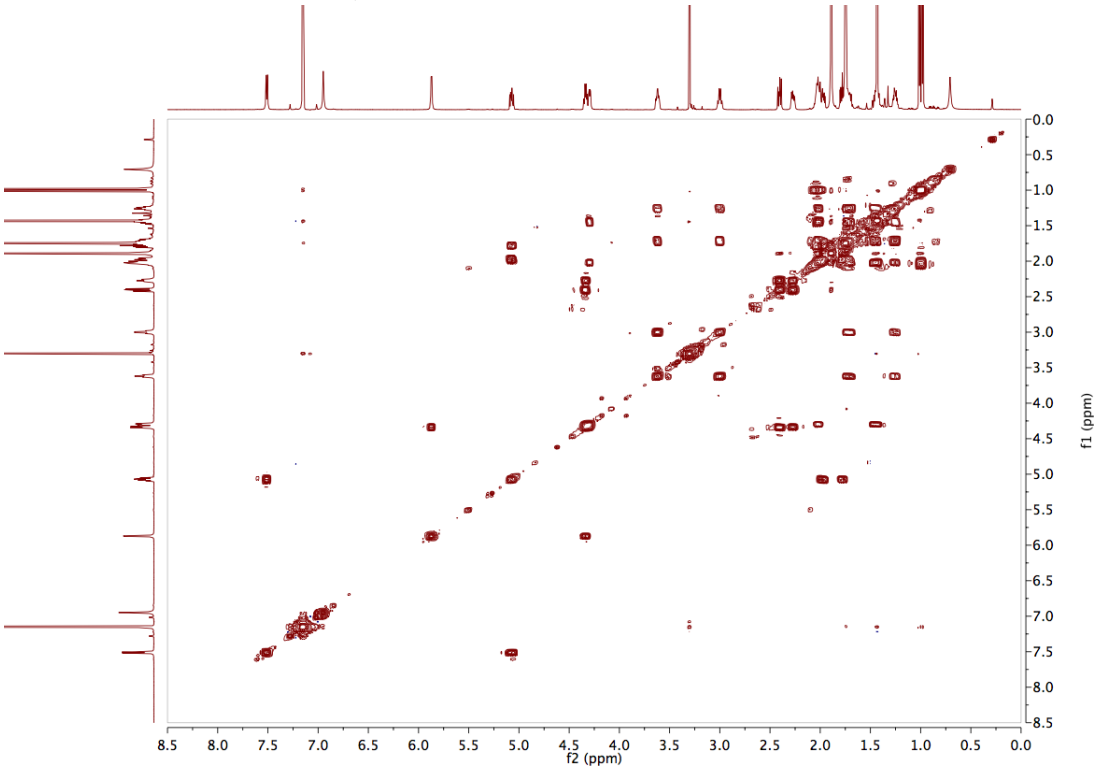

Table S5.28: Peak Assignments for Peptide **25**

Assignment (splitting)	Shift (ppm)	Range (ppm)	H's	*J*'s (Hz)
LeuOMe (s)	3.3	3.32–3.28	3	
LeuNH (d)	7.51	7.54–7.49	1	8.3
LeuHD (dd)	1	1.03–0.96	6	6.54, 17.32
LeuHG, DmaaNMe$_2$ (s)	1.89	1.91–1.87	7	
LeuHB2 (m)	1.97	1.99–1.95	1	
LeuHB1 (m)	1.78	1.82–1.76	1	
LeuHA (ddd)	5.07	5.11–5.04	1	4.80, 8.27, 9.87
DProHG2 (m)	1.71	1.73–1.66	1	
DProHG1 (m)	1.26	1.30–1.21	1	
DProHD2 (td)	3.62	3.65–3.59	1	3.91, 8.91
DProHD1 (q)	3	3.04–2.96	1	8.35
DProHB2 (m)	2.02	2.04–1.99	1	
DProHB1 (m)	1.46	1.48–1.43	1	
DProHA (dd)	4.3	4.31–4.27	1	3.43, 8.54
DmaaNH (d)	5.87	5.89–5.85	2	5.23
DmaaHB2 (dd)	2.41	2.44–2.37	1	8.31, 12.31
DmaaHB1 (dd)	2.27	2.30–2.24	1	6.34, 12.38
DmaaHA (m)	4.34	4.37–4.32	1	
DmaaBoc (s)	1.43	1.44–1.42	9	
AibNH (s)	6.95	6.96–6.93	1	
AibMe (d)	1.75	1.76–1.73	6	5.33

NOESY (600 MHz, 0.01 M in C_6D_6, 20 °C)

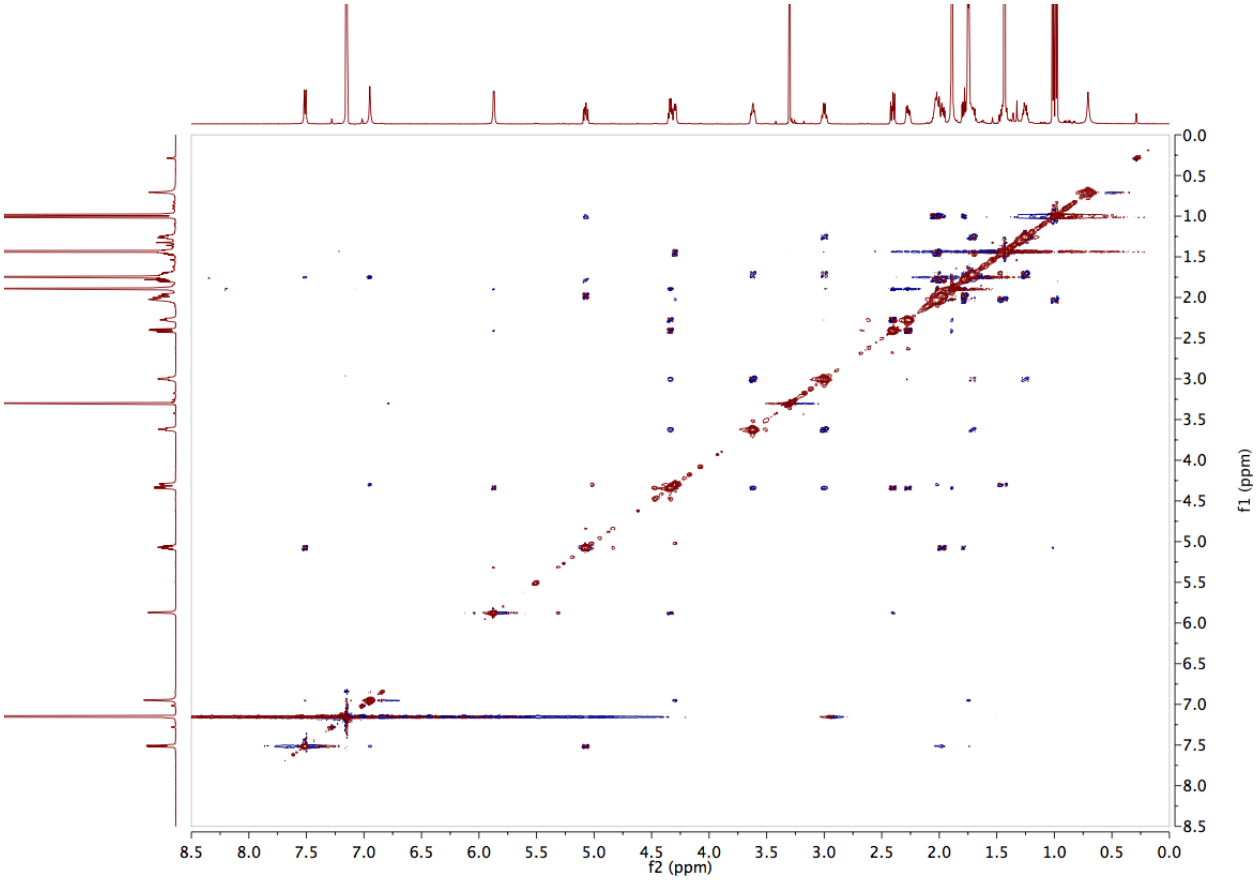

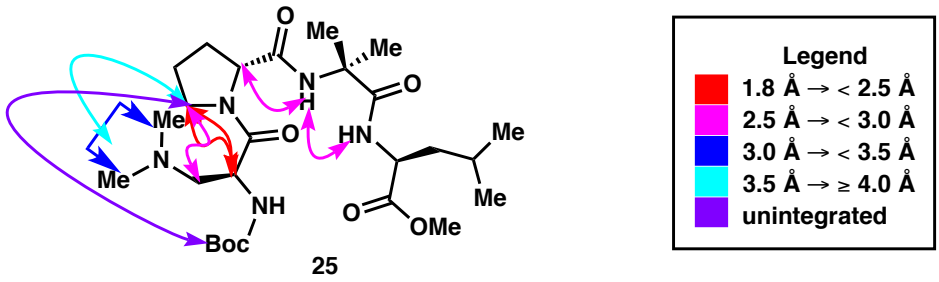

Figure S5.11: Inter-residue nOe Map for Peptide **25**

Table S5.29: Integrated NOESY Cross-peaks for Peptide **25**

	f2	f1	Normalized	Absolute	Assignment	Corrected Distances (Normalized)
1	7.51	1.98	1	788.96	LeuNH-LeuHB2	2.63
	1.98	7.51	1.21	951.33		
2	7.51	1.75	0.99	783.52	LeuNH-LeuHB1	2.66
	1.75	7.51	0.69	541.14		
3	7.51	6.95	0.84	663.63	LeuNH-AibNH	2.59
	6.95	7.51	0.95	751.16		
4	6.95	4.3	1.37	1081.53	AibNH-DProHA	2.53
	4.3	6.95	1.39	1093.24		
5	6.95	1.76	3.11	2451.55	AibNH-AibMe	2.19
	1.74	6.95	2.01	1585.33		
6	5.87	2.28	0.42	328.3	DmaaNH-DmaaHB1	3.02
	2.27	5.87	0.46	364.6		
7	5.87	1.9	0.38	297.36	DmaaNH-DmaaNMe$_2$	3.43
	1.89	5.87	0.25	193.42		
8	5.87	2.41	0.85	674.05	DmaaNH-DmaaHB2	2.65
	2.4	5.87	1.03	809.24		
9	5.07	1	2.07	1630.17	LeuHA-LeuHD	2.79
	1.01	5.07	1.03	810.7		
10	4.34	1.89	2.29	1807.37	DmaaHA-DmaaNMe$_2$	2.64
	1.89	4.34	1.14	896.11		
11	4.34	3.62	3.6	2836.7	DmaaHA-DProHD2	2.22
	3.62	4.33	3.56	2808.34		
12	4.33	3	2.7	2128.97	DmaaHA-DProHD1	2.32
	2.99	4.34	2.66	2099.13		
13	3	1.44	0.5	391.33	DProHD1-DProHB1	3.40
	1.46	3	0.23	177.56		
14	3	2.26	0.77	606.57	DProHD1-DmaaHB1	2.77
	2.27	3	0.78	611.92		
15	2.99	1.89	0.38	296.14	DProHD1-DmaaNMe$_2$	3.50
	1.89	3	0.2	155.29		
16	2.4	1.89	2.48	1953.47	DmaaHB2-DmaaNMe$_2$	2.56
	1.89	2.4	1.19	942.54		
17	2.27	1.89	2.04	1608.18	DmaaHB1-DmaaNMe$_2$	2.65
	1.9	2.27	0.98	770.23		
18	1.78	1	1.52	1197.13	LeuHB1-LeuHD	2.82
	0.99	1.79	1.06	832.35		
19	3.62	3	11.08	8743.76	DProHD1-DProHD2	1.80
	3	3.62	10.83	8546		

Table S5.30: Unintegrated NOESY Cross-peaks for Peptide **25**
LeuNH-LeuHB
AibNH-AibMe
DmaaNH-DmaaNMe$_2$
DmaaHA-DmaaNMe$_2$
DProHD-DmaaBoc

Peptide 30

^{1}H-NMR (600 MHz, 0.01 M in C_6D_6, 24 °C)

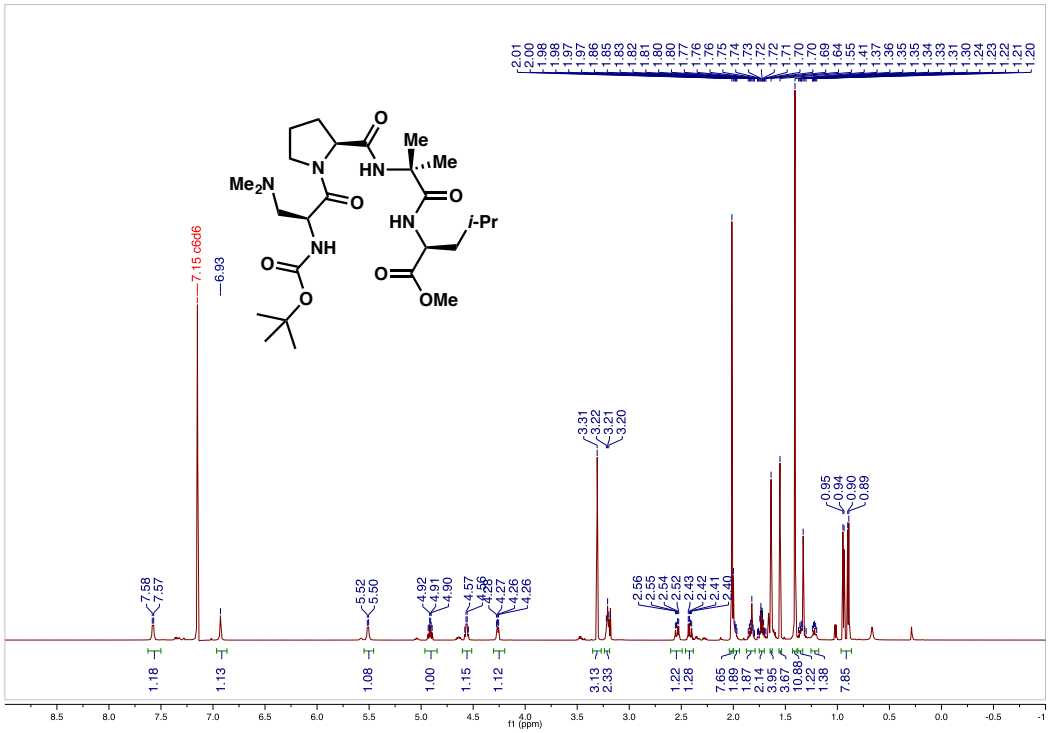

COSY (600 MHz, 0.01 M in C_6D_6, 24 °C)

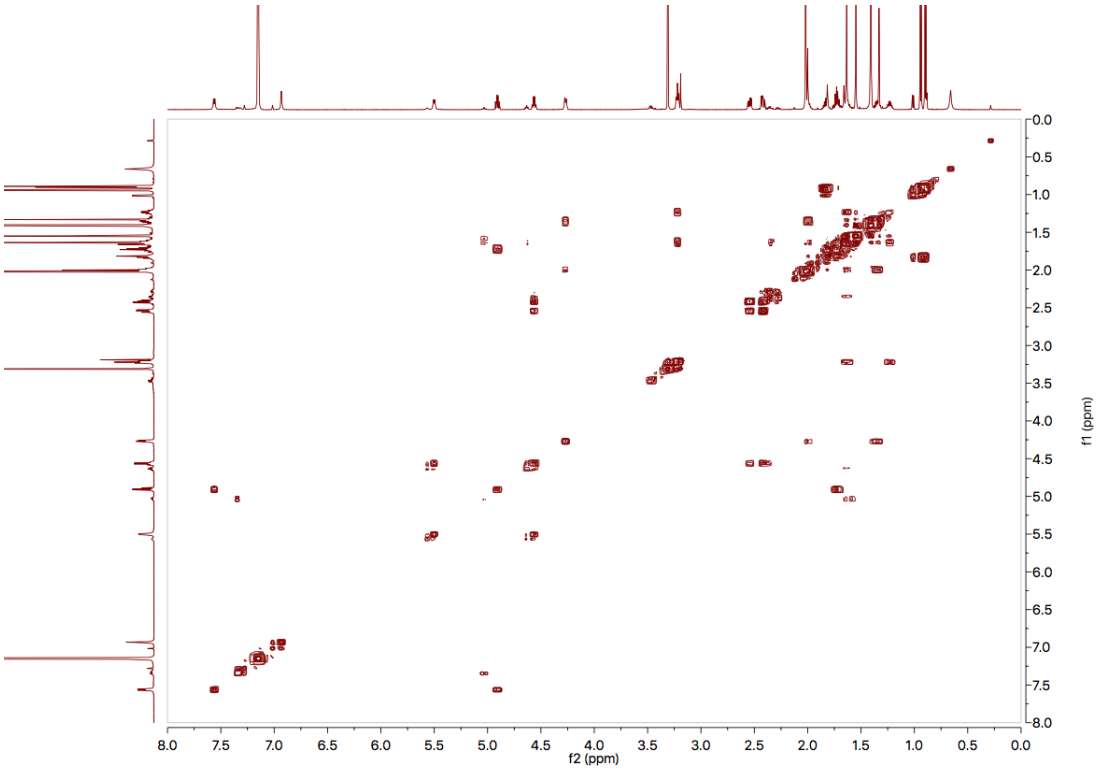

Table S5.31: Peak Assignments for Peptide **30**

Assignment (splitting)	Shift (ppm)	Range (ppm)	H's	*J*'s (Hz)
ProHG2 (m)	1.64	1.68–1.58	1	
ProHG1 (tt)	1.23	1.28–1.18	1	12.27, 6.02
ProHD (m)	3.21	3.25–3.17	2	
ProHB2 (m)	2	2.02–1.96	1	
ProHB1 (m)	1.35	1.39–1.30	1	
ProHA (dd)	4.27	4.30–4.24	1	4.25, 8.07
LeuOMe (s)	3.31	3.33–3.29	3	
LeuNH (d)	7.56	7.59–7.54	1	7.97
LeuHD (dd)	0.92	0.96–0.87	6	6.55, 26.50
LeuHG (m)	1.82	1.88–1.78	1	
LeuHB (m)	1.73	1.78–1.67	2	
LeuHA (td)	4.91	4.94–4.87	1	5.90, 8.40
DmaaNH (d)	5.5	5.52–5.48	1	7.36
DmaaNMe$_2$ (s)	2.02	2.03–2.00	6	
DmaaHB2 (dd)	2.54	2.58–2.51	1	6.33, 12.52
DmaaHB1 (dd)	2.42	2.45–2.39	1	6.95, 12.53
DmaaHA (q)	4.56	4.60–4.53	1	6.92
DmaaBoc (s)	1.41	1.42–1.39	9	
AibNH (s)	6.93	6.95–6.92	1	
AibMe2 (s)	1.63	1.65–1.62	3	
AibMe1 (s)	1.55	1.57–1.53	3	

NOESY (600 MHz, 0.01 M in C_6D_6, 24 °C)

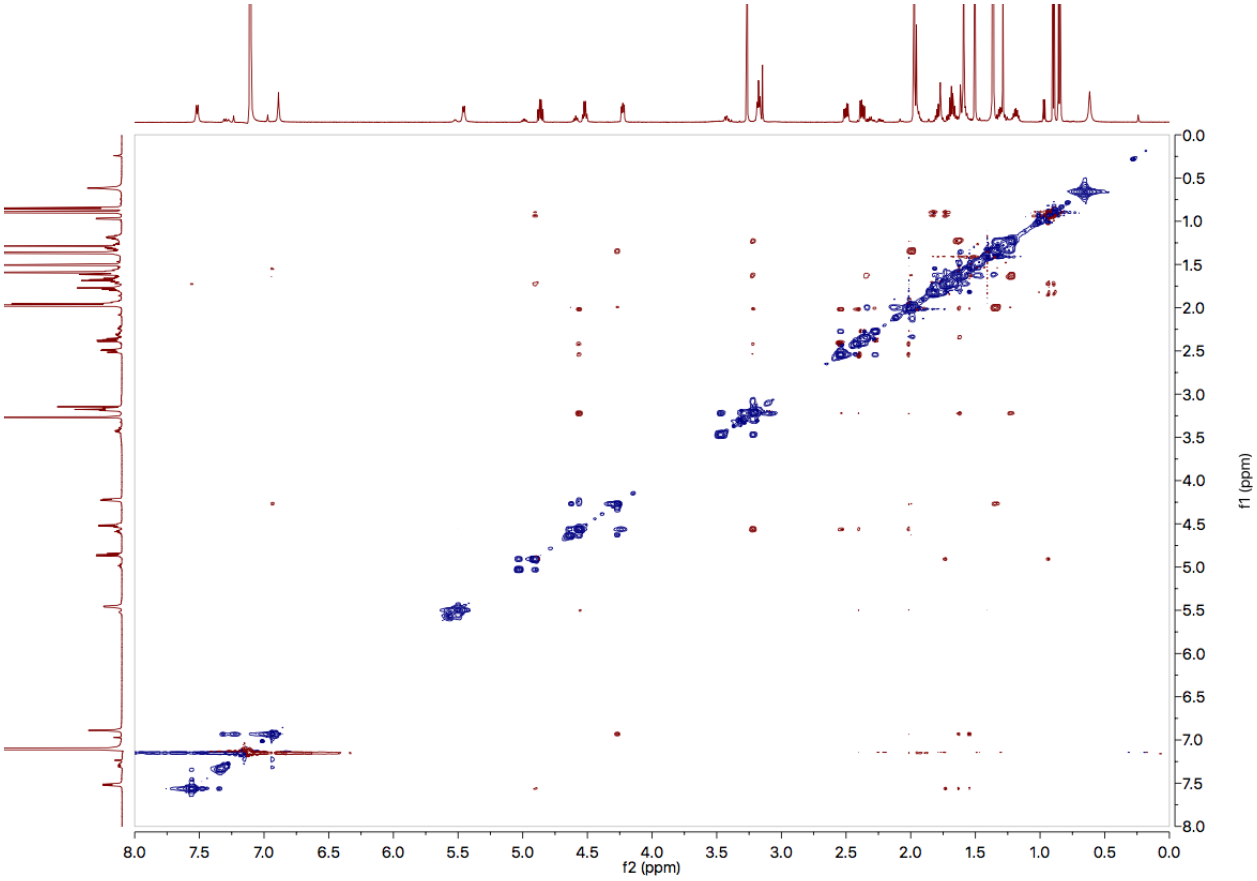

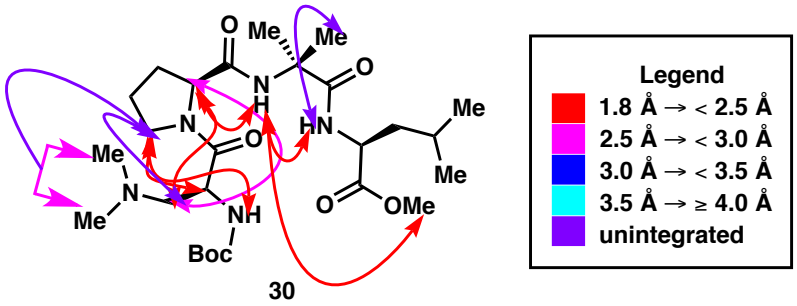

Figure S5.12: Inter-residue nOe Map for Peptide **30**

Table S5.32: Integrated NOESY Cross-peaks for Peptide **30**

	f2	f1	Normalized	Absolute	Assignment	Corrected Distances (Normalized)
1	7.56	1.54	0.9	88.93	LeuNH-LeuOMe	2.65
	1.54	7.56	1.04	102.81		
2	7.56	6.93	1	98.91	LeuNH-AibNH	2.34
	6.93	7.56	0.65	64.2		
3	7.56	1.83	0.97	96.07	LeuNH-LeuHG	2.68
	1.83	7.56	0.88	87.44		
4	7.55	1.72	3.1	306.46	LeuNH-LeuHB	2.22
	1.72	7.56	3.47	342.89		
5	6.93	1.54	1.84	181.97	AibNH-LeuOMe	2.18
	1.53	6.93	3.59	354.6		
6	6.93	1.63	1.39	137.58	AibNH-AibMe2	2.49
	1.63	6.93	2.58	254.78		
7	6.92	4.26	3	296.4	AibNH-ProHA	1.92
	4.27	6.92	6.96	688.86		
8	5.52	2.54	1.26	124.86	DmaaNH-DmaaHB2	2.49
	2.53	5.47	1.64	162.24		
9	5.49	2.41	1.91	189.05	DmaaNH-DmaaHB1	2.33
	2.4	5.47	1.22	120.56		
10	5.49	4.55	1.98	196.16	DmaaNH-ProHD	2.34
	4.56	5.49	2.21	218.89		
11	5.49	2.02	1.01	99.91	DmaaNH-DmaaNMe$_2$	2.96
	2.01	5.47	0.64	63.35		
12	4.9	0.94	3.07	303.73	LeuHA-LeuHD2	2.40
	0.94	4.9	2.53	249.86		
13	4.9	0.89	1.57	155.3	LeuHA-LeuHD1	2.74
	0.89	4.91	0.88	87.51		
14	4.57	3.21	19.68	1946.86	DmaaHA-ProHD	1.81
	3.22	4.55	17.99	1778.93		
15	4.56	2.01	5.5	543.64	DmaaHA-DmaaNMe$_2$	2.33
	2.02	4.55	2.51	248.27		
16	4.27	1.23	0.92	91.4	ProHA-ProHG1	2.81
	1.23	4.27	0.79	77.73		
17	3.22	2.53	1.84	181.7	ProHA-DmaaHB2	2.62
	2.54	3.21	2.28	225.09		
18	3.22	2.41	2.33	230.06	ProHA-DmaaHB1	2.42
	2.39	3.21	1.09	107.76		
19	2.54	2.01	8.56	846.23	DmaaHB2-DmaaNMe$_2$	2.17
	2.01	2.53	3.98	393.85		
20	2.42	2.01	3.78	373.4	DmaaHB1-DmaaNMe$_2$	2.33
	2.01	2.41	3.25	321.89		
21	2.56	2.39	10.55	1043.35	DmaaHB2-DmaaHB1	1.80
	2.4	2.56	9.81	970.46		

Table S5.33: Unintegrated NOESY Cross-peaks for Peptide **30**
LeuNH-AibMe
ProHD-DmaaHB
ProHD-DmaaNMe$_2$

Peptide 32

^{1}H-NMR (600 MHz, 0.01 M in C_6D_6, 24 °C)

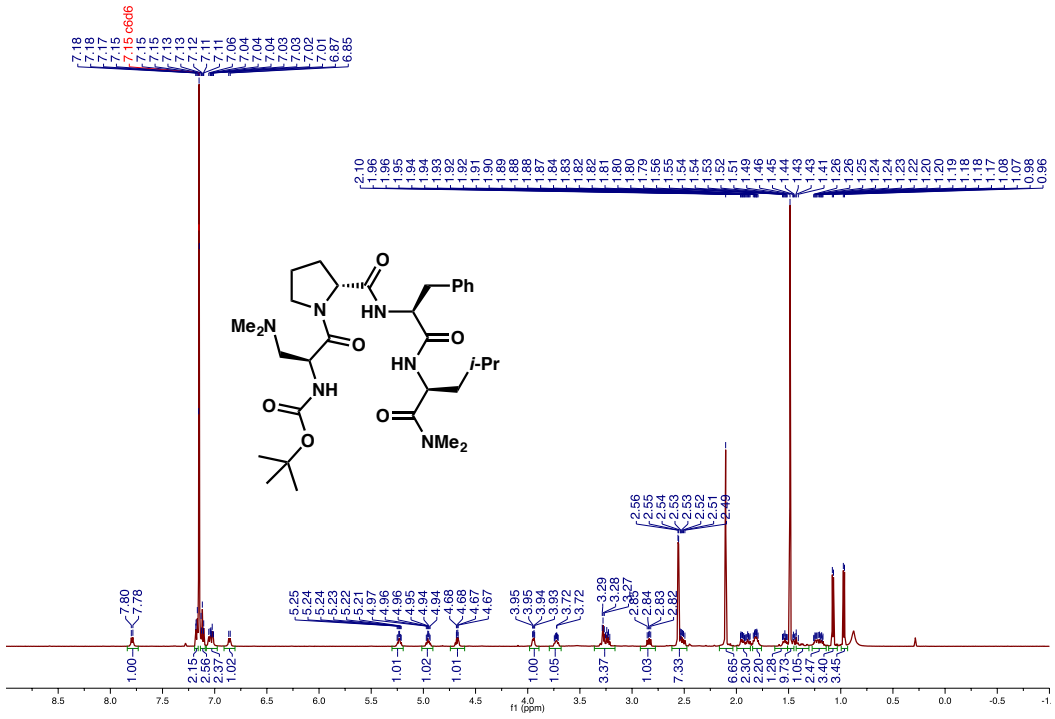

COSY (600 MHz, 0.01 M in C_6D_6, 24 °C)

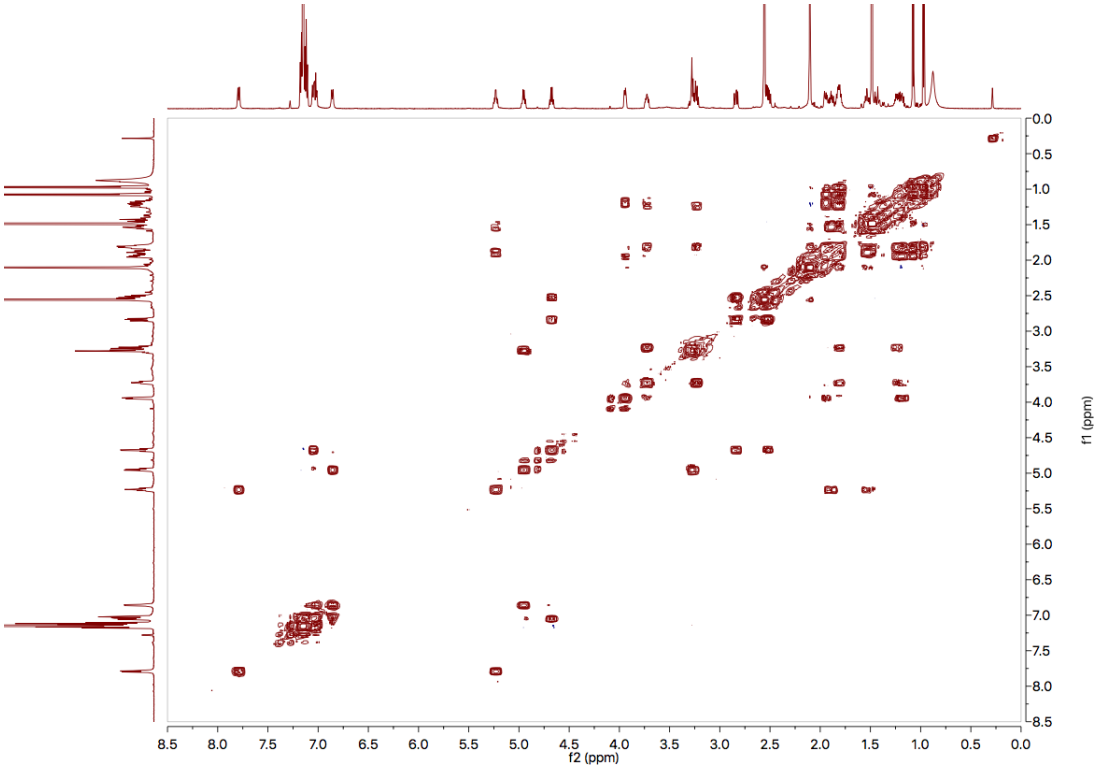

Table S5.34: Peak Assignments for Peptide **32**

Assignment (splitting)	Shift (ppm)	Range (ppm)	H's	*J*'s (Hz)
PheNH (d)	6.86	6.88–6.83	1	8.55
PheHA (td)	4.95	4.99–4.92	1	5.12, 8.28
PheAr (t)	7.12	7.15–7.09	2	7.61
PheAr (m)	7.03	7.04–7.01	1	
PheAr (d)	7.17	7.20–7.15	2	7.14
LeuOMe (d)	2.56	2.58–2.54	6	3.65
LeuNH (d)	7.79	7.82–7.77	1	8.99
LeuHD2 (d)	1.08	1.10–1.05	3	6.48
LeuHD1 (d)	0.97	0.99–0.95	3	6.64
LeuHG, DProHG2 (m)	1.81	1.84–1.78	2	
LeuHB1 (ddd)	1.54	1.58–1.50	1	4.76, 8.82, 13.52
LeuHA (td)	5.23	5.27–5.20	1	4.66, 9.28
DProHG1, DProHB1 (m)	1.21	1.28–1.14	2	
DProHD2 (m)	3.73	3.76–3.69	1	
DProHD1 (d)	3.28	3.30–3.27	1	4.43
DProHB2, LeuHB2 (m)	1.91	1.98–1.82	2	
DProHB (m)	3.23	3.26–3.20	2	
DProHA (dd)	3.94	3.97–3.92	1	3.62, 8.01
DmaaNH (d)	7.05	7.07–7.04	0	7.78
DmaaNMe$_2$ (s)	2.1	2.12–2.09	6	
DmaaHB2 (dd)	2.84	2.87–2.80	1	7.99, 12.23
DmaaHB1 (m)	2.52	2.54–2.48	1	
DmaaHA (td)	4.68	4.71–4.64	1	6.17, 7.83
DmaaBoc (s)	1.49	1.50–1.47	9	

NOESY (600 MHz, 0.01 M in C_6D_6, 24 °C)

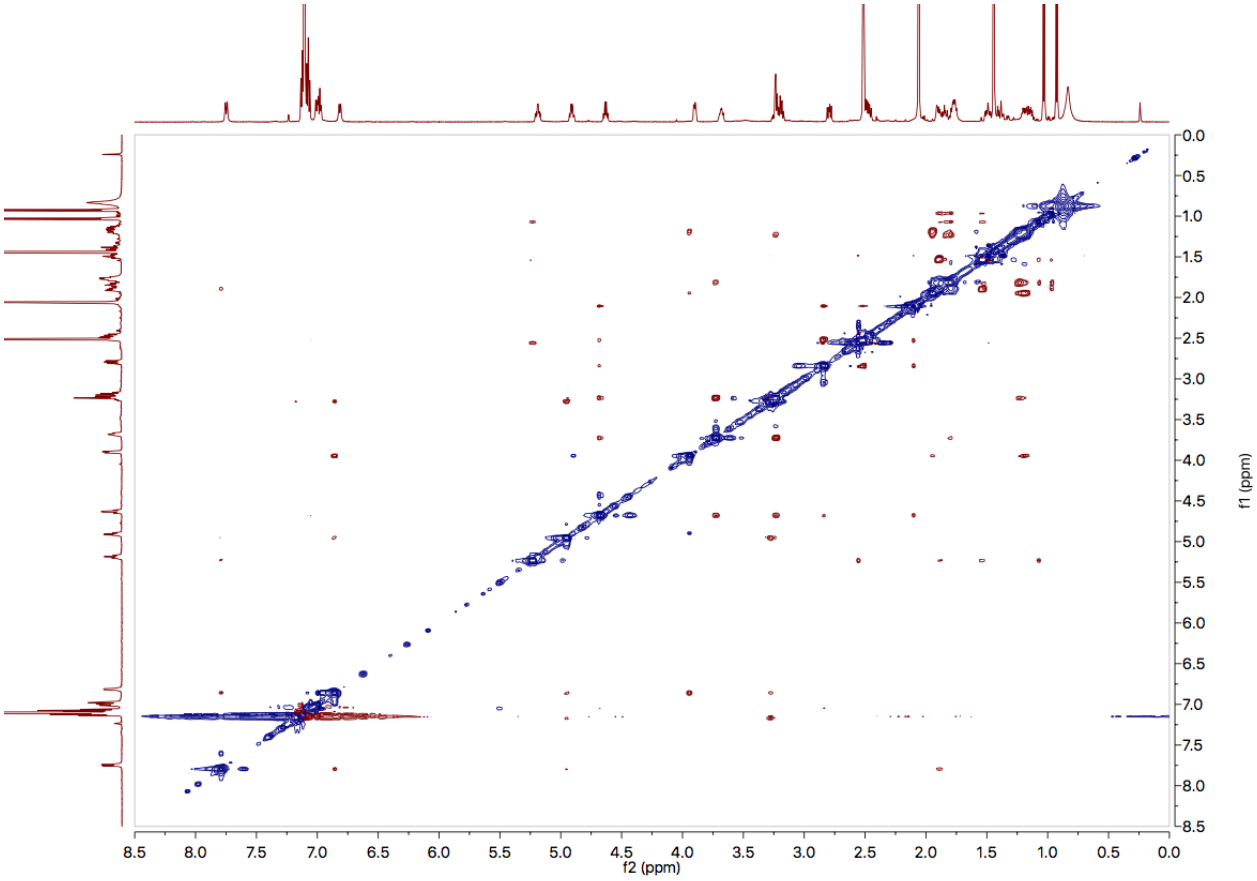

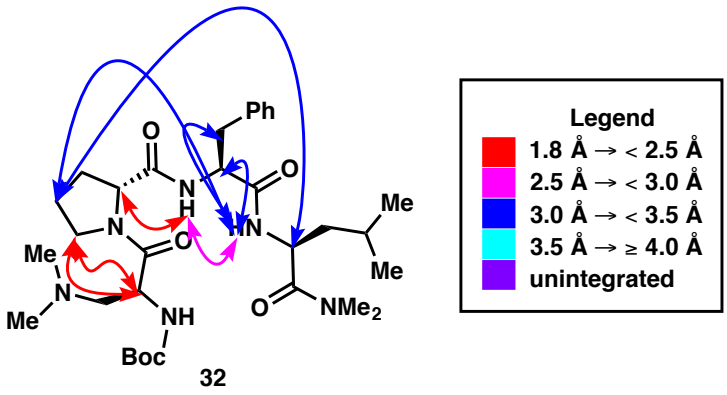

Figure S5.13: Inter-residue nOe Map for Peptide **32**

Table S5.35: Intregrated NOESY Cross-peaks for Peptide **32**

	f2	f1	Normalized	Absolute	Assignment	Corrected Distances (Normalized)
1	7.79	1.89	1.17	318.03	LeuNH-LeuHB2	2.49
	1.9	7.78	1.53	417.27		
2	7.79	6.85	1	272.97	LeuNH-PheNH	2.56
	6.85	7.79	1.16	317.89		
3	7.79	3.27	0.25	66.96	LeuNH-PheHB	3.40
	3.26	7.8	0.29	78.1		
4	7.79	1.79	0.56	152.69	LeuNH-ProHG2	3.01
	1.78	7.8	0.49	133.15		
5	7.79	4.96	0.47	128.32	LeuNH-PheHA	3.07
	4.93	7.79	0.41	112.62		
6	7.05	2.83	0.43	116.16	DmaaNH-DmaaHB2	3.17
	2.84	7.05	0.53	143.41		
7	7.05	2.11	0.12	31.96	DmaaNH-DmaaNMe$_2$	4.36
	2.09	7.03	0.09	23.79		
8	6.85	3.95	3.25	886.36	PheNH-ProHA	2.18
	3.95	6.85	3.46	944.93		
9	5.23	1.08	1.04	284.38	LeuHA-LeuHD2	2.74
	1.07	5.22	1.12	306.18		
10	5.23	1.89	0.44	119.16	LeuHA-LeuHB2	2.83
	1.89	5.23	0.88	239.97		
11	5.23	1.54	1.14	311.02	LeuHA-LeuHB1	2.50
	1.53	5.22	1.48	405.15		
12	5.23	0.96	0.3	81.15	LeuHA-LeuHD1	3.41
	0.96	5.22	0.34	91.97		
13	5.23	1.8	0.43	116.82	LeuHA-ProHG2	3.15
	1.8	5.23	0.4	108.74		
14	4.67	3.72	1.95	533.62	DmaaHA-ProHD2	2.34
	3.72	4.67	3.21	876.95		
15	4.67	3.23	2.43	662.06	DmaaHA-ProHD1	2.28
	3.23	4.67	3.29	898.5		
16	4.66	2.11	1.6	436.42	DmaaHA-DmaaNMe$_2$	2.71
	2.1	4.68	1.45	394.97		
17	2.84	2.09	2.27	619.14	DmaaHB2-DmaaNMe$_2$	2.62
	2.11	2.84	1.48	403.41		
18	3.73	3.22	15.12	4127.81	ProHD2-ProHD1	1.80
	3.23	3.73	12.39	3382.12		

Table S5.36: Unintegrated NOESY Cross-peaks for Peptide **32**
PheNH-PheHB
LeuHB-LeuHD

Peptide 33

^{1}H-NMR (600 MHz, 0.01 M in C_6D_6, 20 °C)

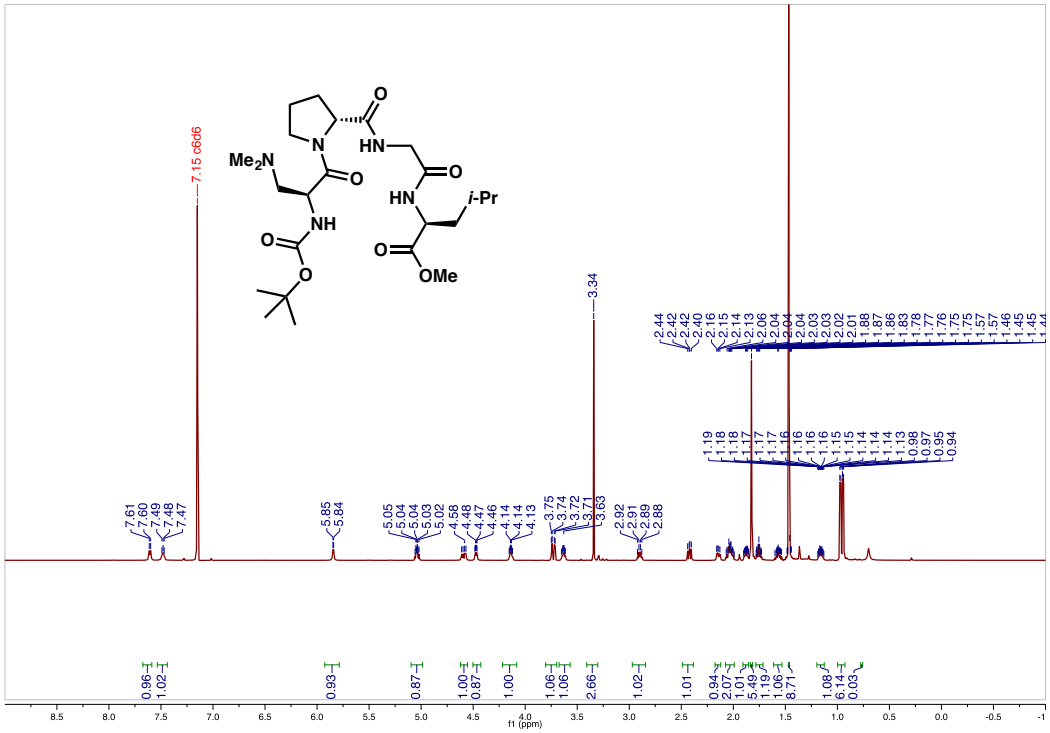

COSY (600 MHz, 0.01 M in C_6D_6, 20 °C)

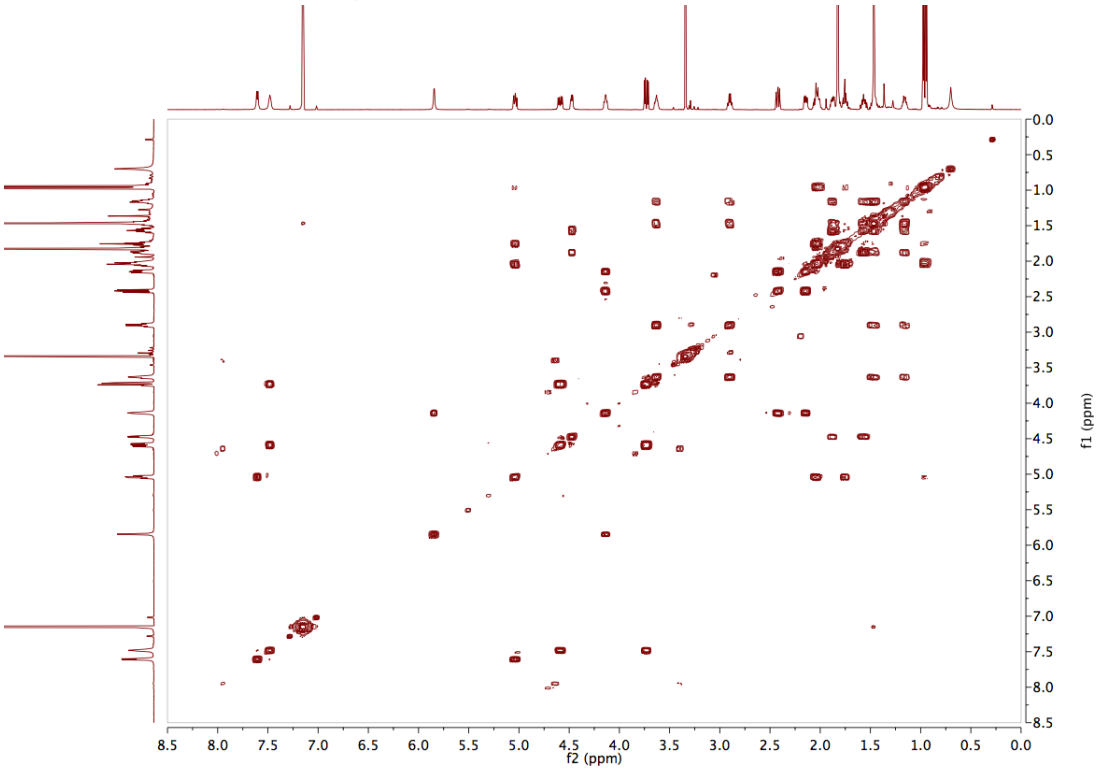

Table S5.37: Peak Assignments for Peptide **33**

Assignment (splitting)	Shift (ppm)	Range (ppm)	H's	*J*'s (Hz)
ProHG2 (m)	1.57	1.62–1.52	1	
LeuOMe (s)	3.34	3.36–3.33	3	
LeuNH (d)	7.61	7.63–7.58	1	7.99
LeuHD (dd)	0.96	0.99–0.88	6	6.44, 15.61
LeuHB2, LeuHG (m)	2.04	2.08–1.99	2	
LeuHB1 (m)	1.76	1.82–1.71	1	
LeuHA (ddd)	5.04	5.07–5.00	1	4.65, 7.95, 10.13
GlyNH (t)	7.48	7.51–7.45	1	6.47
GlyHA2 (dd)	4.59	4.63–4.55	1	7.82, 16.98
GlyHA1 (dd)	3.73	3.77–3.70	1	5.11, 16.99
DProHG1 (m)	1.16	1.20–1.11	1	
DProHD2 (m)	3.63	3.67–3.60	1	
DProHD1 (q)	2.9	2.94–2.86	1	8.16
DProHA (dd)	4.47	4.50–4.43	1	3.76, 8.71
DmaaNH (d)	5.84	5.86–5.82	1	4.06
DmaaHB2 (dd)	2.42	2.46–2.39	1	8.70, 12.24
DmaaHB1 (dd)	2.14	2.18–2.11	1	6.31, 12.26
DmaaHA (m)	4.14	4.17–4.11	1	
$DmaaNMe_2$ (s)	1.83	1.84–1.81	6	
DmaaBoc (s)	1.47	1.48–1.45	9	

NOESY (600 MHz, 0.01 M in C_6D_6, 20 °C)

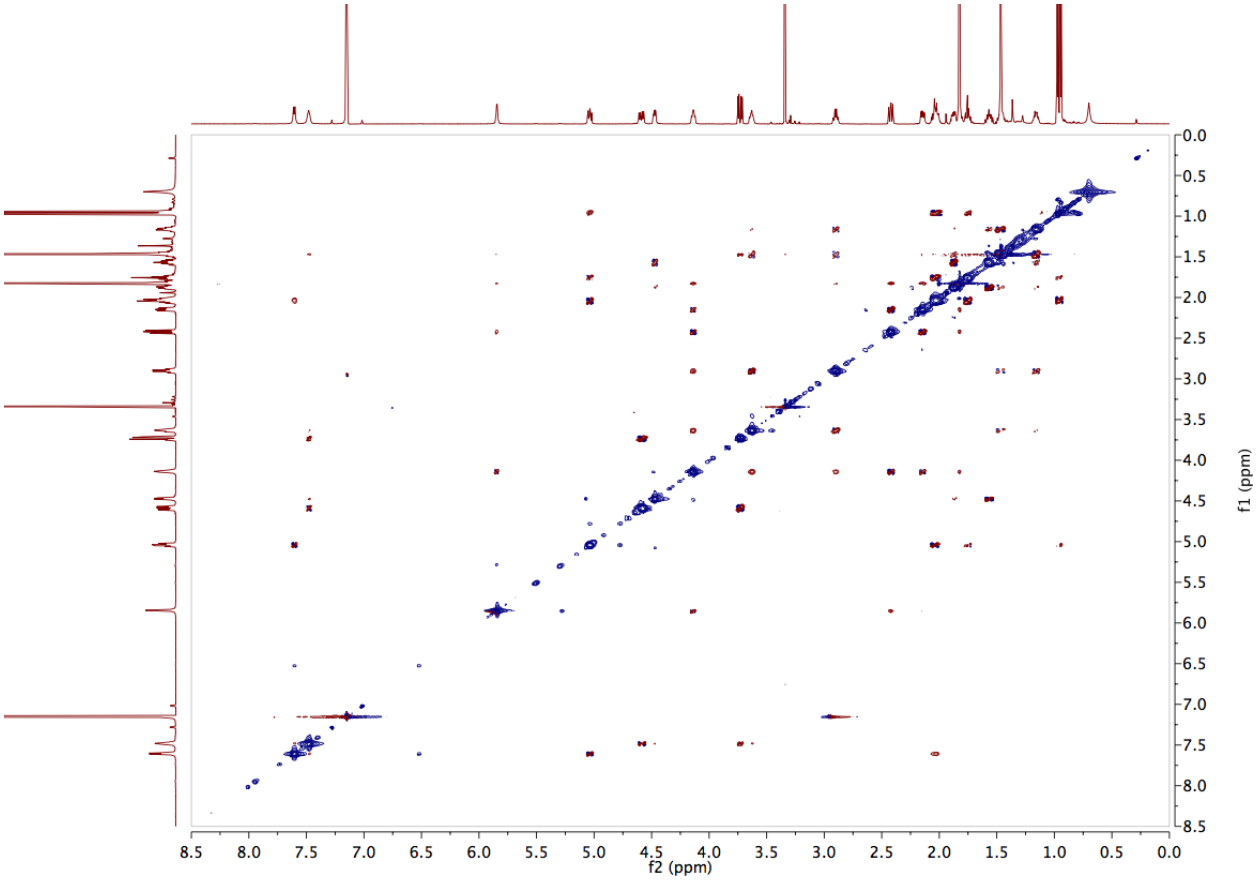

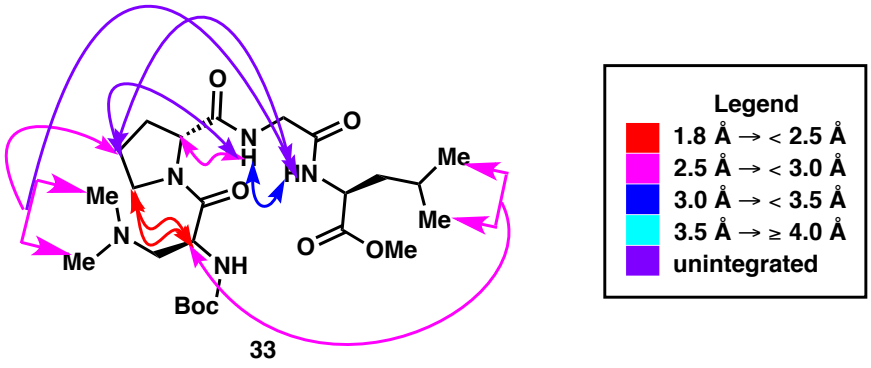

Figure S5.14: Inter-residue nOe Map for Peptide **33**

Table S5.38: Intregrated NOESY Cross-peaks for Peptide **33**

	f2	f1	Normalized	Absolute	Assignment	Corrected Distances (Normalized)
1	7.6	2.04	1	1875.97	LeuNH-LeuHB2	2.45
	2.03	7.6	1.02	1906.64		
2	7.6	7.47	0.14	270.75	LeuNH-GlyNH	3.10
	7.47	7.61	0.12	220.19		
3	7.47	4.45	0.2	378.85	GlyNH-DProHA	2.89
	4.47	7.48	0.2	370.41		
4	5.84	2.42	0.36	682.81	DmaaNH-DmaaHB2	2.55
	2.41	5.85	0.49	921.09		
5	5.85	1.83	0.17	316.9	DmaaNH-DmaaNMe$_2$	3.29
	1.82	5.85	0.1	189.15		
6	5.84	2.15	0.16	299.05	DmaaNH-DmaaHB1	2.95
	2.14	5.85	0.21	385.84		
7	5.02	0.95	0.89	1666.77	LeuHA-LeuHD	2.73
	0.94	5.03	0.47	874.29		
8	4.13	3.63	1.54	2893.5	DmaaHA-DProHD2	2.14
	3.61	4.13	1.49	2793.84		
9	4.13	1.83	0.94	1761.33	DmaaHA-LeuHD	2.59
	1.81	4.13	0.39	740.04		
10	4.13	2.9	1.11	2088.43	DmaaHA-DProHD1	2.26
	2.89	4.14	1	1879.38		
11	2.41	1.83	1.29	2415.41	DmaaHB2-DmaaNMe$_2$	2.45
	1.82	2.42	0.5	941.24		
12	2.14	1.83	1.09	2041.52	DmaaHB1-DmaaNMe$_2$	2.52
	1.82	2.16	0.45	847.67		
13	1.74	0.96	0.76	1420.35	LeuHB1-LeuHD	2.74
	0.95	1.75	0.48	899.02		
14	1.56	1.16	0.55	1029.22	DProHG1-DmaaNMe$_2$	2.51
	1.15	1.57	0.66	1240.01		
15	3.63	2.9	4.17	7818.57	DProHD1-DProHD2	1.80
	2.9	3.63	3.69	6930.23		

Table S5.39: Unintegrated NOESY Cross-peaks for Peptide **33**
LeuNH-DmaaNMe$_2$
LeuNH-DProHG
GlyNH-DProHG
DmaaHA-DmaaNMe$_2$

C. Calculation of ϕ Dihedral Angle From $^3J_{NH\text{-}H\alpha}$ Value

^3J-Values ($^3J_{NH-H\alpha}$) from ^{1}H-NMR spectra were extracted from the N*H*(Dmaa) and N*H*(Leu) resonances and used to solve for the ϕ angles of the two respective residues. The aforementioned dihedrals were solved for using equation S3,[31] which is derived from the studies pioneered by Karplus and co-workers.[32,33] Solutions were found by plotting equation S3 against the extracted ^3J -values and finding their intersection using an online graphing program.[34] Table S5.40 shows all angles calculated from the ^3J -value of each peptide. Those angles in parentheses were eliminated from the realm of possibilities because of their being Ramachandran disallowed on the basis of their positions in Figures S4.04 and S4.05. Resonances with $^3J = 0$ (listed at "undetermined" in Table S5.40) were assigned values of ϕ = –30 °. Informed by our own observations in the solid state and examination of models, pre-helical (type I′) β-turns often adopt ϕ(*i*) and ϕ(*i*+3) at approximately –30° to –90° and –30° to –120°, respectively. These metrics appear to optimize H-bond directionality and minimize repulsive steric and stereoelectronic interactions within the turn. The same issues often mandate ϕ(*i*) and ϕ(*i*+3) for (type II′) β-hairpins to be close to –90° to –150° and –90º to –120º, respectively. Non-hairpin β-turns were observed to have ϕ(*i*) values of approximately –60° to –160° and ϕ(*i*+3) values of –60° to –150°. These estimations of dihedral angles informed the overall assignment of turn-type. These cutoffs are graphically represented in Figure S5.15.

$$J = 6.98\cos^2\left(\phi - \frac{\pi}{3}\right) - 1.38\cos\left(\phi - \frac{\pi}{3}\right) + 1.72 \qquad \text{(S3)}$$

Table S5.40: Peptide $^3J_{NH-H\alpha}$-Values and Calculated ϕ Angles

Peptide	J_i	ϕ(*i*) (eliminated values)	J_{i+3}	ϕ(*i*+3)
3	7.6	–86°, –154°	8.7	–95°, –145°
4	0.0	undetermined	7.8	–89°, –151°
7	0.0	undetermined	6.0	–74º, –166º
15	7.6	–86°, –154°	7.9	–89°, –142°
16	0.0	undetermined	8.9	–96°, –143°
17	0.0	undetermined	7.8	–89°, –151°
18	4.6	–63°, –177° (19°, 102°)	8.0	–89°, –151°
19	3.9	–89°, –142° (12°, 108°)	7.8	–89°, –151°
21	7.1	–82°, –158° (49°, 71°)	7.9	–89°, –142°
22	5.2	–67°, –172° (24°, 95°)	8.2	–90°, –150°
25	5.2	–67°, –172° (24°, 95°)	8.3	–94°, –151°
30	7.4	–89°, –151°	8.0	–89°, –151°
32	7.9	–89°, –142°	9.0	–98°, –142°
33	4.1	–119°, 180° (14°, 106°)	8.0	–89°, –151°

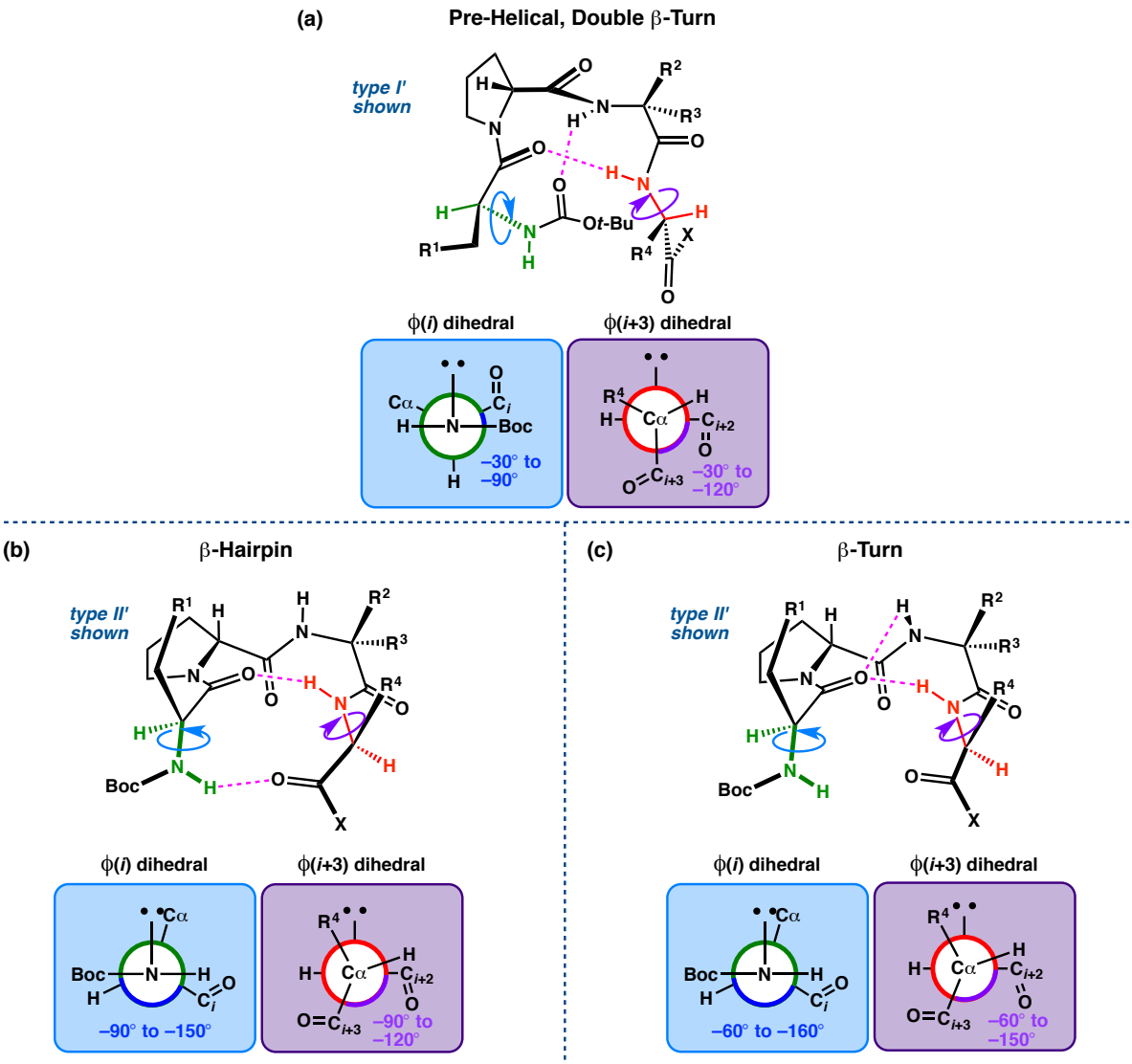

Figure S5.15: Explanation for the predicted ϕ(*i*) and ϕ(*i*+3) dihedrals of **(a)** pre-helical, double β-turns, **(b)** β-hairpins, and **(c)** non-hairpin β–turns (which may sample γ/γ′-turns).

D. Relative Chemical Shift Data & ^{1}H-NMR Overlays of Homologous Series

Table S5.41: Chemical Shift Values for Peptide Amide Protons

Peptide	N*H*(*i*+3) (ppm)	N*H*(*i*+2) (ppm)	N*H*(Dmaa) (ppm)
3	8.07	6.69	7.10
4	7.93	7.67	5.82
7	8.09	7.71	5.71
15	7.77	7.48	5.48
16	7.57	7.06	6.73
17	7.49	7.58	5.75
18	7.60	7.04	5.80
19	7.66	7.23	5.77
21	7.85	6.97	5.48
22	7.52	6.86	5.84
25	7.51	6.95	5.87
30	7.56	6.93	5.50
32	7.79	6.86	7.05
33	7.61	7.48	5.84

Table S5.42: Relative Chemical Shift Values for Peptide Amide Protons*

Peptide	N*H*(*i*+3) (ppm)	N*H*(*i*+2) (ppm)	N*H*(Dmaa) (ppm)
3	8.07	6.69	7.10
4	0.14	–0.98	1.28
7	–0.02	–1.02	1.39
15	0.3	–0.79	1.62
16	0.50	–0.37	0.37
17	0.58	–0.89	1.35
18	0.47	–0.35	1.30
19	0.41	–0.54	1.33
21	0.22	–0.28	1.62
22	0.55	–0.17	1.26
25	0.56	–0.26	1.23
30	0.51	–0.24	1.60
32	0.28	–0.17	0.05
33	0.46	–0.79	1.26

*Values shown are Δδ of N*H*(Leu), N*H*(*i*+2), and N*H*(Dmaa) relative to those in peptide **3**.

Table S5.43: Peak Width at Half-Maximum Intensity for Peptide Amide Protons

Peptide	N*H*(*i*+3) (ppm)	N*H*(*i*+2) (ppm)	N*H*(Dmaa) (ppm)
3	0.025	0.015	0.025
4	0.019	0.013	0.031
7	0.024	0.012	0.016
15	0.019	0.010	0.024
16	0.020	0.014	0.024
17	0.020	0.011	0.020
18	0.020	0.011	0.013
19	0.019	0.009	0.012
21	0.021	obstructed	0.020
22	0.019	0.013	0.016
25	0.018	0.010	0.014
30	0.021	0.009	0.021
32	0.023	0.023	obstructed
33	0.022	0.028	0.014

***i*+2 Series**

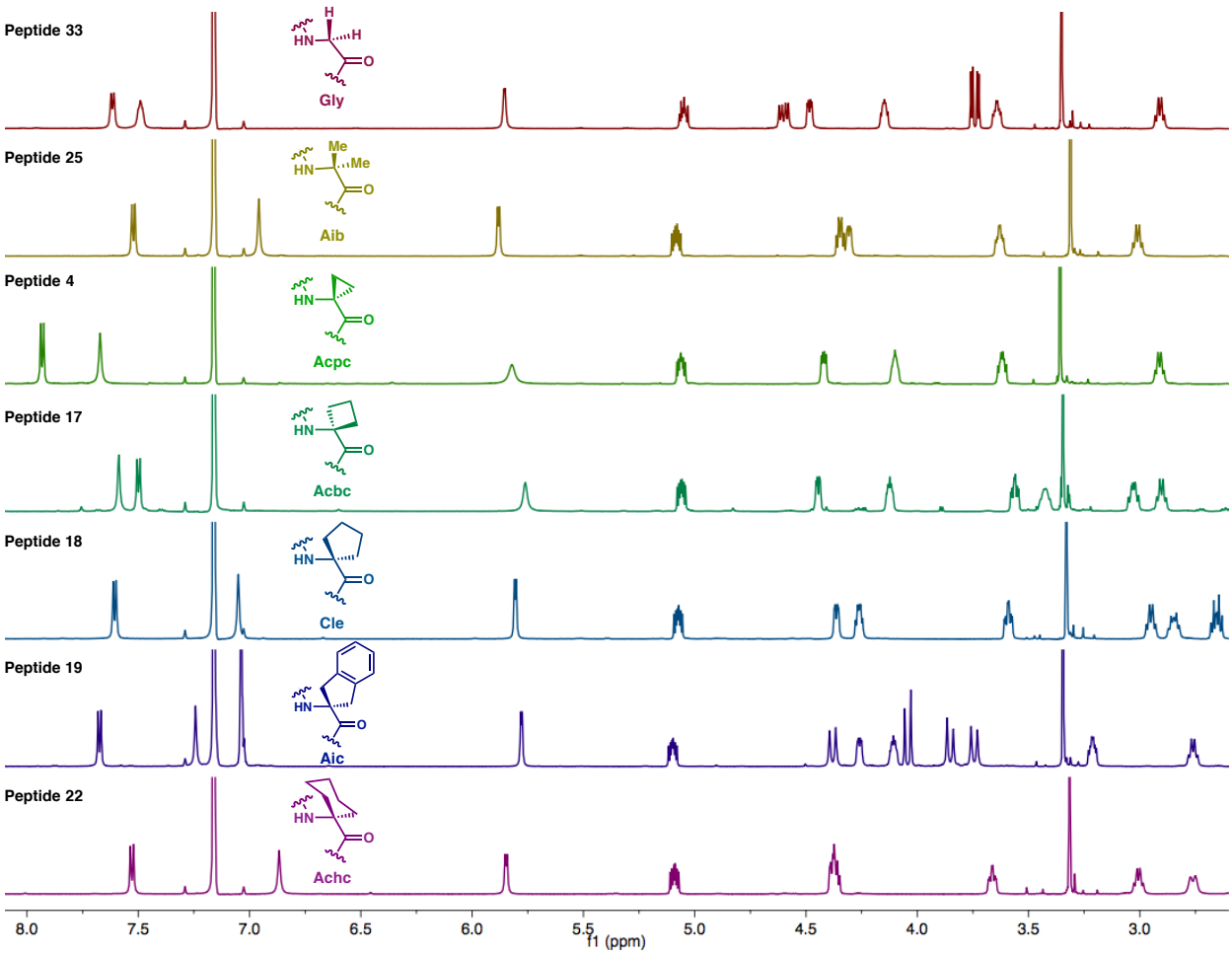

Figure S5.16: Stacked ^{1}H-NMR spectra (600 MHz, 0.01 M in C_6D_6, 20 ºC) of a homologous series of peptides differing only in the *i*+2 residue (Boc-Dmaa-D-Pro-Xaa-Leu-OMe).

L-Pro Series

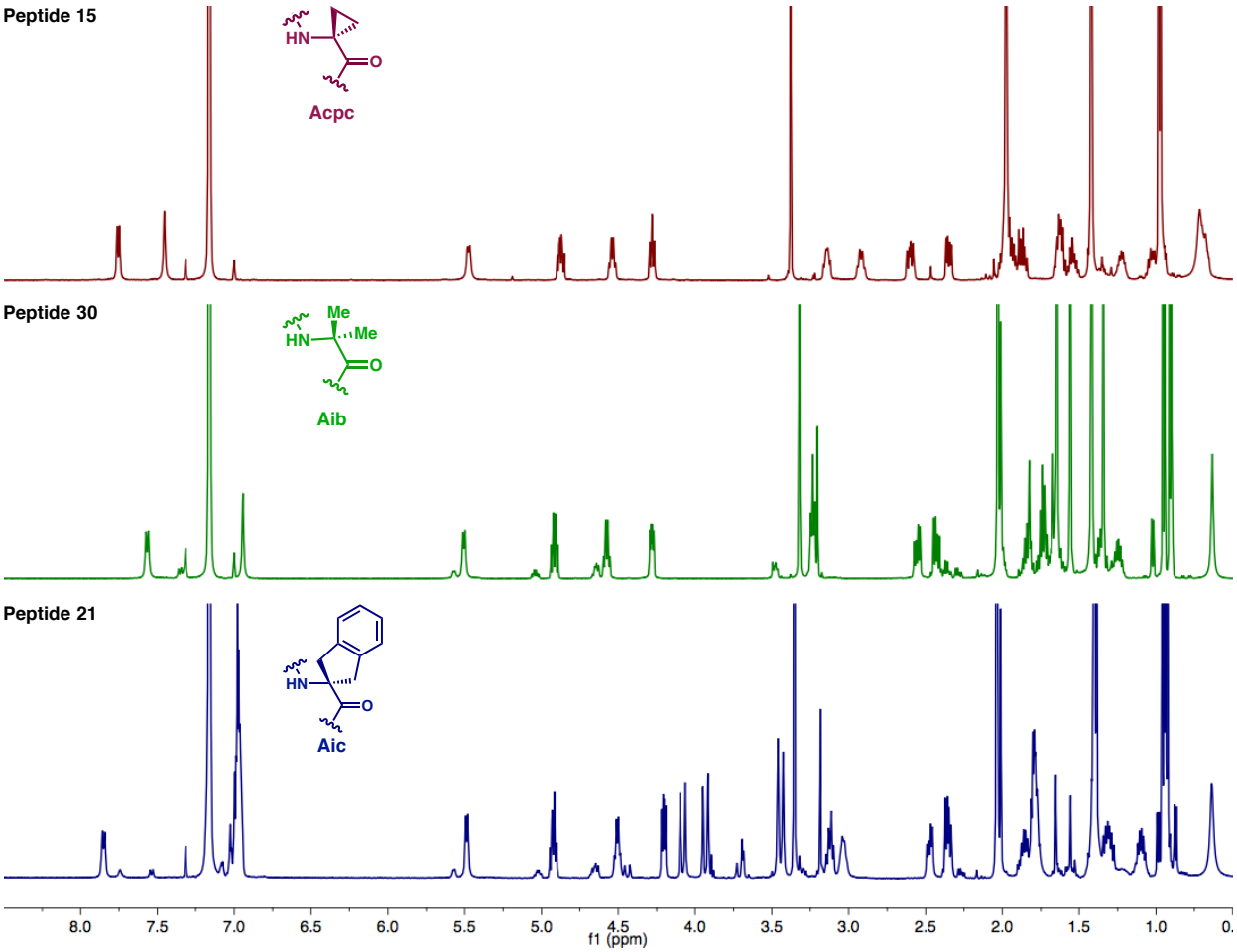

Figure S5.17: Stacked ^{1}H-NMR spectra (600 MHz, 0.01 M in C_6D_6, 20 ºC) of a homologous series of L-Pro-containing peptides differing only in the *i*+2 residue (Boc-Dmaa-Pro-Xaa-Leu-OMe).

VI. DFT Geometry Optimizations of X-Ray Crystal Structures

A. Computational Methods

All *ab initio* computations were performed using Gaussian 09, Revision D.01,[35] which was accessed remotely on OMEGA, a supercomputer cluster owned and operated by the Yale University Faculty of Arts and Sciences High Performance Computing Center.[36] Job files were created locally using GaussView 5.0[37] and transferred to the clusters using a secure file-transfer protocol (SFTP). All jobs reported herein used one node (8 cores) and 32 GB of memory. Computational outputs were rendered using Mercury 3.8 by conversion of the Gaussian output file (.out) to a Protein Data Bank file (.pdb).[16]

Geometry optimization of X-ray crystal structures was accomplished using Density Functional Theory (DFT) at the M06-2X/6-311++G(2d,3p)//B3LYP/6-31+G(d,p) level of theory.[38,39] In most cases, the number of optimization steps was increased to 50 by specifying "opt=(maxcycles=50)" in the route card of the Gaussian job file (.gjf). All such calculations were performed for isolated, gas-phase molecules at 25 ºC (298.15 K) and 1 atm. Vibrational corrections to the total electronic energy were computed using frequency calculations at the B3LYP/6-31+G(d,p) level and were used to derive enthalpy (*H*), entropy (*S*), and Gibbs free energy (*G*) values. The conversion factor of 627.509 kcal/mol per Hartree/particle was used to calculate relative energy values in kcal/mol. Dipole moments from the M06-2X single-point calculations are reported in Debye (D). Overlays of the DFT-optimized structures with the corresponding X-ray crystallographic coordinates were generated using either the "structure overlay" or "molecule overlay" features of Mercury 3.8, both of which provide an RMSD value (in Å) to quantify the fit. The "structure overlay" feature was used to generate backbone and loop region RMSD values, while the "molecule overlay feature was used to generate all-atom RMSDs. Please refer to Section III.A for additional details on structure overlays.

We note that a known DFT optimization protocol for organic X-ray crystal structures has been reported previously.[40] This comprehensive study employed a dispersion corrected functional, B97D3. In a number of cases, we attempted geometry optimizations of our peptide X-ray crystal structures using the D3 dispersion correction,[41] but the resulting structures differed significantly from the X-ray coordinates seemed improbable/unlikely. As such, we continued to use the M06-2X/6-311++G(2d,3p)//B3LYP/6-31+G(d,p) method, which provided structures in good accordance with chemical intuition and previous studies.

B. Optimization of Peptides 3a–c

Table S6.01: B3LYP/6-31+G(d,p) Optimized Coordinates of **3a**

Tag	Symbol	X	Y	Z
1	O	0.029438	–1.784969	0.832165
2	O	–4.56702	–0.10373	1.544639
3	O	–1.5331	2.912301	1.053915
4	O	–0.721522	0.55778	–1.884541
5	O	4.271011	0.73468	–0.665338
6	O	3.748299	–0.408295	1.258207
7	N	–0.986844	–1.434083	2.834271
8	N	–2.695005	–0.372736	0.266245
9	H	–2.070269	0.022668	–0.434845
10	N	–2.887966	2.267335	–0.675164
11	H	–2.850089	1.983126	–1.646407
12	N	0.506421	2.308973	–1.163191
13	N	2.160147	–0.072469	–0.264597
14	H	1.614578	–0.701388	0.324067
15	N	2.607091	–1.960668	–2.535177
16	C	–2.123957	–1.061794	3.67619
17	H	–1.911546	–0.101546	4.161083
18	H	–2.275873	–1.81629	4.45784
19	H	–3.042056	–0.94387	3.104984
20	C	0.308246	–1.387367	3.510797
21	H	1.057771	–1.890679	2.902793
22	H	0.220532	–1.885787	4.481643
23	H	0.624049	–0.349472	3.676438
24	C	–1.01406	–1.645337	1.490869
25	C	–2.376872	–1.712443	0.765181
26	H	–3.172294	–1.974354	1.459936
27	C	–3.759635	0.338819	0.718783
28	C	–3.942047	1.727437	0.139418
29	C	–5.366885	2.105158	–0.250394
30	H	–5.474372	2.723828	–1.13637
31	H	–6.119201	1.335901	–0.11331
32	C	–4.745481	2.703915	0.972491
33	H	–5.07409	2.337366	1.938044
34	H	–4.415255	3.735911	0.938624
35	C	–1.728881	2.77303	–0.147634
36	C	–0.673465	3.199526	–1.192037
37	H	–1.109117	3.155611	–2.197424
38	C	–0.093029	4.596398	–0.877394
39	H	–0.590946	5.377838	–1.457536
40	H	–0.242803	4.804727	0.185966
41	C	1.409131	4.471655	–1.185132
42	H	1.60123	4.597806	–2.257129
43	H	2.012602	5.205743	–0.644203
44	C	1.726002	3.034311	–0.7637
45	H	2.614003	2.619146	–1.240635
46	H	1.859813	2.959722	0.322358
47	C	0.388307	1.020505	–1.563095
48	C	1.665642	0.158488	–1.612841
49	H	2.444144	0.726977	–2.12799
50	C	3.473435	0.12539	0.042316
51	C	5.093193	–0.318186	1.852864
52	C	4.916982	–1.059411	3.181571
53	H	4.158997	–0.568639	3.799857
54	H	5.862012	–1.068894	3.733577
55	H	4.605706	–2.093722	3.006863
56	C	5.466605	1.148243	2.097761
57	H	5.586362	1.686854	1.156763
58	H	6.409249	1.196781	2.653803
59	H	4.694171	1.642552	2.696497
60	C	6.113579	–1.038799	0.964469
61	H	5.786843	–2.064915	0.767637
62	H	7.079448	–1.080318	1.479685
63	H	6.24365	–0.521656	0.013127
64	C	–2.330324	–2.748536	–0.371941
65	H	–1.963061	–3.696002	0.045538
66	H	–1.581456	–2.424249	–1.101135
67	C	–3.677856	–2.993133	–1.07891
68	H	–4.065071	–2.019999	–1.411846
69	C	–4.728559	–3.630019	–0.154105
70	H	–4.370451	–4.59096	0.238579
71	H	–5.658138	–3.823566	–0.701226
72	H	–4.979697	–2.985408	0.693837
73	C	–3.46003	–3.861417	–2.32874
74	H	–2.748946	–3.396266	–3.02054
75	H	–4.400747	–4.019028	–2.868271
76	H	–3.064787	–4.848693	–2.056729
77	C	1.399265	–1.155719	–2.371585
78	H	0.671726	–1.733173	–1.797058
79	H	0.928007	–0.914043	–3.342736
80	C	3.518036	–1.425852	–3.541777
81	H	3.055317	–1.371472	–4.548216
82	H	4.402384	–2.066794	–3.609472
83	H	3.862647	–0.427927	–3.25939
84	C	2.281857	–3.35659	–2.806879
85	H	1.661592	–3.756812	–1.999617
86	H	3.203888	–3.945185	–2.851769
87	H	1.740586	–3.497696	–3.76404

Calculation Type = FREQ
Calculation Method = RB3LYP
Basis Set = 6-31+G(d,p)
Charge = 0
Spin = Singlet
E(RB3LYP) = –1837.84334428 a.u.
RMS Gradient Norm = 0.00000293 a.u.
Imaginary Freq = 0
Dipole Moment = 1.7153 Debye
Point Group = C1
Job cpu time: 6 days 10 hours 30 minutes 38.3 seconds.

Calculation Type = SP
Calculation Method = RM062X
Basis Set = 6-311++G(2d,3p)
Charge = 0
Spin = Singlet
E(RM062X) = –1837.54604149 a.u.
Dipole Moment = 1.6990 Debye
Point Group = C1
Job cpu time: 1 days 12 hours 32 minutes 6.3 seconds.

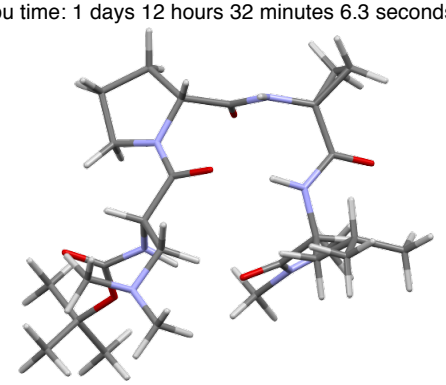

Table S6.02: B3LYP/6-31+G(d,p)-Optimized Coordinates of **3b**

Tag	Symbol	X	Y	Z
1	O	0.246215	–2.076974	0.191209
2	O	4.506326	–0.283624	–1.402201
3	O	0.998948	2.354698	–2.160804
4	O	0.434484	1.299448	1.364685
5	O	–4.239225	0.271559	–0.216557
6	O	–3.226338	–1.600372	–1.077623
7	N	1.39228	–2.706186	–1.669017
8	N	2.660041	–0.140526	–0.066484
9	H	1.940017	0.447027	0.353382
10	N	2.518023	2.642492	–0.469249
11	H	2.577805	2.84011	0.521557
12	N	–0.891965	2.6775	0.167852
13	N	–2.094591	–0.314306	0.350851
14	H	–1.351236	–1.004912	0.23239
15	N	–1.868828	1.277509	3.748029
16	C	2.574951	–2.757001	–2.528945
17	H	3.377778	–2.118481	–2.165823
18	H	2.298423	–2.400761	–3.527624
19	H	2.936087	–3.789393	–2.623159
20	C	0.180829	–3.257719	–2.271572
21	H	–0.614744	–3.282834	–1.530126
22	H	0.384373	–4.270534	–2.638018
23	H	–0.138559	–2.638047	–3.1186
24	C	1.318386	–2.147843	–0.430718
25	C	2.599399	–1.575563	0.2203
26	H	3.49527	–2.006608	–0.221607
27	C	3.62058	0.39301	–0.863994
28	C	3.594998	1.895708	–1.057488
29	C	4.959186	2.578778	–1.086105
30	H	5.010565	3.561974	–0.62815
31	H	5.817316	1.933466	–0.933396
32	C	4.179836	2.419247	–2.353224
33	H	4.509886	1.664538	–3.057804
34	H	3.686195	3.28539	–2.778672
35	C	1.278485	2.768727	–1.042091
36	C	0.254176	3.53546	–0.179209
37	H	0.735435	3.875346	0.744616
38	C	–0.393108	4.706228	–0.95285
39	H	0.27028	5.104735	–1.724055
40	H	–0.623701	5.515538	–0.250957
41	C	–1.686713	4.105299	–1.52921
42	H	–2.438423	4.863219	–1.766888
43	H	–1.457556	3.539157	–2.435834
44	C	–2.159434	3.152569	–0.425816
45	H	–2.751775	3.684102	0.331639
46	H	–2.755161	2.320437	–0.802667
47	C	–0.703682	1.603251	0.966546
48	C	–1.931186	0.747159	1.334917
49	H	–2.836911	1.351785	1.281506
50	C	–3.275427	–0.485377	–0.306497
51	C	–4.384087	–2.018536	–1.889315
52	C	–5.584722	–2.320163	–0.984861
53	H	–5.30616	–3.047106	–0.214829
54	H	–6.392076	–2.753783	–1.585085
55	H	–5.953486	–1.414748	–0.501478
56	C	–4.702223	–0.954004	–2.945605
57	H	–5.067394	–0.036095	–2.483385
58	H	–5.470376	–1.334801	–3.627552
59	H	–3.808421	–0.724405	–3.535166
60	C	–3.877947	–3.302124	–2.553658
61	H	–3.000018	–3.09656	–3.173336
62	H	–4.660175	–3.726202	–3.190971
63	H	–3.604314	–4.045327	–1.798546
64	C	–1.776145	0.197775	2.762992
65	H	–2.542264	–0.580967	2.922764
66	H	–0.79601	–0.277858	2.841639
67	C	–1.03424	1.047104	4.921498
68	H	–1.346177	0.161175	5.509062
69	H	–1.081179	1.920097	5.58122
70	H	0.005296	0.910117	4.61151
71	C	–3.248031	1.572786	4.122673
72	H	–3.855105	1.763312	3.232943
73	H	–3.278062	2.470604	4.748558
74	H	–3.722573	0.743877	4.683921
75	C	2.605102	–1.823392	1.738577
76	H	3.480937	–1.300393	2.145606
77	H	1.714532	–1.351326	2.164905
78	C	2.654268	–3.303895	2.166831
79	H	1.809715	–3.821993	1.692252
80	C	2.463967	–3.41275	3.688287
81	H	3.271259	–2.895572	4.222874
82	H	2.468385	–4.459425	4.012804
83	H	1.514069	–2.966655	4.002538
84	C	3.955477	–4.002417	1.737385
85	H	4.092811	–4.003404	0.650799
86	H	3.962433	–5.047394	2.067434
87	H	4.82882	–3.507579	2.181183

Calculation Type = FREQ
Calculation Method = RB3LYP
Basis Set = 6-31+G(d,p)
Charge = 0
Spin = Singlet
E(RB3LYP) = –1837.84413757 a.u.
RMS Gradient Norm = 0.00000373 a.u.
Imaginary Freq = 0
Dipole Moment = 1.3658 Debye
Point Group = C1
Job cpu time: 6 days 5 hours 36 minutes 55.9 seconds.

Calculation Type = SP
Calculation Method = RM062X
Basis Set = 6-311++G(2d,3p)
Charge = 0
Spin = Singlet
E(RM062X) = –1837.54401280 a.u.
Dipole Moment = 1.3772 Debye
Point Group = C1
Job cpu time: 1 days 2 hours 38 minutes 42.0 seconds.

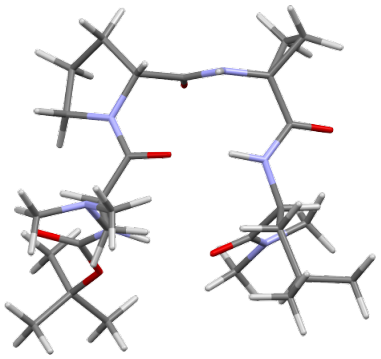

Table S6.03: B3LYP/6-31+G(d,p)-Optimized Coordinates of **3c**

Tag	Symbol	X	Y	Z
1	O	2.466078	0.896135	–1.791502
2	O	3.329082	–0.957984	1.842992
3	O	–0.481828	–3.026455	2.198558
4	O	–1.224408	–0.848688	–0.773897
5	O	–1.129351	2.293468	1.041541
6	O	0.102143	3.406651	–0.551616
7	N	4.588417	0.163603	–1.395542
8	N	1.700634	–1.053644	0.256868
9	H	0.71668	–0.952241	0.023094
10	N	–0.307697	–0.743583	2.19298
11	H	–0.73823	0.12926	1.898993
12	N	–2.813141	–0.587524	0.819162
13	N	–1.488207	2.002463	–1.198791
14	H	–0.986914	1.997979	–2.07697
15	N	–4.532374	0.124844	–2.25156
16	C	5.537602	–0.716729	–0.707499
17	H	5.124749	–1.066681	0.239845
18	H	6.436074	–0.135977	–0.481549
19	H	5.835173	–1.569892	–1.331353
20	C	5.159467	1.326929	–2.06718
21	H	4.382904	1.814425	–2.654738
22	H	5.976486	1.008858	–2.72483
23	H	5.558443	2.04537	–1.33887
24	C	3.22877	0.025168	–1.358383
25	C	2.643155	–1.302039	–0.827733
26	H	3.431106	–1.932399	–0.419886
27	C	2.12984	–0.917669	1.533953
28	C	1.071855	–0.71036	2.598776
29	C	1.408812	–1.230321	3.98289
30	H	0.581328	–1.65524	4.539512
31	H	2.359083	–1.743749	4.073997
32	C	1.431512	0.244028	3.729375
33	H	2.397969	0.729852	3.651417
34	H	0.621414	0.853915	4.117825
35	C	–0.966025	–1.921695	1.974397
36	C	–2.420724	–1.837933	1.49602
37	H	–2.544497	–2.681124	0.808246
38	C	–3.409329	–1.936473	2.680346
39	H	–3.607246	–2.97616	2.947372
40	H	–2.985512	–1.439064	3.560581
41	C	–4.646494	–1.175326	2.18515
42	H	–5.291977	–0.830404	2.997768
43	H	–5.244684	–1.811925	1.523278
44	C	–4.051966	–0.009903	1.382931
45	H	–4.719732	0.317506	0.585744
46	H	–3.812059	0.845979	2.026562
47	C	–2.173361	–0.201032	–0.310956
48	C	–2.614017	1.103684	–1.009651
49	H	–3.346253	1.632003	–0.396515
50	C	–0.836464	2.548222	–0.126983
51	C	1.037508	4.091215	0.367847
52	C	1.853805	3.060168	1.148688
53	H	1.234739	2.528244	1.871726
54	H	2.656912	3.570848	1.691111
55	H	2.301837	2.338603	0.460379
56	C	0.255972	5.041833	1.280005
57	H	–0.348043	5.734708	0.684819
58	H	0.959715	5.631225	1.877546
59	H	–0.399983	4.490423	1.95595
60	C	1.930813	4.867337	–0.602979
61	H	2.446184	4.177562	–1.27692
62	H	2.677592	5.44031	–0.044279
63	H	1.336582	5.564046	–1.20244
64	C	1.94621	–2.030205	–1.994183
65	H	1.121514	–1.397451	–2.339981
66	H	2.660814	–2.09629	–2.827022
67	C	1.422271	–3.443896	–1.667951
68	H	0.778974	–3.374186	–0.781983
69	C	2.554342	–4.435183	–1.354311
70	H	3.244366	–4.52406	–2.204267
71	H	2.149588	–5.432418	–1.149038
72	H	3.135463	–4.13725	–0.475495
73	C	0.561565	–3.956723	–2.833413
74	H	–0.276824	–3.280098	–3.031402
75	H	0.15056	–4.948225	–2.612017
76	H	1.153781	–4.040475	–3.754422
77	C	–3.224672	0.768136	–2.383545
78	H	–3.281046	1.694258	–2.984045
79	H	–2.538739	0.084799	–2.893994
80	C	–4.797381	–0.827627	–3.328723
81	H	–4.851503	–0.347594	–4.324407
82	H	–5.752215	–1.329703	–3.144141
83	H	–4.012678	–1.588486	–3.353337
84	C	–5.615275	1.099438	–2.137058
85	H	–5.422181	1.794912	–1.314597
86	H	–6.557097	0.583239	–1.926794
87	H	–5.746511	1.696367	–3.059879

Calculation Type = FREQ
Calculation Method = RB3LYP
Basis Set = 6-31+G(d,p)
Charge = 0
Spin = Singlet
E(RB3LYP) = –1837.83735371 a.u.
RMS Gradient Norm = 0.00000401 a.u.
Imaginary Freq = 0
Dipole Moment = 5.8323 Debye
Point Group = C1
Job cpu time: 7 days 7 hours 36 minutes 13.4 seconds.

Calculation Type = SP
Calculation Method = RM062X
Basis Set = 6-311++G(2d,3p)
Charge = 0
Spin = Singlet
E(RM062X) = –1837.54323198 a.u.
Dipole Moment = 5.8650 Debye
Point Group = C1
Job cpu time: 1 days 16 hours 3 minutes 42.5 seconds.

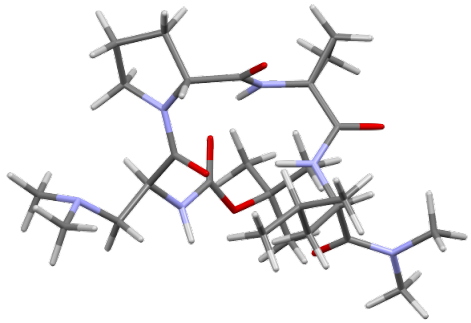

Table S6.04: Comparative Energy Data for **3a–c**

Method		Boc-Dmaa-D-Pro-Acpc-Leu-NMe$_2$ (3)		
		3a	3b	3c
sp of X-ray crystal structure M06-2X/6-311++G(2d,3p)	E(sp, M06-2X, au)	-1837.082149870	-1837.088306590	-1837.055931860
	Relative E(sp, M06-2X, kcal/mol)	3.86	0.00	20.32
	Dipole Moment (D)	1.851	3.203	7.653
opt of X-ray crystal structure B3LYP/6-31+G(d,p)	E(opt, B3LYP, au)	-1837.843344280	-1837.844137570	-1837.837353710
	ZP Correction (au)	0.755768	0.755838	0.755045
	E Correction (au)	0.800094	0.800203	0.799889
	H Correction (au)	0.801039	0.801147	0.800833
	G Correction (au)	0.674431	0.674498	0.673066
	ZPE (au)	-1837.087576280	-1837.088299570	-1837.082308710
	Relative ZPE (kcal/mol)	0.45	0.00	3.76
	E (au)	-1837.043250280	-1837.043934570	-1837.037464710
	Relative E (kcal/mol)	0.43	0.00	4.06
	H (au)	-1837.042305280	-1837.042990570	-1837.036520710
	Relative H (kcal/mol)	0.43	0.00	4.06
	G (au)	-1837.168913280	-1837.169639570	-1837.164287710
	Relative G (kcal/mol)	0.46	0.00	3.36
	S (cal/mol*K)	266.468	266.556	268.909
	Relative S(cal/mol*K)	-0.09	0.00	2.35
	Dipole Moment (D)	1.715	1.366	5.832
sp of optimized structure M06-2X/6-311++G(2d,3p)	E(sp, M06-2X, au)	-1837.546041490	-1837.544012800	-1837.543231980
	ZPE (au)	-1836.790273490	-1836.788174800	-1836.788186980
	Relative ZPE (kcal/mol)	0.00	1.32	1.31
	E (au)	-1836.745947490	-1836.743809800	-1836.743342980
	Relative E (kcal/mol)	0.00	1.34	1.63
	H (au)	-1836.745002490	-1836.742865800	-1836.742398980
	Relative H (kcal/mol)	0.00	1.34	1.63
	G (au)	-1836.871610490	-1836.869514800	-1836.870165980
	Relative G (kcal/mol)	0.00	1.32	0.91
	Dipole Moment (D)	1.699	1.377	5.865

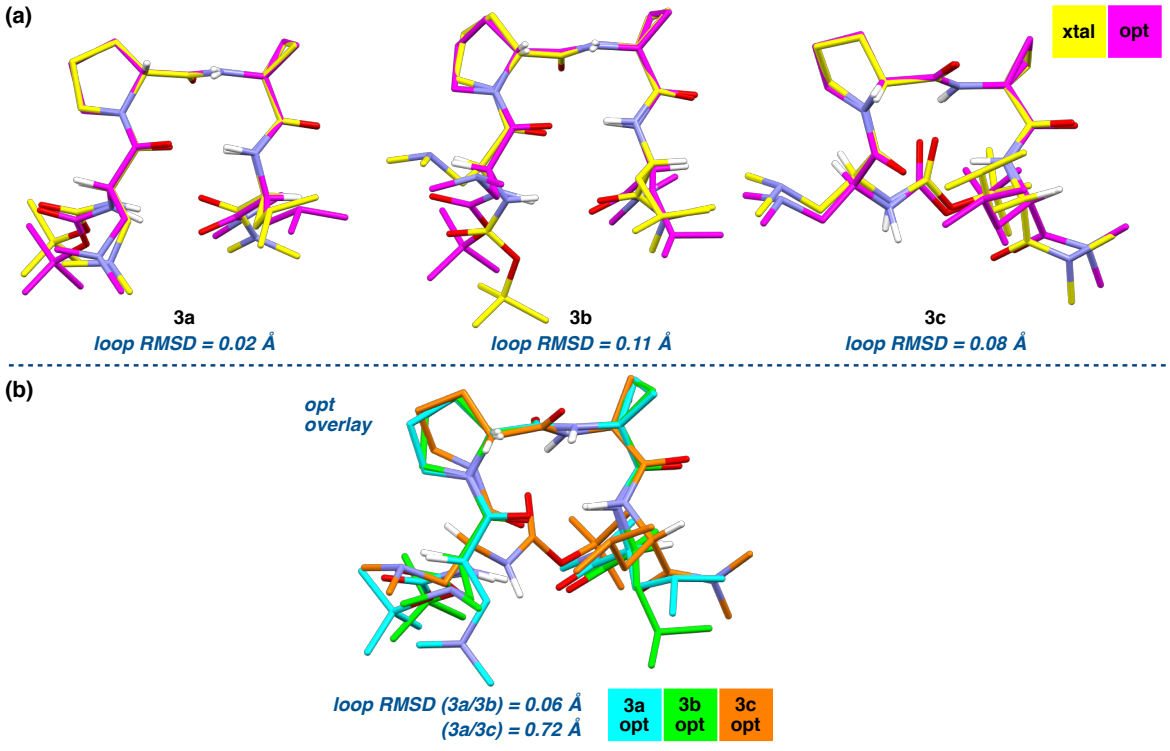

Figure S6.01: (a) Overlays of the DFT-optimized structures of **3a–c** with the corresponding crystal structures. **(b)** Overlay of the optimized structures of **3a–c.**

C. Optimization of Peptides 4a–e

Table S6.05: B3LYP/6-31+G(d,p)-Optimized Coordinates of **4a**

Tag	Symbol	X	Y	Z
1	O	3.544854	–0.562223	1.835642
2	O	–0.058118	–2.993089	2.175299
3	O	–0.983576	–0.885109	–0.812595
4	O	–1.182751	2.245893	1.035254
5	O	–0.01094	3.442058	–0.544016
6	O	2.697224	1.22421	–1.46459
7	O	4.47749	0.010236	–2.143851
8	N	1.937358	–0.899119	0.257429
9	H	0.947637	–0.900879	0.029114
10	N	–0.096165	–0.703628	2.172178
11	H	–0.605905	0.125289	1.877788
12	N	–2.595471	–0.779739	0.777506
13	N	–1.495223	1.932418	–1.206856
14	H	–1.015465	2.006011	–2.093128
15	N	–4.364296	–0.182793	–2.298766
16	C	1.232048	–4.314597	–2.405063
17	H	0.282524	–3.817852	–2.634048
18	H	1.005573	–5.326749	–2.051798
19	H	1.798886	–4.408069	–3.340964
20	C	3.3235	–4.273243	–0.98416
21	H	3.878221	–3.771163	–0.185176
22	H	3.987022	–4.359014	–1.854898
23	H	3.099333	–5.28674	–0.633739
24	C	2.029434	–3.530309	–1.35073
25	H	1.411386	–3.458291	–0.447123
26	C	2.298781	–2.100544	–1.865219
27	H	1.361818	–1.668807	–2.23997
28	H	2.995494	–2.147078	–2.711301
29	C	2.885224	–1.132491	–0.811661
30	H	3.789714	–1.555481	–0.367127
31	C	2.353094	–0.662348	1.529268
32	C	1.272527	–0.539635	2.58584
33	C	1.647489	–1.019354	3.975638
34	H	0.85878	–1.514727	4.530539
35	H	2.640034	–1.443551	4.075538
36	C	1.536775	0.449099	3.711266
37	H	2.455823	1.019501	3.633236
38	H	0.673055	0.985613	4.092531
39	C	–0.640451	–1.936895	1.949282
40	C	–2.092476	–1.988853	1.457644
41	H	–2.131033	–2.838923	0.76841
42	C	–3.076784	–2.180869	2.634017
43	H	–3.177718	–3.234808	2.899291
44	H	–2.708982	–1.646622	3.517707
45	C	–4.376	–1.538602	2.130251
46	H	–5.056575	–1.255945	2.938214
47	H	–4.907809	–2.227432	1.464001
48	C	–3.887198	–0.321749	1.333304
49	H	–4.57703	–0.058627	0.531285
50	H	–3.733096	0.55248	1.978552
51	C	–1.988807	–0.330136	–0.347024
52	C	–2.540962	0.939033	–1.033763
53	H	–3.317978	1.393842	–0.41698
54	C	–0.894612	2.522962	–0.128872
55	C	0.813225	4.244147	0.389585
56	C	1.672128	5.070839	–0.570116
57	H	2.284674	4.413199	–1.192957
58	H	2.333093	5.731591	–0.000359
59	H	1.043174	5.686168	–1.221045
60	C	1.688561	3.328784	1.24696
61	H	1.091206	2.761616	1.961291
62	H	2.40585	3.939881	1.80567
63	H	2.244587	2.633729	0.612698
64	C	–0.10054	5.143503	1.227573
65	H	–0.733519	5.758999	0.57975
66	H	0.512389	5.813519	1.840035
67	H	–0.736876	4.552958	1.889271
68	C	3.31083	0.176764	–1.483382
69	C	4.984655	1.163051	–2.840498
70	H	5.916044	0.836533	–3.302451
71	H	4.272928	1.495586	–3.600477
72	H	5.169905	1.9792	–2.138024
73	C	–3.114611	0.568984	–2.414599
74	H	–3.245508	1.493705	–3.005943
75	H	–2.371045	–0.048883	–2.927988
76	C	–4.544855	–1.137327	–3.391456
77	H	–4.6329	–0.648151	–4.38021
78	H	–5.456491	–1.718033	–3.220257
79	H	–3.700709	–1.831461	–3.422056
80	C	–5.525574	0.695915	–2.175277
81	H	–5.703309	1.293299	–3.090012
82	H	–5.395138	1.392861	–1.341913
83	H	–6.421353	0.099161	–1.977388

Calculation Type = FREQ
Calculation Method = RB3LYP
Basis Set = 6-31+G(d,p)
Charge = 0
Spin = Singlet
E(RB3LYP) = –1818.39243782 a.u.
RMS Gradient Norm = 0.00000473 a.u.
Imaginary Freq = 0
Dipole Moment = 8.1875 Debye
Point Group = C1
Job cpu time: 5 days 15 hours 54 minutes 43.7 seconds.

Calculation Type = SP
Calculation Method = RM062X
Basis Set = 6-311++G(2d,3p)
Charge = 0
Spin = Singlet
E(RM062X) = –1818.11366939 a.u.
Dipole Moment = 8.1820 Debye
Point Group = C1
Job cpu time: 1 days 8 hours 14 minutes 0.2 seconds.

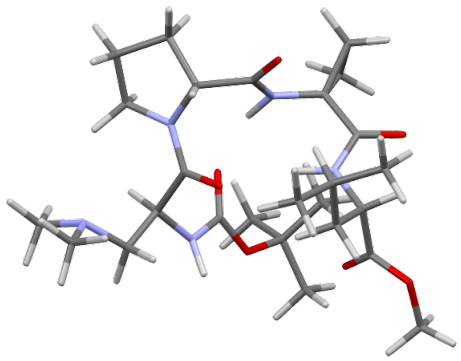

Table S6.06: B3LYP/6-31+G(d,p)-Optimized Coordinates of **4b**

Tag	Symbol	X	Y	Z
1	O	4.47674	0.012165	–2.144687
2	O	2.695765	1.224874	–1.465016
3	O	3.545171	–0.559613	1.835381
4	O	–0.056927	–2.992749	2.176635
5	O	–0.983147	–0.886205	–0.812626
6	O	–1.18405	2.245471	1.035025
7	O	–0.012668	3.442112	–0.54421
8	N	1.937866	–0.89879	0.257451
9	H	0.94817	–0.900641	0.029033
10	N	–0.095707	–0.703289	2.172074
11	H	–0.605955	0.125276	1.877596
12	N	–2.594941	–0.780857	0.7776
13	N	–1.495721	1.931247	–1.207056
14	H	–1.016295	2.00565	–2.093434
15	N	–4.363724	–0.185243	–2.299287
16	C	4.982775	1.165269	–2.841673
17	H	5.167489	1.981724	–2.139413
18	H	4.270602	1.497043	–3.601571
19	H	5.914339	0.839442	–3.303767
20	C	3.310186	0.177909	–1.4838
21	C	2.885872	–1.131522	–0.811637
22	H	3.790807	–1.553506	–0.367028
23	C	2.353476	–0.660869	1.529129
24	C	1.272877	–0.538439	2.585701
25	C	1.648172	–1.017702	3.975593
26	H	0.85977	–1.513426	4.530619
27	H	2.640945	–1.44137	4.075518
28	C	1.53667	0.45063	3.710922
29	H	2.455426	1.02148	3.632699
30	H	0.672697	0.986777	4.092133
31	C	–0.63957	–1.936884	1.949924
32	C	–2.091509	–1.989598	1.458086
33	H	–2.129573	–2.839832	0.769028
34	C	–3.075865	–2.181773	2.634392
35	H	–3.176433	–3.235703	2.899856
36	H	–2.708353	–1.647237	3.518028
37	C	–4.375286	–1.540092	2.130403
38	H	–5.056005	–1.2575	2.938271
39	H	–4.906805	–2.229267	1.46428
40	C	–3.886894	–0.32324	1.333194
41	H	–4.576796	–0.060624	0.531069
42	H	–3.733174	0.551231	1.978197
43	C	–1.988509	–0.331424	–0.347153
44	C	–2.541107	0.937463	–1.034111
45	H	–3.318377	1.391969	–0.417437
46	C	–0.895874	2.522526	–0.1291
47	C	0.810453	4.245123	0.389459
48	C	1.668919	5.072418	–0.570125
49	H	2.281992	4.415174	–1.192867
50	H	2.329342	5.733636	–0.00028
51	H	1.039637	5.687299	–1.221165
52	C	1.686376	3.330694	1.24727
53	H	1.089257	2.76283	1.961255
54	H	2.402717	3.942538	1.806372
55	H	2.243471	2.636257	0.613273
56	C	–0.104339	5.143769	1.227065
57	H	–0.737633	5.758678	0.578993
58	H	0.507836	5.81435	1.83967
59	H	–0.740361	4.552722	1.888614
60	C	2.300305	–2.100542	–1.864793
61	H	1.363033	–1.669758	–2.239881
62	H	2.997158	–2.146929	–2.710769
63	C	2.031988	–3.530252	–1.34963
64	H	1.41365	–3.458227	–0.446221
65	C	3.326543	–4.271953	–0.9823
66	H	3.99043	–4.357584	–1.852777
67	H	3.103068	–5.285478	–0.631513
68	H	3.880591	–3.769082	–0.183343
69	C	1.235531	–4.315738	–2.403779
70	H	1.802802	–4.409454	–3.339394
71	H	0.28577	–3.819773	–2.633468
72	H	1.009563	–5.327809	–2.049951
73	C	–3.114331	0.56704	–2.414986
74	H	–3.245473	1.491618	–3.00652
75	H	–2.370421	–0.050633	–2.928112
76	C	–5.525383	0.69299	–2.17581
77	H	–5.395268	1.389983	–1.34244
78	H	–6.420918	0.09585	–1.977965
79	H	–5.703338	1.290305	–3.090554
80	C	–4.543836	–1.139681	–3.392141
81	H	–4.631928	–0.650379	–4.380831
82	H	–5.455305	–1.720709	–3.221131
83	H	–3.699461	–1.833538	–3.42274

Calculation Type = FREQ
Calculation Method = RB3LYP
Basis Set = 6-31+G(d,p)
Charge = 0
Spin = Singlet
E(RB3LYP) = –1818.39243826 a.u.
RMS Gradient Norm = 0.00000203 a.u.
Imaginary Freq = 0
Dipole Moment = 8.1893 Debye
Point Group = C1
Job cpu time: 5 days 13 hours 35 minutes 22.0 seconds.

Calculation Type = SP
Calculation Method = RM062X
Basis Set = 6-311++G(2d,3p)
Charge = 0
Spin = Singlet
E(RM062X) = –1818.11366318 a.u.
Dipole Moment = 8.1839 Debye
Point Group = C1
Job cpu time: 1 days 10 hours 32 minutes 58.4 seconds.

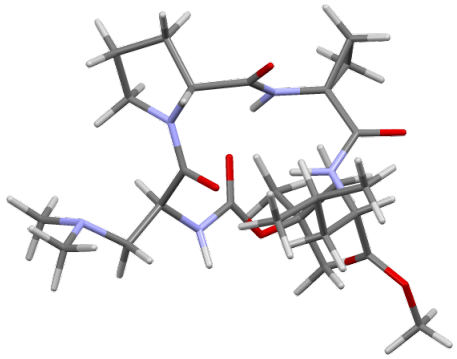

Table S6.07: B3LYP/6-31+G(d,p)-Optimized Coordinates of **4c**

Tag	Symbol	X	Y	Z
1	O	4.476702	0.012808	–2.144536
2	O	2.695189	1.22502	–1.465379
3	O	3.545189	–0.559361	1.835448
4	O	–0.05664	–2.992715	2.176606
5	O	–0.983085	–0.886543	–0.812552
6	O	–1.184405	2.245319	1.035002
7	O	–0.013432	3.442418	–0.54419
8	N	1.937943	–0.898585	0.257477
9	H	0.948242	–0.900706	0.029073
10	N	–0.095695	–0.703266	2.1721
11	H	–0.606031	0.125244	1.877606
12	N	–2.59491	–0.781136	0.777641
13	N	–1.495749	1.930871	–1.207094
14	H	–1.016298	2.005369	–2.093449
15	N	–4.363536	–0.185804	–2.299542
16	C	4.982444	1.165955	–2.841651
17	H	5.166992	1.982519	–2.139477
18	H	4.270177	1.497496	–3.601555
19	H	5.914071	0.840308	–3.303734
20	C	3.309987	0.178266	–1.483866
21	C	2.885981	–1.13122	–0.81161
22	H	3.791005	–1.552988	–0.366986
23	C	2.353508	–0.660696	1.529166
24	C	1.272875	–0.538286	2.585715
25	C	1.536566	0.450954	3.710824
26	H	2.455258	1.021885	3.632536
27	H	0.672537	0.987069	4.091945
28	C	1.648187	–1.017345	3.975655
29	H	0.859817	–1.51305	4.530738
30	H	2.640982	–1.440934	4.075657
31	C	–0.639433	–1.936905	1.949978
32	C	–2.091421	–1.989758	1.458285
33	H	–2.12953	–2.840128	0.769399
34	C	–3.075701	–2.181711	2.634687
35	H	–2.708209	–1.646846	3.51814
36	H	–3.17613	–3.235561	2.900495
37	C	–4.37519	–1.540306	2.130578
38	H	–4.906654	–2.229676	1.46461
39	H	–5.055939	–1.257615	2.93838
40	C	–3.886936	–0.323562	1.333093
41	H	–4.576853	–0.061213	0.530892
42	H	–3.733343	0.55107	1.977903
43	C	–1.988496	–0.331783	–0.34714
44	C	–2.541098	0.93703	–1.03423
45	H	–3.318479	1.391533	–0.417688
46	C	–0.896241	2.522442	–0.129116
47	C	0.809871	4.24526	0.389452
48	C	1.685855	3.330735	1.247087
49	H	1.08888	2.76308	1.961344
50	H	2.402527	3.942498	1.805855
51	H	2.242607	2.636118	0.61299
52	C	1.668273	5.072584	–0.570155
53	H	2.281484	4.415397	–1.192817
54	H	2.328556	5.733959	–0.000334
55	H	1.038931	5.687311	–1.221277
56	C	–0.104785	5.143896	1.227234
57	H	–0.737987	5.75902	0.579281
58	H	0.507456	5.81426	1.840004
59	H	–0.740898	4.55278	1.888638
60	C	2.300628	–2.10044	–1.864701
61	H	1.363241	–1.669917	–2.239779
62	H	2.997455	–2.146679	–2.710703
63	C	2.032711	–3.53019	–1.349449
64	H	1.414384	–3.458258	–0.446023
65	C	3.327467	–4.27153	–0.982124
66	H	3.99137	–4.357015	–1.852602
67	H	3.104275	–5.285107	–0.631309
68	H	3.881405	–3.768496	–0.183193
69	C	1.236412	–4.315954	–2.403499
70	H	0.286496	–3.820273	–2.633158
71	H	1.010749	–5.328072	–2.049614
72	H	1.803645	–4.40956	–3.33915
73	C	–3.114118	0.566456	–2.415145
74	H	–3.245165	1.490933	–3.006856
75	H	–2.370153	–0.051316	–2.92807
76	C	–4.543571	–1.140168	–3.39247
77	H	–4.631455	–0.650807	–4.381141
78	H	–5.455121	–1.721113	–3.221641
79	H	–3.699263	–1.834109	–3.422977
80	C	–5.525201	0.692438	–2.176138
81	H	–5.395199	1.389367	–1.342702
82	H	–6.420755	0.095284	–1.978447
83	H	–5.703032	1.289812	–3.090852

Calculation Type = FREQ
Calculation Method = RB3LYP
Basis Set = 6-31+G(d,p)
Charge = 0
Spin = Singlet
E(RB3LYP) = –1818.39243834 a.u.
RMS Gradient Norm = 0.00000253 a.u.
Imaginary Freq = 0
Dipole Moment = 8.1888 Debye
Point Group = C1
Job cpu time: 6 days 10 hours 41 minutes 12.6 seconds.

Calculation Type = SP
Calculation Method = RM062X
Basis Set = 6-311++G(2d,3p)
Charge = 0
Spin = Singlet
E(RM062X) = –1817.74111503 a.u.
Dipole Moment = 10.5122 Debye
Point Group = C1
Job cpu time: 1 days 5 hours 13 minutes 17.2 seconds.

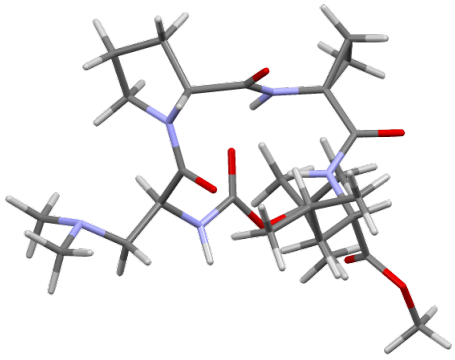

Table S6.08: B3LYP/6-31+G(d,p)-Optimized Coordinates of **4d**

Tag	Symbol	X	Y	Z
1	O	4.476103	0.01349	–2.146054
2	O	2.695385	1.226101	–1.465537
3	O	3.545401	–0.559164	1.835637
4	O	–0.055358	–2.992729	2.175265
5	O	–0.982675	–0.886481	–0.812828
6	O	–1.18502	2.244973	1.035198
7	O	–0.014201	3.442391	–0.543846
8	N	1.938241	–0.897324	0.257324
9	H	0.948522	–0.89997	0.029033
10	N	–0.095505	–0.703316	2.171967
11	H	–0.606091	0.125176	1.877896
12	N	–2.594772	–0.782036	0.777167
13	N	–1.496364	1.930731	–1.206907
14	H	–1.017172	2.005774	–2.093346
15	N	–4.363465	–0.186753	–2.299623
16	C	4.981579	1.16657	–2.843504
17	H	5.912999	0.840843	–3.305957
18	H	5.166425	1.983199	–2.141489
19	H	4.268985	1.498031	–3.603139
20	C	3.309919	0.179207	–1.484479
21	C	2.886267	–1.130122	–0.811707
22	H	3.791436	–1.551437	–0.366933
23	C	2.353745	–0.660193	1.529174
24	C	1.273024	–0.53809	2.585688
25	C	1.53643	0.451185	3.7108
26	H	2.455029	1.022297	3.632637
27	H	0.672297	0.987119	4.09195
28	C	1.64837	–1.017096	3.97563
29	H	0.86007	–1.512947	4.530687
30	H	2.641273	–1.440424	4.075661
31	C	–0.638697	–1.937123	1.94919
32	C	–2.090763	–1.990403	1.457921
33	H	–2.128924	–2.84096	0.769277
34	C	–3.074647	–2.182306	2.634666
35	H	–3.174815	–3.236139	2.900693
36	H	–2.707029	–1.64718	3.517882
37	C	–4.374479	–1.541353	2.130747
38	H	–5.055082	–1.258658	2.938672
39	H	–4.905872	–2.231094	1.465124
40	C	–3.8868	–0.32471	1.332799
41	H	–4.576986	–0.062911	0.530643
42	H	–3.733392	0.550205	1.977279
43	C	–1.988292	–0.332181	–0.347376
44	C	–2.541414	0.93658	–1.034157
45	H	–3.318809	1.390703	–0.417362
46	C	–0.896956	2.522281	–0.12889
47	C	0.808612	4.245412	0.390052
48	C	1.68484	3.330977	1.247551
49	H	1.08791	2.762694	1.961376
50	H	2.401006	3.942835	1.806841
51	H	2.242085	2.636897	0.613305
52	C	1.666784	5.073353	–0.569242
53	H	2.280165	4.416558	–1.192153
54	H	2.326904	5.734662	0.000839
55	H	1.037276	5.688159	–1.220125
56	C	–0.106519	5.143431	1.227957
57	H	–0.740027	5.758323	0.580077
58	H	0.505398	5.814032	1.840787
59	H	–0.74234	4.551925	1.889273
60	C	2.301185	–2.099996	–1.864369
61	H	1.36364	–1.669921	–2.239596
62	H	2.998018	–2.146407	–2.710344
63	C	2.033702	–3.529593	–1.348482
64	H	1.415498	–3.457529	–0.445003
65	C	3.328725	–4.270478	–0.981108
66	H	3.992251	–4.356487	–1.851816
67	H	3.105806	–5.283814	–0.629449
68	H	3.882904	–3.766776	–0.182772
69	C	1.237466	–4.315988	–2.402139
70	H	0.287416	–3.820612	–2.631865
71	H	1.012084	–5.328005	–2.047797
72	H	1.804625	–4.409833	–3.337795
73	C	–3.114481	0.566218	–2.415116
74	H	–3.246107	1.490902	–3.006384
75	H	–2.370231	–0.050927	–2.928378
76	C	–5.525587	0.690859	–2.175915
77	H	–5.395666	1.387899	–1.342569
78	H	–6.420763	0.093228	–1.977921
79	H	–5.70402	1.288085	–3.090629
80	C	–4.543109	–1.140953	–3.392773
81	H	–4.631506	–0.651365	–4.381297
82	H	–5.454264	–1.72251	–3.221895
83	H	–3.698374	–1.834351	–3.423607

Calculation Type = FREQ
Calculation Method = RB3LYP
Basis Set = 6-31+G(d,p)
Charge = 0
Spin = Singlet
E(RB3LYP) = –1818.39243850 a.u.
RMS Gradient Norm = 0.00000790 a.u.
Imaginary Freq = 0
Dipole Moment = 8.1910 Debye
Point Group = C1
Job cpu time: 6 days 6 hours 56 minutes 9.8 seconds.

Calculation Type = SP
Calculation Method = RM062X
Basis Set = 6-311++G(2d,3p)
Charge = 0
Spin = Singlet
E(RM062X) = –1818.11367125 a.u.
Dipole Moment = 8.1855 Debye
Point Group = C1
Job cpu time: 1 days 0 hours 42 minutes 4.7 seconds.

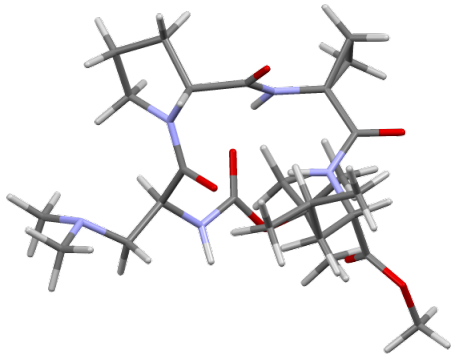

Table S6.09: B3LYP/6-31+G(d,p)-Optimized Coordinates of **4e**

Tag	Symbol	X	Y	Z
1	O	3.19681	1.713609	–2.810539
2	O	1.137858	1.100736	–2.141697
3	O	2.382822	2.965365	1.733918
4	O	1.574601	–1.172601	3.44984
5	O	0.523564	–1.56805	–0.050394
6	O	–3.646578	0.475531	–0.386941
7	O	–2.297976	2.16455	–1.166621
8	N	1.944651	1.073414	0.536587
9	H	1.440298	0.193052	0.471565
10	N	0.06109	0.234232	2.456786
11	H	–0.772518	0.257183	1.883998
12	N	–1.242373	–1.986303	1.297586
13	N	–1.59079	0.061327	–1.321942
14	H	–0.710193	0.488688	–1.605141
15	N	–1.411004	–3.594085	–2.159928
16	C	2.720441	1.76275	–4.169836
17	H	3.57499	2.086805	–4.762853
18	H	1.895834	2.473687	–4.258514
19	H	2.382319	0.774119	–4.489222
20	C	2.296884	1.36033	–1.874133
21	C	2.924873	1.393365	–0.483231
22	H	3.192747	2.443586	–0.315541
23	C	1.774872	1.898236	1.605705
24	C	0.769004	1.46852	2.655054
25	C	1.070013	1.889366	4.080213
26	H	0.792104	1.18002	4.851069
27	H	2.010261	2.408432	4.226679
28	C	–0.007337	2.598916	3.322884
29	H	0.202769	3.598501	2.958691
30	H	–1.04256	2.386078	3.572614
31	C	0.540183	–0.996731	2.818277
32	C	–0.346594	–2.196905	2.453713
33	H	0.350125	–3.013352	2.237439
34	C	–1.316661	–2.577229	3.5938
35	H	–0.832079	–3.218228	4.332852
36	H	–1.662594	–1.673107	4.108554
37	C	–2.485698	–3.251815	2.860435
38	H	–2.227596	–4.287486	2.611769
39	H	–3.408548	–3.26545	3.446787
40	C	–2.630951	–2.426803	1.573623
41	H	–3.016105	–3.022732	0.744674
42	H	–3.287862	–1.560495	1.71031
43	C	–0.701122	–1.699906	0.084026
44	C	–1.637892	–1.376419	–1.095692
45	H	–2.67367	–1.607996	–0.852334
46	C	–2.60817	0.873861	–0.908714
47	C	–3.237811	3.264771	–0.8773
48	C	–2.456881	4.495008	–1.346991
49	H	–1.518594	4.592277	–0.793072
50	H	–3.052794	5.398663	–1.185384
51	H	–2.222296	4.418252	–2.412821
52	C	–3.515019	3.342549	0.628231
53	H	–4.06647	2.4673	0.974946
54	H	–4.107421	4.238361	0.843085
55	H	–2.574523	3.419115	1.183837
56	C	–4.520743	3.090314	–1.697599
57	H	–4.280925	2.992101	–2.761441
58	H	–5.154792	3.974722	–1.573185
59	H	–5.080502	2.210472	–1.377038
60	C	4.241918	0.583476	–0.337444
61	H	4.67579	0.908651	0.615009
62	H	4.931281	0.907096	–1.126584
63	C	4.144734	–0.955751	–0.328558
64	H	3.396795	–1.248574	0.419108
65	C	5.494989	–1.544149	0.114017
66	H	6.292512	–1.276544	–0.591511
67	H	5.447687	–2.637598	0.163588
68	H	5.785523	–1.176735	1.104403
69	C	3.719314	–1.549286	–1.681592
70	H	2.706237	–1.249015	–1.963996
71	H	3.723045	–2.643974	–1.634178
72	H	4.410191	–1.246761	–2.479082
73	C	–1.197359	–2.156364	–2.343772
74	H	–1.738216	–1.759362	–3.220492
75	H	–0.131201	–1.972611	–2.500122
76	C	–0.430719	–4.404287	–2.87798
77	H	–0.494287	–4.284975	–3.976902
78	H	–0.589811	–5.462026	–2.644687
79	H	0.578658	–4.133244	–2.557206
80	C	–2.774028	–4.000609	–2.490924
81	H	–3.501101	–3.409819	–1.925942
82	H	–2.919684	–5.053073	–2.22788
83	H	–3.004089	–3.878475	–3.567263

Calculation Type = FREQ
Calculation Method = RB3LYP
Basis Set = 6-31+G(d,p)
Charge = 0
Spin = Singlet
E(RB3LYP) = –1818.39233242 a.u.
RMS Gradient Norm = 0.00010016 a.u.
Imaginary Freq =
Dipole Moment = 5.6562 Debye
Point Group = C1
Job cpu time: 6 days 22 hours 45 minutes 30.9 seconds.

Calculation Type = SP
Calculation Method = RM062X
Basis Set = 6-311++G(2d,3p)
Charge = 0
Spin = Singlet
E(RM062X) = –1818.11185055 a.u.
Dipole Moment = 5.6228 Debye
Point Group = C1
Job cpu time: 1 days 4 hours 39 minutes 13.2 seconds.

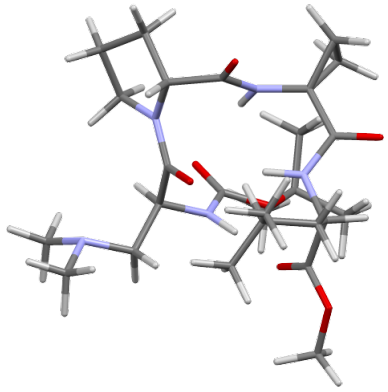

Table S6.10: Comparative Energy Data for **4a–e**

Method		Boc-Dmaa-D-Pro-Acpc-Leu-Ome (4)				
		4a	4b	4c	4d	4e
sp of X-ray crystal structure M06-2X/6-311++G(2d,3p)	E(sp, M06-2X, au)	-1817.585822240	-1817.751115040	-1817.741115030	-1817.751423580	-1817.741043650
	Relative E(sp, M06-2X, kcal/mol)	103.92	0.19	6.47	0.00	6.51
	Dipole Moment (D)	9.687	9.6794	10.5122	9.6553	9.989
opt of X-ray crystal structure B3LYP/6-31+G(d,p)	E(opt, B3LYP, au)	-1818.392437820	-1818.392438260	-1818.392438340	-1818.392438500	-1818.392332420
	ZP Correction (au)	0.714796	0.714795	0.714795	0.714798	0.714856
	E Correction (au)	0.757846	0.757845	0.757847	0.757848	0.757761
	H Correction (au)	0.758790	0.758789	0.758791	0.758793	0.758705
	G Correction (au)	0.635144	0.635137	0.635128	0.635128	0.634436
	ZPE (au)	-1817.677641820	-1817.677643260	-1817.677643340	-1817.677640500	-1817.677476420
	Relative ZPE (kcal/mol)	0.00	0.00	0.00	0.00	0.10
	E (au)	-1817.634591820	-1817.634593260	-1817.634591340	-1817.634590500	-1817.634571420
	Relative E (kcal/mol)	0.00	0.00	0.00	0.00	0.01
	H (au)	-1817.633647820	-1817.633649260	-1817.633647340	-1817.633645500	-1817.633627420
	Relative H (kcal/mol)	0.00	0.00	0.00	0.00	0.01
	G (au)	-1817.757293820	-1817.757301260	-1817.757310340	-1817.757310500	-1817.757896420
	Relative G (kcal/mol)	0.00	0.00	-0.01	-0.01	-0.38
	S (cal/mol*K)	260.234	260.250	260.270	260.274	261.547
	Relative S(cal/mol*K)	0.00	0.02	0.04	0.04	1.31
	Dipole Moment (D)	8.188	8.189	8.189	8.191	5.656
sp of optimized structure M06-2X/6-311++G(2d,3p)	E(sp, M06-2X, au)	-1818.113669390	-1818.113663180	-1818.113662940	-1818.113671250	-1818.111850550
	ZPE (au)	-1817.398873390	-1817.398868180	-1817.398867940	-1817.398873250	-1817.396994550
	Relative ZPE (kcal/mol)	0.00	0.00	0.00	0.00	1.18
	E (au)	-1817.355823390	-1817.355818180	-1817.355815940	-1817.355823250	-1817.354089550
	Relative E (kcal/mol)	0.00	0.00	0.00	0.00	1.09
	H (au)	-1817.354879390	-1817.354874180	-1817.354871940	-1817.354878250	-1817.353145550
	Relative H (kcal/mol)	0.00	0.00	0.00	0.00	1.09
	G (au)	-1817.478525390	-1817.478526180	-1817.478534940	-1817.478543250	-1817.477414550
	Relative G (kcal/mol)	0.00	0.00	-0.01	-0.01	0.70
	Dipole Moment (D)	8.182	8.184	8.183	8.186	5.623

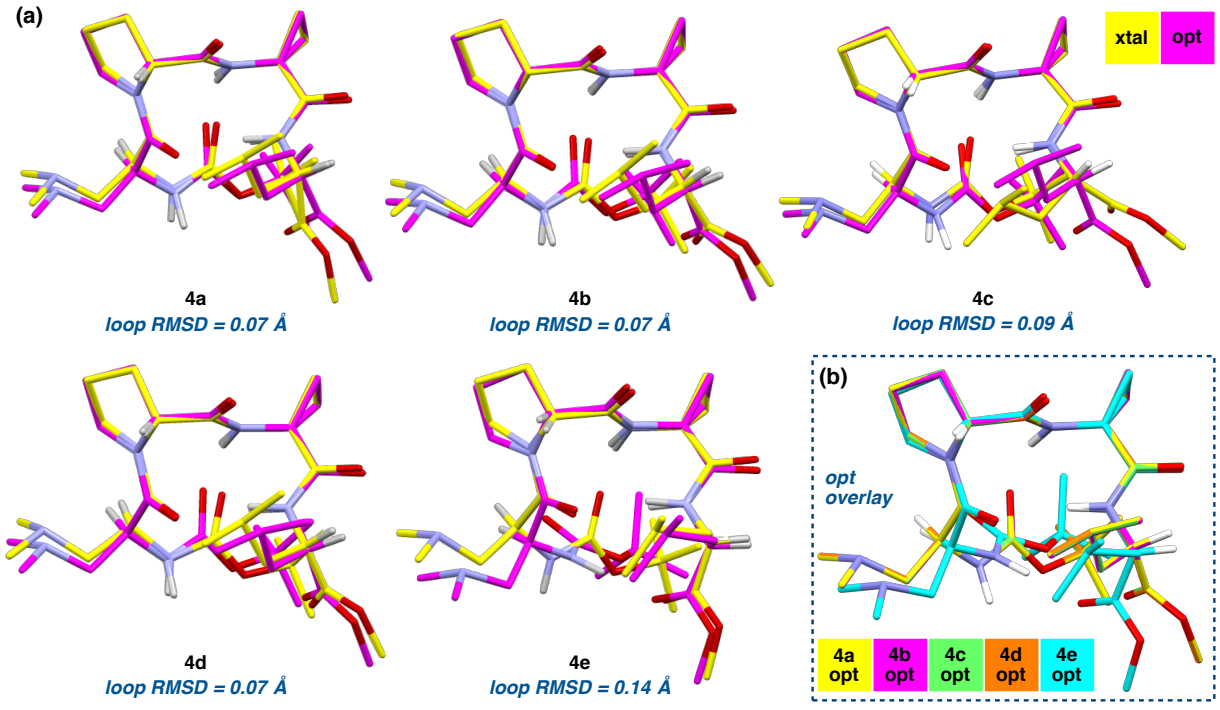

Figure S6.02: (a) Overlays of the DFT-optimized structures of **4a–e** with the corresponding crystal structures. **(b)** An overlay of the optimized structures shows that **4a–d** converged (loop RMSDs < 0.001 Å), while **4e** was a discrete conformer.

D. Optimization of Peptide 7a,b

Table S6.11: B3LYP/6-31+G(d,p)-Optimized Coordinates of **7a**

Tag	Symbol	X	Y	Z
1	O	–2.416299	4.470603	0.212378
2	O	–3.386963	2.848177	1.456112
3	O	–4.32789	0.911308	–1.692655
4	O	–1.431023	–2.521587	–1.141081
5	O	–0.356121	–0.22192	1.44637
6	O	2.702931	–1.117008	–1.263358
7	O	2.987556	1.115948	–1.733103
8	N	–2.478467	0.877006	–0.359761
9	H	–1.891256	0.360993	0.288854
10	N	–2.964888	–1.769177	0.386836
11	H	–3.082154	–1.542226	1.366149
12	N	0.432688	–2.32043	1.153902
13	N	3.365805	1.16216	2.806962
14	N	2.288323	0.507864	0.291192
15	H	2.518381	1.459604	0.547248
16	C	–2.906464	5.459084	1.138232
17	H	–2.512565	5.271496	2.14017
18	H	–3.998377	5.439133	1.17186
19	H	–2.550695	6.415888	0.756892
20	C	–2.741819	3.18731	0.489048
21	C	–2.168276	2.263972	–0.58337
22	H	–2.575692	2.573353	–1.550049
23	H	–1.083126	2.404661	–0.61263
24	C	–3.578961	0.309051	–0.919787
25	C	–3.8633	–1.129881	–0.537352
26	C	–5.336912	–1.501746	–0.423969
27	H	–5.594202	–2.204948	0.362518
28	H	–6.041349	–0.695661	–0.596723
29	C	–4.532508	–1.993475	–1.586135
30	H	–4.691069	–1.51982	–2.548399
31	H	–4.226046	–3.03286	–1.612236
32	C	–1.783548	–2.359111	0.019941
33	C	–0.932935	–2.874733	1.20077
34	H	–1.39994	–2.584161	2.147985
35	C	–0.699425	–4.39904	1.113462
36	H	–0.58544	–4.804311	2.125628
37	H	–1.535704	–4.915255	0.635485
38	C	0.614749	–4.525326	0.324681
39	H	1.117663	–5.482745	0.487837
40	H	0.416591	–4.40674	–0.743253
41	C	1.453468	–3.342987	0.825583
42	H	2.017926	–3.612801	1.728717
43	H	2.135627	–2.957245	0.066765
44	C	0.609191	–0.990646	1.308091
45	C	2.047543	–0.425172	1.377885
46	H	2.772169	–1.24086	1.31378
47	C	2.179876	0.314632	2.727249
48	H	1.297936	0.950601	2.8434
49	H	2.149865	–0.440852	3.536808
50	C	3.283979	2.08123	3.940195
51	H	2.37176	2.680695	3.867893
52	H	4.141683	2.760516	3.922174
53	H	3.279126	1.560281	4.916778
54	C	4.612868	0.402184	2.830685
55	H	4.681884	–0.272085	3.706299
56	H	5.459855	1.093496	2.86477
57	H	4.71252	–0.19976	1.923528
58	C	2.668499	0.066173	–0.943878
59	C	3.360664	0.931945	–3.152226
60	C	2.198919	0.292925	–3.919509
61	H	2.014192	–0.729164	–3.586487
62	H	2.437108	0.27589	–4.988421
63	H	1.283889	0.8784	–3.785372
64	C	3.594919	2.37119	–3.618576
65	H	2.684295	2.966772	–3.504994
66	H	3.88496	2.377968	–4.67377
67	H	4.392548	2.842413	–3.036076
68	C	4.65114	0.111667	–3.253122
69	H	5.442744	0.570705	–2.651431
70	H	4.986822	0.090749	–4.295491
71	H	4.496314	–0.913727	–2.914811

Calculation Type = FREQ
Calculation Method = RB3LYP
Basis Set = 6-31+G(d,p)
Charge = 0
Spin = Singlet
E(RB3LYP) = –1661.12003269 a.u.
RMS Gradient Norm = 0.00000278 a.u.
Imaginary Freq = 0
Dipole Moment = 7.2557 Debye
Point Group = C1
Job cpu time: 2 days 20 hours 39 minutes 12.6 seconds.

Calculation Type = SP
Calculation Method = RM062X
Basis Set = 6-311++G(2d,3p)
Charge = 0
Spin = Singlet
E(RM062X) = –1660.87600910 a.u.
Dipole Moment = 7.2674 Debye
Point Group = C1
Job cpu time: 0 days 11 hours 55 minutes 23.5 seconds.

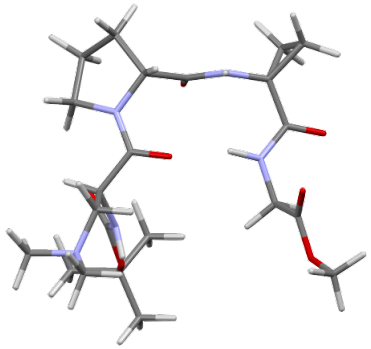

Table S6.12: B3LYP/6-31+G(d,p)-Optimized Coordinates of **7b**

Tag	Symbol	X	Y	Z
1	O	–3.395104	–2.757253	–2.751483
2	O	–2.303499	–2.401288	–0.803459
3	O	–4.231176	0.698629	–0.285113
4	O	–1.327421	3.928643	–1.186744
5	O	0.821295	0.623476	–1.750062
6	O	0.731906	0.022886	1.717722
7	O	0.722257	–2.273834	1.838036
8	N	–2.241948	0.403025	–1.351157
9	H	–1.245491	0.592788	–1.385777
10	N	–0.972192	2.237316	0.319081
11	H	–0.289864	1.597828	0.721246
12	N	1.77011	2.158124	–0.378677
13	N	4.145473	–1.952877	–1.281304
14	N	1.914318	–1.273496	0.256442
15	H	2.240086	–2.207373	0.036455
16	C	–3.47145	–4.161536	–2.442276
17	H	–4.036812	–4.316392	–1.520188
18	H	–2.469437	–4.581978	–2.325981
19	H	–3.984636	–4.617469	–3.288541
20	C	–2.785332	–1.977458	–1.831187
21	C	–2.792114	–0.525193	–2.302723
22	H	–2.225688	–0.471469	–3.237926
23	H	–3.828268	–0.252177	–2.522514
24	C	–3.03121	0.961812	–0.393075
25	C	–2.361709	1.941425	0.549222
26	C	–2.833518	1.90339	1.996789
27	H	–2.072472	2.076625	2.751389
28	H	–3.577095	1.149858	2.232624
29	C	–3.242359	3.038612	1.112464
30	H	–2.768406	4.004702	1.241083
31	H	–4.262552	3.05395	0.746112
32	C	–0.56956	3.159546	–0.604139
33	C	0.938119	3.244904	–0.922524
34	H	0.985043	3.229812	–2.014328
35	C	1.586449	4.511507	–0.329629
36	H	2.406844	4.838798	–0.978414
37	H	0.869269	5.331019	–0.254277
38	C	2.132521	4.031765	1.024752
39	H	1.327487	3.993328	1.766478
40	H	2.923253	4.673814	1.422153
41	C	2.640554	2.611105	0.730833
42	H	3.690041	2.627702	0.409254
43	H	2.540166	1.944074	1.589827
44	C	1.657275	0.90395	–0.881293
45	C	2.631307	–0.180381	–0.373994
46	H	3.339588	0.260346	0.335532
47	C	3.390003	–0.741535	–1.595344
48	H	2.643118	–0.987521	–2.354416
49	H	4.034365	0.058627	–2.007083
50	C	5.327621	–1.692992	–0.462511
51	H	6.057792	–1.03338	–0.969575
52	H	5.825307	–2.638779	–0.229698
53	H	5.043836	–1.226471	0.484928
54	C	4.493191	–2.696124	–2.491598
55	H	3.585883	–2.935324	–3.05345
56	H	4.981417	–3.635335	–2.214606
57	H	5.177099	–2.136391	–3.157048
58	C	1.081174	–1.090539	1.315111
59	C	–0.233033	–2.392448	2.965771
60	C	–0.376081	–3.90991	3.106299
61	H	–0.791492	–4.34152	2.191214
62	H	–1.048398	–4.142979	3.937721
63	H	0.594928	–4.374779	3.303697
64	C	0.392	–1.780857	4.223181
65	H	1.358595	–2.24811	4.439587
66	H	–0.26906	–1.955016	5.078851
67	H	0.533564	–0.704704	4.107967
68	C	–1.574398	–1.752373	2.602054
69	H	–1.502959	–0.664879	2.576515
70	H	–2.318118	–2.0326	3.356151
71	H	–1.920025	–2.103376	1.626099

Calculation Type = FREQ
Calculation Method = RB3LYP
Basis Set = 6-31+G(d,p)
Charge = 0
Spin = Singlet
E(RB3LYP) = –1661.12599990 a.u.
RMS Gradient Norm = 0.00000368 a.u.
Imaginary Freq = 0
Dipole Moment = 9.2507 Debye
Point Group = C1
Job cpu time: 3 days 7 hours 3 minutes 8.3 seconds.

Calculation Type = SP
Calculation Method = RM062X
Basis Set = 6-311++G(2d,3p)
Charge = 0
Spin = Singlet
E(RM062X) = –1660.88689919 a.u.
Dipole Moment = 9.2029 Debye
Point Group = C1
Job cpu time: 0 days 19 hours 21 minutes 23.1 seconds.

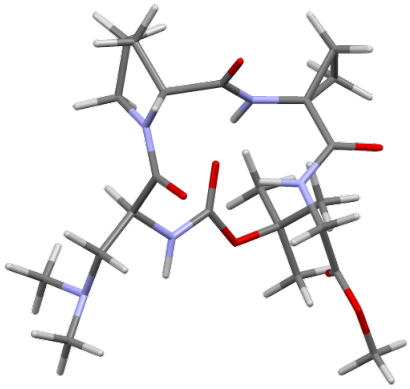

Table S6.13: Comparative Energy Data for **7a,b**

Method		Boc-Dmaa-D-Pro-Acpc-Gly-Ome (7) 7a	7b
sp of X-ray crystal structure M06-2X/6-311++G(2d,3p)	E(sp, M06-2X, au)	-1660.520970810	-1660.491425800
	Relative E(sp, M06-2X, kcal/mol)	0.00	18.54
	Dipole Moment (D)	7.912	8.906
opt of X-ray crystal structure B3LYP/6-31+G(d,p)	E(opt, B3LYP, au)	-1661.120032690	-1661.125999900
	ZP Correction (au)	0.601558	0.602213
	E Correction (au)	0.639248	0.639432
	H Correction (au)	0.640192	0.640376
	G Correction (au)	0.525694	0.529866
	ZPE (au)	-1660.518474690	-1660.523786900
	Relative ZPE (kcal/mol)	3.33	0.00
	E (au)	-1660.480784690	-1660.486567900
	Relative E (kcal/mol)	3.63	0.00
	H (au)	-1660.479840690	-1660.485623900
	Relative H (kcal/mol)	3.33	0.00
	G (au)	-1660.594338690	-1660.596133900
	Relative G (kcal/mol)	3.33	0.00
	S (cal/mol*K)	240.982	232.588
	Relative S(cal/mol*K)	0.00	-8.39
	Dipole Moment (D)	7.256	9.251
sp of optimized structure M06-2X/6-311++G(2d,3p)	E(sp, M06-2X, au)	-1660.876009100	-1660.886899190
	ZPE (au)	-1660.274451100	-1660.284686190
	Relative ZPE (kcal/mol)	6.42	0.00
	E (au)	-1660.236761100	-1660.247467190
	Relative E (kcal/mol)	6.72	0.00
	H (au)	-1660.235817100	-1660.246523190
	Relative H (kcal/mol)	6.72	0.00
	G (au)	-1660.350315100	-1660.357033190
	Relative G (kcal/mol)	4.22	0.00
	Dipole Moment (D)	7.267	9.203

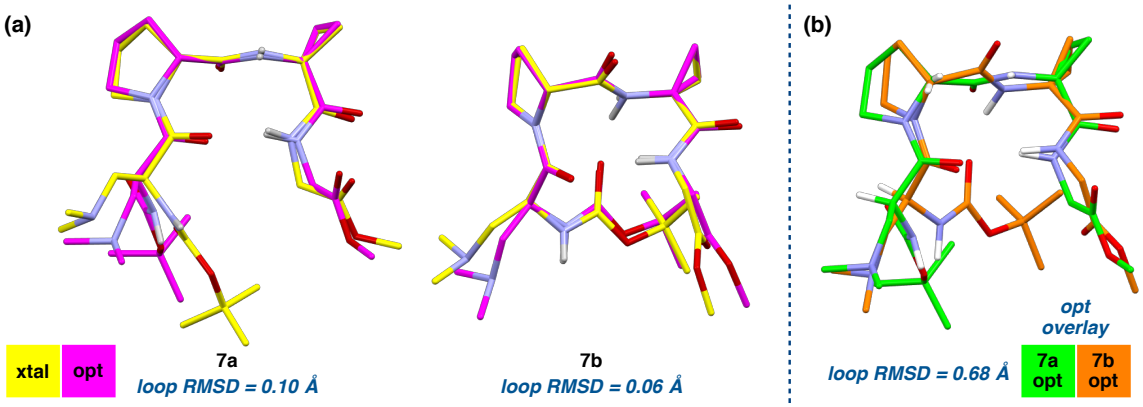

Figure S6.03: (a) Overlays of DFT-optimized structures of **7a**,**b** with the corresponding crystal structures. **(b)** Overlay of the optimized structures of **7a** and **7b**.

E. Optimization of Peptide 15

Table S6.14: B3LYP/6-31+G(d,p)-Optimized Coordinates of **15**

Tag	Symbol	X	Y	Z
1	O	0.740287	–3.016366	–1.977885
2	O	–0.431123	–2.497986	–0.120751
3	O	4.622126	–1.732047	–0.962051
4	O	2.958037	2.249505	0.568163
5	O	0.131074	0.656575	–0.950604
6	O	–4.359848	1.228165	–0.169876
7	O	–4.177024	–0.964998	–0.833999
8	N	2.471979	–1.071203	–0.567872
9	H	1.786111	–0.322903	–0.632572
10	N	3.003929	1.491689	–1.59613
11	H	2.421613	1.408699	–2.41973
12	N	0.082288	2.767112	–0.160855
13	N	–2.382349	0.076385	–0.036518
14	H	–1.929726	–0.823343	–0.159304
15	N	–2.295811	0.474358	2.93309
16	C	4.183357	–3.567334	1.944138
17	H	5.116259	–3.485448	2.513354
18	H	3.684744	–4.494421	2.257673
19	H	4.455296	–3.652829	0.888636
20	C	3.284247	–2.348297	2.204571
21	H	3.810392	–1.454136	1.846481
22	C	1.936169	–2.441144	1.463566
23	H	1.273388	–1.639167	1.807475
24	H	1.440334	–3.383309	1.735092
25	C	2.010956	–2.367934	–0.071619
26	H	2.708619	–3.112874	–0.462996
27	C	3.74959	–0.8607	–0.977385
28	C	4.076471	0.540256	–1.467131
29	C	5.186168	0.633427	–2.505515
30	H	5.61073	–0.311151	–2.826735
31	H	5.063642	1.393058	–3.27172
32	C	5.447583	1.075428	–1.099969
33	H	5.501344	2.13617	–0.882634
34	H	6.050945	0.430964	–0.470693
35	C	2.493286	2.233037	–0.564725
36	C	1.285341	3.118989	–0.94518
37	H	1.052204	2.996577	–2.010702
38	C	1.528083	4.59882	–0.589251
39	H	2.214395	4.645747	0.262005
40	H	1.97131	5.14877	–1.423464
41	C	0.140419	5.121041	–0.18473
42	H	0.189502	6.015821	0.44157
43	H	–0.45815	5.359911	–1.071202
44	C	3.032644	–2.170917	3.710987
45	H	3.977498	–2.0809	4.258297
46	H	2.439977	–1.271977	3.915673
47	H	2.490894	–3.032112	4.123665
48	C	–0.476444	3.928774	0.556417
49	H	–0.165395	3.911677	1.608293
50	H	–1.567598	3.926013	0.515403
51	C	–0.421134	1.512664	–0.240561
52	C	–1.654753	1.147789	0.599777
53	H	–2.342447	1.993467	0.642718
54	C	–3.705656	0.201251	–0.32832
55	C	–5.589496	–1.119347	–1.22312
56	C	–5.642319	–2.572381	–1.703995
57	H	–4.963718	–2.724148	–2.548994
58	H	–6.658173	–2.823619	–2.024829
59	H	–5.351291	–3.254892	–0.899951
60	C	–6.498133	–0.921179	–0.004485
61	H	–6.193078	–1.588066	0.808436
62	H	–7.5306	–1.165544	–0.277121
63	H	–6.463166	0.109396	0.351159
64	C	–5.931164	–0.157191	–2.366715
65	H	–5.887763	0.881003	–2.034815
66	H	–6.941912	–0.369169	–2.732252
67	H	–5.233624	–0.293669	–3.199946
68	C	0.633897	–2.631594	–0.695398
69	C	–0.499088	–3.214351	–2.689195
70	H	–1.103053	–3.978076	–2.194022
71	H	–0.208318	–3.53869	–3.687812
72	H	–1.061362	–2.278805	–2.733661
73	C	–1.190845	0.76996	2.032151
74	H	–0.570152	–0.127942	1.949384
75	H	–0.539665	1.577017	2.424831
76	C	–1.846738	–0.28374	4.09646
77	H	–1.353721	–1.204687	3.771909
78	H	–2.711481	–0.559527	4.707904
79	H	–1.141216	0.281638	4.737059
80	C	–3.051305	1.658532	3.326846
81	H	–2.429029	2.402049	3.865338
82	H	–3.870318	1.360956	3.988155
83	H	–3.499555	2.138154	2.452943

Calculation Type = FREQ
Calculation Method = RB3LYP
Basis Set = 6-31+G(d,p)
Charge = 0
Spin = Singlet
E(RB3LYP) = –1818.38899011 a.u.
RMS Gradient Norm = 0.00000230 a.u.
Imaginary Freq = 0
Dipole Moment = 4.8298 Debye
Point Group = C1
Job cpu time: 5 days 2 hours 58 minutes 12.9 seconds.

Calculation Type = SP
Calculation Method = RM062X
Basis Set = 6-311++G(2d,3p)
Charge = 0
Spin = Singlet
E(RM062X) = –1818.10654798 a.u.
Dipole Moment = 4.7547 Debye
Point Group = C1
Job cpu time: 1 days 6 hours 26 minutes 55.3 seconds.

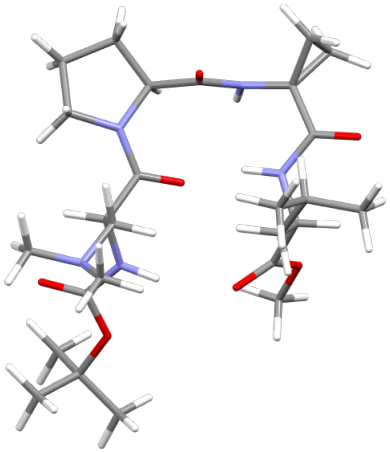

F. Optimization of Peptide 16a–c

Table S6.15: B3LYP/6-31+G(d,p)-Optimized Coordinates of **16a**

Tag	Symbol	X	Y	Z
1	O	0.281707	2.01012	0.887747
2	O	–4.092797	1.49178	–1.119025
3	O	–1.050153	–1.077737	–2.650375
4	O	–0.362073	–1.47972	0.973668
5	O	3.72862	1.572525	–0.461666
6	O	4.480174	–0.586835	–0.247838
7	N	–2.392127	0.624328	0.126874
8	H	–1.782399	–0.169289	0.322037
9	N	–2.609173	–1.835597	–1.163832
10	H	–2.726198	–2.401629	–0.333579
11	N	0.782798	–2.46212	–0.705392
12	N	2.392569	0.045712	0.463923
13	H	1.74074	0.824304	0.575031
14	N	–0.742565	3.407587	–0.583802
15	C	0.541546	3.969611	–0.997124
16	H	1.330571	3.584568	–0.354919
17	H	0.502622	5.063083	–0.926547
18	H	0.757318	3.695238	–2.03694
19	C	–1.900499	3.953745	–1.292827
20	H	–2.783583	3.326735	–1.185452
21	H	–1.662421	4.003654	–2.360848
22	H	–2.120498	4.971777	–0.944872
23	C	–0.762374	2.443119	0.375673
24	C	–2.118543	1.870262	0.848695
25	H	–2.931728	2.548111	0.598978
26	C	–3.370112	0.536884	–0.8089
27	C	–3.634824	–0.842485	–1.443135
28	C	–5.081216	–1.332255	–1.08533
29	H	–5.096739	–2.419558	–0.958822
30	H	–5.548432	–0.860244	–0.217455
31	C	–5.570387	–0.88379	–2.487931
32	H	–6.177732	–1.606163	–3.040546
33	H	–6.09071	0.074791	–2.451902
34	C	–4.092656	–0.73	–2.932493
35	H	–3.817804	0.196423	–3.436494
36	H	–3.723337	–1.580215	–3.509594
37	C	–1.38506	–1.861225	–1.766039
38	C	–0.457778	–2.997523	–1.288614
39	H	–0.975304	–3.59656	–0.531171
40	C	0.043147	–3.867622	–2.464045
41	H	0.179505	–4.89745	–2.114999
42	H	–0.665993	–3.882141	–3.295117
43	C	1.39569	–3.240758	–2.842481
44	H	1.23008	–2.359788	–3.468017
45	H	2.05178	–3.934413	–3.375784
46	C	1.982537	–2.816911	–1.491535
47	H	2.516088	–3.648102	–1.010356
48	H	2.667381	–1.971919	–1.567346
49	C	0.729003	–1.747367	0.441861
50	C	2.058386	–1.248953	1.041582
51	H	2.867057	–1.924168	0.75985
52	C	3.614658	0.271466	–0.093173
53	C	4.958264	2.082003	–1.095219
54	C	4.628405	3.56097	–1.317576
55	H	3.76052	3.668569	–1.975225
56	H	5.479944	4.068281	–1.78169
57	H	4.406499	4.053959	–0.366271
58	C	5.1967	1.376242	–2.43516
59	H	5.432524	0.321476	–2.288974
60	H	6.033177	1.855487	–2.955438
61	H	4.309321	1.458405	–3.071544
62	C	6.147359	1.934338	–0.1388
63	H	5.92242	2.408898	0.822049
64	H	7.023396	2.433278	–0.567291
65	H	6.389713	0.884822	0.032421
66	C	–2.082933	1.641612	2.370626
67	H	–1.284685	0.925488	2.588632
68	H	–1.786673	2.586509	2.846907
69	C	–3.407685	1.157446	2.991571
70	H	–3.709991	0.239794	2.467888
71	C	–4.544691	2.182951	2.849564
72	H	–4.270378	3.135387	3.32217
73	H	–5.455992	1.822422	3.340121
74	H	–4.79589	2.383153	1.803282
75	C	–3.185434	0.798972	4.470024
76	H	–2.405303	0.038101	4.584032
77	H	–4.103842	0.411252	4.925147
78	H	–2.877262	1.681675	5.045068
79	C	1.961469	–1.1974	2.575582
80	H	2.825334	–0.627457	2.95988
81	H	1.05533	–0.649455	2.843432
82	C	1.091526	–2.613308	4.3552
83	H	1.519107	–2.023885	5.190148
84	H	1.012632	–3.65447	4.68573
85	H	0.083091	–2.244033	4.149709
86	C	3.215925	–3.132602	3.34128
87	H	3.796864	–3.098986	2.415156
88	H	3.114433	–4.18194	3.63678
89	H	3.798251	–2.607478	4.12396
90	N	1.894332	–2.547321	3.13952

Calculation Type = FREQ
Calculation Method = RB3LYP
Basis Set = 6-31+G(d,p)
Charge = 0
Spin = Singlet
E(RB3LYP) = –1877.16009531 a.u.
RMS Gradient Norm = 0.00000509 a.u.
Imaginary Freq = 0
Dipole Moment = 1.3233 Debye
Point Group = C1
Job cpu time: 7 days 15 hours 46 minutes 12.3 seconds.

Calculation Type = SP
Calculation Method = RM062X
Basis Set = 6-311++G(2d,3p)
Charge = 0
Spin = Singlet
E(RM062X) = –1876.84766105 a.u.
Dipole Moment = 1.3218 Debye
Point Group = C1
Job cpu time: 1 days 14 hours 2 minutes 1.4 seconds.

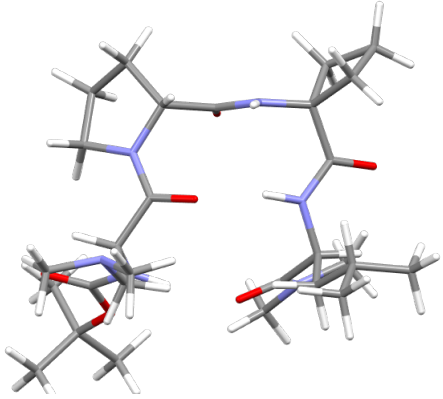

Table S6.16: B3LYP/6-31+G(d,p)-Optimized Coordinates of **16b**

Tag	Symbol	X	Y	Z
1	O	0.330406	–1.744351	0.907338
2	O	–4.381417	–0.422652	1.618737
3	O	–1.72747	2.601516	1.064655
4	O	–0.627431	0.421815	–1.905522
5	O	3.990873	–0.184972	1.183577
6	O	4.370049	0.960969	–0.771765
7	N	–2.536691	–0.631817	0.295243
8	H	–1.961413	–0.228174	–0.442175
9	N	–2.943064	1.929628	–0.7496
10	H	–2.831251	1.669583	–1.721823
11	N	0.454815	2.230803	–1.097917
12	N	2.333082	0.022015	–0.287998
13	H	1.847433	–0.628811	0.328914
14	N	–0.67225	–1.262821	2.88881
15	C	–1.819018	–0.887623	3.71641
16	H	–1.704337	0.153683	4.040421
17	H	–1.859116	–1.526028	4.607218
18	H	–2.761183	–0.960072	3.17832
19	C	0.626861	–1.016331	3.512447
20	H	1.408384	–1.520282	2.946812
21	H	0.605877	–1.397001	4.538581
22	H	0.84623	0.05864	3.541532
23	C	–0.708072	–1.620338	1.577621
24	C	–2.073152	–1.882742	0.901122
25	H	–2.823333	–2.155904	1.640641
26	C	–3.650305	0.015366	0.724521
27	C	–4.037875	1.312735	–0.008585
28	C	–5.293766	1.173164	–0.932773
29	H	–5.094493	1.135357	–2.009515
30	H	–5.883418	0.299233	–0.646837
31	C	–5.862642	2.485643	–0.335169
32	H	–5.659779	3.354261	–0.968163
33	H	–6.923969	2.483351	–0.073127
34	C	–4.849485	2.346044	0.831666
35	H	–5.282226	1.848154	1.700718
36	H	–4.296262	3.230415	1.150207
37	C	–1.853627	2.492955	–0.152072
38	C	–0.786071	3.034455	–1.129173
39	H	–1.181919	3.0095	–2.151849
40	C	–0.3194	4.451119	–0.733533
41	H	–0.879225	5.222636	–1.268866
42	H	–0.484681	4.584711	0.339741
43	C	1.186211	4.460654	–1.044557
44	H	1.364944	4.647377	–2.110116
45	H	1.731134	5.217027	–0.472965
46	C	1.618496	3.036555	–0.682538
47	H	2.529947	2.711897	–1.185225
48	H	1.772752	2.932036	0.398158
49	C	0.439954	0.953954	–1.550016
50	C	1.780971	0.195977	–1.621794
51	H	2.494566	0.820964	–2.166236
52	C	3.639741	0.309797	–0.029464
53	C	5.352365	–0.013857	1.719775
54	C	5.656662	1.47399	1.929816
55	H	5.711899	2.003274	0.977658
56	H	6.615398	1.580189	2.448952
57	H	4.882171	1.936307	2.551124
58	C	6.371838	–0.692364	0.797942
59	H	6.092933	–1.737293	0.628364
60	H	7.359435	–0.674448	1.271592
61	H	6.433487	–0.18316	–0.164555
62	C	5.273083	–0.743072	3.064451
63	H	4.518849	–0.282756	3.710169
64	H	6.240864	–0.694707	3.573367
65	H	5.009229	–1.794685	2.917398
66	C	–1.945576	–3.010025	–0.138074
67	H	–1.495362	–3.879839	0.359675
68	H	–1.230202	–2.693275	–0.903459
69	C	–3.269154	–3.435756	–0.803291
70	H	–3.733826	–2.538655	–1.236081
71	C	–2.979095	–4.411762	–1.95529
72	H	–2.305585	–3.967309	–2.696658
73	H	–3.902556	–4.700723	–2.469671
74	H	–2.506397	–5.329525	–1.582241
75	C	–4.265464	–4.053511	0.191953
76	H	–3.832086	–4.937588	0.678128
77	H	–5.17752	–4.375033	–0.323544
78	H	–4.56482	–3.346278	0.971532
79	C	1.601741	–1.144768	–2.360703
80	H	0.928469	–1.766847	–1.766514
81	H	1.097336	–0.951627	–3.325624
82	C	2.638728	–3.279814	–2.784149
83	H	2.061679	–3.713928	–1.96245
84	H	3.601225	–3.799065	–2.835468
85	H	2.095899	–3.47407	–3.731026
86	C	3.714253	–1.272497	–3.564871
87	H	3.23108	–1.266724	–4.563068
88	H	4.642804	–1.846514	–3.640809
89	H	3.987439	–0.247966	–3.300569
90	N	2.863279	–1.860178	–2.535223

Calculation Type = FREQ
Calculation Method = RB3LYP
Basis Set = 6-31+G(d,p)
Charge = 0
Spin = Singlet
E(RB3LYP) = –1877.16026864 a.u.
RMS Gradient Norm = 0.00000197 a.u.
Imaginary Freq = 0
Dipole Moment = 1.7800 Debye
Point Group = C1
Job cpu time: 7 days 21 hours 49 minutes 57.1 seconds.

Calculation Type = SP
Calculation Method = RM062X
Basis Set = 6-311++G(2d,3p)
Charge = 0
Spin = Singlet
E(RM062X) = –1876.85098237 a.u.
Dipole Moment = 1.7670 Debye
Point Group = C1
Job cpu time: 1 days 17 hours 1 minutes 44.2 seconds.

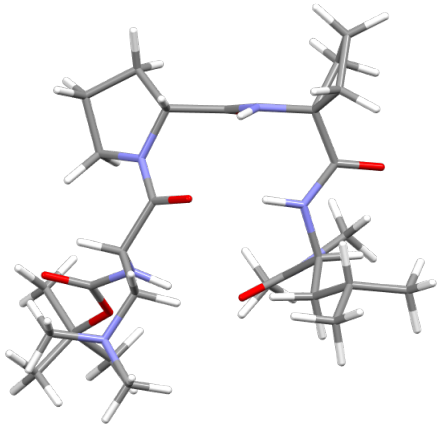

Table S6.17: B3LYP/6-31+G(d,p)-Optimized Coordinates of **16c**

Tag	Symbol	X	Y	Z
1	O	2.471349	1.370032	–1.565859
2	O	3.457404	–1.508857	1.374367
3	O	–0.220063	–3.446379	1.354529
4	O	–1.255879	–0.665557	–0.934333
5	O	–1.391452	2.442861	1.331568
6	O	–0.209104	3.593585	–0.27233
7	N	4.591422	0.537086	–1.466845
8	N	1.762488	–1.039827	–0.065238
9	H	0.773026	–0.856937	–0.202666
10	N	–0.128306	–1.246112	1.947279
11	H	–0.619199	–0.359349	1.946696
12	N	–2.722683	–0.852986	0.781685
13	N	–1.767748	2.15064	–0.909541
14	H	–1.262611	2.160069	–1.786033
15	N	–4.83461	0.238085	–1.837666
16	C	5.548723	–0.507749	–1.091439
17	H	5.157906	–1.118776	–0.276516
18	H	6.458654	–0.020319	–0.730359
19	H	5.821113	–1.141594	–1.945744
20	C	5.162322	1.831951	–1.824351
21	H	4.375833	2.468593	–2.226772
22	H	5.94721	1.693198	–2.576633
23	H	5.604325	2.323019	–0.94731
24	C	3.231811	0.407315	–1.414389
25	C	2.636022	–1.006303	–1.233414
26	H	3.42284	–1.736928	–1.057066
27	C	2.255313	–1.298666	1.167798
28	C	1.271492	–1.263402	2.352622
29	C	1.651014	–0.114962	3.348576
30	H	2.276557	0.683115	2.943371
31	H	0.752342	0.324968	3.792703
32	C	2.334809	–1.155513	4.274062
33	H	3.419681	–1.158397	4.154114
34	H	2.087591	–1.091995	5.337755
35	C	1.656925	–2.291392	3.465093
36	H	0.759076	–2.687341	3.944966
37	H	2.288531	–3.117518	3.139257
38	C	–0.760807	–2.348034	1.459925
39	C	–2.246474	–2.212392	1.110848
40	H	–2.398326	–2.869218	0.247717
41	C	–3.144413	–2.634768	2.295193
42	H	–3.28222	–3.717302	2.322379
43	H	–2.680269	–2.331884	3.241102
44	C	–4.441589	–1.847604	2.065277
45	H	–5.042455	–1.736729	2.972282
46	H	–5.058576	–2.345116	1.308358
47	C	–3.951317	–0.496711	1.526724
48	H	–4.681265	–0.037055	0.861506
49	H	–3.711335	0.202129	2.337795
50	C	–2.208722	–0.202121	–0.292538
51	C	–2.807893	1.158684	–0.710706
52	H	–3.463178	1.545744	0.070338
53	C	–1.120383	2.708539	0.16345
54	C	0.701816	4.315384	0.640642
55	C	1.574224	5.108585	–0.33526
56	H	2.111299	4.426787	–1.000303
57	H	2.301578	5.709453	0.220011
58	H	0.960531	5.781262	–0.942552
59	C	1.549124	3.318203	1.43388
60	H	0.939207	2.763166	2.147954
61	H	2.321857	3.862659	1.987776
62	H	2.038245	2.618537	0.749915
63	C	–0.111417	5.249111	1.542829
64	H	–0.735223	5.916843	0.939381
65	H	0.57115	5.86634	2.136889
66	H	–0.751891	4.68361	2.222132
67	C	–3.591242	0.987148	–2.029252
68	H	–3.775597	1.987453	–2.45862
69	H	–2.949794	0.442886	–2.730083
70	C	–5.176329	–0.589819	–2.993066
71	H	–5.376079	0.003992	–3.905245
72	H	–6.073391	–1.175523	–2.768971
73	H	–4.360786	–1.286708	–3.204504
74	C	–5.947682	1.110386	–1.46902
75	H	–5.689799	1.712518	–0.59249
76	H	–6.824737	0.506131	–1.21666
77	H	–6.228711	1.804918	–2.283554
78	C	1.8557	–1.380248	–2.508993
79	H	1.020893	–0.678754	–2.610857
80	H	2.514648	–1.209581	–3.37216
81	C	1.331646	–2.830316	–2.554669
82	H	0.763741	–3.018182	–1.634996
83	C	0.368068	–2.994235	–3.740744
84	H	–0.472758	–2.29671	–3.662155
85	H	–0.03839	–4.011334	–3.779107
86	H	0.878801	–2.804584	–4.694254
87	C	2.466221	–3.864573	–2.632279
88	H	3.075492	–3.710562	–3.533139
89	H	2.060852	–4.881595	–2.675274
90	H	3.129851	–3.820063	–1.76243

Calculation Type = FREQ
Calculation Method = RB3LYP
Basis Set = 6-31+G(d,p)
Charge = 0
Spin = Singlet
E(RB3LYP) = –1877.15280365 a.u.
RMS Gradient Norm = 0.00000230 a.u.
Imaginary Freq = 0
Dipole Moment = 5.3348 Debye
Point Group = C1
Job cpu time: 7 days 13 hours 21 minutes 15.4 seconds.

Calculation Type = SP
Calculation Method = RM062X
Basis Set = 6-311++G(2d,3p)
Charge = 0
Spin = Singlet
E(RM062X) = –1876.84358068 a.u.
Dipole Moment = 5.3907 Debye
Point Group = C1
Job cpu time: 1 days 9 hours 57 minutes 20.4 seconds.

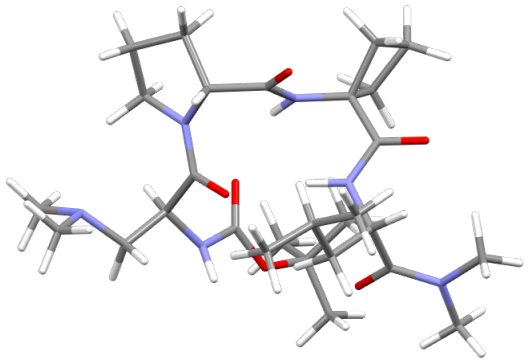

Table S6.18: Comparative Energy Data for **16a–c**

Method		Boc-Dmaa-D-Pro-Acbc-Leu-NMe_2 (16)		
		16a	16b	16c
sp of X-ray crystal structure M06-2X/6-311++G(2d,3p)	E(sp, M06-2X, au)	-1876.248550570	-1876.352670060	-1876.434337570
	Relative E(sp, M06-2X, kcal/mol)	116.58	51.25	0.00
	Dipole Moment (D)	2.252	1.296	8.828
opt of X-ray crystal structure B3LYP/6-31+G(d,p)	E(opt, B3LYP, au)	-1877.160095310	-1877.160268640	-1877.152803650
	ZP Correction (au)	0.784781	0.784804	0.783972
	E Correction (au)	0.830262	0.830166	0.830001
	H Correction (au)	0.831206	0.831110	0.830945
	G Correction (au)	0.701878	0.702579	0.699899
	ZPE (au)	-1876.375314310	-1876.375464640	-1876.368831650
	Relative ZPE (kcal/mol)	0.09	0.00	4.16
	E (au)	-1876.329833310	-1876.330102640	-1876.322802650
	Relative E (kcal/mol)	0.17	0.00	4.58
	H (au)	-1876.328889310	-1876.329158640	-1876.321858650
	Relative H (kcal/mol)	0.17	0.00	4.58
	G (au)	-1876.458217310	-1876.457689640	-1876.452904650
	Relative G (kcal/mol)	-0.33	0.00	3.00
	S (cal/mol*K)	272.194	270.516	275.81
	Relative S(cal/mol*K)	1.68	0.00	5.29
	Dipole Moment (D)	1.323	1.780	5.335
sp of optimized structure M06-2X/6-311++G(2d,3p)	E(sp, M06-2X, au)	-1876.847661050	-1876.850982370	-1876.843580680
	ZPE (au)	-1876.062880050	-1876.066178370	-1876.059608680
	Relative ZPE (kcal/mol)	2.07	0.00	4.12
	E (au)	-1876.017399050	-1876.020816370	-1876.013579680
	Relative E (kcal/mol)	2.14	0.00	4.54
	H (au)	-1876.016455050	-1876.019872370	-1876.012635680
	Relative H (kcal/mol)	2.14	0.00	4.54
	G (au)	-1876.145783050	-1876.148403370	-1876.143681680
	Relative G (kcal/mol)	1.64	0.00	2.96
	Dipole Moment (D)	1.322	1.767	5.391

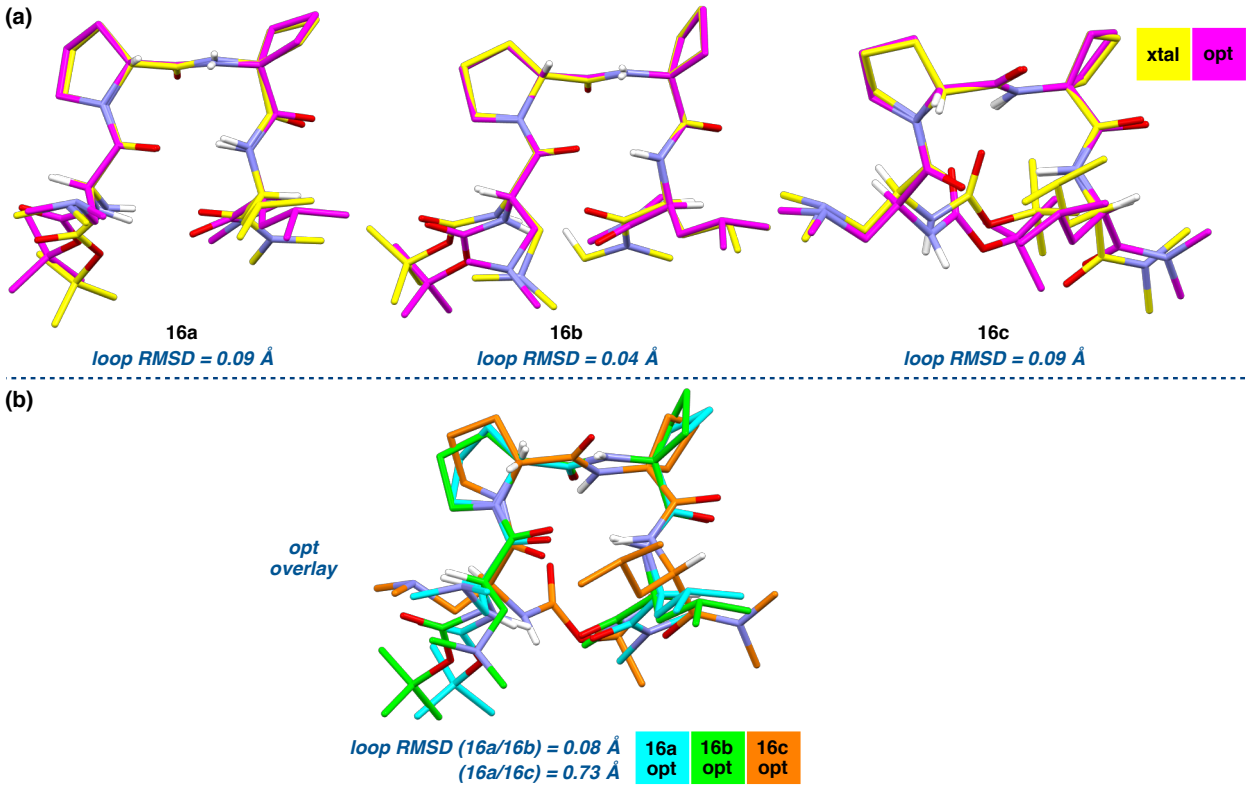

Figure S6.04: (a) Overlays of the DFT-optimized structures of **16a–c** with the corresponding crystal structures. **(b)** Overlay of the optimized structures of **16a–c**.

G. Optimization of Peptide 19a,b

Table S6.19: B3LYP/6-31+G(d,p)-Optimized Coordinates of **19a**

Tag	Symbol	X	Y	Z	Tag	Symbol	X	Y	Z
1	O	–0.42224	1.309583	2.959007	63	C	–3.785644	3.878125	–2.561177
2	O	0.398875	3.040366	4.150578	64	H	–4.717606	4.23317	–2.081358
3	O	3.350483	0.155962	2.212549	65	H	–3.791739	4.217066	–3.601879
4	O	2.956902	0.996888	–1.946886	66	H	–2.935319	4.345108	–2.056876
5	O	–0.616774	1.838449	–0.810049	67	C	1.575591	3.743173	1.470657
6	O	–3.767771	–1.876469	–0.406404	68	H	1.465638	4.509462	2.246801
7	O	–3.064671	–1.51542	1.752655	69	H	0.672969	3.782313	0.846801
8	N	1.629431	1.275369	1.221241	70	C	2.807381	4.059691	0.599259
9	H	0.970316	1.319735	0.450209	71	H	2.931423	3.24816	–0.129464
10	N	1.573191	–0.503857	–0.901475	72	C	2.559375	5.35883	–0.184663
11	H	0.63451	–0.877574	–0.925793	73	H	1.660331	5.284091	–0.80714
12	N	–0.584641	0.314816	–2.483573	74	H	3.405052	5.585719	–0.843176
13	N	–2.644237	0.025738	0.200086	75	H	2.427816	6.211094	0.494802
14	H	–2.150465	0.498375	0.947292	76	C	4.100702	4.161944	1.423303
15	N	–3.644765	2.423991	–2.52414	77	H	4.016272	4.940538	2.192706
16	C	–1.476863	1.192638	3.938517	78	H	4.94675	4.421889	0.777489
17	H	–2.091022	0.357334	3.603733	79	H	4.352417	3.220008	1.920601
18	H	–2.05946	2.116093	3.982148	80	C	–3.213166	–1.193225	0.445541
19	H	–1.053678	0.991721	4.925334	81	C	–3.596245	–2.785829	2.298195
20	C	0.481197	2.286243	3.202561	82	C	–2.908234	–3.975531	1.621036
21	C	1.615817	2.367584	2.176863	83	H	–3.171125	–4.037976	0.564323
22	H	2.530888	2.278428	2.768986	84	H	–3.218872	–4.902426	2.114579
23	C	2.519234	0.256422	1.30877	85	H	–1.82064	–3.891473	1.716477
24	C	2.410973	–0.872365	0.249683	86	C	–5.119941	–2.825915	2.143089
25	C	1.765933	–2.135062	0.906268	87	H	–5.572731	–1.934366	2.589151
26	H	2.040046	–2.158956	1.967398	88	H	–5.513398	–3.7032	2.667345
27	H	0.670311	–2.113189	0.856493	89	H	–5.411664	–2.88522	1.093784
28	C	2.402871	–3.288871	0.162751	90	C	–3.203033	–2.702464	3.775055
29	C	1.996086	–4.619221	0.081471	91	H	–3.535543	–3.603451	4.299347
30	H	1.089992	–4.95741	0.578463	92	H	–3.66936	–1.83558	4.253068
31	C	2.772561	–5.522057	–0.657403	93	H	–2.117577	–2.619749	3.884579
32	H	2.464737	–6.560883	–0.735744					
33	C	3.938794	–5.091003	–1.298691					
34	H	4.53136	–5.798172	–1.872309					
35	C	4.346328	–3.7532	–1.210466					
36	H	5.252624	–3.422784	–1.711546					
37	C	3.572987	–2.855167	–0.476293					
38	C	3.806635	–1.385075	–0.214148					
39	H	4.174935	–0.822601	–1.072791					
40	H	4.511912	–1.242781	0.612341					
41	C	1.878554	0.416325	–1.85681					
42	C	0.774546	0.729761	–2.886904					
43	H	0.808644	1.817161	–2.991868					
44	C	0.987113	0.014101	–4.241217					
45	H	0.690244	0.68566	–5.053844					
46	H	2.034276	–0.25322	–4.397559					
47	C	0.041939	–1.197756	–4.179198					
48	H	–0.223041	–1.583788	–5.166975					
49	H	0.502426	–2.014684	–3.612747					
50	C	–1.181342	–0.659098	–3.426372					
51	H	–1.873741	–0.146928	–4.106295					
52	H	–1.729121	–1.439654	–2.893372					
53	C	–1.214232	0.989504	–1.488616					
54	C	–2.662238	0.631746	–1.124903					
55	H	–3.079491	–0.11824	–1.794784					
56	C	–3.530095	1.904819	–1.161133					
57	H	–4.512334	1.672395	–0.712935					
58	H	–3.046273	2.65794	–0.532742					
59	C	–4.711904	1.770886	–3.27934					
60	H	–4.580686	0.685017	–3.273461					
61	H	–4.686144	2.107066	–4.320536					
62	H	–5.716235	1.991781	–2.869739					

Calculation Type = FREQ
Calculation Method = RB3LYP
Basis Set = 6-31+G(d,p)
Charge = 0
Spin = Singlet
E(RB3LYP) = –2049.48741410 a.u.
RMS Gradient Norm = 0.00000185 a.u.
Imaginary Freq = 0
Dipole Moment = 8.8503 Debye
Point Group = C1
Job cpu time: 10 days 15 hours 50 minutes 12.7 seconds.

Calculation Type = SP
Calculation Method = RM062X
Basis Set = 6-311++G(2d,3p)
Charge = 0
Spin = Singlet
E(RM062X) = –2049.16094379 a.u.
Dipole Moment = 8.7942 Debye
Point Group = C1
Job cpu time: 1 days 10 hours 33 minutes 25.0 seconds.

Table S6.20: B3LYP/6-31+G(d,p)-Optimized Coordinates of **19b**

Tag	Symbol	X	Y	Z
1	O	–4.324992	0.133797	–2.960147
2	O	–2.410329	1.054465	–2.190971
3	O	–1.52703	–3.179565	–1.845203
4	O	–0.810541	–2.683676	2.22091
5	O	–1.396035	0.857992	1.471937
6	O	1.580719	1.21028	–0.262678
7	O	2.761679	3.132983	–0.676578
8	N	–1.903924	–1.258559	–0.677277
9	H	–1.554851	–0.587674	0.00054
10	N	0.476291	–1.525501	0.717133
11	H	0.936986	–0.635545	0.546392
12	N	0.553599	0.673633	2.595141
13	N	1.258905	3.140503	0.954813
14	H	1.413263	4.137075	0.843805
15	N	–0.962329	4.897183	0.478094
16	C	–4.471594	1.235134	–3.875136
17	H	–4.558883	2.177589	–3.328409
18	H	–5.384496	1.029154	–4.433448
19	H	–3.61232	1.287784	–4.548097
20	C	–3.236729	0.16528	–2.15834
21	C	–3.231538	–1.039032	–1.213942
22	H	–3.485465	–1.919322	–1.808778
23	C	–1.152826	–2.328697	–1.03481
24	C	0.278201	–2.411246	–0.442702
25	C	0.689954	–3.877146	–0.110431
26	H	0.438143	–4.145447	0.915885
27	H	0.132755	–4.544341	–0.777811
28	C	2.166323	–3.917136	–0.427337
29	C	3.125052	–4.852589	–0.040246
30	H	2.855612	–5.688769	0.600246
31	C	4.444744	–4.703379	–0.487323
32	H	5.200501	–5.424691	–0.188759
33	C	4.795856	–3.63097	–1.314306
34	H	5.822062	–3.524459	–1.655115
35	C	3.831037	–2.691722	–1.702871
36	H	4.106662	–1.861132	–2.348018
37	C	2.521164	–2.839217	–1.250163
38	C	1.304172	–1.9909	–1.546102
39	H	0.889014	–2.251648	–2.52694
40	H	1.491035	–0.913732	–1.540761
41	C	–0.104073	–1.718595	1.931533
42	C	0.209353	–0.694959	3.034135
43	H	–0.700051	–0.65887	3.643322
44	C	1.429376	–1.114139	3.883812
45	H	2.178212	–1.598883	3.24697
46	H	1.144448	–1.821267	4.665103
47	C	1.972024	0.21847	4.421044
48	H	1.37403	0.557239	5.275191
49	H	3.015716	0.158607	4.74186
50	C	1.784563	1.175033	3.235956
51	H	1.672181	2.218188	3.539336
52	H	2.628386	1.116054	2.538291
53	C	–0.334469	1.371908	1.844181
54	C	–0.055758	2.854642	1.536139
55	H	–0.054561	3.361861	2.511671
56	C	–1.181953	3.45717	0.672081
57	H	–1.177837	2.9525	–0.297858
58	H	–2.157026	3.242855	1.135365
59	C	–1.465027	5.690389	1.598245
60	H	–2.563961	5.619966	1.708729
61	H	–1.201522	6.742649	1.453123
62	H	–1.011603	5.363345	2.539181
63	C	–1.524509	5.372665	–0.785383
64	H	–1.099961	4.805998	–1.618263
65	H	–1.27071	6.428696	–0.923275
66	H	–2.625597	5.275832	–0.82802
67	C	–4.278971	–0.830361	–0.09234
68	H	–3.980004	0.047653	0.494487
69	H	–5.240402	–0.593267	–0.565498
70	C	–4.458657	–2.033761	0.855523
71	H	–3.477799	–2.281409	1.28046
72	C	–5.386901	–1.63761	2.014949
73	H	–4.99403	–0.773357	2.562587
74	H	–5.497463	–2.4634	2.726413
75	H	–6.388775	–1.37738	1.648223
76	C	–4.994093	–3.278537	0.130295
77	H	–5.962897	–3.071313	–0.343979
78	H	–5.140584	–4.101323	0.839007
79	H	–4.305953	–3.636158	–0.641781
80	C	1.836576	2.388265	–0.035111
81	C	3.624156	2.581435	–1.74594
82	C	4.492737	3.785772	–2.118359
83	H	3.87247	4.617572	–2.465129
84	H	5.184036	3.510521	–2.920735
85	H	5.07719	4.123909	–1.257414
86	C	4.48615	1.444378	–1.189237
87	H	5.039725	1.782705	–0.307159
88	H	5.214943	1.139191	–1.947342
89	H	3.884808	0.575955	–0.918681
90	C	2.762595	2.145148	–2.934693
91	H	2.109905	1.311752	–2.6732
92	H	3.412608	1.835126	–3.759607
93	H	2.144888	2.978445	–3.284334

Calculation Type = FREQ
Calculation Method = RB3LYP
Basis Set = 6-31+G(d,p)
Charge = 0
Spin = Singlet
E(RB3LYP) = –2049.48700001 a.u.
RMS Gradient Norm = 0.00000295 a.u.
Imaginary Freq = 0
Dipole Moment = 9.9607 Debye
Point Group = C1
Job cpu time: 12 days 1 hours 15 minutes 7.8 seconds.

Calculation Type = SP
Calculation Method = RM062X
Basis Set = 6-311++G(2d,3p)
Charge = 0
Spin = Singlet
E(RM062X) = –2049.16582187 a.u.
Dipole Moment = 9.8465 Debye
Point Group = C1
Job cpu time: 1 days 15 hours 40 minutes 24.0 seconds.

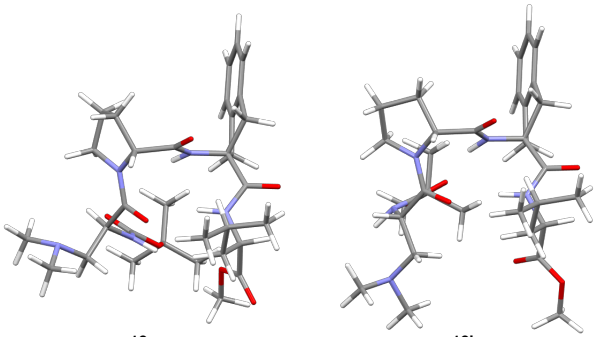

19a **19b**

Table S6.21: Comparative Energy Data for **19a,b**

Method		Boc-Dmaa-D-Pro-Aic-Leu-OMe (19) 19a	19b
sp of X-ray crystal structure M06-2X/6-311++G(2d,3p)	E(sp, M06-2X, au)	-2048.734794180	-2048.742395710
	Relative E(sp, M06-2X, kcal/mol)	4.77	0.00
	Dipole Moment (D)	10.915	10.730
opt of X-ray crystal structure B3LYP/6-31+G(d,p)	E(opt, B3LYP, au)	-2049.487414100	-2049.487000010
	ZP Correction (au)	0.796772	0.796893
	E Correction (au)	0.844042	0.843961
	H Correction (au)	0.844986	0.844905
	G Correction (au)	0.709116	0.710702
	ZPE (au)	-2048.690642100	-2048.690107010
	Relative ZPE (kcal/mol)	0.00	0.34
	E (au)	-2048.643372100	-2048.643039010
	Relative E (kcal/mol)	0.00	0.21
	H (au)	-2048.642428100	-2048.642095010
	Relative H (kcal/mol)	0.00	0.21
	G (au)	-2048.778298100	-2048.776298010
	Relative G (kcal/mol)	0.00	1.26
	S (cal/mol*K)	285.963	282.455
	Relative S(cal/mol*K)	0.00	-3.51
	Dipole Moment (D)	8.850	9.961
sp of optimized structure M06-2X/6-311++G(2d,3p)	E(sp, M06-2X, au)	-2049.160943790	-2049.165821870
	ZPE (au)	-2048.364171790	-2048.368928870
	Relative ZPE (kcal/mol)	2.99	0.00
	E (au)	-2048.316901790	-2048.321860870
	Relative E (kcal/mol)	3.11	0.00
	H (au)	-2048.315957790	-2048.320916870
	Relative H (kcal/mol)	3.11	0.00
	G (au)	-2048.451827790	-2048.455119870
	Relative G (kcal/mol)	2.07	0.00
	Dipole Moment (D)	8.794	9.847

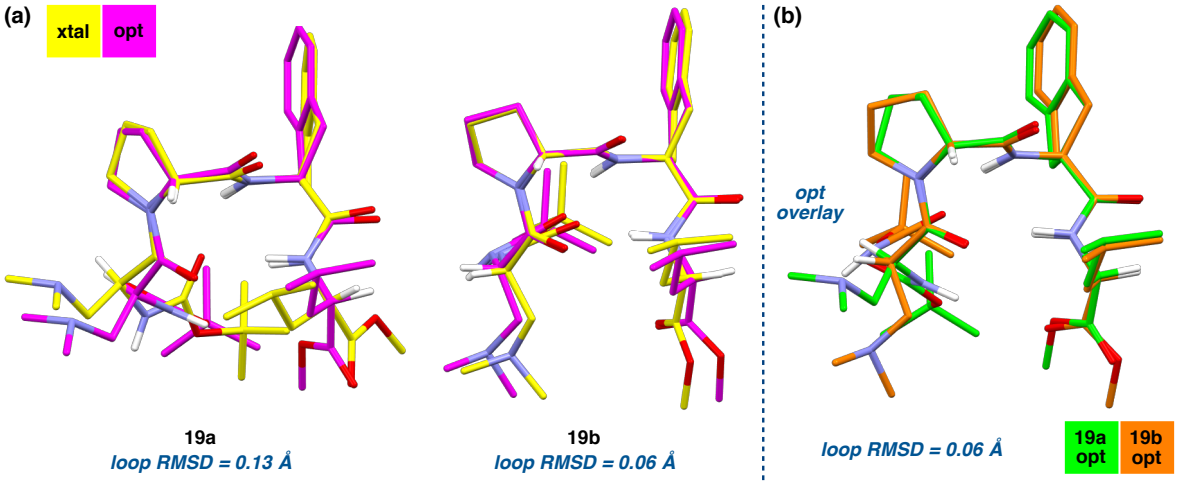

Figure S6.05: (a) Overlays of the DFT-optimized structures of **19a**,**b** with the corresponding crystal structures. **(b)** Overlay of the optimized structures of **19a** and **19b**.

H. Optimization of Peptide 29a,b

Table S6.22: B3LYP/6-31+G(d,p)-Optimized Coordinates of **29a**

Tag	Symbol	X	Y	Z
1	S	–4.074342	–2.118753	–1.593252
2	O	0.327635	–1.52435	1.27616
3	O	–3.898521	0.886475	2.163748
4	O	–0.712333	3.042837	0.573127
5	O	–0.468024	0.22146	–1.70433
6	O	4.591008	0.29845	–0.893496
7	O	4.047837	–0.540143	1.174456
8	N	–0.350663	–0.516937	3.197082
9	N	–2.3242	0.128257	0.699712
10	H	–1.78484	0.299596	–0.147221
11	N	–2.469469	2.479054	–0.788349
12	H	–2.673056	2.14553	–1.720789
13	N	0.867194	2.040847	–1.745171
14	N	2.442016	–0.297882	–0.350431
15	H	1.864365	–0.779023	0.339918
16	N	2.732133	–2.473014	–2.384608
17	C	1.02464	–0.469699	3.690527
18	H	1.642315	–1.164094	3.124706
19	H	1.032956	–0.740942	4.751523
20	H	1.436959	0.541445	3.583644
21	C	–1.319341	0.180677	4.041551
22	H	–2.305209	0.236386	3.58563
23	H	–0.975109	1.207792	4.211906
24	H	–1.394683	–0.322805	5.01329
25	C	–0.587699	–1.057694	1.973448
26	C	–2.037155	–1.103803	1.429476
27	H	–2.763895	–1.157811	2.239751
28	C	–3.241196	1.031748	1.129914
29	C	–3.518088	2.265055	0.222127
30	C	–4.824053	1.966432	–0.543192
31	H	–5.098501	2.827154	–1.162448
32	H	–5.628808	1.775874	0.169493
33	H	–4.720242	1.08254	–1.182066
34	C	–3.700741	3.517504	1.097548
35	H	–2.780264	3.763215	1.628349
36	H	–4.492378	3.336195	1.826266
37	H	–3.980615	4.363449	0.461473
38	C	–1.170515	2.817169	–0.543903
39	C	–0.297053	2.93912	–1.811038
40	H	–0.895103	2.682192	–2.692549
41	C	0.339207	4.342565	–1.94205
42	H	–0.268306	5.114187	–1.463014
43	H	0.433286	4.596597	–3.003927
44	C	1.72733	4.187061	–1.297857
45	H	2.440861	4.942551	–1.638481
46	H	1.638165	4.251023	–0.210204
47	C	2.150835	2.770405	–1.701481
48	H	2.623875	2.762278	–2.693073
49	H	2.838358	2.307983	–0.993785
50	C	0.679134	0.701032	–1.719308
51	C	1.928514	–0.200869	–1.709036
52	H	2.714843	0.276285	–2.297444
53	C	3.773523	–0.154175	–0.096706
54	C	5.416963	–0.478097	1.715704
55	C	6.348551	–1.38675	0.905331
56	H	5.936125	–2.399301	0.849465
57	H	7.324085	–1.442057	1.400697
58	H	6.488931	–1.006742	–0.107251
59	C	5.907191	0.974006	1.752774
60	H	6.033081	1.372847	0.745402
61	H	6.869863	1.02049	2.273505
62	H	5.195731	1.602381	2.299059
63	C	5.237228	–1.023125	3.135824
64	H	4.545782	–0.395568	3.706481
65	H	6.200482	–1.037493	3.655235
66	H	4.840579	–2.042517	3.109787
67	C	–2.198414	–2.350261	0.52577
68	H	–1.493426	–2.269788	–0.304823
69	H	–1.888127	–3.226186	1.106539
70	C	–3.602279	–2.564919	0.02975
71	C	–4.671013	–3.109237	0.699401
72	H	–4.602306	–3.463764	1.722889
73	C	–5.868684	–3.165265	–0.077694
74	H	–6.808652	–3.563831	0.287372
75	C	–5.701804	–2.66566	–1.342063
76	H	–6.430512	–2.593268	–2.137881
77	C	1.582925	–1.577538	–2.310697
78	H	0.821446	–2.038627	–1.677554
79	H	1.118407	–1.41781	–3.304128
80	C	3.688132	–2.095301	–3.420893
81	H	3.237653	–2.094402	–4.434377
82	H	4.521273	–2.804698	–3.421744
83	H	4.104477	–1.105794	–3.217897
84	C	2.312269	–3.862167	–2.534316
85	H	1.655217	–4.143099	–1.705871
86	H	3.190646	–4.515037	–2.508169
87	H	1.773404	–4.052657	–3.484094

Calculation Type = FREQ
Calculation Method = RB3LYP
Basis Set = 6-31+G(d,p)
Charge = 0
Spin = Singlet
E(RB3LYP) = –2272.94624711 a.u.
RMS Gradient Norm = 0.00000304 a.u.
Imaginary Freq = 0
Dipole Moment = 1.9118 Debye
Point Group = C1
Job cpu time: 7 days 20 hours 35 minutes 25.5 seconds.

Calculation Type = SP
Calculation Method = RM062X
Basis Set = 6-311++G(2d,3p)
Charge = 0
Spin = Singlet
E(RM062X) = –2272.65153093 a.u.
Dipole Moment = 1.9213 Debye
Point Group = C1
Job cpu time: 1 days 14 hours 38 minutes 39.1 seconds.

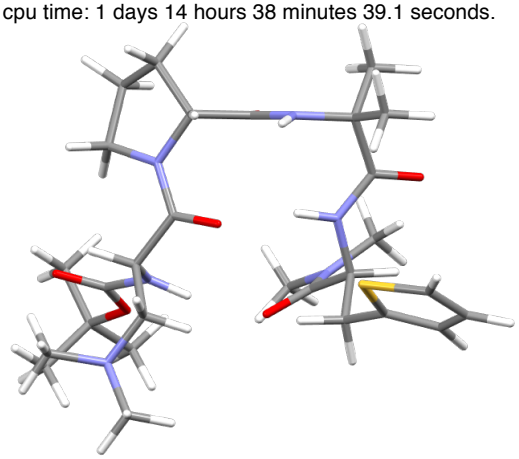

Table S6.23: B3LYP/6-31+G(d,p)-Optimized Coordinates of **19b**

Tag	Symbol	X	Y	Z
1	S	–4.074746	–2.116787	–1.593101
2	O	0.327527	–1.524372	1.276008
3	O	–3.898475	0.886377	2.163934
4	O	–0.711883	3.04278	0.573369
5	O	–0.468097	0.22159	–1.704191
6	O	4.590985	0.298403	–0.893713
7	O	4.047949	–0.539857	1.174406
8	N	–0.350875	–0.517764	3.197275
9	N	–2.324208	0.128279	0.69979
10	H	–1.784744	0.299737	–0.147053
11	N	–2.469284	2.479344	–0.787922
12	H	–2.673025	2.145903	–1.720361
13	N	0.867276	2.040849	–1.74505
14	N	2.442057	–0.297977	–0.350456
15	H	1.864461	–0.779091	0.339954
16	N	2.73165	–2.473281	–2.384593
17	C	1.024447	–0.470834	3.690693
18	H	1.641616	–1.166565	3.125946
19	H	1.032421	–0.740488	4.752083
20	H	1.43766	0.539791	3.582308
21	C	–1.319515	0.179634	4.041961
22	H	–2.30526	0.235967	3.585847
23	H	–0.974978	1.206524	4.213054
24	H	–1.395272	–0.324436	5.013365
25	C	–0.587867	–1.058001	1.97341
26	C	–2.037305	–1.10394	1.429359
27	H	–2.764099	–1.158035	2.23958
28	C	–3.241144	1.031759	1.130108
29	C	–3.517824	2.265359	0.222635
30	C	–4.823956	1.967246	–0.542588
31	H	–5.098275	2.828185	–1.161595
32	H	–5.628654	1.776671	0.170155
33	H	–4.720419	1.083486	–1.181693
34	C	–3.700072	3.517633	1.098405
35	H	–2.779494	3.762969	1.629197
36	H	–4.491722	3.336336	1.82711
37	H	–3.979757	4.363819	0.462565
38	C	–1.170246	2.817273	–0.543621
39	C	–0.29693	2.939164	–1.810855
40	H	–0.895094	2.682195	–2.692274
41	C	0.339388	4.342559	–1.942036
42	H	0.433441	4.596437	–3.003957
43	H	–0.268079	5.114282	–1.463102
44	C	2.150962	2.770327	–1.701362
45	H	2.624071	2.762058	–2.692916
46	H	2.838411	2.307943	–0.99357
47	C	0.679103	0.70104	–1.719194
48	C	1.727523	4.187062	–1.297894
49	H	2.441084	4.942474	–1.63863
50	H	1.638423	4.251149	–0.210243
51	C	1.928412	–0.200963	–1.709001
52	H	2.714709	0.276105	–2.297522
53	C	3.773557	–0.154145	–0.096812
54	C	5.417168	–0.478021	1.715435
55	C	6.348498	–1.38688	0.904993
56	H	5.935858	–2.399348	0.849182
57	H	7.324056	–1.442384	1.400289
58	H	6.488882	–1.006929	–0.107609
59	C	5.237557	–1.022919	3.135622
60	H	4.546219	–0.395258	3.706294
61	H	6.200871	–1.037305	3.65492
62	H	4.840832	–2.042285	3.109718
63	C	5.907621	0.974009	1.752328
64	H	6.033349	1.372783	0.744908
65	H	6.870414	1.020383	2.272848
66	H	5.19637	1.602515	2.298737
67	C	–2.198545	–2.350279	0.525487
68	H	–1.493403	–2.269811	–0.304974
69	H	–1.888432	–3.226264	1.106262
70	C	–3.602326	–2.56491	0.029254
71	C	–4.670734	–3.110681	0.698254
72	H	–4.601729	–3.466613	1.721235
73	C	–5.86846	–3.166185	–0.07879
74	H	–6.808208	–3.56569	0.285816
75	C	–5.701943	–2.664742	–1.342479
76	H	–6.43077	–2.591576	–2.138117
77	C	1.5826	–1.577623	–2.310565
78	H	0.821132	–2.038575	–1.67731
79	H	1.117989	–1.417854	–3.303951
80	C	2.311495	–3.862308	–2.534639
81	H	1.77262	–4.052455	–3.48448
82	H	1.654347	–4.14329	–1.706287
83	H	3.189726	–4.51538	–2.508611
84	C	3.687793	–2.095534	–3.420746
85	H	3.237343	–2.094232	–4.434244
86	H	4.520724	–2.805176	–3.421772
87	H	4.104401	–1.106202	–3.217448

Calculation Type = FREQ
Calculation Method = RB3LYP
Basis Set = 6-31+G(d,p)
Charge = 0
Spin = Singlet
E(RB3LYP) = –2272.94624707 a.u.
RMS Gradient Norm = 0.00000205 a.u.
Imaginary Freq = 0
Dipole Moment = 1.9101 Debye
Point Group = C1
Job cpu time: 10 days 6 hours 22 minutes 41.3 seconds.

Calculation Type = SP
Calculation Method = RM062X
Basis Set = 6-311++G(2d,3p)
Charge = 0
Spin = Singlet
E(RM062X) = –2272.65152997 a.u.
Dipole Moment = 1.9196 Debye
Point Group = C1
Job cpu time: 1 days 14 hours 33 minutes 9.2 seconds.

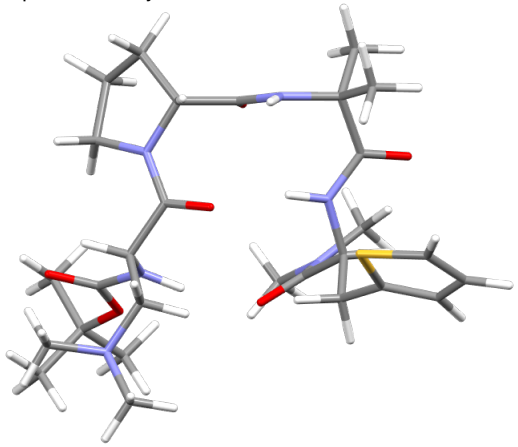

Table S6.24: Comparative Energy Data for **29a,b**

Method		Boc-Dmaa-D-Pro-Aib-2-Thi-NMe_2 (29) 29a	29b
sp of X-ray crystal structure M06-2X/6-311++G(2d,3p)	E(sp, M06-2X, au)	-2272.191896760	-2272.196580950
	Relative E(sp, M06-2X, kcal/mol)	2.94	0.00
	Dipole Moment (D)	2.689	2.401
opt of X-ray crystal structure B3LYP/6-31+G(d,p)	E(opt, B3LYP, au)	-2272.946247110	-2272.946247070
	ZP Correction (au)	0.740439	0.740443
	E Correction (au)	0.786097	0.786098
	H Correction (au)	0.787041	0.787042
	G Correction (au)	0.656491	0.656516
	ZPE (au)	-2272.205808110	-2272.205804070
	Relative ZPE (kcal/mol)	0.00	0.00
	E (au)	-2272.160150110	-2272.160149070
	Relative E (kcal/mol)	0.00	0.00
	H (au)	-2272.159206110	-2272.159205070
	Relative H (kcal/mol)	0.00	0.00
	G (au)	-2272.289756110	-2272.289731070
	Relative G (kcal/mol)	0.00	0.02
	S (cal/mol*K)	274.766	274.716
	Relative S(cal/mol*K)	0.00	0.05
	Dipole Moment (D)	1.912	1.910
sp of optimized structure M06-2X/6-311++G(2d,3p)	E(sp, M06-2X, au)	-2272.651530930	-2272.651529970
	ZPE (au)	-2271.911091930	-2271.911086970
	Relative ZPE (kcal/mol)	0.00	0.00
	E (au)	-2271.865433930	-2271.865431970
	Relative E (kcal/mol)	0.00	0.00
	H (au)	-2271.864489930	-2271.864487970
	Relative H (kcal/mol)	0.00	0.00
	G (au)	-2271.995039930	-2271.995013970
	Relative G (kcal/mol)	0.00	0.02
	Dipole Moment (D)	1.921	1.920

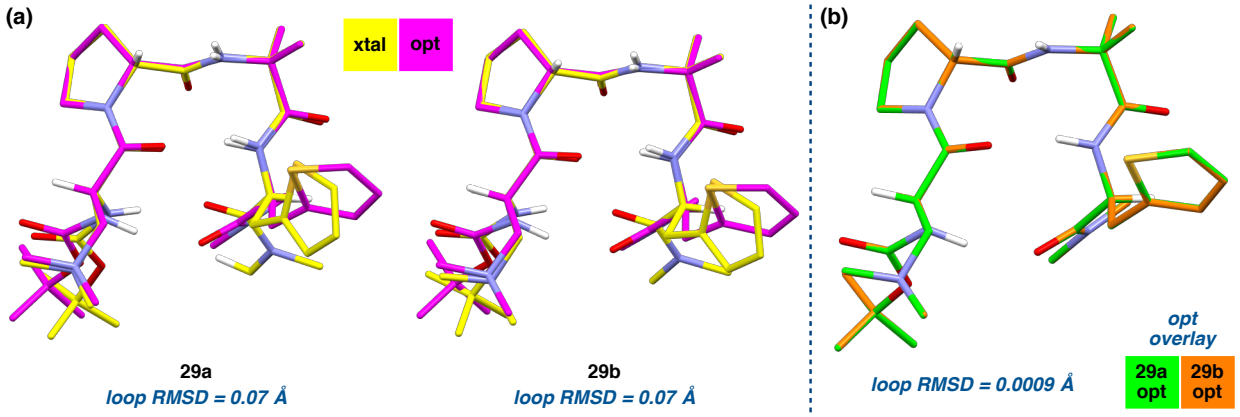

Figure S6.06: (a) Overlays of the DFT-optimized structures of **29a**,**b** with the corresponding crystal structures. **(b)** An overlay of the two computed structures shows that **29a** and **29b** converged on DFT optimization.

I. Optimization of Peptide 30

Table S6.25: B3LYP/6-31+G(d,p)-Optimized Coordinates of **30**

Tag	Symbol	X	Y	Z
1	O	4.447356	–3.43181	0.148726
2	O	3.728099	–2.382677	–1.719346
3	O	5.10058	0.01424	0.343904
4	O	1.842839	2.870802	1.007263
5	O	–0.139117	0.656304	–0.598106
6	O	–4.717679	0.442872	–0.436339
7	O	–3.91437	–1.571895	–1.198336
8	N	2.881971	–0.255888	–0.018068
9	H	2.006428	0.120155	–0.366507
10	N	2.648718	2.328511	–1.074326
11	H	2.354938	2.204104	–2.033579
12	N	–0.78184	2.794947	–0.229569
13	N	–2.613121	–0.308573	0.089002
14	H	–1.893193	–0.94862	–0.223117
15	N	–2.739715	0.622776	3.184878
16	C	5.251686	–4.30466	–0.66757
17	H	5.995864	–3.723419	–1.216878
18	H	4.625472	–4.851964	–1.376557
19	H	5.735852	–4.988533	0.028988
20	C	3.740626	–2.492828	–0.51087
21	C	2.92207	–1.630071	0.461036
22	H	3.437232	–1.648759	1.424516
23	C	4.029189	0.463677	–0.066904
24	C	4.007705	1.858233	–0.750158
25	C	4.743057	1.686222	–2.096569
26	H	4.233266	0.960011	–2.740157
27	H	5.7542	1.319368	–1.913705
28	H	4.802628	2.648879	–2.615834
29	C	4.757214	2.874653	0.129008
30	H	4.827674	3.831191	–0.399389
31	H	5.762143	2.497685	0.326544
32	H	4.243427	3.031803	1.077727
33	C	1.706941	2.797319	–0.20963
34	C	0.424173	3.316682	–0.892259
35	H	0.406511	3.013723	–1.947317
36	C	0.284662	4.847764	–0.745654
37	H	0.793111	5.163969	0.170853
38	H	0.730403	5.379695	–1.589919
39	C	–1.229566	5.07243	–0.613915
40	H	–1.478614	6.023811	–0.136192
41	H	–1.711142	5.050718	–1.598187
42	C	–1.688736	3.868699	0.217597
43	H	–1.558962	4.05719	1.290929
44	H	–2.731826	3.604767	0.031563
45	C	–0.957758	1.457791	–0.117049
46	C	–2.15642	0.936584	0.681575
47	H	–2.998003	1.628222	0.635801
48	C	–3.833224	–0.400685	–0.523601
49	C	–5.142098	–1.969445	–1.915869
50	C	–4.756608	–3.331764	–2.49854
51	H	–3.896386	–3.236384	–3.168003
52	H	–5.595285	–3.745054	–3.067438
53	H	–4.497771	–4.034741	–1.701064
54	C	–6.305622	–2.110183	–0.928515
55	H	–6.037999	–2.79766	–0.119435
56	H	–7.176155	–2.522704	–1.449712
57	H	–6.579691	–1.145668	–0.498932
58	C	–5.443953	–0.966515	–3.034606
59	H	–5.707536	0.010964	–2.628543
60	H	–6.281164	–1.334605	–3.637277
61	H	–4.575074	–0.85768	–3.691955
62	C	1.484149	–2.171024	0.60134
63	H	0.938402	–1.46848	1.243834
64	H	1.007388	–2.127766	–0.385591
65	C	1.340496	–3.593979	1.177508
66	H	1.918442	–4.284573	0.548481
67	C	1.872466	–3.707688	2.615114
68	H	2.945166	–3.503092	2.674904
69	H	1.709194	–4.717479	3.0079
70	H	1.353608	–3.005109	3.279926
71	C	–0.13243	–4.029246	1.108752
72	H	–0.514998	–3.994235	0.082404
73	H	–0.764304	–3.37727	1.725292
74	H	–0.256918	–5.053281	1.477749
75	C	–1.707041	0.761405	2.174927
76	H	–1.052736	–0.116825	2.220637
77	H	–1.090771	1.627046	2.446956
78	C	–3.550688	1.811834	3.39888
79	H	–2.901524	2.684763	3.528139
80	H	–4.133177	1.690138	4.31854
81	H	–4.264453	2.022071	2.580573
82	C	–3.531401	–0.601936	3.149659
83	H	–4.301319	–0.614377	2.360954
84	H	–4.036261	–0.72416	4.115148
85	H	–2.873171	–1.46254	2.99926

Calculation Type = FREQ
Calculation Method = RB3LYP
Basis Set = 6-31+G(d,p)
Charge = 0
Spin = Singlet
E(RB3LYP) = –1819.62621480 a.u.
RMS Gradient Norm = 0.00000240 a.u.
Imaginary Freq = 0
Dipole Moment = 4.8642 Debye
Point Group = C1
Job cpu time: 4 days 5 hours 47 minutes 9.7 seconds.

Calculation Type = SP
Calculation Method = RM062X
Basis Set = 6-311++G(2d,3p)
Charge = 0
Spin = Singlet
E(RM062X) = –1819.33477044 a.u.
Dipole Moment = 4.8658 Debye
Point Group = C1
Job cpu time: 1 days 5 hours 2 minutes 34.3 seconds.

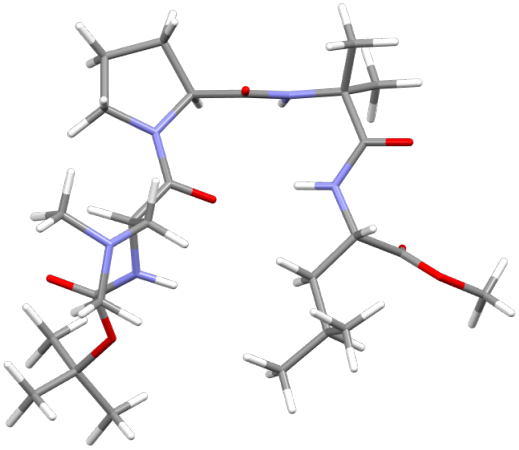

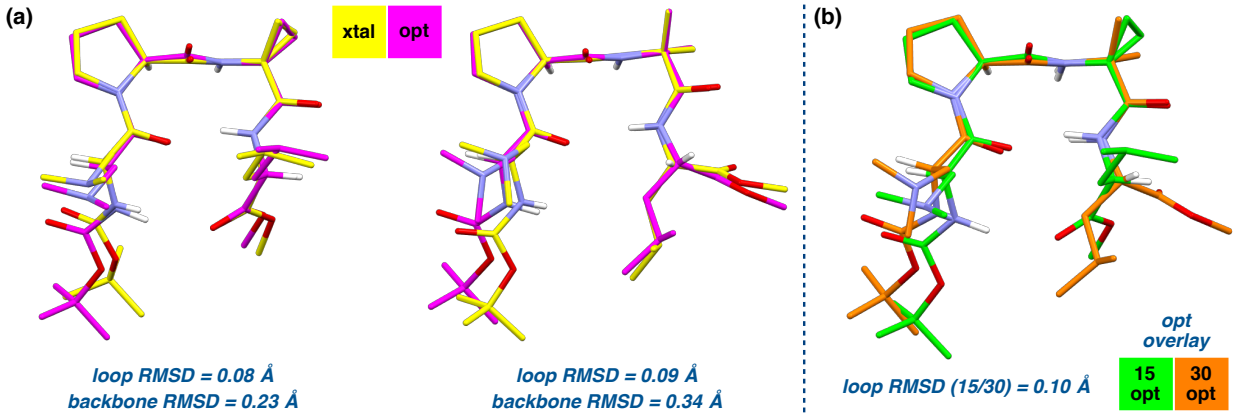

Figure S6.07: (a) Overlays of the X-ray crystal structures **15** and **30** with the corresponding DFT-optimized structures. Loop and backbone RMSDs are provided. **(b)** Overlay of the optimized structures of **15** and **30**.

VII. Catalyst-Substrate Titration Data

A. General Information

Data were acquired for this catalyst-substrate titration study according to the NMR methods detailed in Section V. Characterization and NMR spectra of quinazolinones **1** and **38** and mixtures **3+1** and **3+38** are provided in this section.

B. Complex 3+1

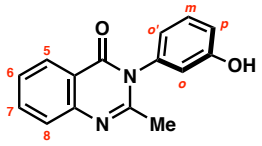

1

Full ^{1}H-NMR Characterization of Substrate 1 (600 MHz, 0.01 M in C_6D_6, 25 ºC)**:** d 8.41 (dd, *J* = 7.9, 1.5 Hz, 1H, **5**), 7.73 (d, *J* = 8.2 Hz, 1H, **8**), 7.27 (ddd, *J* = 8.4, 7.1, 1.6 Hz, 1H, **7**), 7.06–6.96 (m, 1H, **6**), 6.94 (t, *J* = 8.0 Hz, 1H, ***m***), 6.68 (dd, *J* = 8.1, 2.4 Hz, 1H, ***o'***), 6.60 (s, 1H, **OH**), 6.39 (t, *J* = 2.2 Hz, 1H, ***o***), 6.18 (dd, *J* = 7.8, 1.9 Hz, 1H, ***p***), 1.89 (s, 3H, **Me**).

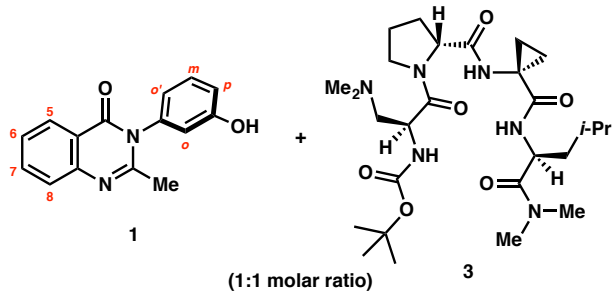

1 **3**

(1:1 molar ratio)

Full ^{1}H-NMR Characterization of 3+1 Complex (600 MHz, 0.01 M in C_6D_6, 25 ºC)**:** δ 8.46 (dd, *J* = 8.0, 1.5 Hz, 1H, **5**), 8.10 (d, *J* = 8.8 Hz, 1H, N*H*$_{Leu}$), 7.76 (d, *J* = 7.9 Hz, 1H, **8**), 7.67 (s, 1H, N*H*$_{Acpc}$), 7.41 (d, *J* = 8.0 Hz, 1H, N*H*$_{Dmaa}$), 7.32 (ddd, *J* = 8.4, 7.1, 1.5 Hz, 1H, **7**), 7.13–7.09 (m, 1H, **6**), 7.06–6.97 (m, 1H, ***m***), 6.89 (ddd, *J* = 8.4, 2.4, 1.1 Hz, 1H, ***o'***), 6.73 (q, *J* = 2.4 Hz, 1H, ***o***), 6.26–6.20 (m, 1H, ***p***), 5.15 (td, *J* = 9.4, 4.8 Hz, 1H, α_{Leu}), 4.69 (dd, *J* = 14.5, 6.4 Hz, 1H, α_{Dmaa}), 3.98 (dd, *J* = 8.3, 4.5 Hz, 1H, $\alpha_{D\text{-}Pro}$), 3.77 (q, *J* = 7.4 Hz, 1H, $\delta_{D\text{-}Pro}$), 3.40 (dt, *J* = 9.8, 6.6 Hz, 1H, $\delta'_{D\text{-}Pro}$), 3.14 (t, *J* = 10.8 Hz, 1H, β_{Dmaa}), 2.69 (s, 3H, NMe_{Leu}), 2.58 (s, 3H, NMe'_{Leu}), 2.39 (dd, *J* = 12.2, 4.7 Hz, 1H, β'_{Dmaa}), 2.08 (s, 6H, 2x NMe_{Dmaa}), 2.05 (s, 3H, **Me**), 2.03–1.92 (m, 1H, β_{Leu}), 1.92 (dd, *J* = 13.1, 3.1 Hz, 1H, β_{Acpc}), 1.91–1.83 (m, 1H, β'_{Acpc}), 1.74–1.63 (m, 3H, γ_{Leu} + $\beta_{D\text{-}Pro}$ + $\gamma_{D\text{-}Pro}$), 1.50 (s, 9H, *t*-Bu_{Dmaa}), 1.48–1.38 (m, 2H, β'_{Leu} + $\beta'_{D\text{-}Pro}$), 1.39–1.20 (m, 1H, $\gamma'_{D\text{-}Pro}$), 1.16–1.01 (m, 2H, β''_{Acpc}), 0.83 (d, *J* = 6.6 Hz, 6H, δ_{Leu}). ***Note:** Quinazolinone **1** is completely soluble in C_6D_6 in the presence of equimolar **3**, while it is only partially soluble alone at 0.01 M in C_6D_6.

^{1}H-NMR (600 MHz, 0.01 M in C_6D_6, 25 °C)

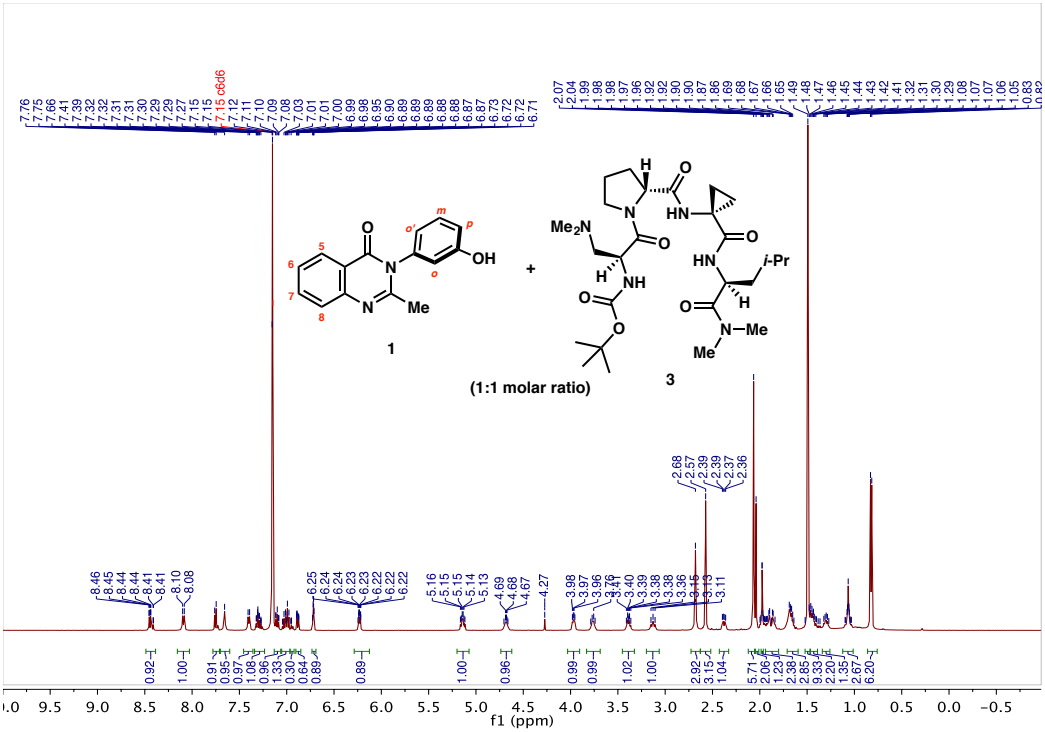

COSY (600 MHz, 0.01 M in C_6D_6, 25 °C)

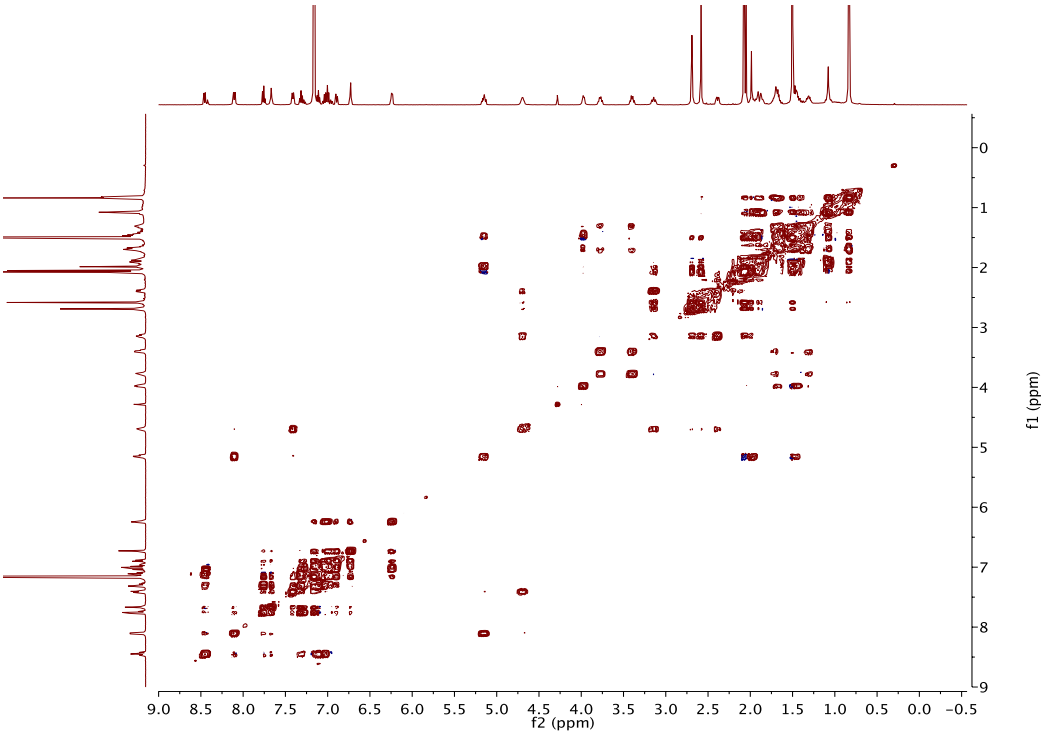

NOESY (600 MHz, 0.01 M in C_6D_6, 25 °C)

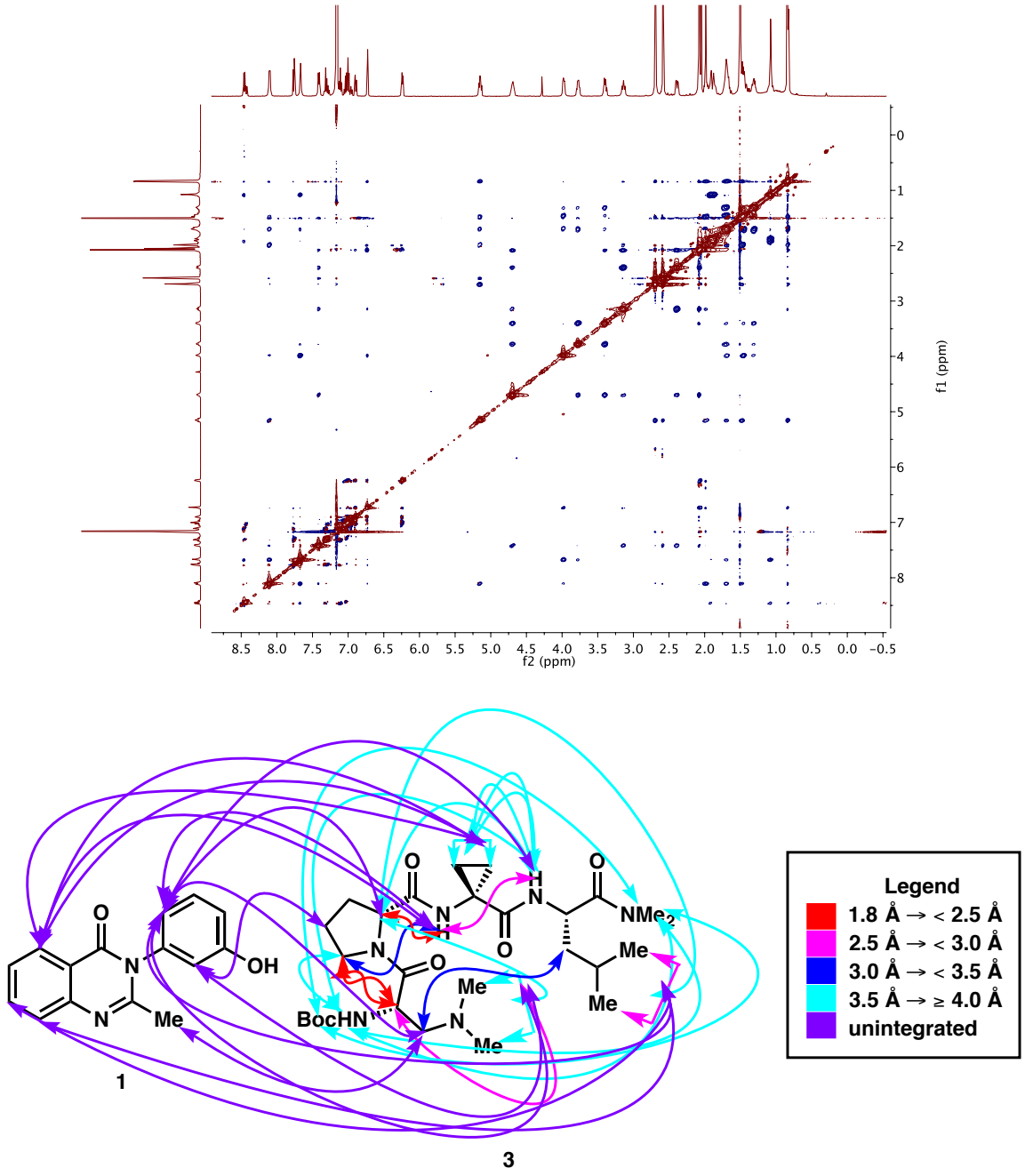

Figure S7.01: Inter-residue and Intermolecular nOe Map for Peptide **3**+**1**

Table S7.02: Integrated NOESY Cross-peaks for Peptide **3**+**1**

	f2	f1	Normalized	Absolute	Assignment	Distance (Absolute)
1	8.1	1.91	–0.02	–0.05	LeuNH-AcpcHB2b	4.71
	1.91	8.11	–0.02	–0.05		
2	8.1	2.58	–0.05	–0.11	LeuNH-LeuNMe1	4.13
	2.57	8.11	–0.05	–0.11		
3	8.1	1.08	–0.03	–0.07	LeuNH-AcpcHB1	4.51
	1.08	8.1	–0.03	–0.06		
4	8.1	1.87	–0.03	–0.06	LeuNH-AcpcHB2a	4.57
	1.86	8.11	–0.03	–0.06		
5	8.1	2.69	–0.04	–0.08	LeuNH-LeuNMe2	4.35
	2.69	8.11	–0.04	–0.08		
6	8.1	2.08	–0.04	–0.09	LeuNH-DmaaMe	4.27
	2.09	8.11	–0.05	–0.09		
7	8.1	1.69	–0.52	–1.08	LeuNH-LeuHC	2.82
	1.69	8.1	–0.51	–1.07		
8	8.1	7.67	–1	–2.08	LeuNH-AcpcNH	2.53
	7.67	8.1	–1	–2.09		
9	8.1	1.98	–1.04	–2.18	LeuNH-LeuHB2	2.51
	1.98	8.11	–1.06	–2.2		
10	8.1	3.98	–0.11	–0.24	LeuNH-DProHA	3.61
	3.97	8.1	–0.12	–0.25		
11	8.1	7.41	–0.1	–0.2	LeuNH-DmaaNH	3.69
	7.41	8.1	–0.11	–0.23		
12	7.67	3.78	–0.15	–0.31	AcpcNH-DProHD2	3.45
	3.77	7.67	–0.16	–0.33		
13	7.67	1.88	–0.01	–0.02	AcpcNH-AcpcHB2a	5.28
	1.87	7.67	–0.02	–0.03		
14	7.67	1.91	–0.03	–0.07	AcpcNH-AcpcHB2b	4.51
	1.91	7.67	–0.03	–0.06		
15	7.67	2.08	–0.02	–0.04	AcpcNH-DmaaMe	4.71
	2.08	7.66	–0.03	–0.06		
16	7.66	3.97	–2.59	–5.4	AcpcNH-DProHA	2.16
	3.97	7.67	–2.61	–5.43		
17	7.42	2.08	–0.18	–0.37	DmaaNH-DmaaMe	3.42
	2.07	7.4	–0.15	–0.31		
18	7.41	2.59	–0.21	–0.43	DmaaNH-LeuNMe1	3.28
	2.58	7.41	–0.21	–0.44		

19	7.41	2.39	–0.51	–1.06	DmaaNH-DmaaHB1	2.83
	2.38	7.41	–0.51	–1.07		
20	7.41	3.79	–0.06	–0.13	DmaaNH-DProHD2	3.99
	3.77	7.41	–0.07	–0.14		
21	7.41	2.69	–0.03	–0.07	DmaaNH-LeuNMe2	4.45
	2.69	7.41	–0.03	–0.07		
22	7.41	3.15	–0.47	–0.99	DmaaNH-DmaaHB2	2.86
	3.14	7.41	–0.47	–0.98		
23	5.15	0.83	–2.01	–4.19	LeuHA-LeuHD	2.25
	0.83	5.15	–2	–4.18		
24	5.15	2.58	–0.43	–0.89	LeuHA-LeNMe1	2.93
	2.58	5.15	–0.4	–0.84		
25	5.15	2.69	–2.59	–5.4	LeuHA-LeuNMe2	2.16
	2.69	5.15	–2.61	–5.43		
26	4.69	3.77	–1.76	–3.68	DmaaHA-DProHD2	2.30
	3.77	4.7	–1.77	–3.7		
27	4.69	2.07	–1.68	–3.51	DmaaHA-DmaaMe	2.32
	2.08	4.69	–1.68	–3.5		
28	4.68	3.39	–2.4	–5	DmaaHA-DProHD1	2.19
	3.39	4.69	–2.39	–4.99		
29	3.98	2.08	–0.03	–0.06	DProHA-DmaaMe	4.57
	2.08	3.98	–0.03	–0.06		
30	3.98	0.84	–0.07	–0.14	DProHA-LeuHD	3.96
	0.83	3.98	–0.07	–0.14		
31	3.98	1.08	–0.02	–0.05	DProHA-AcpcHB1	4.79
	1.08	3.98	–0.02	–0.04		
32	3.97	1.31	–0.28	–0.59	DProHA-DProHC1	3.12
	1.31	3.97	–0.28	–0.59		
33	3.97	3.4	–0.1	–0.21	DProHA-DProHD1	3.71
	3.39	3.98	–0.1	–0.21		
34	3.4	1.45	–0.27	–0.57	DProHD1-LeuHB1	3.12
	1.45	3.4	–0.29	–0.61		
35	3.14	1.98	–0.27	–0.56	DmaaHB2-LeuHB2	3.14
	1.98	3.14	–0.28	–0.58		
36	3.14	2.08	–1.75	–3.64	DmaaHB2-DmaaMe	2.30
	2.08	3.14	–1.77	–3.68		
37	3.13	0.84	–0.12	–0.25	DmaaHB2-LeuHD	3.58
	0.83	3.14	–0.13	–0.27		

38	2.69	0.83	–0.41	–0.85	LeuNMe2-LeuHD	2.92
	0.83	2.69	–0.43	–0.9		
39	2.68	1.45	–0.15	–0.32	LeuNMe2-LeuHB1	3.42
	1.46	2.69	–0.17	–0.36		
40	2.68	1.51	–0.2	–0.42	LeuNMe2-BocMe	3.28
	1.5	2.69	–0.22	–0.46		
41	2.58	1.51	–0.46	–0.96	LeuNMe1-BocMe	2.87
	1.5	2.58	–0.48	–1		
42	2.38	1.5	–0.15	–0.32	DmaaHB1-BocMe	3.37
	1.5	2.39	–0.2	–0.42		
43	2.06	0.83	–0.42	–0.88	DmaaHB1-DmaaMe	2.92
	0.83	2.07	–0.42	–0.87		
44	3.77	3.39	–7.67	–15.97	DProHD1-DProHD2	1.80
	3.39	3.77	–7.68	–16		

C. Complex 3+38

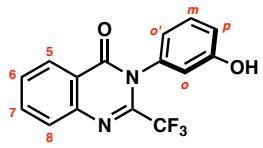

38

Full ^{1}H-NMR Characterization of Substrate 38: (600 MHz, 0.01 M in C_6D_6, 25 ºC) δ 8.23 (dd, *J* = 8.0, 1.5 Hz, 1H, **5**), 7.65 (dt, *J* = 8.1, 0.8 Hz, 1H, **8**), 7.16–7.13 (m, 1H, **7**), 6.97 (ddd, *J* = 8.2, 7.3, 1.2 Hz, 1H, **6**), 6.92 (t, *J* = 8.1 Hz, 1H, ***m***), 6.52 (ddd, *J* = 8.3, 2.4, 0.9 Hz, 1H, ***o′***), 6.45 (ddt, *J* = 7.9, 2.0, 1.0 Hz, 1H, **O*H***), 6.41 (d, *J* = 2.3 Hz, 1H, ***o***), 5.10 (s, 1H, ***p***).

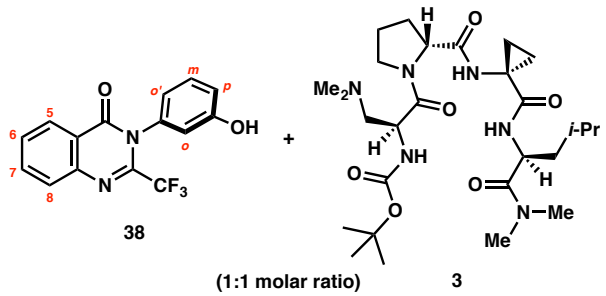

38 (1:1 molar ratio) 3

Full ^{1}H-NMR Characterization of 3+38 Complex (600 MHz, 0.01 M in C_6D_6, 25 ºC)**:** δ 8.30 (dd, *J* = 41.2, 8.3 Hz, 1H, **5**), 8.12 (d, *J* = 8.7 Hz, 1H, N*H*$_{Leu}$), 7.68 (dd, *J* = 15.6, 8.1 Hz, 1H, **8**), 7.47–7.36 (m, 1H, N*H*$_{Dmaa}$), 7.24–7.18 (m, 1H, **7**), 7.13–7.07 (m, 1H, **6**), 7.07–6.98 (m, 1H, ***m***), 6.96–6.90 (m, 2H, ***o′***, ***p***), 6.89 (s, 1H, N*H*$_{Acpc}$), 6.48 (dd, *J* = 31.2, 7.7 Hz, 1H, ***o***), 5.08 (td, *J* = 9.5, 4.9 Hz, 1H, α_{Leu}), 4.79–4.63 (m, 1H, α_{Dmaa}), 3.99–3.86 (m, 1H, $\alpha_{D\text{-}Pro}$), 3.76 (t, *J* = 9.8, 6.6 Hz, 1H, $\delta_{D\text{-}Pro}$), 3.51–3.34 (m, 1H, $\delta'_{D\text{-}Pro}$), 3.22–3.05 (m, 1H, β_{Dmaa}), 2.68 (s, 3H, NMe$_{Leu}$), 2.57 (s, 3H, NMe′$_{Leu}$), 2.37–2.31 (m, 1H, β'_{Dmaa}), 2.07 (s, 6H, 2x NMe$_{Dmaa}$), 1.93–1.82 (m, 3H, β_{Leu}, β_{Acpc}, β'_{Acpc}), 1.77–1.69 (m, 1H, γ_{Leu}), 1.69–1.58 (m, 1H, $\beta_{D\text{-}Pro}$), 1.50 (s, 9H, *t*-Bu$_{Dmaa}$), 1.48–1.37 (m, 3H, $\gamma_{D\text{-}Pro}$, β'_{Leu}, $\beta'_{D\text{-}Pro}$), 1.37–1.25 (m, 1H, $\gamma'_{D\text{-}Pro}$), 1.14–0.95 (m, 2H, β''_{Acpc}), 0.86–0.63 (m, 6H, δ_{Leu}).

^{1}H-NMR (600 MHz, 0.01 M in C_6D_6, 25 °C)

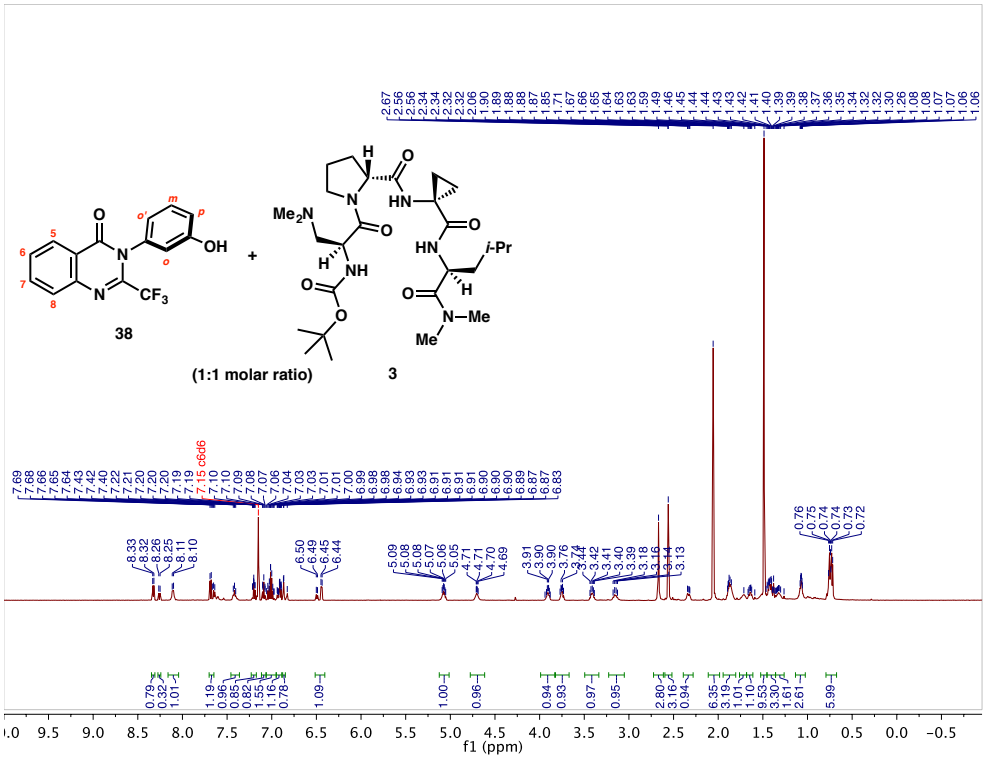

COSY (600 MHz, 0.01 M in C_6D_6, 25 °C)

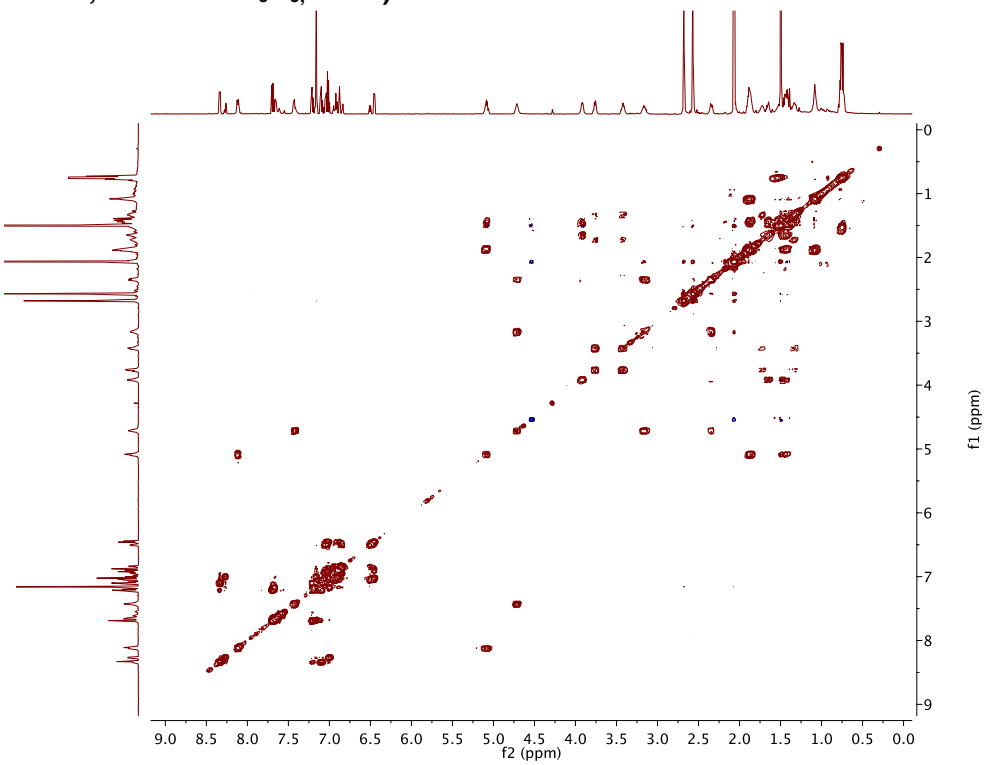

NOESY (600 MHz, 0.01 M in C_6D_6, 25 °C)

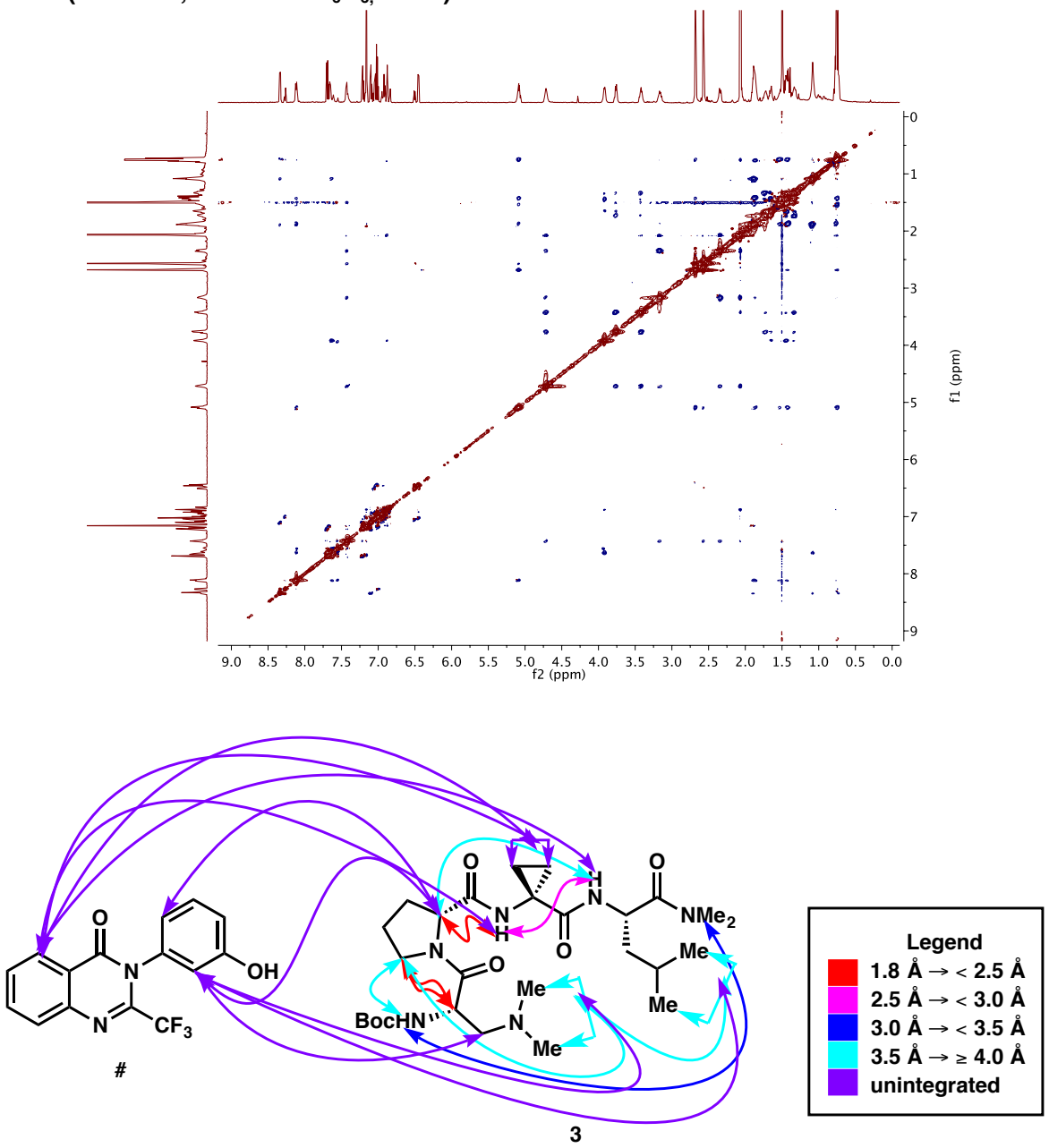

Figure S7.02: Inter-residue and Intermolecular nOe Map for Peptide **3**+**38**

Table S7.02: Integrated NOESY Cross-peaks for Peptide **3**+**38**

	f2	f1	Normalized	Absolute	Assignment	Distance (Absolute)
1	8.12	1.55	–0.51	–0.46	LeuNH-LeuHC	3.13
	1.54	8.12	–0.53	–0.48		
2	8.12	7.64	–0.85	–0.77	LeuNH-AcpcNH	2.85
	7.64	8.12	–0.99	–0.9		
3	8.12	2.68	–0.16	–0.15	LeuNH-LeuNMe2	4.21
	2.68	8.12	–0.01	–0.01		
4	8.12	3.92	–0.21	–0.19	LeuNH-DProHA	3.66
	3.92	8.12	–0.2	–0.18		
5	7.63	3.92	–3.96	–3.59	AcpcNH-DProHA	2.23
	3.92	7.63	–3.98	–3.61		
6	7.63	1.08	–1.43	–1.3	AcpcNH-AcpcHB2	2.58
	1.08	7.65	–1.88	–1.71		
7	7.42	3.77	–0.2	–0.18	DmaaNH-DProHD2	3.71
	3.76	7.43	–0.18	–0.16		
8	7.42	3.17	–1.09	–0.99	DmaaNH-DmaaHB2	2.77
	3.15	7.43	–1.1	–1		
9	7.42	2.35	–1.15	–1.04	DmaaNH-DmaaHB1	2.74
	2.35	7.42	–1.19	–1.08		
10	7.42	2.57	–0.57	–0.51	DmaaNH-LeuNMe1	3.03
	2.58	7.44	–0.7	–0.64		
11	5.09	2.68	–4.61	–4.18	LeuHA-LeuNMe2	2.17
	2.69	5.08	–4.71	–4.27		
12	5.09	0.75	–3.61	–3.28	LeuHA-LeuHD	2.27
	0.76	5.1	–3.48	–3.16		
13	5.09	2.57	–0.43	–0.39	LeuHA-LeuNMe1	3.23
	2.57	5.09	–0.43	–0.39		
14	5.09	1.54	–0.99	–0.9	LeuHA-LeuHC	2.93
	1.53	5.08	–0.57	–0.52		
15	4.71	3.76	–3.57	–3.24	DmaaHA-DProHD2	2.27
	3.76	4.71	–3.55	–3.22		
16	4.71	3.42	–4.8	–4.35	DmaaHA-DProHD1	2.16
	3.42	4.71	–4.88	–4.42		
17	4.71	2.07	–3.96	–3.59	DmaaHA-DmaaMe	2.23
	2.08	4.71	–4.11	–3.73		
18	3.92	1.34	–0.55	–0.5	DProHA-DProHC1	3.09
	1.33	3.92	–0.59	–0.53		

19	3.76	1.65	–0.65	–0.59	DProHD2-DProHB2	3.01
	1.65	3.76	–0.67	–0.61		
20	3.42	2.07	–0.69	–0.62	DProHD1-DmaaMe	2.92
	2.08	3.42	–0.92	–0.83		
21	3.17	2.08	–4.48	–4.06	DmaaHB2-DmaaMe	2.17
	2.08	3.16	–5.05	–4.58		
22	2.68	0.75	–0.85	–0.77	LeuNMe-LeuHD	2.76
	0.76	2.66	–1.38	–1.26		
23	2.34	2.06	–3.19	–2.89	DmaaHB1-DmaaMe	2.31
	2.08	2.33	–3.23	–2.93		
24	2.06	0.77	–0.74	–0.67	DmaaMe-LeuHD	2.93
	0.75	2.08	–0.82	–0.74		
25	1.43	0.76	–3.81	–3.45	LeuHB1-LeuHD	2.24
	0.75	1.43	–3.94	–3.57		
26	3.76	3.42	–14.34	–13	DProHD1-DProHD2	1.80
	3.41	3.76	–14.53	–13.18		

D. Chemical Shift Analysis of 3+1 and 3+38

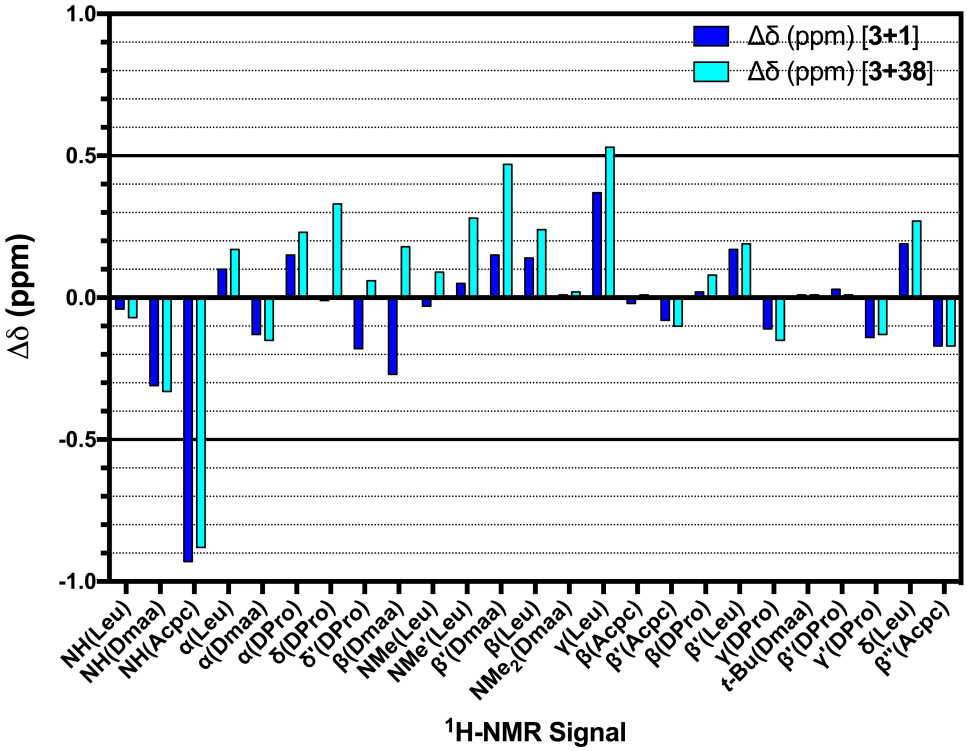

Figure S7.03: Chemical shift analysis of peptide **3** in complexes **3+1** and **3+38**. Negative Δδ values indicate downfield shifts.

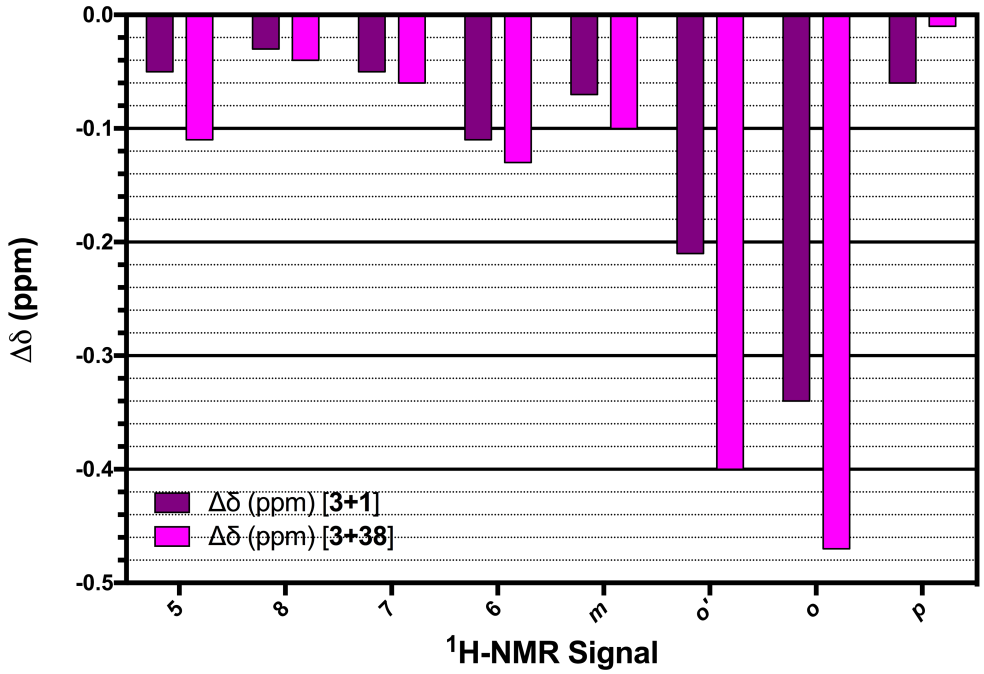

Figure S7.04: Chemical shift analysis of quinazolinones **1** and **38** in complexes **3+1** and **3+38**. Negative Δδ values indicate downfield shifts.

VIII. Atroposelective Bromination Data

A. Synthesis of 3-Arylquinazolinone 1[4,5]

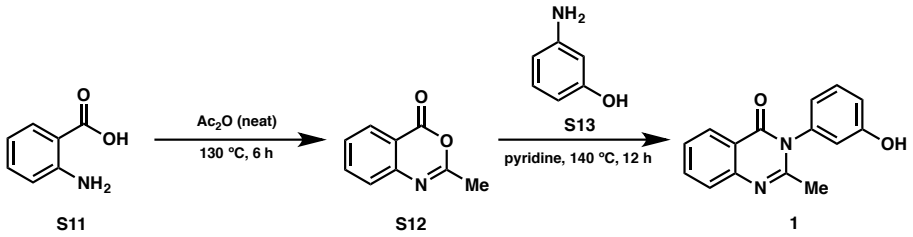

S11 S12 1

2-Methyl-4*H*-benzo-[*d*][1,3]oxazin-4-one (S12):[42] Anthranilic acid (**S11**, 8.23 g, 60.0 mmol) was added to an oven-dried 40 mL sealed tube (thick-walled) equipped with a magnetic stir bar. The off-white solid was suspended in acetic anhydride (36 mL, 380 mmol), and the vessel was purged with nitrogen, sealed tightly, and submerged into an oil bath at 130 ºC. The cloudy suspension quickly became a clear, deep yellow solution, which was allowed to stir at 130 °C for 6 h. The reaction solution was allowed to cool to room temperature, and the contents of the sealed tube were transferred to a round bottom flask washing with copious PhMe. Removal of solvent under reduced pressure yielded benzoxazinone **S12** (9.50 g, 98% yield) which was used without further purification.

3-(3-Hydroxyphenyl)-2-methylquinazolin-4(3*H*)-one (1):[43] Benzoxazinone **S12** (2.99 g, 18.6 mmol) and *m*-aminophenol (**S13**, 2.43 g, 22.3 mmol) were added to an oven-dried 40 mL sealed tube (thick-walled) equipped with a magnetic stir bar. The solid mixture was dissolved in pyridine (16.7 mL, 1.2 M w.r.t. **S12**). The vessel was purged with nitrogen, sealed tightly, and submerged in an oil bath at 145 °C. The cloudy, deep red suspension began to clarify upon heating. The deep red solution was allowed to stir for 12 h at 145 ºC, after which the vessel was cooled to room temperature. The contents of the sealed tube were transferred to a round bottom flask, washing with copious PhMe, and the solvent was removed under reduced pressure. The crude product was purified by automated flash chromatography using a gradient of 10–100% EtOAc/hexanes. Fractions were pooled and concentrated *in vacuo* to provide a pale yellow solid, which was suspended in hot CH_2Cl_2 and vacuum filtered to remove insoluble side-products. The filtrate was allowed to cool to 0 ºC, precipitating 2.56 g (61% yield) of pure **1** as a white solid. **TLC:** R_f = 0.21 (50% EtOAc/hexanes). **IR** (FT-ATR, cm^{-1}): 3310, 3090, 2819, 1661, 1591, 1570, 1291, 1112, 933. **^{1}H-NMR** (400 MHz, DMSO-d_6): δ 9.85 (s, 1H), 8.10 (dd, *J* = 7.9, 1.5 Hz, 1H), 7.84 (ddd, *J* = 8.4, 7.1, 1.6 Hz, 1H), 7.66 (dd, *J* = 8.3, 1.1 Hz, 1H), 7.52 (ddd, *J* = 8.3, 7.2, 1.2 Hz, 1H), 7.36 (t, *J* = 8.0 Hz, 1H), 6.92 (ddd, *J* = 8.3, 2.4, 1.0 Hz, 1H), 6.84 (ddd, *J* = 7.8, 2.0, 0.9 Hz, 1H), 6.80 (t, *J* = 2.1 Hz, 1H), 2.17 (s, 3H). **^{13}C-NMR** (151 MHz, DMSO-d_6): δ 161.6, 158.7, 154.9, 147.7, 139.2, 134.9, 130.7, 127.1, 126.8, 126.7, 120.9, 119.2, 116.4, 115.8, 24.2. **HRMS:** Exact mass calculated for $[C_{15}H_{12}N_2O_2 + H]^+$ requires *m/z* = 253.0977. Found 253.0975 (ESI+).

B. Peptide Screening Procedure[4,5]

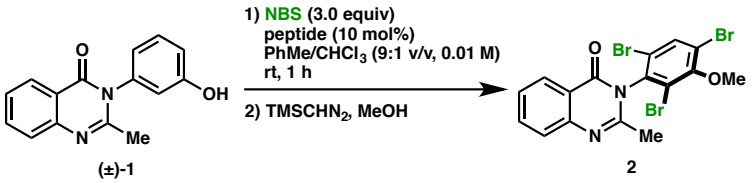

To an oven-dried 20 mL vial equipped with a magnetic stir bar was added 3-(3-hydroxyphenyl)-2-methyl-quinazolin-4(3*H*)-one (**1**, 12.6 mg, 0.050 mmol) and peptide catalyst (0.005 mmol, 10 mol% w.r.t. **1**). The solid mixture was suspended in 5 mL of PhMe/$CHCl_3$ (9:1 v/v, 0.01 M w.r.t. **1**), and the resulting suspension was allowed to stir vigorously at rt. *N*-Bromosuccinimide (NBS, 26.7 mg, 0.15 mmol, 3.0 equiv w.r.t. **1**) was added in one portion to the stirring solution at rt. The vial was sealed with a cap, and the reaction solution was allowed to stir for 60 minutes. (Note: A color change from colorless to yellow was observed within 15 minutes. In some cases, the clear yellow or pale yellow reaction solutions turned cloudy.) The reaction was quenched by addition of 1 mL of MeOH followed by (trimethylsilyl)diazomethane solution ($TMSCHN_2$, 2.0 M in hexanes) until the bright yellow color persisted in solution (Note: the yellow reaction solution became clear and colorless before turning bright yellow). The solution was allowed to stir 15–20 minutes at rt, after which glacial acetic acid was added dropwise until the solution became clear and colorless. The solvent was removed *in vacuo*, and the crude reaction mixture was purified by flash chromatography through a pipette silica plug (1 x 6 cm SiO_2) washing with EtOAc/hexanes (1:1 v/v). The fractions were pooled and concentrated *in vacuo*. The resulting white foam (or clear oil) was dried thoroughly on high vacuum to provide 3-(2,4,6-tribromo-3-methoxyphenyl)-2-methyl-quinazolin-4(3*H*)-one (**2**), which was analyzed by chiral HPLC to assess the enantioselectivity of the reaction. **Chiral HPLC** (Chiralcel OJ-H column, 10% EtOH/hexanes eluent, 2 μL injection, 1 mL/min flow rate, regulated at 20 °C, 230 nm)**:** major enantiomer t_R = 9.7 min, minor enantiomer t_R = 12.6 min.

Note: Conversion of **1** was always complete, and thus only er/ee values were tabulated in Table 7.01.

C. Tabulated ee vs. τ(*i*+2) Data[44]

Table S8.01: ee, er, and $\Delta\Delta G^{\ddagger}$ as a Function of τ(*i*+2)

i+2 Residue	Peptide Sequence	τ(*i*+2)	Average τ(*i*+2)	major	minor	er	ee (%)	log er	$\Delta\Delta G^{\ddagger}$(kcal/mol)
Acpc	Boc-Dmaa-D-Pro-Acpc-Leu-NMe_2 (**3a**)	118.1							
	Boc-Dmaa-D-Pro-Acpc-Leu-NMe_2 (**3b**)	116.5	117.3	92.0	8.0	11.5	83.9	1.06	1.43
	Boc-Dmaa-D-Pro-Acpc-Leu-NMe_2 (**3c**)	117.4							
	Boc-Dmaa-D-Pro-Acpc-Leu-OMe (**4a**)	117.0							
	Boc-Dmaa-D-Pro-Acpc-Leu-OMe (**4b**)	117.7							
	Boc-Dmaa-D-Pro-Acpc-Leu-OMe (**4c**)	117.0	117.4	94.6	5.4	17.5	89.1	1.24	1.68
	Boc-Dmaa-D-Pro-Acpc-Leu-OMe (**4d**)	117.3							
	Boc-Dmaa-D-Pro-Acpc-Leu-OMe (**4e**)	118.0							
	Boc-Dmaa-D-Pro-Acpc-Gly-OMe (**7a**)	117.0	116.4	88.9	11.1	8.0	77.7	0.90	1.22
	Boc-Dmaa-D-Pro-Acpc-Gly-OMe (**7b**)	115.7							
	Boc-Dmaa-D-Pro-Acpc-Nle-NMe_2 (**8**)	117.4	117.4	92.4	7.6	12.2	84.7	1.08	1.46
	Boc-Dmaa-D-Pro-Acpc-Val-NMe_2 (**9**)	117.7	117.7	93.6	6.4	14.6	87.1	1.17	1.57
	Boc-Dmaa-D-Pro-Acpc-Val-OMe (**10**)	117.2	117.2	90.9	9.1	10.0	81.8	1.00	1.35
	Boc-Dmaa-D-Pro-Acpc-Chg-NMe_2 (**11**)	117.4	117.4	93.0	7.0	13.3	85.9	1.12	1.52
	Boc-Dmaa-D-Pro-Acpc-Phe-NMe_2 (**12**)	116.9	116.9	88.1	11.9	7.4	76.1	0.87	1.17
	Boc-Dmaa-D-Pro-Acpc-Phe-OMe (**13**)	116.9	116.9	85.8	14.2	6.0	71.6	0.78	1.05
Acbc	Boc-Dmaa-D-Pro-Acbc-Leu-NMe_2 (**16a**)	111.8							
	Boc-Dmaa-D-Pro-Acbc-Leu-NMe_2 (**16b**)	114.4	112.9	85.0	15.0	5.7	70.0	0.75	1.02
	Boc-Dmaa-D-Pro-Acbc-Leu-NMe_2 (**16c**)	112.5							
	Boc-Dmaa-D-Pro-Acbc-Leu-OMe (**17a**)	112.3	112.3	82.9	17.1	4.8	65.7	0.69	0.93
	Boc-Dmaa-D-Pro-Acbc-Leu-OMe (**17b**)	112.3							
Aic	Boc-Dmaa-D-Pro-Aic-Leu-OMe (**19a**)	110.6	107.6	60.9	39.1	1.6	21.3	0.19	0.26
	Boc-Dmaa-D-Pro-Aic-Leu-OMe (**19b**)	104.5							
Cle	Boc-Dmaa-D-Pro-Cle-Leu-OMe (**18a**)	111.7	111.5	70.1	29.9	2.3	40.1	0.37	0.50
	Boc-Dmaa-D-Pro-Cle-Leu-OMe (**18b**)	111.3							
Achc	Boc-Dmaa-D-Pro-Achc-Leu-OMe (**22a**)	110.8	110.3	68.1	31.9	2.1	36.2	0.33	0.44
	Boc-Dmaa-D-Pro-Achc-Leu-OMe (**22b**)	109.8							
Aib	Boc-Dmaa-D-Pro-Aib-Leu-NMe_2 (**24**)	112.0	112.0	74.8	25.2	3.0	49.5	0.47	0.64
	Boc-Dmaa-D-Pro-Aib-Leu-OMe (**25**)	111.7	111.7	67.5	32.5	2.1	34.9	0.32	0.43
	Boc-Dmaa-D-Pro-Aib-Val-OMe (**26**)	112.0	112.0	67.8	32.2	2.1	35.6	0.32	0.44
	Boc-Dmaa-D-Pro-Aib-Phe-OMe (**27**)	111.0	111.0	65.8	34.2	1.9	31.5	0.28	0.38
	Boc-Dmaa-D-Pro-Aib-2-Thi-NMe_2 (**29a**)	110.9	111.3	71.2	28.8	2.5	42.3	0.39	0.53
	Boc-Dmaa-D-Pro-Aib-2-Thi-NMe_2 (**29b**)	111.6							
Mono	Boc-Dmaa-D-Pro-Ala-Phe-OMe (**31**)	111.8	111.8	71.7	28.3	2.5	43.3	0.40	0.54
Gly	Boc-Dmaa-D-Pro-Gly-Leu-OMe (**33a**)	115.7	115.6	91.0	9.0	10.1	81.4	1.00	1.36
	Boc-Dmaa-D-Pro-Gly-Leu-OMe (**33b**)	115.4							

Note: $\Delta\Delta G^{\ddagger}$ values were calculated using the following formula, where R = 1.99 x 10^{-3} kcal/(mol*K) and T = 298.15 K:

$$-\Delta\Delta G^{\ddagger} = \mathrm{RT}\ln(\mathrm{er})$$

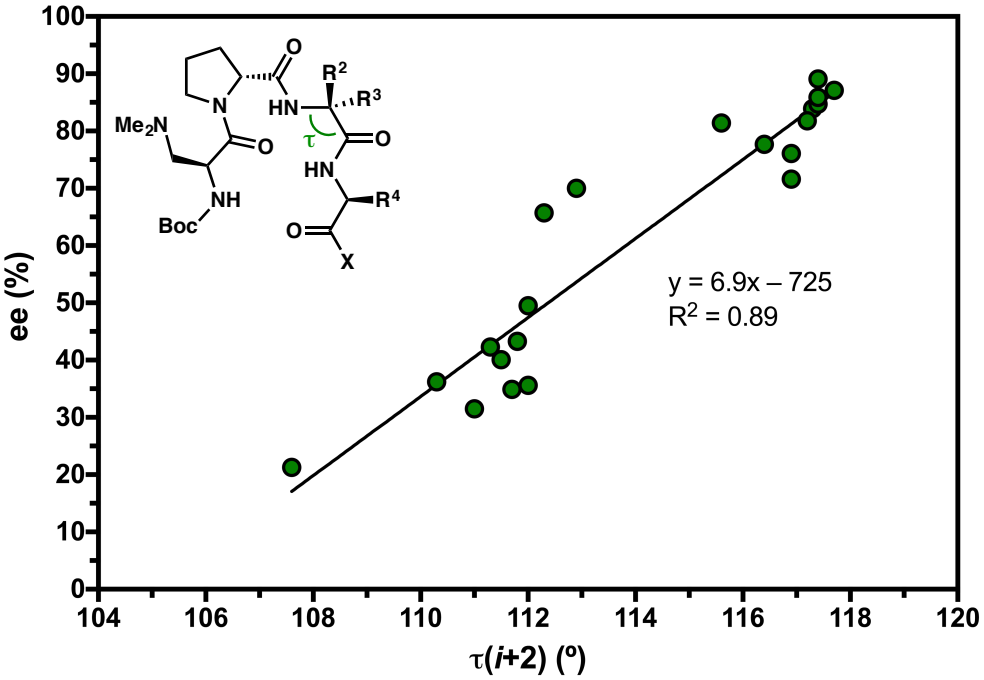

Figure S8.01: A plot of ee vs. τ(*i*+2) reveals a linear correlation. This chart is reproduced from Figure 20 in the manuscript. Only peptides corresponding to the scheme provided (top right corner) in were considered for this analysis (Table S8.01).

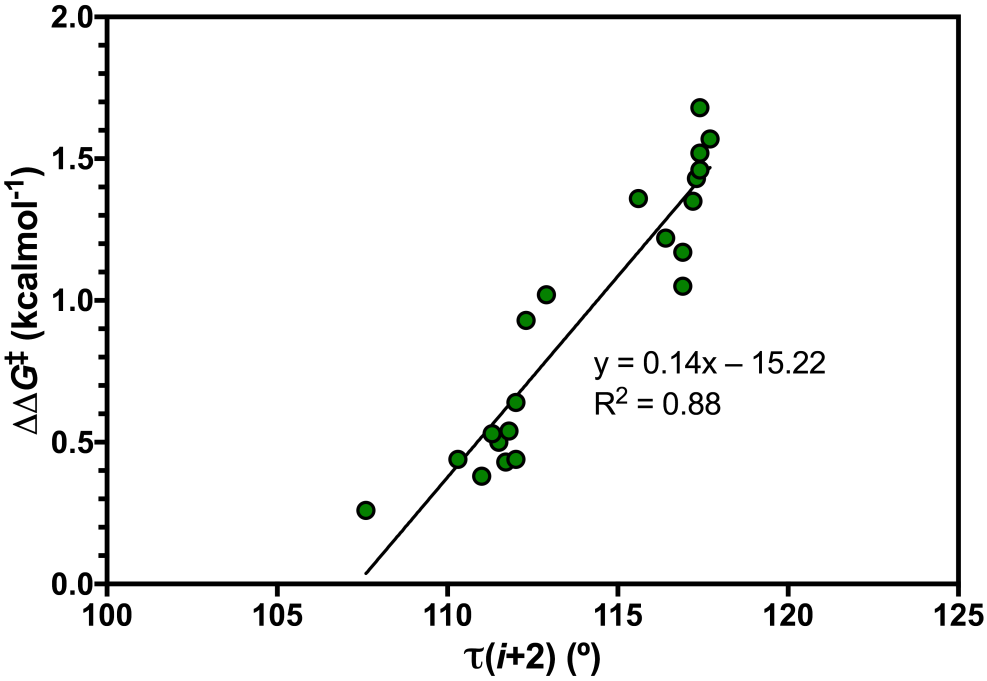

Figure S8.02: Plot of $\Delta\Delta G^{\ddagger}$ vs. τ(*i*+2).

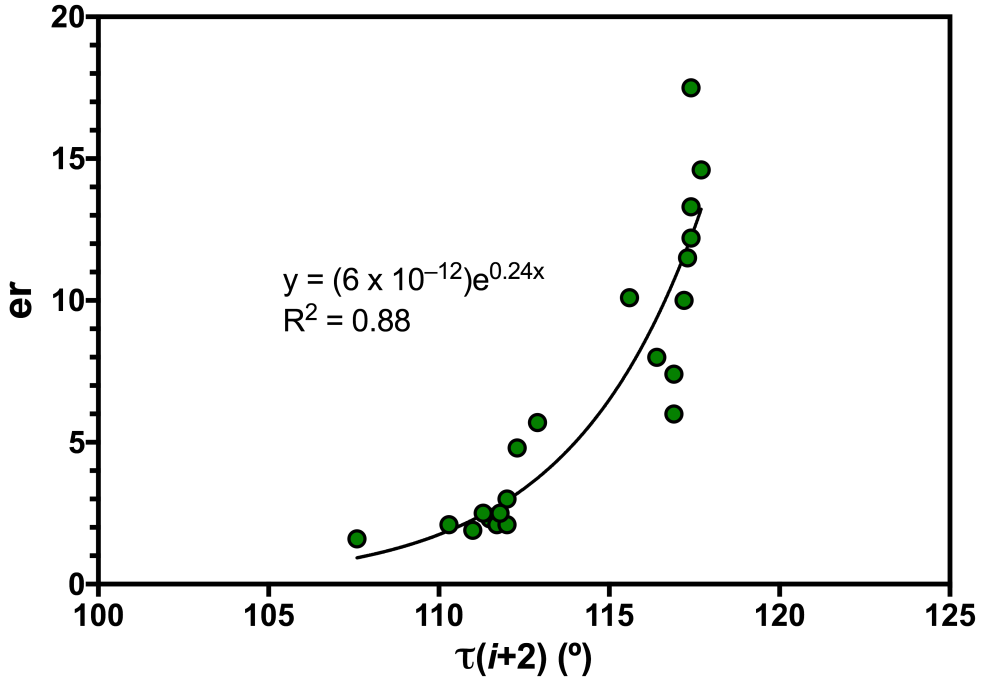

Figure S8.03: Plot of er vs. τ(*i*+2).

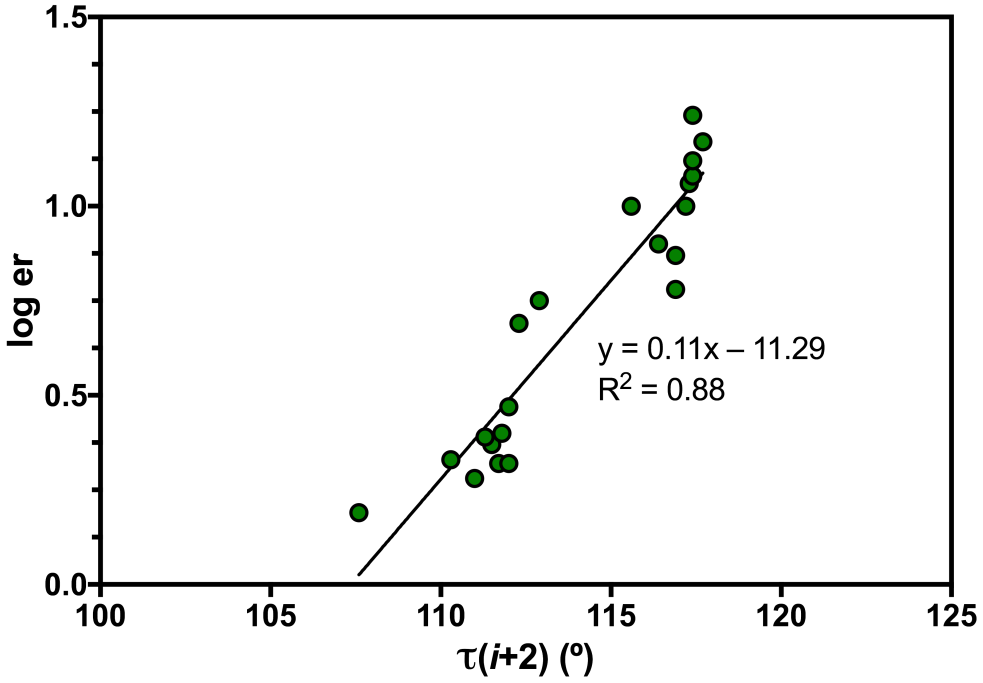

Figure S8.04: Plot of log er vs. τ(*i*+2).

IX. References

1. Fulmer, G. R.; Miller, A. J. M.; Sherden, N. H.; Gottlieb, H. E.; Nudelman, A.; Stoltz, B. M.; Bercaw, J. E.; Goldberg, K. I. *Organometallics* **2010**, *29*, 2176–2179.
2. (a) Montalbetti, C. A. G. N.; Falque, V. *Tetrahedron* **2005**, *61*, 10827–10852. (b) El-Faham, A.; Albericio, F. *Chem. Rev.* **2011**, *111*, 6557–6602.
3. Zhang, L.-H.; Kauffman, G. S.; Pesti, J. A.; Yin, J. *J. Org. Chem.* **1997**, *62*, 6918–6920.
4. Diener, M. E.; Metrano, A. J.; Kusano, S.; Miller, S. J. *J. Am. Chem. Soc.*, **2015**, *137*, 12369–12377.
5. Metrano, A. J.; Abascal, N. C.; Mercado, B. Q.; Paulson, E. K.; Miller, S. J. *Chem. Commun.* **2016**, *52*, 4816–4819.
6. Metrano, A. J.; Miller, S. J. *J. Org. Chem.* **2014**, *79*, 1542–1554.
7. Barrett, K. T.; Miller, S. J. *J. Am. Chem. Soc.* **2013**, *135*, 2963–2966.
8. Blank, J. T.; Miller, S. J. *Biopolymers (Pept. Sci.)* **2006**, *84*, 38–47.
9. Jarvo, E. R.; Copeland, G. T.; Papaioannou, N.; Bonitatebus, P. J.; Miller, S. J. *J. Am. Chem. Soc.* **1999**, *121,* 11638–11643.
10. Jakobsche, C. E.; Peris, G.; Miller, S. J. *Angew. Chem. Int. Ed.* **2008**, *47*, 6707–6711.
11. Blank, J. T.; Guerin, D. J.; Miller, S. J. *Org. Lett.* **2000**, *2,* 1247–1249.
12. CrystalClear and CrystalStructure, Rigaku/MSC, The Woodlands, TX, 2005.
13. *APEX2* and *SADABS*, Bruker AXS Inc., Madison, WI, 2014.
14. Sheldrick, G. M. *Acta Crystallogr.* **2008**, *A64*, 112–122.
15. CYLview was used to render X-ray crystal data: CYLview, 1.0b; Legault, C. Y. L., Universite de Sherbrooke, 2009 (http://www.cylview.org).
16. Mercury CSD 3.8, Macrae, C. F.; Bruno, I. J.; Chisholm, J. A.; Edgington, P. R.; McCabe, P.; Pidcock, E.; Rodriguez-Monge, L.; Taylor, R.; van de Streek, J.; Wood, P. A. *J. Appl. Cryst.*, **2008**, *41*, 466–470.
17. Prism 7.0a, GraphPad Software, Inc., La Jolla, CA, 2016.
18. (a) Wilmot, C. M.; Thornton, J. M. *J. Mol. Biol.* **1988**, *203*, 221–232. (b) Hutchinson, E. G.; Thornton, J. M. *Protein Sci.* **1994**, *3*, 2207–2216.
19. Toniolo, C.; Benedetti, E. *Trends Biochem. Sci.* **1991**, *16*, 350–353.
20. Gunasekaran, K.; Ramakrishnan, C.; Balaram, P. *Protein Eng.* **1997**, *10*, 1131–1141.
21. Shoulders, M. D.; Kotch, F. W.; Choudhary, A.; Guzei, I. A.; Raines, R. T. *J. Am. Chem. Soc.* **2010**, *132*, 10857–10865.
22. (a) Zhou, A. Q.; O'Hern, C. S.; Regan, L. *Protein Sci.* **2011**, *20*, 1166–1171. (b) Sony Malathy, S. M.; Saraboji, K.; Sukumar, N.; Ponnuswamy, M. N. *Biophys. Chem.* **2005**, *120*, 24–31.
23. (a) Dunbrack, R. L.; Sapovalov, M. V. *Proteins: Struct., Funct., Bioinf.* **2011**, *66*, 279–303. (b) Zhou, A. Q.; O'Hern, C. S.; Regan, L. *Biophys. J.* **2012**, *102*, 2345–2352. (c) Zhou, A. Q.; Caballero, D.; O'Hern, C. S.; Regan, L. *Biophys. J.* **2013**, *105*, 2403–2411. (d) Caballero, D.; Smith, W. W.; O'Hern, C. S.; Regan, L. *Proteins: Struct., Funct., Bioinf.* **2015**, *83*, 1488–1499. (e) Caballero, D.; Virrueta, A.; O'Hern, C. S.; Regan, L. *Protein Eng. Des. Sel.* **2016**, *29*, 367–376.
24. (a) Steiner, T. *Angew. Chem. Int. Ed.* **2002**, *41*, 48–76. (b) Gellman, S. H.; Dado, G. P.; Liang, G.-B.; Adams, B. R. *J. Am. Chem. Soc.* **1991**, *113*, 1164–1173.
25. (a) Choudhary, A.; Gandla, D.; Krow, G. R.; Raines, R. T. *J. Am. Chem. Soc.* **2009**, *131*, 7244–7246. (b) Bartlett, G. J.; Choudhary, A.; Raines, R. T.; Woolfson, D. N.; *Nature Chem. Biol.* **2010**, *6*, 615–620. (c) Jakobsche, C. E.; Choudhary, A.; Miller, S. J.; Raines, R. T. *J. Am. Chem. Soc.* **2010**, *132*, 6651–6653. (d) Grünenfelder, C. E.; Kisunzu, J. K.; Trapp, N.; Kastl, R.; Wennemers,

H. *Biopolymers (Pept. Sci.)* **2016**, *ASAP*, DOI: 10.1002/bip.22912. (e) Newberry, R. W.; Orke, S. J.; Raines, R. T. *Org. Lett.* **2016**, *18*, 3614–3617.

26. (a) MacArthur, M. W.; Thornton, J. M. *J. Mol. Biol.* **1996**, *264*, 1180–1195. For related examples, see: (b) Cruz-Cabeza, A. J.; Day, G. M.; Motherwell, W. D. S.; Jones, W. *Cryst. Growth Des.* **2006**, *6*, 1858–1866. (c) Alemán, C.; Jiménez, A. I.; Cativiela, C.; Pérez, J. J.; Casanovas, J. *J. Phys. Chem. B* **2005**, *109*, 11836–11841.
27. (a) Steiner, T. *Acta Crystallogr.* **2000**, *B56*, 673–676. (b) Nangia, A. *Acc. Chem. Res.* **2008**, *41*, 595–604. (c) Cruz-Cabeza, A. J.; Bernstein, J. *Chem. Rev.* **2013**, *114*, 2170–2191.
27. Jeener, J.; Meier, B. H.; Bachmann, P.; Ernst, R. R. *J. Chem. Phys.* **1979**, *71*, 4546–4553.
28. Borgia, B. A.; Gochin, M.; Kehrwood, D. J; James, T. L. *Prog. NMR Spectrosc.,* **1990**, *22*, 83–100.
29. Macura, S.; Farmer, II, B. T.; Brown, L. R. *J. Mag. Res.*, **1986**, *70*, 493–499.
30. Stothard, P. *Biotechniques* **2000**, *28*, 1102–1104.
31. Wang, A. C.; Bax, A. *J. Am. Chem. Soc.* **1996**, *118*, 2483–2494.
32. Karplus, M. *J. Chem. Phys.* **1959**, *30*, 11–15.
33. Karplus, M. *J. Am. Chem. Soc.* **1963**, *85*, 2870–2871.
34. Online graphing software (https://www.desmos.com/calculator/xjx15igpsf).
35. Gaussian 09, Revision **D.01**, Frisch, M. J.; Trucks, G. W.; Schlegel, H. B.; Scuseria, G. E.; Robb, M. A.; Cheeseman, J. R.; Scalmani, G.; Barone, V.; Mennucci, B.; Petersson, G. A.; Nakatsuji, H.; Caricato, M.; Li, X.; Hratchian, H. P.; Izmaylov, A. F.; Bloino, J.; Zheng, G.; Sonnenberg, J. L.; Hada, M.; Ehara, M.; Toyota, K.; Fukuda, R.; Hasegawa, J.; Ishida, M.; Nakajima, T.; Honda, Y.; Kitao, O.; Nakai, H.; Vreven, T.; Montgomery, J. A., Jr.; Peralta, J. E.; Ogliaro, F.; Bearpark, M.; Heyd, J. J.; Brothers, E.; Kudin, K. N.; Staroverov, V. N.; Kobayashi, R.; Normand, J.; Raghavachari, K.; Rendell, A.; Burant, J. C.; Iyengar, S. S.; Tomasi, J.; Cossi, M.; Rega, N.; Millam, J. M.; Klene, M.; Knox, J. E.; Cross, J. B.; Bakken, V.; Adamo, C.; Jaramillo, J.; Gomperts, R.; Stratmann, R. E.; Yazyev, O.; Austin, A. J.; Cammi, R.; Pomelli, C.; Ochterski, J. W.; Martin, R. L.; Morokuma, K.; Zakrzewski, V. G.; Voth, G. A.; Salvador, P.; Dannenberg, J. J.; Dapprich, S.; Daniels, A. D.; Farkas, Ö.; Foresman, J. B.; Ortiz, J. V.; Cioslowski, J.; Fox, D. J. Gaussian, Inc., Wallingford CT, 2013.
36. All computational work was supported by the facilities and staff of Yale University Faculty of Arts and Sciences High Performance Computing Center, and by the National Science Foundation under grant number CNS 08-21132 that partially funded acquisition of the facilities.
37. GaussView 5.0, Gaussian, Inc., Wallingford, CT, 2008.
38. (a) J. A. Pople, J. A.; Gill, P. M. W.; Johnson, B. G. *Chem. Phys. Lett.* **1992**,*199*, 557–560. (b) Parr R. G.; Yang, W. *Density-Functional Theory of Atoms and Molecules*; Oxford University Press: Oxford, 1989.
39. Zhao, Y.; Truhlar, D. G. *Theor. Chem. Acc.* **2008**, *120*, 215–241.
40. Thompson, H. P. G.; Day, G. M. *Chem. Sci.* **2014**, *5*, 3173–3182.
41. (a) Grimme, S.; Antony, J.; Ehrlich, S.; Krieg, H. *J. Chem. Phys.*, **2010**, *132*, 154104–1–19. (b) S. Grimme, Ehrlich, S.; Goerigk, L. *J. Comp. Chem.* **2011**, *32*, 1456–1465.
42. Nagase, T.; Mizutani, T.; Ishikawa, S.; Sekino, E.; Sasaki, T.; Fujimura, T.; Ito, S.; Mitobe, Y.; Miyamoto, Y.; Yoshimoto, R.; Tanaka, T.; Ishihara, A.; Takenaga, N.; Tokita, S.; Fukami, T.; Sato, F. *J. Med. Chem.* **2008**, *51*, 4780–4789.
43. Ponomarev, I. I.; Razorenov, D. Y.; Petrovskii, P. V. *Russ. Chem. Bull.* **2009**, *58*, 2376–2384.
44. (a) Milo, A.; Bessm E. N.; Sigman, M. S. *Nature*, **2014**, *507*, 210–214. (b) Gustafson, J. L.; Sigman, M. S.; Miller, S. J. *Org. Lett.* **2010**, *12*, 2794–2797. (c) Sigman, M. S.; Harper, K. C.; Milo, A. *Acc. Chem. Res.* **2016**, *49*, 1292–1301.